AUGUST 2024
ENERGINET ELTRANSMISSION A/S

HESSELØ SOUTH - INTEGRATED 3D GEOMODEL

REPORT

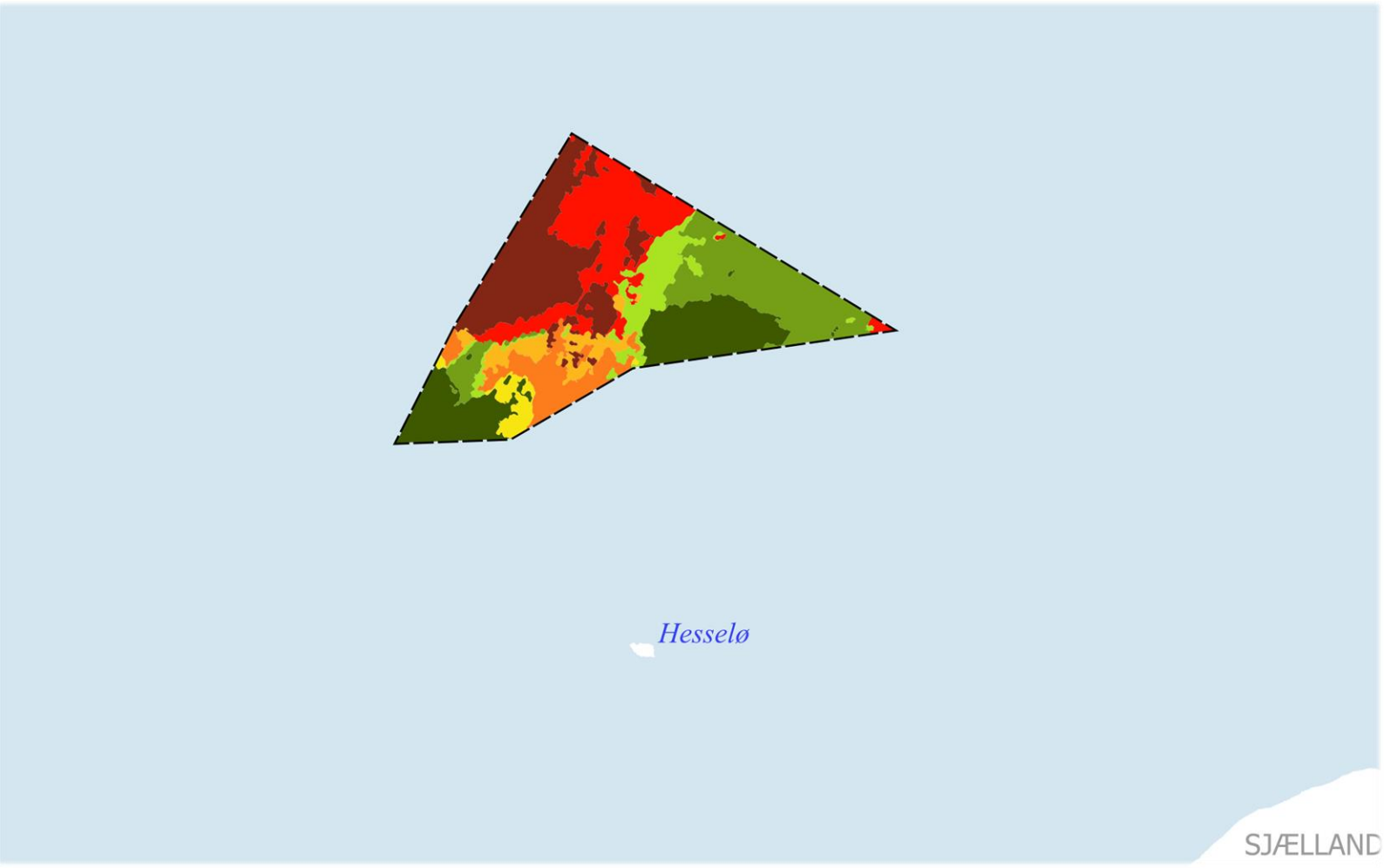

COWI

ADDRESS COWI A/S
Parallelvej 2
2800 Kongens Lyngby
Denmark

TEL +45 56 40 00 00
FAX +45 56 40 99 99
WWW cowi.com

AUGUST 2024
ENERGINET

HESSELØ SOUTH - INTEGRATED 3D GEOMODEL

REPORT

PROJECT NO.	DOCUMENT NO.
A268907	A268907-REP-001

VERSION	DATE OF ISSUE	DESCRIPTION	PREPARED	CHECKED	APPROVED
3.0	29.08.2024	Report	CONN, MALA, ATHN, KAWE, SPSO	KAPN, KTAA	OFN

CONTENTS

APPENDICES

1 Executive Summary

As part of Denmark's plan for expansion of the energy supply from offshore wind farms (OWF) towards 2030, The Danish Energy Agency is planning to tender out the Hesselø South OWF project site in 2024 for design and installation of wind turbines. The site is located in the Danish Inner Seas (Kattegat), covers approximately 166 km² and is planned for a capacity of 0.8-1.2 GW.

This report describes the work and outcome of the Integrated Geological Model (IGM) for the Hesselø South OWF project site. The 3D IGM covers the site down to a minimum depth of 100 mbsb (m below seabed) and is based on integrated interpretation of geophysical and geotechnical data.

The geotechnical site investigations and reporting is made by Gardline and geophysical investigations and reporting by GEOxyz, both investigations finalized in 2023. Seismic 2D UHRS data cover the site down to minimum 100 mbsb with a line spacing of 250 m by 1000 m (870 line-km in total) and SBP data cover the top 10 mbsb with a line spacing of 62.5 m by 1000 m (3858 line-km in total). The geotechnical data comprise offshore and onshore testing from eight (8) boreholes, 32 cone penetration tests (CPT), four (4) P-S logs and several classification tests, advanced laboratory tests and chemical tests.

The result is an IGM containing detailed information on the spatial distribution of the soil units as well as the characteristic geotechnical parameters. It contains thirteen (13) integrated soil units consisting of Holocene, Pleistocene, or Miocene deposits.

The sediments generally comprise relative soft Holocene and Late Weichselian soils overlaying competent Pleistocene soils. The thickness of the soft soils is found to depths of more than 30 m below seabed in the Western and Northern part of the site. Toward East and South consolidated Pleistocene layers generally of more than 25 m thickness is interpreted. Pre-quaternary layers is generally found deeper than 45 m but found shallower central at the site and toward south.

Potential geohazards include shallow gas in Holocene deposits. Further, glacial deformation can create a lager variability in geotechnical properties of the

Pleistocene soils whereas faulting is found to be confined to the pre-quaternary layers.

Enclosures provided with this report present the soil units as surface maps with respect to depth below seabed, elevation, thickness, and lateral extent. Furthermore, 13 cross sections are provided showing the soil units, seismic data, and geotechnical data. Appendices include presentation of geotechnical data and interpretations, and the Conceptual Geological Model.

Based on the IGM a geotechnical zonation has been made outlining eight (8) different geotechnical zones with regards to ground conditions for WTG foundation design. The zones have been defined based on selected criteria for thicknesses of soft sediments and glacial impacted layers as well as depth to the pre-quaternary deposits. The geotechnical zonation map shows that the conditions for WTG foundations are best in the eastern and southwestern part of the site, while the poorest conditions are found in the north.

Also, a high-level leg penetration analysis is made for two different types of vessels. The results show a higher leg penetration risk in the geotechnical zones with thick layers of normally consolidated soft clays.

All enclosures and grids are provided digitally. The Integrated Geological Model is delivered as a digital 3D model in a Kingdom suite project.

2 Introduction

The Integrated Geological Model (IGM) for the former Hesselø OWF was finalized in 2022. A key finding was that low strength deposits were prevalent with cumulated thicknesses of more than 35 m in more than half of the area of investigation. The Danish Energy Agency therefore decided to carry out new investigations just south of the former Hesselø site. The new site is called Hesselø South.

This report presents the Integrated Geological Model from the new Hesselø South OWF project site. The IGM was made by COWI January-Juli 2024 and is based on the geophysical investigations (finalized in 2023) and preliminary geotechnical investigations (finalized in 2023) procured by Energinet Eltransmission A/S.

The result is an IGM; a 3D digital ground model with spatial distribution of the interpreted geological units across the site down to a depth of minimum 100 m bsb (below seabed). Besides the IGM a geotechnical characterization of each soil unit is provided together with a geotechnical zonation map. Furthermore, a Leg Penetration Analysis (LPA) is provided.

The purpose of this work is to provide an overview of the site with respect to WTG (Wind Turbine Generator) foundation conditions. The results thus provide an important basis for the tenderers, who are applying for a licence to develop and construct the OWF, and for the assessment of the soil-related risks and requirements for installation and design of the WTG foundations.

The deliverables include a digital 3D ground model (Kingdom Suite), all soil unit interfaces as grids and this report including appendices and charts. Please see section 12 for detailed information on the appendices, charts, and deliverables.

2.1 The project site

The Hesselø South OWF project site is situated just south of the former Hesselø OWF project site, approximately 30 km offshore the northern coast of Zealand in the inner waters of Kattegat.

The Hesselø South OWF project site covers 166 km² and is shown in Figure 2-1 together with the former Hesselø OWF project site. The coordinates for the vertices of the area are listed in Table 2-1.

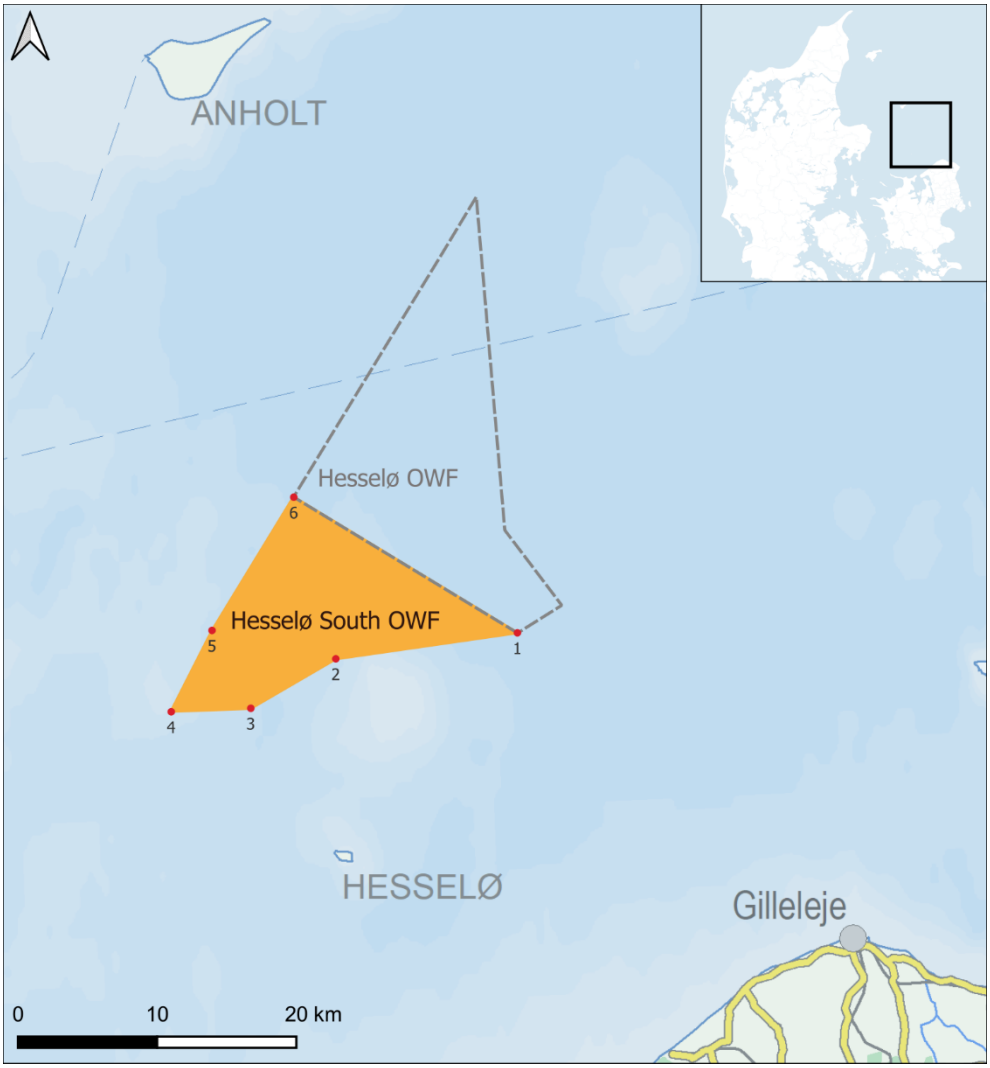

Figure 2-1 *Hesselø South OWF project site shown in orange. Vertices for the area are shown as red dots. The former Hesselø OWF site (grey) is situated just north of the Hesselø South OWF project site.*

Table 2-1 *Coordinates for the 6 vertices of the Hesselø South OWF project site.*

Point ID	Easting EUREF89 Zone 32N [meter]	Northing EUREF89 Zone 32N [meter]	Longitude EUREF89	Latitude EUREF89
1	680400	6247230	11° 55.099' E	56° 20.121' N
2	667356	6245357	11° 42.383' E	56° 19.400' N
3	661231	6241793	11° 36.317' E	56° 17.608' N
4	655523	6241583	11° 30.781' E	56° 17.610' N
5	658472	6247391	11° 33.847' E	56° 20.679' N
6	664326	6256983	11° 39.884' E	56° 25.724' N

2.2 Scope of Work

The results presented in this report will be part of the Hesselø South OWF tender process, informing development tenderers about the local geology, associated geotechnical properties and potential geohazards as well as supporting

subsequent development of the Hesselø South OWF project site. A key objective of the present work is to ensure the applicability for sub-selection of a specific OWF site within the area of investigation.

The output of the assignment must be applied for

- Sub-selection of specific OWF area within the area of investigation.
- Initial determination of foundation concept and design.
- Assessment of the soil-related risks for installation of foundations.
- Initial planning of the layout for turbines.

These applications are relevant for both the license tender process and the subsequent development performed by the nominated developer.

The Integrated Geological Model comprises a Conceptual Geological Model, a digital, spatial geological model, and a geotechnical characterization of the soil units in the model.

Furthermore, a Geotechnical Zonation Map and a Leg Penetration Analysis are provided.

3 Basis

The data packages have been received successively from Energinet. An overview of the data received from Energinet is listed below, divided into the geotechnical and geophysical data packages including reports.

Geotechnical data packages	
Datatype	Year
Danish Offshore Wind 2030 - Lot 1 - Hesselø South, Volume II Measured and Derived Final Results, Revision 2, Gardline. AGS data and Excel files providing results from offshore and onshore works of the geotechnical site investigation for Lot 1 documented in the report.	2024
Geophysical data packages	
Datatype	Year
GEOxyz: Kingdom Project with 2D Ultra High Resolution Seismic (2D UHRS) Line spacing 250*1000 m Sub Bottom profiler (SBP) Line spacing 62.5*1000 m SEG-Y data was also delivered separately from the Kingdom project Multi Beam Echo Sounder (MBES), 0.25 m x 0.25 m bin size / 16 x pings per 1.0 m x 1.0 m	2024
GEOxyz: Geodatabase with Multi Beam Echo Sounder (MBES), 0.25 m x 0.25 m bin size / 16 x pings per 1.0 m x 1.0 m Side Scan Sonar (SSS) and Magnetometer (MAG) with between 50 to 62.5 m line spacing. Tracklines, maps and results from geophysical surveys (MBES, SSS, MAG)	2024

Reports		
Author	Title	Year
GEUS	Screening of seabed geological conditions for the offshore wind farm area Hesselø South and the adjacent cable corridor area	2023
GEOxyz	Geophysical Surveys for Danish Offshore Wind 2030 - Hesselø South	2023

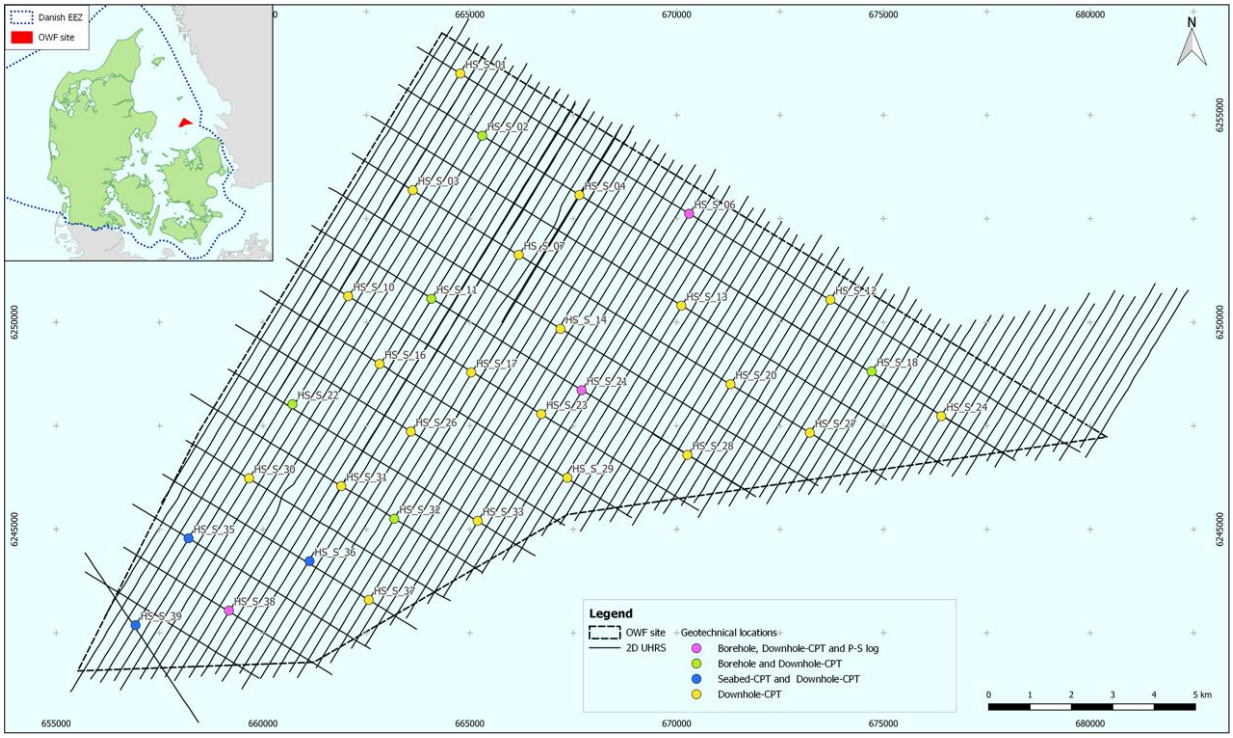

Figure 3-1 Overview map of the Hesselø South OWF project site with locations for the 2D UHRS seismic lines and geotechnical data (borehole, CPT and P-S log).

3.1 Geotechnical basis

The geotechnical basis for the project can generally be divided into two categories:

- Offshore sampling and in-situ testing
- Laboratory testing and description

The site investigation work has been performed by Gardline from March 2023 to August 2023, focusing on the Hesselø South area. The campaign consisted of in-situ testing and laboratory testing. The in-situ works include borehole sampling (BH), different CPT types and wireline logging. The laboratory works consist of soil description and classification testing as well as a comprehensive onshore laboratory test programme performed mainly by Gardline, but with the chemical testing and rock UCS performed by GEOLABS and the advanced tests performed by GEO.

The geotechnical work has been summarised in a factual report.

3.1.1 In-situ works

The offshore works consist of in-situ testing (seabed and downhole CPTs), P-S logging, and borehole drilling incl. sampling. The acquired samples are used for testing in the onshore laboratory programme.

An overview of the positions for CPT, including seabed (CPT), downhole (dCPT) and boreholes (with sampling) is shown in Table 3-1, Figure 3-1, and on Enclosure 1.02.

Several locations across the Hesselø South OWF project site have multiple CPTs due to premature CPT refusal, which means that the total number of unique locations surveyed is 32. Of these 32 locations, 8 locations have been surveyed with minimum one (1) CPT and one (1) borehole, while 24 have been surveyed with minimum one (1) CPT but no borehole.

For boreholes a target depth of 70 m was considered. For CPTs a target depth of 55 m was considered. However, it is noted that most of the seabed CPTs have not reached the target depth due to stop criteria, like CPT refusal or rod deviation.

The distances between CPTs and boreholes performed at the same location and the distances between extra repeated CPTs performed at the same location are maximum 13.6 m.

Table 3-1 Summary of in-situ geotechnical tests.

Test type	Quantity*
Seabed Cone Penetration Test (CPT)	6 (incl. 3 retests)
Composite Cone Penetration Test and sampling boreholes (BH)	8
Downhole Cone Penetration Test (dCPT)	28 (incl. 4 retests)
P-S logging	At 4 BHs (incl. 1 bump-over)

**Only counting locations with usable data.*

3.1.2 Laboratory works

The laboratory works consist of classification testing, advanced laboratory testing and chemical testing. The performed laboratory tests available are summarized in Table 3-2.

All laboratory works are performed using samples acquired from the geotechnical composite downhole CPT and boreholes.

Table 3-2 Summary of performed laboratory tests.

Test type	Quantity*
Water content	146
Bulk and dry density	Bulk density 170, dry density 53
Particle density	33
Atterberg limits	38

Test type	Quantity*
Particle size distribution	51
Maximum and minimum dry density	2
Carbonate content	18
Acid & Water-soluble Sulphate	18
Acid & Water-soluble Chloride	18
Loss on ignition (Organic content)	8
Thermal conductivity	6
Oedometer (incremental load)	19
Laboratory miniature vane test	7
Laboratory hand penetrometer	166
Laboratory torvane test	65
Unconsolidated Undrained (UU) triaxial test	23
Point load tests (PLT)	34 (excl. 4 invalid tests)
Unconfined compressive strength (UCS)	9 incl. 3 with strain gauges
Consolidated Isotropically Undrained (CIU) triaxial tests	17 (1 excluded due to soil type)
Consolidated Isotropically Drained (CID) triaxial tests	4
Consolidated Anisotropically Undrained (CAU) triaxial tests	12 (1 excluded due to test conditions)
Cyclic Consolidated Anisotropically Undrained (CAUcyc) triaxial tests	11
Direct simple shear (DSS) tests	14
Direct simple shear cyclic (CSS) tests	12 (4 sets of 3)

**Numbers based on available quantity of test results in available AGS data file, and numbers therefor can differ when comparing to numbers presented in Factual Report, cf. Ref. /1/, due to discrepancies between the Factual Report and related AGS data file.*

3.2 Geophysical and hydrographical basis

The geophysical basis for this report is a geophysical survey including 2D UHRS and SBP, acquired in 2023 by GEOxyz.

The main objectives from these surveys from GEOxyz are:

- Initial marine archaeological site assessment.

- Planning of environmental investigations.
- Planning of initial geotechnical investigations.
- Decision of foundation concept and preliminary foundation design.
- Assessment of installation conditions for foundations and inter-array cables.
- Site information enclosed the tender for the offshore wind farm concession.
- Acquiring high resolution bathymetric data to ascertain water depth and changes in topography across the sites using multibeam echosounder (MBES) data.
- Acquiring high frequency (900 kHz) side scan sonar (SSS) data to identify seabed objects and features.
- Acquiring low frequency (300 kHz) side scan sonar (SSS) data to distinguish seabed sediments.
- Acquiring magnetometer data to identify cables, pipelines, potential UXOs and other ferrous objects on and below the seabed.
- Acquiring high-resolution and 2D ultra high-resolution seismic data, in order to locate structural complexities or geohazards within the shallow geological succession, such as faulting, accumulations of shallow gas, buried channels, soft sediments, hard sediments, high boulder density estimation, mobile sediments, etc.

The work described above and below has been performed by GEOxyz, and the outcome of the site investigations (SI's) has been documented in Ref. /10/.

3.2.1 Bathymetry

MBES data were acquired for the entire Hesselø South area with a line spacing of between 50 and 62 m, deviating from the original plan for line spacing of 62.5 m due to conditions in the area. The Bathymetry was delivered with a grid size of 0.25x0.25 m.

The bathymetry can be found in enclosure 1.01. As can be seen from the enclosure the water depth varies between approx. 18 to 33 meters.

3.2.2 Subsurface data

The 2D UHRS data were acquired with NW-SE orientated lines with a line spacing of 250 m, and cross lines were oriented in a NE-SW with a line spacing of 1000 m (See enclosure 1.02). Lines with a planned length below 4 km were extended outside the survey area to the minimum length of 4 km.

The SBP mainlines were also acquired with a NW-SE orientation with a line spacing of 62.5 m and with crosslines with an orientation of NE-SW and a line spacing of 1000 m (see enclosure 1.02).

The quality of the data is described in section 9.3.

4 Geological Setting

In this section the geological setting for the Hesselø South OWF project site is presented.

4.1 Pre-Quaternary Geology

The Hesselø South OWF project site is located near the south-western boundary of the Baltic Shield between the southern part of Sweden, the Kattegat, and the northern part of Jutland (Figure 2-1). The area is strongly influenced by the Sorgenfrei Tornquist zone, a southeast to northwest oriented fault system, where one of the major faults, the Grenå-Helsingborg fault crosses the middle of the Hesselø South OWF project site, see Figure 4-1.

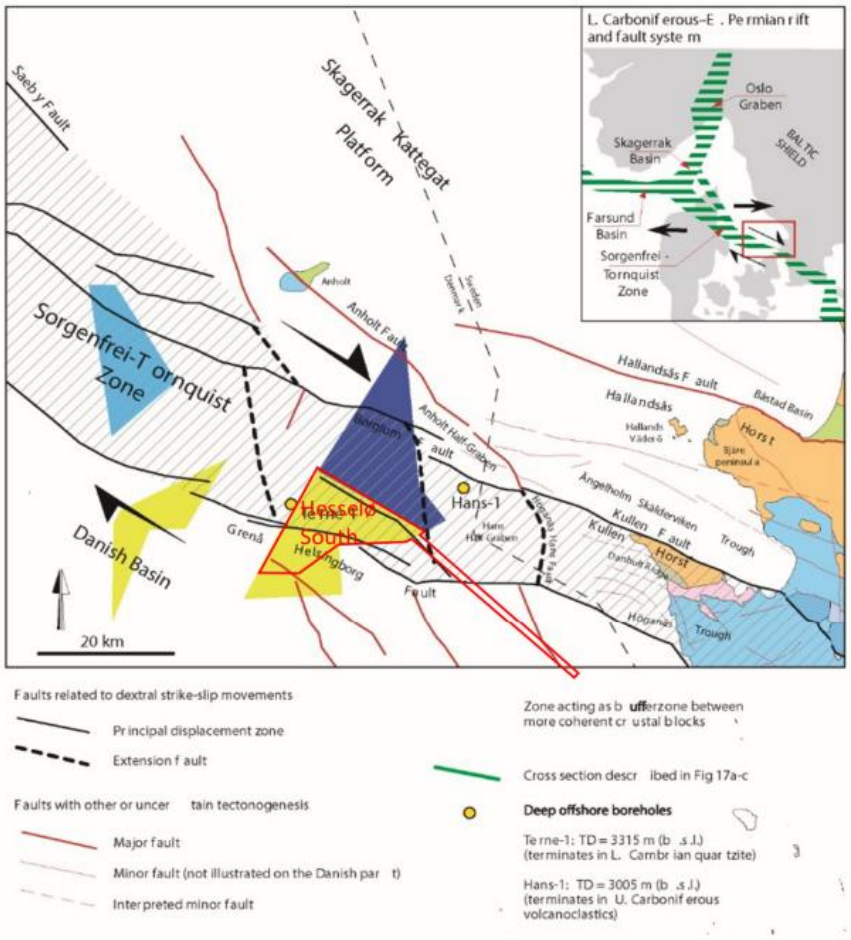

Figure 4-1: Map of the regional structures in the southern part of Kattegat, modified by GEUS from Ref. /9/.. The Hesselø South OWF project site and cable corridor is marked with a red outline. The former Hesselø OWF project site is marked with a blue area and on-going investigation areas (Kattegat and Hesselø South) are marked with a yellow area. The already existing Anholt OWF is marked by a turquoise area.

In the Late Cretaceous – Early Paleogene, the previous subsiding depocenter became inverted, primarily along pre-existing faults, due to a change in the regional stress orientation dominated by compression associated with the Alpine Orogeny and the opening of the North Atlantic.

The Hesselø South OWF project site is located on a NW-dipping crystalline anticlinorium, and the bedrock is expected to be Upper Cretaceous and Jurassic sandy mudstone, see Figure 4-2, Ref. /9/.

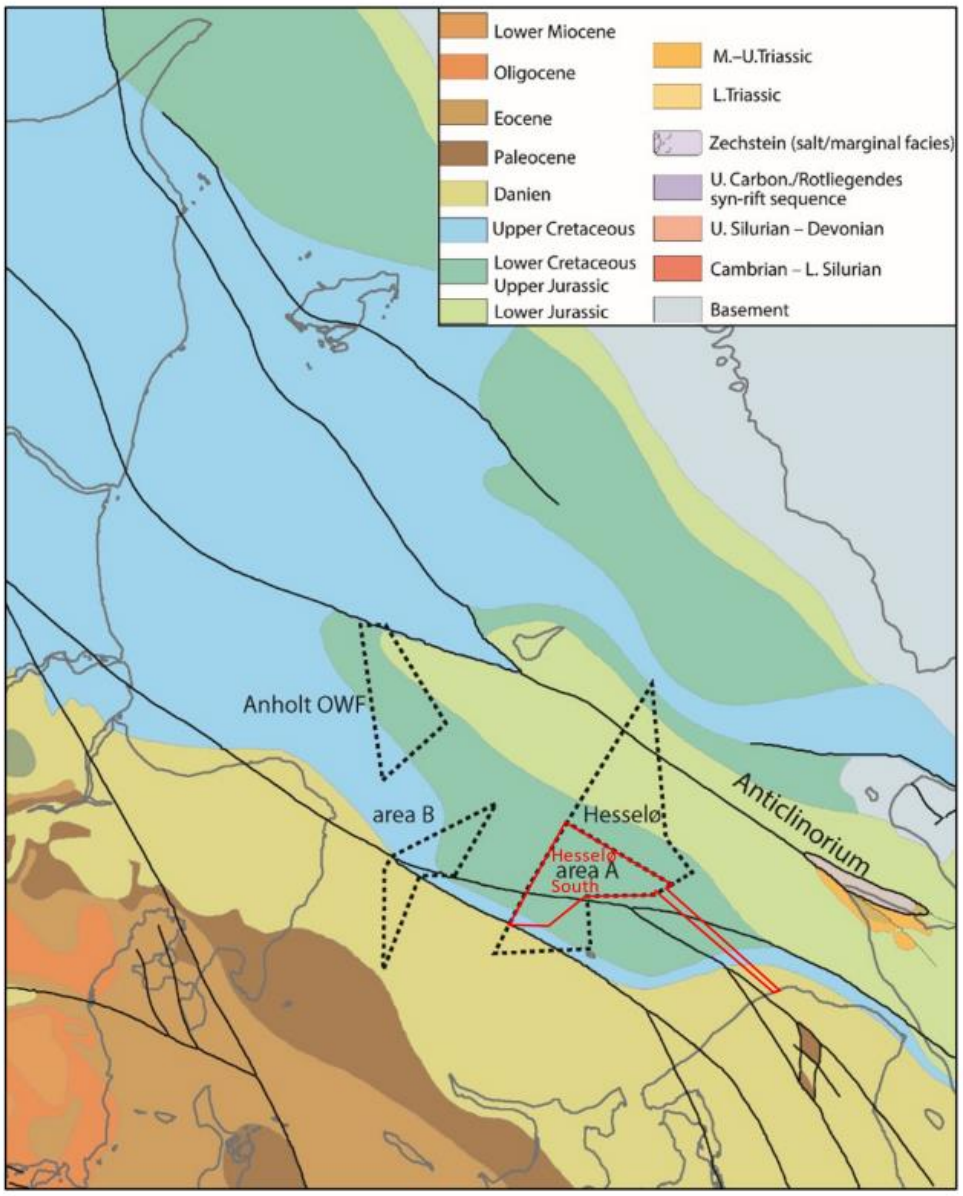

Figure 4-2: Map of the major faults and the Pre-Quaternary of Kattegat. The Hesselø South OWF project site and the corresponding cable corridor is marked by a red line (Ref. /9/).

4.2 Quaternary Geology

During the Quaternary period several glacial events have been identified in the northern Danish area. The different glacial events are separated by interglacial or interstadial marine or glaciolacustrine conditions. In Figure 4-3 the extent of the three major ice advances, the Elsterian, the Saalian, and the Weichselian ice advance can be seen. The Hesselø South OWF project site is marked by a star and during the largest extent of all three ice advances the OWF has had a subglacial setting.

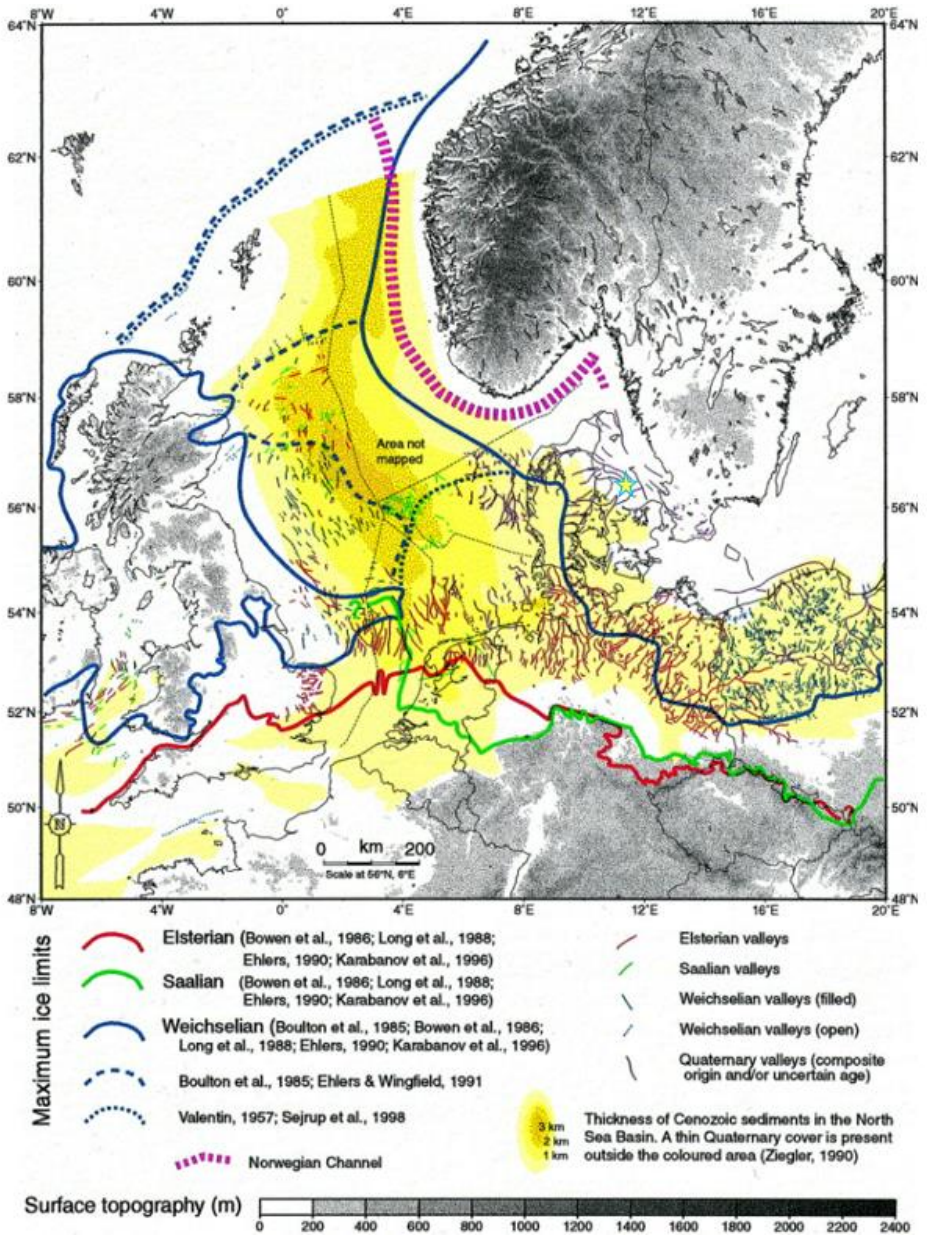

Figure 4-3: The extent of the three major ice advances along with known associated tunnel valleys. Hesselø South OWF is marked by a light-blue star (Ref. /9/).

Till from the Weichselian glaciation is found south of Anholt along with late glacial and Holocene deposits. The Scandinavian Ice Sheet reached its maximum extent in Denmark about 22 ka BP followed by stepwise retreat. Around 18 ka

BP the sea began to inundate northern Denmark which led to rapid deglaciation. At ca. 17 ka BP the ice margin had retreated to the Halland coastal moraines along the Swedish west coast (Ref. /9/). In the Danish area the ice cap steadily retreated, which caused the opening of the Kattegat depression and a transgression of the area. A glaciomarine environment was established where the glacier was in direct contact to the sea. Therefore, discharge of meltwater-borne sediments could be dispersed from the glacier to the sea and drop stones rafted by calving icebergs should be expected. Thick glaciomarine deposits related to the late glacial are reported from the area (Ref. /9/).

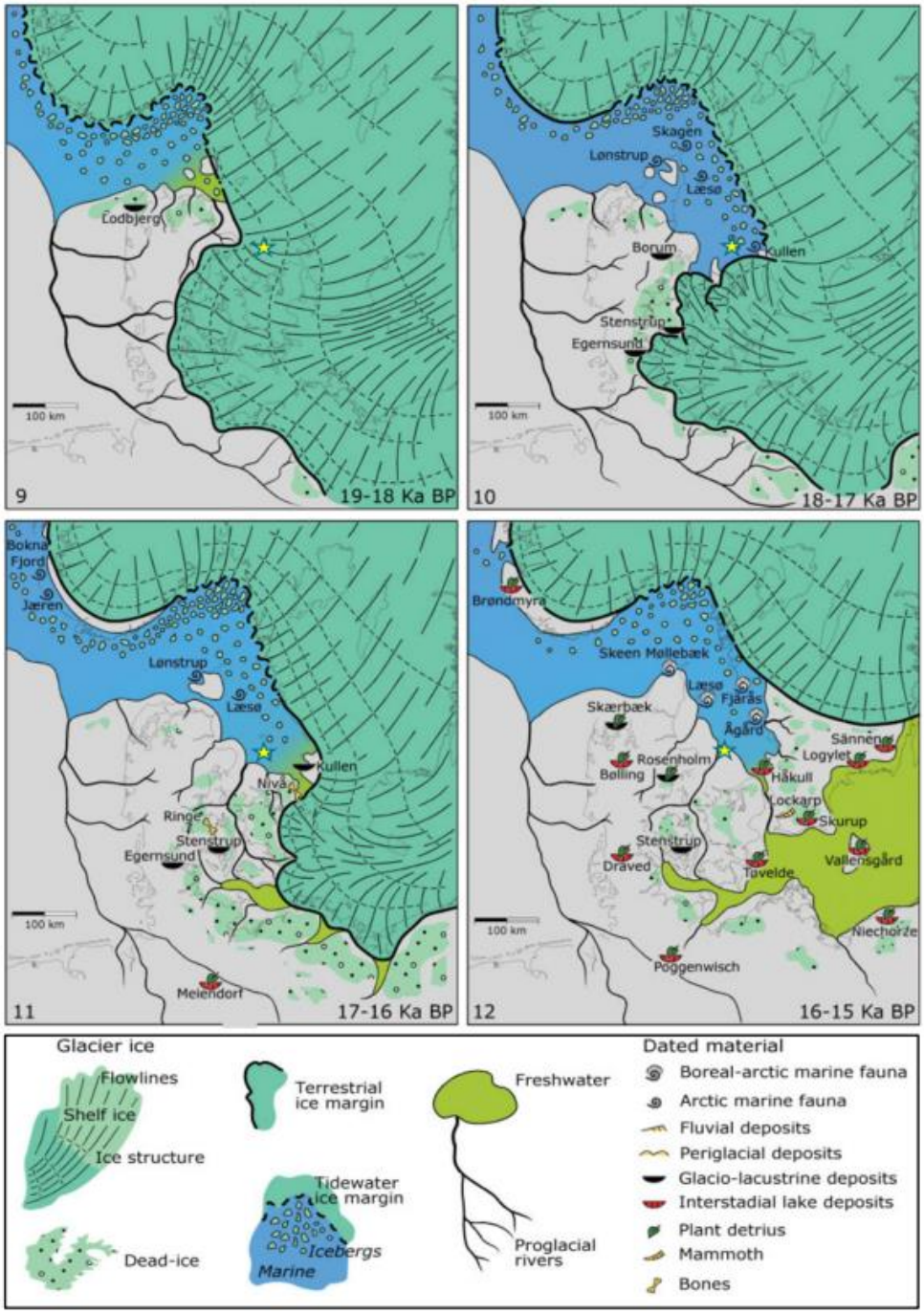

Figure 4-4: Paleogeographical reconstructions of the last deglaciation of southern Scandinavia. Hesselø South OWF site is marked by a star. (Ref. /9/).

5 Conceptual Geological Model

The Conceptual Geological Model is compiled as hand-drawn geological profiles summarizing the geology across the entire Hesselø South OWF project site. It is based on units from the Integrated Geological Model, geological cross sections, and layer thickness maps extracted from the spatial model.

The colours in the conceptual model differ from the colours in the spatial model, as the units have been grouped in colours according to age and lithology, whereas they have been chosen for ease of interpretation in the spatial model. The Conceptual Geological Model can be seen in Figure 5-1 and Figure 5-2 and in better resolution in Appendix G.

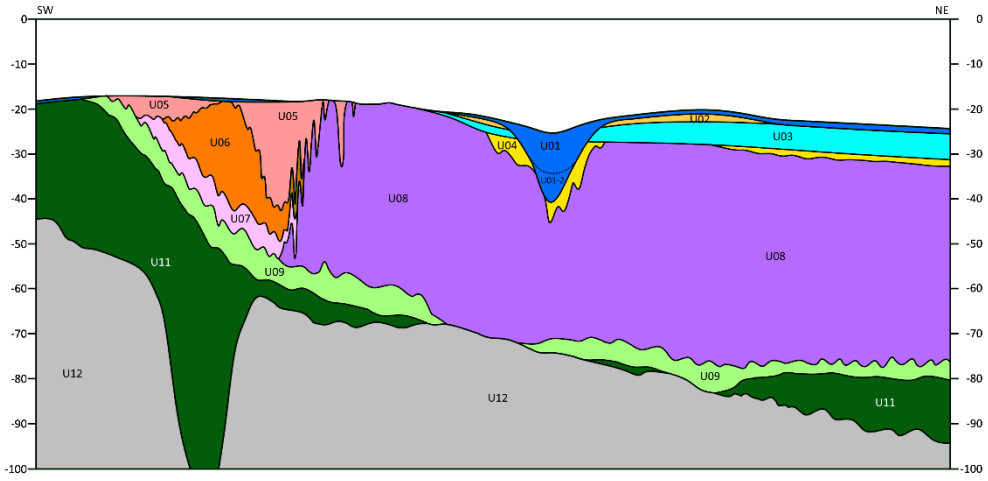

Figure 5-1 Conceptual model cross section oriented from southwest to northeast through the Hesselø South OWF project site.

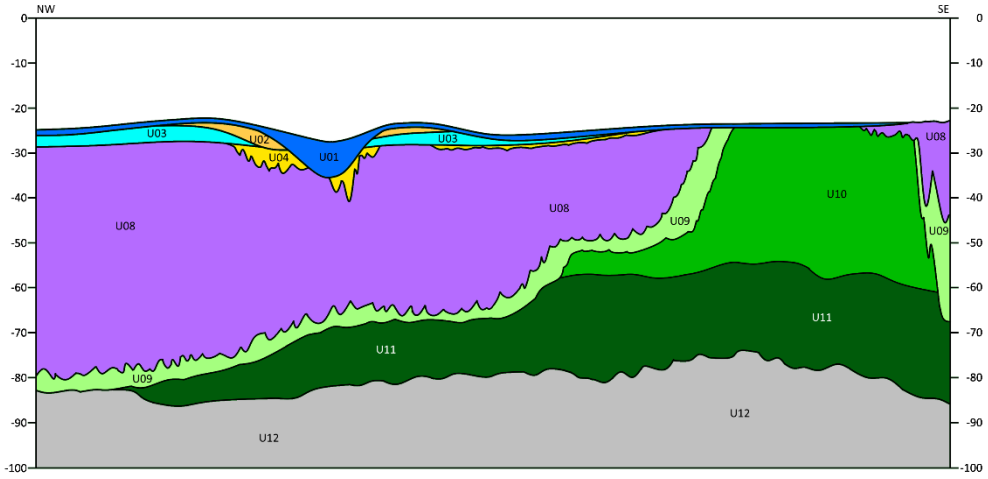

Figure 5-2 Conceptual model cross section oriented from northwest to southeast through the Hesselø South OWF project site.

The Conceptual Geological Model presents all the interpreted and integrated model units. Thickness, depth and location are only indicative for the individual units. The model consists of the units presented in Table 5-1 below.

Table 5-1: List of units constituting the model with assigned age, depositional environment, and relation to the units from the former Hesselø model.

Unit (colour in Conceptual model)	Age	Depositional environment	Primary soil type	Equivalent units in the former Hesselø model
U01/ U01-2	Holocene	Post glacial, marine	CLAY	A
U02	Early Holocene	Post glacial, deltaic marine	SAND	B
U03	Early Holocene	Post glacial, deltaic marine	CLAY	B
U04	Early Holocene	Post glacial, fluvial to shallow marine	SAND	C
U05	Late Weichselian	Late glacial, glaciolacustrine	SAND/CLAY	Unit not present
U06	Late Weichselian	Late glacial, glaciolacustrine	SAND	Unit not present
U07	Late Weichselian	Late glacial, glaciolacustrine	CLAY	Unit not present
U08	Late Weichselian	Late glacial, glaciomarine	SAND/CLAY	D1, D2, E1, E2, F
U09	Late Weichselian	Glacial, subglacial (mostly deformed glaciomarine)	CLAY	H
U10	Weichselian	Glacial, glaciofluvial	SAND	H
U11	Weichselian or Early Pleistocene	Glacial, mixed environments	TILL	H
U12	Jurassic to Early Cretaceous	Marine	SANDSTONE/ MUDSTONE	I

The model can be divided into four primary stratigraphical groups. The Holocene, The Late Weichselian, the Weichselian and Early Pleistocene, and the Jurassic and Early Cretaceous.

The Holocene comprises U01/U01.2, U02, U03 and U04, and constitutes a relatively shallow part of the model, that represents the post glacial deposits. U01/U01.2 represents deposits from the Littorina transgression to present marine conditions. U02, U03, U04 represents the transition from terrestrial and fluvial to shallow marine conditions in Early Holocene.

The Late Weichselian comprises U05, U06, U07, U08, U09 and constitute the main part of the model and are related to the period of deglaciation (late glacial) where depositional rates were high, filling in thick beds of primarily glaciomarine deposits. Units U05, U06, and U07 are interpreted to represent glaciolacustrine deposits. U08 and part of U07, U06 and U05 have been heavily deformed, most likely by late glacial soft-sediment deformation processes (SSDS), see Figure 5-3, Figure 5-4, and section 9.8.5. U09 has been glacially overridden and is expected to mainly consist of glaciomarine deposits which have been mixed with other deposit types and may have slightly higher strength caused by the glacial compaction. The deformation structures have a southern limit which is likely to be related to the southern extent of the Sorgenfrei-Tornquist Zone (see Figure 5-3 and the white line in Figure 5-5 for comparison). The glacier that deposited and/or deformed U09 is interpreted to have covered the entire site. A subsequent glacial advance is expected to have partly eroded and squeezed into the deposits of U08 from southern and eastern directions, see Figure 5-3, Figure 5-4, and Figure 5-5. By this event a depression was formed into the southern central part of the area, which was afterwards filled up by the glaciolacustrine deposits of U07, U06, and U05.

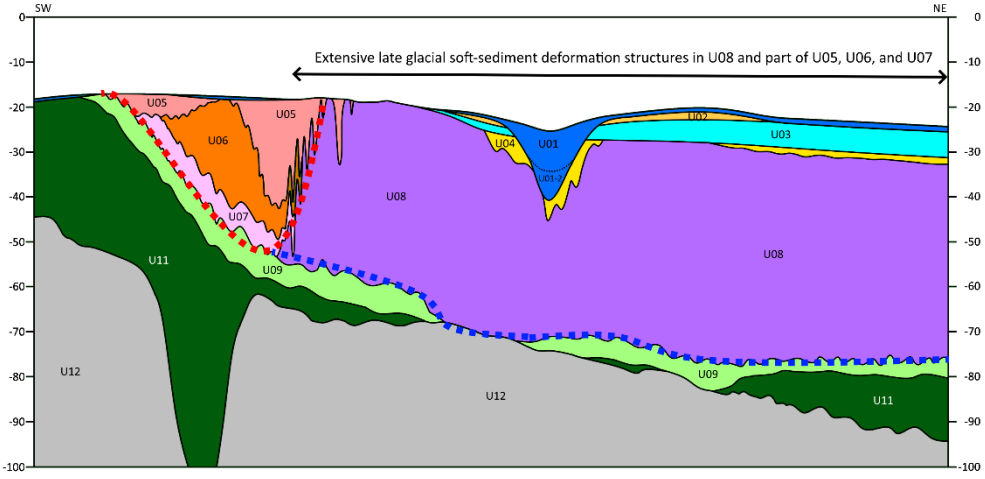

Figure 5-3 *Conceptual model cross section oriented from southwest to northeast through the Hesselø South OWF project site. Extent of SSDS indicated with arrows. Dashed lines indicate latest glacier advances into the area – the blue prior to deposition of U08, the red prior to deposition of U07.*

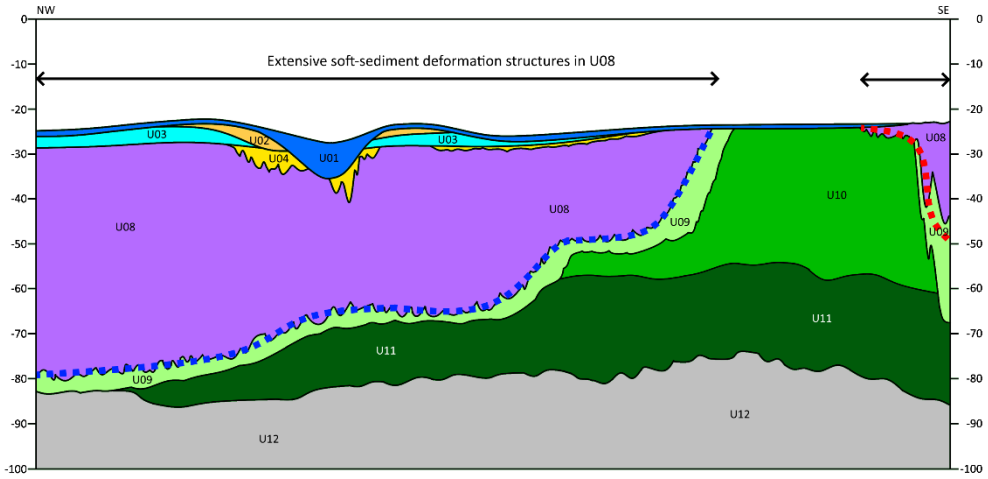

Figure 5-4 *Conceptual model cross section oriented from northwest to southeast through the Hesselø South OWF project site. Extent of SSDS indicated with arrows. Dashed lines indicate latest glacier advances into the area – the blue represents the first of the two advances; the red represents the second of the two advances.*

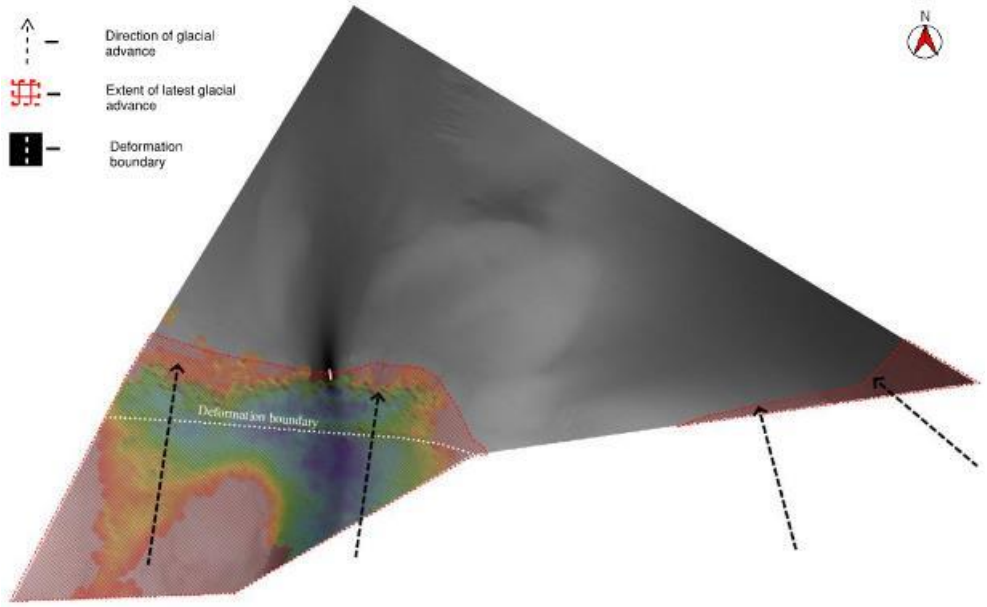

Figure 5-5 *Interpreted extent of the latest glacial advance in the areas (red dashed line in Figure 5-3 and Figure 5-4,). The coloured map indicated combined base of the glaciolacustrine units U07, U06 and U05 which is approximately equivalent to the depression in which the glacial advance formed. Black dashed lines indicate expected direction the glacial advance. White line indicates the southern limit of the SSDS.*

The Weichselian and Early Pleistocene comprise units U10 and U11 and constitute glacial deposits which have been glacially overridden and compacted. U10 comprises glaciofluvial sand deposits which are most likely of Weichselian age. U11 is a complex unit with internal layers of mixed depositional

environments and lithologies. Parts of U11 may have been glacially overridden several times.

The Jurassic and Early Cretaceous comprises U12 and consist of mudstone, siltstone, sandstone, and slightly indurated clay. Faulting to different degrees has been observed within U12. Some of the faulting is most likely related to the Sorgenfrei-Tornquist Zone. None of the faults have been observed to be impacting the overlying Pleistocene units.

6 Methodology for integration of geophysical and geotechnical data

The methodology used for the performed work with interface between geophysics and geotechnics is an iterative process, from which the geophysical and geotechnical findings support each other to obtain an Integrated Geological Model representing the site conditions.

The steps in the iterative work process between geophysics and geotechnics for the work covered in this report are the following:

1 The geophysical and geotechnical work is initially assessed in each discipline for establishing a basis to work from.

   1a) A preliminary geophysical model was received for the Hesselø South OWF project site. Initial work included understanding the interpreted seismic units, the stratigraphical model and identify where additional stratigraphic units need to be interpreted.

   1b) The geotechnical basis is established by generating a stratigraphy for each available test location across the Hesselø South OWF project site. In addition, classification parameters are determined to support this selection. The soil behaviour type index, I_c, (cf. section 7.2.1) with depth is shared with the geophysical team as basis for merging the two models and initial interpretation.

2 The geophysical and geotechnical disciplines share horizons and stratigraphy at the test locations across the Hesselø South OWF project site.

3 Each discipline reviews the received information from the other discipline for re-evaluation and update the models for alignment. This is supported through meetings between the disciplines. The integrated ground model will mainly be influenced by geotechnical relevance, hence the selection of relevant horizons to interpretate is driven by the geotechnical relevant boundaries.

4 Steps 2 and 3 are repeated until an alignment between the geophysical and geotechnical interpretation is made. When the work for updating the model is finalised, the documentation and post processing of the result is completed within each discipline.

5 In parallel with the individual work for each discipline, the zonation is ongoing between the disciplines, where input from both parties is considered.

The iterative process used for the project is visualised by a flowchart in Figure 6-1.

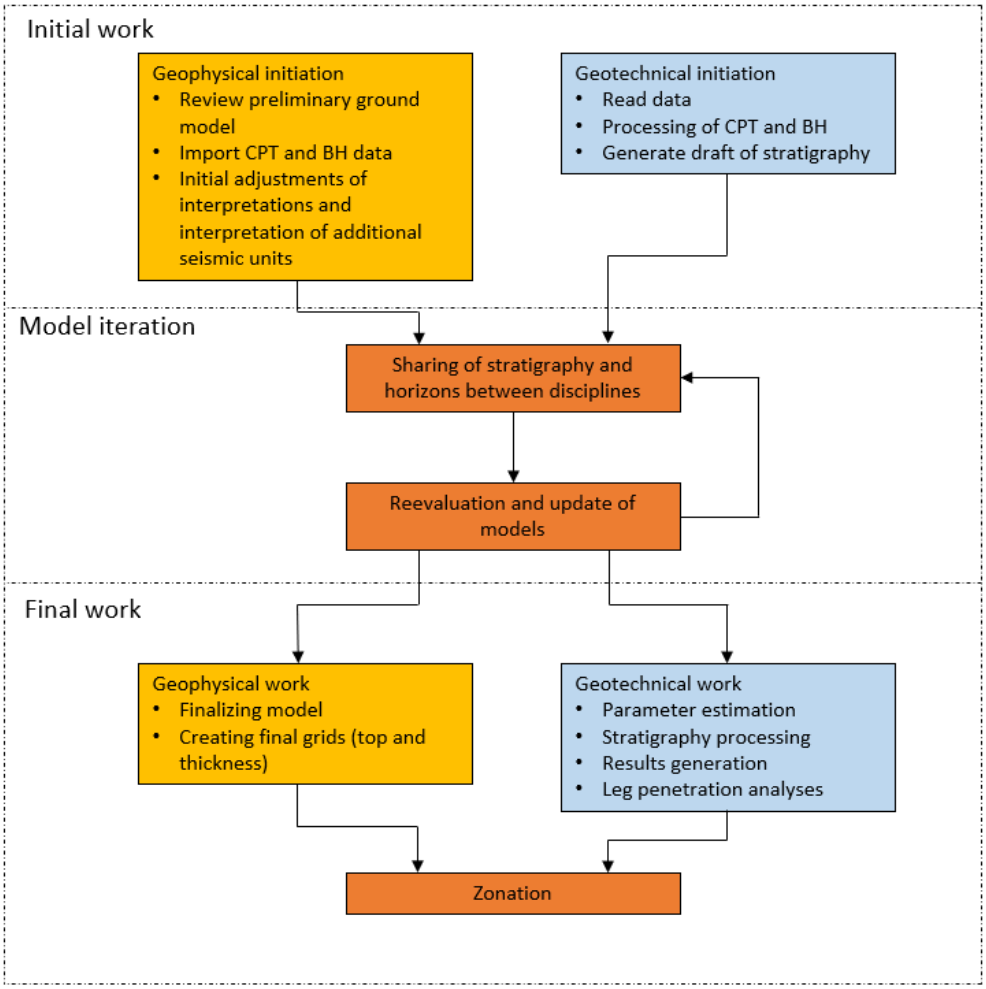

Figure 6-1 Flowchart visualising the work iteration between disciplines.

7 Geotechnical interpretation

In this section it is described how the geotechnical data have been evaluated to characterize the model units in the IGM and the layering of geotechnical units at each geotechnical survey location. The layering and soil characterization interpreted at survey locations has served as input to the Integrated Geological Model, cf. section 9.

For each geotechnical survey location, a geotechnical interpretation of the stratigraphy has been carried out. This interpretation has considered input from borehole logs, CPT logs (using CPT correlations as presented in section 7.2) and geophysical data (to link geotechnical units across the Hesselø South OWF project site). One geotechnical interpretation of the stratigraphy has been prepared for each geotechnical survey location. This also implies that at geotechnical survey locations where borehole and CPT data are available, or CPT data from multiple tests are available, the information from these tests has been combined into one interpreted stratigraphy. A total of 32 unique geotechnical interpretations of stratigraphy have been developed, cf. Appendix A, where geophysical data has been included for the stratigraphy estimation. All these interpretations have been applied as input to the Integrated Geological Model.

The following sections describe the procedure for the geotechnical stratigraphic interpretation in further detail.

7.1 Geotechnical unit overview

The development of the soil stratigraphy can generally be divided into two parts:

- based on borehole log descriptions,
- based on CPT classification and correlation.

The work documented in Ref. /1/ can be considered the basis. The soil descriptions provided in the borehole logs provide descriptions of soil type/class as well as estimates of soil age and depositional environment. In addition, the seismic horizons interpreted from the geophysical data also serves as input into the definition of geotechnical units.

An overview of the defined geotechnical units is presented in Table 7-1 based on the defined units in the integrated ground model. Additionally, the table presents the amount of available CPT data for each geotechnical unit. The integrated model unit ID refers to the presented integrated model units in section 9.9. Unit U01 and U01.2 have been combined for the geotechnical assessment due to the similarity of the units and the limited amount of data present for U01.2. Figures for verifying a similar behaviour for the established geotechnical units are presented in Appendix B.1. This is done by gathering all available CPT data from the site in the same figure for each unit to verify that the layers categorised as the same unit have the same behaviour from measured properties.

The following is noted with regards to the defined units:

- U01 split between sand and clay at seabed. The unit is mainly found within the first meters below seabed with few exceptions of deeper occurrences. The unit is a marine Holocene deposit.

- U02 consist of shallow sand found at shallow depths (up to approximately 10 m). The unit is an Early Holocene fluvial/delta deposit.

- U03 is a normal consolidated clay layer with the presence of few small interbedded sand layers. The unit is found at shallow depths (up to approximately 10 m). The unit is an Early Holocene deltaic to estuarine deposit.

- U04 is dominated by sand with few exceptions of small interbedded clay layers. The unit is found at shallow depths (up to approximately 10 m). The unit is an Early Holocene fluvial to estuarine deposit.

- U05 consist of a split of both sand and clay material. The unit is found at shallow depths (up to approximately 10 m). The unit is a Late Weichselian glaciolacustrine deposit.

- U06 is a sand layer found at depths up to approximately 27 m. The unit is a Late Weichselian glaciolacustrine deposit.

- U07 is found as thick clay layer which for some locations are found up to large depth (approximately 30 m below seabed). The unit is a Late Weichselian glaciolacustrine deposit.

- U08 is dominated as a normal consolidated clay layer with interbedded sand layers located across the site. The unit is found to be very thick at areas of the site varying from close to seabed down to approximately 45 m for some geotechnical locations. The unit is a Late Weichselian glaciomarine deposit.

- U09 is a clay expected to be similar to unit U08 with more silty parts and slightly more consolidated. The unit is found to be very thick at areas of the site varying from close to seabed down to approximately 45 m for some geotechnical locations. The unit is a Weichselian sub to proglacial deposit.

- U10 is a high strength glacial sand layer which for some locations are found already from near the seabed. The unit is measured down to approximately 32 m below seabed. The unit is a Weichselian periglacial to proglacial deposit.

- U11 is a split between glacial sand and clay. The material is overconsolidated and based on geotechnical locations the unit is found from seabed at some locations, and down to approximately 62 m below seabed. The unit is a Weichselian to Early Pleistocene mixed glacial deposit.

- U12 is pre-quaternary material with limited measurements. The limited measurements indicate high strength material, which from borehole logs is interpreted as sandstone and mudstone. From the geotechnical data, the unit is found present from approximately 25 m depth and down to the end of geotechnical tests (maximum depth measured is approximately 70 m below seabed). The unit is a Jurassic to Early Cretaceous marine deposit.

Table 7-1 Overview of identified integrated model units and considered geotechnical units.

Geophysical unit	Geotechnical unit	Geotechnical material	Total length of CPT measurement [m]	Percent of total CPT length in geophysical unit [%]
U01 U01.2	UC01	Clay	44.2	74.6
	US01	Sand	15.0	25.4
U02	US02	Sand	15.6	100.0
U03	UC03	Clay	34.3	90.1
	US03*	Sand	3.8	9.9
U04	UC04*	Clay	0.7	4.1
	US04	Sand	16.5	95.9
U05	UC05	Clay	5.0	42.2
	US05	Sand	6.9	57.8
U06	US06	Sand	37.8	100.0
U07	UC07	Clay	37.3	98.6
	US07*	Sand	0.5	1.4
U08	UC08	Clay	233.4	85.5
	US08	Sand	39.6	14.5
U09	UC09	Clay	34.9	97.4
	US09*	Sand	0.9	2.6
U10	UC10*	Clay	2.9	2.6
	US10	Sand	110.8	97.4
U11	UC11	Clay	43.2	41.7
	US11	Sand	60.5	58.3
U12	UC12	Weak Rock	12.5	100.0

**Geotechnical unit established to group measurements of sub-material.*

7.2 Stratigraphic interpretation based on CPT

The process of determining the stratigraphy for all survey locations based on the CPT data is described in the following steps:

1 Load raw CPT data from AGS-file.

2 Calculate additional parameters for soil interpretation and classification.

3 Calculate soil behaviour type for each depth with available CPT data.

4 Select stratigraphy based on calculated parameters and soil behaviour type related to depth.

5 Define geotechnical unit for all defined layers.

Initially, the raw CPT data are loaded into a script designed to classify the soils (Step 1). Some postprocessing of the raw data are performed to derive additional parameters required for classifying the soil using the Robertson-method (Step 2). These parameters are shown below, cf. Ref. /2/.

Corrected cone resistance: $q_t = q_c + u_2 \cdot (1 - a)$

Friction ratio: $R_f = \frac{f_s}{q_t}$

Normalised cone resistance: $Q_{tn} = \left(\frac{q_t - \sigma_{v0}}{P_a}\right) \cdot \left(\frac{P_a}{\sigma'_{v0}}\right)^n$

Stress exponent: $n = 0.381 I_c + 0.05 \left(\frac{\sigma'_{v0}}{P_a}\right) - 0.15 \leq 1.0$

Normalised pore pressure ratio: $B_q = \frac{u_2 - u_0}{q_t - \sigma_{v0}}$

Normalised friction ratio: $F_r = \left(\frac{f_s}{q_t - \sigma_{v0}}\right) \cdot 100$

Soil behaviour type index: $I_c = [(3.47 - \log Q_{tn})^2 + (\log F_r + 1.22)^2]^{0.5}$

Where:

f_s is the measured CPT sleeve friction,

q_c is the measured CPT cone tip resistance,

u_2 is the measured pore pressure immediately behind cone tip,

u_0 is the hydrostatic pore pressure,

σ_{v0} is the total vertical in-situ stress,

σ'_{v0} is the effective vertical in-situ stress,

a is the area ratio of the adopted CPT cone,

P_a is the atmospheric pressure.

From the available parameters, an initial estimation of the soil behaviour type for each layer is made based on different classification methods (Step 3). Three different classification methods are used for evaluating the variation in the soil behaviour type (SBT):

- Using soil behaviour type index.
- Using normalised cone resistance and friction ratio.
- Using normalised cone resistance and pore pressure ratio.

The three considered classification methods are described in section 7.2.1, 7.2.2 and 7.2.3, respectively.

Based on the measurements from the CPT (cone resistance, sleeve friction and pore pressure) and the estimated SBT, the soil layering can be determined, and the geotechnical units can be defined (Step 4 and 5).

Once the soil stratigraphy and the associated geotechnical units have been defined, layer specific information can be determined in the postprocessing. For each soil layer, the associated CPT data can be used to estimate the strength and stiffness parameters for that specific soil layer. The methods adopted for defining strength and stiffness properties can be found in section 8.

7.2.1 Soil behaviour type index

The estimation of the SBT is based on the soil behaviour type index I_c value using Table 7-2 as seen below. Table 7-2 shows that the correlation between the soil behaviour type index and SBT only applies for SBT zones 2-7, i.e., zones 1, 8 and 9 are not considered here.

This method considers both the normalised cone resistance and the normalised friction ratio, whilst pore pressure is not accounted for.

Table 7-2 Soil behaviour types (SBT) based on I_c, cf. Ref. /2/.

Zone	Soil Behaviour type	I_c
1	Sensitive, fine grained	N/A
2	Organic soils – clay	> 3.6
3	Clays – silty clay to clay	2.95 - 3.6
4	Silt mixtures – clayey silt to silty clay	2.6 - 2.95
5	Sand mixtures – silty sand to sandy silt	2.05 - 2.60
6	Sands – clean sand to silty sand	1.31 - 2.05
7	Gravelly sand to dense sand	< 1.31
8	Very stiff sand to clayey sand	N/A
9	Very stiff, fine grained	N/A

7.2.2 Normalised cone resistance and friction ratio

SBT is estimated based on Ref. /2/ where normalised cone penetration resistance, Q_{tn}, and normalised friction ratio, F_r, are used as basis, cf. Figure 7-1.

As seen from Figure 7-1, information about OCR/age and sensitivity can also be deduced from the plot. However, this type of information shall be treated with some caution, and it has not been used actively to establish geological age or degree of pre-consolidation for the soils.

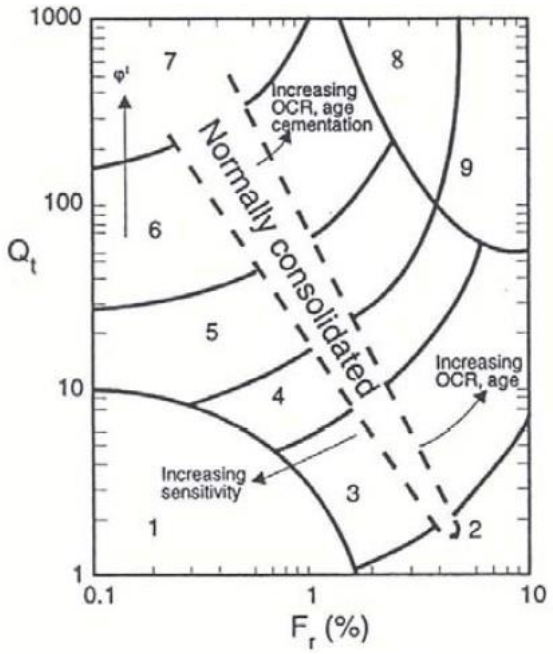

Figure 7-1 Robertson Q_t – F_r classification chart for soil behaviour type, cf. Ref. /2/. As recommended in Ref. /2/ the normalised cone resistance (Q_{tn}) is considered instead of Q_t when evaluating the soil behaviour type.

7.2.3 Normalised cone resistance and pore pressure ratio

SBT is estimated based on Ref. /2/ were normalised cone penetration resistance, Q_{tn}, and normalised pore pressure ratio, B_q, are used as basis, cf. Figure 7-2.

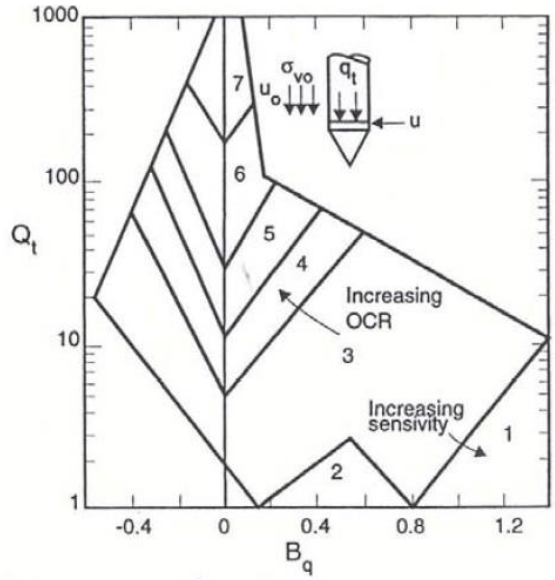

Figure 7-2 *Robertson Q_t – B_q classification chart for soil behaviour type, cf. Ref. /2/. As recommended in Ref. /2/ the normalised cone resistance (Q_{tn}) is considered instead of Q_t when evaluating the soil behaviour type.*

7.3 Classification of soils using CPT, borehole logs and geophysical horizons

For the classification of soils used for the definition of the stratigraphy and the geotechnical units, the following is noted:

- In the borehole logs, the soil types given are evaluated based on classification tests (particle size distribution, Atterberg limits, etc.) and based on geological evaluation.
- Classification based on CPT interpretation, cf. section 7.2, generally takes into consideration the mechanical behaviour of the soil.

Hence, the source of the interpreted stratigraphy from borehole log and CPT is different and each geotechnical investigation type is valuable for a detailed understanding of the soil characteristics and behaviour.

At the survey locations the maximum distance between the performed tests is found as 13.6 m. Some lateral variation of the stratigraphy may be present between the locations for borehole and CPT. However, given the short distance between borehole and CPT, such lateral variation is expected to be insignificant.

The variation in soil behaviour type (based on normalised cone resistance together with normalised friction ratio or normalised pore pressure, cf. section 7.2.2 and 7.2.3) interpreted from CPT of selected geotechnical units are presented in Figure 7-3 to Figure 7-6 as an example for the geotechnical units US10 for a sand and UC08 as a clay. The scatter of CPT data is presented with a colour scale to indicate where a high density of the data is located within the chart. It is observed that UC08 mainly plot in soil behaviour type zone 3 representing "Clay – silty clay to clay", cf. Figure 7-3 and Figure 7-4. Additionally, it is seen the scatter mainly plot in the normally consolidated area in the chart. The concentrated area in the soil behaviour type plot covered by the clay unit highlights the similarity in behaviour of this unit across the OWF site.

Geotechnical unit US10 is considered for the example of sand, and generally fall within the soil behaviour zone 6 representing "Sands – clean sand to silty sand", cf. Figure 7-5 and Figure 7-6. Further, it is noted from the normalised friction ratio plot that the soil behaviour type shows a tendency to have experienced some over consolidation.

The same Robertson charts for all other geotechnical units are presented in Appendix B.2.

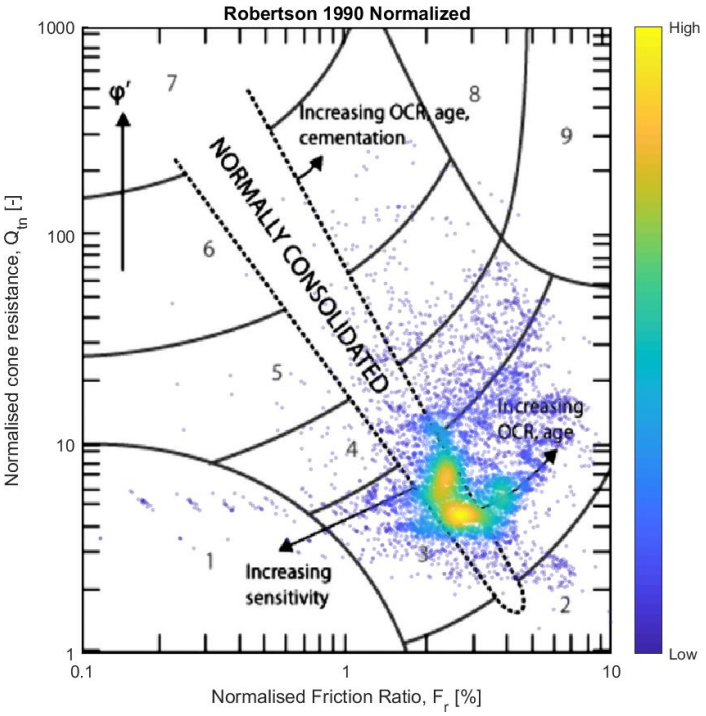

Figure 7-3 *Robertson Q_{tn} – F_r classification chart for soil behaviour type plotted for all CPT survey locations for the geotechnical unit UC08.*

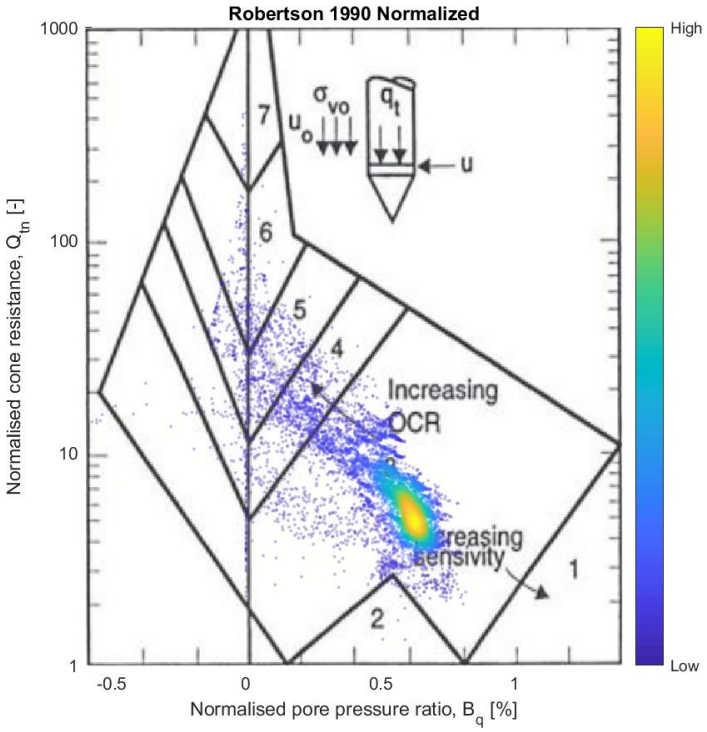

Figure 7-4 Robertson Q_{tn} – B_q classification chart for soil behaviour type plotted for all CPT survey locations for the geotechnical unit UC08.

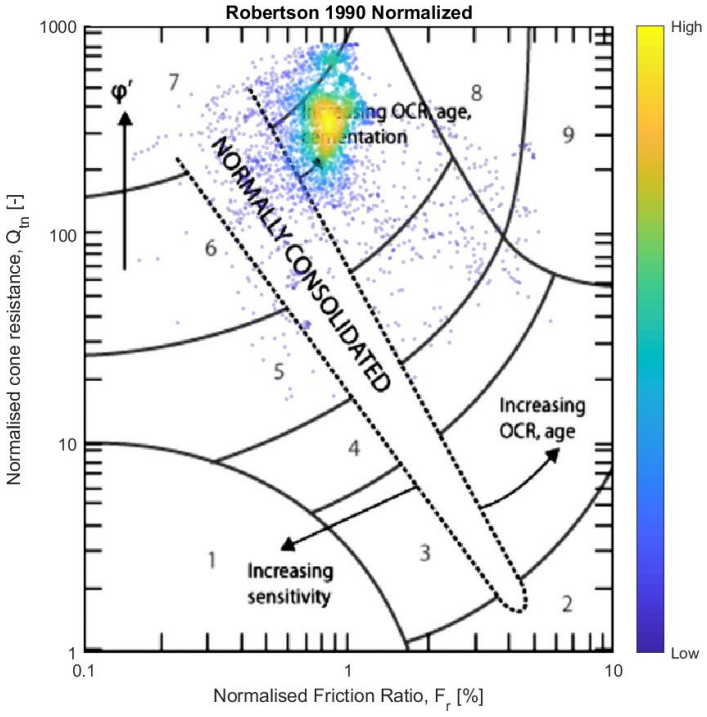

Figure 7-5 Robertson Q_{tn} – F_r classification chart for soil behaviour type plotted for all CPT survey locations for the geotechnical unit US10.

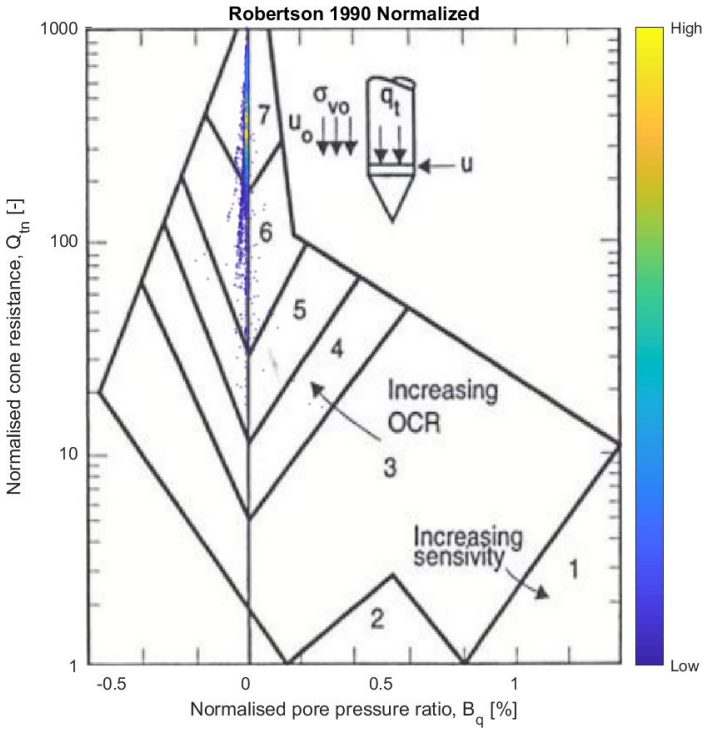

Figure 7-6 *Robertson Q_{tn} – B_q classification chart for soil behaviour type plotted for all CPT survey locations for the geotechnical unit US10.*

8 Geotechnical properties and variation

Following the definition of soil layers and stratigraphy based on CPT and borehole data outlined in section 7.3, this section addresses the methodologies considered for determination of geotechnical properties and associated variation including the assignment of these properties to the geotechnical units. The results for all geotechnical units are presented in Appendix D.

The determination of geotechnical properties is based on both selected CPT correlations and the available laboratory test data from the performed campaign, cf. Ref. /1/. For the CPT data, the geotechnical properties are determined based on selected correlations, while the properties derived on the basis of onshore laboratory testing are generally taken as-is from the outcome of the testing. The only performed processing of the data are:

- For triaxial tests and DSS tests a re-evaluation of the peak value is performed if the peak is located after 10% strain level for triaxial test or 15% for DSS test or UU test.

- The undrained shear strength from UU tests and DSS tests have been calibrated by multiplying with a factor of 1.2, cf. Ref. /3/. The lack of consolidation of the sample before shear result in lack of radial stresses which exist in the in-situ conditions. This means it will most likely show a false low strength as the sample is not brought to the actual in-situ condition, hence the applied factor is used for considering this and having comparable strength values between the different types of tests.

- The friction angle determined from the laboratory campaign has been reevaluated for the effective cohesion to be zero.

- The G_{max} results from the P-S logging have been determined from the shear wave velocities received in digital format per test depth. For depths with no density data, no shear modulus has been provided in the AGS file, despite P-S logging results being available.

Beside the above points, no additional interpretation has been imposed on the laboratory testing.

The use of CPT correlations to derive soil parameters is an efficient way of assessing the soil characteristics reducing the need for soil sampling and subsequent onshore laboratory testing. It must, however, be emphasized that these correlations shall ideally be benchmarked using additional results from testing of soil specimens under controlled laboratory conditions. The assessed soil properties based on the CPT correlations are shown for all CPT survey locations in Appendix C.

The relevant geotechnical properties assessed in the following are divided into three categories:

- State properties,

- Strength properties,
- Stiffness properties.

Table 8-1 provides an overview of the parameters that will be determined including the data sources considered for each of these. The abbreviation presented in the brackets represent the naming in the plots. The focus is to provide estimates for traditional soil parameters including the expected ranges of variation for the different geotechnical units. These parameters provide an estimate of the soils' ability to withstand loads and a general understanding of the deformation characteristics of the soil. Results from the CPT correlations are made with a 90% transparent scatter for being able to determine the concentrated areas in the plots.

In addition, an overview of the ranges of classification, strength, and stiffness properties per geotechnical unit are presented in section 8.4.

Table 8-1 Overview of data sources adopted for assessing geotechnical properties.

Category	Soil property	Data source
State	Over-consolidation ratio	CPT correlation
	Relative density	CPT correlation
Strength	Undrained shear strength	CPT correlation Triaxial testing (CAU, CIU, UU) Direct Simple Shear (DSS) Unconfined compressive strength (UCS) Pocket penetrometer (PP) Laboratory vane test (Vane)
	Friction angle	CPT correlation Triaxial testing (CIDU)
Stiffness	Small-strain shear modulus	CPT correlation P-S logging (PS)

8.1 Presentation of CPT properties

As outlined in section 8, the soil parameters are derived partly using CPT correlations and partly using results from the laboratory testing when available.

This section presents the data from the CPTs across the Hesselø South OWF project site. The results are presented per geotechnical unit.

Figure 8-1 shows an example of range of basic CPT measurements for geotechnical unit UC08 which include soil behaviour type index, cone tip resistance, cone shaft resistance, friction ratio and pore water pressure. The presented example shows that the CPT measurements in this layer generally plots within a consistent trend.

In Appendix B.1 the variation of measured CPT parameters is presented for the considered geotechnical units.

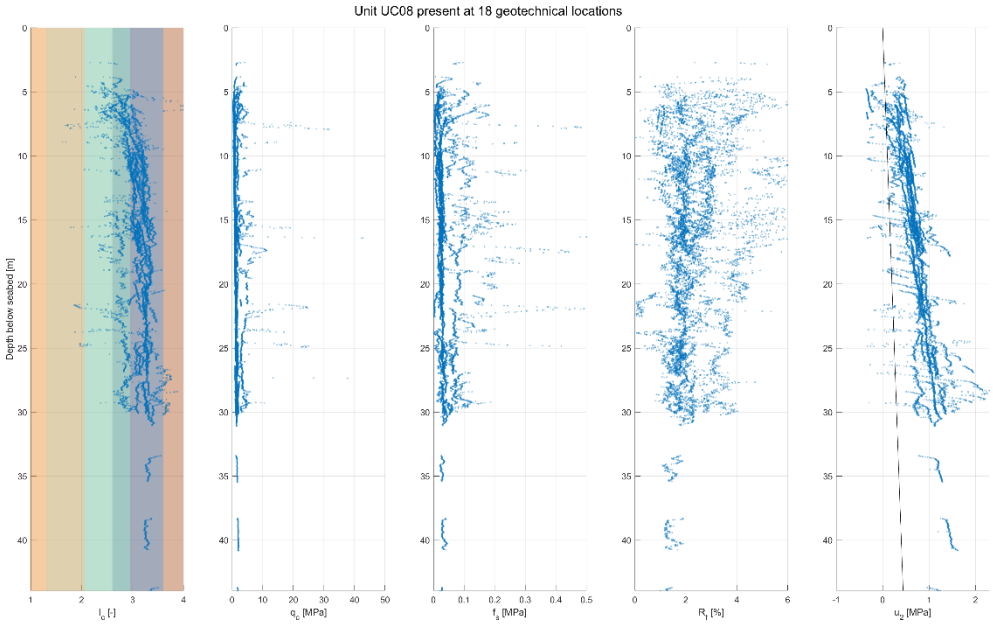

Figure 8-1 Range of CPT parameters for geotechnical unit UC08.

8.2 Presentation of state properties

As outlined above in section 8, state parameters such as over-consolidation ratio (for cohesive soils) and relative density (for non-cohesive soils) have been determined from CPT correlations.

The assessment of these parameters serves as input to the overall understanding of the in-situ soil state, which is crucial for assessing the general soil behaviour. This section presents the methods adopted for the analyses of these parameters as well as the outcome.

8.2.1 Over-consolidation ratio

The over-consolidation ratio, OCR, is determined by a CPT correlation commonly used in the industry. The method considered for the parameter estimation is the Mayne (2019) methodology which is representative for both sand, clay, and mixed soil conditions due to the correction from the *m'* exponent.

The Mayne methodology adopts the following formula, cf. Ref. /5/:

$$OCR = k\left(\frac{(q_t - \sigma_{v0})^{m'} * \left(\frac{p_a}{100}\right)^{1-m'}}{\sigma'_{v0}}\right)$$

where q_t is the corrected cone resistance, σ_{v0} is the total in-situ vertical stress, σ'_{v0} is the effective in-situ vertical stress, p_a is the atmospheric pressure, k is a dimensionless constant which is set to 0.33, and m' is an exponent which can be calculated from below formula, where I_c is the soil behaviour type index, cf. Ref. /5/.

$$m' = 1 - \frac{0.28}{1 + (I_c/2.65)^{25}}$$

Figure 8-2 presents the variation of OCR (interpreted based on CPT) with depth for the geotechnical unit UC08. It is observed the OCR value for the clay generally indicate normal- to slightly over-consolidated state with higher values near the top. It should be kept in mind the OCR value is less reliable in the depths near seabed due to the low overburden pressure.

In Appendix D.1, the variation of OCR with depth is presented for the individual geotechnical units.

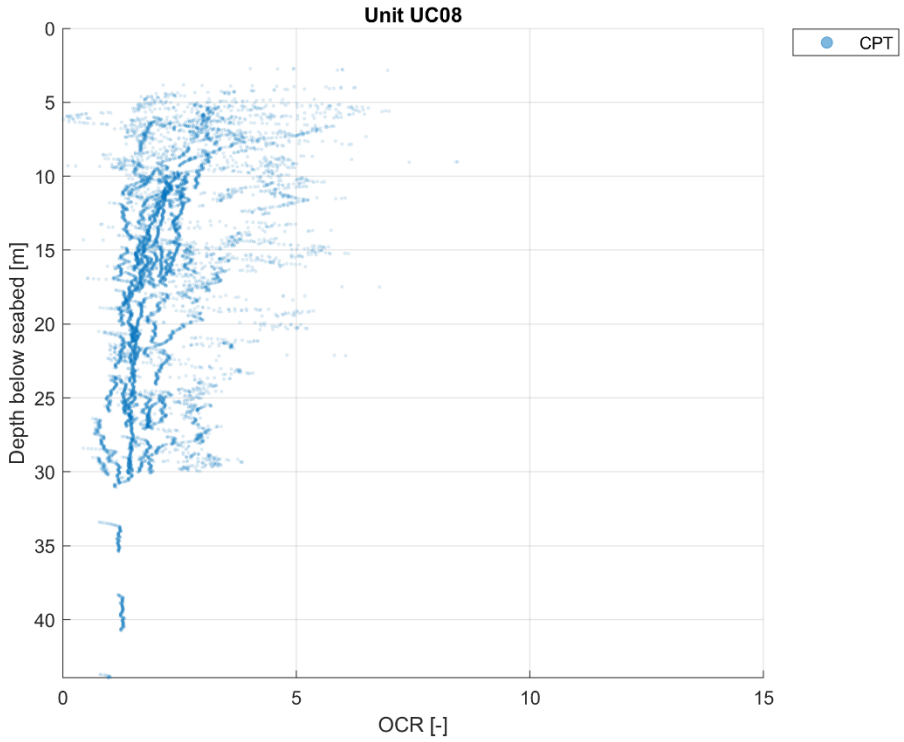

Figure 8-2 Range of OCR for geotechnical unit UC08.

8.2.2 Relative density

The relative density, I_D, is determined for the non-cohesive soils by the Jamiolkowski (2003) CPT correlation which is commonly used in the industry, as no laboratory testing is used for calibration of the parameter.

The Jamiolkowski (2003) correlation is determined from the below formulas, cf. Ref. /6/:

$$I_{D,sat} = I_{D,dry} * \frac{-1.87 + 2.32 \ln\left(\frac{q_t}{(p_a * \sigma'_{v0})^{0.5}}\right)}{100} + I_{D,dry}$$

$$I_{D,dry} = \frac{100}{2.96} \ln\left(\frac{q_t/p_a}{24.94\,(\sigma'_m/p_a)^{0.46}}\right)$$

where q_t is the corrected cone resistance, σ'_m is the in-situ mean effective stress, σ'_{v0} is the effective in-situ vertical stress and p_a is the atmospheric pressure. By assuming a value for K_0 of 1.0, which means the material is considered as slightly over-consolidated, the in-situ mean effective stress σ'_m is set equal to the effective in-situ vertical stress σ'_{v0}.

In Figure 8-3, an example of the variation of relative density (interpreted based on CPT) with depth is presented for the geotechnical unit US10. It is observed that the relative density of the geotechnical unit varies within the range 70% to 130% with the highest concentration of scatter located around 100%. It should be noted the values above 100% is due to the formula from the CPT correlation. In Appendix D.2, the variation of relative density with depth is presented for all geotechnical sand units. For a number of locations some shallow intervals give a calculated relative density of less than 30–40%, which is deemed not being realistic for an offshore sediment subjected to wave action. Correlations exists, that can consider the shallow pressure conditions on the CPT, but these correlations are not incorporated here as they are only relevant for the shallow depths.

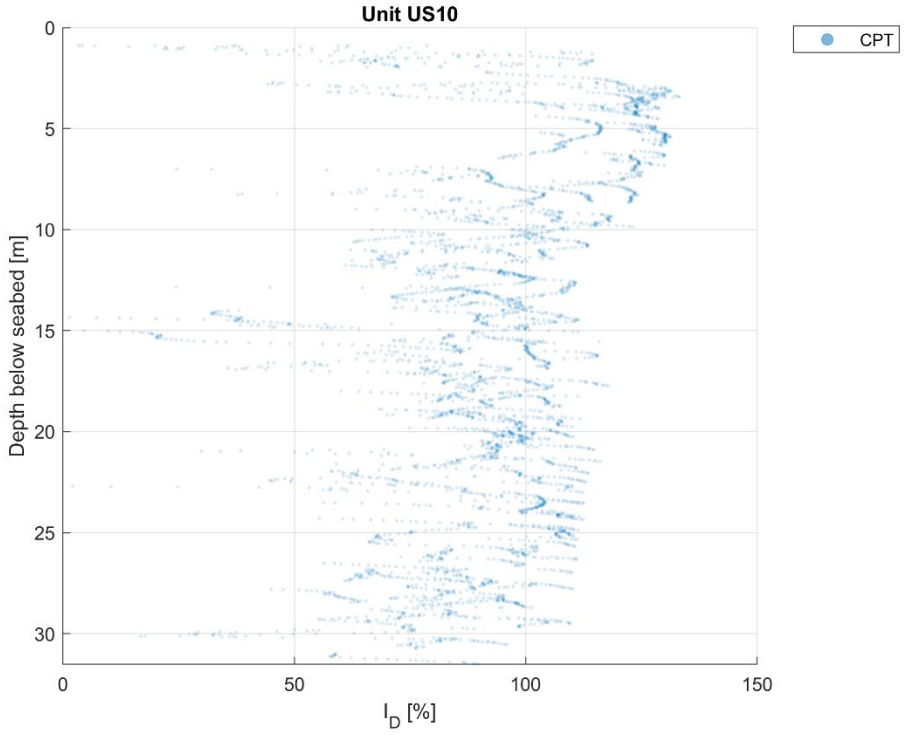

Figure 8-3 Range of estimated I_D using CPT correlations for geotechnical unit US10.

8.3 Presentation of strength and stiffness properties

Following the state parameters described in section 8.2, strength and stiffness parameters such as undrained shear strength (for cohesive soils), friction angle (for non-cohesive soils) and small-strain shear modulus (all soils) have been determined from CPT correlations, supplemented by laboratory testing, cf. Ref. /1/. In addition, the small-strain shear modulus has also been evaluated based on P-S logging. The CPT correlations have been selected based on which of the considered literature correlations match the laboratory testing best.

The assessment of these parameters serves as input to the overall understanding of the soil behaviour during loading, e.g., in relation to placement of wind turbine foundations or jack-up operations on the Hesselø South OWF project site. This section presents the method adopted for the analyses of these parameters as well as the outcome.

To determine just one representative value (soil strength/stiffness) per geotechnical unit per survey location, the average value for each geotechnical unit is determined. When deriving the average value for the sand and clay layers, the peaks and troughs in the CPT trace (usually found close to the layer boundaries) are removed to reduce the impact of this data on the average value, i.e., to obtain the most representative value.

8.3.1 Friction angle

The peak friction angle, φ'_p, is calculated for non-cohesive soils according to the method of Schmertmann (1978) assuming that the sand is "Uniform medium sand" to "Well-graded fine sand", cf. Ref. /4/. The Schmertmann correlation have been selected as representative for the Hesselø South OWF project site based on visual inspections of the comparison between CPT correlated values and the laboratory test results from the same positions and depths.

$$\varphi'_p = 31.5 + 0.12\, I_D$$

where I_D is the relative density determined from the Jamiolkowski (2003), which was presented in section 8.2.

As the relative density calculated from CPT correlation for few layers are found above 100%, and values larger than 100% is considered for the correlation, a line representing the friction angle for a relative density of 100% is added to the figures.

Further to the CPT correlation, the friction angle is obtained through triaxial testing, CIDU. The CIDU triaxial tests have been reassessed for assuming no effective cohesion in the derivation of the strength parameter by considering the following equations:

$$M = \frac{q}{p'}$$

$$\varphi'_p = \text{asin}\left(\frac{3M}{6+M}\right)$$

where q is the deviatoric stress at failure and p' is the effective mean stress at failure. Hereby it is assumed that the effective cohesion is zero.

Using CPT data for all survey locations as well as the available laboratory test data, the range of friction angle for geotechnical unit US06 is shown in Figure 8-4. It is observed that the friction angle interpreted based on CPT generally estimates larger values than the result from the one CIDU test available for the unit. However, when the laboratory result is matched against the local CPT measurement a general good match is found.

In Appendix D.3, the variation of friction angle with depth is presented for all geotechnical sand units.

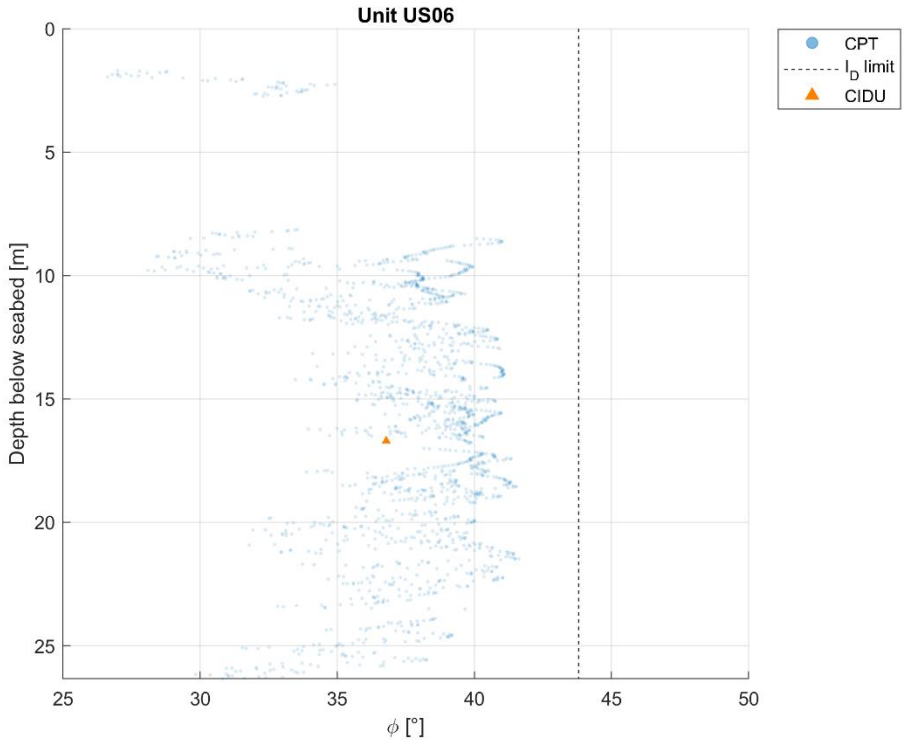

Figure 8-4 Range of φ for geotechnical unit US06.

8.3.2 Undrained shear strength

The undrained shear strength, c_u, is determined for cohesive soils according to Ref. /2/ as:

$$c_u = \frac{q_t - \sigma'_{v0}}{N_{kt}} = \frac{q_{net}}{N_{kt}}$$

For determination of undrained shear strength in fine grained materials, a cone factor has been determined for each unit containing laboratory data. These values are determined from visual inspections of CPT vs laboratory data, and

they are found to ensure a proper match between the undrained shear strength determined based on CPT, and the undrained shear strength from the consolidated undrained triaxial tests (CIU and CAU). In addition to the consolidated undrained triaxial tests, the correlations have also been established partly from the unconsolidated undrained triaxial tests (UU) and direct simple shear tests (DSS), where a multiplication factor of 1.2 have been used on the UU tests, cf. section 8. From the visual inspection, a constant cone factor, N_{kt}, is found to be 15 for all clay layers at the site. It should be noted the factor is based on a high-level assessment with limited/no data available in some geotechnical units, hence a more detailed assessment should be performed for future foundation design. The selection of cone factor is presented in Appendix E.

Further, the simpler laboratory tests, Torvane and Pocket Penetrometer (PP) tests, are available for determination of undrained shear strength. These have not been considered when estimating the cone factor but are included in the figures presenting the data per geotechnical unit.

Using CPT data for all survey locations as well as the available laboratory test data, the range of undrained shear strength is shown in Figure 8-5 for the geotechnical clay unit UC08. It is observed that the unit shows general increasing strength with depth but with few strength variations being present at most depths. Further, it is observed that the CPT predicted strength matches generally well with the strength derived from consolidated triaxial tests and DSS tests. In contrast, pocket penetrometer tests and unconsolidated undrained triaxial tests generally have larger spread of the results and sometimes yield higher strength than the CPT predictions. In this regard it is emphasized that consolidated triaxial tests and DSS tests are considerably more reliable than the other laboratory tests.

In Appendix D.4, the variation of undrained shear strength with depth is presented for each of the individual geotechnical clay units.

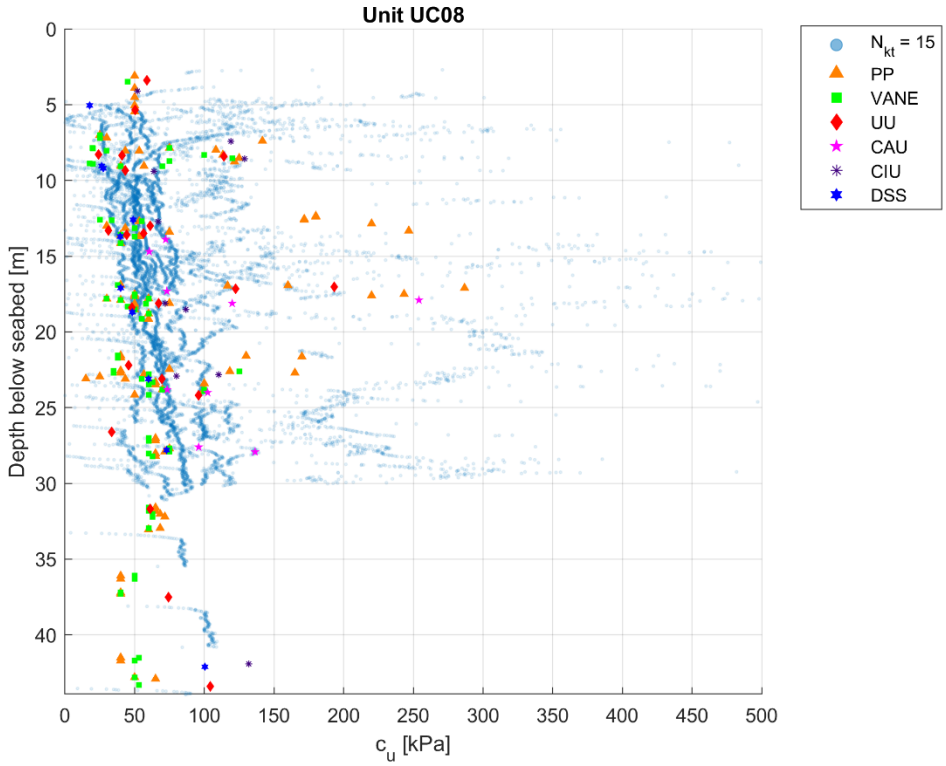

Figure 8-5 *Range of c_u for the geotechnical clay unit UC08 using CPT correlation (blue dots) and laboratory test results.*

8.3.3 Small-strain shear modulus

The small-strain shear modulus, G_{max}, is determined in all soils from below expression derived for elastic theory, cf. Ref. /2/:

$$G_{max} = \rho \, V_s^2$$

where ρ is the bulk density of the material and V_s is the shear wave velocity.

The shear wave-velocity, V_s, is for non-cohesive soils estimated from CPT using the following equation, cf. Ref. /2/:

$$V_s = 277 \, q_c^{0.13} \, {\sigma'_{v0}}^{0.27}$$

where q_c is the measured CPT cone tip resistance and σ'_{v0} is the effective in situ vertical stress.

For cohesive soils, the shear wave velocity, V_s, is estimated from CPT using the following equation, cf. Ref. /2/:

$$V\_s = (10.1 \log q_c - 11.4)^{1.67} \left(\frac{f_s}{q_c}\right)^{0.3}$$

where q_c is the measured CPT cone tip resistance, and f_s is the measured CPT sleeve friction.

Further to the CPT correlation, the small-strain shear modulus is obtained through P-S logging.

Using CPT data for all survey locations as well as the available P-S logging data, the range of small-strain shear modulus for the geotechnical unit UC08 is shown in Figure 8-6. It is noted that the small-strain shear modulus from PS logging differs with some measurements matching with the values interpreted from the CPT correlation. No explanation of the discrepancies between correlation and some test results are found when comparing tests from different locations or looking into the data quality of the test results. In Appendix D.5, the variation of small-strain shear modulus with depth is presented for all the individual geotechnical units.

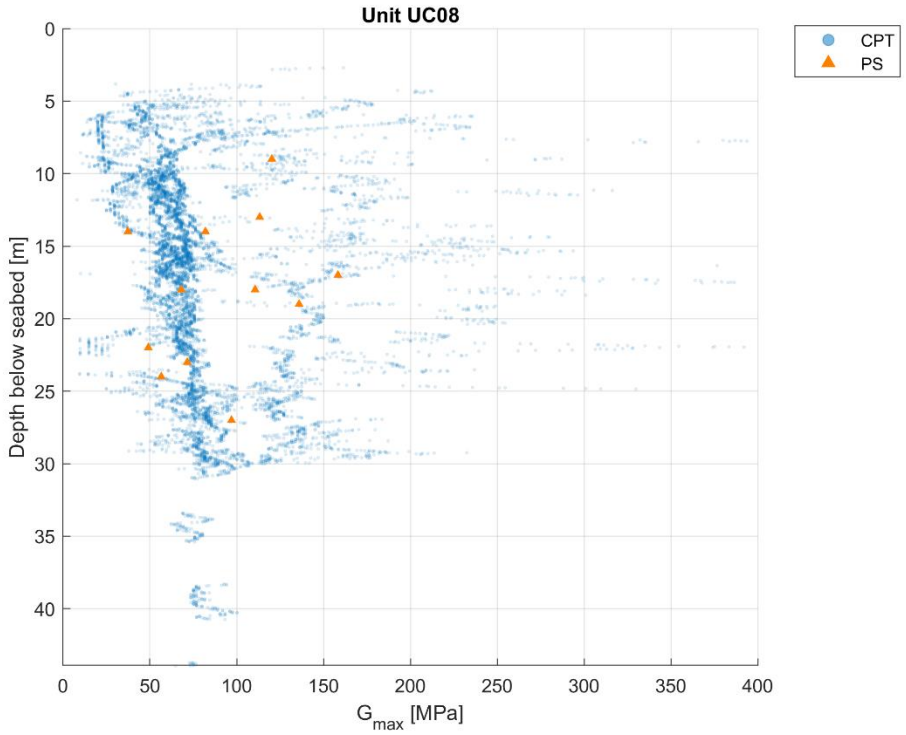

Figure 8-6 Range of G_{max} for the geotechnical unit UC08.

8.4 Range of soil parameters per geotechnical unit

In Appendix F the range, average and standard deviation values from the laboratory results of classification, strength and stiffness parameters are presented for the geotechnical units.

9 Integrated Geological Model

In this section it is described how the Integrated Geological Model has been developed. The interpretations are based on the geotechnical results from Gardline (Ref. /1/) and geophysical results from GEOxyz (Ref. /10/).

9.1 Datum, coordinate system and software

The model is set up with datum ETRS89 (EPSG:25832) and GRS80 Spheroid. The coordinate system used is the UTM projection in Zone 32 N. Units are in meters and vertical reference is MSL, height model DTU21 MSL.

The software used for interpretations is the IHS Markit Kingdom suite 2023. Seismic data were delivered in two data packages: 2D-UHRS and SBP data. The 2D UHRS was delivered in both a time and a depth version. No velocity model accompanied the 2D-UHRS data, only a description of applied interval velocities. The SBP data were delivered in time and depth. No velocity model accompanied the SBP, but a unity velocity of 1600 m/s had been applied.

A Kingdom project has been set up using the 2D UHRS seismic data. Horizons from the initial interpretation provided by GEOxyz have been imported and used as a basis for the integrated interpretation. The horizon interpreted on the SBP data were transposed and integrated into the 2D-UHRS data. Geotechnical data and borehole information have been imported into the Kingdom project from the delivered AGS files.

Existing horizons have been modified and new horizons have been interpreted along clear reflectors in the seismic data.

9.2 Assessment of the existing geophysical model

The received geophysical model (Ref. /10/) was based on the two seismic datasets, 2D-UHRS and SBP data. One horizon, H05, was identified in the SBP data and was transposed to the 2D-UHRS data. On the 2D-UHRS data initial interpretations of the intermediate and deep units were made.

In Table 9-1 a list of the initially identified horizons from GEOxyz can be seen. Two horizons, H15 and H18, interpreted by GEOxyz are not stated in the table, as they constitute the top of unit III and an internal unit in unit II, respectively.

Table 9-1: Initial units as interpreted by GEOxyz (Ref. /10/).

Data type	Unit name	Unit boundary (Horizons) Top	Base
SBP	I, H, Holocene	Seabed	H05
2D-UHRS	II, LG, late Glacial	Seabed, H05	H20
	III, GL, Glacial	H05, H20	H30
	IV, BR, Bedrock	H20, H30	-

The interpreted unit boundaries in the existing SBP and 2D-UHRS-based geophysical model, were generally interpreted along some of the most clear and continuous reflectors identified in the seismic dataset. Across the entire site, a need for either updating or adding horizons was identified. This applies both for late glacial deposits and glacial deposits.

In some places, the existing interpretations were seen to be based on multiples in the data which has been corrected. Further info on multiples in the seismic data can be found in section 9.3.

9.3 Limitations and uncertainties in the data

The 2D-UHRS data have areas where there are significant limitations to the quality of the seismic signal leading to higher uncertainty and therefor also higher risk of incorrect interpretations. Some of those areas are related to gas blanking or gas related multiples. This is further described in section 9.8.1.

In general, a high degree of multiples and related effects interfere with the seismic signal. Multiples of overlying seismic reflectors have a large impact on the interpretability of the units in several parts of the Hesselø South OWF project site.

Figure 9-1 shows two cross sections where several multiples are disturbing the data. The upper profile shows multiples of the lower boundary of B03, in the figure marked by red lines. The bottom profile shows four multiples of B03 along with seabed multiples. This is one of the areas most affected by disturbance of multiples found in the Hesselø South OWF project site. The figure also shows an example of an attempt to remove a multiple, which still leads to a disturbance in the data. The multiples have been marked by red arrows only, not to mask the reflectors in the data.

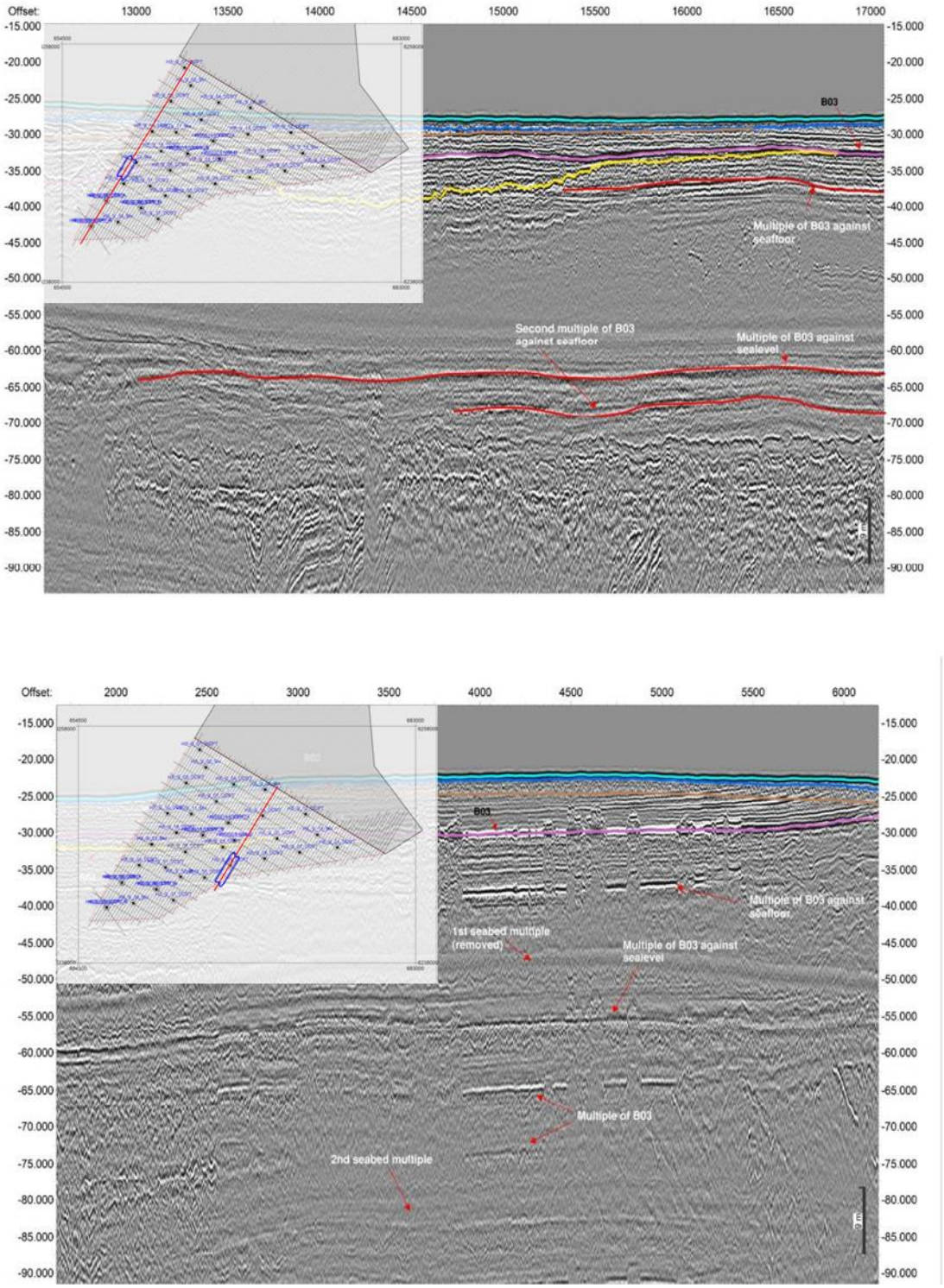

Figure 9-1 *Top: Line A_HS_L005_UHR_T_MIG_STK. Example of a cross section where multiples of B03 have been highlighted in red.*
Bottom: Line A_HS_L033_UHR_T_MIG_STK. Example of one of the worst parts in the area regarding multiples. A ringing effect is seen and B03 and seabed multiples are seen several times in the data. An attempt has been made to remove the seabed multiple, however, it is still seen to interfere with the data.

9.4 Setup of the Integrated Geological Model

The model is set up by combining SEGY files with geotechnical data as well as the initial interpretations in the Kingdom software as basis for the Integrated Geological Model.

The preliminary interpretations from the 2D-UHRS data have in some places been kept and redefined in others. Also, additional units have been found relevant to add to the model. The preliminary interpretation of H05 (GEOxyz), which was the only horizon interpreted in the SBP data, was transposed onto the 2D-UHRS data, so that it could be visualized with the rest of the model.

In the 2D-UHRS data it was possibly to interpret U01.2 as a separate unit. U01 and U01.2 are closely related units, which is why they have been given the same unit number.

The additional interpreted units are mainly based on their geotechnical significance but have only been interpreted if it was possible to identify a clear seismic reflector or unique seismic facies with a wide extent.

9.5 Interpolation and adjustment of surfaces

Geotechnical data (Ref. /1/) were imported into Kingdom and an integrated interpretation was performed, establishing a correlation between seismic reflectors and the stratigraphy based on the CPT and borehole logs, (section 7). The geotechnical data were imported in depth and converted to TWT (in ms) using a time-depth ratio calculation (section 9.7).

An overview of the resulting units in the Integrated Geological Model and its relation to the previous model is presented in Table 9-2.

Table 9-2: Table over initial and final surfaces and units.

Initial Units	Initial horizons	Updated integrated model units	Base of unit	Chrono-stratigraphic group
I	H05	U01	B01	Holocene
II	H15/H20	U01.5	B01.5	Early Holocene
		U02	B02	Early Holocene
		U03	B03	Early Holocene
	H15	U04	B04	Early Holocene
		U05	B05	Late Weichselian
		U06	B06	Late Weichselian

Initial Units	Initial horizons	Updated integrated model units	Base of unit	Chrono-stratigraphic group
		U07	B07	Late Weichselian
	H20, H18	U08	B08	Late Weichselian
III	H30	U09	B09	Weichselian
		U10	B10	Weichselian
		U11	B11	Weichselian to Early Pleistocene
IV	-	U12	-	Jurassic to Early Cretaceous

9.6 Uncertainty in the grids

Grids for top of units (elevation relative to MSL and depth below seabed) and thickness (isochore) of units are delivered with the IGM.

For grids to be continuous across gaps between survey lines, a search radius of 130 m were applied in the interpolations. This is a little larger than half of the survey line spacing for 2D-UHRS (250 m). Subsequently all grids have been adjusted from the overlying grids.

A grid cell size of 10x10 m has been chosen to accommodate file size as well as accuracy and lateral resolution of the 2D-UHRS seismic data. This applies along the seismic lines where the uncertainty is lowest. However, in areas far from the seismic lines (maximum distance is up to approximately 125 meters) the cell size is evaluated as being relatively small, indicating a higher certainty than the actual seismic data provides. The uncertainty becomes larger as the distance to the seismic lines increases independent of cell size and it is therefore important to note the location of the seismic lines when working with the grids in detail.

9.7 Depth conversion

The 2D-UHRS and SBP data were delivered both in the time and depth domain however no velocity model was received. All interpretations carried out on the data after the delivery, was performed in the time domain and later converted to the depth domain. This was done to ensure that interpretations were available both in the time and depth domain, should any further work be needed.
To convert the reinterpreted and the new horizons from time to depth a velocity model was created for the 2D-UHRS data. No velocity model was created for the SBP data since the horizon, H05 (now B01), was transposed to the 2D-UHRS data.

The velocity model was created using the Dynamic Depth Conversion (DDC) tool in the Kingdom software. The model is a simple two-layer model, using the velocities 1600 m/s and 1800 m/s. The seafloor was corrected against the delivered bathymetry, which was extended to cover all 2D-UHRS seismic lines. From the extended math calculator, a collective base of units from Seabed to B09 was created using the Merge-Max function. These units were given a velocity of 1600 m/s, and the underlying units a velocity of 1800 m/s. This velocity model corresponds to the one described in Ref. /10/, where the boundary between 1600 and 1800 m/s was set at H20, the horizon closely corresponding to B09. The sample size for the velocity model was set to 0.05 m. Using this velocity model a seismic volume in depth was created and the interpreted horizons were converted from time to depth using the model values.

9.8 Potential geohazards; shallow gas, peat, faults, and sub-surface boulders

The potential geohazards are presented and are based on the seismic and the geotechnical data (Ref. /1/).

Interpretation	Description	Associated units	Geohazard potential
Shallow gas	Strong soft-kick reflectors and acoustic blanking from locally produced gas is seen in the lower part of U03 and in U04. Produces several multiples in the seismic data.	U03 and U04	Higher uncertainty of the thickness of masked layers. Primary units affected are U04, U08, U09, U10, U11).
Peat	Strong soft-kick reflections at lower boundary of U03 may be associated with organic content and potential peat layers. Produces several multiples in the seismic data.	U03 and U04	Strong soft-kick
Faults	Extensive faulting in Pre-Quaternary related to the Grenå-Helsingborg fault.	U12 (Pre-Quaternary)	Since the faulting is confined to the bedrock it does not pose any geohazard.

Boulders, cobbles, and patches of gravel	Few diffractions seen in SBP from shells and rock fragments. Possible boulders in till.	U01 and U11	No potential hazard from the small fragments. Possible boulders in U11 pose a potential geohazard for installation of WTG foundation.
Glacial deformation	Deformation in the glacial and some of the late glacial deposits.	U09, U10, and U11	Some unpredictability in soil characterization. Units may vary in strength in different areas due to mixing.
Late glacial soft-sediment deformation	Deformation in the late glacial deposits.	U08 and part of U05, U06, and U07.	Unpredictability in soil characterization. Hard to identify lithological changes within deformed layers.

9.8.1 Shallow gas

Gas in the sediment can be seen as a disturbance and blanking of the below seismic signal. Large areas of gas disturbance and blanking have been mapped in the data and the extend of this can be seen on Figure 9-4 (see also Enclosure 5.01). The gas is generally found at the base of U03 where it is disturbing the interpretation of both B03 and the underlying units. Gas blanking also attenuate the seismic data below the gas. This naturally has an impact on the interpretation of the underlying units.

In some locations the presence of gas can be seen as illustrated in Figure 9-2 where it is seen disturbing the bottom of U03 and the top of U08. The gas is here seen creating a ”mirroring effect” with a mirror plane along B03. This effect is caused by a lower velocity in the gas filled sediment, compared to the surrounding sediments. Since the signal takes longer to reach the acoustic receivers, this causes the apparent placement of the otherwise flat B03 to be pulled down into the top of U08 in an almost 1 to 1 mirroring of the top of the gas. This effect is important to identify, because it obscures the seismic data and could potentially create the illusion that an additional unit is present below B03.

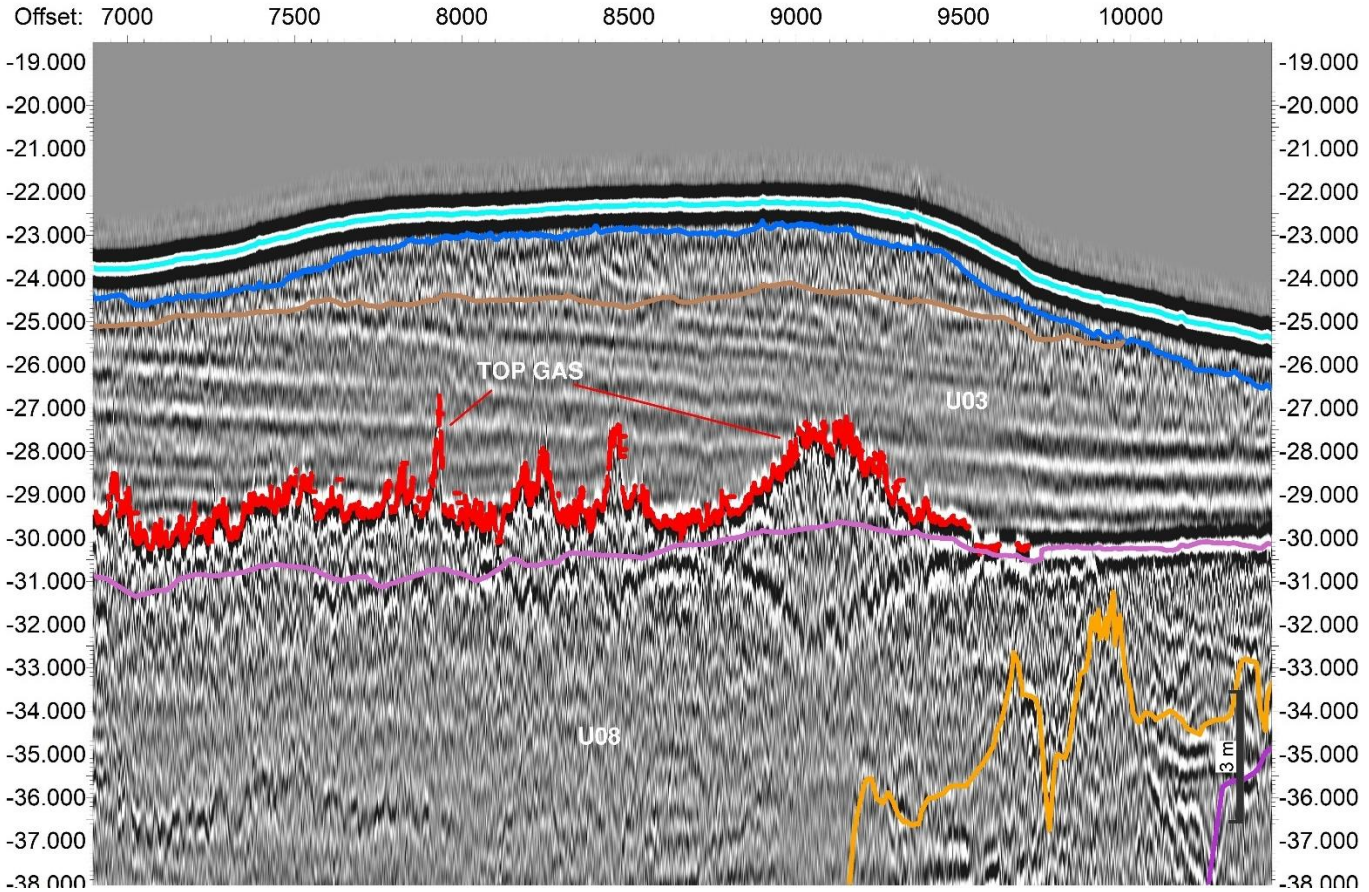

Figure 9-2: *Line A_HS_X014_UHR_T_MIG_STK: Example of gas presence at the base of U03. The gas creates a blanking of the seismic signal below and creates a visual "mirroring effect" (mirroring of the red line).*

An example of a seismic profile heavily affected by the seismic blanking can be seen in Figure 9-3. In the figure the top of the gas has been marked by a red line and the multiples created in the seismic data have also been marked as well. This shows that the gas has both made a first and a second multiple against the seabed and the top of the water column respectively. When this is combined with a seabed multiple, it makes it very difficult to decipher what reflections are real and what are noise below -30 m MLS Datum.

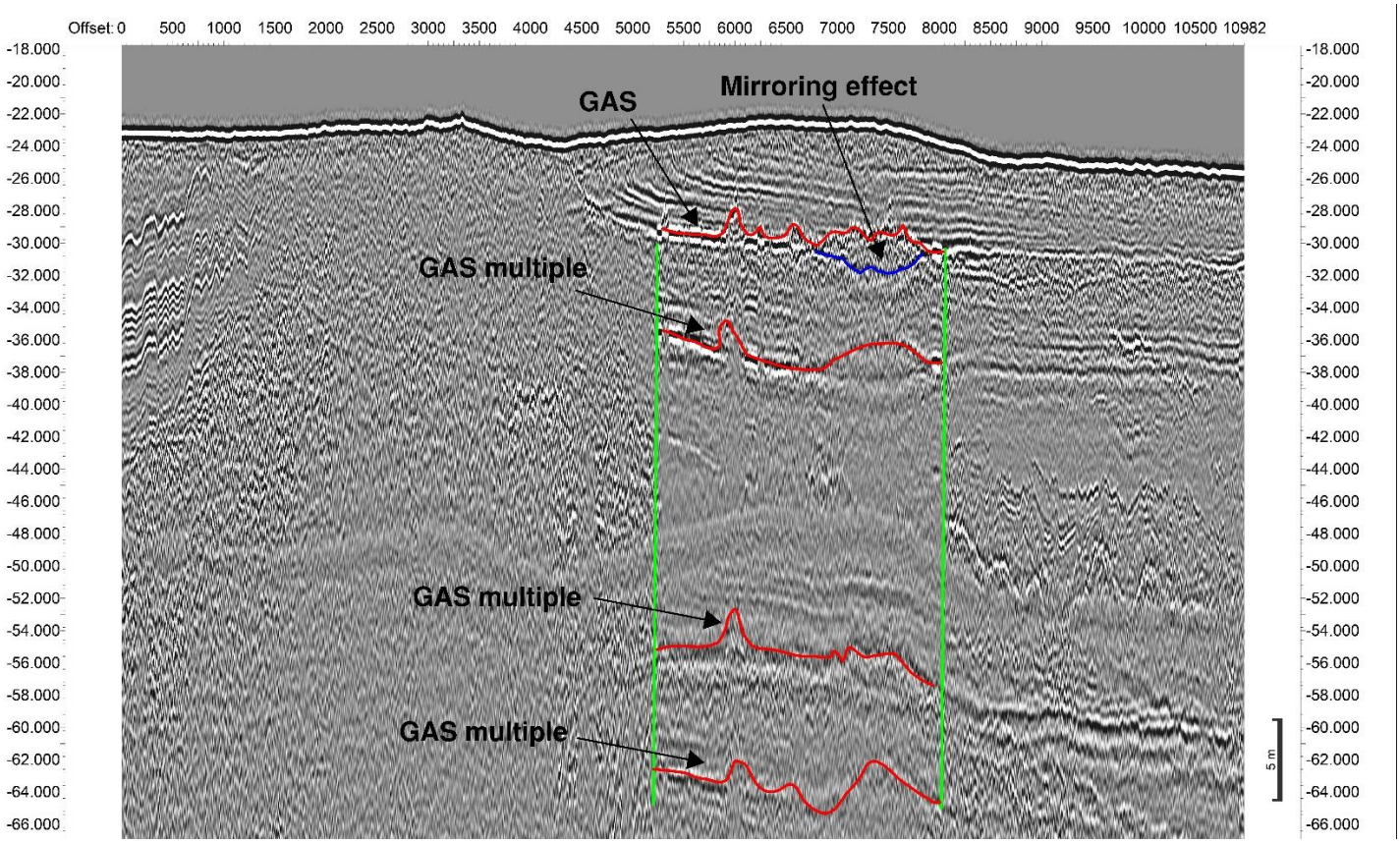

Figure 9-3: Line A_HS_L031_UHR_T_MIG_STK. Example of the severe effects the gas occurrences have on the seismic data. In this example the seismic signal has been blanked (attenuated) and multiples of the gas is present which can be mistaken for actual reflectors.

The total extent of the gas found in the 2D-UHRS data can be seen in Figure 9-4 (see also enclosure 5.01). Due to the effects described above, a higher uncertainty in the interpretations below B03 should be expected in this area.

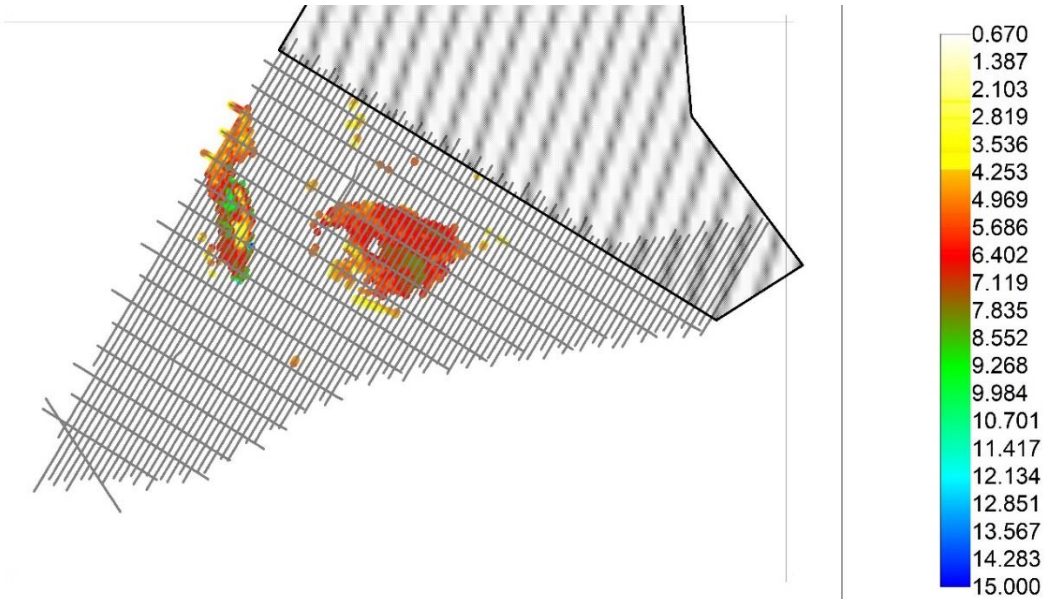

Figure 9-4: Base map of the extent of the gas blanking displayed in mbsb.

9.8.2 Faulting

Extensive faulting has been observed in U12 and has been mapped by GEOxyz on several lines. The faults are proposed to be created by a reactivation of the Grenå-Helsingborg Fault zone that runs NW to SE through the centre of the Hesselø South OWF project area (Ref. /9/). Figure 9-5 shows the faulting observed in U12 along with the interpretations made by GEOxyz.

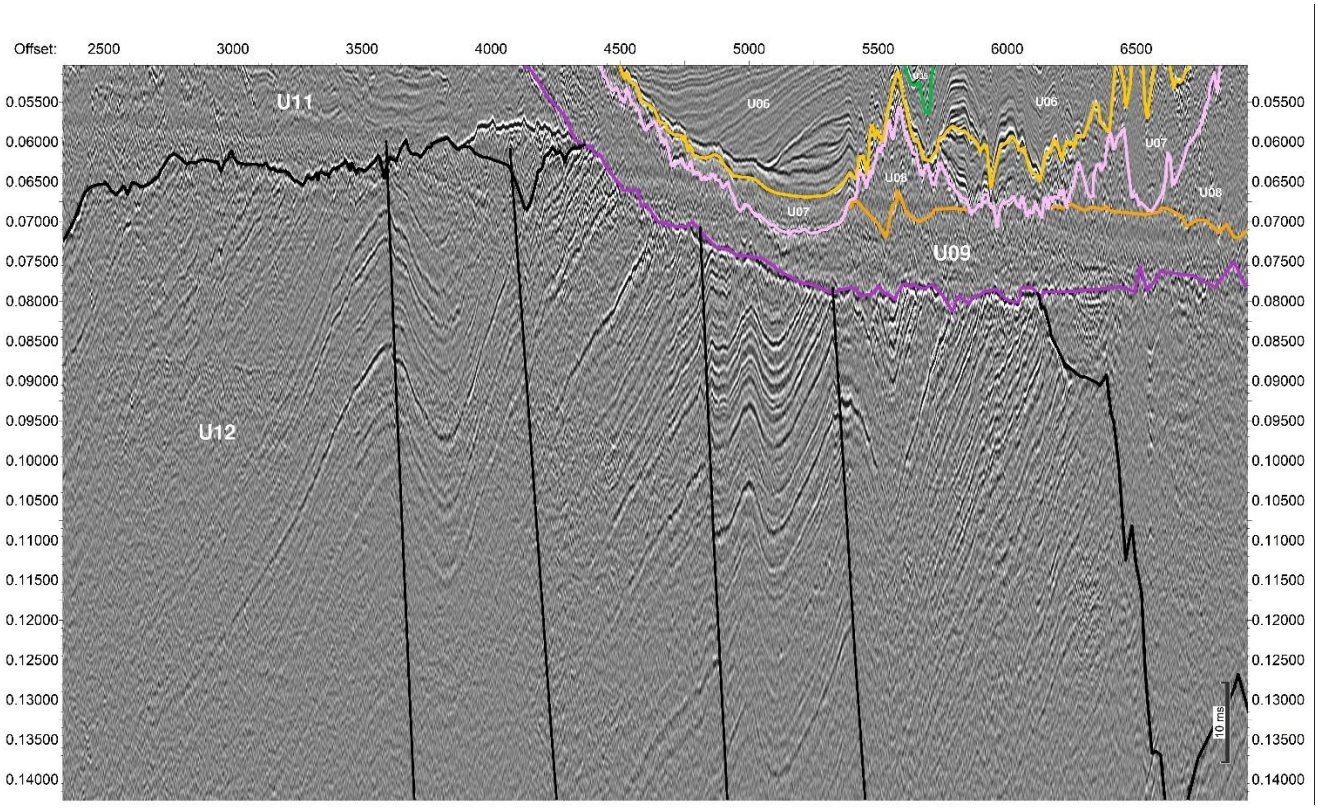

Figure 9-5: Line A_HS_L016_UHR_T_MIG_STK. Example of faults in U12. The faults are mapped by GEOxyz and are shown as black lines.

Faults are not interpreted across the entire area as it is not everywhere possible due to the limited data quality in parts of the area. This means that it has not been possible to make a complete and detailed interpretation of the extent and nature of the faults. However, U12 should be assumed to include faults across the entire Hesselø South OFW project site.

No clear faulting has been identified in the Quaternary sediments. However, Soft-Sediment Deformation Structures (SSDS) related to the Sorgenfrei Tornquist Zone are found in U08, see section 9.8.5.

9.8.3 Boulders, cobbles, and patches of gravel

Diffraction hyperbolas have been identified in the SBP data across U01 and are interpreted as being potential boulders. An example of the diffractors in the SBP data can be seen in Figure 9-6.

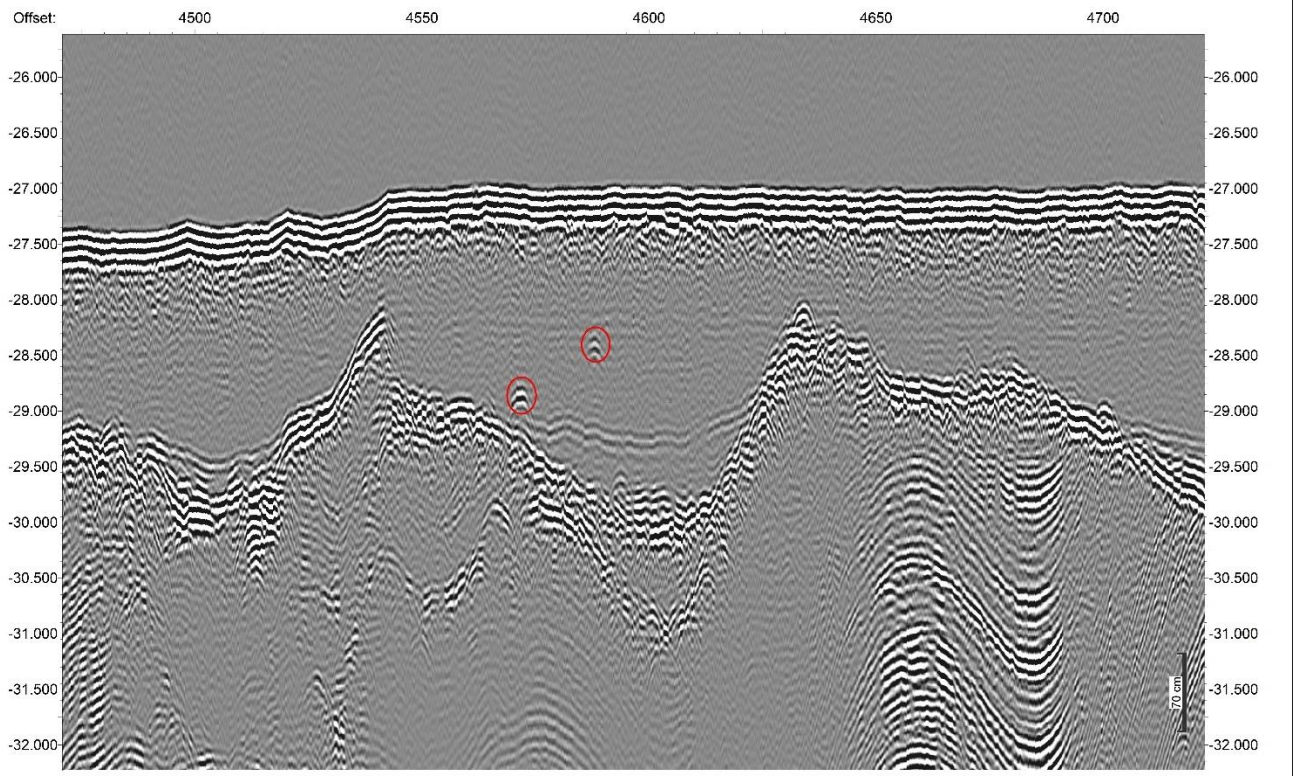

Figure 9-6: Line 0287_C_HS_G06_L672S: Example of small diffractions seen in the SBP data, suspected to be potential boulders.

Subsurface boulders in the 2D-UHRS have not been interpreted individually and can primarily be expected in the till unit, U11, which has been in direct contact with the ice that has truncated the bedrock.

9.8.4 Glacial deformation

Deformation of units overridden by ice is observed in the Hesselø South OWF project site. The units where the deformation is observed are U09, U10, and U11. An example of glacial deformation can be seen in Figure 9-7, where the chaotic internal structures of U10 is especially visible. The three glacially deformed units seem to be evenly disturbed across the site, even though it can be hard to determine due to poor seismic data quality with e.g. multiples.

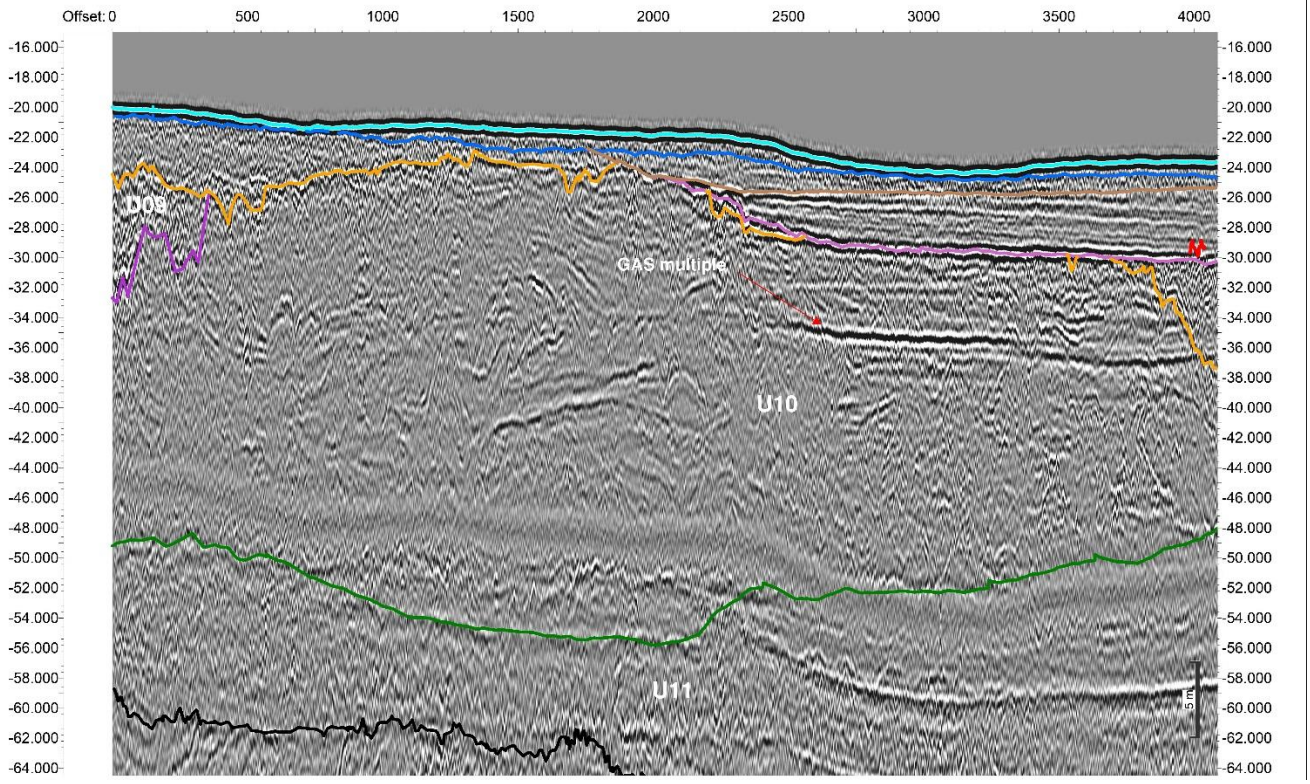

Figure 9-7: Line A_HS_L038B_UHR_T_MIG_STK. Example of glacial deformation in U10. The seismic facies show chaotic reflectors which represent disturbed deposits. An overview of the seismic facies is found in section 9.9.

9.8.5 Late glacial deformation of soft sediments

Soft-Sediments Deformation Structures (SSDS) are complex deformations in soft sediments often triggered by tectonic movements, see Ref. /11/. Thick beds of glaciomarine clays were deposited with high sedimentation rates in the late glacial period within the site. At the same time offloading by melting of the ice sheet initiated the lithosphere uplift (isostatic rebound). The tectonic setting around the Sorgenfrei-Tornquist Zone is likely to have influenced the lithosphere movements during the most active periods of the isostatic rebound. SSDS have been described from Lønstrup Klint, an onshore location within the Sorgenfrei-Tornquist Zone (Ref. /12/). These lithospheric movements are considered to have resulted in comprehensive deformation of structures which is observed in the late glacial deposits within the site.

A major part of the glaciomarine clays of U08 displays comprehensive deformation features which are interpreted to be related to SSDS, see Figure 9-8. The northern part of U05, U06, and U07 also display deformation structures which are interpreted to be related to SSDS but less comprehensive than U08.

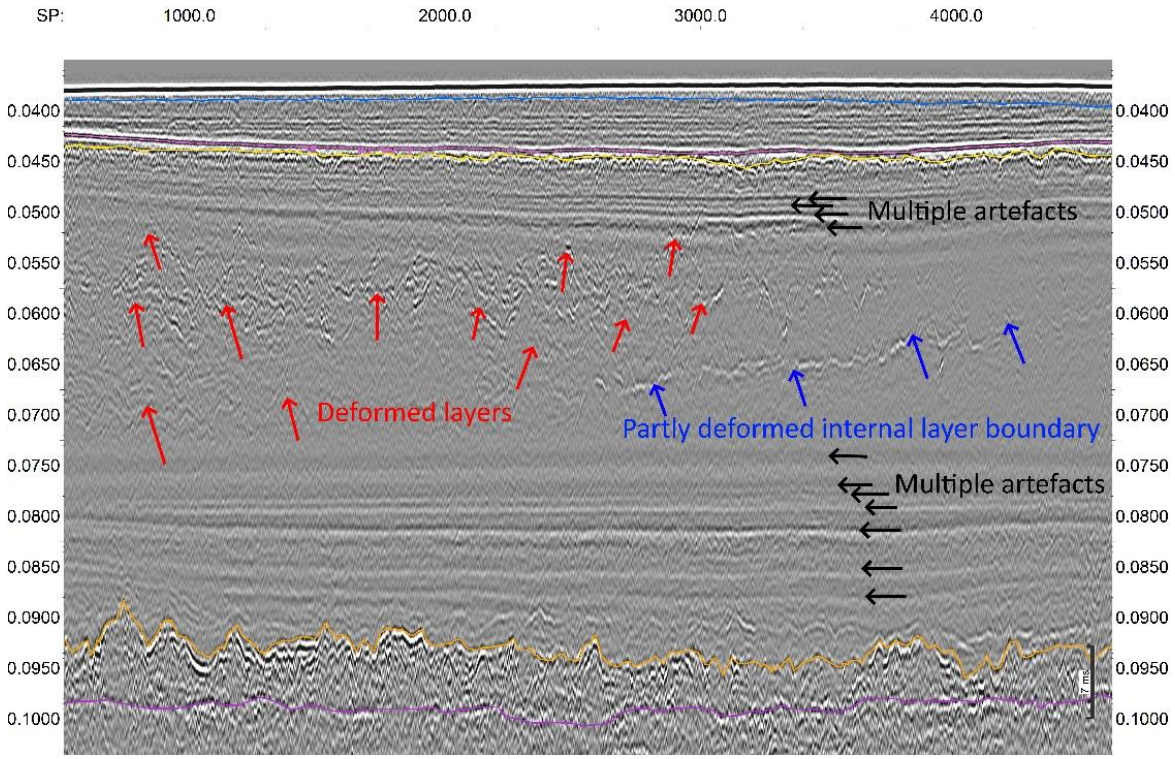

Figure 9-8: Line A_HS_L008_UHR_T_MIG_STK. Deformation structures as seen across U08. Vertical scale in ms (TWT).

9.9 Model stratigraphy

The stratigraphy of Hesselø South OWF project site has been divided into 12 units with a further subdivision of U01 into U01.2. A summarized description of the different units can be found in Table 9-3. Cross sections from the Conceptual Geological Model are shown in Figure 5-1 and Figure 5-2 (see Appendix G for higher resolution).

Cross sections through the digital 3D IGM, displaying the distribution and stratigraphy of the units are presented in enclosures 6.01-6.13.

The stratigraphy interpreted in the data collected for the Hesselø South OWF has been guided by scientific papers and reports, amongst others from the desktop study conducted by GEUS (Ref. /8/ and Ref. /9/). The units have been appointed an age based on the seismic characteristics, the lithology, and the specific characteristics of the unit.

The 12 units have been divided into four chronostratigraphic groups named as follows: Holocene, Late Weichselian, Weichselian/Pleistocene, and Jurassic to Early Cretaceous. The Weichselian/Pleistocene group was created for the units that was overridden by ice sheets at some point after deposition. No interglacial units were identified, and it is therefore difficult to assign a unit to one of each of the three major glaciations, because the area was in a subglacial setting during each of the three glaciations. The units assigned to Weichselian/Pleistocene could therefore in theory be assigned to either the Weichselian, the Saalian, or the Elsterian glaciation.

None of the units found in the Hesselø South OWF project site have been interpreted as belonging to the interglacial periods Eem or Holstein. However, there is a possibility that they are present within the Hesselø South OWF project site, but do not stand out clear enough to be distinguished and separated from the glacial units.

Deformation has been identified in the units older than Late Weichselian. Especially in the till unit, U11, the deformation of the unit is so pronounced, that older deposits might occur on top of younger deposits. The laws of superposition have potentially also been violated in heavily folded areas of the Pre-Quaternary unit U12.

Table 9-3 Summary of units in the Integrated Geological Model. The cell with unit name has been coloured in same colours as in the Conceptual Geological Model, see section 5.

Unit	Base Horizon	Seismic facies	Soil Type according to the borehole descriptions. (Ordered by frequency)	Chronostratigraphic group	Depositional Environment
U01	B01	Acoustically semi-transparent. In thicker deposits internal parallel reflectors are present. Mostly low amplitude reflectors.	Sandy CLAY, Silty CLAY, CLAY, SAND	Holocene	Marine
U01.2	B01.2	Chaotic to semi parallel facies of low to medium amplitude. Semi-transparent facies are also seen.	CLAY		
U02	B02	Chaotic to sub parallel reflectors, with areas of acoustic transparency. Low to medium amplitude reflectors.	SAND, Silty SAND, sandy SILT		Deltaic marine
U03	B03	Parallel reflectors with areas of transparency. Low to medium amplitude reflectors.	Sandy CLAY, Silty CLAY, Sandy Gravelly CLAY, Silty Sandy CLAY, Silty Gravelly CLAY, SAND, Silty SAND		Deltaic marine
U04	B04	Facies of chaotic to transparent in the N to NW. Clear internal structures in the thicker parts of the N-S channel. Medium to high amplitude.	Silty Gravelly SAND, Silty SAND		Fluvial, estuarine to shallow marine
U05	B05	Draping subparallel reflectors in the western part and has parallel reflectors in the eastern part. Low to high amplitude reflectors.	Silty SAND, Silty CLAY	Late Weichselian	Glaciolacustrine
U06	B06	Consists mainly of parallel reflectors with low to high amplitude reflections but does also include areas with almost transparent to chaotic facies	Silty SAND, SAND		Glaciolacustrine
U07	B07	Primarily subparallel reflectors of low to high amplitude. Also found as semi-chaotic to semi-transparent facies.	Silty Gravelly CLAY, Silty CLAY, Sandy Gravelly CLAY, CLAY		Glaciolacustrine
U08	B08	Parallel to sub-parallel reflectors. Areas of deformation is seen. Blanking from multiple removal is disturbing the seismic facies across the site.	Silty SAND, Gravelly CLAY, Silty Gravelly SAND, Silty Sandy Gravelly CLAY, SAND, CLAY, Sandy, Silty Gravelly CLAY, Silty Sandy Cobbly CLAY, Silty Sandy Gravelly Cobbly CLAY		Glaciomarine

Unit	Base Horizon	Seismic facies	Soil Type according to the borehole descriptions. (Ordered by frequency)	Chronostratigraphic group	Depositional Environment
U09	B09	Chaotic seismic facies to semi-transparency.	Silty CLAY, Silty Gravelly CLAY,		Subglacial
U10	B10	Areas of parallel and semi-parallel reflectors and more deformed and chaotic areas.	Clayey SAND, Gravelly SAND, Silty SAND, SAND	Weichselian to Pleistocene	Glacial fluvial
U11	B11	Chaotic seismic facies with deformation structures.	Silty Sandy Gravelly CLAY (TILL), Sandy Gravelly CLAY (TILL), Silty Sandy CLAY, Silty Gravelly SAND, Clayey SAND, Silty CLAY, Clayey Silty SAND,		Mixed glacial
U12		Sub-parallel to hummocky reflectors. Areas of chaotic and blanking facies occur but is most likely due to the quality of the data.	SANDSTONE, SILTSTONE, MUDSTONE	Jurassic to Early Cretaceous	Marine

9.9.1 Holocene

The units assigned to the chronostratigraphic group Holocene represent an environmental transition from terrestrial over near coastal to marine. The marine U01 is seen across the entire site while the near coastal U02 and U03 are only found in the northern part of the site. The lower fluvial, estuarine to shallow marine U04 is eroding into the underlying units.

U01 – Post glacial marine

U01 represents the most recent deposits in the model and is a recent Holocene marine deposit. The unit mainly consists of very weak to extremely weak silty CLAY but is also occasionally found either as sandy or purely as sand (HS_S_14_DCPT). The unit is present across most of the Hesselø South OWF site and is only locally not present due to erosion. U01 has a thickness of up to 18 m but is generally found ranging from 0-4 m. The thickest deposits are found in an erosional channel feature running approximately N-S in the western part of the OWF where it reaches maximum thickness in the southern part of the channel, see enclosure 4.01. The channel is proposed to be an Early Holocene channel that has been infilled with the sediments of U01. The channel must have been formed after the deposition of unit U03, which has clear signs of erosion and with the younger and overlying units seemingly draping onto the erosional top. Where the units U01.2, U02, U03 or U04 are directly underlying U01, an erosional contact is found.

U01 is generally easy to correlate with geotechnical data since it's a layer of low strength typically overlying sand of U02 or U04.

The unit is interpreted on the SBP dataset and is recognised by its generally transparent seismic facies, but can be seen having parallel internal reflectors, especially in the thickest parts of the unit. These internal reflectors can indicate lenses of more sandy material. Diffraction hyperbolas are present within this unit and are likely due to the presence of coarse material (i.e., gravel-sized shells, shell, and rock fragments).

Figure 9-9 shows an example of the seismic facies of U01, and the lithology of the unit at the position of borehole HS_S_32_BH.

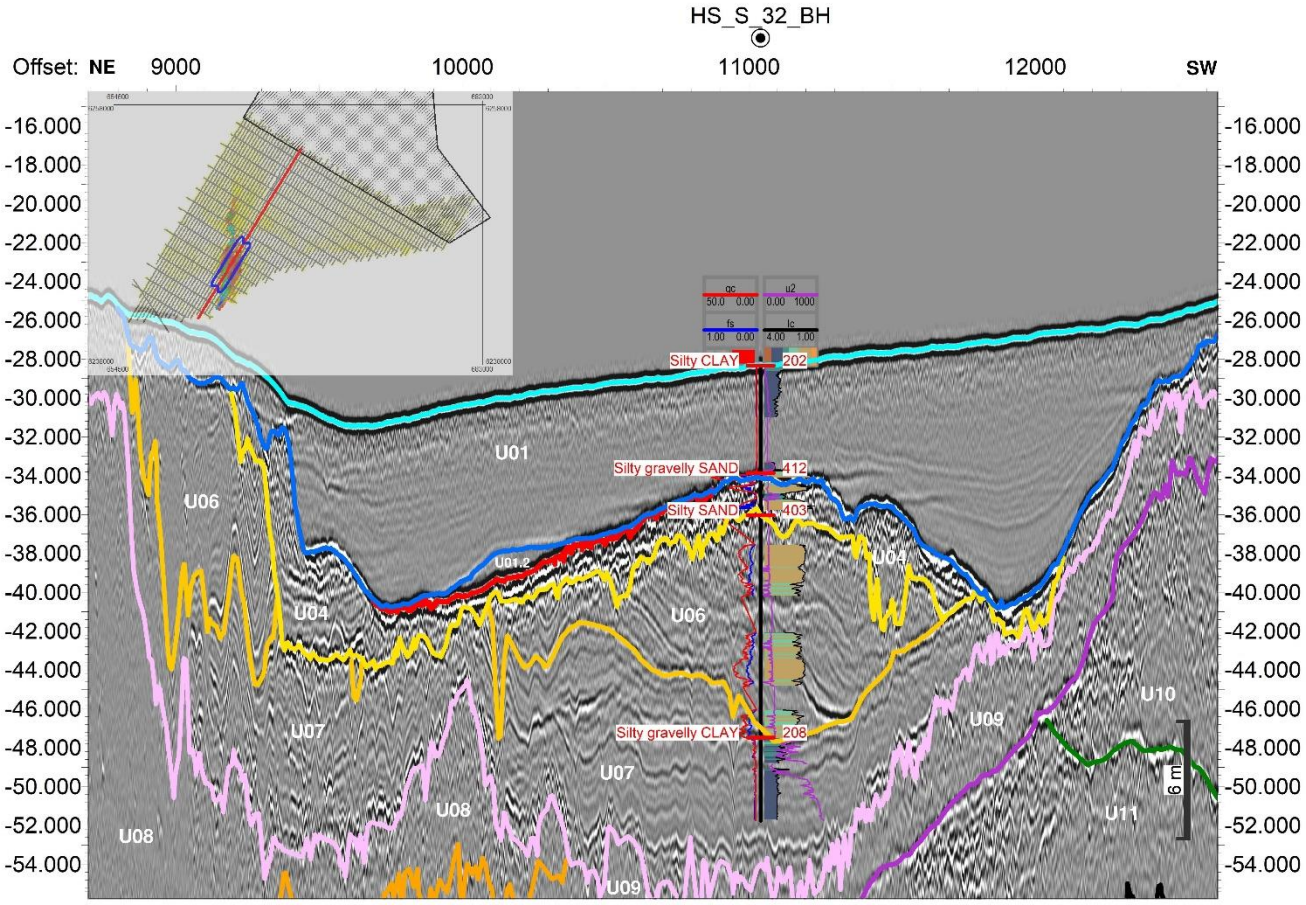

Figure 9-9: Line A_HS_L021_UHR_T_MIG_STK. Example of U01 which is seen between the Seabed (turquoise) and B01 (blue). The unit has a silty CLAY composition in HS_S_32_BH and is seen having a seismic facies of low amplitude reflectors which are semi-transparent to subparallel.

Enclosure 2.01 shows the depth below seabed of the top of unit U01, enclosure 3.01 the elevation of the top of the unit, and enclosure 4.01 the thickness (isochore) of unit U01.

U01.2

The unit is found locally in a thin line running N-S and is discontinuous approximately at the middle of the site where it is truncated by U01. In Figure 9-10 an example of U01.2 can be seen. This example shows an area where the unit has it greatest thickness, but it is generally seen as a thin layer marking the change from U01 to the underlying units.

The unit is seen as having chaotic to semi-parallel reflectors generally with low amplitude, but with more signal than the overlying U01. In Figure 9-10 the change from U01 to U01.2 is easy to see, but in other cases the boundary is marked by a faint reflector but with the same seismic facies at both sides of the reflector. U01.2 is only penetrated by one geotechnical test location (HS_S_11_BH), but it is located in an area with only very limited thickness of the unit. No significant change can be seen going from U01 to U01.2 and they are both categorized as CLAY.

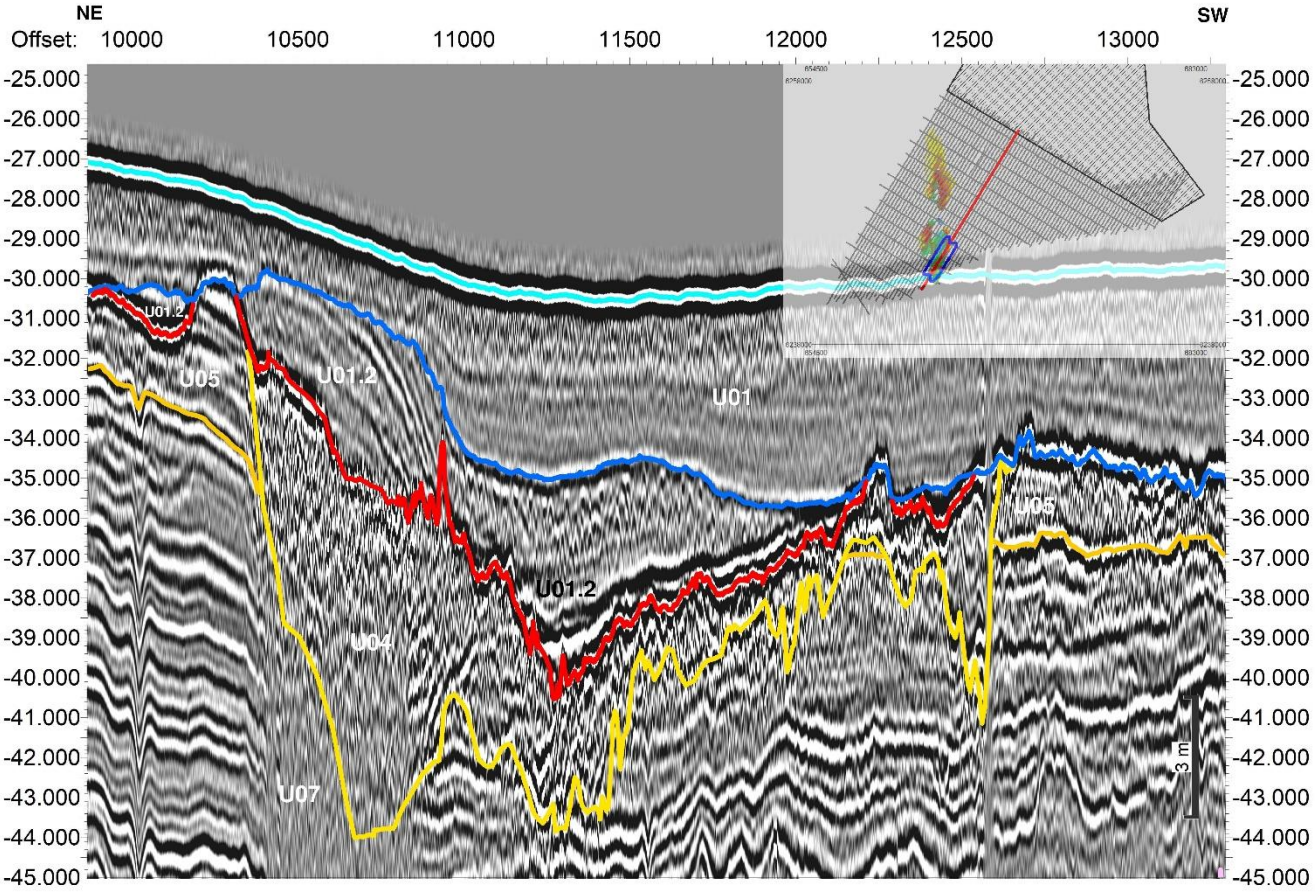

Figure 9-10: A_HS_L025A_UHR_T_MIG_STK. Example of U01.2, bounded to the top by B01 (Blue) and by B01.5 (Red). The seismic facies is chaotic to semi-parallel/draping. In the left-hand side of the figure gas blanking is seen below U01.2.

The thickness of U01.2 is up to approximately 6 m thick, and the thickest deposits are found in the southern part of the unit ranging generally from 2.5 to 6 m. In the northern extend of U01.2 the thickness is smaller ranging from 0.2 to approximately 3 m, see enclosure 4.02.

We only have one geotechnical location with samples from U01.2, here it is hard to distinguish from the overlying U01. The base of U01.2 is typically overlying the sandy U04 and is well-defined.

Enclosure 2.02 shows the depth below seabed of the top of unit U01.2, enclosure 3.02 the elevation of the top of the unit, and enclosure 4.02 the thickness (isochore) of unit U01.2.

U02

The unit is found from the northwestern part of the area and towards the middle of the site (enclosure 2.03). It is interpreted as an outbuilding structure related to a channel mouth, relatable to a delta style deposit, and consists mainly of SAND and silty SAND, with occasional sandy SILT. Internal outbuilding structures can be seen in the units' seismic facies, and it is in some places toplapping onto U01. The seismic facies vary across the site and is chaotic to sub parallel, with areas of acoustic transparency. U02 is highly related to the underlying U03. Together the two units display low angel clinoforms where U02 represents the top part consisting mainly of sand and U03 represents the lower part consisting mainly of silt and clay. In other places the change from U02 to the underlying U03 can be seen as a change from more chaotic to more subparallel reflectors, however, not a very profound change. The change is visible in the geotechnical data were a change from sandy to clayey material is evident, as seen in HS_S_14_DCPT. In Figure 9-11 an example of the seismic facies of U02 can be seen in a location where the clinoforms are divided in U02 (upper part) and U03 (lower part).

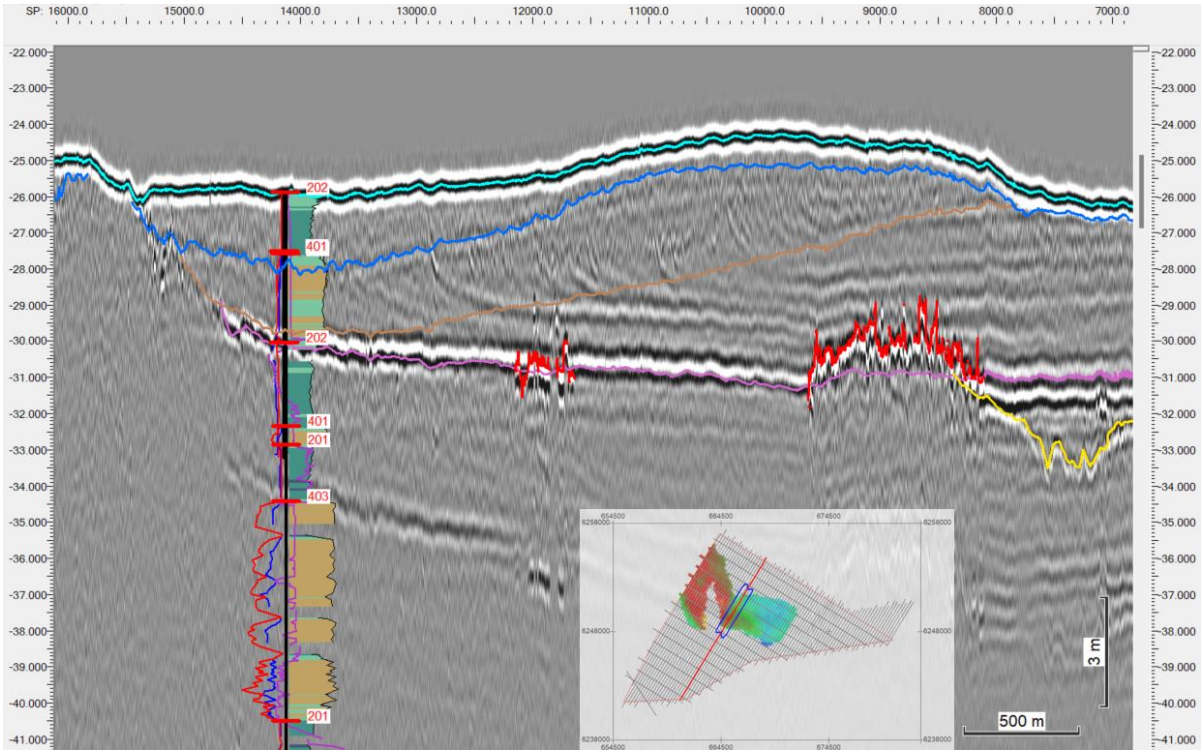

Figure 9-11: Line A_HS_L020_UHR_T_MIG_STK. Example of U02 which is seen between B01 (blue) and B02 (Brown). The seismic facies is seen to be laminated in some cases and chaotic to blanking in others. The unit is penetrated by HS_S_17_DCPT which shows a Sandy Gravelly CLAY lithology.

The unit is ranging between approximately 0.2 and 5 m in thickness, and is found to be thickest in the westernmost lobe of the unit, where it is generally above 3 m. The thinnest areas are found in the northern part of the unit (enclosure 4.03).

U02 is deposited together with U03 in deltaic environment where U02 represents the upper more proximal sandy sequence and U03 represent the more distal fine-grained part of the deposits. The split between the two units (U02 and U03) is well-defined in the geotechnical data but can be a challenge to locate accurately in the seismic data.

Enclosure 2.03 shows the depth below seabed of the top of unit U02, enclosure 3.03 the elevation of the top of the unit, and enclosure 4.03 the thickness (isochore) of unit U02.

U03

The unit is present only in the northern part of the Hesselø South OWF project area. The unit is found to primarily consist of Silty or Sandy CLAY and has parallel to subparallel internal reflectors. In Figure 9-12 an example of the seismic facies can be seen along with the geotechnical information from HS_S_02_BH and HS_S_04_DCPT. Geotechnically it can be hard to differentiate between U03 and the overlying U01, but when the sandy U02 is present, the three units constitute a change from CLAY to SAND to CLAY.

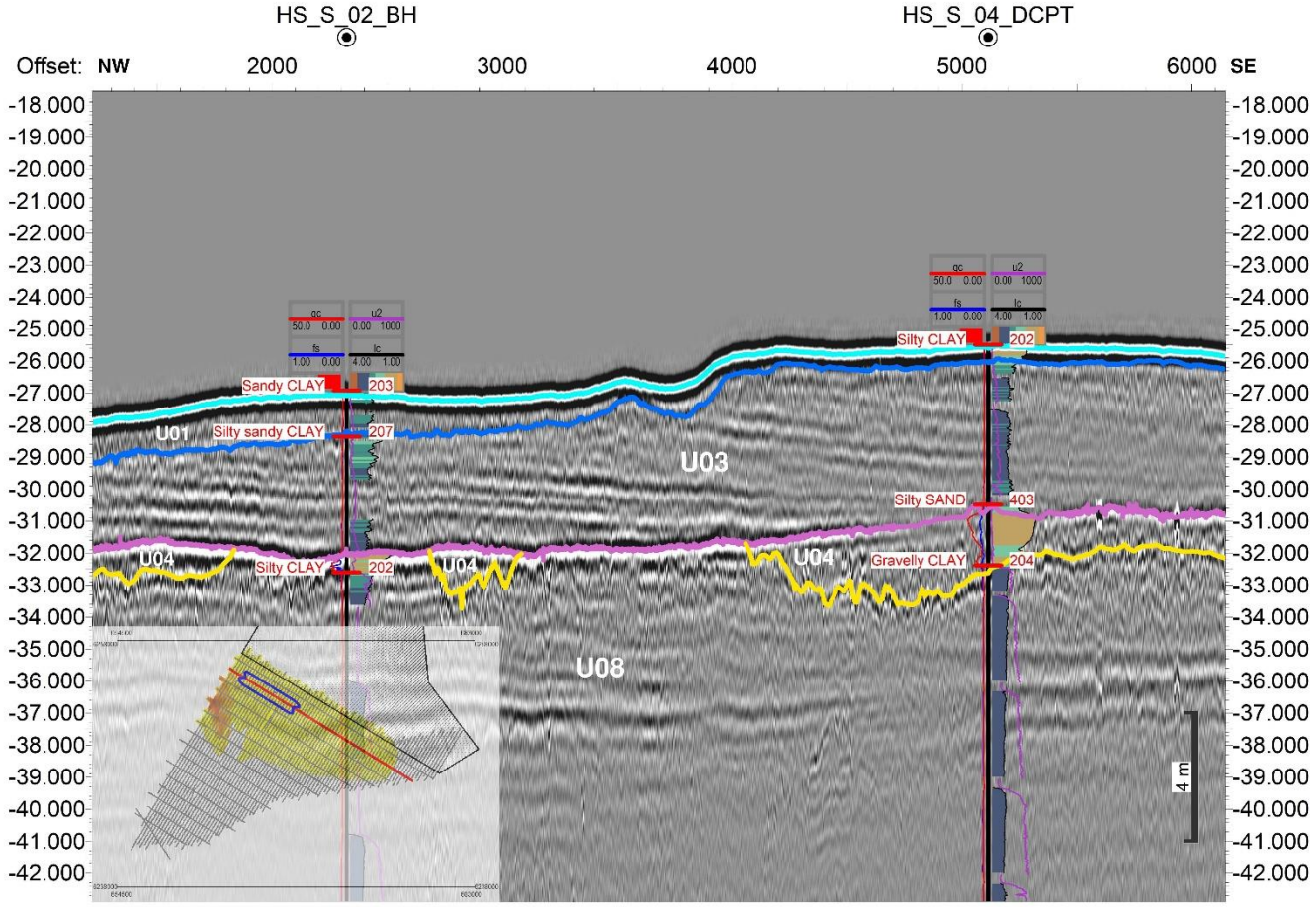

Figure 9-12: Line A_HS_X016_UHR_T_MIG_STK. Example of U03 which in this case is bounded to the top by B01 (blue) and to the bottom by B03 (purple). The facies is seen as having parallel reflectors to transparency. Two wells are penetrating the unit in this example, and HS_S_02_BH shows a lithology of Silty Sandy CLAY while HS_S_04_DCPT shows Silty CLAY.

The unit is overlying U04 and U08 and the changes from U03 into the lower units are marked by a clear erosive boundary. The unit has been interpreted as being a deltaic or estuarine deposit.

U03 is found to be up to 7.6 m thick, and the thickest deposits are found in a local part of the western part of the unit, and in the middle. In the northeast, the unit is locally

missing due to truncation by the upper U01. The elevation of the upper boundary of B03 is not varying much but has generally a deepening towards the east and west sides of its extent, see enclosure 3.04. At the base of U03, gas is present across quite a large area, see enclosure 5.01 or Figure 9-4 in section 9.8.1, where a more detailed description of the shallow gas is provided.

The lower boundary of U03 is typically well defined when it overlies the sand of U04.

Enclosure 2.04 shows the depth below seabed of the top of unit U03, enclosure 3.04 the elevation of the top of the unit, and enclosure 4.04 the thickness (isochore) of unit U03.

U04

The unit is found mainly in the northern part of the Hesselø South OWF site, but also in a N-S trending channel incision. The interpretation of this unit is proposed as a fluvial/estuarine Early Holocene unit.

The geotechnical data describes this unit as Silty Gravelly SAND or silty SAND. The seismic facies differs from being chaotic and without structure in the northern and northwestern part of the OWF area, to having clear internal structures in the thicker parts of the N-S channel. The unit has a clear erosional contact to U03 in the top and an erosional contact to the underlying units (U06, U08). An example of U04 can be seen in Figure 9-13 around the location of borehole HS_S_03_DCPT which shows the lithology of U04 to be Silty Gravelly SAND. As also seen in Figure 9-2, the mirroring effect of the gas can easily be mistaken as the same signature as U04, which is important to have in mind when interpreting the unit.

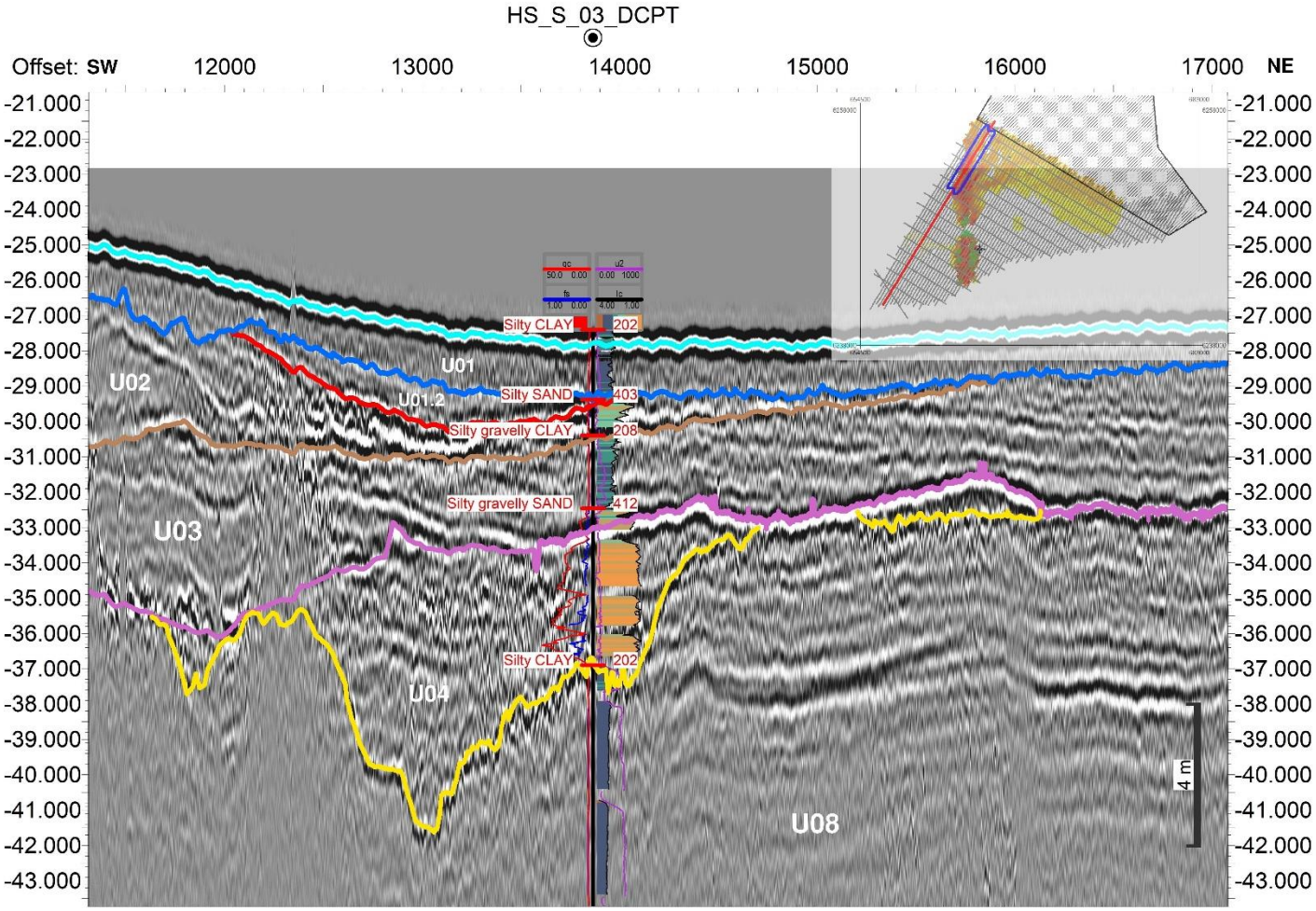

Figure 9-13: Line A_HS_L006_UHR_T_MIG_STK. Example of U04 which in this example is bounded to the top by B02 (brown) and B01 (blue) and to the base by B04 (yellow). The seismic facies is seen as having a structured infill of sub-parallel to chaotic reflectors. HS_S_S03_DCPT is penetrating the unit and shows a lithology of Silty Gravelly SAND.

The unit is found to be 15 m at the thickest place (enclosure 4.05) but is most generally found below 3 m in thickness. The thickest areas are located in a N-S running channel feature.

U04 is a well-defined layer in both seismic sections and geotechnical data and consistently mapped as a fluvial sand layer.

Enclosure 2.05 shows the depth below seabed of the top of unit U04, enclosure 3.05 the elevation of the top of the unit, and enclosure 4.05 the thickness (isochore) of unit U04.

9.9.2 Late Weichselian

The units assigned to the chronostratigraphic group Late Weichselian group are related to last glacial maximum, which occurred in last phase of the Weichselian around 20,000 years ago. Late Weichselian includes deposits from the latest glacial readvances during general glacial retreat. U09 was deposited or deformed into its present shape by subglacial conditions. The subsequent unit U08 was deposited under glaciomarine

conditions. U07, U06 and U05 were deposited under glaciolacustrine conditions. A late glacial readvance formed the depression which the glaciolacustrine units fill up.

U05

The unit is found locally in the southwestern part of the study area and is an infill in a larger glaciolacustrine infill unit. U05 is identified as having a finer grained composition than the underlying infill unit, U06, and is found having the geotechnical parameters of Silty SAND to silty CLAY. The clay material is found in the western part of the basin while the sand is found in the eastern. The clayey parts are of medium to high strength with lose to medium dense SAND lenses. The sandy parts of the unit consist of medium dense to very dense SAND. The unit has draping subparallel reflectors in the western part while it is seen more as having parallel reflectors in the east. The unit has a clear erosive contact to the underlying unit U06, which could represent a major erosive event between the two units. An example of U05 can be seen in Figure 9-14, where both seismic facies of parallel and semi-parallel reflectors can be seen. HS_S_31_DCPT is seen penetrating U05, and it shows a Silty SAND lithology. Strongly wavy to increasingly chaotic reflections can be seen in the northeastern part of the unit which is interpreted to reflect soft-sediments deformation structures (SSDS) which seem to be limited the Sorgenfrei-Tornquist Zone – see section 9.8.5. SSDS can be seen in the northwestern side of the section in Figure 9-14.

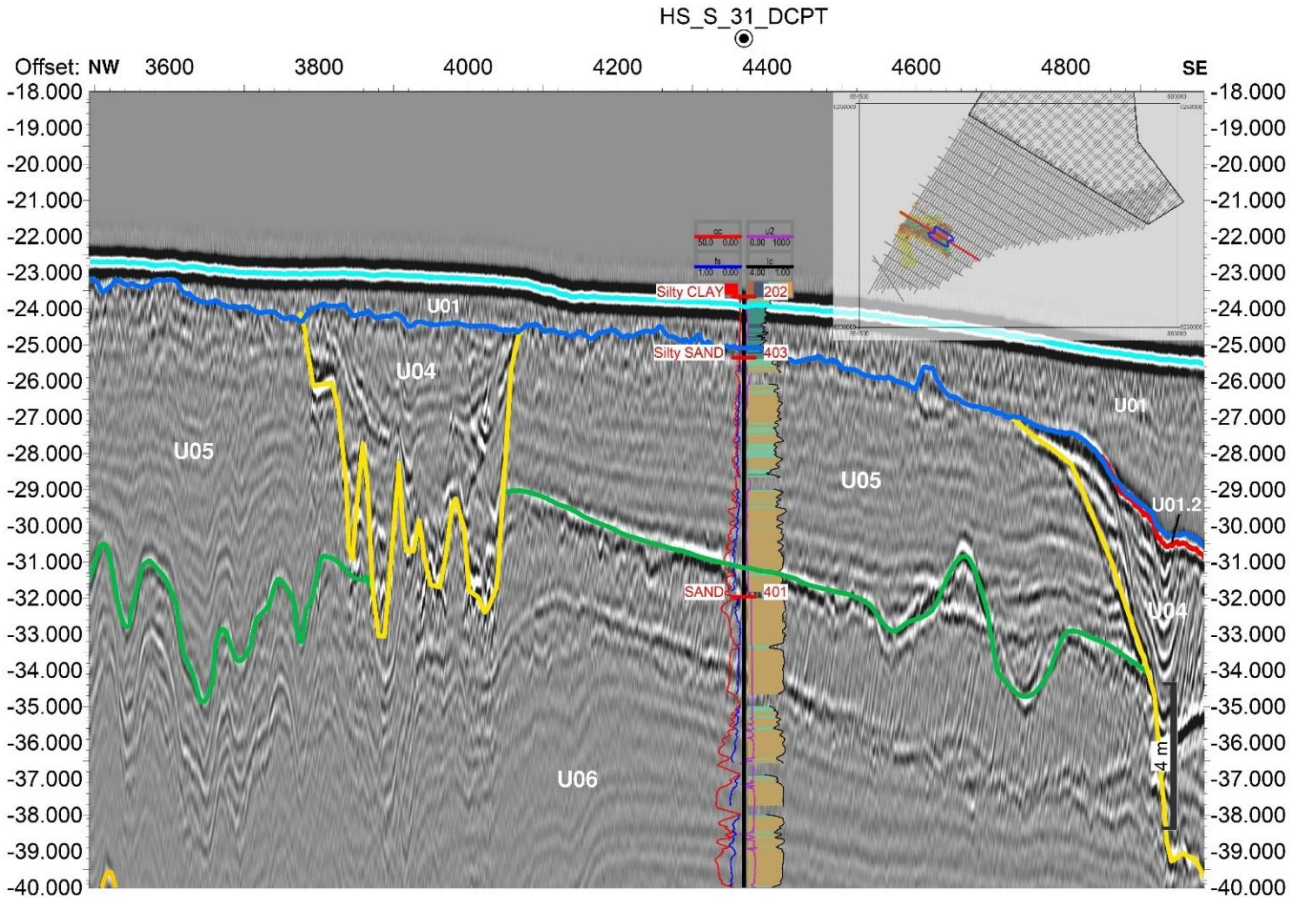

Figure 9-14: Line A_HS_X007_UHR_T_MIG_STK. Example of unit U05 which in this example is bounded to the top by B01 (blue) and to the bottom by B05 (green). It is seen cut into by U04 (B04 is yellow). The seismic reflectors seen in the unit are parallel to sub-parallel. HS_S_31_DCPT is penetrating U05 and shows a Silty SAND lithology.

The thickness of U05 is locally up to 21 m and the deepest areas are found approximately W-E in the area occupied by U05. The thicknesses are generally above 9 m but are found thinner in the periphery of the unit and in the southern lobe.

U05 is the uppermost of the three glaciolacustrine layers and is well-defined in the seismic section. In the geotechnical data it can in some areas be hard to distinguish from the underlying U06, where U05 consists of sand like U06. In other areas where U05 consists of clay, the boundary to U06 is clear in the geotechnical data.

Enclosure 2.06 shows the depth below seabed of the top of unit U05, enclosure 3.06 the elevation of the top of the unit, and enclosure 4.06 the thickness (isochore) of unit U05.

U06

The unit is found locally in the southwestern part of the study area and is a lower part of the basin including U05. The unit consists mainly of parallel reflectors with low to high amplitude reflections but does also include areas with almost transparent to chaotic facies. The unit consists of SAND to silty SAND and marks a change from silty CLAY to SAND in the top in the western part of the basin. In the western part at H_S_32_BH there is no change from the Silty SAND of U05 to the Silty SAND of U06. To the bottom the unit marks a change from SAND to CLAY and Silty Gravelly CLAY where underlain by U07. The unit is medium dense to very dense SAND. In Figure 9-15 an example of U06 can be seen, where the parallel reflectors can be seen, along with a more deformed part under U04. A DCPT and a borehole is penetrating the unit in this example and HS_S_31_DCPT shows a lithology consisting of SAND, while HS_S_32_BH shows Silty SAND.

The unit is interpreted to be a sandy part of a glaciolacustrine deposition environment, deposited in an environment with higher energy than the clayey components of the glaciolacustrine infill units, parts of U05 and U07. Strongly wavy to increasingly chaotic reflections can be seen in the northeastern part of the unit which is interpreted to reflect soft-sediments deformation structures (SSDS) which seem to be limited to the Sorgenfrei-Tornquist Zone – see section 9.8.5.

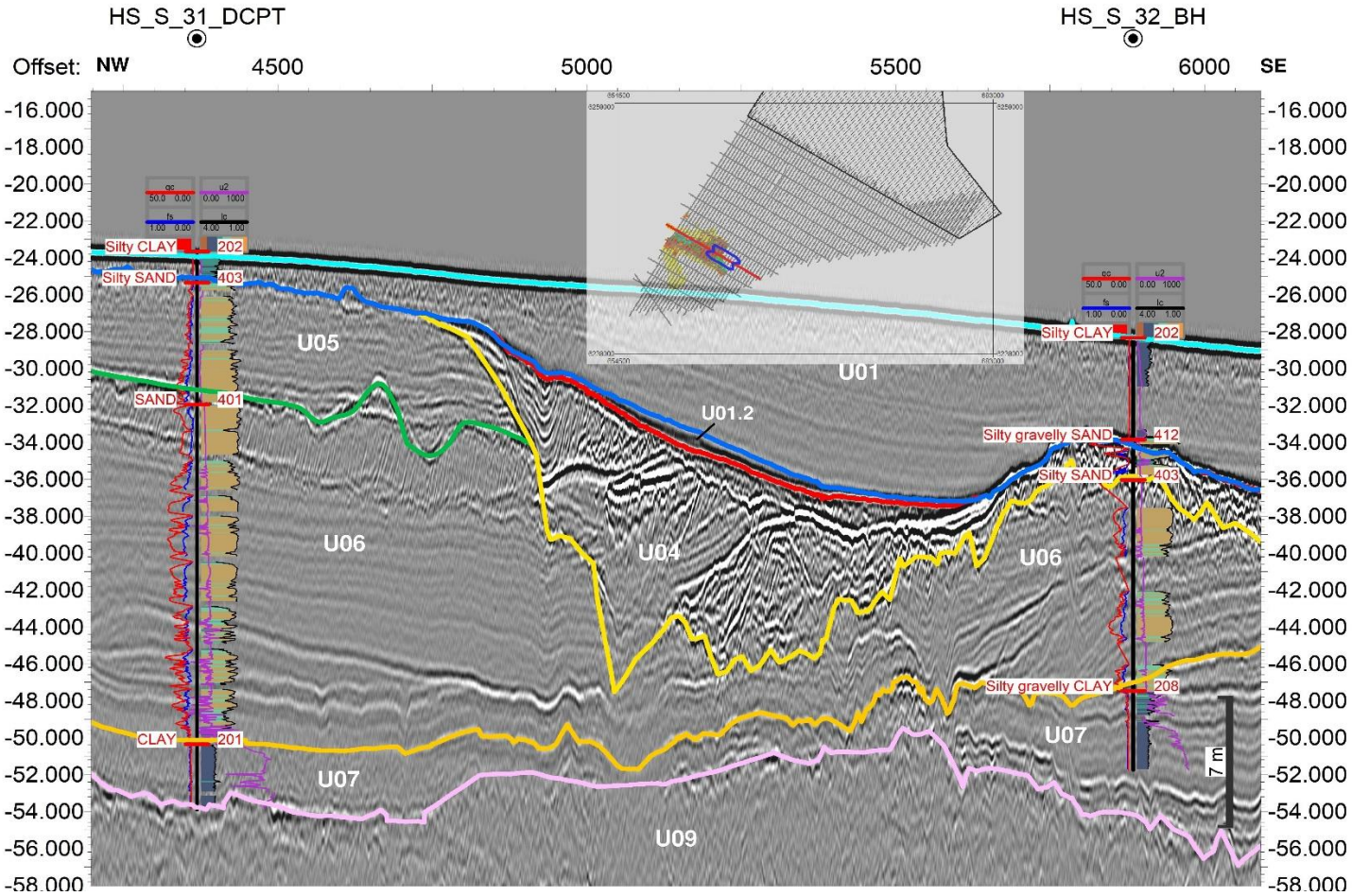

Figure 9-15: Line A_HS_X007_UHR_T_MIG_STK. Example of U06 where it is in this example seen bounded to the top by B05 (Green) and B04 (Yellow) and B06 (Gold) to the bottom. The seismic facies shows parallel to subparallel reflectors and areas with deformation. Penetrating the unit is HS_S_31_DCPT showing a SAND lithology and HS_S_32_BH showing a Silty SAND lithology.

The thickness of U06 is up to 25 m, the thickest area is seen in the left side of Figure 9-15, and is generally thicker in the middle of the infilled area. The thinnest parts are found at the sides of the infilled area, since the unit is generally slopping downwards towards the centre of infill.

U06 consist of sand in contrast to the clay of the underlying U07 and the lower boundary of U06 is therefore easy to identify in geotechnical data. The reflection pattern of U06 can in some areas be difficult to distinguish form U07 and some places its easier.

Enclosure 2.07 shows the depth below seabed of the top of unit U06, enclosure 3.07 the elevation of the top of the unit, and enclosure 4.07 the thickness (isochore) of unit U06.

U07

The unit is found locally in the southwestern part of the study area and is lower part of the basin including U05 and U06. The unit primarily has subparallel reflectors of low to high amplitude but is also found as semi-chaotic to semi-transparent. The geotechnical data shows that the unit has a lithology of CLAY to Silty Gravelly CLAY, and it marks a change from SAND and Silty SAND at the top. In Figure 9-16 an example of U07 can be

seen, where the semi-parallel reflectors are visible. HS_S_33_DCPT is penetrating U07 and is showing a lithology of Silty Gravelly CLAY with a transition to Silty CLAY. U07 is interpreted as a glaciolacustrine unit, and marks the bottom of the glaciolacustrine infill units, Unit D1-2. U07 is of high to very high strength. The unit has been interpreted as the CLAY base of a lacustrine sediment infilled depression left by the latest glacial readvance in the area. Strongly wavy to increasingly chaotic reflections can be seen in the northeastern part of the unit which is interpreted to reflect soft-sediments deformation structures (SSDS) which seem to be limited the Sorgenfrei-Tornquist Zone – see section 9.8.5. SSDS can be seen in the northeastern side of the section in Figure 9-7.

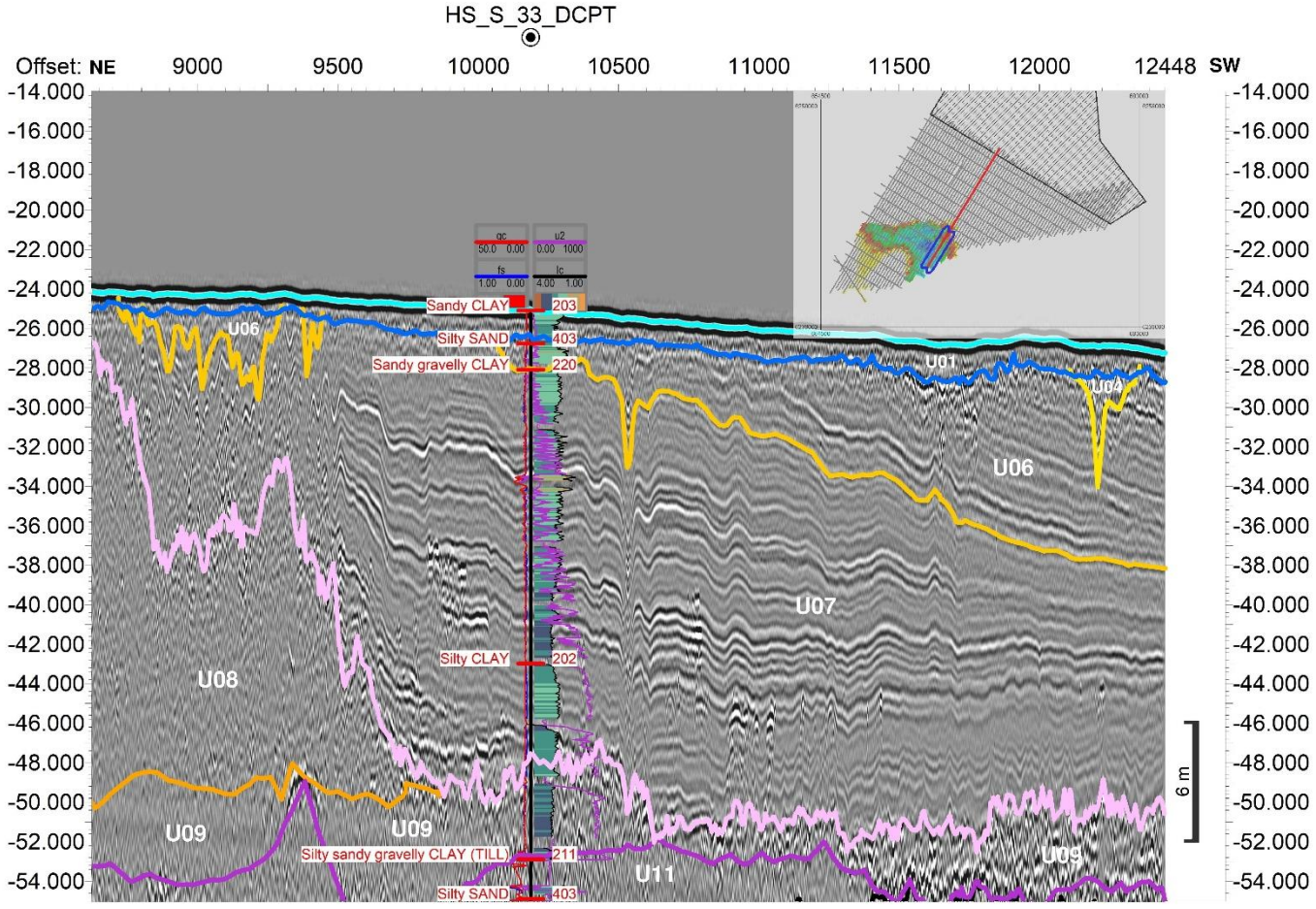

Figure 9-16: Line A_HS_L028_UHR_T_MIG_STK. Example of U07, in this example bounded by B06 (Gold) and B01 (blue) to the top and B07 (Pink) to the bottom. The seismic facies is semi-parallel. HS_S_33_DCPT is indicating a Silty Gravelly CLAY lithology changing into a Silty Clay lithology at 17.9 m.

The thickness of U07 is up to 26 m, and it is found the thickest in the east where it is ranging from 10-25 m thickness. Figure 9-16 shows an example of the thickest infill area. In the W and SW area the general thickness of the unit is below 6 m with some local areas of up to 10 m thickness.

U07 often resemblance U06 in the seismic section and the boundary between the two is primarily driven by the geotechnical data. The CPT signature of U07 often resemblances that of U08 but is clearly distinguishable in the seismic sections.

Enclosure 2.08 shows the depth below seabed of the top of unit U07, enclosure 3.08 the elevation of the top of the unit, and enclosure 4.08 the thickness (isochore) of unit U07.

U08

The unit is found almost across the entire site, except in the south, where it is eroded by younger sediments. The seismic facies of the unit is often found to be transparent to blank due to removal of multiples in the processing stage. Both areas of internal parallel to subparallel reflectors and areas with visual deformation of the unit can be seen. In Figure 9-17 the seismic facies of U08 are seen where blanking areas along with areas with internal structures can be seen. HS_S_06_BH is penetrating the unit, and the lithology has here been interpreted as Silty CLAY.

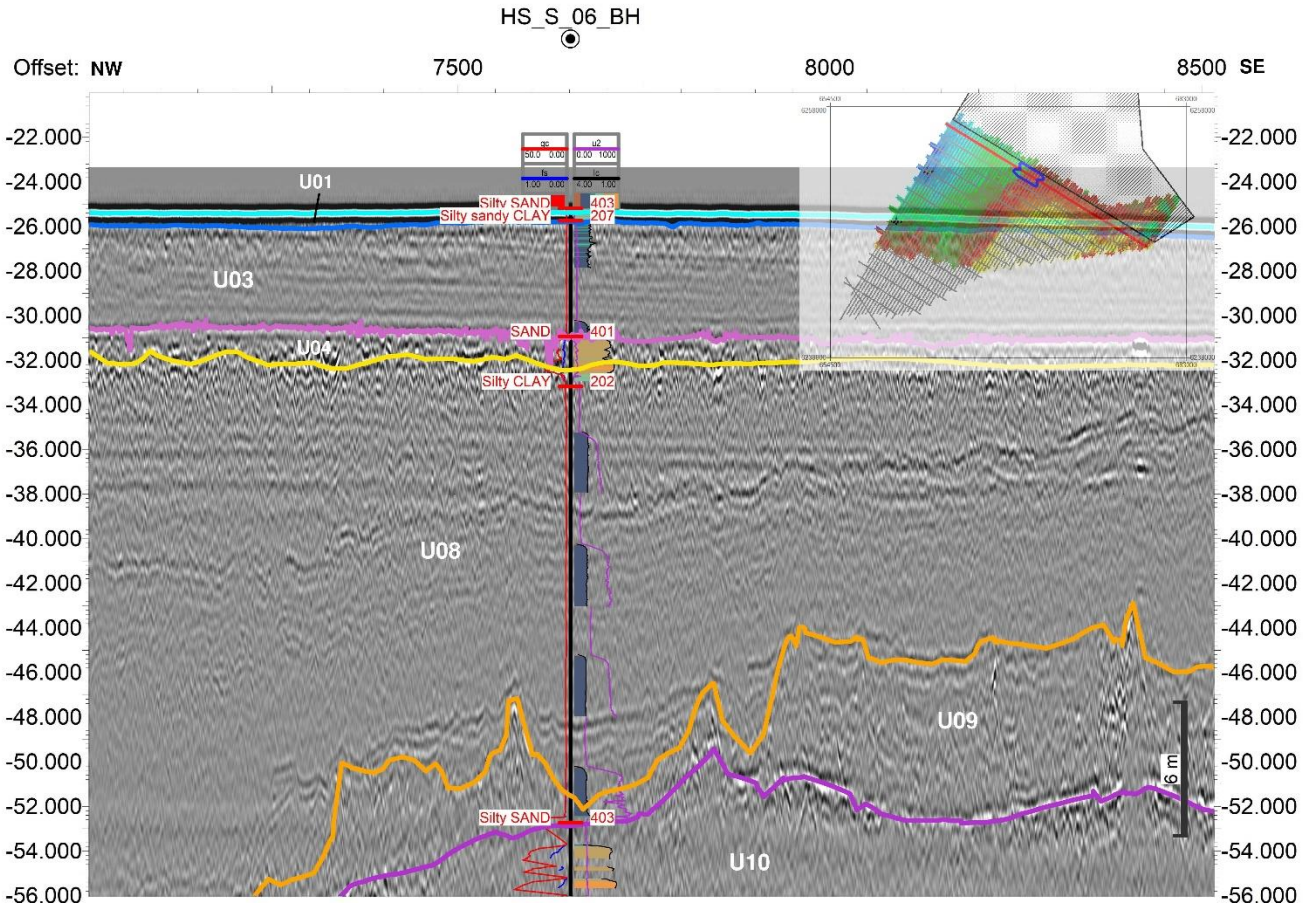

Figure 9-17: Line A_HS_X017C_UHR_T_MIG_STK. Example of U08, in this example bounded by B04 (Yellow) to the top and B08 (Orange) to the bottom. Reflector structure is best seen at the top of the unit. HS_S_06_BH is penetrating U08 and the lithology is interpreted as Silty CLAY.

The unit varies in lithology across its extend and is generally found to be clayey in the north and sandier towards the south, see Figure 9-18. The sandier content to the south may indicate that the input to the glaciomarine sea of U08 came from the south. Possibly the input came from a nearby glacier front, see Figure 4-4.

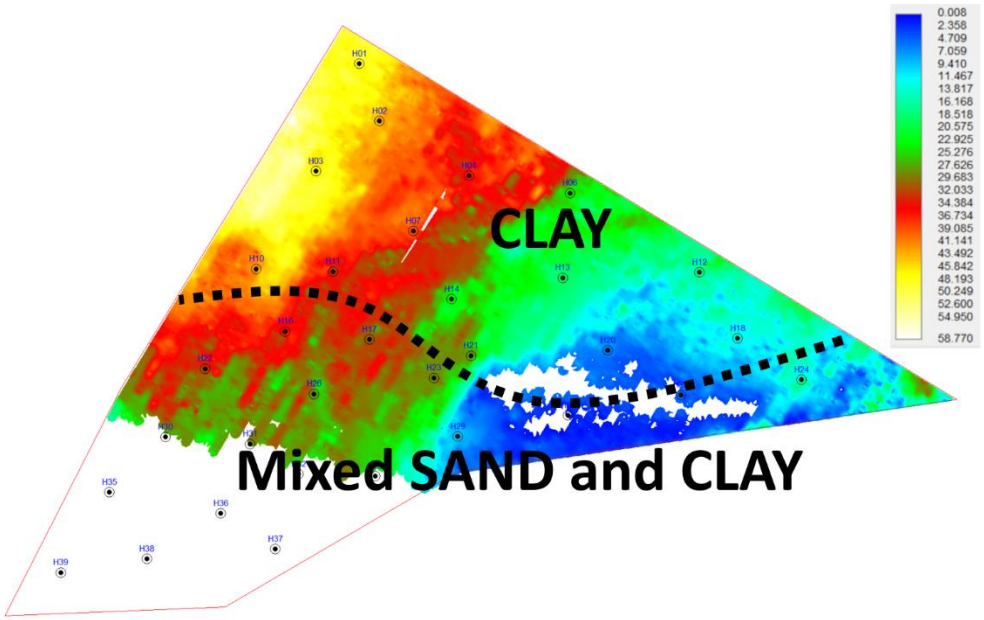

Figure 9-18: B08 (base of U08), depth below seabed (mbsb). Black dashed line indicates the approximate split of U08 of where the unit contains just clay and where it contains mixed layers of sand and clay.

U08 is thickening towards the west and is generally thinner than 20 m in the east and thickening evenly to up to 53 m in the western part of the area. Some thicker parts of up to 36 m are seen in the very NE of the Hesselø South OWF project site. It is seen in incisions which contains completely sub-parallel reflectors indicating a glaciolacustrine setting.

U08 has an erosive base and is found cutting into the underlying U09. U08 is generally seen deformed in various degrees throughout the site, but the exact type of deformation is hard to distinguish due to the quality of the seismic data. The unit is interpreted to be a late glacial glaciomarine deposit of the Weichselian ice advance and is therefore not considered to have been overridden by an ice sheet (except from the areas to the south where the latest readvance formed basin for U07, U06 and U05).

The chaotic reflections which are dominating U08 is interpreted to reflect soft-sediments deformation structures (SSDS) which is interpreted to have impacted U08 to a comprehensive degree. Few areas with less deformation can been seen e.g. in the northern corner of the site – here it is only the uppermost part of U08 that appear undeformed or only lightly deformed. Another example can be seen Figure 9-17 where U08 do display internal layer boundaries.

The base of U08 is well-defined in the seismic sections and characterized by a strong and often highly undulating reflector. In most of the area U08 consists of clay and has a faint laminated to chaotic or featureless interior. In the southern part, where U08 consists of intermixed clay and sand, the interior is mostly chaotic to featureless with scattered amplitude spikes and discontinuous short reflectors. It's not possible to separate the two different parts of U08. In some locations it can be difficult to separate U08 from the underlying U09 based on the geotechnical data where both layers are characterized by relatively weak clay. In other areas U09 has higher strength.

Enclosure 2.09 shows the depth below seabed of the top of unit U08, enclosure 3.09 the elevation of the top of the unit, and enclosure 4.09 the thickness (isochore) of unit U08.

U09

The unit is present across most of the Hesselø South OWF site but is absent in the most southern part and in the middle of the survey area in the west, along with some local spots. In the south the unit is simply terminating against U01 near the seabed, while it in the rest of the OWF area is truncated by U08.

The unit has a chaotic seismic facies and is at the base often recognized by a high amplitude reflector which marks an erosive surface. In Figure 9-19 an example of the chaotic seismic facies can be found. In the right side of the figure, approximately starting at 2800 m, an area of seismic blanking occurs, due to gas in the overlying units. This affects the interpretation of the unit in the western part of the survey area, and higher uncertainty should thus be expected here.

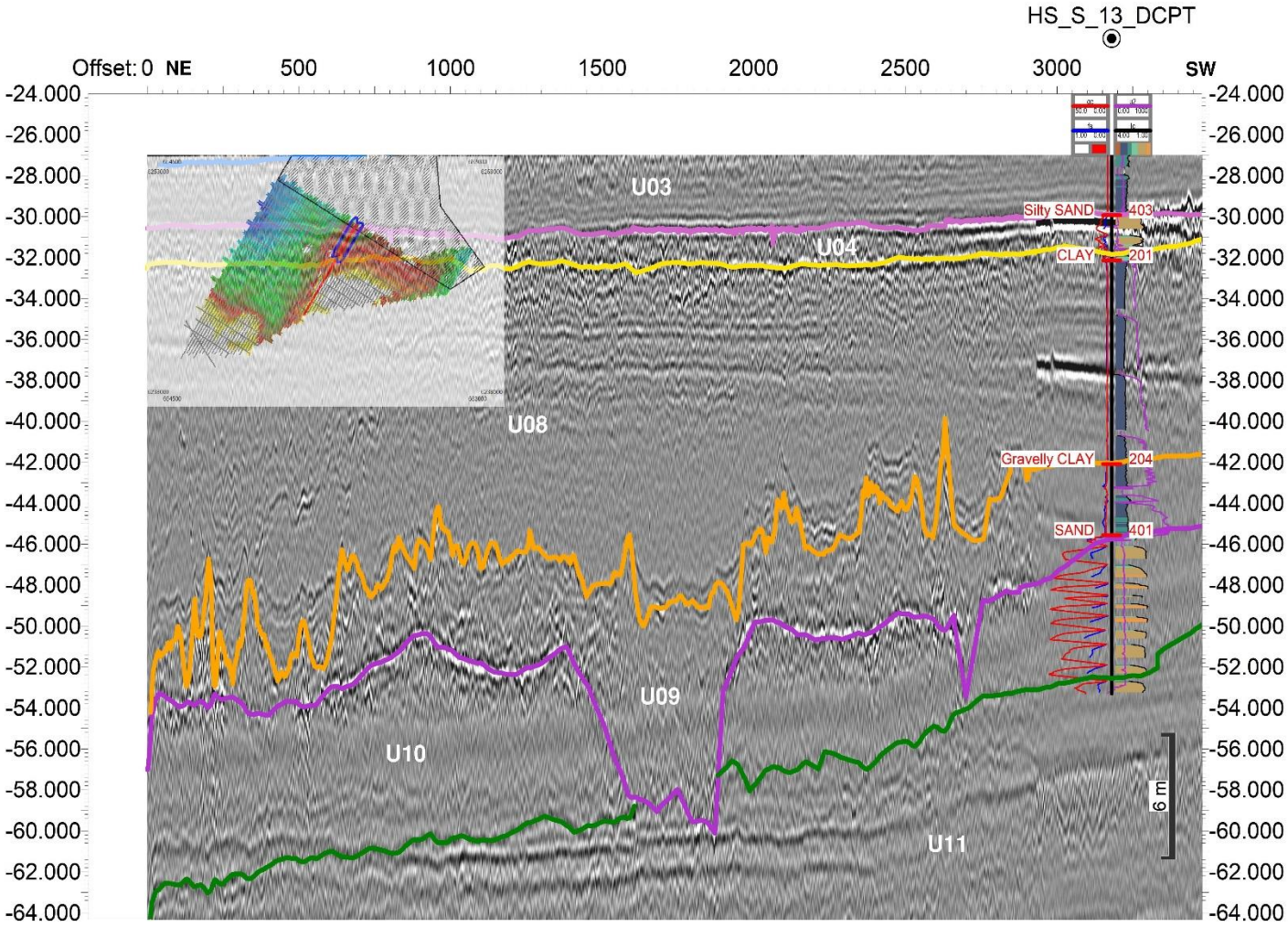

Figure 9-19: Line A_HS_L034_UHR_T_MIG_STK. Example of U09, where it in this example is bounded by B08 (Orange) to the top and B09 (Purple) at the base. The unit has a chaotic seismic facies and blanking due to gas is seen in the right side of the figure. HS_S13_DCPT is penetrating U09 and the lithology in the unit is interpreted as Gravelly CLAY.

Figure 9-19 shows HS_13_DCPT, and U09 is interpreted as having a Gravelly CLAY lithology, which is distinguishable by the change from cleaner CLAY to the top and the change to SAND at the bottom.

The unit has been interpreted as being a late subglacial deposit from late readvances of the Weichselian ice sheet. The unit is showing signs of over-consolidation in the strength parameters but is not as strong a layer as the older glacial units (U10, U11). The unit is of medium strength but has been grouped with the soft sediment units because it is weaker than the other over-consolidated units.

The thickness of the unit is generally found to be below 10 m, but in the NW thicknesses of up to 30 m can be found locally for the unit.

Top of U09 is defined by a strong undulating reflector which makes the unit stand out compared to the overlying U08. U09 generally has higher amplitudes compared to U08 and display a chaotic interior with discontinuous steeply sloping reflectors.
Geotechnically U09 is mainly characterized as a weak unit, however, some test locations indicate higher strength. Base of U09 is characterized by increasing strength with depth.

Enclosure 2.10 shows the depth below seabed of the top of unit U09, enclosure 3.10 the elevation of the top of the unit, and enclosure 4.10 the thickness (isochore) of unit U09.

9.9.3 Weichselian and Early Pleistocene

This unit contains all the Pleistocene deposits up to the late Weichselian. The reason for combining all the Pleistocene units is that it can be difficult to tell exactly which glacial period each unit are deposited during. All units within this group have been glacially overridden and are assumed to have been over-consolidated by subglacial compaction. Glaciotectonic complexes of varying material can be found in deposits from the Pleistocene period.

U10

The unit is found in the NE part of the site and covers approximately half of the Hesselø South OWF area. Where the unit is not present it has been eroded by U09 and U08, and U10 is only present where these units are found to be shallow or not present.

Geotechnically the unit consists of different variations of SAND, that appears both as clayey, gravelly, and silty compositions throughout the site.
In Figure 9-20 the seismic facies of U10 can be seen. The unit consists of some parts with parallel to semi-parallel reflectors and more chaotic and deformed parts. Figure 9-20 shows signs of fluvial deposition in the top of U10 and more deformed material, probably still of fluvial composition at the base. In this example HS_S_28_DCPT is penetrating U10 and shows a generally sandy lithology but with both a large part being Clayey Gravelly SAND, and a part being Silty SAND. The change from U10 to U11 is indicated by a lithological change from a sandy material to TILL.

The unit is interpreted to be a glaciofluvial deposit from meltwater from the Weichselian ice sheet. The glaciofluvial deposit has later been overridden by readvances of the ice

sheet, which is seen by the internal deformation in the unit and the fact that it is located below the subglacial unit of U09.

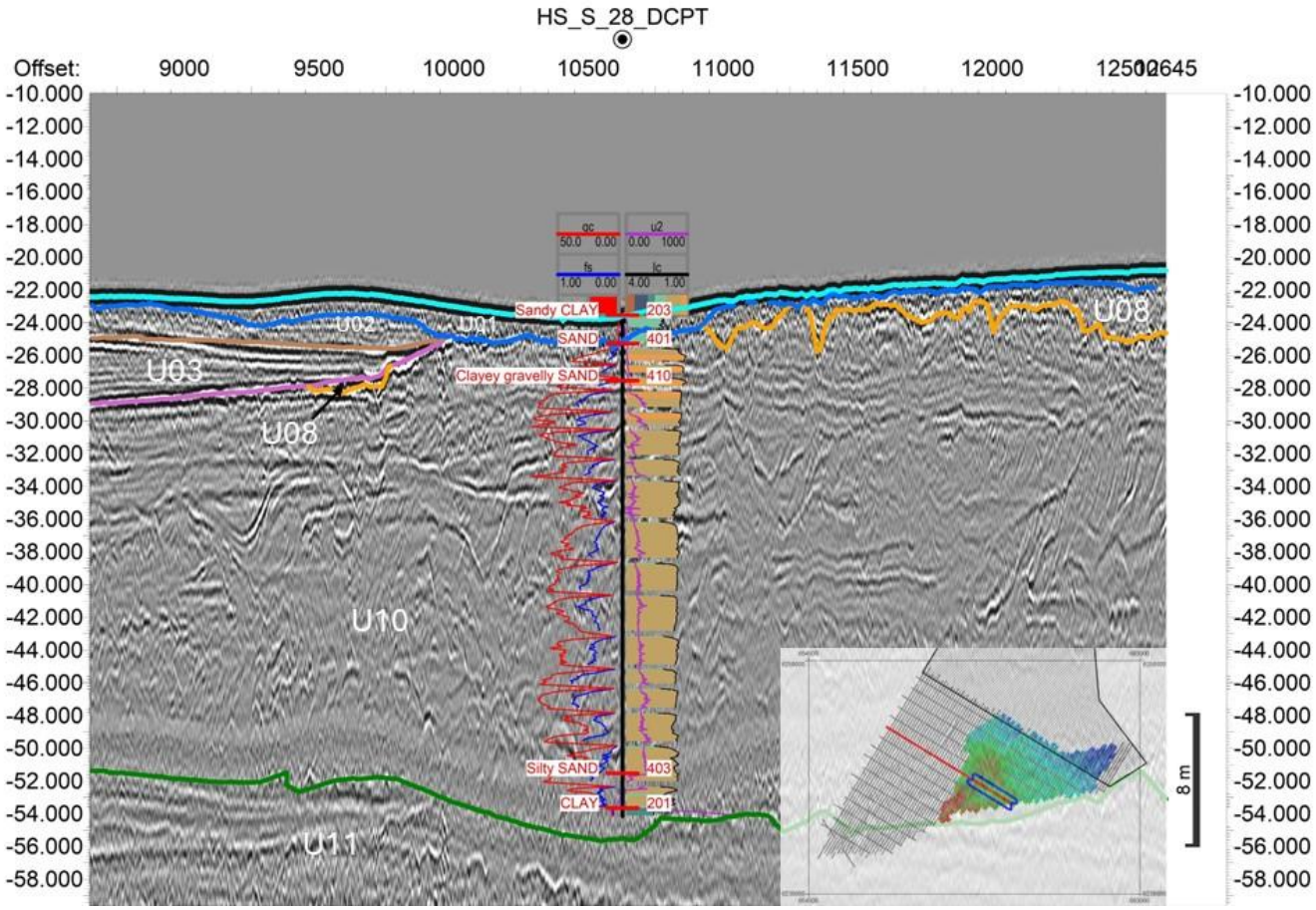

Figure 9-20: Line A_HS_X012_UHR_T_MIG_STK. Example of U10, in this example bounded to the top by B08 (Orange) and B03 (Purple) and to the bottom by B10 (Green). The seismic facies consists of semi-parallel reflectors and large areas of deformation. HS_S_28_DCPT is penetrating U10 and is interpreted as SAND, Clayey Gravelly SAND, and Silty SAND.

The thickness of the unit is found to be up to 36 m, and the thickest parts of the unit is found in the middle of the survey area in the W, closest to the extent of the OWF site. For the northernmost area of the 2 parts of the unit, the thickness is generally decreasing towards the NW to below 10 m. In the southern part the thickness is up to 30 m and is generally above 10 m.

U10 is relatively well-defined in both seismic sections and geotechnical data. The seismic signature of U10 stands out in comparison with the above-lying units and comprises complex reflection patterns including many steeply sloping reflectors which can be interpreted as bar migration deposits from the fluvial environment. Geotechnically, U10 consists of compact sand. U10 is overlying U11 and at the interface the seismic signature changes to parallel, plan reflections and here the CPT data indicates clayey deposits. In other locations U11 comprises layers which resemble U10. However, in these areas the sandy layers are partly covered by clayey layers also belonging to U11. Here it has been decided to include the sand layers in U11 and not in U10.

Enclosure 2.11 shows the depth below seabed of the top of unit U10, enclosure 3.11 the elevation of the top of the unit, and enclosure 4.11 the thickness (isochore) of unit U10.

U11

The unit is found in most of the site except at the border of the western part of Hesselø South OWF area and other smaller local areas. When U11 is not present, it has been fully eroded by B09.

U11 is complex glacial unit including parts which has been geotechnically determined to be a TILL. This is the only identified TILL unit in the Hesselø South OWF area and is identified as an especially competent unit.

In Figure 9-21 an example of U11 can be seen, and generally the seismic facies of the unit are chaotic and highly deformed, but occasionally larger scale deformation structures can be seen internally in the unit. In this example HS_S_21_BH is seen penetrating U11, and a varying lithology consisting of Silty, sandy, gravelly, and clayey TILL is found.

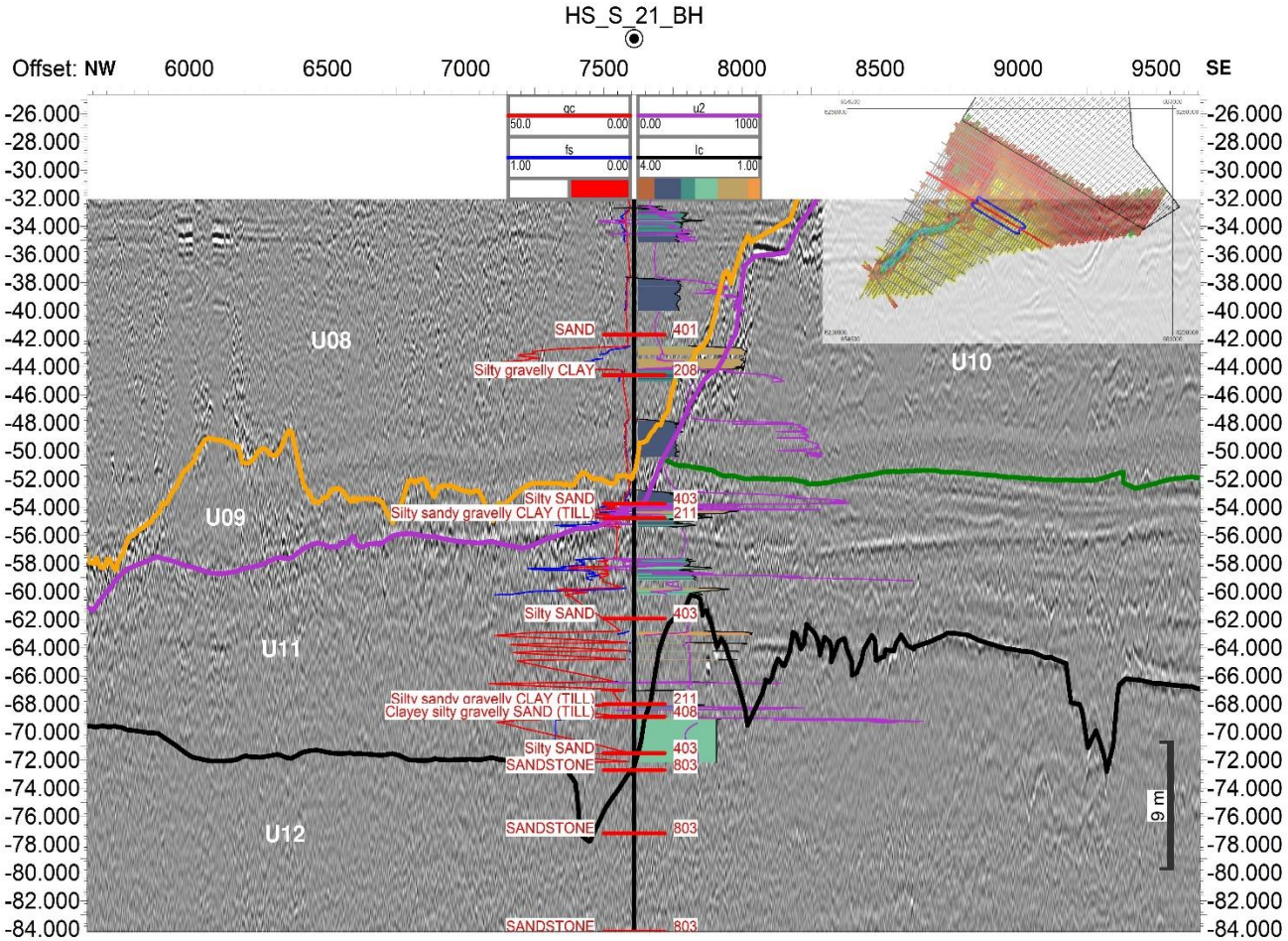

Figure 9-21: Line A_HS_X012_UHR_T_MIG_STK. Example of U11, in this example seen bounded by B09 (Purple) and B10 (Green) to the top and B11 (Black) to the bottom. The seismic facies consists of chaotic and deformed reflectors. HS_S_21_BH is penetrating the unit and shows a varying lithology of silty, sandy, gravelly and clayey TILL.

The unit is interpreted as being a subglacially deposited till unit, which shows signs of over-consolidation. The deposits of U11 may not just belong to one glacial event and could potentially include deposits from more than one ice age.

The thickness of the unit is found to be up to 129 m, where it is thickest. These thick deposits are found in a tunnel valley running SW-NE approximately halfway through the site. A cross-section from the deepest part of the tunnel valley can be seen in Figure 9-22, where the parallel internal reflectors of U12 are seen truncated by B11. In areas outside the tunnel valley the unit is generally thickest in the southwest, 30 to 60 m, and in the east where it is found to be up to 40 m but generally around 15 to 30m. Lowest thicknesses are seen in the middle section of the Hesselø South OWF area in a S to N oriented area and the unit is absent in a large fraction of the westernmost part of the site.

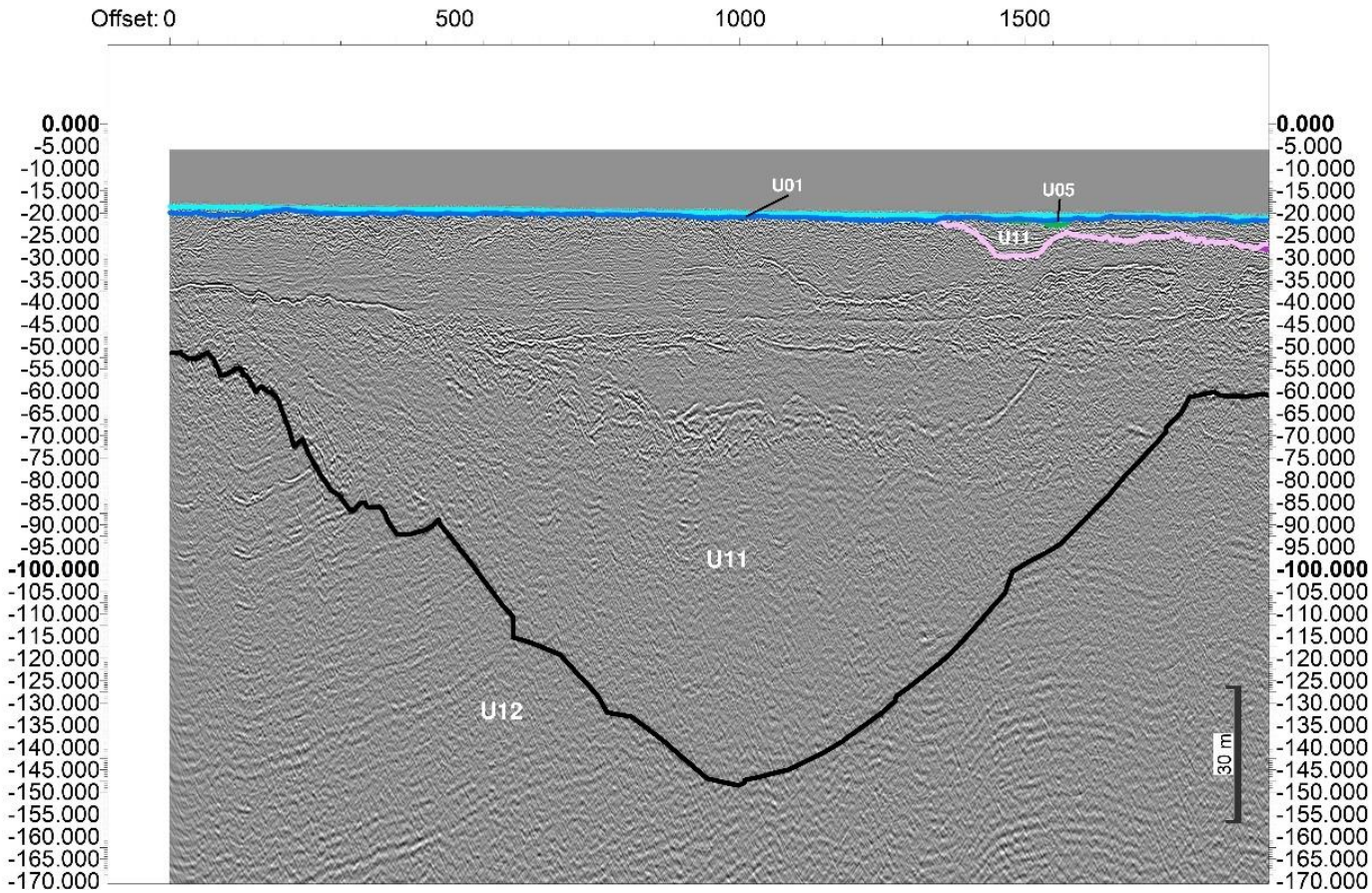

Figure 9-22: Line A_HS_X003_UHR_T_MIG_STK. Example of the deepest incision of U11 into U12. The parallel internal reflectors of U12 are seen being truncated by B11.

U11 is a mixed unit comprising many different types of deposits, however, all considered glacially compacted and with high strength. In the seismic sections U11 can appear chaotic with high amplitudes in some areas and in other areas range from nearly transparent to plan and parallel bedded. The interface to the underlying U12 is mostly a distinct surface both in the seismic sections and in the geotechnical data.

Enclosure 2.12 shows the depth below seabed of the top of unit U11, enclosure 3.12 the elevation of the top of the unit, and enclosure 4.12 the thickness (isochore) of unit U11.

9.9.4 Jurassic to Early Cretaceous

Jurassic and Cretaceous deposits are known to underly the Quaternary sediments in the Hesselø OWF project site (Figure 2-1). A clear angular unconformity can be seen across the border of the lowest base horizons interpreted and in the seismic data below this horizon (Figure 9-22, Figure 9-23, Figure 9-24). This has been interpreted to consist of Jurassic and Cretaceous deposits and is named U12.

U12

The unit is found across the entire Hesselø South OWF project site and is the basal unit of the IGM. The unit is underlying B12 and B09, and these horizons have been used to define the top. No base has been identified because it lies below the penetration depth of the 2D-UHRS data. In Figure 9-23 a good example of the seismic facies of U12 is seen, where it consists of subparallel reflectors. The facies are not always seen as nicely across the site, and large areas of chaotic reflectors are also found. Folding of U12 is identified in the area, and where the reflectors have been inclined and truncated by the upper units, angular unconformity can be found. An example of this can be seen in Figure 9-24.

The few instances where a borehole has penetrated U12 it has either been interpreted as SANDSTONE, SILTSTONE, or MUDSTONE. In Figure 9-21 a borehole penetrating SANDSTONE can be seen. According to GEUS, Ref. /8/, Sandy mudstone from the Jurassic and glauconitic Sandstone from the Lower Cretaceous can be expected in the area. They propose that the bedrock with strongly dipping reflectors is an indication of the Jurassic deposits.

Faulting is seen inside U12 throughout the site which is described further in section 9.8.2.

U12 is well-defined in both the seismic sections and in the geotechnical data.

Enclosure 2.13 shows the depth below seabed of the top of unit U12 and enclosure 3.13 shows the elevation of the top of unit U12.

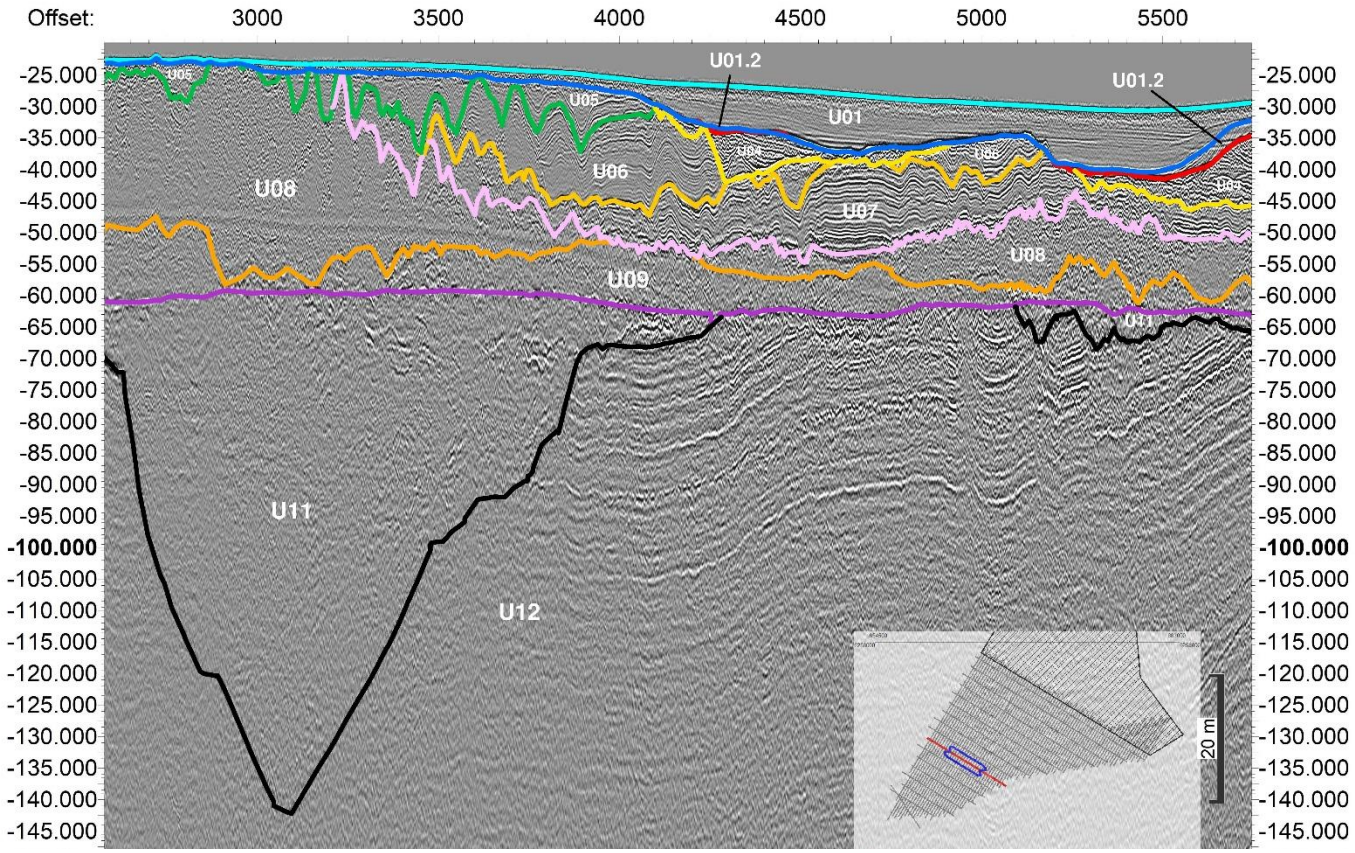

Figure 9-23: Line A_HS_X008_UHR_T_MIG_STK. Example of U12, bounded to the top by B12 and with no visible base due to the limited seismic penetration depth of the 2D-UHRS data. The seismic facies is seen as undulating with semi-parallel to parallel reflectors.

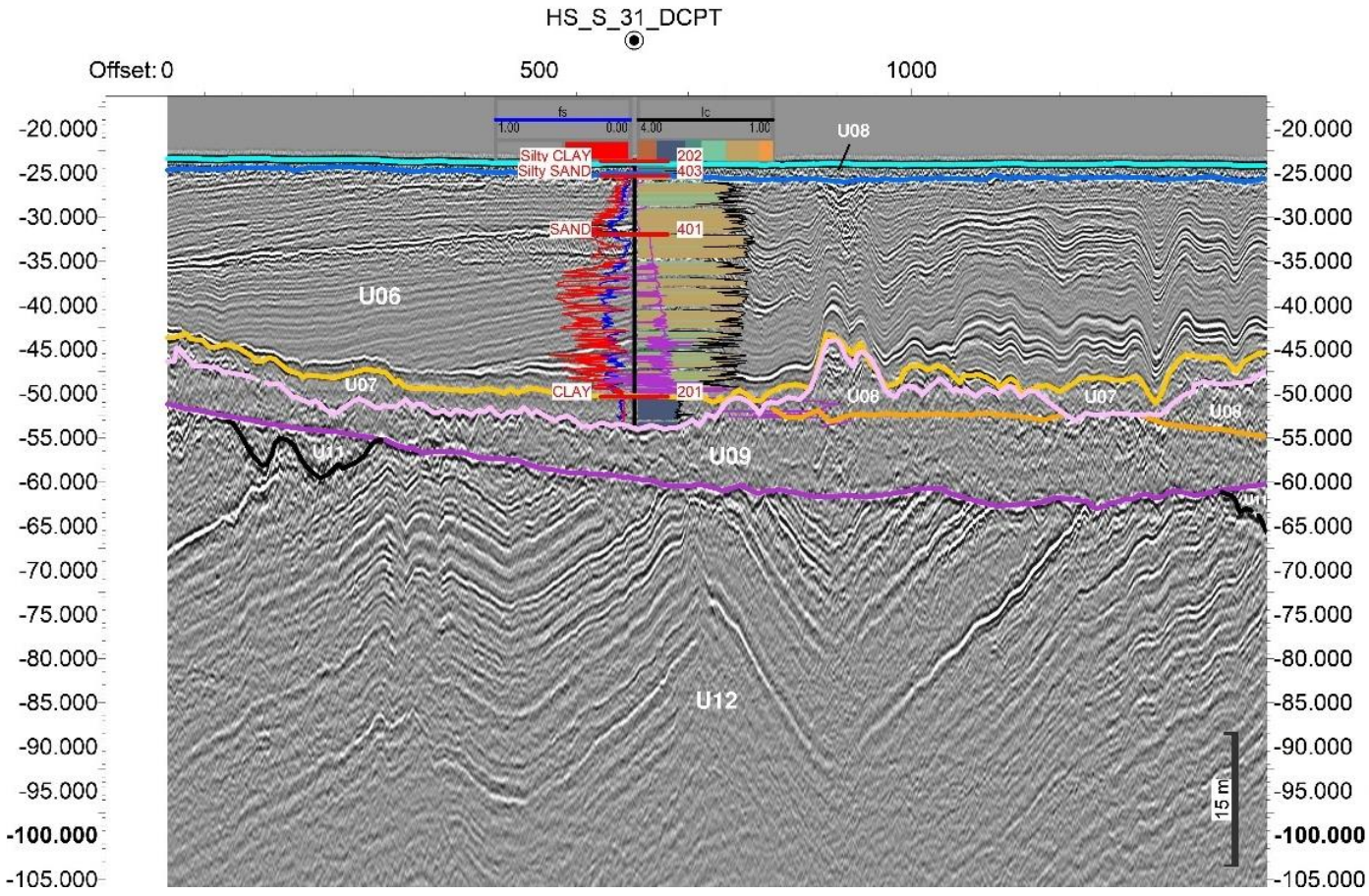

Figure 9-24: Line A_HS_I002A_UHR_T_MIG_STK: Example of folding structures in U12 and angular unconformities at the top of U12/base of U09.

10 Geotechnical zonation and representative soil profiles

Based on the geotechnical and geophysical data, and the interpreted model, a soil zonation has been made. The soil zonation provides the basis for clustering the main geological deposits and structures relevant for the wind turbine foundations.

The soil zonation is further simplified into one single map dividing the entire site into eight (8) different geotechnical zones. The simplification is made by selecting the most significant parameters in relation to foundation conditions.

The purpose of the geotechnical zonation map is to provide a geological overview of the Hesselø South OWF project site with regards to foundation conditions. The map should ideally divide the Hesselø South OWF project site into a limited number of provinces with similar foundation conditions.

The workflow of the process is presented in Figure 10-1.

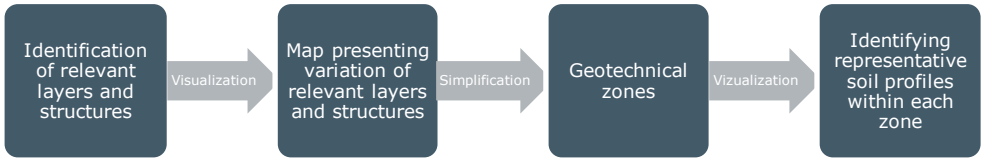

Figure 10-1 Workflow for dividing the area into geotechnical zones.

10.1.1 Identification of relevant layers and structures

For the geotechnical zonation of the Hesselø South OWF project site, relevant layers and structures have been identified. For the identification of these relevant layers and structures, focus have been on the following:

- Soils present at depths less than 50 m below seabed, as this depth range is considered important for wind turbine foundations.
- Mapping extent of weaker soil layers.
- Mapping thickness of competent glacial layers across the Hesselø South OWF project site.
- Depth to Pre-Quaternary layers

Regarding weaker soil layers, it is noted that they vary greatly in thickness across the Hesselø South OWF project site with cumulative thickness ranging from 0 to approximately 60 m. The weaker geotechnical units consist of normally consolidated to slightly over-consolidated clays. These weak units are identified as a primary parameter in establishing a foundation design as the amount of these affect the required foundation size and as most likely the foundation as minimum would need to embed a certain distance into more competent layers located below these weaker soil layers. The

units identified as the weakest are the Holocene units U01, U01.2, and U03, and the Late Weichselian units U05, U07, U08, and U09. It must be noted the wording "weaker" is indicative for the grouping of units when comparing to high strength glacial impacted clays, and as strength properties vary within this grouping of units, some units like U08 and U09 will not necessarily have a soft response. For U08 it has earlier been noted that unit U08 become gradually sandier towards south, see Figure 9-18. This part of U08 has been evaluated conservatively in the zonation and the actual conditions could potentially have more beneficial foundation conditions depending on the sand content.

The thickness of the underlying competent glacial layers is considered the second most important parameter for establishing a foundation design. The competent glacial layers comprise primarily dense to very dense sand and over-consolidated clay. Thicknesses of these layers range from 0 m to more than 100 m. The units identified as competent glacial units are U10 and U11.

The depth to the Pre-Quaternary layers (U12) is considered the third most important parameter for establishing a foundation design. The Pre-Quaternary layers consist mainly of SANDSTONE and MUDSTONE. Depth of U12 ranges approximately from 25 m to more than 100 m. The Pre-Quaternary layers pose a potentially installation risk (related to impact driving) and hence the depth to Pre-Quaternary layers together with the thickness of glacial layers and thickness of weaker soil layers are of relevance to understand the risk related to installation.

The three parameters mentioned above are all considered relevant when dividing the site into zones of comparable soil conditions.

Given the above considerations three maps have been prepared. These maps are considered to provide valuable input for the geotechnical zonation. The presented maps are as follows:

- Figure 10-2 presents a map showing the combined thickness of ground model units interpreted as soft sediments, namely unit U01, U03, U05, U07, U08 and U09. The map hence shows the thickness of layers considered as poor material for foundation design and when present for large thickness can result in relative heavy WTG foundations.

- Figure 10-3 presents a map showing the combined thickness of ground model units categorised as competent glacial layers namely unit U10 and U11. The map hence shows the thickness of layers considered as good material for foundation design and when present for large thickness can result in lighter WTG foundations.

- Figure 10-4 presents a map showing the depth below seabed to top of pre-quaternary layer, namely unit U12. The map hence shows the depth to the high strength layers which potentially can result in foundation installation difficulties.

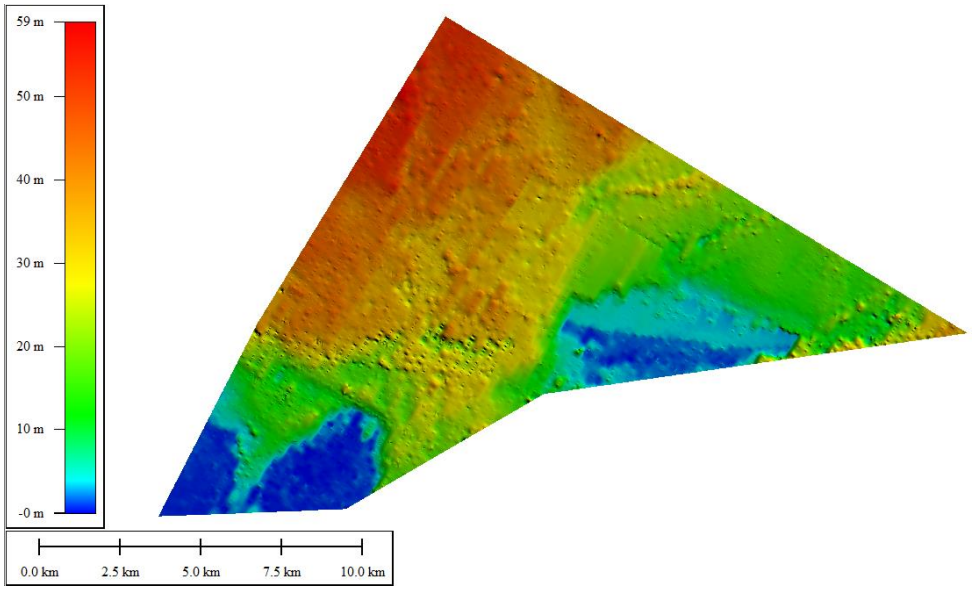

Figure 10-2 Combined thickness of soft sediments derived from units U01, U03, U05, U07, U08 and U09.

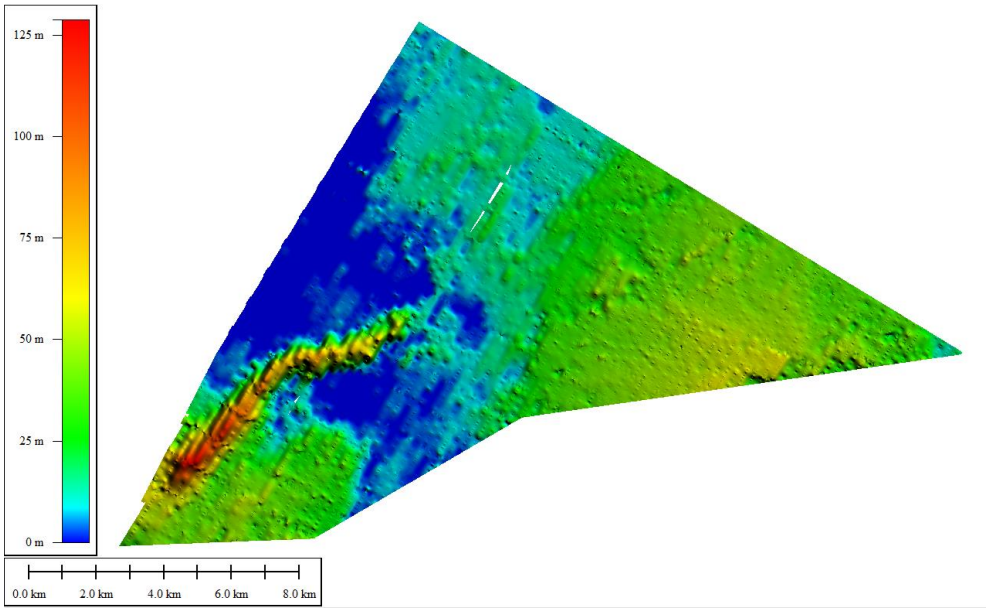

Figure 10-3 Combined thickness of competent glacial material, defined by unit U10 and U11.

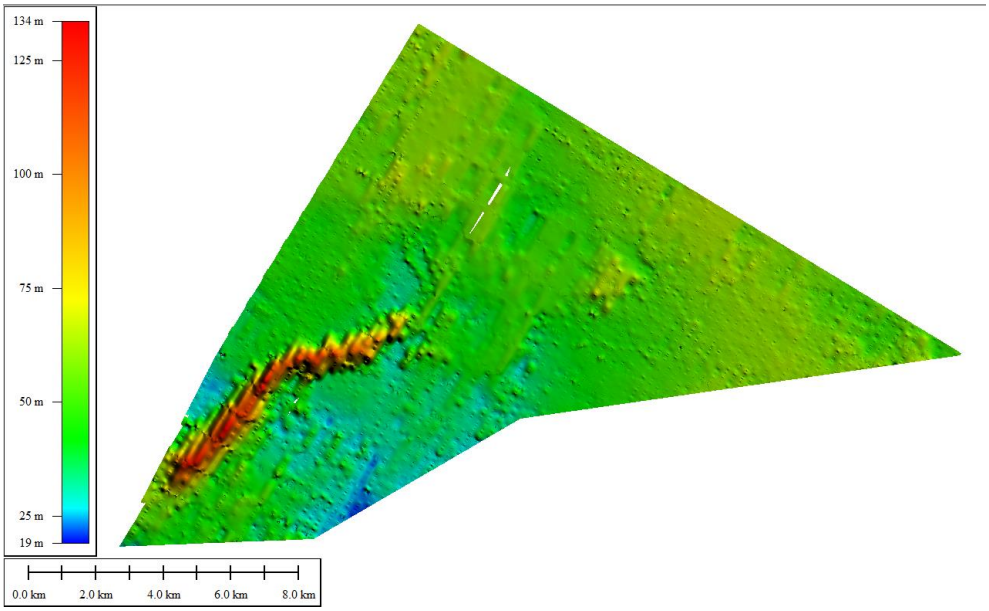

Figure 10-4 Depth below seabed to top of pre-quaternary material and deeper units defined as top of unit U12.

10.2 Variation of model units based on selected criteria

Based on Figure 10-2 to Figure 10-4, the following criteria relevant for foundation design have been defined for the combined thickness of potential soft clay layers (U01, U03, U05, U07, U08 and U09), for the combined thickness of glacial impacted layers (U10 and U11), and for the depth to top of pre-quaternary layers (U12). These criteria are as follows:

- Combined thickness of soft sediments (U01, U03, U05, U07, U08 and U09) between 10 m and 30 m.
- Combined thickness of soft sediments (U01, U03, U05, U07, U08 and U09) greater than 30 m.
- Combined thickness of glacial impacted layers less than 10 m.
- Combined thickness of glacial impacted layers between 10 m and 15 m.
- Combined thickness of glacial impacted layers between 15 m and 30 m.
- Depth below seabed to top of pre-quaternary material and deeper units less than 35 m.
- Depth below seabed to top of pre-quaternary material and deeper units between 35 m and 45 m.

The above-mentioned criteria are in Figure 10-5 plotted on a map of the Hesselø South OWF project site. This map is also provided by Enclosure 7.02.

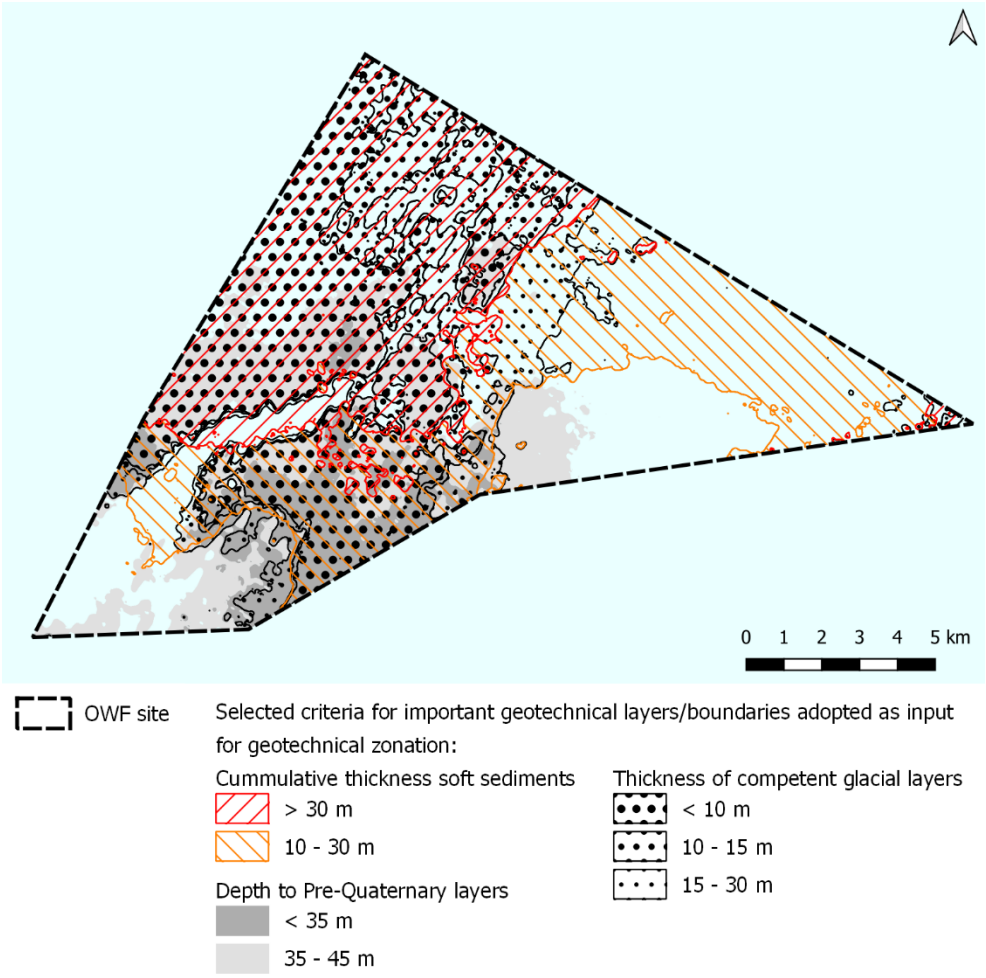

Figure 10-5 Map showing extent of the selected variation criteria across the site of relevant model units (see also Enclosure 7.02).

10.3 Geotechnical zones

Geotechnical zones have been established based on the content of Figure 10-5. The geotechnical zones represent a simplification of Figure 10-5 aiming to have a limited number of geotechnical zones. For the simplification the following has been considered:

- For areas with combined thickness of soft sediments larger than 30 m, the thickness of glacial impacted layers has been considered higher importance than the depth to top of pre-quaternary layers.

- The glacial thickness values used as criteria for splitting the zone with combined thickness of soft sediments larger than 30 m is selected to be 10 m, while for the remaining part of the site 15 m and 30 m thickness is considered as criteria.

- Depth to top of pre-quaternary material is split from criteria of 35 m and 45 m due to installation risks associated with expected high-level foundation geometries.

Based on the above considerations eight (8) geotechnical zones as presented in Figure 10-6 have been defined. Due to uncertainties in the seismic interpretation and the

gridding minor areas have been disregarded. In practice this means that all elements in map smaller than 50.000 m² has been filtered out. This also results in a more comprehensible map. The geotechnical zonation map is also added as Enclosure 7.01. The characteristics of the geotechnical zones are described in detail in section 10.4. Geotechnical zones I to III generally show good ground conditions for WTG foundation design and installation, with the conditions being most competent for Geotechnical zone I. Geotechnical zones IV to VI are categorised by medium ground conditions for WTG foundation design, which combined with depth to top of pre-quaternary material potentially can result in foundation installation difficulties. For Geotechnical zones VII and VIII thick deposits of soft clay are anticipated and hence in these zones heavy WTG foundations are expected to be required.

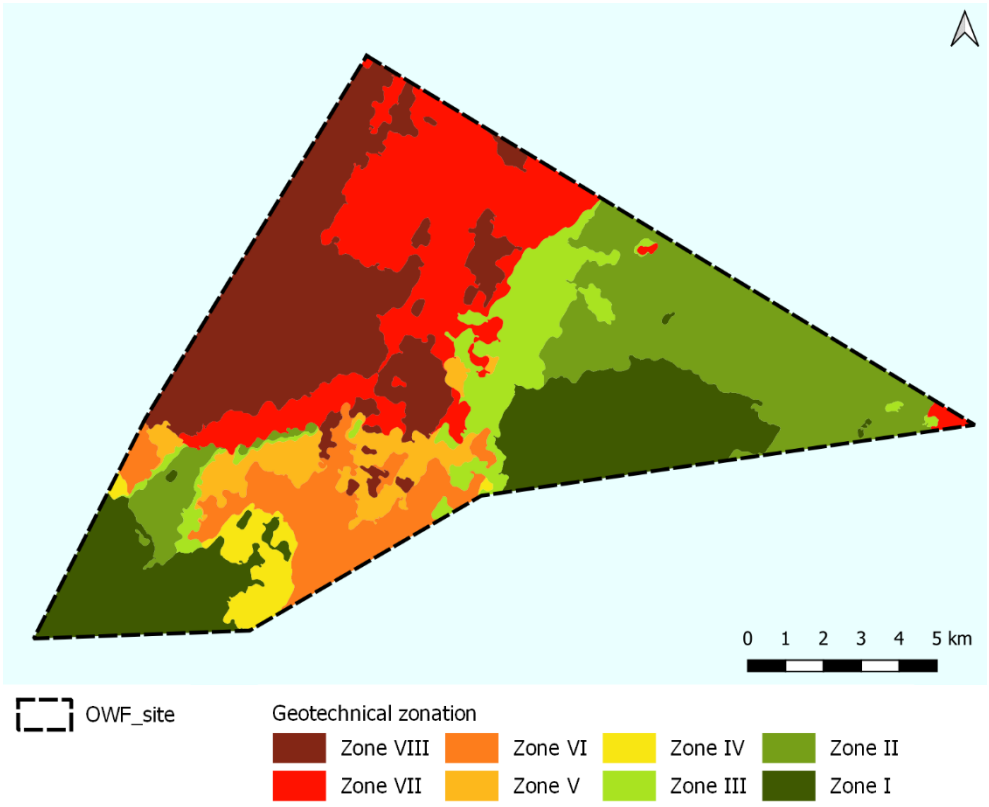

Figure 10-6 Geotechnical zonation (see also Enclosure 7.01).

10.4 Representative soil profile for the geotechnical zones

The eight (8) geotechnical zones are described in the following subsections, and further representative soil profiles are also presented. The representative profiles are selected based on geotechnical location tests present within each zone. It should be noted not all CPT tests are performed down to sufficient depth for presenting the trend which the geotechnical zone is categorising. A summary of the following sections is found in section 10.4.9. Table 10-1 presents an overview of which geotechnical locations are present within each of the defined geotechnical zones together with the percentage distribution between the established zones at the site.

Table 10-1 Overview of geotechnical test locations within each geotechnical zone.

Geotechnical zone	Geotechnical locations within zone	Coverage [%]
I	HS_S_20, HS_S_27, HS_S_28, HS_S_35, HS_S_38, HS_S_39	18.6
II	HS_S_06, HS_S_12, HS_S_13, HS_S_18, HS_S_24, HS_S_30	19.3
III	HS_S_21, HS_S_29	7.7
IV	HS_S_36	2.6
V	HS_S_31	4.6
VI	HS_S_32, HS_S_33, HS_S_37	7.9
VII	HS_S_02, HS_S_04, HS_S_07, HS_S_14, HS_S_23	17.9
VIII	HS_S_01, HS_S_03, HS_S_10, HS_S_11, HS_S_16, HS_S_17, HS_S_22, HS_S_26	21.5

10.4.1 Geotechnical zone I

This zone is characterised by having less than 10 m of cumulative thickness of soft sediments (unit U01, U03, U05, U07, U08 and U09), thickness of competent glacial layers being larger than 30 m and the top of pre-quaternary layers being located deeper than 35 m below seabed.

The representative profile for this zone is selected as HS_S_28 where the CPT profile is presented in Figure 10-7 and the stratigraphy in table format is presented in Table 10-2.

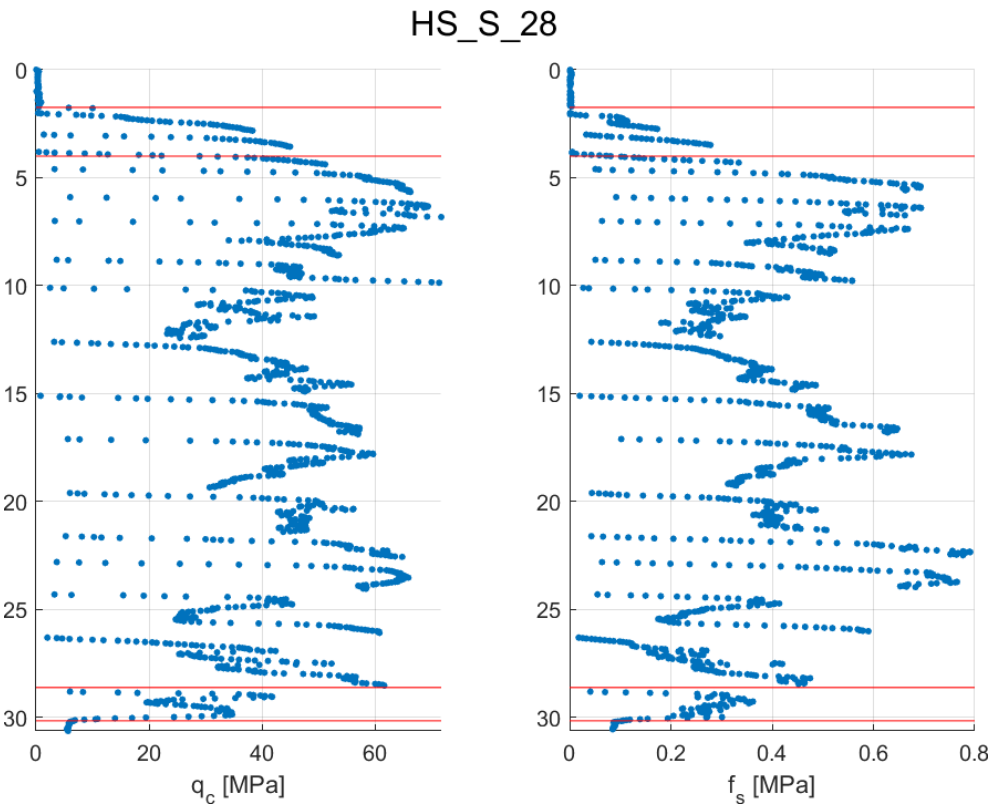

Figure 10-7 q_c and f_s from CPT measurements for HS_S_28 found as representative for zone I. More information about the location can be found in Appendix A.

Table 10-2 Soil stratigraphy for HS_S_28 found as representative for zone I.

Layer	Top [m]	Bottom [m]	Unit	Geotechnical material
1	0.0	1.7	UC01	Clay
2	1.7	4.0	US10	Sand
3	4.0	28.6	US10	Sand
4	28.6	30.2	US10	Sand
5	30.2	30.6	UC10	Clay

10.4.2 Geotechnical zone II

This zone is characterised by having between 10 m and 30 m of cumulative thickness of soft sediments (unit U01, U03, U05, U07, U08 and U09), thickness of competent glacial layers being larger than 30 m and the top of pre-quaternary layers being located deeper than 45 m below seabed.

The representative profile for this zone is selected as HS_S_06 where the CPT profile is presented in Figure 10-8 and the stratigraphy in table format is presented in Table 10-3.

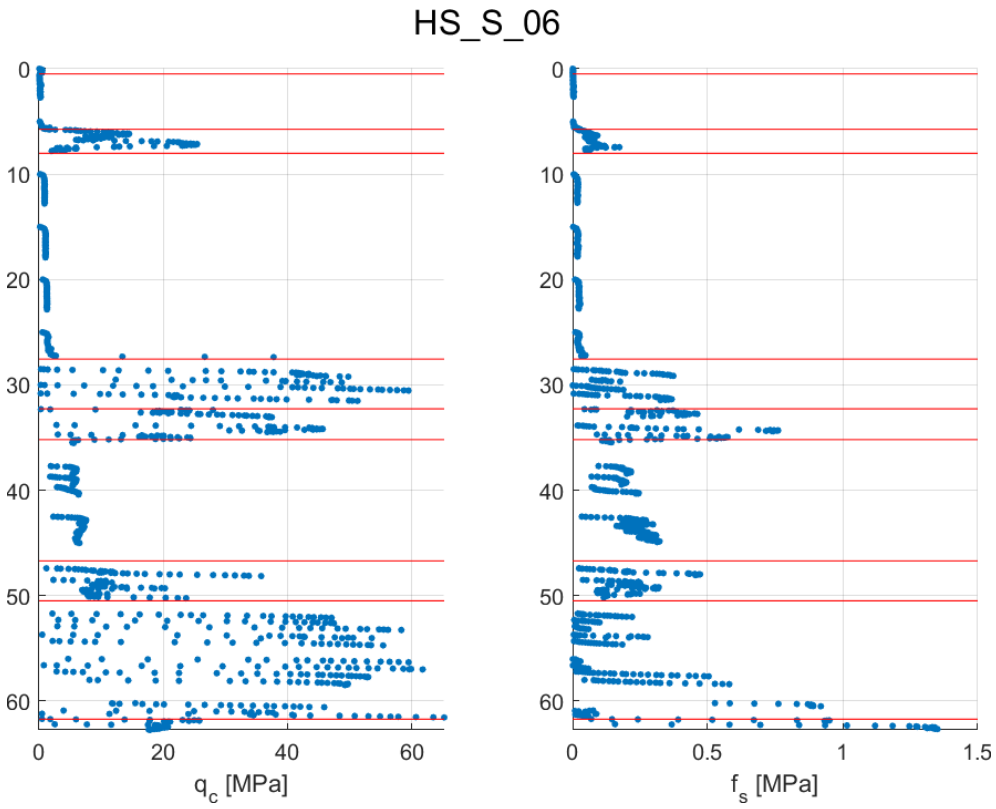

Figure 10-8 *q_c and f_s from CPT measurements for HS_S_06 found as representative for zone II. More information about the location can be found in Appendix A.*

Table 10-3 *Soil stratigraphy for HS_S_06 found as representative for zone II.*

Layer	Top [m]	Bottom [m]	Unit	Geotechnical material
1	0.0	0.49	US01	Sand
2	0.49	5.74	UC03	Clay
3	5.74	8.02	US04	Sand
4	8.02	27.55	UC08	Clay
5	27.55	32.27	US10	Sand
6	32.27	35.19	US11	Sand
7	35.19	46.7	UC11	Clay
8	46.7	50.49	UC11	Clay
9	50.49	61.72	US11	Sand
10	61.72	62.74	UC12	Clay

10.4.3 Geotechnical zone III

This zone is characterised by having between 10 m and 30 m of cumulative thickness of soft sediments (unit U01, U03, U05, U07, U08 and U09), thickness of competent glacial material between 15 m and 30 m, and the depth to top of the pre-quaternary layer being larger than 35 m below seabed.

The representative profile for this zone is selected as HS_S_21 where the CPT profile is presented in Figure 10-9 and the stratigraphy in table format is presented in Table 10-4.

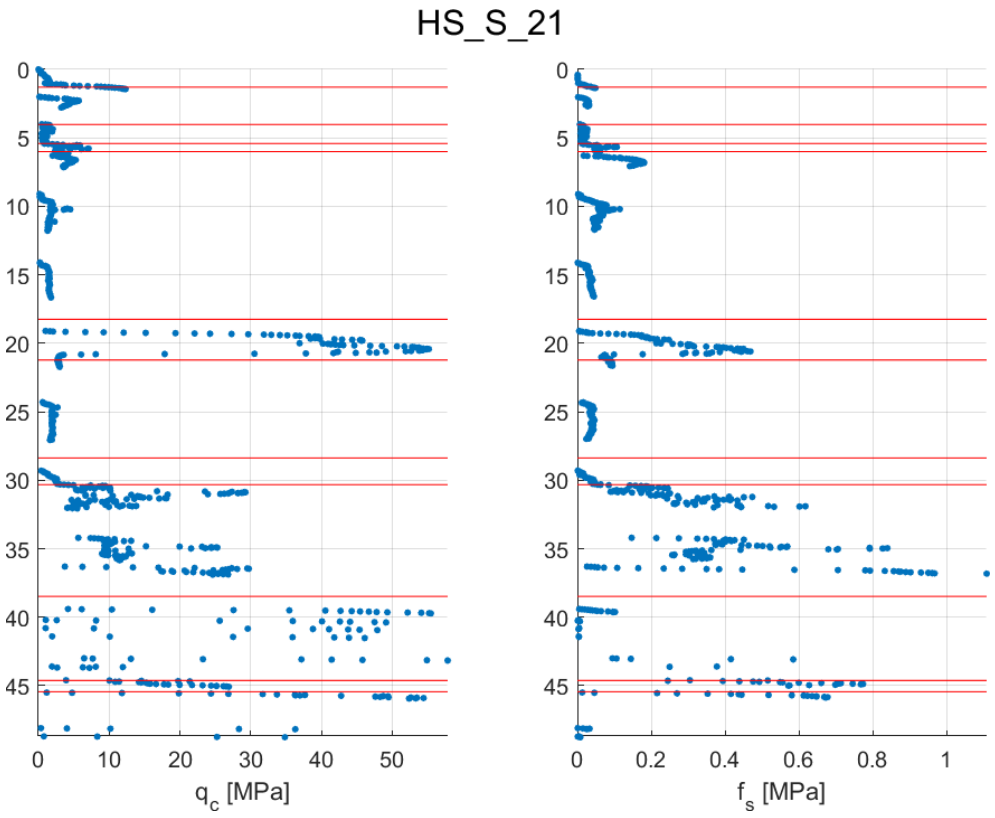

Figure 10-9 q_c *and* f_s *from CPT measurements for HS_S_21 found as representative for zone III. More information about the location can be found in Appendix A.*

Table 10-4 Soil stratigraphy for HS_S_21 found as representative for zone III.

Layer	Top [m]	Bottom [m]	Unit	Geotechnical material
1	0.0	1.3	US01	Sand
2	1.3	4.0	US02	Sand
3	4.0	5.4	UC03	Clay
4	5.4	6.0	US04	Sand
5	6.0	18.3	UC08	Clay
6	18.3	21.2	US08	Sand
7	21.2	28.4	UC08	Clay
8	28.4	30.3	UC09	Clay
9	30.3	38.5	UC11	Clay
10	38.5	44.6	US11	Sand
11	44.6	45.4	UC11	Clay
12	45.4	48.8	US11	Sand

10.4.4 Geotechnical zone IV

This zone is characterised by having less than 10 m cumulative thickness of soft sediments (unit U01, U03, U05, U07, U08 and U09), thickness of competent glacial material larger than 15 m, and the depth to top of the pre-quaternary layer being less than 35 m below seabed. The lowest depth of the pre-quaternary layer within the geotechnical zone is found to be 23 m below seabed.

The representative profile for this zone is selected as HS_S_36 where the CPT profile is presented in Figure 10-10 and the stratigraphy in table format is presented in Table 10-5.

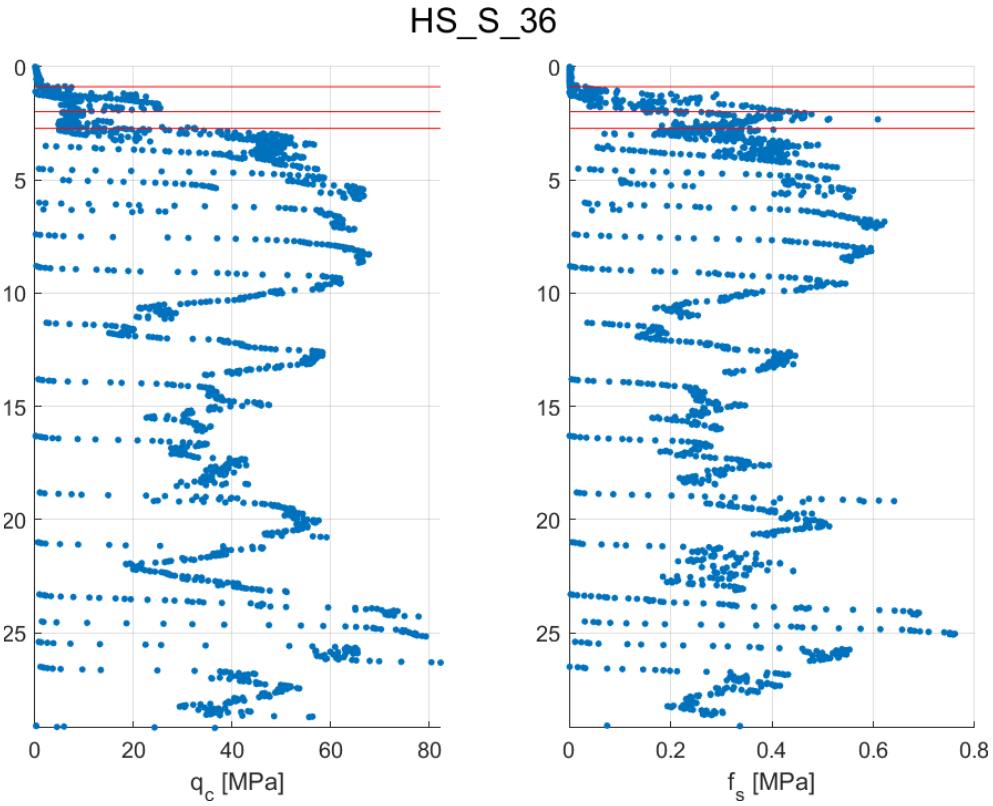

Figure 10-10 *q_c and f_s from CPT measurements for HS_S_36 found as representative for zone IV. More information about the location can be found in Appendix A.*

Table 10-5 *Soil stratigraphy for HS_S_36 found as representative for zone IV.*

Layer	Top [m]	Bottom [m]	Unit	Geotechnical material
1	0.0	0.9	US01	Sand
2	0.9	2.0	US10	Sand
3	2.0	2.7	UC10	Clay
4	2.7	29.2	US10	Sand

10.4.5 Geotechnical zone V

This zone is characterised by having between 10 m and 30 m of cumulative thickness of soft sediments (unit U01, U03, U05, U07, U08 and U09), thickness of competent glacial material being less than 15 m, and the depth to top of the pre-quaternary layer being larger than 35 m below seabed.

The representative profile for this zone is selected as HS_S_31 where the CPT profile is presented in Figure 10-11 and the stratigraphy in table format is presented in Table 10-6.

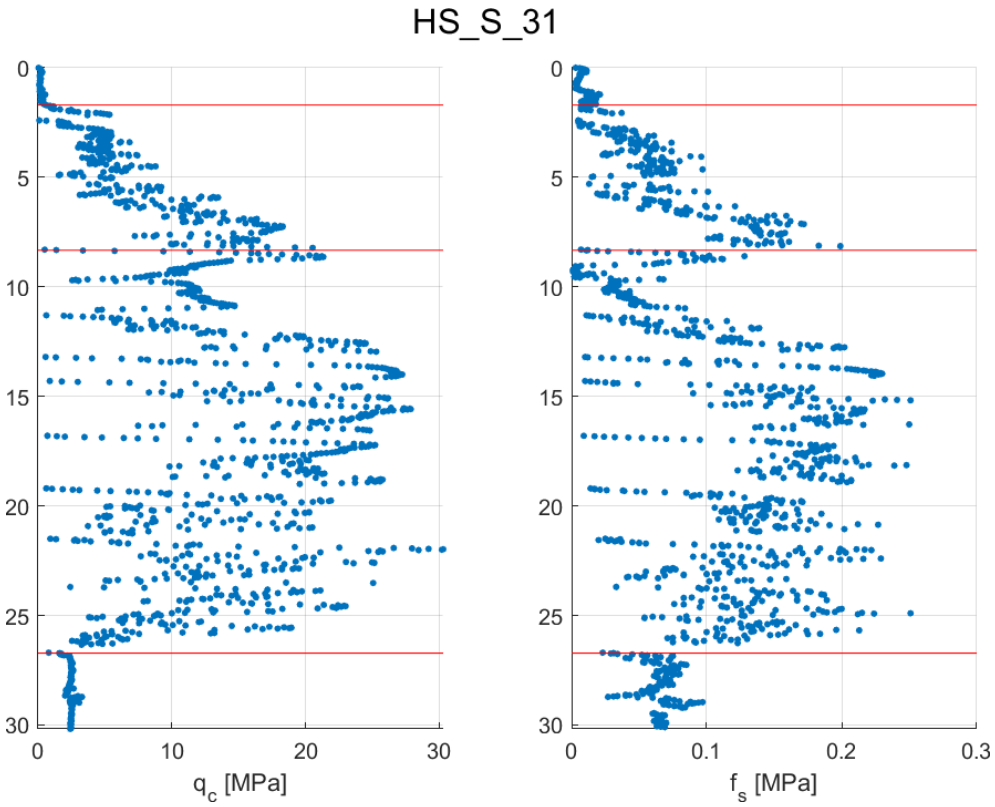

Figure 10-11 q_c *and* f_s *from CPT measurements for HS_S_31 found as representative for zone V. More information about the location can be found in Appendix A.*

Table 10-6 Soil stratigraphy for HS_S_31 found as representative for zone V.

Layer	Top [m]	Bottom [m]	Unit	Geotechnical material
1	0.0	1.7	UC01	Clay
2	1.7	8.33	US05	Sand
3	8.3	26.7	US06	Sand
4	26.7	30.2	UC07	Clay

10.4.6 Geotechnical zone VI

This zone is characterised by having between 10 m and 30 m of cumulative thickness of soft sediments (unit U01, U03, U05, U07, U08 and U09), thickness of competent glacial material less than 30 m, and the depth to top of the pre-quaternary layer less than 35 m below seabed. The lowest depth of the pre-quaternary layer within the geotechnical zone is found to be 20 m below seabed.

The representative profile for this zone is selected as HS_S_37 where the CPT profile is presented in Figure 10-12 and the stratigraphy in table format is presented in Table 10-7.

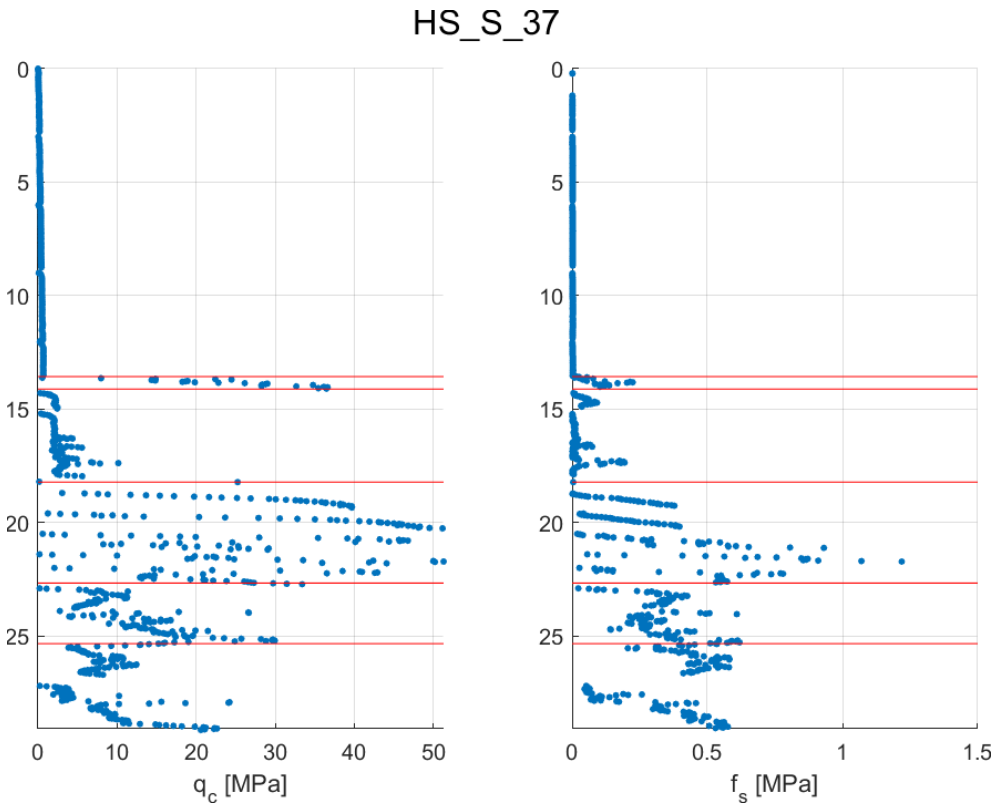

Figure 10-12 *q_c and f_s from CPT measurements for HS_S_37 found as representative for zone VI. More information about the location can be found in Appendix A.*

Table 10-7 *Soil stratigraphy for HS_S_37 found as representative for zone VI.*

Layer	Top [m]	Bottom [m]	Unit	Geotechnical material
1	0.0	13.6	UC01	Clay
2	13.6	14.1	US07	Sand
3	14.1	18.2	UC09	Clay
4	18.2	22.7	US10	Sand
5	22.7	25.3	UC11	Clay
6	25.3	29.1	UC12	Clay

10.4.7 Geotechnical zone VII

This zone is characterised by having more than 30 m of cumulative thickness of soft sediments (unit U01, U03, U05, U07, U08 and U09) and having more than 10 m thickness of underlying glacial material.

The representative profile for this zone is selected as HS_S_02 where the CPT profile is presented in Figure 10-13 and the stratigraphy in table format is presented in Table 10-8.

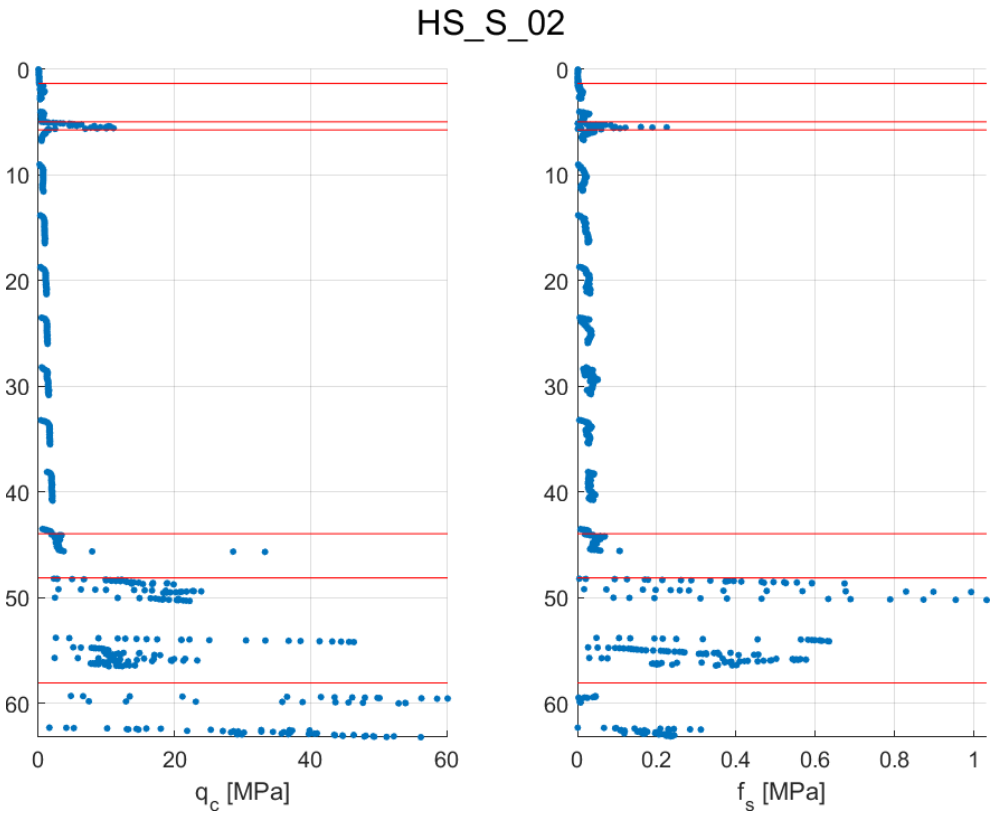

Figure 10-13 *q_c and f_s from CPT measurements for HS_S_02 found as representative for zone VII. More information about the location can be found in Appendix A.*

Table 10-8 *Soil stratigraphy for HS_S_10 found as representative for zone VII.*

Layer	Top [m]	Bottom [m]	Unit	Geotechnical material
1	0.0	1.3	UC01	Clay
2	1.3	5.0	UC03	Clay
3	5.0	5.7	US03	Sand
4	5.7	44.0	UC08	Clay
5	44.0	48.1	UC09	Clay
6	48.1	58.1	UC11	Clay
7	58.1	63.2	US11	Sand

10.4.8 Geotechnical zone VIII

This zone is characterised by having more than 30 m of cumulative thickness of soft sediments (unit U01, U03, U05, U07, U08 and U09) and having less than 10 m thickness of underlying glacial material.

The representative profile for this zone is selected as HS_S_10 where the CPT profile is presented in Figure 10-14 and the stratigraphy in table format is presented in Table 10-9. The soil profile represents a clay dominated position with thin interbedded sand layers. It should be noted the amount and thickness of interbedded sand layers vary within the zone.

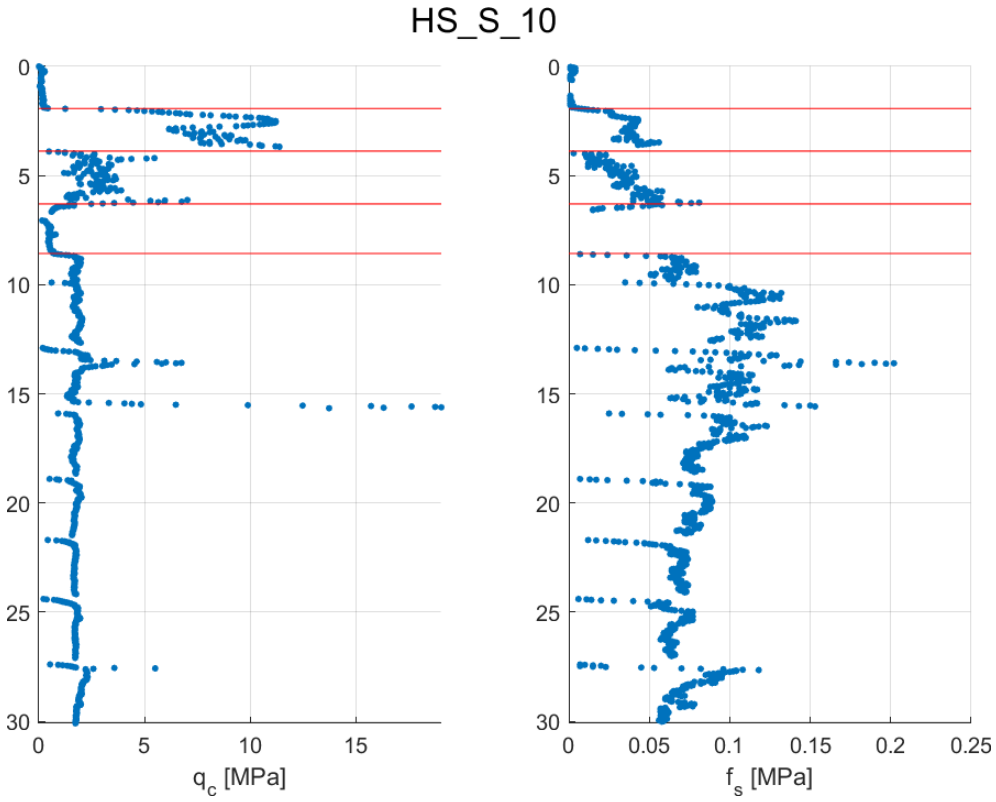

Figure 10-14 q_c *and* f_s *from CPT measurements for HS_S_10 found as representative for zone VIII. More information about the location can be found in Appendix A.*

Table 10-9 *Soil stratigraphy for HS_S_10 found as representative for zone VIII.*

Layer	Top [m]	Bottom [m]	Unit	Geotechnical material
1	0.0	1.9	UC01	Clay
2	1.9	3.9	US02	Sand
3	3.9	6.3	US02	Sand
4	6.3	8.6	UC03	Clay
5	8.6	30.1	UC08	Clay

10.4.9 Summary

Based on the previous sections per geotechnical zone, a summary for the geotechnical zonation can be found in Table 10-10.

Table 10-10 Summary of geotechnical zonation.

Geotechnical zone	Representative location	Description
I	HS_S_28	Cumulative thickness soft sediments < 10m Thickness of competent glacial layers > 30m Depth to Pre-Quaternary layers > 35m
II	HS_S_06	Cumulative thickness soft sediments 10m – 30m Thickness of competent glacial layers > 30m Depth to Pre-Quaternary layers > 45m
III	HS_S_21	Cumulative thickness soft sediments 10m – 30m Thickness of competent glacial layers 15m – 30m Depth to Pre-Quaternary layers > 35m
IV	HS_S_36	Cumulative thickness soft sediments < 10m Thickness of competent glacial layers > 15m Depth to Pre-Quaternary layers < 35m
V	HS_S_31	Cumulative thickness soft sediments 10m – 30m Thickness of competent glacial layers < 15m Depth to Pre-Quaternary layers > 35m
VI	HS_S_37	Cumulative thickness soft sediments 10m – 30m Thickness of competent glacial layers < 30m Depth to Pre-Quaternary layers < 35m
VII	HS_S_02	Cumulative thickness soft sediments > 30m Thickness of competent glacial layers > 10m
VIII	HS_S_10	Cumulative thickness soft sediments > 30m Thickness of competent glacial layers < 10m

11 Leg penetration analysis

This section describes a high-level leg penetration risk assessment. The assessment is performed to provide an indication of potential geotechnical risks associated with jack-up operations at the Hesselø South OWF project site.

The assessment is intended to provide an overview of the potential behaviour of two selected generic vessel configurations, which can inform on potential jack-up risks during the next project phases and provide a basic understanding of how the risks vary from different vessel configurations across the site.

In general, a leg penetration analysis performed at an offshore wind farm site, can help in:

- determining whether a jack-up is suitable for operating at a site or not,
- knowing what leg penetration behaviour and risks to anticipate,
- identifying and being able to mitigate possible geotechnical hazards.

Furthermore, leg penetration analysis is part of site-specific assessment that needs to be performed for all offshore wind farm sites once the project has matured further.

11.1 Selection of vessels

To provide a range of possibilities in terms of leg penetration behaviour and a good basic understanding of jack-up operations at the Hesselø South OWF project site, two different vessel configurations have been selected for the current study.

To select the appropriate vessel configurations, experience from previous leg penetration analyses (performed by COWI) has been used as database. The specifications of the vessels considered are confidential, however the selected vessels are characterized by they shall give insight into the possible range of penetration behaviours, where the limits of the range roughly correspond to a generic installation vessel and a generic operation and maintenance (O&M) vessel. The range of penetration behaviour was deduced from several leg penetration analyses for representative soil conditions at the Hesselø South OWF project site.

The first vessel (further denoted Generic Installation Vessel) is a four-legged vessel, equipped with a large spudcan and a maximum preload of 105 MN, whereas the second vessel (further denoted Generic O&M Vessel) is a four-legged vessel, equipped with a smaller spudcan and a maximum preload of 7 MN.

The foundation pressure applied to the seabed is dependent on the spudcan area and geometry, which is confidential. The ratio of foundation pressure between the Generic Installation Vessel and the Generic O&M Vessel is around a factor 2.

The final decision on the type of vessel to be adopted for the Hesselø South OWF project site is based on several factors, such as:

- vessel suppliers tendering for the installation/maintenance work,
- type of foundation solution,
- crane capacity, incl. lifting height and (horizontal) reach,
- deck size and capacity with regard to planned operations, e.g., how many installation units can be stored at once,
- amount and complexity of structural adjustments to be made to adopt vessel to planned operations,
- available leg length for soil penetration depth based on expected water depth and required air gap at site,
- speed, capacity, and size of the vessel,
- distance to the port,
- installation method, etc.

These are only a few of the factors that should be considered when selecting a certain jack-up vessel for installation works. All of them contribute to the final cost (and required duration) of the installation and should therefore be given special attention.

11.2 Geotechnical risks during jack-up

The main geotechnical risks that can be encountered during jack-up operations at an offshore wind site will be elaborated in the following subsections, cf. Ref. /13/. These are intended to give a high-level understanding of the spudcan behaviour and potential effects on the operations and how these effects may generally be handled or mitigated. During operations it is the responsibility of the owners, operators, and crew on jack-ups to exercise sound judgement based on their education, training and experience, while taking into account leg penetration assessments provided, including related recommendations.

The term "preloading" should be well understood before discussing the risks. Preloading is defined by the installation of the spudcans by vertical loading of the soil beneath a jack-up leg spudcan with the objective of ensuring sufficient foundation capacity under assessment situations through to the time when the maximum load is applied and held. In general preloading shall be carried out corresponding to at least 1.5 times the actual maximum load during operations. It is to be noted that the terms that describe the risk types used in this report might differ from the terms presented in various literature, therefore the description of the risks, failure mechanisms and particularities are more important than the actual terms. To highlight the most important characteristics of each of the risks, these have been gathered in Table 11-1.

Table 11-1 Overview of main characteristics of the geotechnical risks during jack-up.

Risk	Description	Circumstance	Effect	Observation	Consequence
Leg scour	Formation of local scour hole around spudcan	Cohesionless soil at seabed	Loss/reduction of soil bearing capacity	To be monitored continuously	Small [1)]
Squeezing	Thin and soft soil layer is squeezed horizontally	Thin, soft layer in between strong/stiff layers	Controllable leg settlements during initial preloading operations	Controllable penetration rate	Small
Fast leg penetration	Leg footing penetrates rapidly through strong layer and down to a soft layer	Thicker, soft layer below a strong/stiff layer	Structural damage, stability issues, personnel safety	Occurs during preloading before reaching maximum preload	Medium
Punch through	Leg footing penetrates rapidly through strong layer and down to a soft layer	Thicker, soft layer below a strong/stiff layer	Structural damage, significant stability issues, personnel safety	Occurs during operations after reaching maximum preload	High
Deep penetration	Leg has insufficient length to reach a stable penetration level	Penetration depth larger than available leg length	Non-operational, Lack of stability, risk for adjacent structures	To be mitigated before operations start	High
Difficulties during leg extraction	High resistance when attempting to extract legs after operations	Large suction below spudcan and large weight of soil above spudcan (can be caused by deep penetration in soft soils)	Operational downtime, structural damage, soil alteration at the location due to mitigation measures	To be mitigated before operations start	High

1) Consequence is generally small when (initial phase of) operations consider scour adequately but can be large when scour occurs (very) fast or when their circumstance exists in combination with a soil stratigraphy where scour can result in a later risk of punch through, and insufficient attention should have been paid to the (possible) existence of these circumstances. Scour is dependent on the current velocity (at seabed), and this could consequently be larger at a later moment in time than during the preloading phase.

Further to Table 11-1, other risks for jack-up assessment can be mentioned from seabed conditions as an effect from large seabed slopes, previous jack-up footprints and boulders, or deterioration of soil stiffness and strength from previous jack-up at the location. However, these are not considered for the categorisation of jack-up risks in the performed analyses, hence no further considerations of these have been performed.

11.2.1 Leg scour

Under certain flow and seabed conditions, seabed erosion may occur when temporarily introducing spudcans and/or jack-up legs. The presence of a spudcan/leg will cause the water flow in its vicinity to change. This local change in the flow will cause an increase in the sediment transport capacity on the seabed close to the structure, which can lead to the formation of a local scour hole.

When scour occurs the maximum bearing capacity of the soil beneath the spudcan will decrease due to loss of supporting soil. If the bearing capacity drops to a level below the footing load, additional penetration will occur.

Furthermore, scour may cause the spudcan to be loaded eccentrically and exert a corresponding load and bending moment on the spudcan and leg.

Relevant scour typically occurs when one or more of the situations below are encountered:

- shallow water depths at jack-up locations,
- (very) shallow spudcan penetrations into seabed,
- cohesionless soil at seabed level.

Some of the most common mitigation measures are:

- if possible, planning of operations for periods when current velocities are lowest and during benign weather,
- monitor scour during operations and take actions in accordance with observations,
- for operations with long durations, scour protection such as gravel beds, prefabricated mattresses and front mats can be used,
- excavation to obtain larger initial penetration.

11.2.2 Squeezing

The potential for squeezing is present when a relative thin and soft layer is sandwiched between the leg footing and a harder layer or when the thin, soft layer is present between two stronger layers. The thin soil layer can in such cases squeeze laterally between the hard layers, when the vertical stress on this layer is large enough and occurs over sufficiently large finite area.

Ref. /14/ presents two criteria to be used to make an initial check for a possible risk of squeezing, see equations and figure below. If both geometrical criteria are satisfied, there is a potential risk of squeezing.

$$B > 3.45\,T$$

$$\frac{D}{B} \leq 2.5$$

B is the width of the spudcan

T is the thickness of the soft layer

D is the thickness of the soil above the soft layer

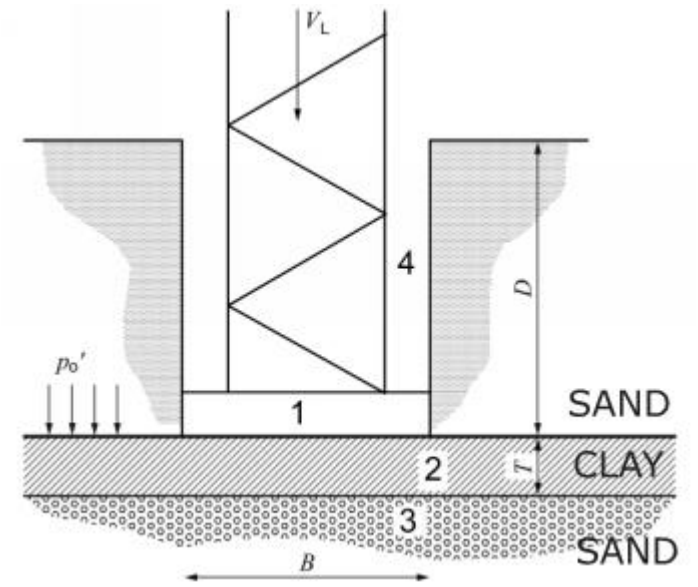

Figure 11-1 Sketch illustrating relevant parameters regarding squeezing, Ref. /14/.

It is important to note, however, that an actual risk of squeezing will only be present if the strength of the soft layer is insufficient relative to the vertical stress to be imposed on it. The difference in strength of the two materials (strong vs soft) should therefore be considered on top of the criteria shown above, which only relate to the geometry of the spudcan and soil situation.

The risk of squeezing generally leads to controllable leg settlements occurring during initial preloading operations. Therefore, most of the times no measures are taken to mitigate it.

11.2.3 Fast leg penetration

Fast leg penetration occurs in circumstances where a leg footing is temporarily supported by a stronger layer of soil that overlies a weaker layer and where the vertical footing load, as it is increased up to the preload, subsequently exceeds the bearing capacity of the soil, allowing the leg to penetrate rapidly through the stronger upper layer into the layer below.

In principle this is a punch through, see section 11.2.4, but as it occurs at a load level below the preload, the situation can be managed and is thus generally only referred to as fast (or rapid) leg penetration.

In such circumstances the upper soil layer may for instance be sand or stiff clay overlying soft clay. This type of failure is different to a squeezing failure described in section 11.2.2, as in this case the soil mass fails through large continuous soil failure surfaces rather than by many small internal soil shear failures within the weaker layer, which (only) cause the soil of the weaker layer to displace laterally. The penetration rates for squeezing are usually more controllable than penetration rates for fast leg penetration.

As the risk of fast leg penetration is defined to occur during preloading, it is important to make sure close and continuous monitoring is performed according to standards and the preloading is performed without jacking up completely out of the water (with zero air gap), such that in case a leg experiences fast/larger penetration than the others, the situation can be handled and the vessel will not tilt more than the allowable limit.

11.2.4 Punch through

The failure mechanism of punch through is the same as described above for fast leg penetration and occurs in circumstances where a leg footing has become temporarily supported by a stronger layer of soil that overlies a weaker layer, and where the vertical footing load, as it is increased, subsequently exceeds the foundation bearing capacity allowing the footing to penetrate rapidly through the upper layer into the layer below.

The main difference between fast leg penetration and punch through is that the former is defined as occurring before reaching the maximum preload, therefore occurring during close and continuous monitoring and with zero air gap, whereas the latter describes the potential occurrence of the same phenomenon, but after preloading (when the jack-up has an air gap), this making it (more/very) dangerous for the operations, possibly resulting in significant tilting of the jack-up with all related consequences. Because they are described by the same failure mechanism, sometimes both types of risk are referred to as “rapid penetration”.

Depending on the local soil conditions in terms of stratigraphy and strength of materials, it is sometimes difficult to predict which of the two

types of risks (fast leg penetration and punch through) is expected at a certain location. Conducting a leg penetration analysis using a range of parameters usually helps in identifying the expected risk, provided that the soil data are reliable.

The quality of soil data is therefore one of the most important factors in estimating the penetration behaviour that will occur during jack-up operations.

When the soil conditions show a significant reduction in soil strength with penetration depth, then there is a potential for punch through to occur. However, Ref. /15/ suggests several procedures to mitigate punch through:

- carry out a detailed soil survey at the Hesselø South OWF project site,
- if spudcan data from previous penetrations at the location is available, use this to back analyse and confirm the prediction methods for bearing capacity,
- ensure procedures for reducing the spudcan loads during the potential punch through phases, including the use of buoyancy (preload in water) and zero air gap (prevent vertical displacement using buoyancy of the hull) and preloading of one leg at a time,
- consider the use of jetting system (if available) to penetrate the harder soils.

To conclude, an important observation provided in Ref. /15/ states that "*Whereas mitigation techniques exist to allow for the possibility of punch-through during the installation phase, there is none for the in-service condition. It is vital, therefore, that soil data are assessed carefully, and that actual penetration behaviour is used to verify predicted behaviour.*"

Therefore, reliable soil data is the most important factor in estimation and mitigation of potential risk of punch through.

11.2.5 Deep penetration

The risk of deep penetration exists when the leg penetration is larger than the available leg length of the jack up vessel.

Deep penetration occurs when the soil conditions are so soft, that they do not provide sufficient bearing capacity to reach the maximum preloading. This means that there is no available leg length left, but the leg has not reached a stable penetration level.

It is important to highlight situations in which the leg length of the vessel to be used may not be sufficient, as there will then generally be the need

to employ a different vessel at the specific location/site. However, in some cases the selection of another vessel can be avoided. This is the case when there is the possibility to operate at a given location with smaller operational loads than considered for the initial assessment and these loads, and the related preloads, lead to less and feasible leg penetrations.

Deep penetrations may also pose a potential risk for adjacent structures.

11.2.6 Difficulties during leg extraction

The process of extracting the legs after operations at a certain location might sometime prove to be difficult and it is important to include this in the risk overview, such that the right measures are taken beforehand.

When extracting a leg and spudcan from a deep penetration in clay, the weight of the leg and the soil above the spudcan is to be overcome, together with the mobilised friction in the soil above the spudcan, and the suction below the spudcan. When the spudcan is in low permeable clay, the water cannot run freely to the bottom of the spudcan during extraction.

This implies that no equalising water pressure can develop below the spudcan during spudcan extraction. Thus, a resulting suction is developed below the spudcan, acting downwards, counteracting the retraction process.

According to Ref. /14/, leg extraction difficulties can be caused by conditions including the following:

- deeply penetrated spudcan in soft clay or loose silt,
- skirted or caisson-type spudcan where uplift resistance can be greater than the installation reaction,
- sites where the soil exhibits increased strength with time (this of course depends on the duration of the operations).

Ref. /14/ suggests jetting and/or excavation of the surface soils as mitigation measures against difficulties during leg extraction. A remark is added regarding soil alteration at the location due to these mitigation measures, which can affect future emplacement of jack-ups at the specific site. Another mitigation measure to prevent difficulties during leg extraction can be performance of stomping movement to reduce the suction underneath the spudcan.

11.3 Risk categories across the Hesselø South OWF project site

At the Hesselø South OWF project site, 32 unique soil investigation locations have been grouped into four different categories. For each of the categories, the primary geotechnical risks are defined and a graphical representation of all the locations and their corresponding category is presented in the end of current section and in Enclosure 7.03 and 7.04 considering the Generic Installation Vessel and the Generic O&M Vessel, respectively. In addition to the individual location specific assessments, a risk categorisation of the site based on the integrated ground model and same criteria as for the location specific assessment is performed to split the site into zones representing the jack-up assessment risks, which is presented together with the result from soil investigation locations.

It is important to acknowledge that the assessment presented here, and the associated evaluation of the geotechnical risk(s) is based on local soil data for the location specific categorisation, and cautious assumptions for the zonation of the site. Hence, the outcome from the location specific assessments should be seen as the most representative as these applies to specific conditions at the location, while the zonation across the site is based on global trends for the units present at the site which potentially can be found different in case a geotechnical test is performed and different design soil profiles is found representative.

When estimating the risk(s) at each location during this categorisation process, the CPT results and borehole logs have been considered, together with the soil strength of the layers which is derived based on CPT results as outlined in chapter 7 and 8. The strength of sand layers is characterized by friction angle and the strength of clay layers by the undrained shear strength.

To categorize the geotechnical locations, the following factors have been considered:

- Stratigraphy at each location, based on CPT results and borehole data. For categorization purposes, only the first 30 meters starting from the seabed have been considered, as the influence on the penetration behaviour for larger depths is considered negligible in relation to the currently assumed vessel configurations and spudcan geometries.

- The strength properties used for the assessment requires a constant value per layer. For estimating this, the required strength parameters for sand and clay are determined from the average of the value when disregarding the lowest and highest 10% of the data within the considered layer for removing small outliers. The derived strength profiles considered for the assessment are presented in Appendix H.

- Penetration risk analysis was performed following ISO guidelines, as per Ref. /16/.

In Table 11-2 below, a summary of the four categories across the Hesselø South OWF project site when considering operations with both vessels, including their description and corresponding risks, is presented. It must be noted that the outcome from a leg penetration analysis is dependent on the combination of stratigraphy, layer thicknesses, strength properties, vessel configurations etc. Hence, generic values for presented criteria in Table 11-2 are based on sensitivity analyses, COWI's experience, and assumptions with slightly conservatism included.

For dividing the Hesselø South OWF project site into different zones representing the different risk categories for jack-up assessment, the same criteria from Table 11-2 is considered to define a risk associated to each of the ground model units. Thicknesses and depths of layers presenting a risk across the site is evaluated from the integrated ground model, while the geotechnical clay layers presenting a risk based on the strength is evaluated from derived undrained shear strength values in section 8.3.2 and presented in Appendix D.4. A list of the ground model units and description of their consideration in the leg penetration zonation is listed in Table 11-3. It should be noted the layers marked with risks in Table 11-3 need to fulfil the criteria in Table 11-2 for being categorised with a risk in the leg penetration zonation.

Table 11-2 Jack-up assessment summary table presenting categories and corresponding potential risks.

Category	Description	Potential risk(s)
1	Category 1 comprises locations where in the first 30 meters below the seabed, where mainly sand and/or very competent silt/clay layers are encountered. For locations where soft clay layers are present, the criteria presented for category 2 to 4 are not fulfilled. › If sand is encountered at seabed level, there might be a risk of scour.	› Leg scour
2	Category 2 comprises locations where in the first 30 meters below the seabed only sand is encountered, except for an interbedded thin clay layer, which presents the potential for squeezing. › If sand is encountered at seabed level, there might be a risk of scour. According to Ref. /14/ and considering the spudcan geometry of both vessels, the following criteria has been applied in order to select locations within Category 2: › Thickness of clay layer to be: › < 3.2 m (Generic Installation Vessel), › < 1.0 m (Generic O&M Vessel). › Top of clay layer to be: › ≤ 27.6 m depth (Generic Installation Vessel), › ≤ 8.7 m depth (Generic O&M Vessel). The formula given in Ref. /14/ is not dependent on the strength of clay layer. In the current assessment it was however considered relevant to consider that only a clay layer	› Leg scour › Squeezing

Category	Description	Potential risk(s)
	with a corresponding conservative c_u as per below has the potential of squeezing [1]: › < 350 kPa (Generic Installation Vessel) › < 200 kPa (Generic O&M Vessel)	
3	Category 3 comprises location where in the first 30 meters below the seabed thick clay layer is present but no sand layer with sufficient thickness overlies. › If sand is encountered at seabed level, there might be a risk of scour. To select locations within Category 3, the following criteria has been applied: › Depth of soft clay layer base to be [2]: › > 25.0 m (Generic Installation Vessel), › > 15.0 m (Generic O&M Vessel). › Strength of clay layer c_u [1]: › < 175 kPa (Generic Installation Vessel), › < 100 kPa (Generic O&M Vessel). › Thickness of potential interbedded sand layer(s) (for the sand layer not being able to create punch through or fast leg penetration) [1]: › < 1.0 m (Generic Installation Vessel), › < 0.5 m (Generic O&M Vessel). In the event of deep penetration occurring, the spudcan can penetrate deep into clay layer, thus leading to potential retraction difficulties, due to suction below spudcan and weight of soil above spudcan.	› Leg scour › Deep penetration › Difficulties during leg extraction
4	Category 4 comprises locations where in the first 30 meters below the seabed, sand is encountered and overlies a thick clay layer, which presents potential for rapid penetration, i.e., the risk of fast leg penetration (if rapid penetration occurs during preloading) or punch through (if rapid penetration occurs during operations). › If sand is encountered at seabed level, there might be a risk of scour. To select locations within Category 4, the following criteria has been applied: › Thickness of clay layer to be (in order not to consider squeezing): › > 3.2 m (Generic Installation Vessel), › > 1.0 m (Generic O&M Vessel). › Strength of clay layer c_u [1]: › < 175 kPa (Generic Installation Vessel), › < 100 kPa (Generic O&M Vessel). › Thickness of overlying sand layer (for the sand layer being able to affect the spudcan behaviour) [1]: › > 1.0 m (Generic Installation Vessel), › > 0.5 m (Generic O&M Vessel).	› Leg scour › Fast leg penetration › Punch through › Deep penetration › Difficulties during leg extraction

Category	Description	Potential risk(s)
	In the event of fast leg penetration or punch through occurring, the spudcan can penetrate deep into clay layer, thus leading to potential retraction difficulties, due to suction below spudcan and weight of soil above spudcan.	

(1) *Value derived from sensitivity analysis of parameter.*

(2) *Deep penetration depends on the combined thickness of water depth, soil penetration and required air gap for vessel during jack-up operation compared to the available leg length from vessel. Due to the available leg length for soil penetration is site dependent and vessel dependent, a generic value is estimated for the performed assessment.*

Table 11-3 Overview of integrated ground model unit risk consideration for jack-up assessments.

Ground model unit	Unit description	Generic Installation Vessel	Generic O&M Vessel
U01 U01.2	Very low strength clay with parts being sand.	No sand overlying layer, hence only risk from category 2 and 3 is possible.	No sand overlying layer, hence only risk from category 2 and 3 is possible.
U02	Categorised as sand layer, not considered posing a risk.	-	-
U03	Very low strength clay with parts being sand.	Strength significantly below lowest criteria, hence risk from both risk category 2, 3 and 4 is possible.	Strength significantly below lowest criteria, hence risk from both risk category 2, 3 and 4 is possible.
U04	Categorised as sand layer with minor areas of being clay. Not considered posing a risk.	-	-
U05	Split between low strength clay and sand. Due to the unit partly contains clay material, the entire unit is considered as a risk.	Strength significantly below lowest criteria, hence risk from both risk category 2, 3 and 4 is possible.	Strength significantly below lowest criteria, hence risk from both risk category 2, 3 and 4 is possible.
U06	Categorised as sand layer, not considered posing a risk.	-	-
U07	Low strength clay with small interbedded sand layers. Considered as a risk.	Strength below lowest criteria, hence risk from both risk category 2, 3 and 4 is possible.	Strength below lowest criteria, hence risk from both risk category 2, 3 and 4 is possible.
U08	Low strength clay with small interbedded sand layers. Considered as a risk.	Strength below lowest criteria, hence risk from both risk category 2, 3 and 4 is possible.	Strength below lowest criteria, hence risk from both risk category 2, 3 and 4 is possible.
U09	Medium strength clay with small interbedded sand layers. Considered as a risk.	Strength below lowest criteria, hence risk from both risk category 2, 3 and 4 is possible.	Strength below criterion for squeezing, hence risk from risk category 2 is possible.
U10	Categorised as sand layer with minor areas of being clay. Not considered posing a risk.	-	-
U11	Clay within unit represented from high strength properties, hence not considered posing a risk.	-	-
U12	Very high strength clay, not considered posing a risk.	-	-

Considering that operations at the offshore wind site are performed with either one of the vessels selected in the study, the outcome of the analyses and the final categorisation per geotechnical location and risk zonation are shown in Figure 11-2 and Figure 11-3. These figures are presented in larger format in Enclosure 7.03 and 7.04, respectively. It is observed that the categorisation based on the integrated ground model generally matches well with the categorisation based on local geotechnical investigation data. However, at few locations the categorization differs. In this regards it is noted that the leg penetration risk assessment is sensitive to the local stratigraphy and the presence and thickness of sand layers above soft clay layers. Hence, the difference in categorisation for few locations is as expected due to the ground model is not capable of capturing interbedded layers within soil units. This limitation of the ground model must be kept in mind when obtaining information about jack-up assessment at the site from the presented results, and a location specific leg penetration assessment must be performed prior to jack-up to verify the actual soil conditions and potentially interbedded layers.

Comparison of the results of the leg penetration analysis shown on Enclosures 7.03 and 7.04 with the zonation presented in Figure 10-6 (and Enclosure 7.01) shows that the higher leg penetration risk mainly occurs in the geotechnical zones with thick layers of normally consolidated soft clays, which is also expected based on the considered criteria for the leg penetration analyses and the descriptions for the geotechnical zones defined from the zonation.

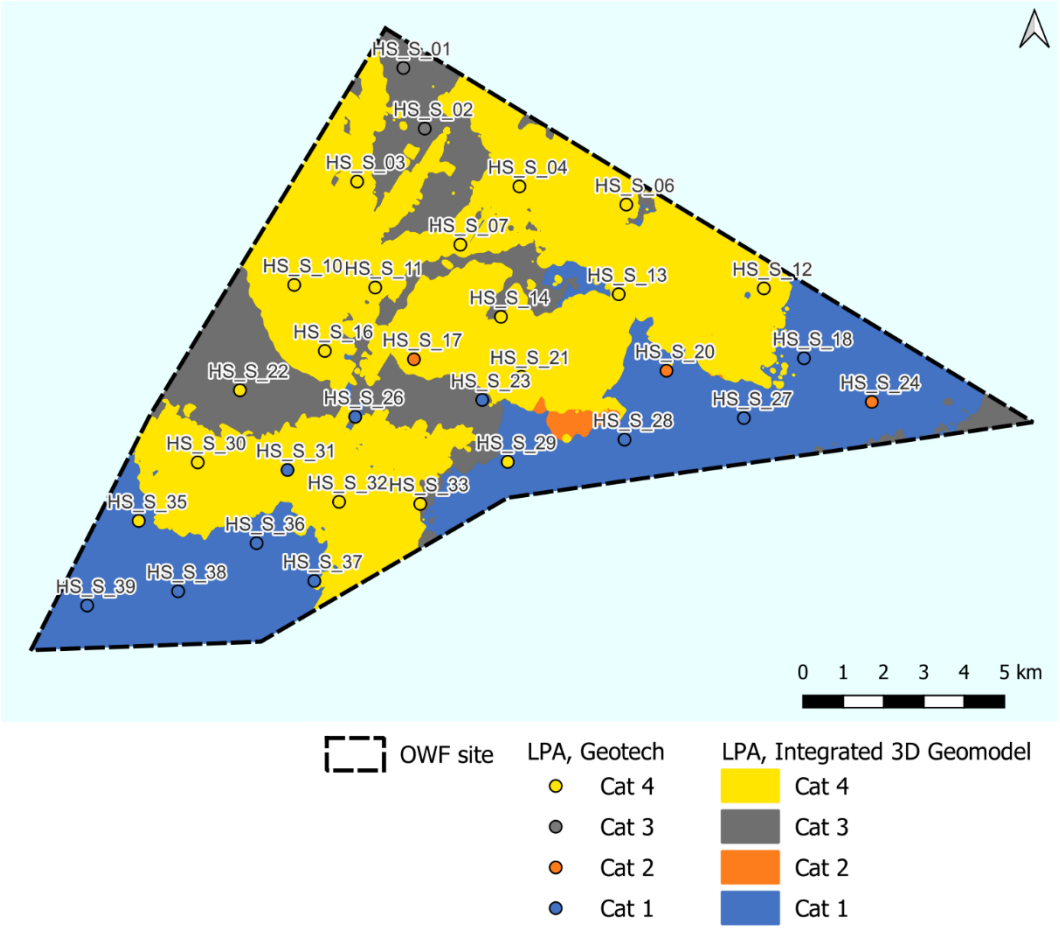

Figure 11-2 Results from leg penetration analysis for Generic Installation Vessel.

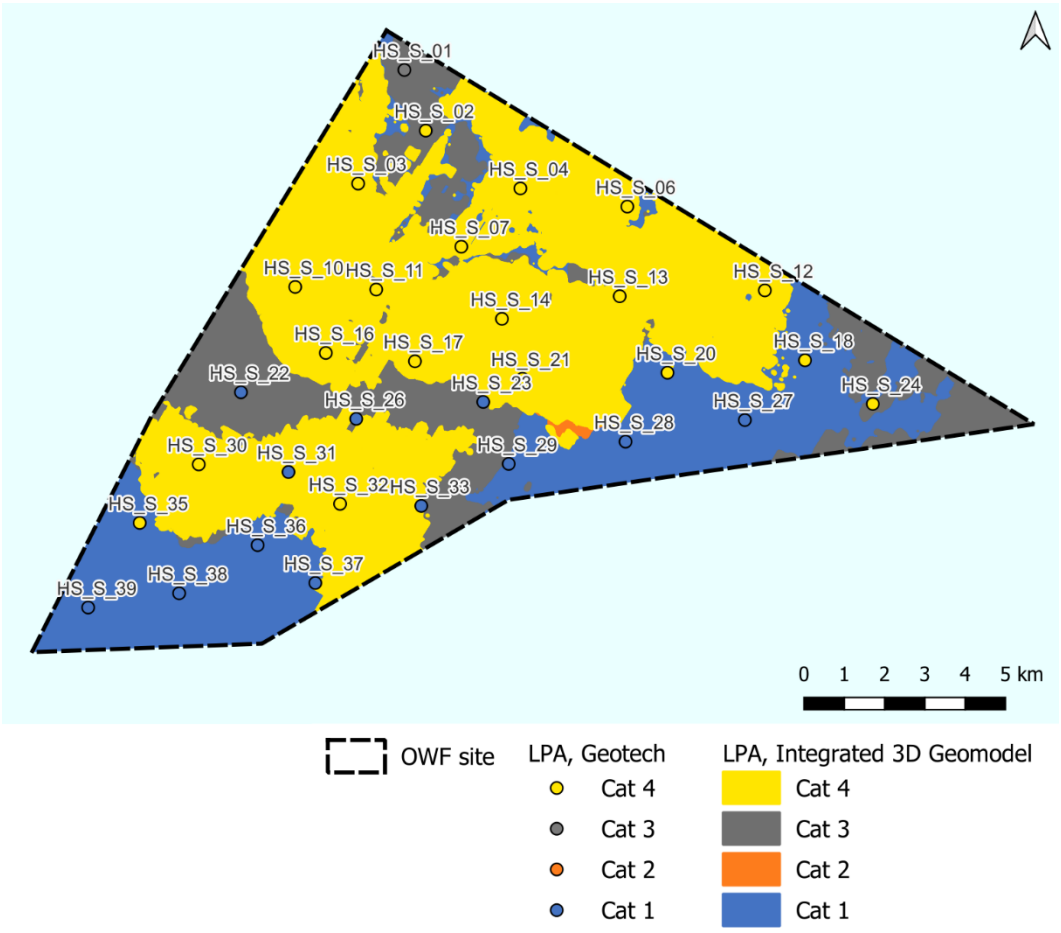

Figure 11-3 Results from leg penetration analysis for Generic O&M Vessel.

12 List of charts, appendices, and deliverables

Below is a complete list of appendices and enclosures delivered with this report.

Appendices	
Number	Title
Appendix A	Interpreted stratigraphy at CPT locations
Appendix B	CPT for geotechnical units
Appendix C	Calculated soil properties per CPT location
Appendix D	CPT plots per geotechnical unit including properties from laboratory testing
Appendix E	Cone factor assessment
Appendix F	Range of soil properties per geotechnical unit
Appendix G	Conceptual geological model
Appendix H	Soil profiles for LPA assessment

Enclosures	
Number	Title
1.01	Overview map Bathymetry
1.02	Overview map Cross sections, 2D UHRS Survey lines and GT locations
2.01	Depth to top of soil unit U01 [mbsb]
2.02	Depth to top of soil unit U01.2 [mbsb]
2.03	Depth to top of soil unit U02 [mbsb]
2.04	Depth to top of soil unit U03 [mbsb]
2.05	Depth to top of soil unit U04 [mbsb]
2.06	Depth to top of soil unit U05 [mbsb]
2.07	Depth to top of soil unit U06 [mbsb]
2.08	Depth to top of soil unit U07 [mbsb]
2.09	Depth to top of soil unit U08 [mbsb]
2.10	Depth to top of soil unit U09 [mbsb]
2.11	Depth to top of soil unit U10 [mbsb]
2.12	Depth to top of soil unit U11 [mbsb]
2.13	Depth to top of soil unit U12 [mbsb]
3.01	Elevation of top of soil unit U01 [DTU21 MSL]
3.02	Elevation of top of soil unit U01.2 [DTU21 MSL]
3.03	Elevation of top of soil unit U02 [DTU21 MSL]
3.04	Elevation of top of soil unit U03 [DTU21 MSL]
3.05	Elevation of top of soil unit U04 [DTU21 MSL]
3.06	Elevation of top of soil unit U05 [DTU21 MSL]
3.07	Elevation of top of soil unit U06 [DTU21 MSL]
3.08	Elevation of top of soil unit U07 [DTU21 MSL]
3.09	Elevation of top of soil unit U08 [DTU21 MSL]
3.10	Elevation of top of soil unit U09 [DTU21 MSL]
3.11	Elevation of top of soil unit U10 [DTU21 MSL]
3.12	Elevation of top of soil unit U11 [DTU21 MSL]
3.13	Elevation of top of soil unit U12 [DTU21 MSL]
4.01	Isochore of soil unit U01 [m]
4.02	Isochore of soil unit U01.2 [m]
4.03	Isochore of soil unit U02 [m]
4.04	Isochore of soil unit U03 [m]
4.05	Isochore of soil unit U04 [m]
4.06	Isochore of soil unit U05 [m]
4.07	Isochore of soil unit U06 [m]
4.08	Isochore of soil unit U07 [m]
4.09	Isochore of soil unit U08 [m]
4.10	Isochore of soil unit U09 [m]
4.11	Isochore of soil unit U10 [m]

Enclosures	
Number	Title
4.12	Isochore of soil unit U11 [m]
5.01	Geohazards - shallow gas [mbsb]
6.01	Cross section A_HS_L005_UHR_T_MIG_STK
6.02	Cross section A_HS_L007_UHR_T_MIG_STK
6.03	Cross section A_HS_L013_UHR_T_MIG_STK
6.04	Cross section A_HS_L020_UHR_T_MIG_STK
6.05	Cross section A_HS_L028_UHR_T_MIG_STK
6.06	Cross section A_HS_L034_UHR_T_MIG_STK
6.07	Cross section A_HS_X003_UHR_T_MIG_STK
6.08	Cross section A_HS_X005_UHR_T_MIG_STK
6.09	Cross section A_HS_X007_UHR_T_MIG_STK
6.10	Cross section A_HS_X010_UHR_T_MIG_STK
6.11	Cross section A_HS_X012_UHR_T_MIG_STK
6.12	Cross section A_HS_X014_UHR_T_MIG_STK
6.13	Cross section A_HS_X017C_UHR_T_MIG_STK
7.01	Geotechnical zonation
7.02	Variation of relevant geotechnical layers/boundaries
7.03	Jack-up Risk Assessment. Generic Installation Vessel
7.04	Jack-up Risk Assessment. O&M Vessel

Digital deliverables	
Item	Format
Kingdom Suite Project (version 2024) including spatial geological model	Kingdom project
All soil unit interfaces as depth grids [mbsb]	GeoTIFF and AXCII.xyz
All soil unit interfaces as elevation grids. Top of units [DTU21 MSL]	GeoTIFF and AXCII.xyz
All soil units as isochore grids [vertical layer thickness, m]	GeoTIFF and AXCII.xyz
Shallow gas interfaces as elevation grid [mbsb]	GeoTIFF and AXCII.xyz
Geotechnical zones	ESRI Shapefile
Jackup risk assessment categories - Polygons	ESRI Shapefile
Jackup risk assessment categories - Points	ESRI Shapefile

13 Conclusions

A 3D Integrated Geological Model (IGM) has been established for the entire Hesselø South OWF project site. The model comprises an integrated interpretation of the newly (2023) gathered geotechnical and seismic data. The report provides detailed geotechnical and geological information on the geological layers in the model including stratigraphical descriptions, lithological descriptions, and geotechnical characteristics.

The result is an IGM which contains detailed information on the spatial distribution of the layers as well as the characteristic geotechnical parameters. It contains thirteen (13) integrated soil units consisting of Holocene, Pleistocene, or Miocene deposits.

The sediments generally comprise relative soft Holocene and Late Weichselian soils overlaying competent Pleistocene soils. The thickness of the soft soils is found to depths of more than 30 m below seabed in the Western and Northern part of the site. Toward East and South consolidated Pleistocene layers generally of more than 25 m thickness is interpreted. Pre-quaternary layers is generally found deeper than 45 m but found shallower central at the site and toward south.

Potential geohazards include shallow gas in Holocene deposits. Further, glacial deformation can create a lager variability in geotechnical properties of the Pleistocene soils whereas faulting is found to be confined to the pre-quaternary layers.

A Conceptual Geological Model is also provided which visualizes the geological layers and their variation for the entire site in two conceptual profiles.

The digital IGM is delivered as a 3D layered model in a Kingdom suite project. Enclosures provided with the report present the soil units with respect to depth below seabed, thickness, elevation for top of unit, and lateral extent. Appendices present the geotechnical interpretations.

Thirteen (13) cross sections distributed over the entire Hesselø South OWF project site show the layering in the model. The cross sections follow the seismic survey lines and display CPT logs (q_c, f_s, u_2, and I_c) and geological descriptions from boreholes at top of layers from boreholes located on the seismic survey lines.

The enclosures are also supporting the geotechnical zonation where thickness and depth of grouped units of importance from the IGM are presented and integrated into eight (8) geotechnical zones. In establishing the geotechnical zones focus has been on the low and high strength deposits and geological structures assessed to be

important for the foundation design and installation works. The soil zonation maps have been simplified into a single map showing the eight selected geotechnical zones which provide a geological/geotechnical overview of the entire site relevant for foundation conditions. Geotechnical zone I to III generally show good ground conditions for WTG foundation design and installation, with the conditions being most competent for Geotechnical zone I. Geotechnical zone IV to VI are categorised by medium ground conditions for WTG foundation design, which combined with depth to top of pre-quaternary material potentially can result in foundation installation difficulties. For Geotechnical zones VII and VIII thick deposits of soft clay are anticipated and hence in these zones heavy WTG foundations are expected to be required. Zones VII and VIII are dominating the northern part of the Hesselø South OWF site, while zones I to III are dominating the eastern and southwestern parts. Zone IV to VI dominates in a central area within the southern part of the site.

The leg penetration risk has been assessed for each of the geotechnical survey locations for two generic vessels – an installation vessel and an O&M vessel – and a risk category has been assigned for each survey location. This has been applied to the integrated ground model to cover the Hesselø South OWF project site with zones representing the assessed jack-up risks. The results from the performed assessment show large differences of jack-up behaviour across the Hesselø South OWF project site, which is also in accordance with expectations based on the learnings from performed geotechnical zonation. The highest leg penetration risks are seen in the geotechnical zones with thick layers of normally consolidated soft clays (particularly zones VII and VIII, but also in zones II, III, V and VI).

With respect to the purpose of the pre-investigations initiated by Energinet Eltransmission A/S the new IGM therefore provides a strong basis for developers to evaluate the ground conditions in relation to the positioning of WTG's and the foundation design.

References

Ref. /1/ Danish Offshore Wind 2030 - Lot 1 - Hesselø South, Volume II Measured and Derived Final Results, Revision 2, Gardline, May 2024.

Ref. /2/ Robertson and Cabal, 2015: Guide to Cone Penetration Testing, 6th Edition.

Ref. /3/ DNV-RP-C207, Statistical representation of soil data, September 2021.

Ref. /4/ Lunne, T., Robertson, P. K., and Powell, J. J. M., 1997: Cone Penetration Testing in Geotechnical Practice, 1st edition.

Ref. /5/ Mayne, P. W & Sharp, J. 2019 - CPT Approach to Evaluating Flow Liquefaction Using Yield Stress Ratio.

Ref. /6/ Jamiolkowski, M., Lo Presti, D. C. F. & Manassero, M. 2003 - Evaluation of Relative Density and Shear Strength of Sands from CPT and DMT.

Ref. /7/ Huuse, M. L. A., 2000: Overdeepened Quaternary valleys in the eastern Danish North Sea: morphology and origin. Quaternary Science Reviews, 19, 1233-1253

Ref. /8/ GEUS. Screening of seabed geological conditions for the offshore wind farm area Hesselø South and the adjacent cable corridor area, Desk study for Energinet. 2023

Ref. /9/ GEUS. General geology of southern Kattegat, the Hesselø wind farm area, Desk study. 2020

Ref. /10/ GEOxyz. Geophysical Surveys for Danish Offshore Wind 2030 – Hesselø South, Rev 2.0, BE5376H-711-01-RR, 19/12/2023

Ref. /11/ Müller, K., Winsemann, J., Pisarska-Jamroży, M., Lege, T., Spies, T., Brandes, C., 2021: The Challenge to Distinguish Soft-Sediment Deformation Structures (SSDS) Formed by Glaciotectonic, Periglacial and Seismic Processes in a Formerly Glaciated Area: A Review and Synthesis. 10.1017/9781108779906.007.

Ref. /12/ Brandes, C., Steffen, H., Sandersen, P.B.E., Wu, P., Winsemann, J., 2018: Glacially induced faulting along the NW segment of the Sorgenfrei-Tornquist Zone, northern Denmark: Implications for neotectonics and Late glacial fault-bound basin formation, Quaternary Science Reviews, Volume 189, Pages 149-168, ISSN 0277-3791, https://doi.org/10.1016/j.quascirev.2018.03.036.

Ref. /13/ LOC, January 2013, Geotechnical engineering for jack-ups, Ref no. LOC/CM/MANUAL/2013/R0.1-4.

Ref. /14/ European Standard EN ISO 19905-1, Petroleum and natural gas industries – Site-specific assessment of mobile offshore units – Part 1: Jack-ups, February 2016.

Ref. /15/ MSL Engineering Ltd., 2004, Guidelines for jack-up rigs with particular reference to foundation integrity (HSE Research Report 289).

Ref. /16/ ISO 19905-1:2016: Petroleum and natural gas industries, Site-specific assessment of mobile offshore units, Part 1: Jack-ups.

Appendix A Interpreted stratigraphy at CPT locations

The CPT measurements and general CPT correlations (from left: soil behaviour type, soil behaviour type index, measured cone tip resistance, measured cone skin resistance, friction ratio and measured pore water pressure) together with stratigraphy per geotechnical test location is presented in this Appendix as shown in the example in Figure A-1. The soil behaviour type have three different methodologies, where the blue dots represent the soil behaviour type based on Ic, the red dots represent the normalised cone resistance and friction ratio chart, and the yellow dots represent the normalised cone resistance and pore pressure chart, cf. the presented methodologies in section 7.2.1, 7.2.2, and 7.2.3, respectively.

The figures show the interpreted soil stratigraphy, where each considered layer boundary is marked with a red line. Additionally, interpreted horizons from the Kingdom model and the borehole logs received within the AGS-file is presented in as purple horizontal dashed lines and green dashed lines, respectively. Identifications of units, horizons and borehole log numbers are presented in the right side of the figures. The numbering from the borehole logs is presented in Table A-1 corresponding to the received values in the AGS-file together with the acquired description from the AGS-file.

On a few locations it is interpreted that two consecutive layers with same units are present, which is also illustrated in Figure A-1 for layer US03. This is due to an observation, that the soil behaviour/properties change. However, in interaction with the geophysical interpreted horizons, it is not assessed, that these layers should be divided any further or processed differently.

All figures per geotechnical test location are presented in the following pages.

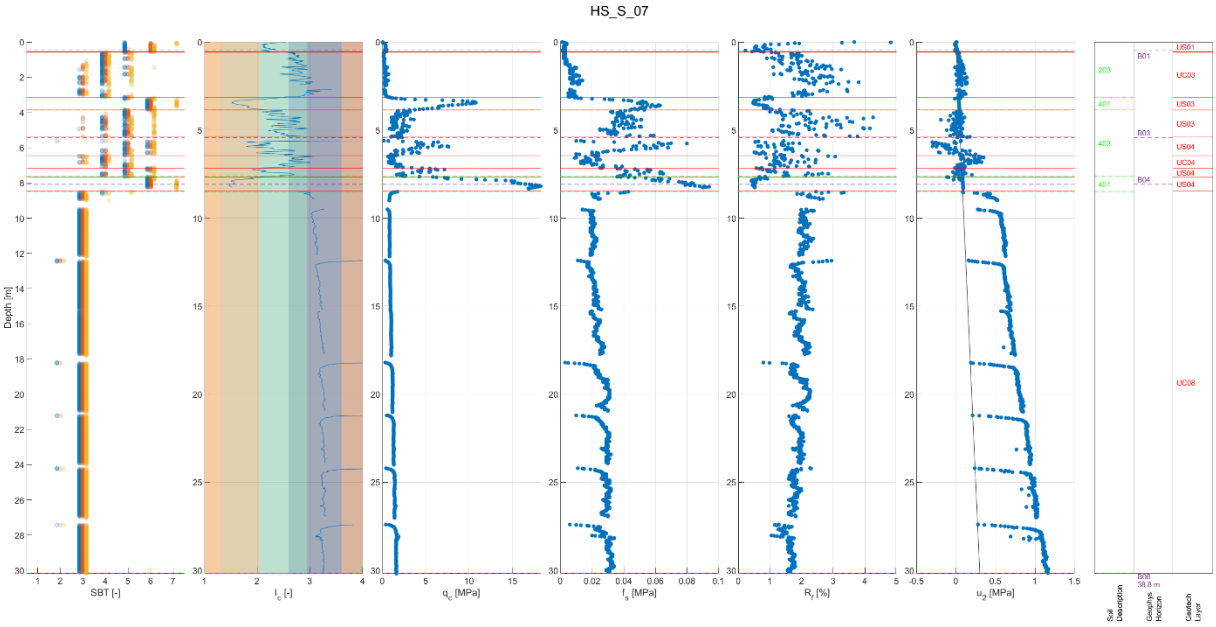

Figure A-1 *Example of interpreted stratigraphy for HS_S_07.*

Table A-1 *Borehole legends and descriptions from received AGS-file.*

Legend	Description	Legend	Description
201	CLAY	402	Clayey SAND
202	Silty CLAY	403	Silty SAND
203	Sandy CLAY	404	Gravelly SAND
204	Gravelly CLAY	407	clayey silty SAND
207	Silty sandy CLAY	408	clayey silty gravelly SAND
208	Silty gravelly CLAY	409	clayey silty gravelly cobbly SAND
211	Silty sandy gravelly CLAY	410	Clayey gravelly SAND
214	Silty sandy gravelly cobbly CLAY	412	Silty gravelly SAND
220	Sandy gravelly CLAY	501	GRAVEL
303	Sandy SILT	802	SILTSTONE
306	Clayey sandy SILT	803	SANDSTONE
401	SAND		

HS_S_01

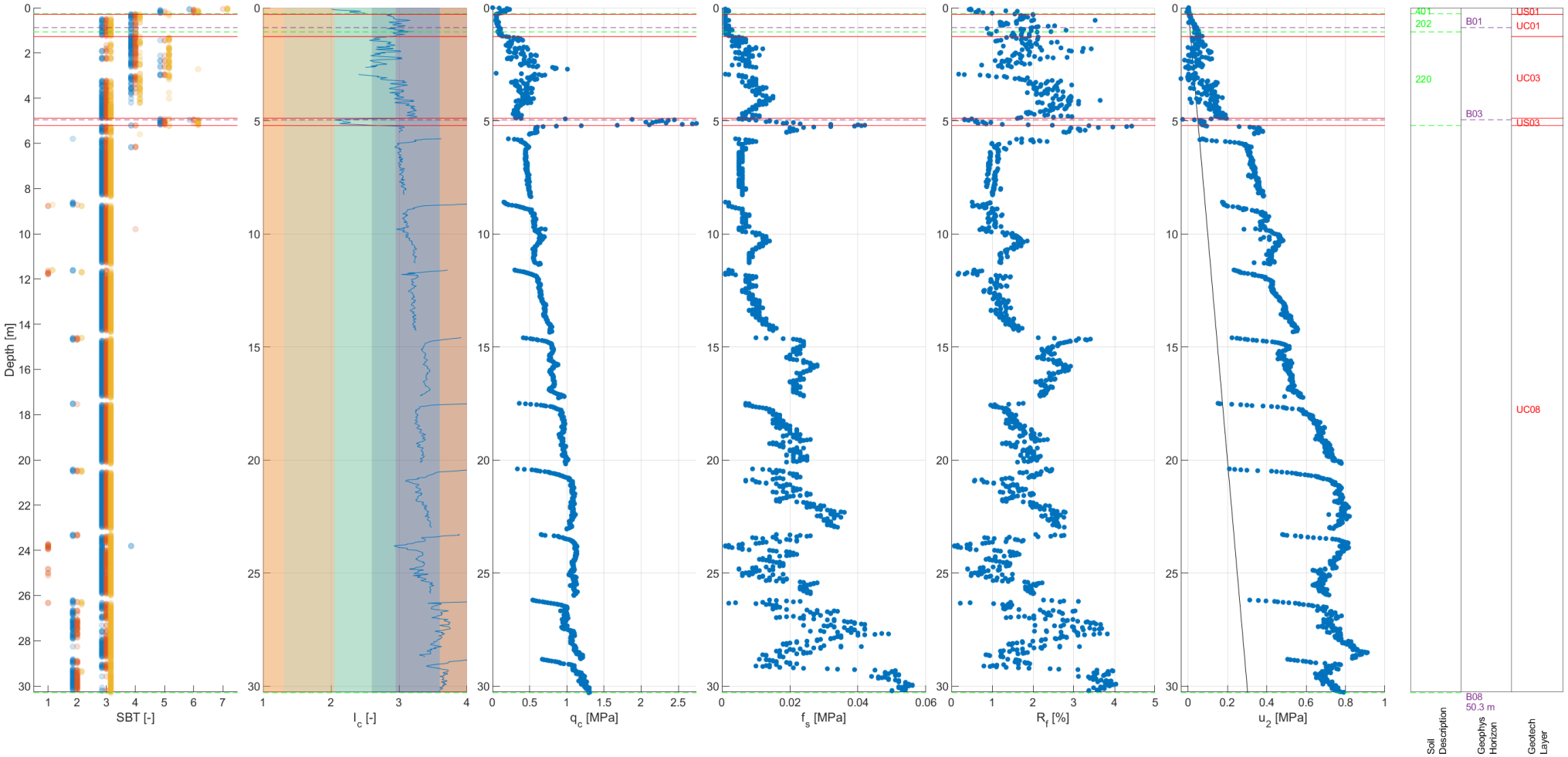
Depth [m]
SBT [-]
I_c [-]
q_c [MPa]
f_s [MPa]
R_f [%]
u_2 [MPa]
401
202
220
B01
B03
B08
50.3 m
US01
UC01
UC03
US03
UC08
Soil Description
Geophys Horizon
Geotech Layer

HS_S_02

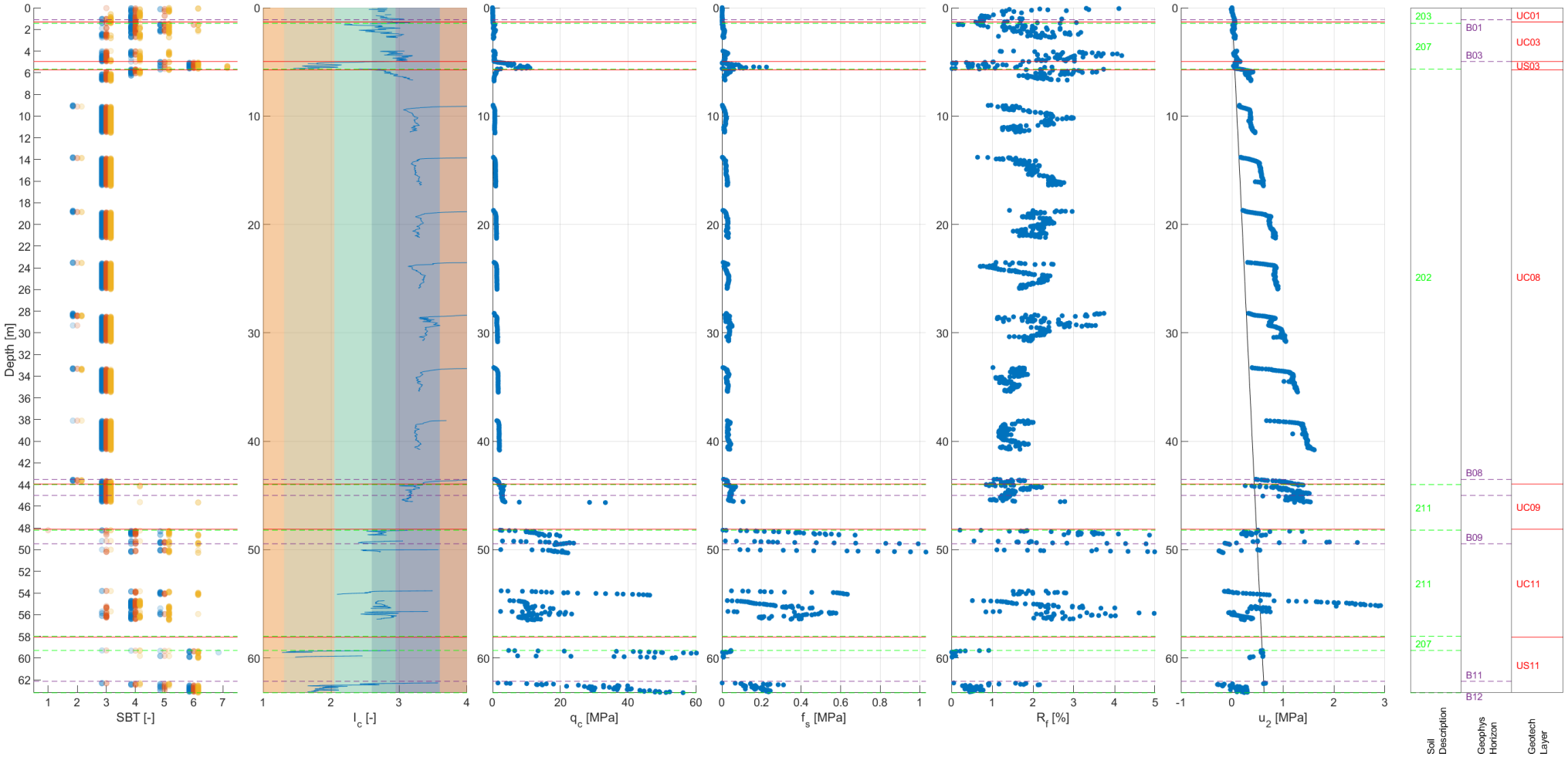
Depth [m]
SBT [-]
I_c [-]
q_c [MPa]
f_s [MPa]
R_f [%]
u_2 [MPa]
Soil Description
Geophys Horizon
Geotech Layer
203
207
202
211
211
207
B01
B03
B08
B09
B11
B12
UC01
UC03
US03
UC08
UC09
UC11
US11

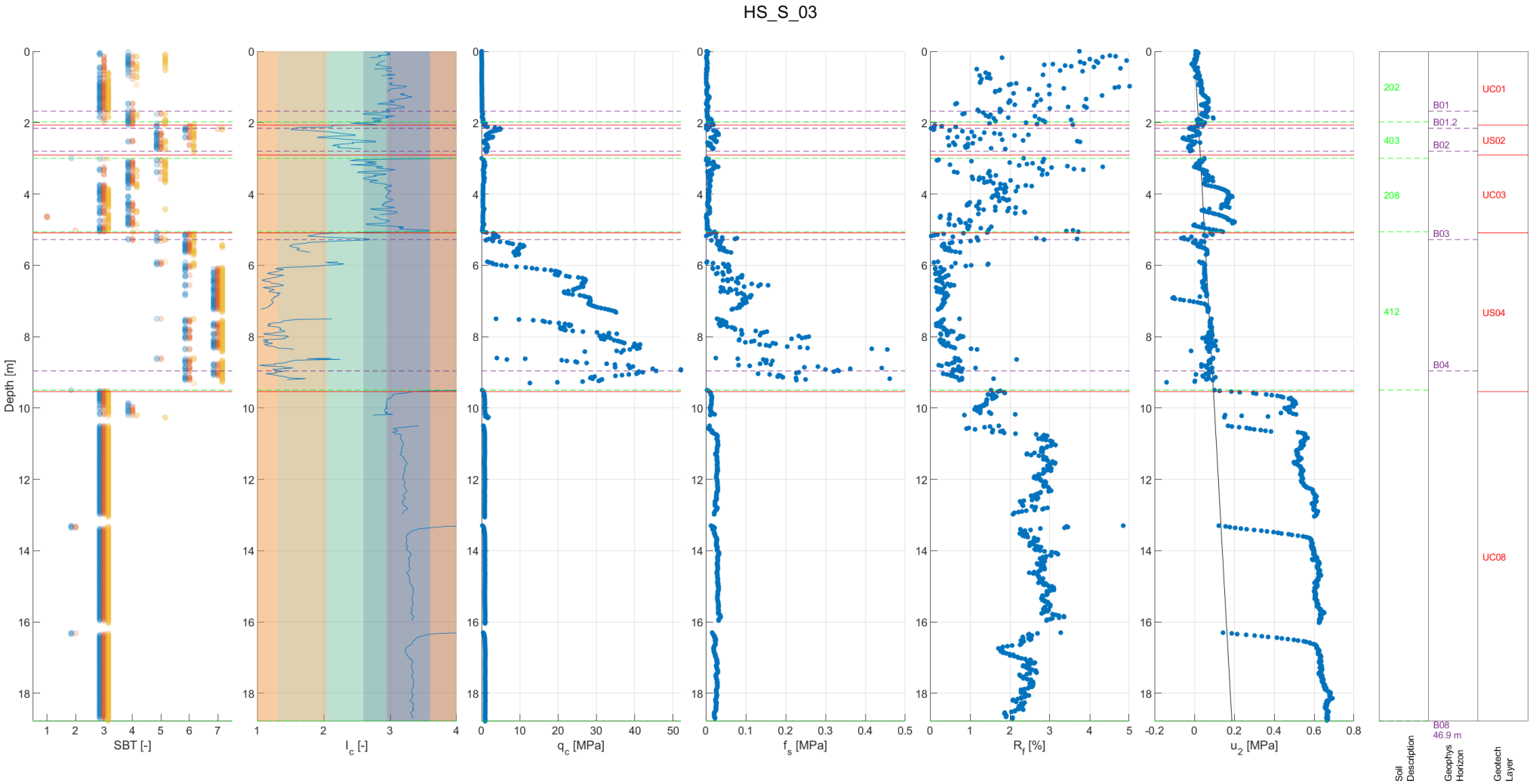
HS_S_03
Depth [m]
SBT [-]
I_c [-]
q_c [MPa]
f_s [MPa]
R_f [%]
u_2 [MPa]
202
403
208
412
B01
B01.2
B02
B03
B04
B08
46.9 m
UC01
US02
UC03
US04
UC08
Soil Description
Geophys Horizon
Geotech Layer

HS_S_04

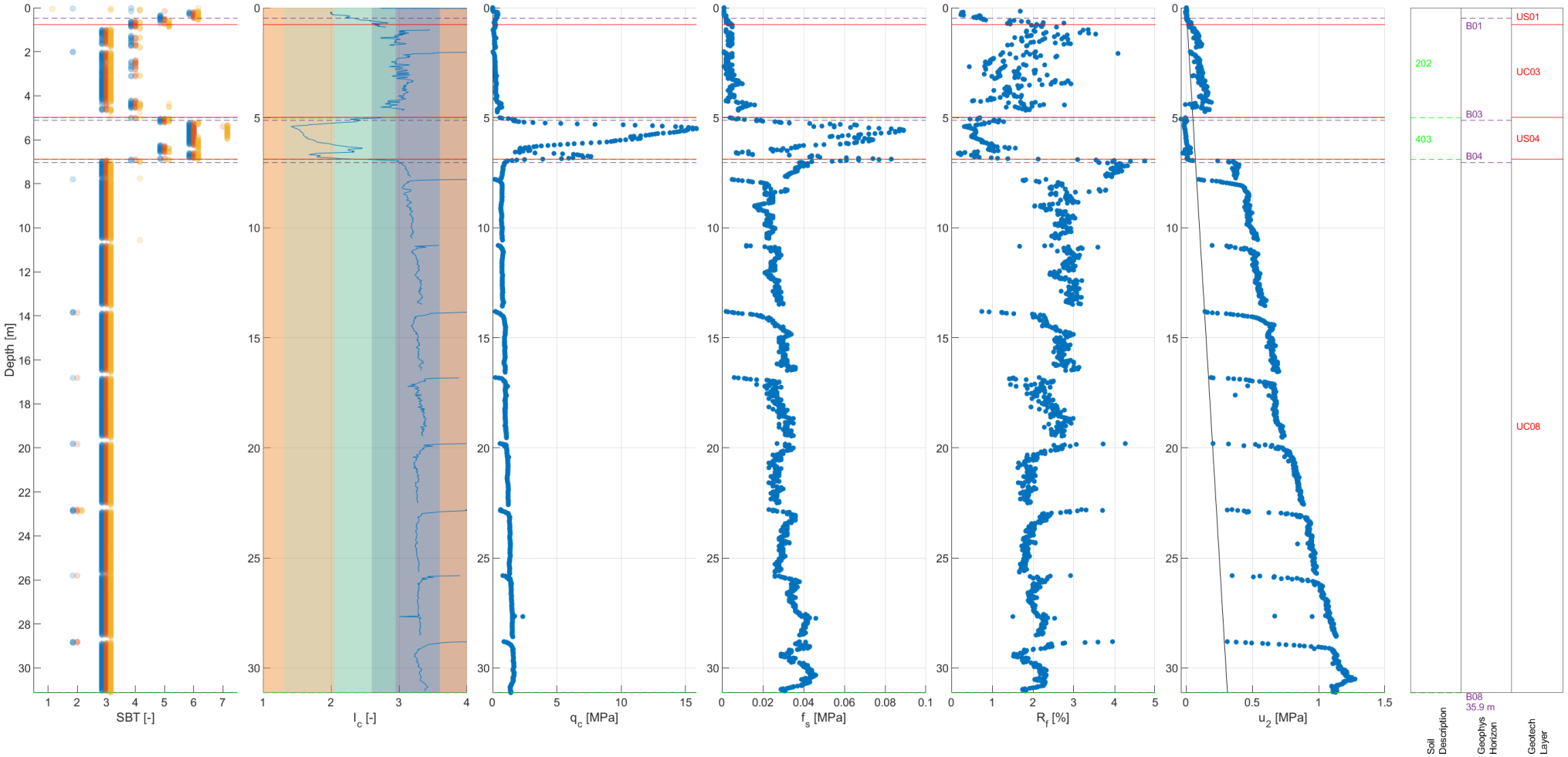
Depth [m]
SBT [-]
I_c [-]
q_c [MPa]
f_s [MPa]
R_f [%]
u_2 [MPa]
US01
B01
UC03
202
B03
US04
403
B04
UC08
B08
35.9 m
Soil Description
Geophys Horizon
Geotech Layer

HS_S_06

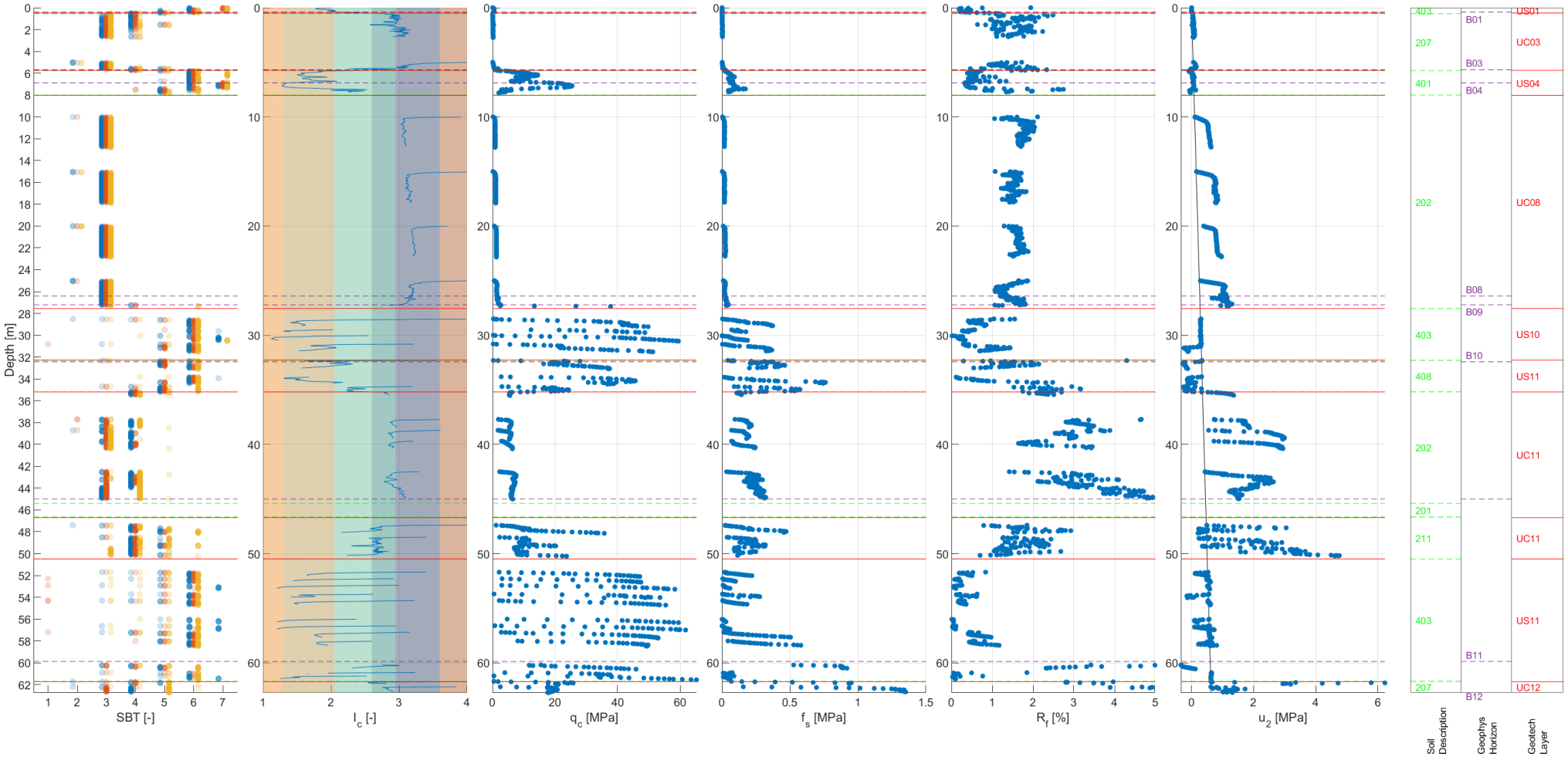
Depth [m]
SBT [-]
I_c [-]
q_c [MPa]
f_s [MPa]
R_f [%]
u_2 [MPa]
Soil Description
Geophys Horizon
Geotech Layer
403
207
401
202
403
408
202
201
211
403
207
B01
B03
B04
B08
B09
B10
B11
B12
US01
UC03
US04
UC08
US10
US11
UC11
UC11
US11
UC12

HS_S_07

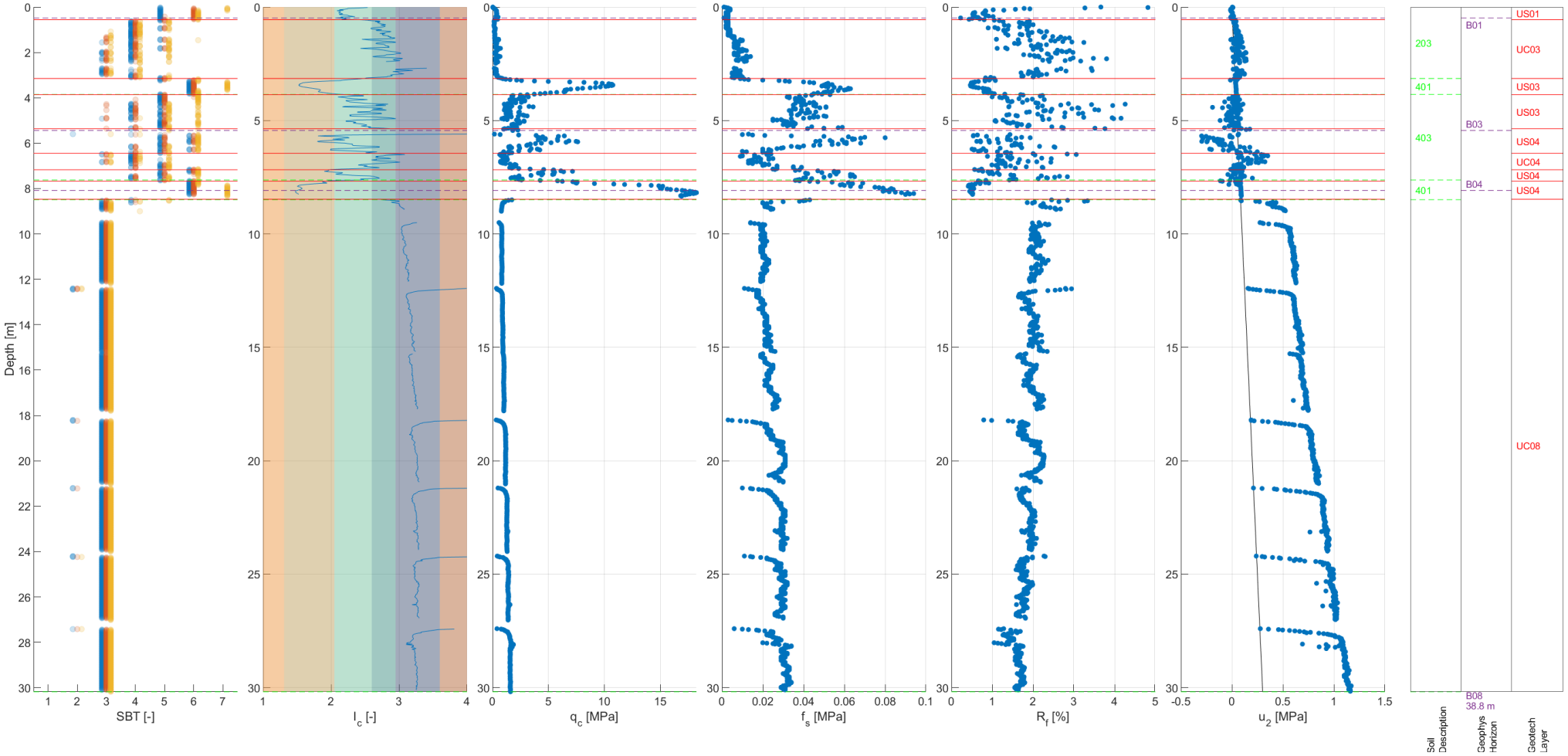
Depth [m]
SBT [-]
I_c [-]
q_c [MPa]
f_s [MPa]
R_f [%]
u_2 [MPa]
Soil Description
Geophys Horizon
Geotech Layer
203
401
403
401
B01
B03
B04
B08
38.8 m
US01
UC03
US03
US03
US04
UC04
US04
US04
UC08

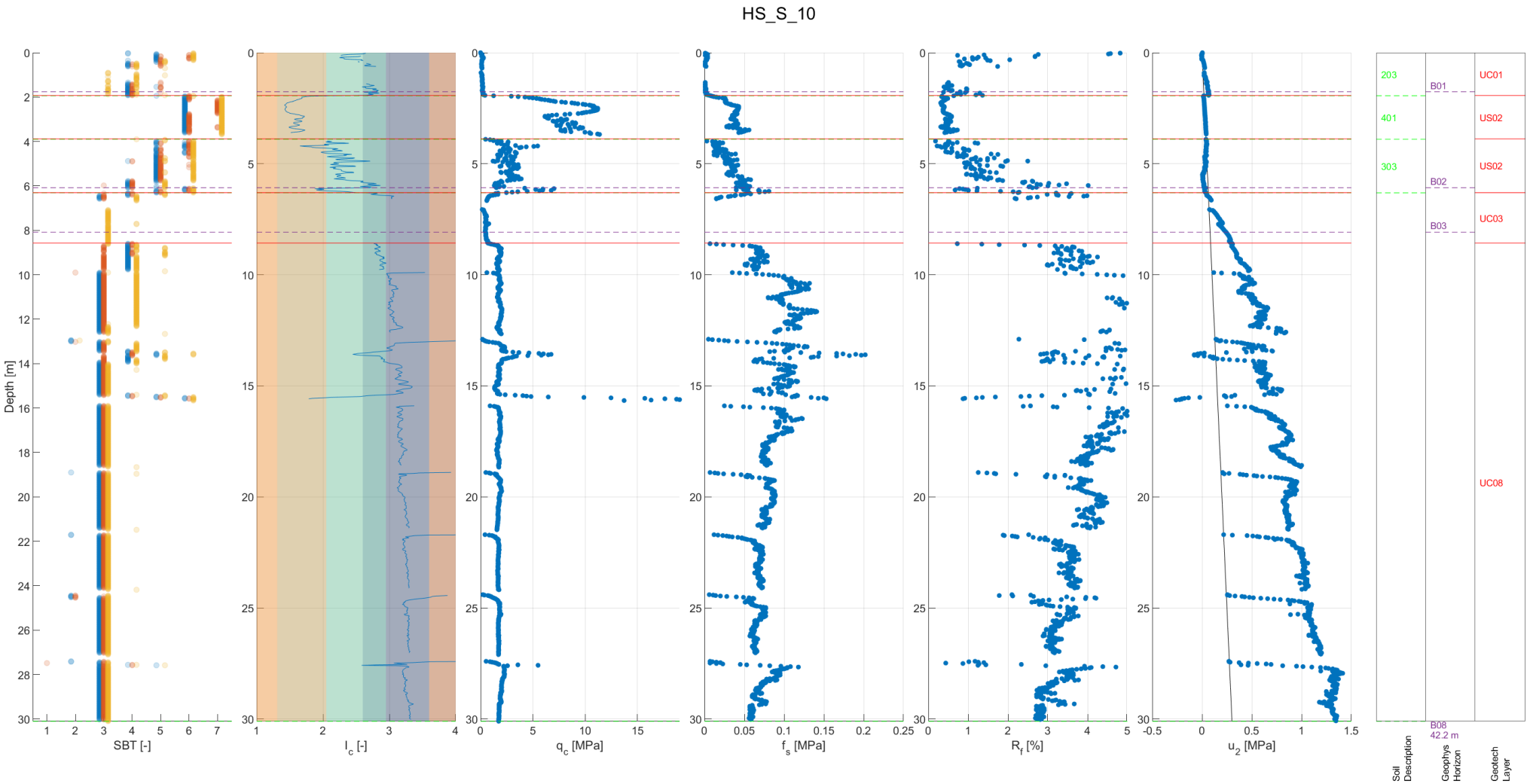
HS_S_10
Depth [m]
SBT [-]
I_c [-]
q_c [MPa]
f_s [MPa]
R_f [%]
u_2 [MPa]
203
401
303
B01
B02
B03
B08
42.2 m
UC01
US02
US02
UC03
UC08
Soil Description
Geophys Horizon
Geotech Layer

HS_S_11

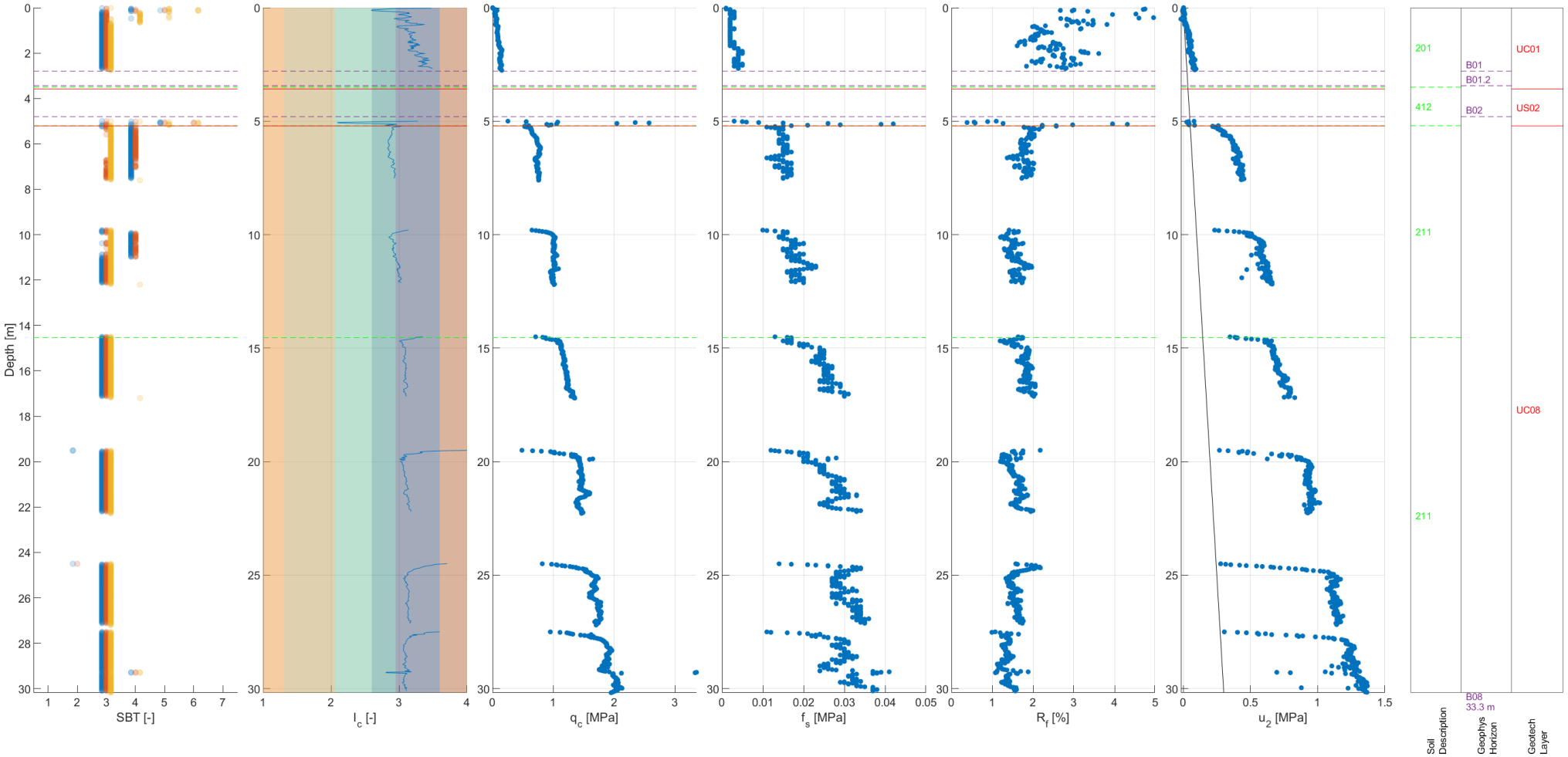
Depth [m]
SBT [-]
I_c [-]
q_c [MPa]
f_s [MPa]
R_f [%]
u_2 [MPa]
201
412
211
211
B01
B01.2
B02
B08
33.3 m
UC01
US02
UC08
Soil Description
Geophys Horizon
Geotech Layer

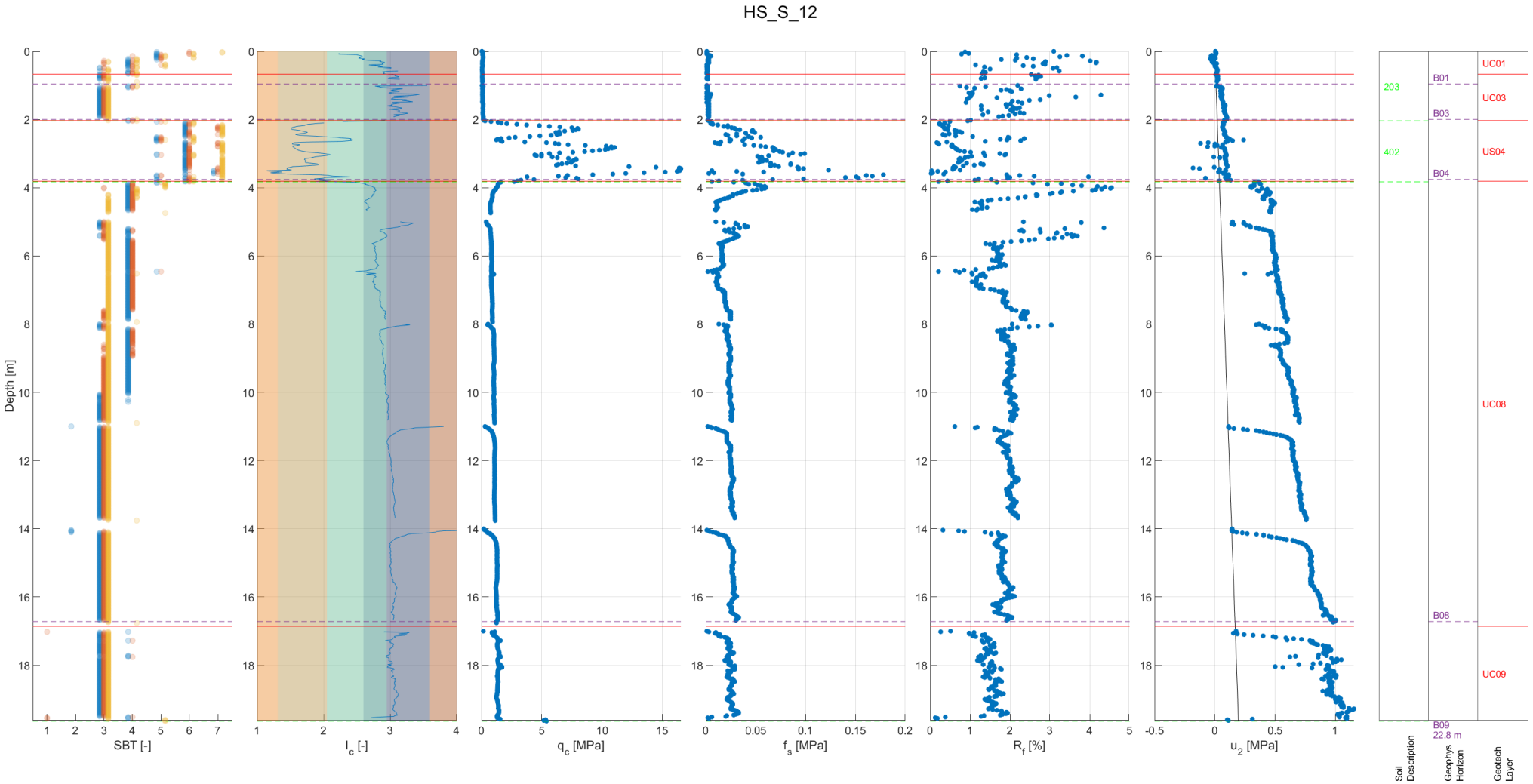
HS_S_12
Depth [m]
SBT [-]
I_c [-]
q_c [MPa]
f_s [MPa]
R_f [%]
u_2 [MPa]
203
402
B01
B03
B04
B08
B09
22.8 m
UC01
UC03
US04
UC08
UC09
Soil Description
Geophys Horizon
Geotech Layer

HS_S_13

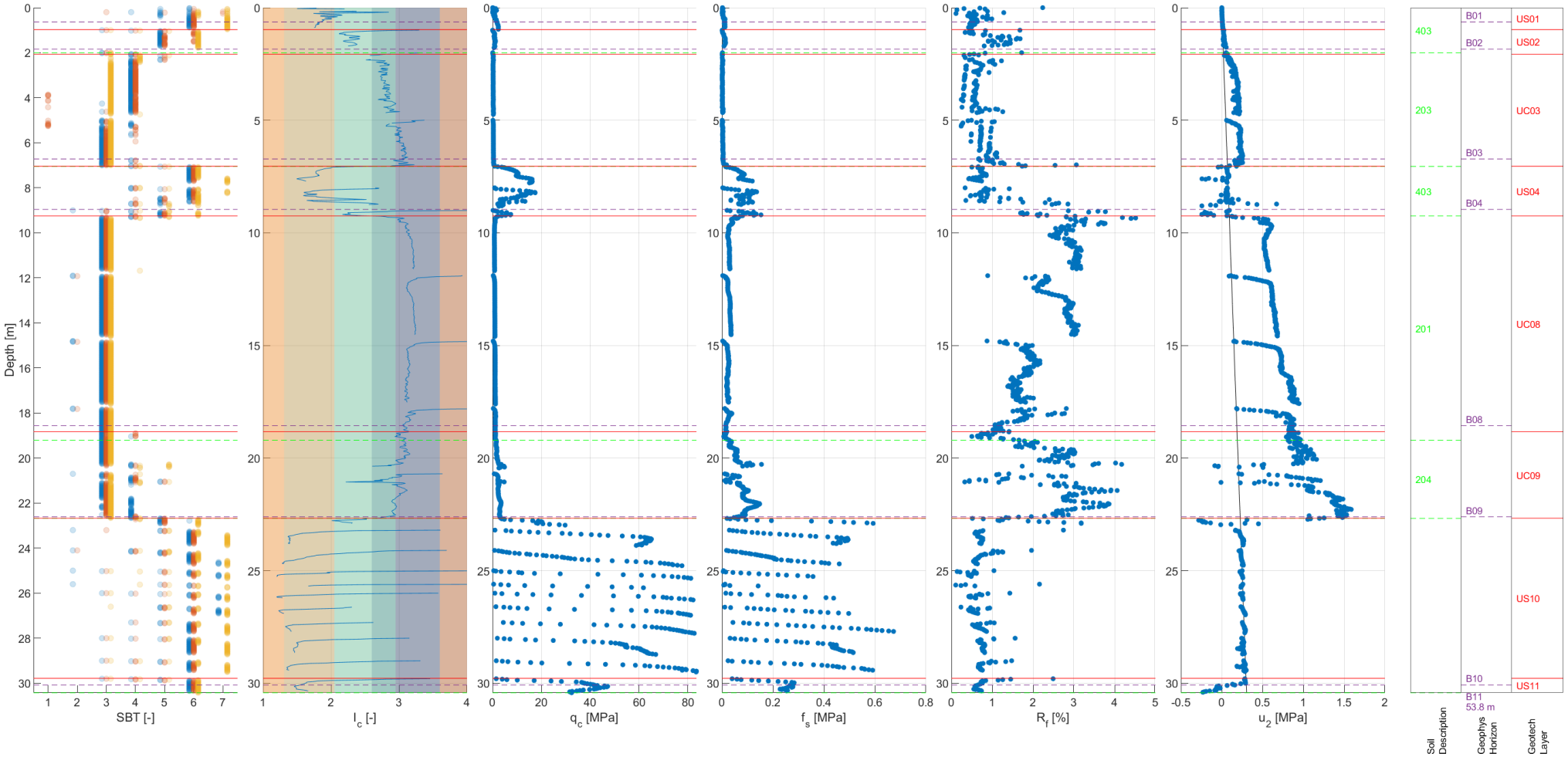
Depth [m]
SBT [-]
I_c [-]
q_c [MPa]
f_s [MPa]
R_f [%]
u_2 [MPa]
403
203
403
201
204
B01
B02
B03
B04
B08
B09
B10
B11
53.8 m
US01
US02
UC03
US04
UC08
UC09
US10
US11
Soil Description
Geophys Horizon
Geotech Layer

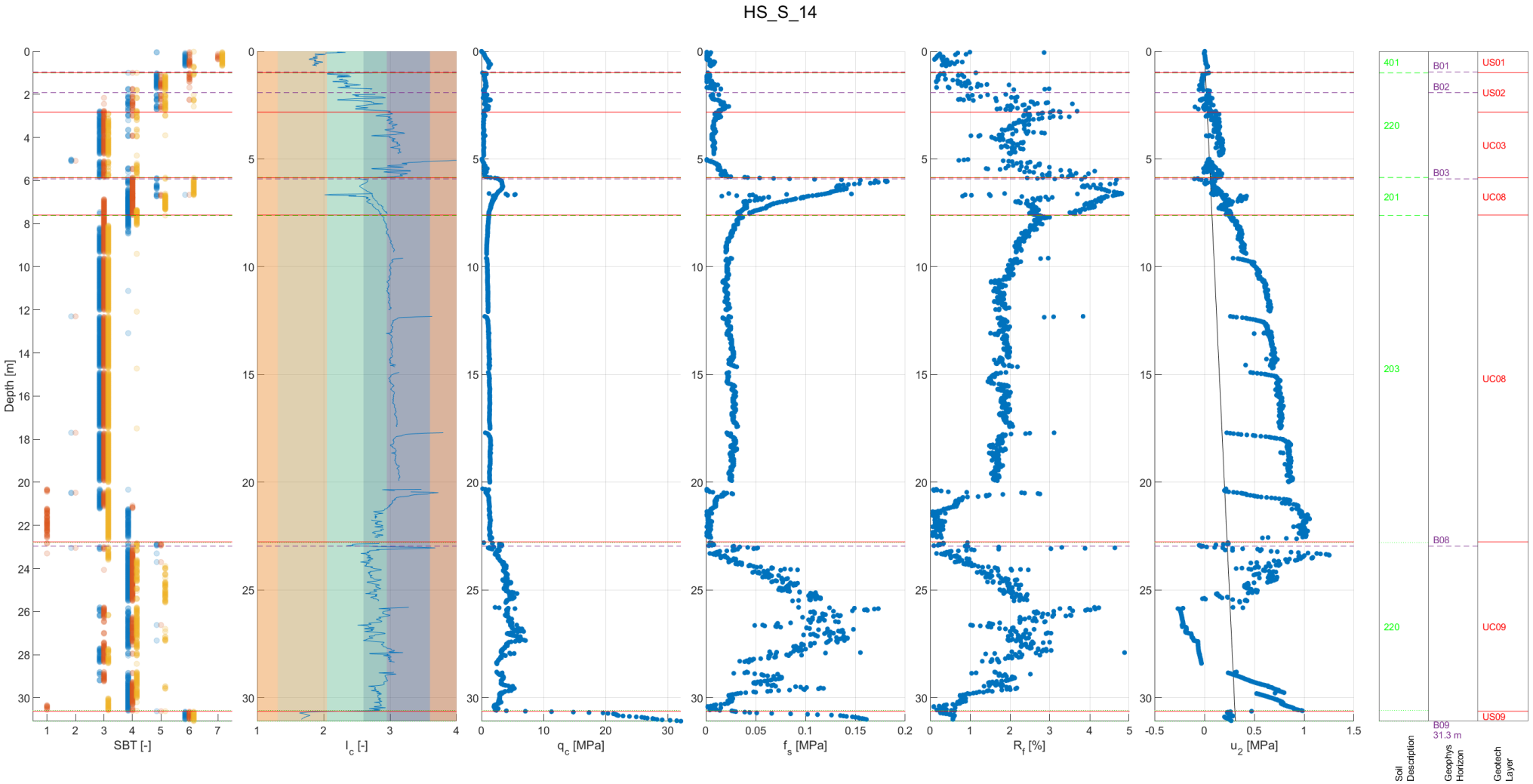
HS_S_14
Depth [m]
SBT [-]
I_c [-]
q_c [MPa]
f_s [MPa]
R_f [%]
u_2 [MPa]
401
220
201
203
220
B01
B02
B03
B08
B09
31.3 m
US01
US02
UC03
UC08
UC08
UC09
US09
Soil Description
Geophys Horizon
Geotech Layer

HS_S_16

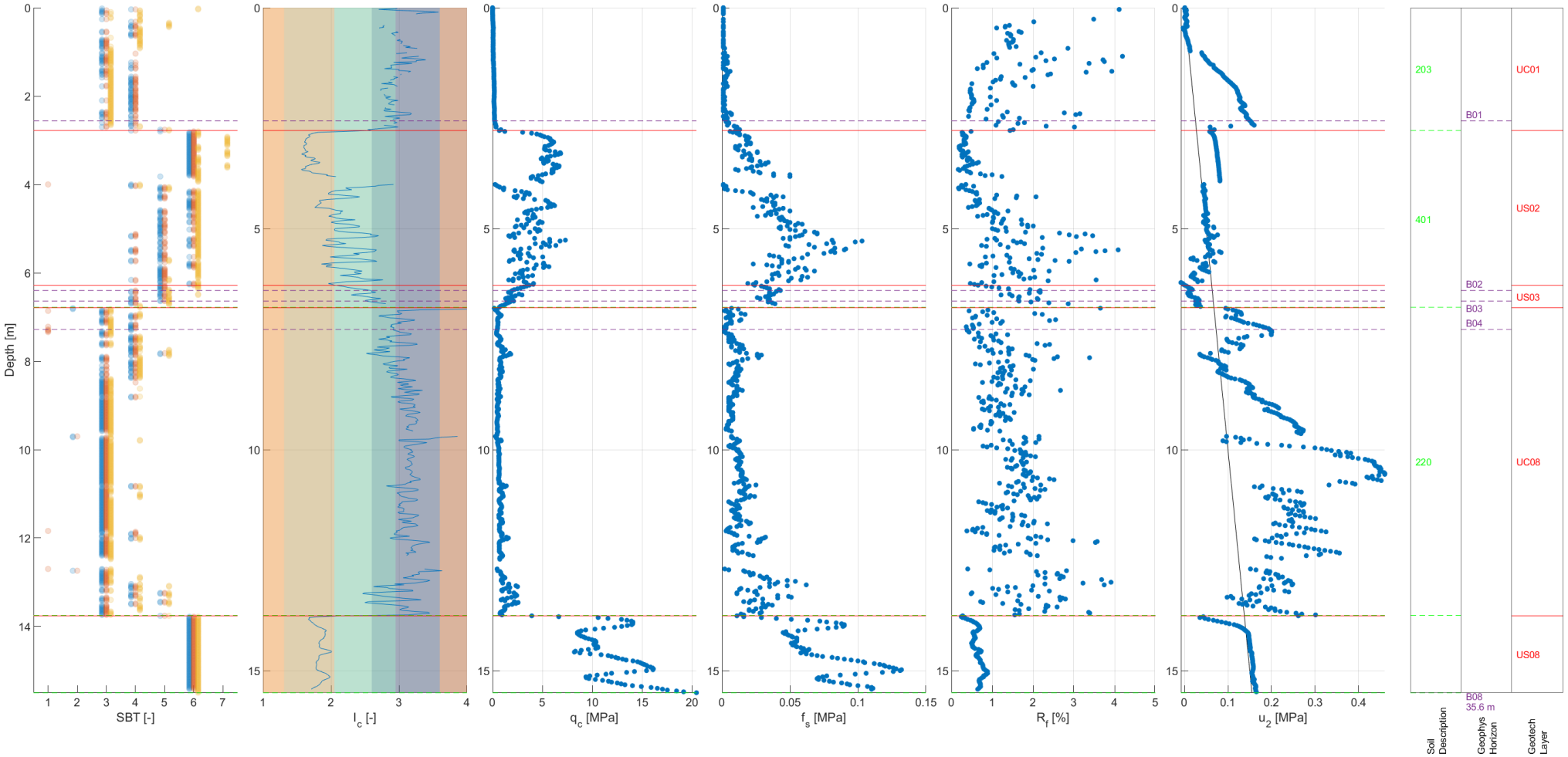
Depth [m]
SBT [-]
I_c [-]
q_c [MPa]
f_s [MPa]
R_f [%]
u_2 [MPa]
203
401
220
B01
B02
B03
B04
B08
35.6 m
UC01
US02
US03
UC08
US08
Soil Description
Geophys Horizon
Geotech Layer

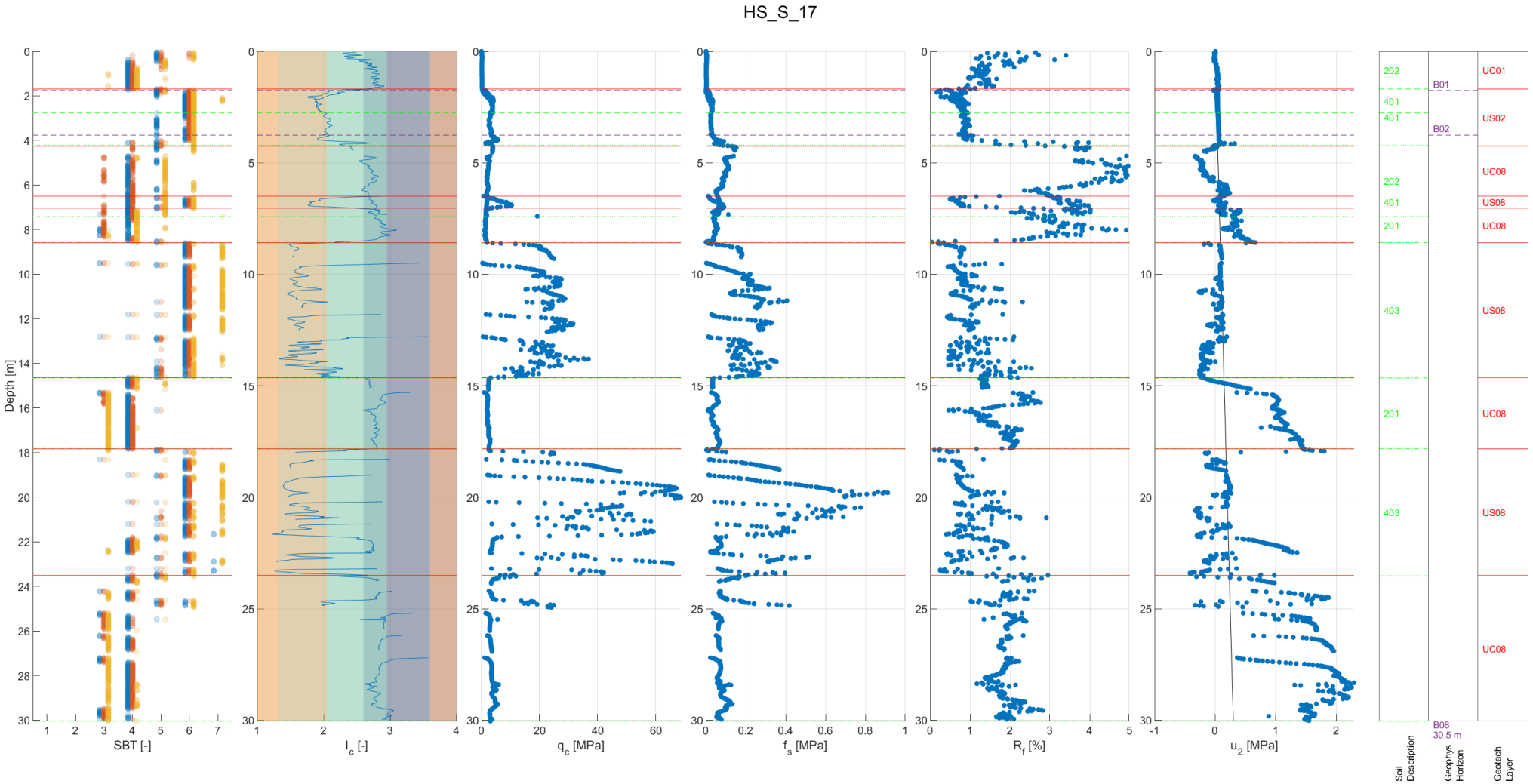
HS_S_17
Depth [m]
SBT [-]
I_c [-]
q_c [MPa]
f_s [MPa]
R_f [%]
u_2 [MPa]
Soil Description
Geophys Horizon
Geotech Layer
202
401
401
202
401
201
403
201
403
B01
B02
B08
30.5 m
UC01
US02
UC08
US08
UC08
US08
UC08
US08
UC08

HS_S_18

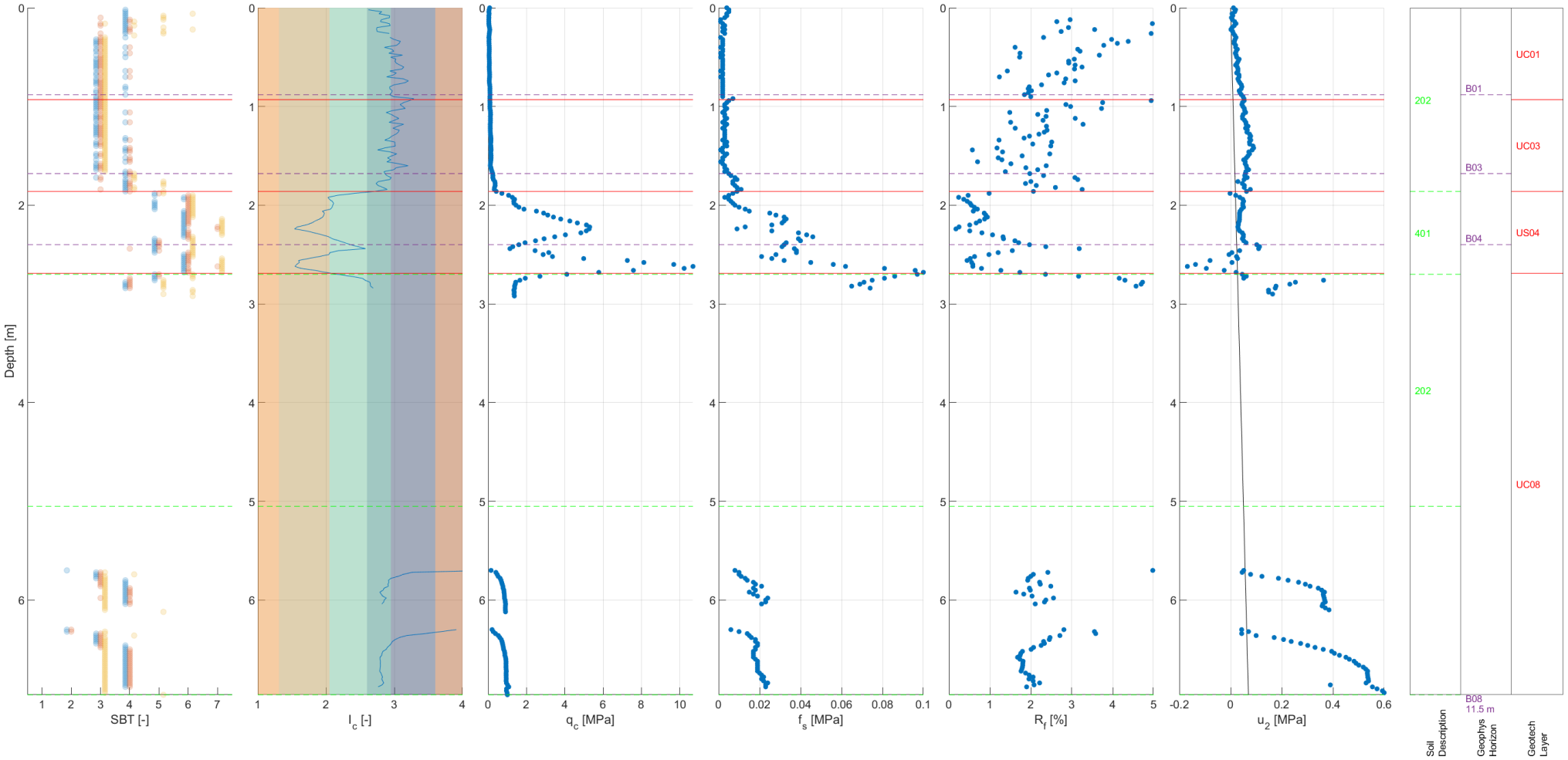
Depth [m]
SBT [-]
I_c [-]
q_c [MPa]
f_s [MPa]
R_f [%]
u_2 [MPa]
Soil Description
Geophys Horizon
Geotech Layer
202
401
202
B01
B03
B04
B08
11.5 m
UC01
UC03
US04
UC08

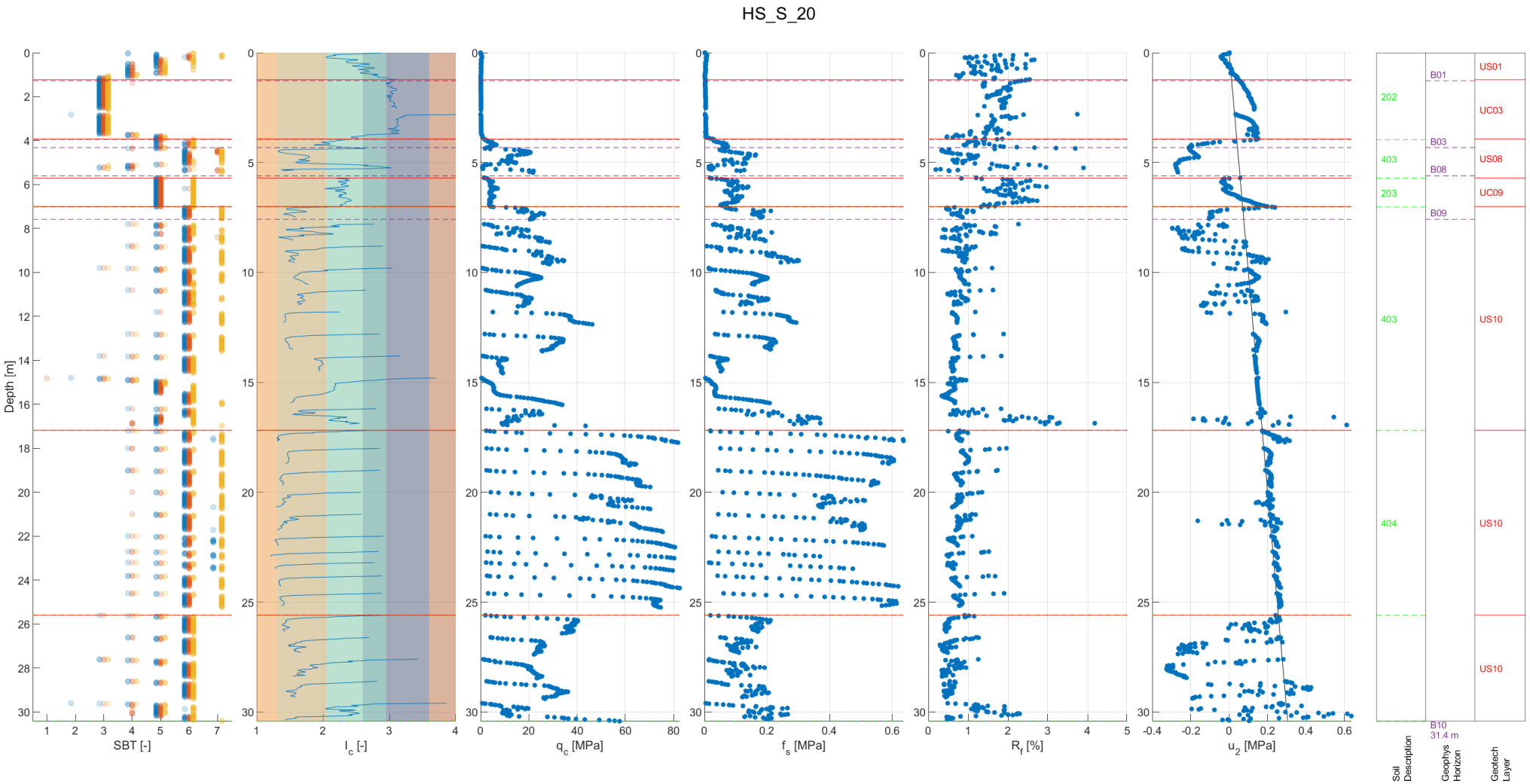
HS_S_20
Depth [m]
SBT [-]
I_c [-]
q_c [MPa]
f_s [MPa]
R_f [%]
u_2 [MPa]
Soil Description
Geophys Horizon
Geotech Layer
202
403
203
403
404
B01
B03
B08
B09
B10
31.4 m
US01
UC03
US08
UC09
US10
US10
US10

HS_S_21

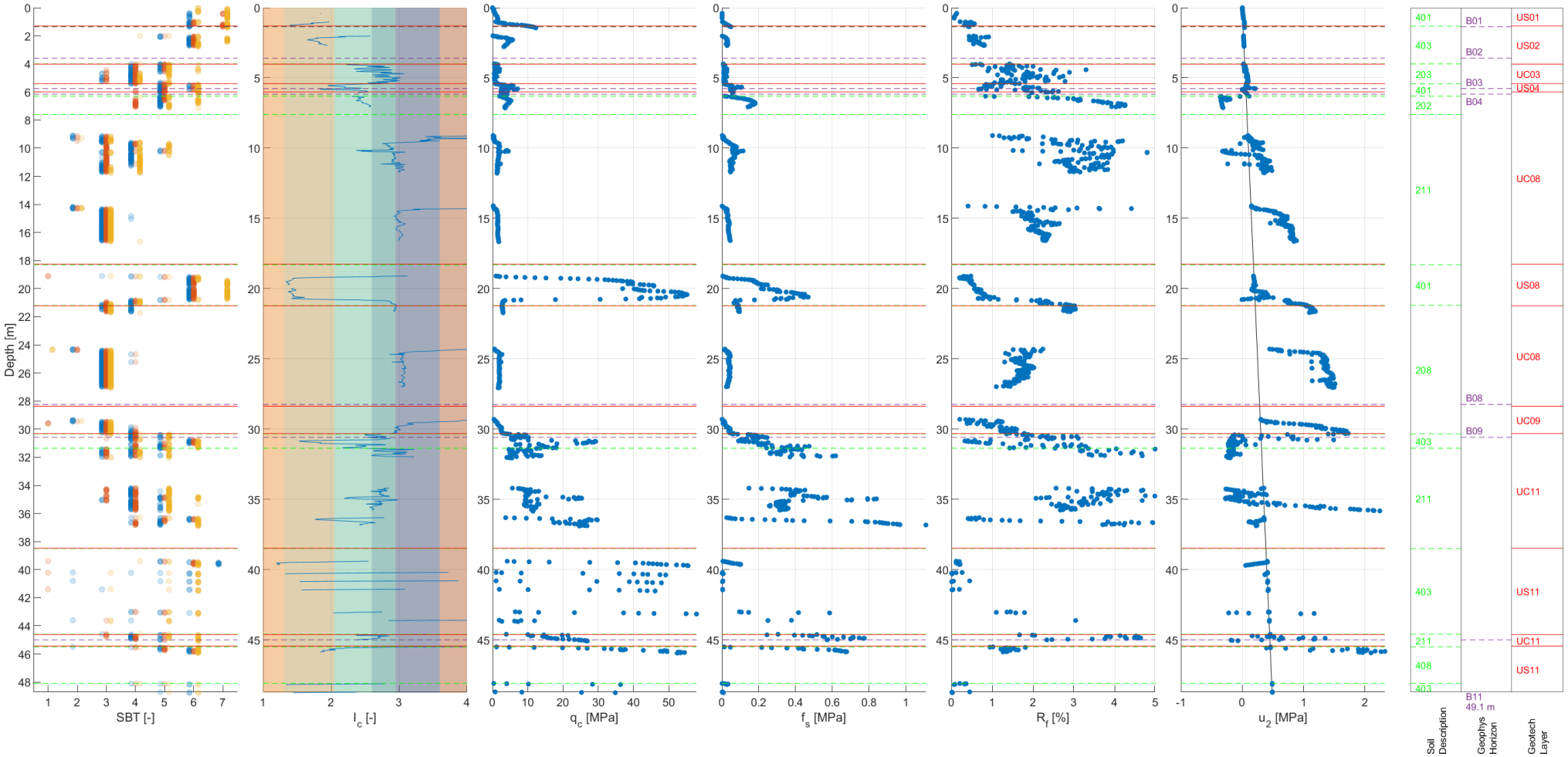
Depth [m]
SBT [-]
I_c [-]
q_c [MPa]
f_s [MPa]
R_f [%]
u_2 [MPa]
Soil Description
Geophys Horizon
Geotech Layer
B01
B02
B03
B04
B08
B09
B11
49.1 m
US01
US02
UC03
US04
UC08
US08
UC08
UC09
UC11
US11
UC11
US11

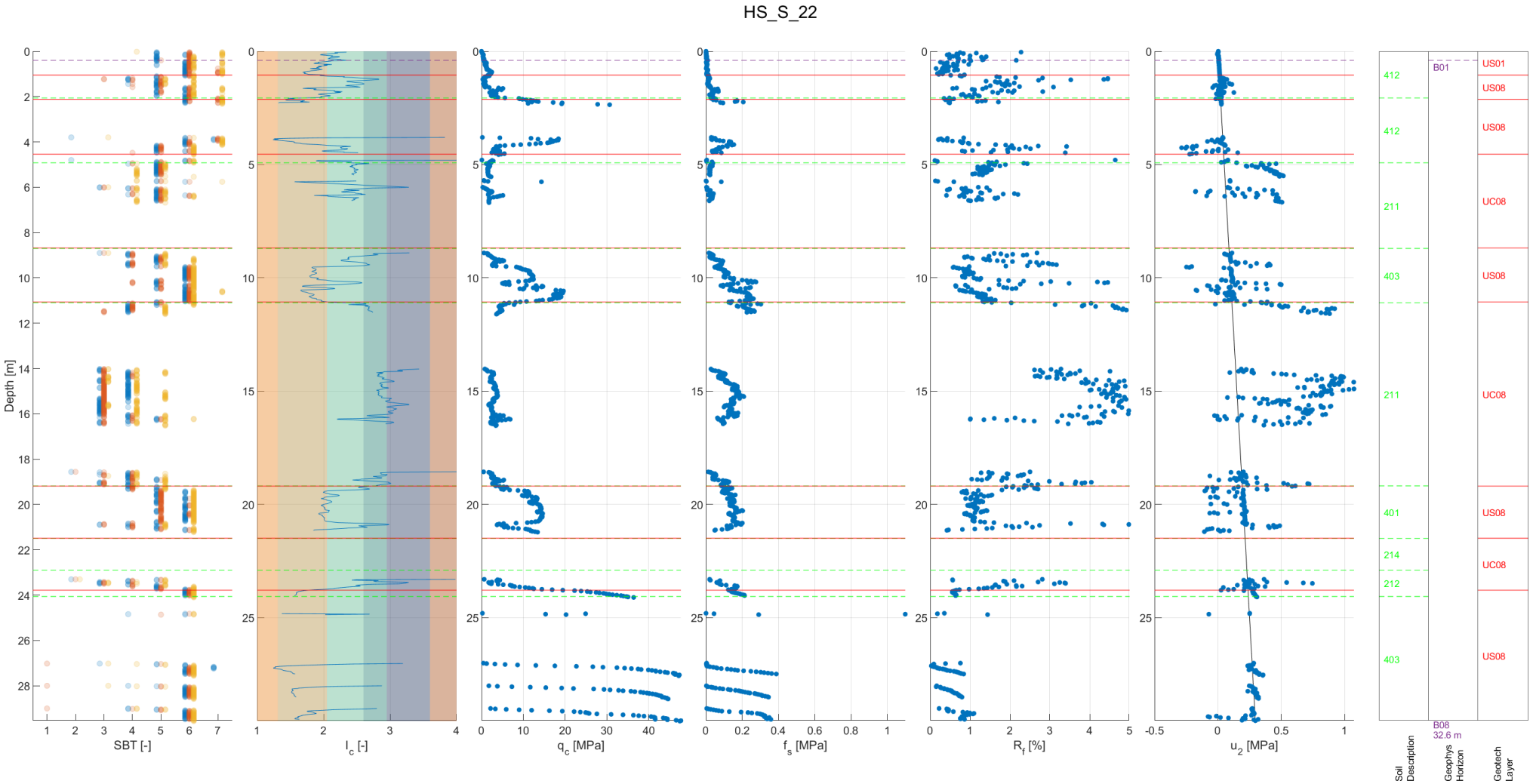
HS_S_22
Depth [m]
SBT [-]
I_c [-]
q_c [MPa]
f_s [MPa]
R_f [%]
u_2 [MPa]
412
412
211
403
211
401
214
212
403
B01
B08
32.6 m
US01
US08
US08
UC08
US08
UC08
US08
UC08
US08
Soil Description
Geophys Horizon
Geotech Layer

HS_S_23

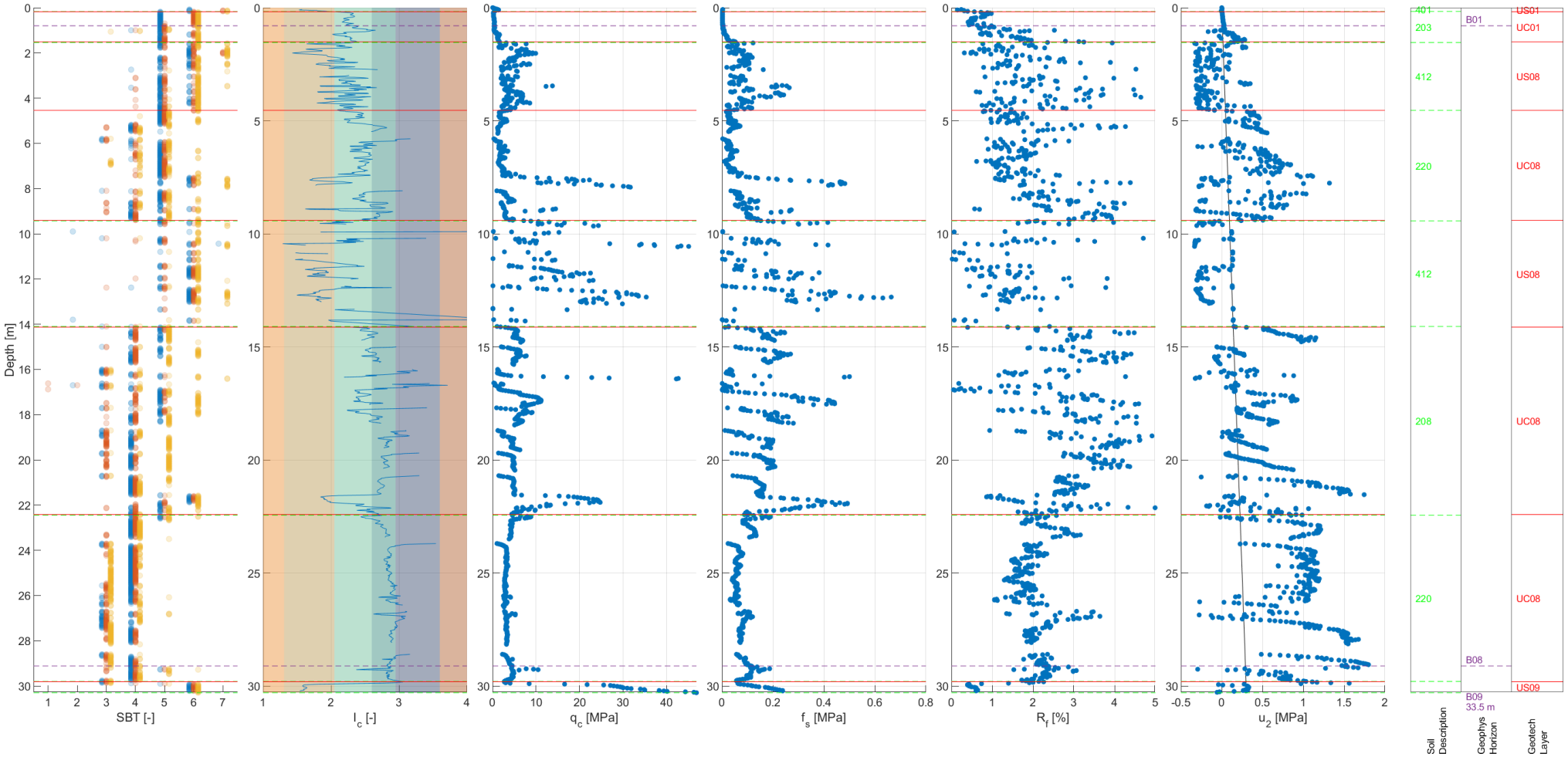
Depth [m]
SBT [-]
I_c [-]
q_c [MPa]
f_s [MPa]
R_f [%]
u_2 [MPa]
401
203
412
220
412
208
220
B01
B08
B09
33.5 m
US01
UC01
US08
UC08
US08
UC08
UC08
US09
Soil Description
Geophys Horizon
Geotech Layer

HS_S_24

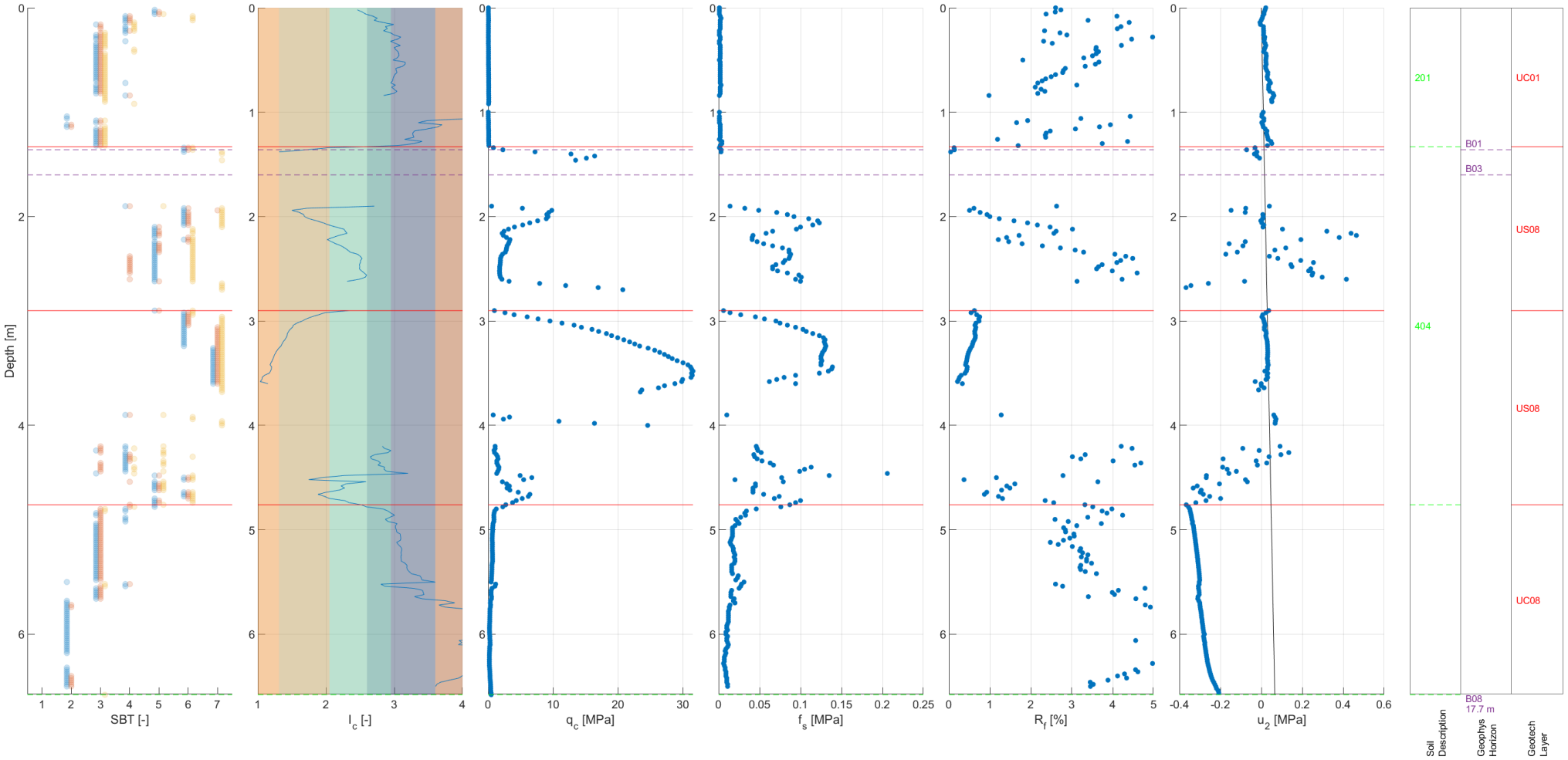
Depth [m]
SBT [-]
I_c [-]
q_c [MPa]
f_s [MPa]
R_f [%]
u_2 [MPa]
201
404
B01
B03
B08
17.7 m
UC01
US08
US08
UC08
Soil Description
Geophys Horizon
Geotech Layer

HS_S_26

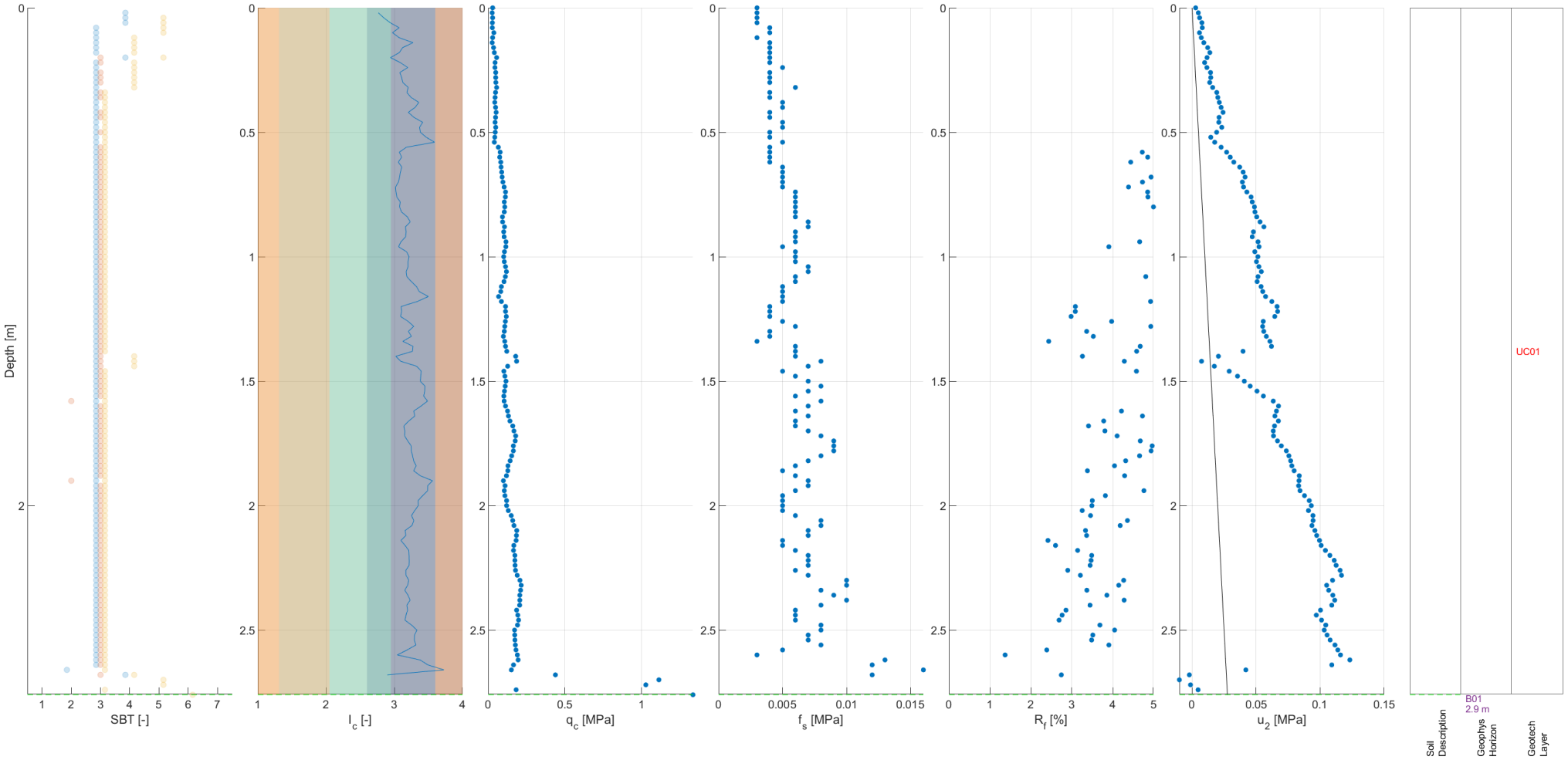
Depth [m]
SBT [-]
I_c [-]
q_c [MPa]
f_s [MPa]
R_f [%]
u_2 [MPa]
UC01
B01
2.9 m
Soil Description
Geophys Horizon
Geotech Layer

HS_S_27

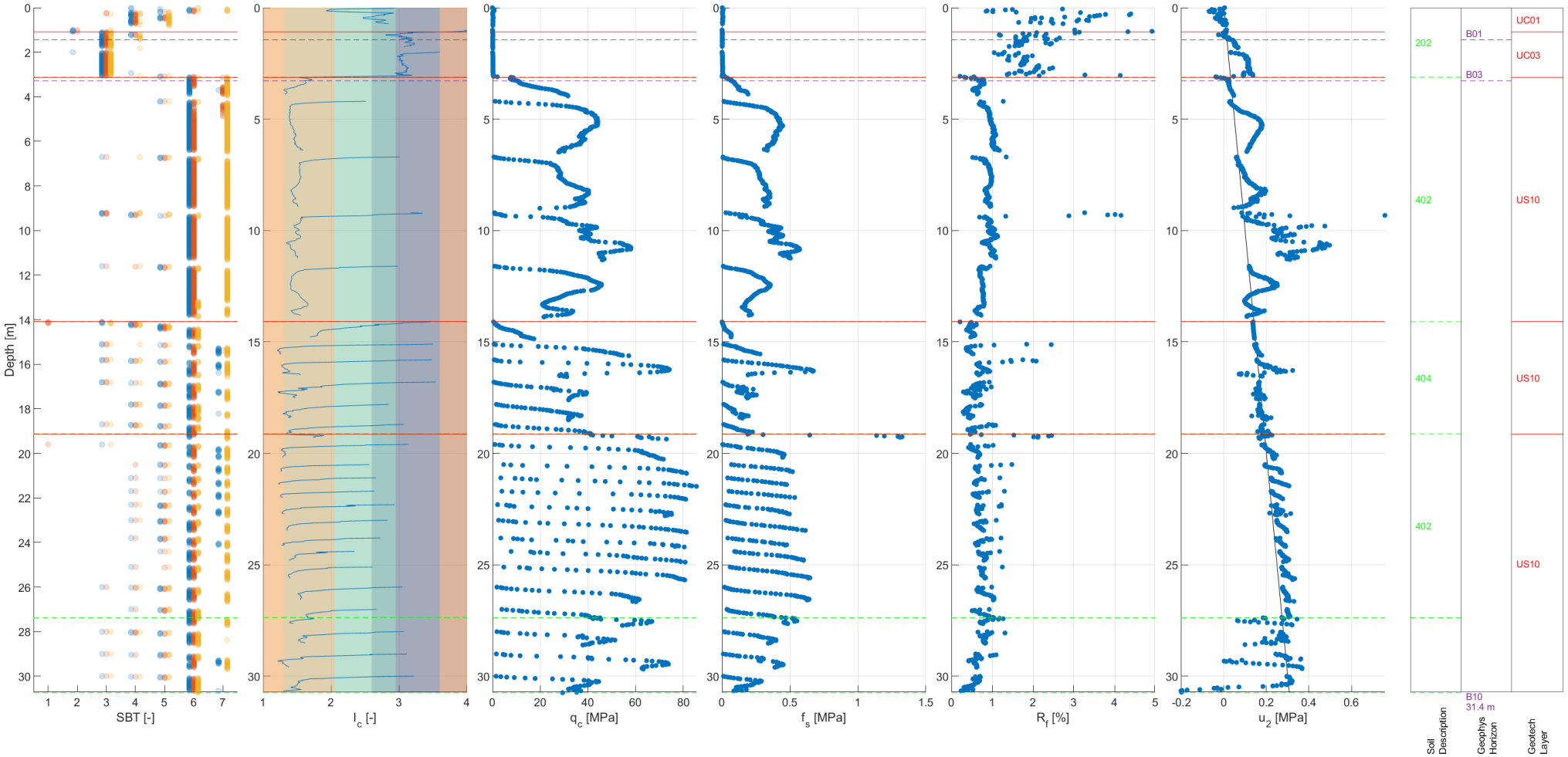
Depth [m]
SBT [-]
I_c [-]
q_c [MPa]
f_s [MPa]
R_f [%]
u_2 [MPa]
202
402
404
402
B01
B03
B10
31.4 m
UC01
UC03
US10
US10
US10
Soil Description
Geophys Horizon
Geotech Layer

HS_S_28

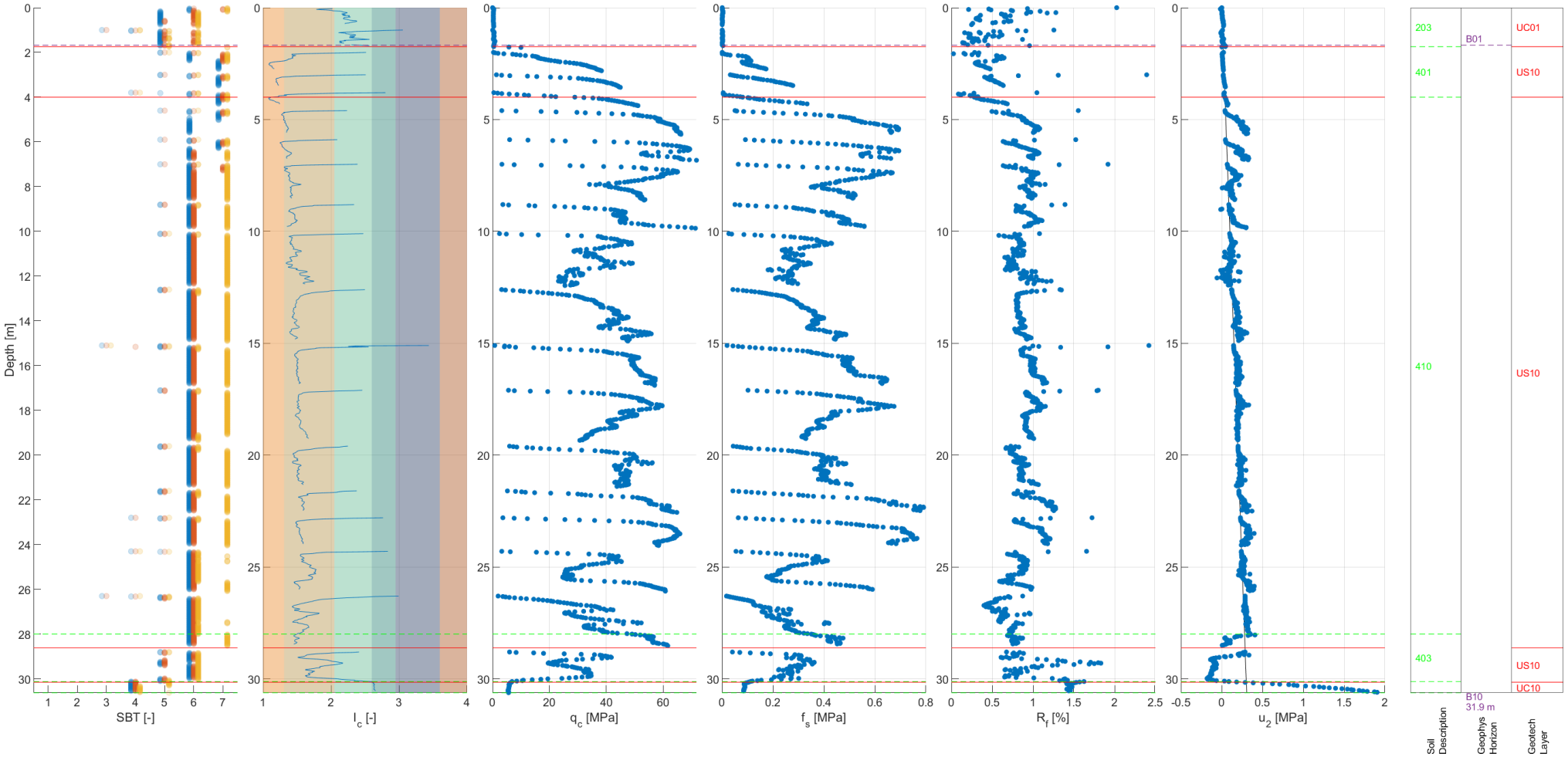
Depth [m]
SBT [-]
I_c [-]
q_c [MPa]
f_s [MPa]
R_f [%]
u_2 [MPa]
203
401
410
403
B01
B10
31.9 m
UC01
US10
US10
US10
UC10
Soil Description
Geophys Horizon
Geotech Layer

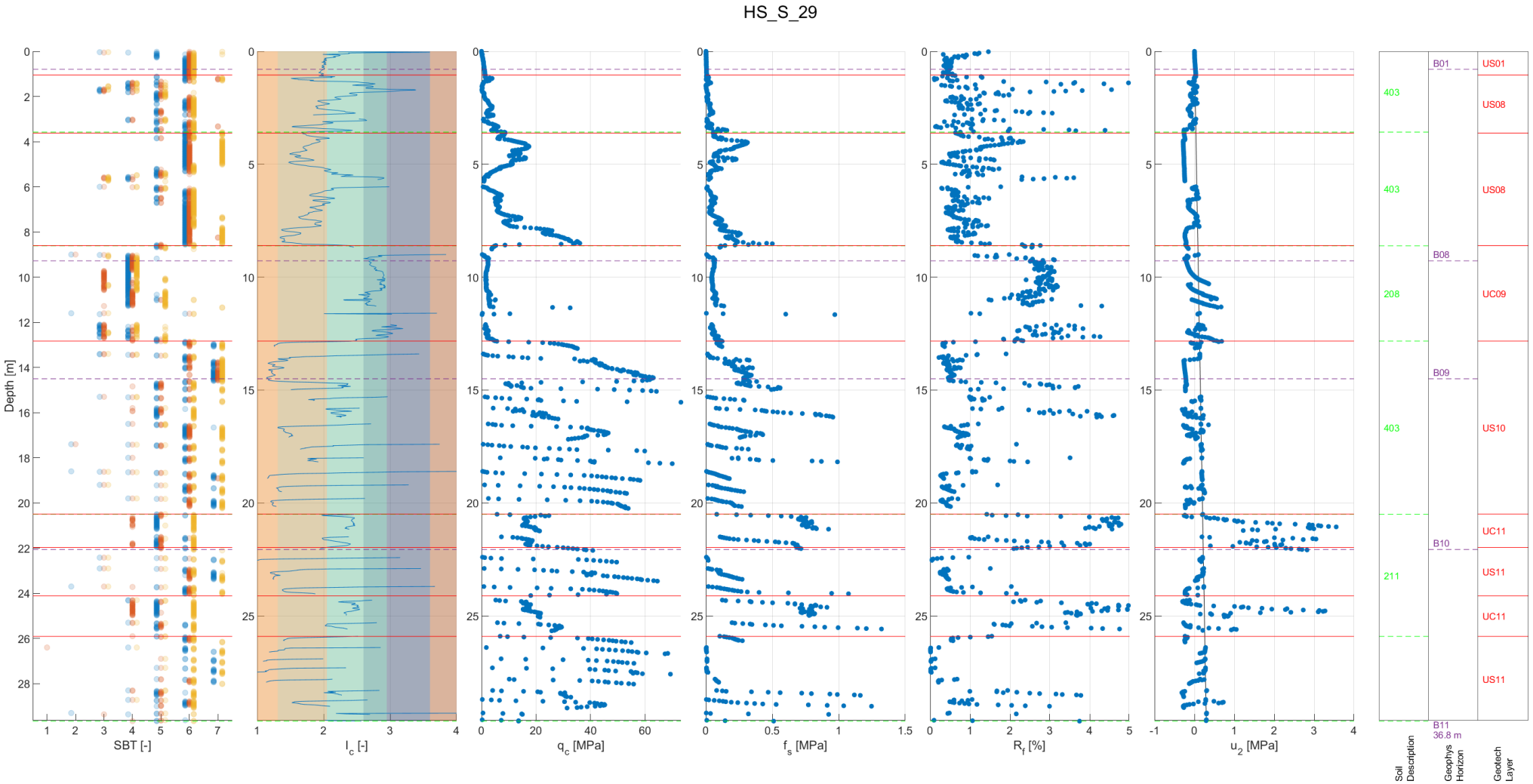
HS_S_29
Depth [m]
SBT [-]
I_c [-]
q_c [MPa]
f_s [MPa]
R_f [%]
u_2 [MPa]
Soil Description
Geophys Horizon
Geotech Layer
403
403
208
403
211
B01
B08
B09
B10
B11
36.8 m
US01
US08
US08
UC09
US10
UC11
US11
UC11
US11

HS_S_30

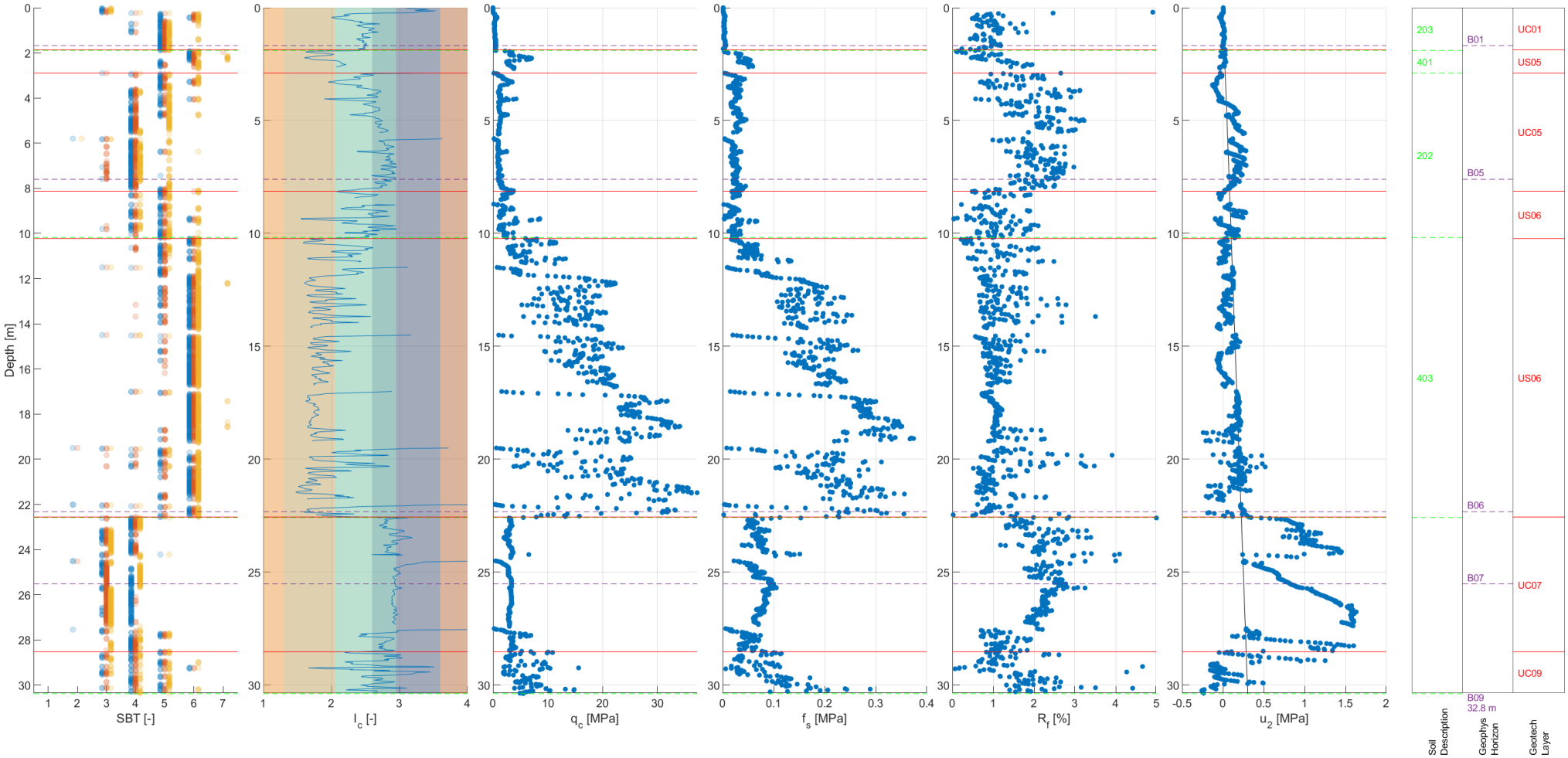
Depth [m]
SBT [-]
I_c [-]
q_c [MPa]
f_s [MPa]
R_f [%]
u_2 [MPa]
203
401
202
403
B01
B05
B06
B07
B09
32.8 m
UC01
US05
UC05
US06
US06
UC07
UC09
Soil Description
Geophys Horizon
Geotech Layer

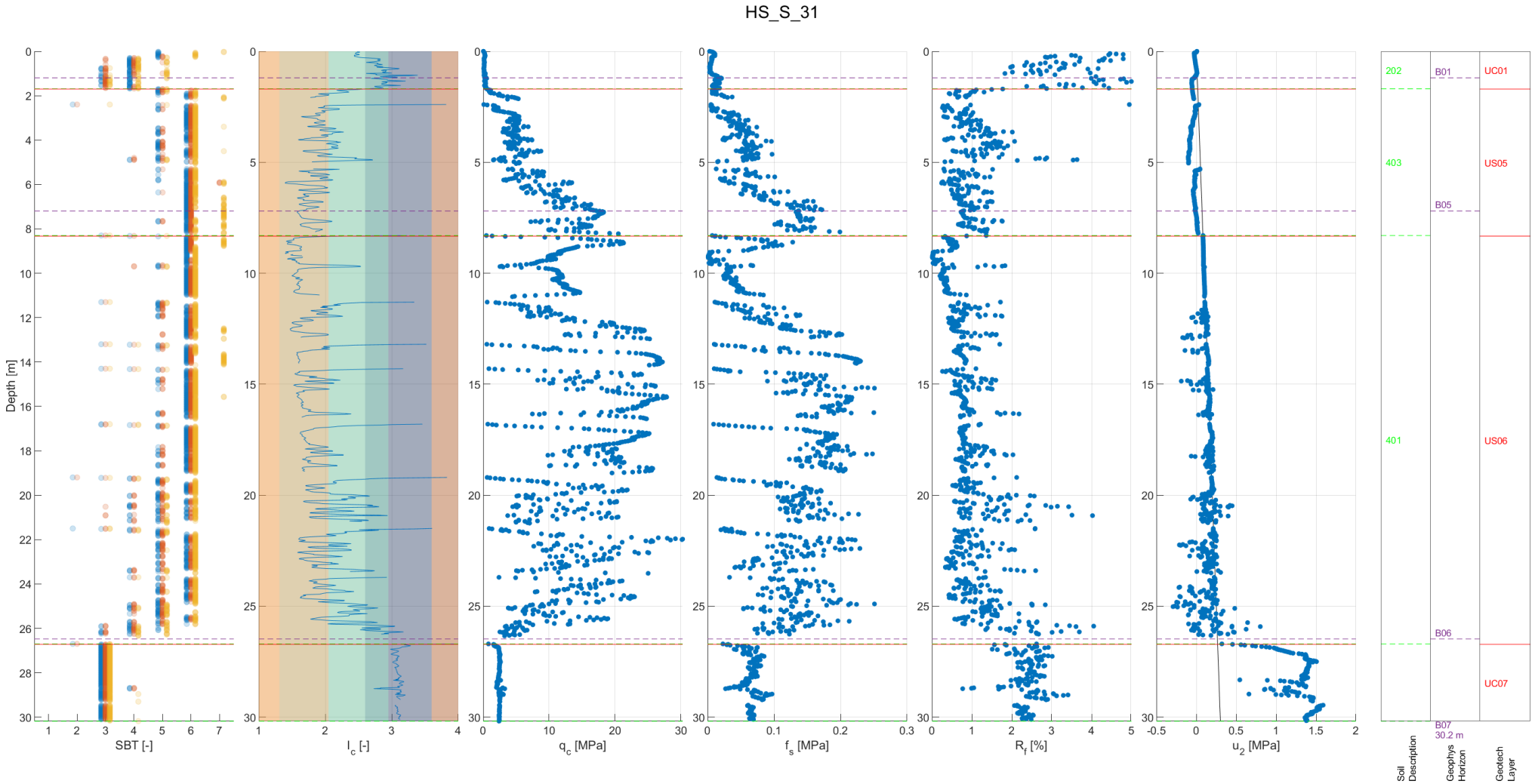
HS_S_31
Depth [m]
SBT [-]
I_c [-]
q_c [MPa]
f_s [MPa]
R_f [%]
u_2 [MPa]
202
403
401
B01
B05
B06
B07
30.2 m
UC01
US05
US06
UC07
Soil Description
Geophys Horizon
Geotech Layer

HS_S_32

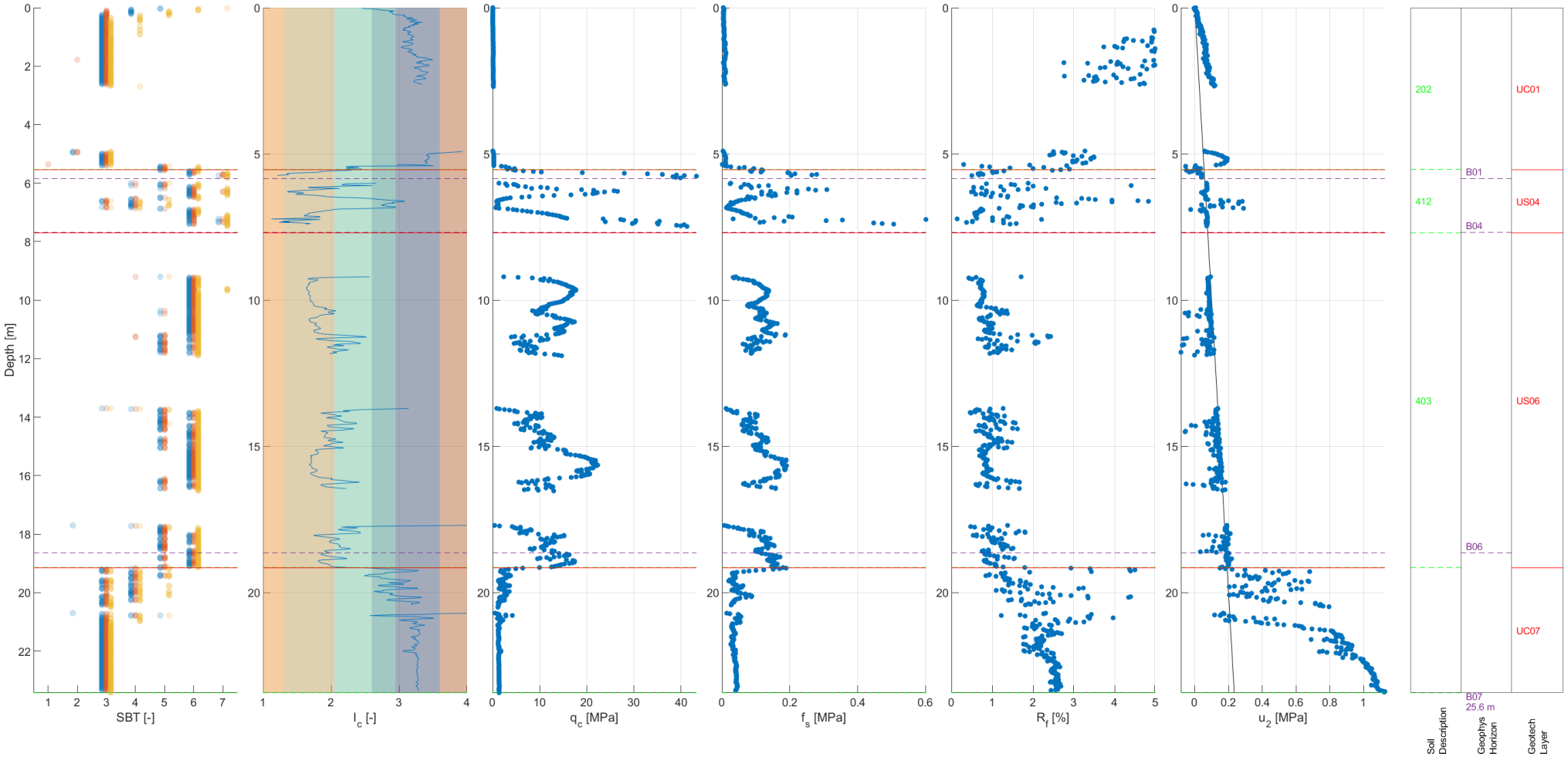
Depth [m]
SBT [-]
I_c [-]
q_c [MPa]
f_s [MPa]
R_f [%]
u_2 [MPa]
202
412
403
B01
B04
B06
B07
25.6 m
UC01
US04
US06
UC07
Soil Description
Geophys Horizon
Geotech Layer

HS_S_33

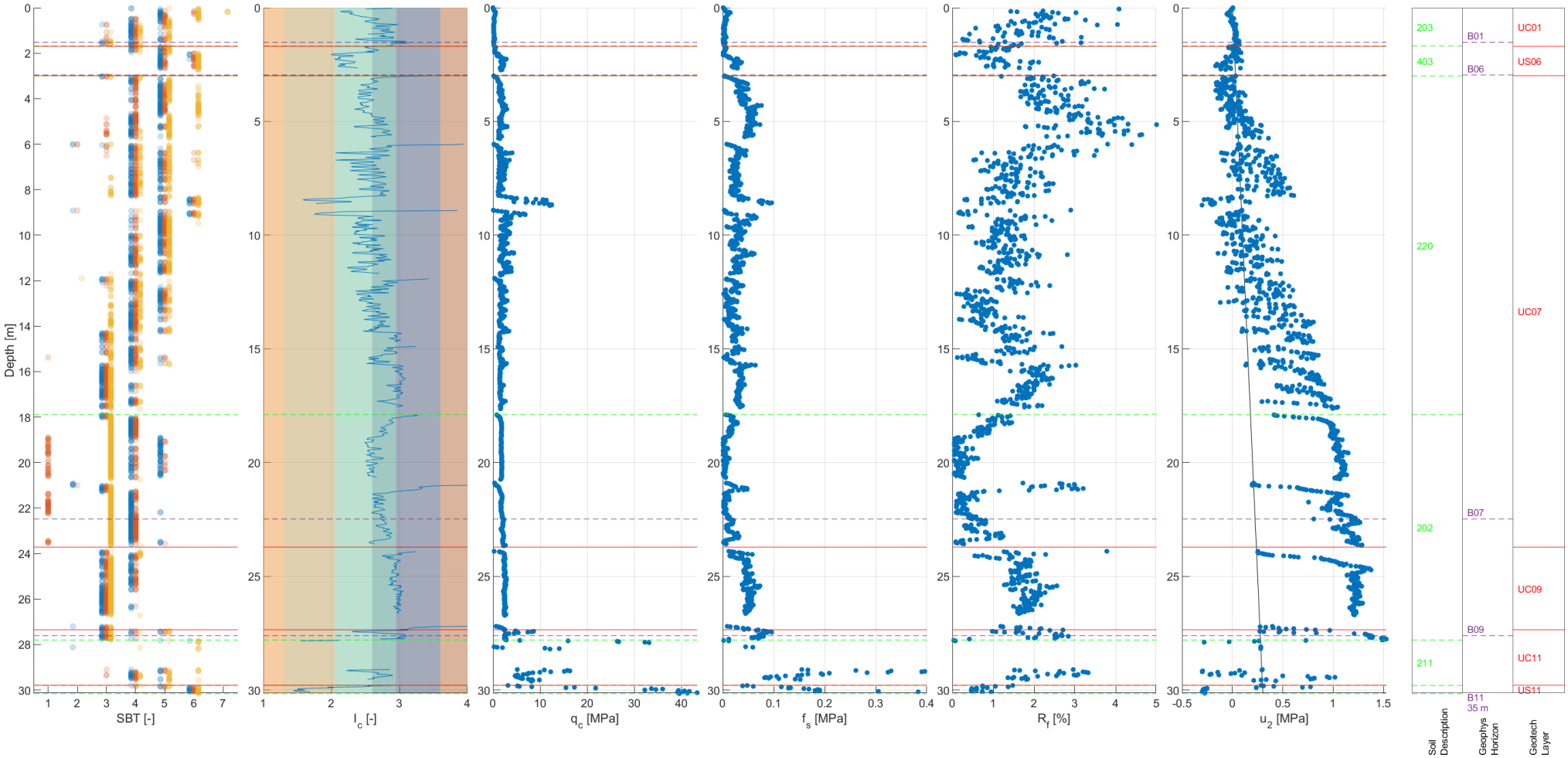
Depth [m]
SBT [-]
I_c [-]
q_c [MPa]
f_s [MPa]
R_f [%]
u_2 [MPa]
203
403
220
202
211
B01
B06
B07
B09
B11
35 m
UC01
US06
UC07
UC09
UC11
US11
Soil Description
Geophys Horizon
Geotech Layer

HS_S_35

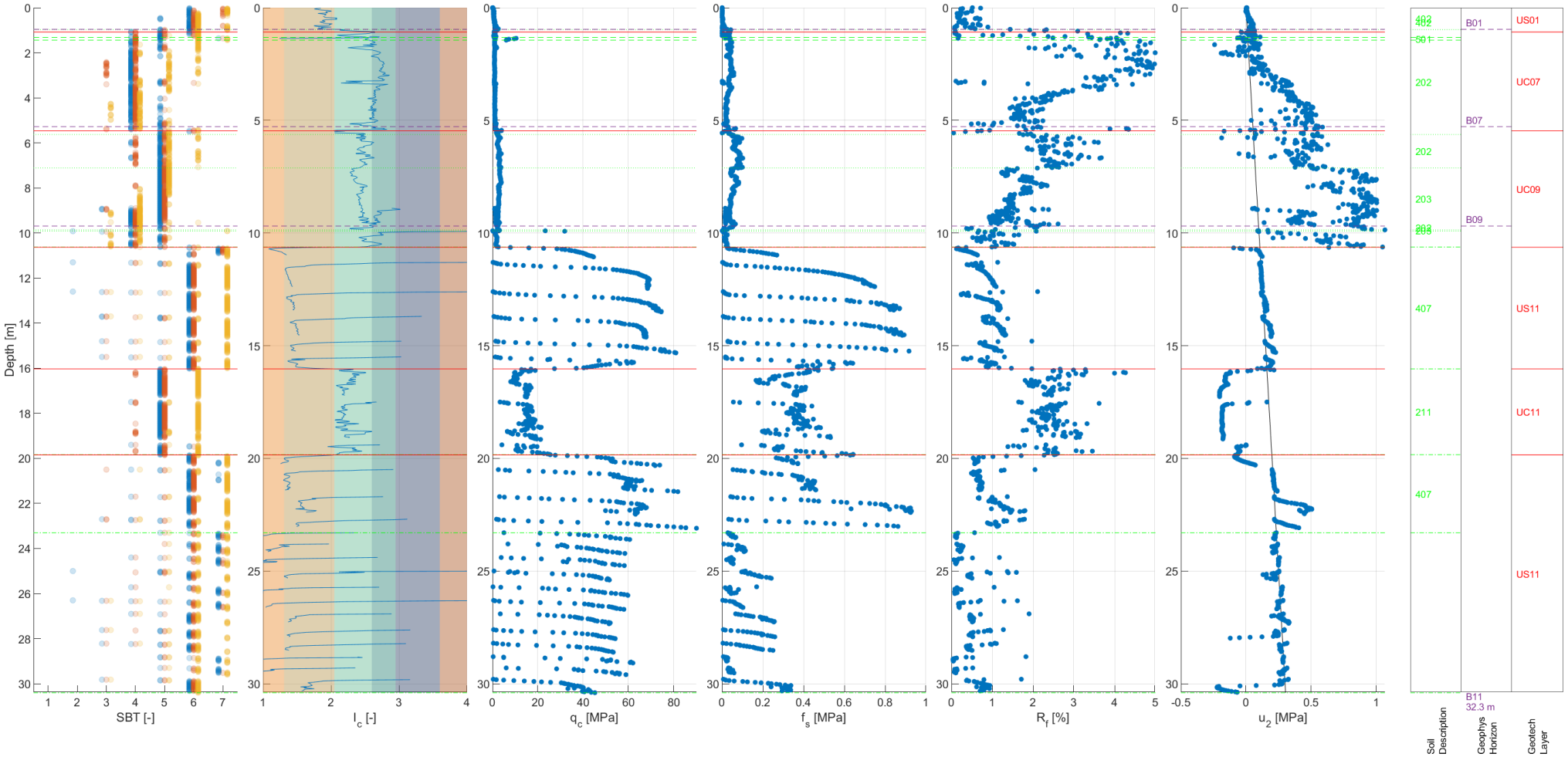
Depth [m]
SBT [-]
I_c [-]
q_c [MPa]
f_s [MPa]
R_f [%]
u_2 [MPa]
B01
B07
B09
B11
32.3 m
US01
UC07
UC09
US11
UC11
US11
Soil Description
Geophys Horizon
Geotech Layer

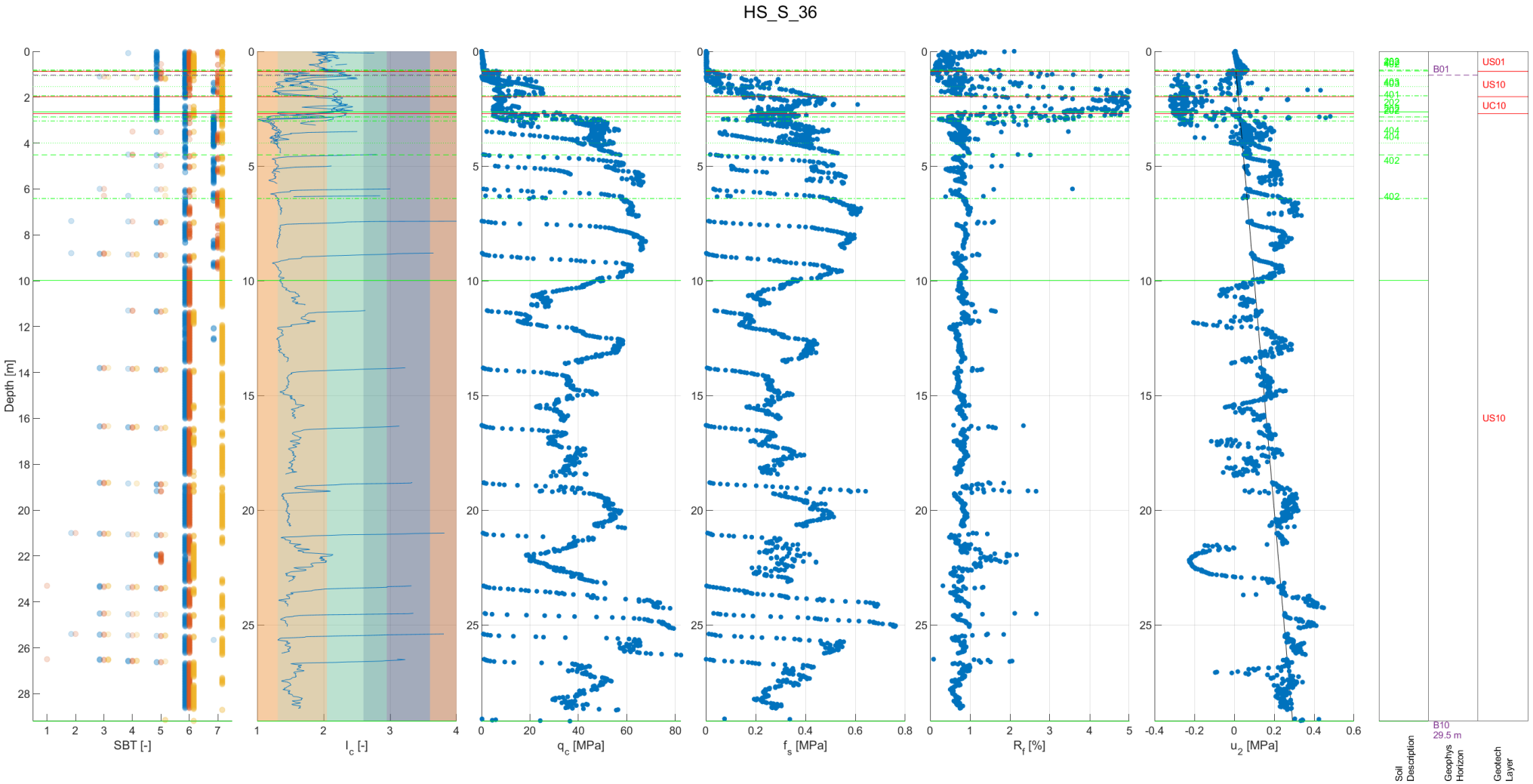
HS_S_36
Depth [m]
SBT [-]
I_c [-]
q_c [MPa]
f_s [MPa]
R_f [%]
u_2 [MPa]
B01
B10
29.5 m
US01
US10
UC10
US10
Soil Description
Geophys Horizon
Geotech Layer

HS_S_37

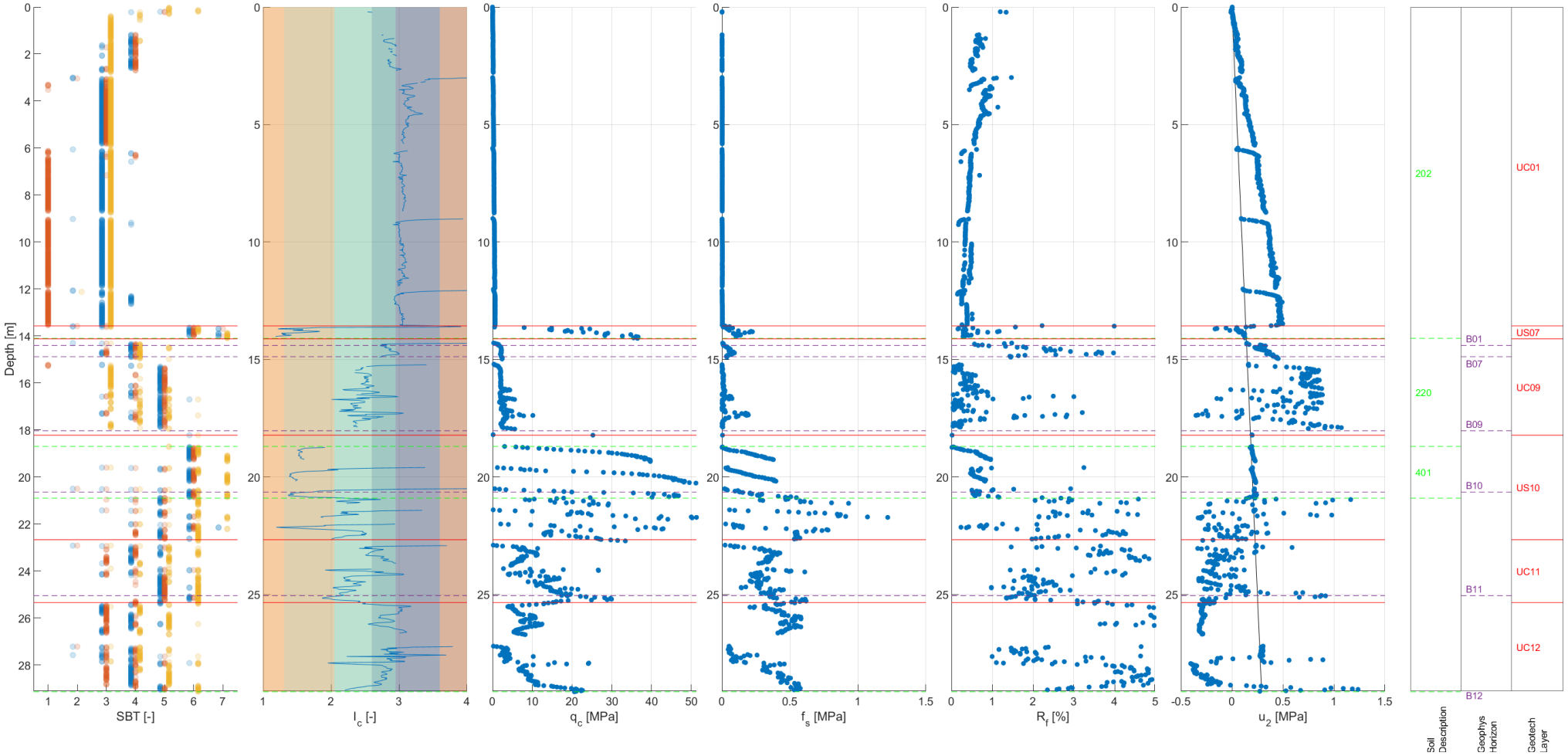
Depth [m]
SBT [-]
I_c [-]
q_c [MPa]
f_s [MPa]
R_f [%]
u_2 [MPa]
202
220
401
B01
B07
B09
B10
B11
B12
UC01
US07
UC09
US10
UC11
UC12
Soil Description
Geophys Horizon
Geotech Layer

HS_S_38

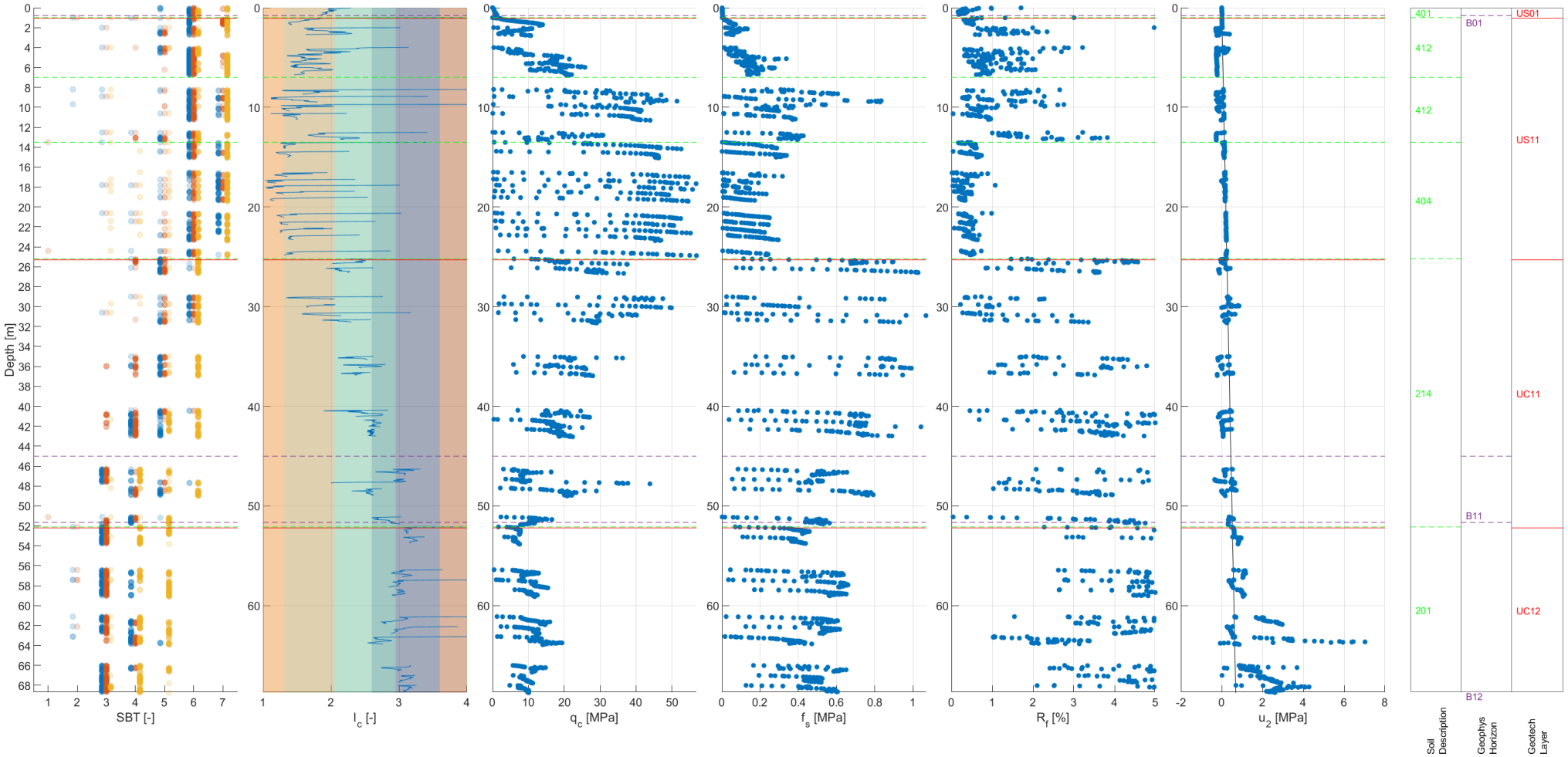
Depth [m]
SBT [-]
I_c [-]
q_c [MPa]
f_s [MPa]
R_f [%]
u_2 [MPa]
401
412
412
404
214
201
US01
B01
US11
B11
UC11
UC12
B12
Soil Description
Geophys Horizon
Geotech Layer

HS_S_39

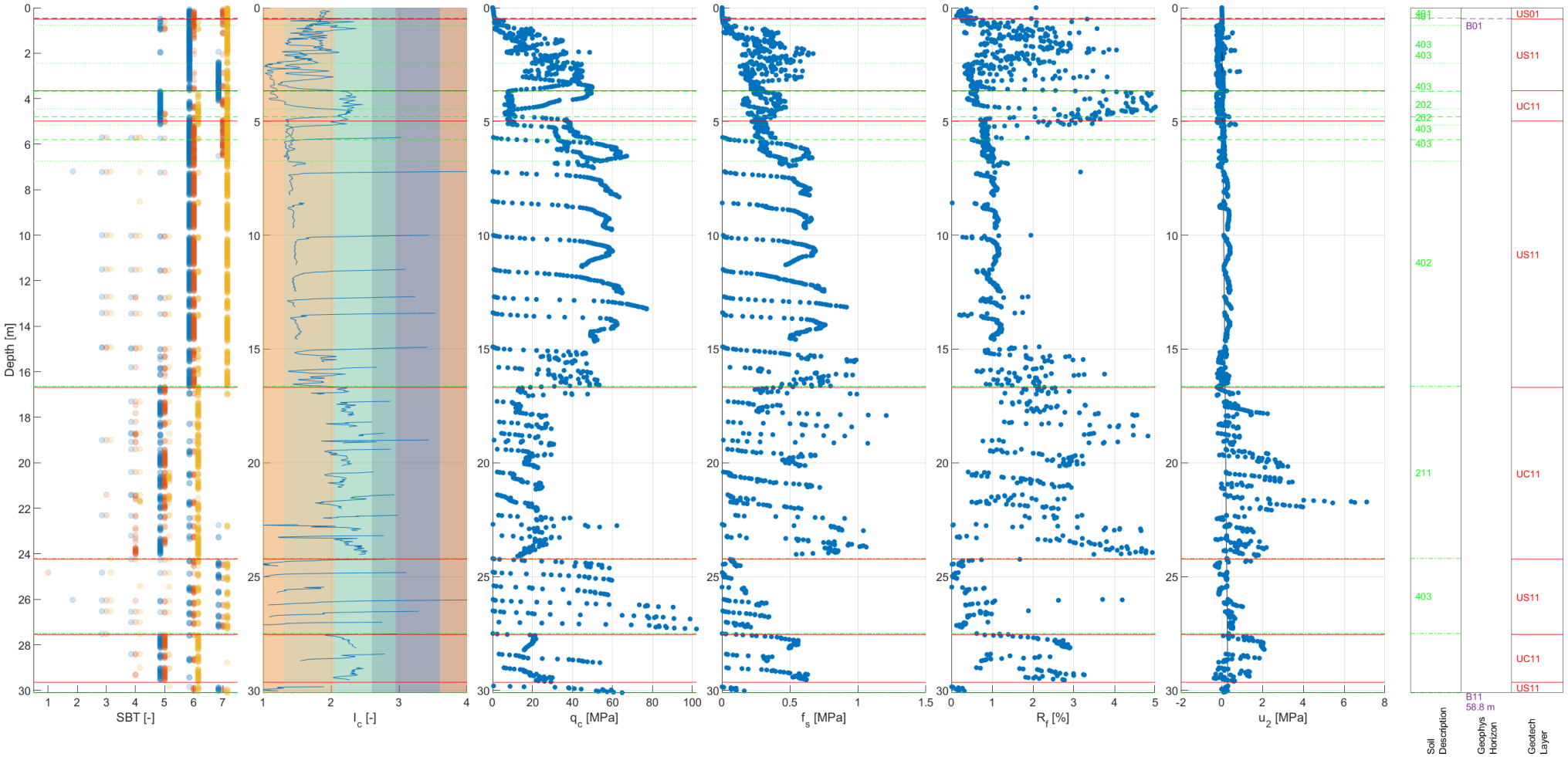
Depth [m]
SBT [-]
I_c [-]
q_c [MPa]
f_s [MPa]
R_f [%]
u_2 [MPa]
401
403
403
403
202
202
403
403
402
211
403
US01
US11
UC11
US11
UC11
US11
UC11
US11
B01
B11
58.8 m
Soil Description
Geophys Horizon
Geotech Layer

Appendix B CPT for geotechnical units

This appendix presents the CPT data available from each of the geotechnical units and present the data in Robertson soil classification charts. The scatter data in the Robertson SBT charts are considering a colour for indicating the density of data in different areas. For presenting the data per unit, the first 20 cm of each CPT push has been removed from the data sample as these are not found representative for the actual unit properties.

B.1 CPT data presented by geotechnical units

CPT data are presented in graphs on the following pages.

Unit UC01 present at 19 geotechnical locations

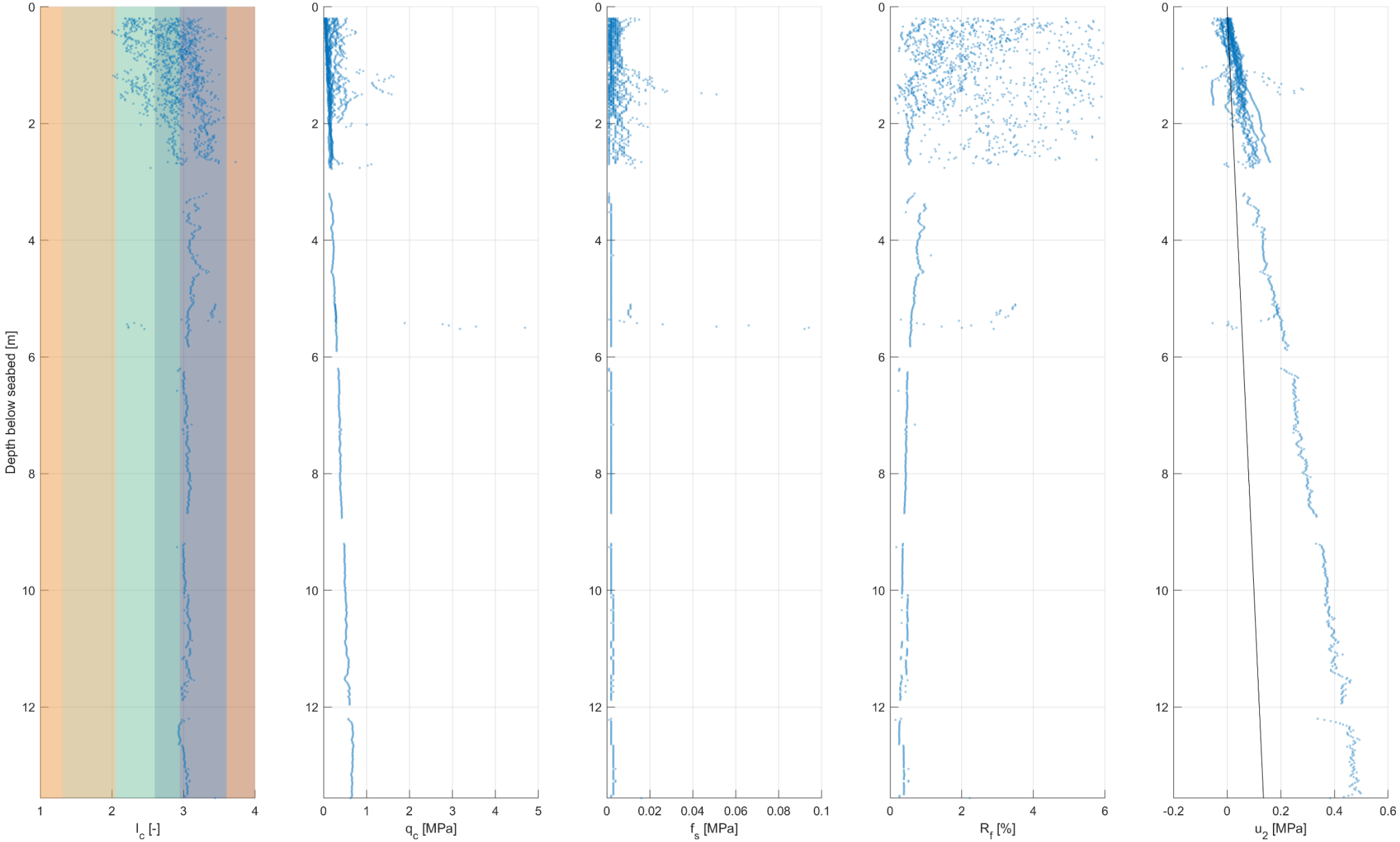

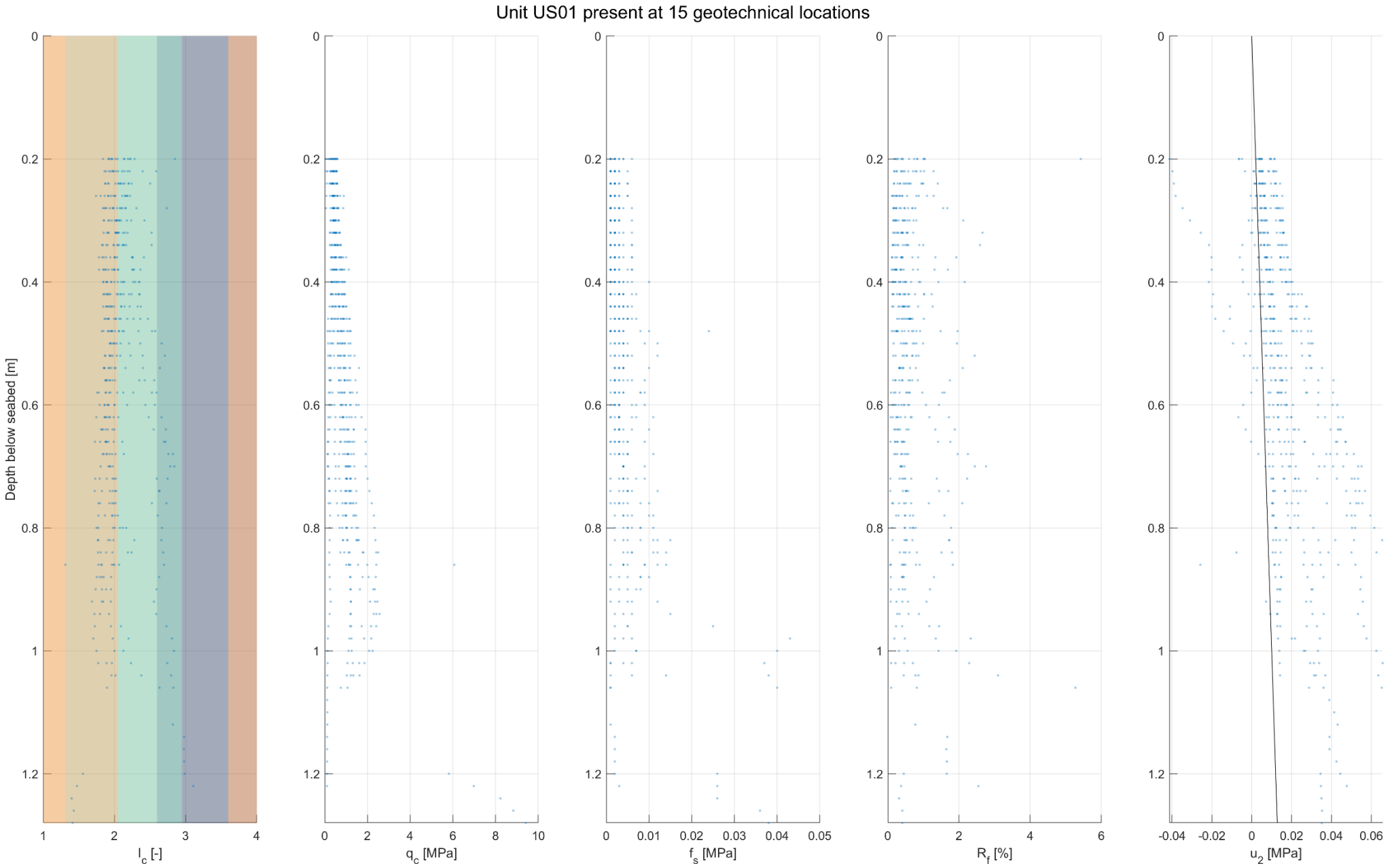
Unit US01 present at 15 geotechnical locations
Depth below seabed [m]
0
0.2
0.4
0.6
0.8
1
1.2
1
2
3
4
I_c [-]
0
2
4
6
8
10
q_c [MPa]
0
0.01
0.02
0.03
0.04
0.05
f_s [MPa]
0
2
4
6
R_f [%]
-0.04
-0.02
0
0.02
0.04
0.06
u_2 [MPa]

Unit US02 present at 8 geotechnical locations

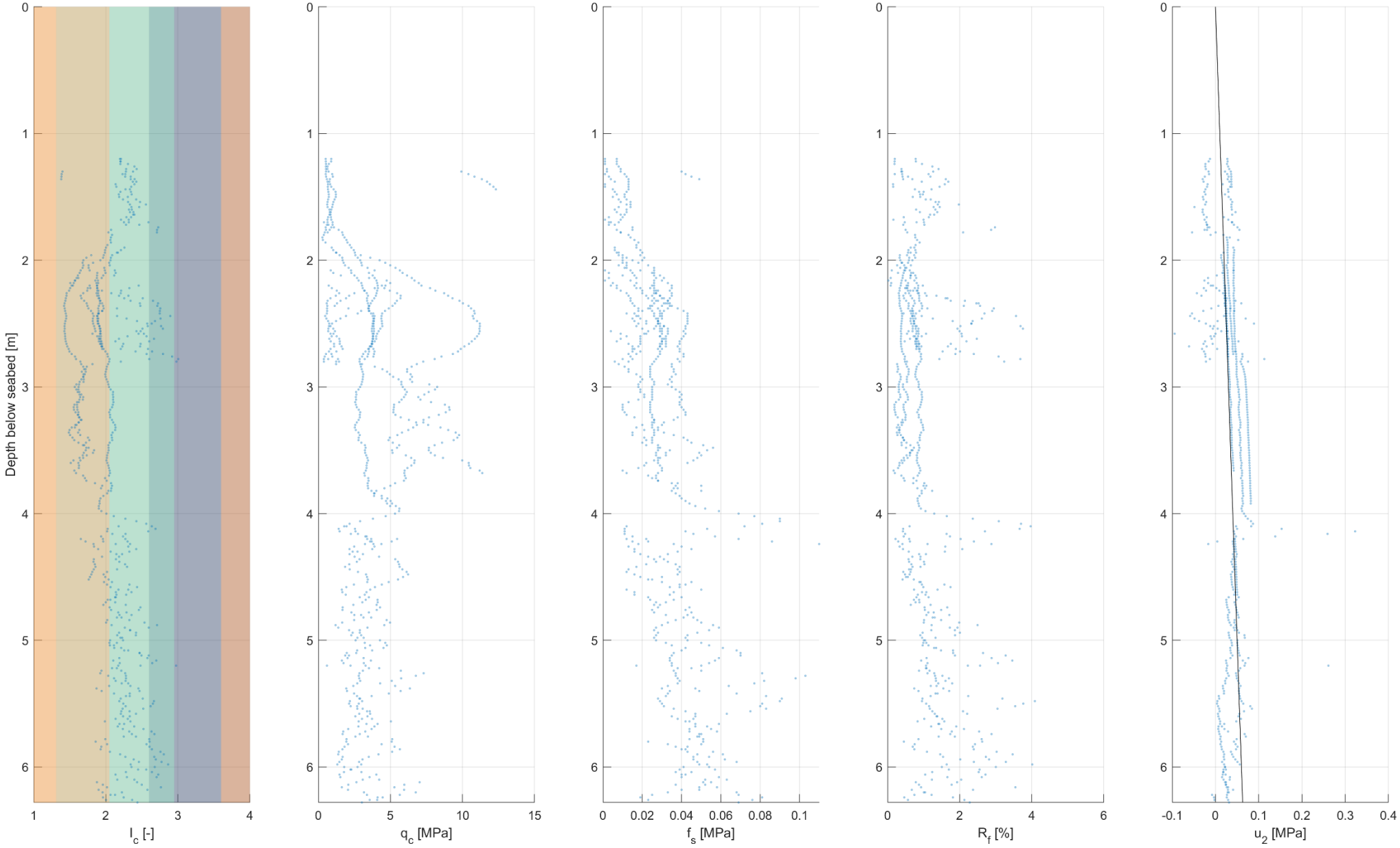

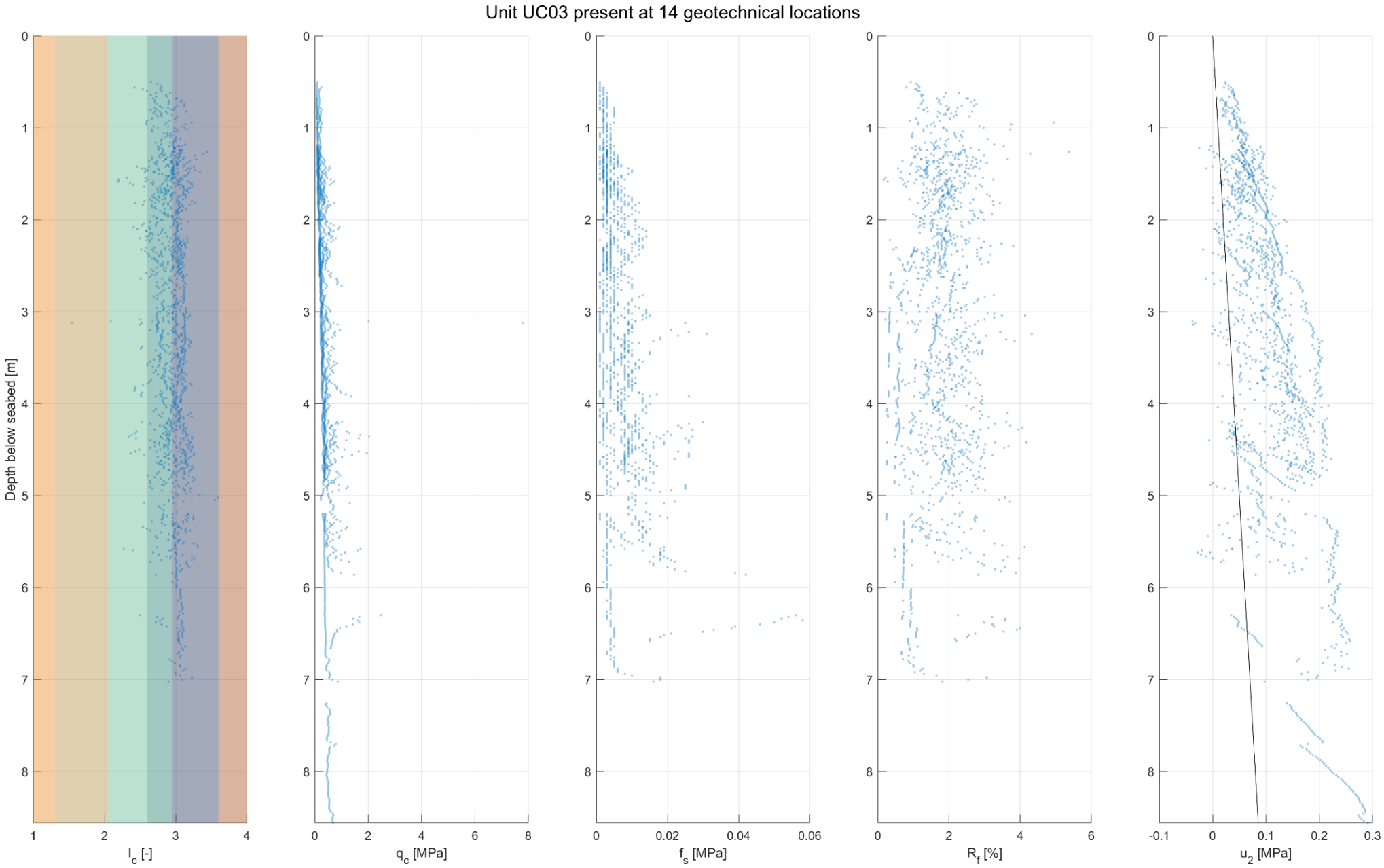
Unit UC03 present at 14 geotechnical locations
Depth below seabed [m]
I_c [-]
q_c [MPa]
f_s [MPa]
R_f [%]
u_2 [MPa]

Unit US03 present at 4 geotechnical locations

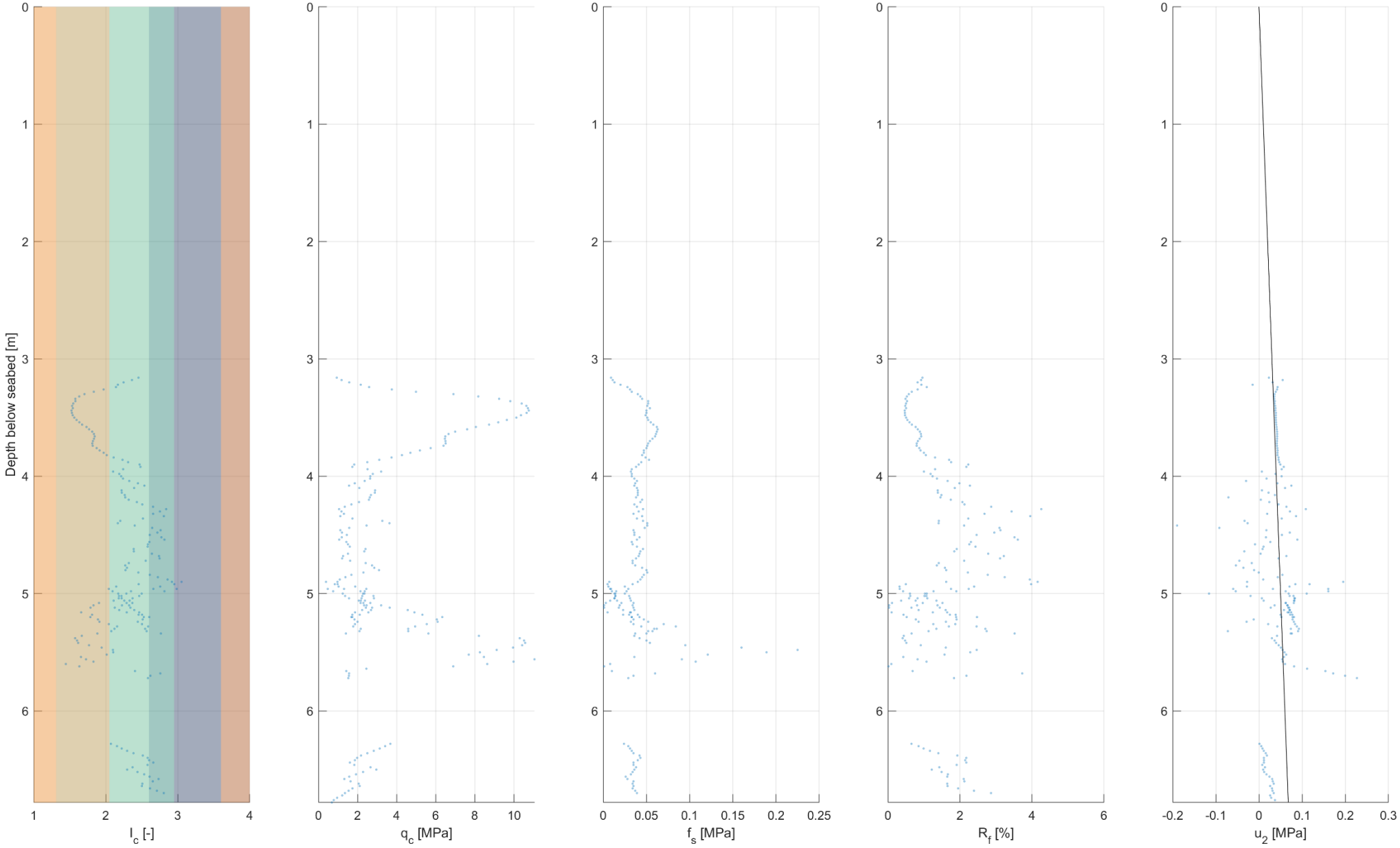

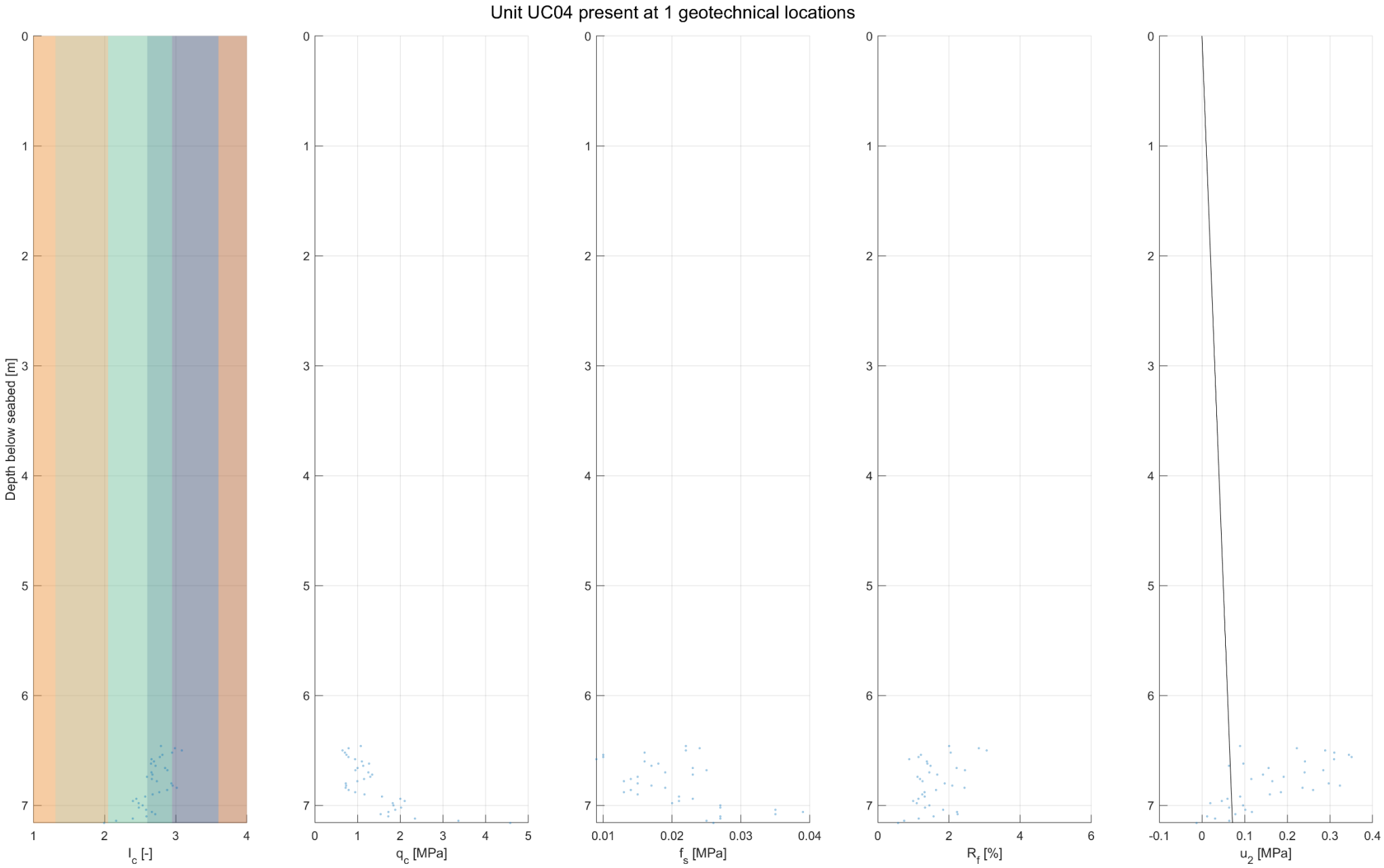
Unit UC04 present at 1 geotechnical locations
Depth below seabed [m]
0
1
2
3
4
5
6
7
1
2
3
4
I_c [-]
0
1
2
3
4
5
q_c [MPa]
0.01
0.02
0.03
0.04
f_s [MPa]
0
2
4
6
R_f [%]
-0.1
0
0.1
0.2
0.3
0.4
u_2 [MPa]

Unit US04 present at 9 geotechnical locations

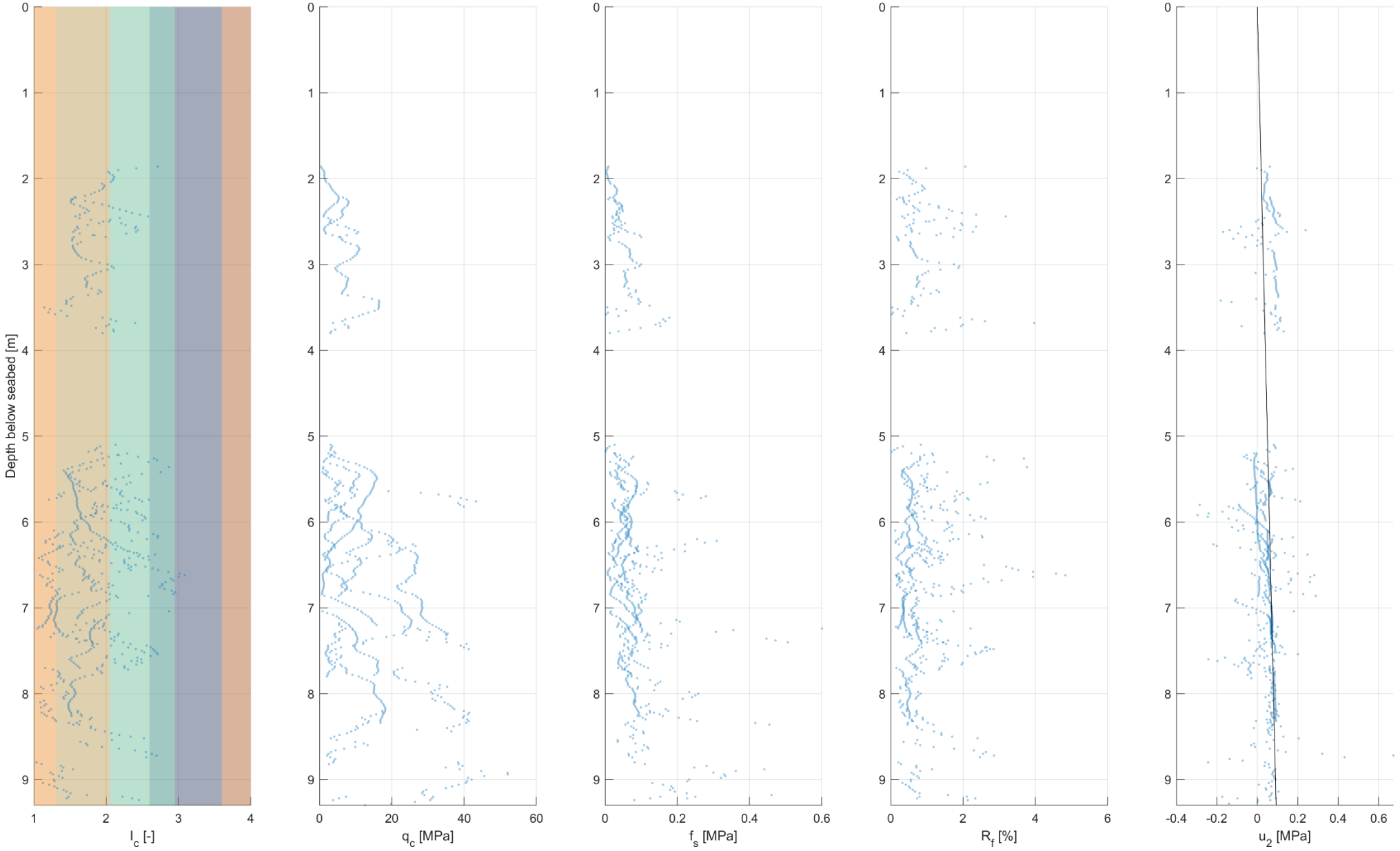

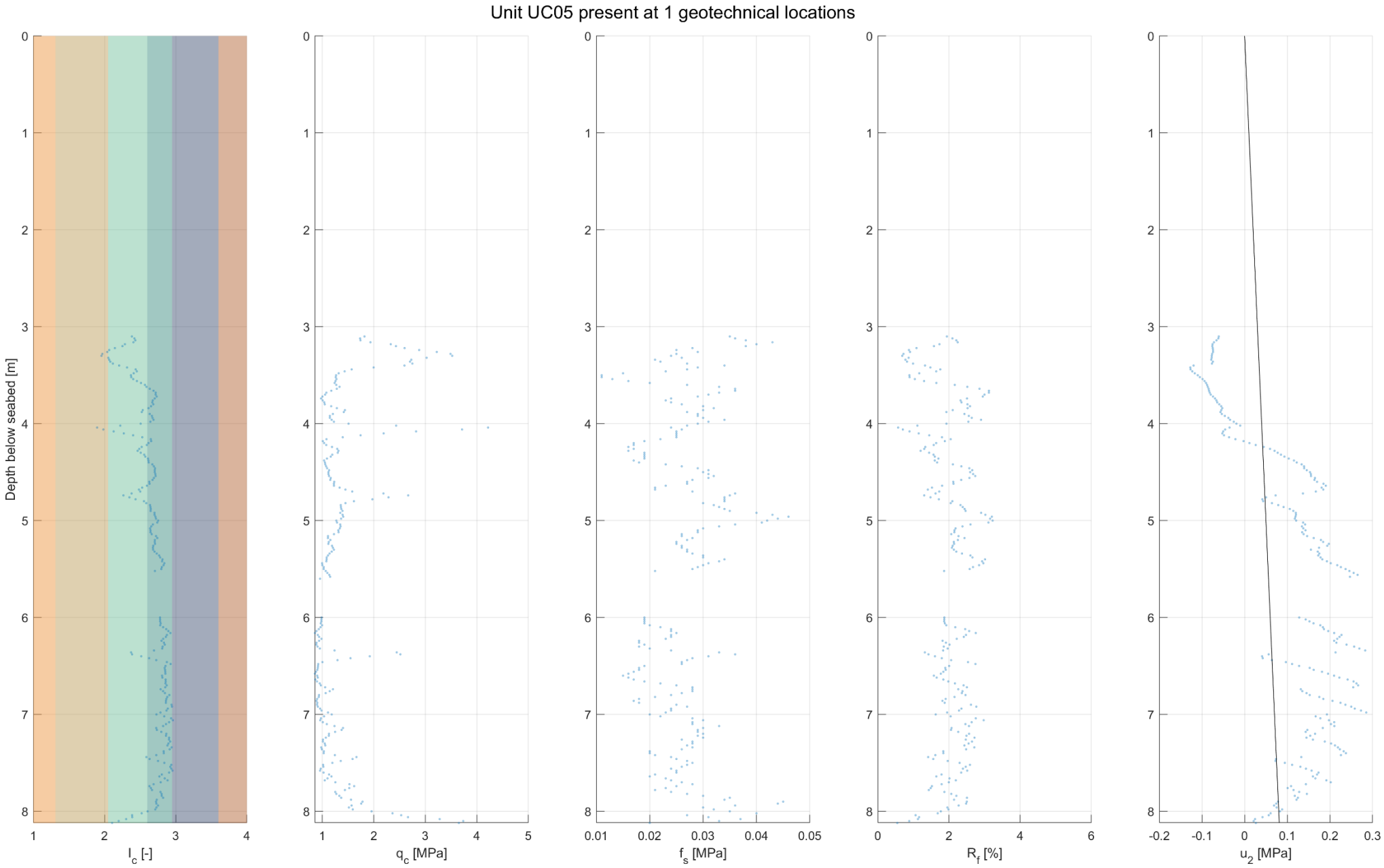
Unit UC05 present at 1 geotechnical locations
Depth below seabed [m]
0
1
2
3
4
5
6
7
8
1
2
3
4
I_c [-]
1
2
3
4
5
q_c [MPa]
0.01
0.02
0.03
0.04
0.05
f_s [MPa]
0
2
4
6
R_f [%]
-0.2
-0.1
0
0.1
0.2
0.3
u_2 [MPa]

Unit US05 present at 2 geotechnical locations

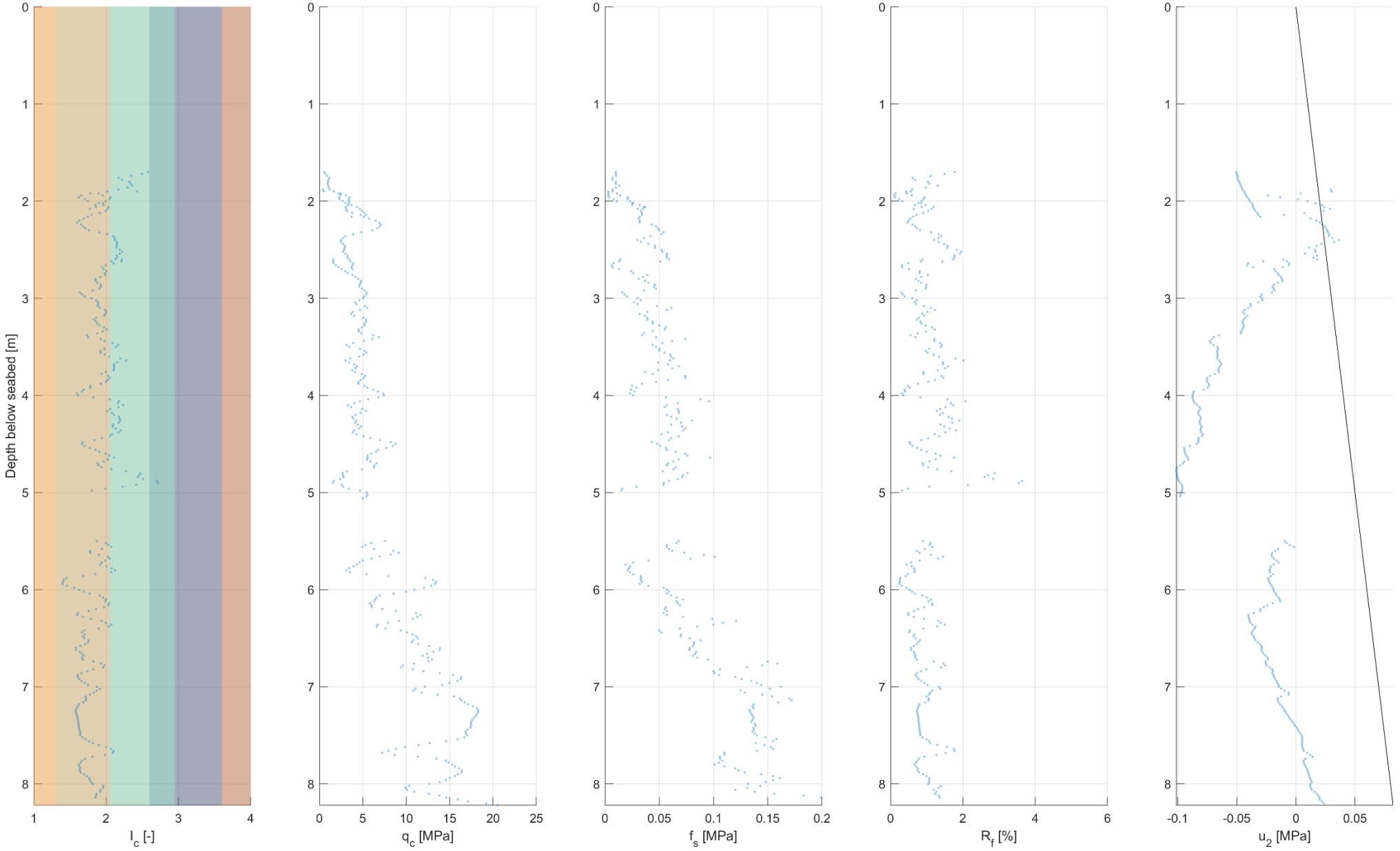

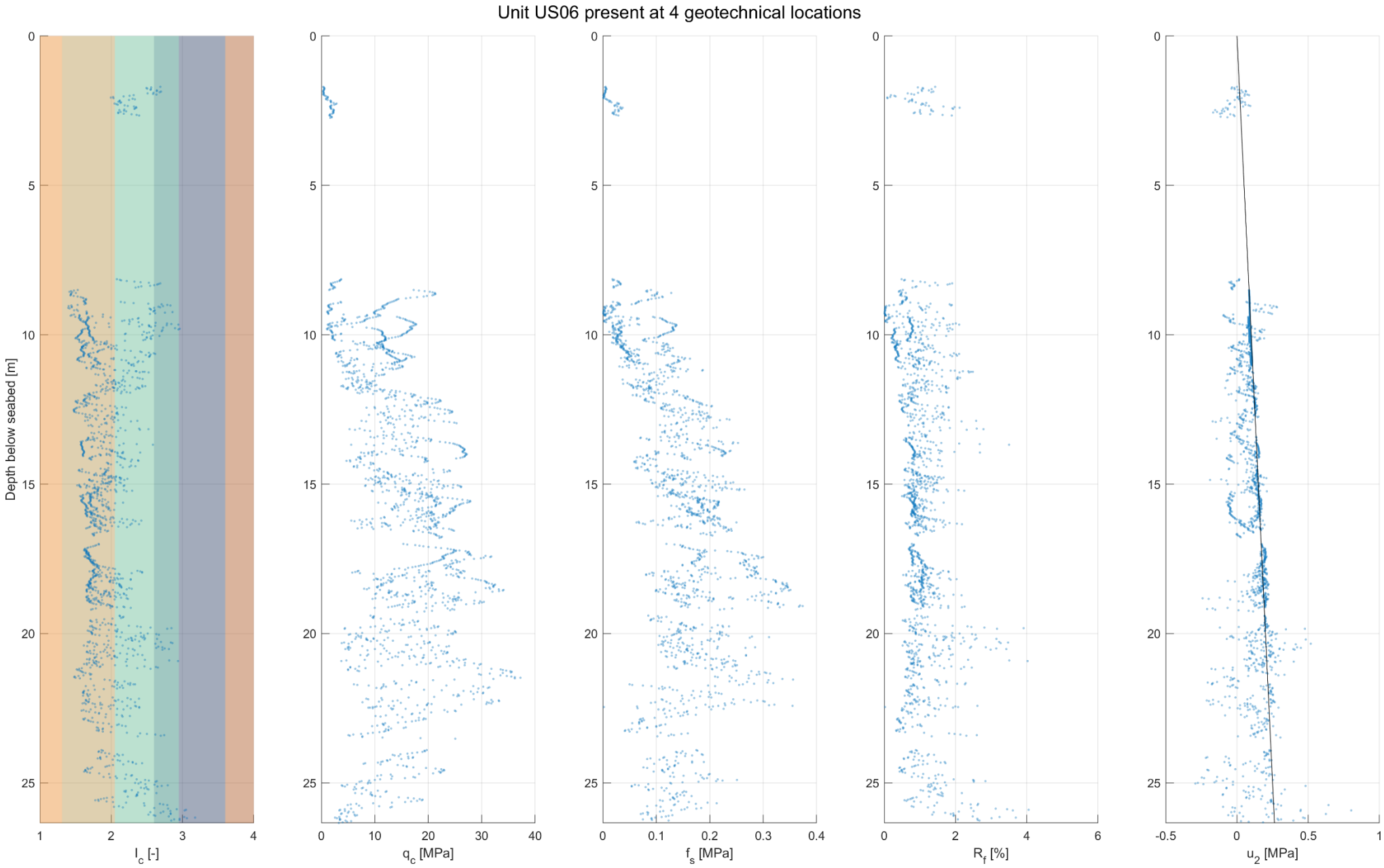
Unit US06 present at 4 geotechnical locations
Depth below seabed [m]
0
5
10
15
20
25
1
2
3
4
I_c [-]
0
10
20
30
40
q_c [MPa]
0
0.1
0.2
0.3
0.4
f_s [MPa]
0
2
4
6
R_f [%]
-0.5
0
0.5
1
u_2 [MPa]

Unit UC07 present at 5 geotechnical locations

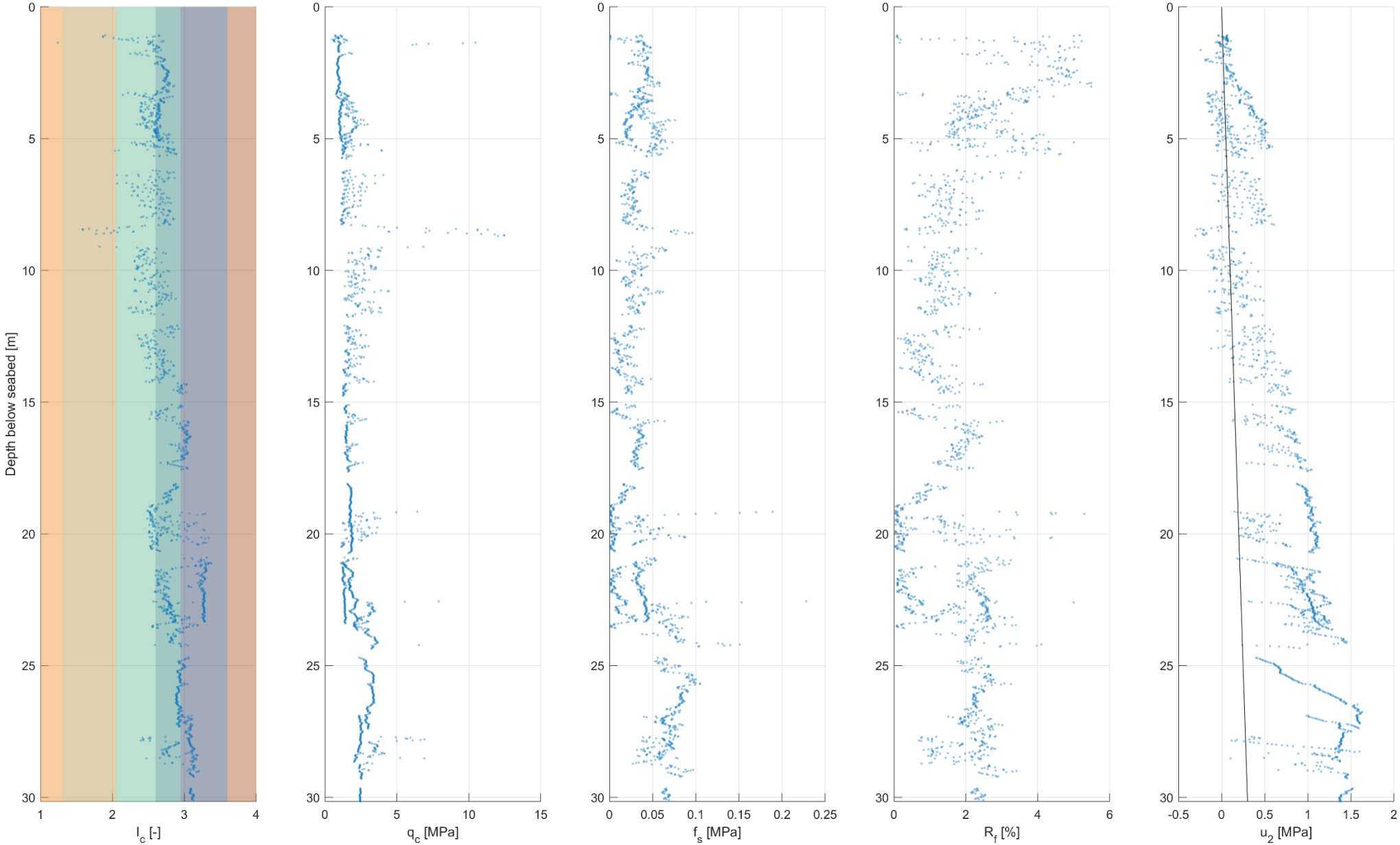

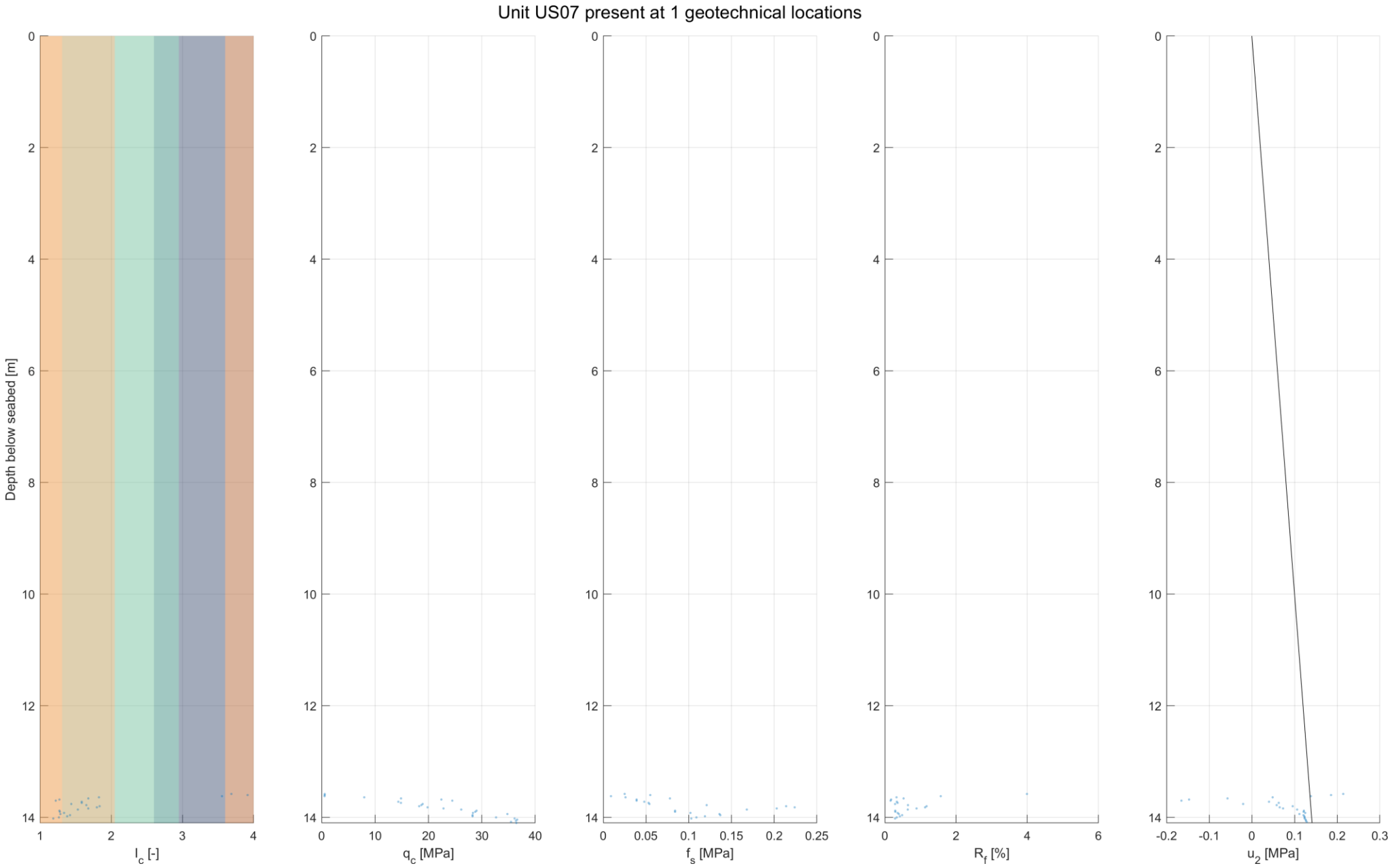
Unit US07 present at 1 geotechnical locations
Depth below seabed [m]
0
2
4
6
8
10
12
14
1
2
3
4
I_c [-]
0
10
20
30
40
q_c [MPa]
0
0.05
0.1
0.15
0.2
0.25
f_s [MPa]
0
2
4
6
R_f [%]
-0.2
-0.1
0
0.1
0.2
0.3
u_2 [MPa]

Unit UC08 present at 18 geotechnical locations

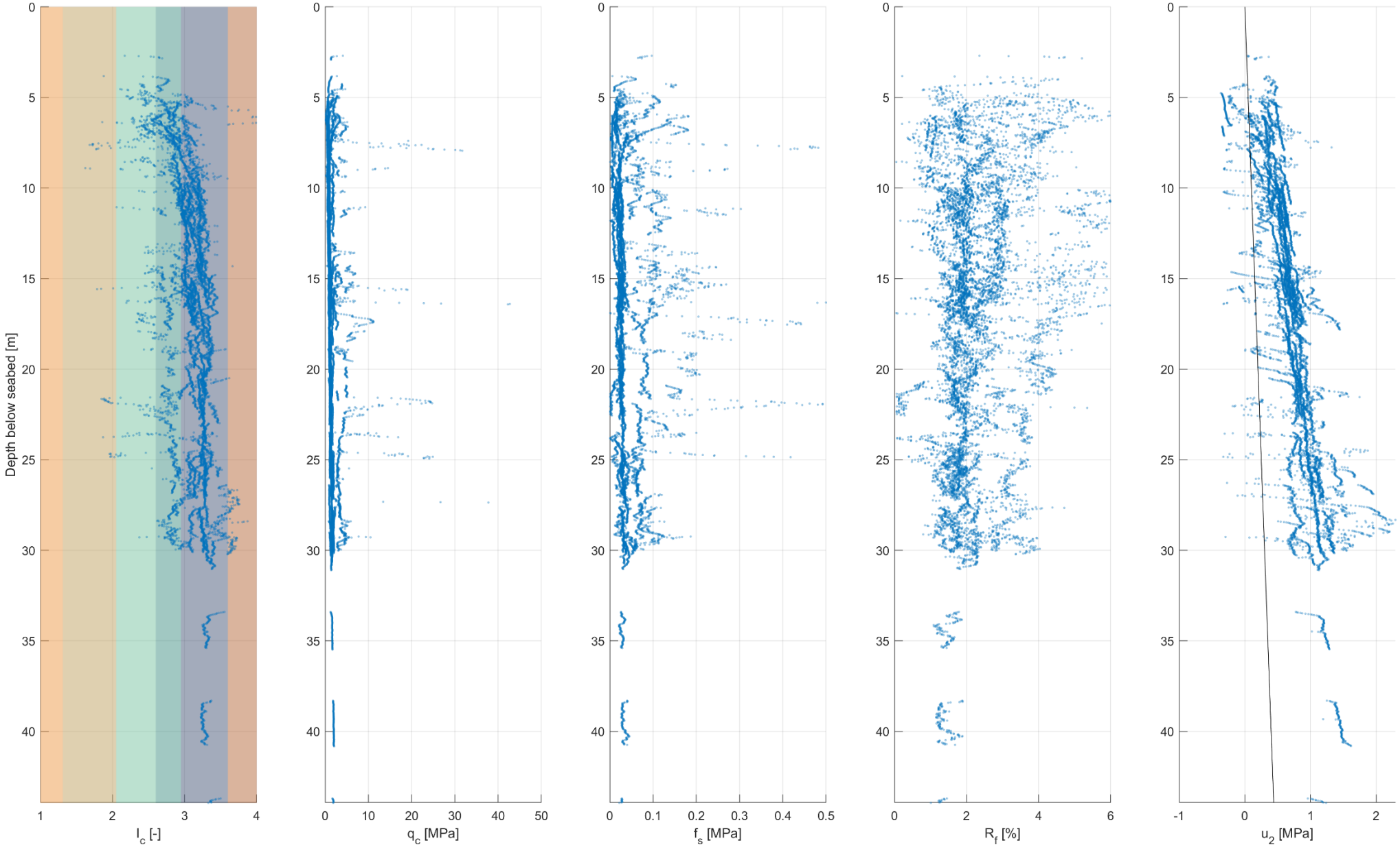

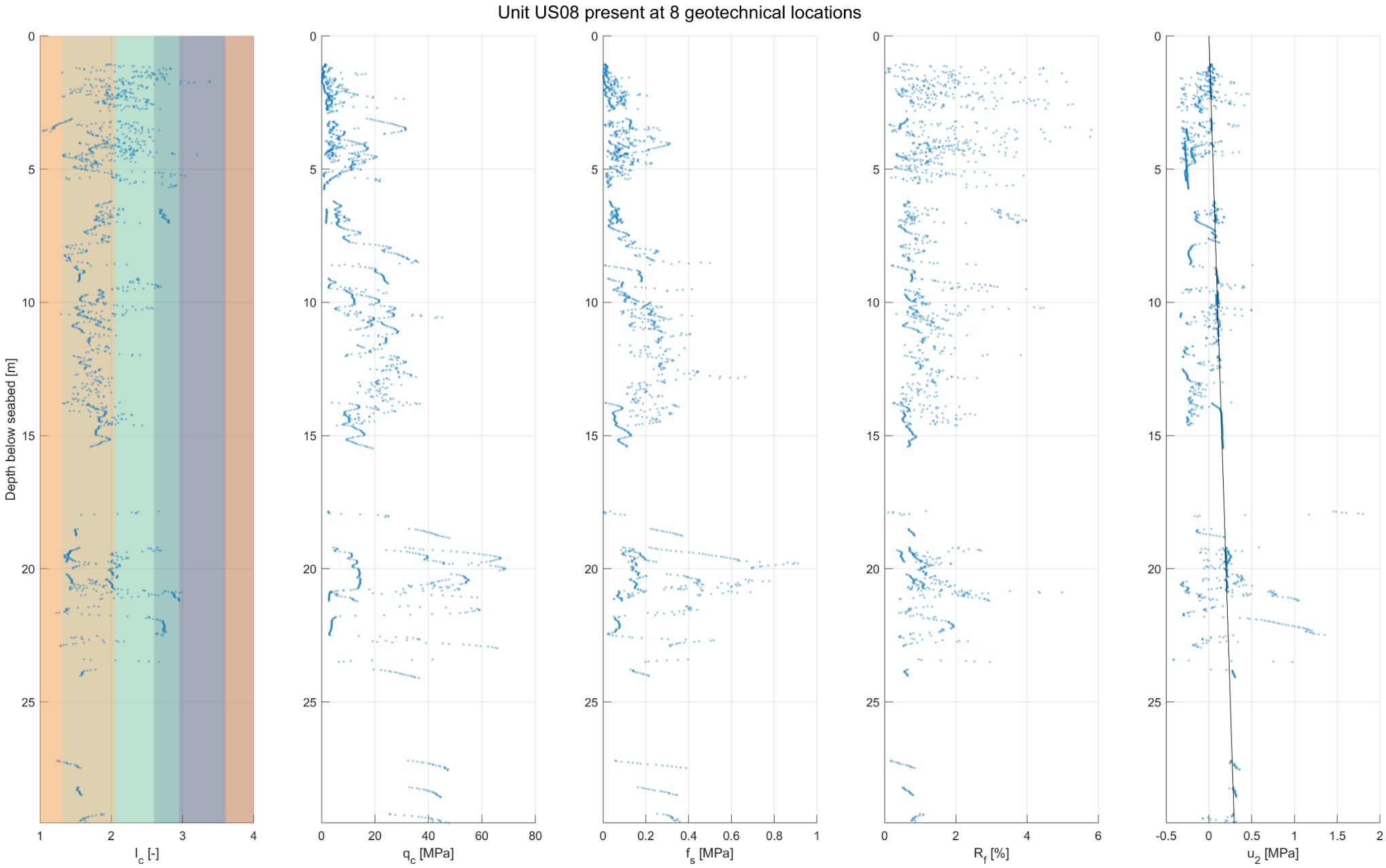
Unit US08 present at 8 geotechnical locations
Depth below seabed [m]
0
5
10
15
20
25
1
2
3
4
I_c [-]
0
20
40
60
80
q_c [MPa]
0
0.2
0.4
0.6
0.8
1
f_s [MPa]
0
2
4
6
R_f [%]
-0.5
0
0.5
1
1.5
2
u_2 [MPa]

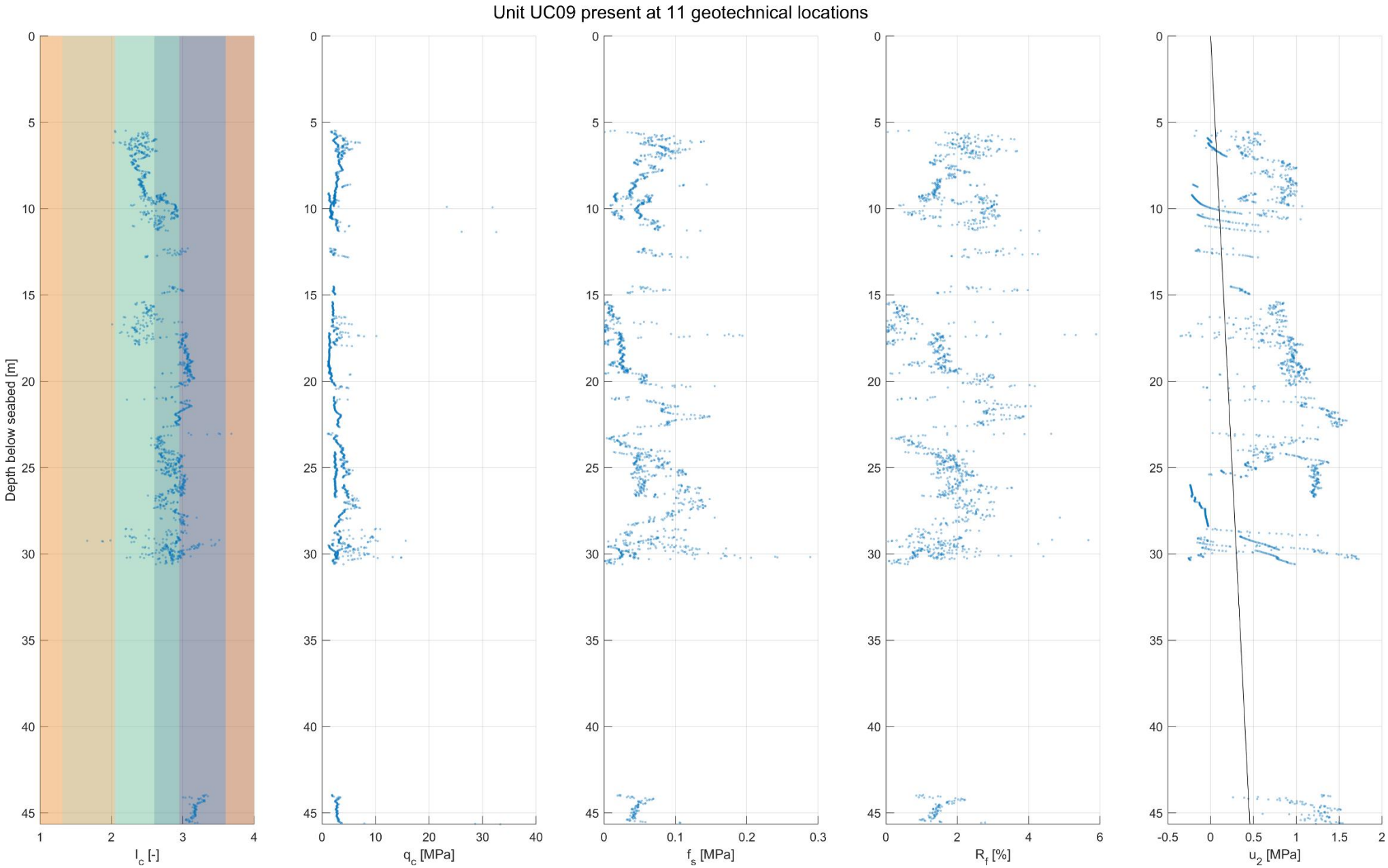
Unit UC09 present at 11 geotechnical locations
Depth below seabed [m]
I_c [-]
q_c [MPa]
f_s [MPa]
R_f [%]
u_2 [MPa]

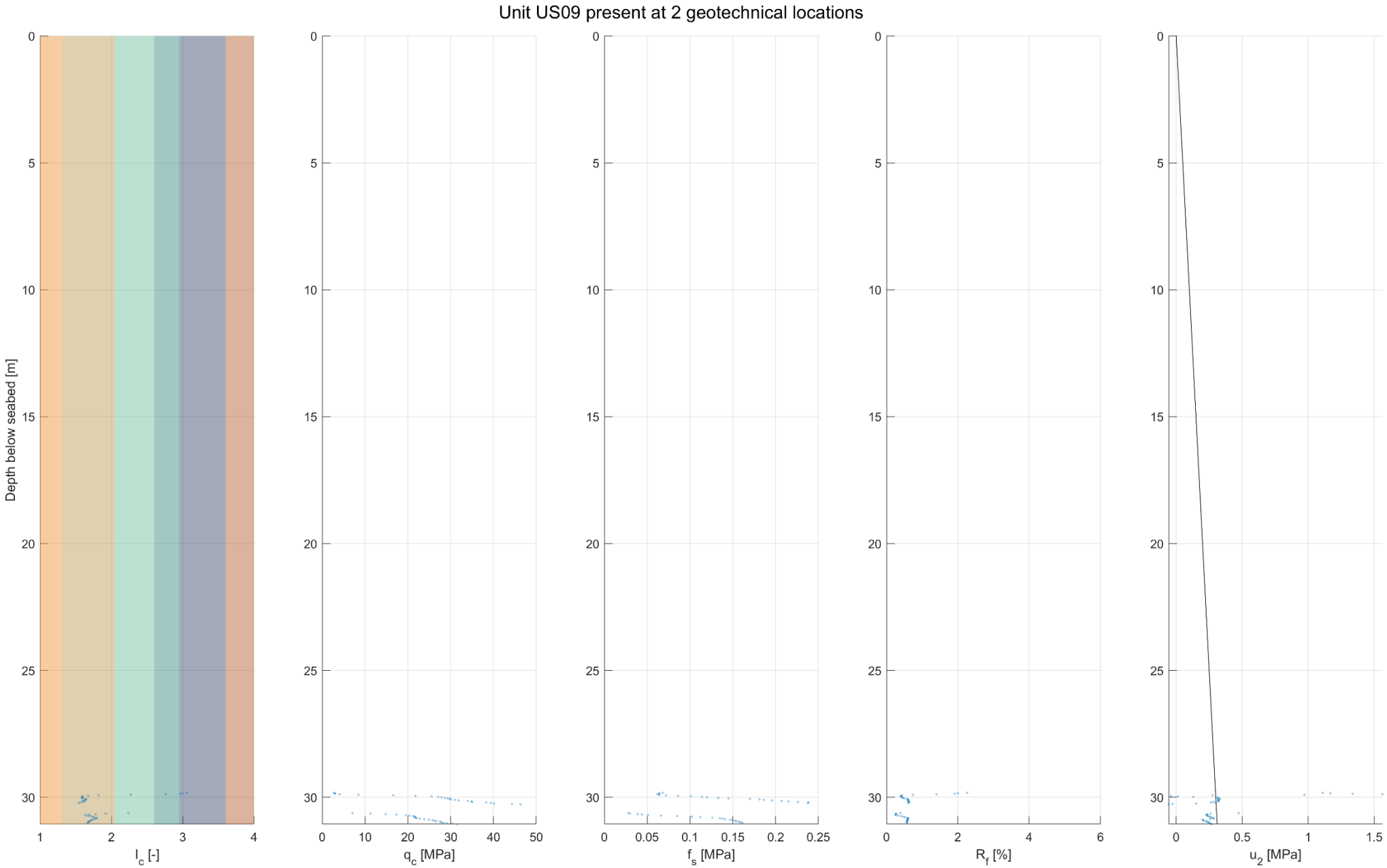
Unit US09 present at 2 geotechnical locations
Depth below seabed [m]
0
5
10
15
20
25
30
1
2
3
4
I_c [-]
0
10
20
30
40
50
q_c [MPa]
0
0.05
0.1
0.15
0.2
0.25
f_s [MPa]
0
2
4
6
R_f [%]
0
0.5
1
1.5
u_2 [MPa]

Unit UC10 present at 2 geotechnical locations

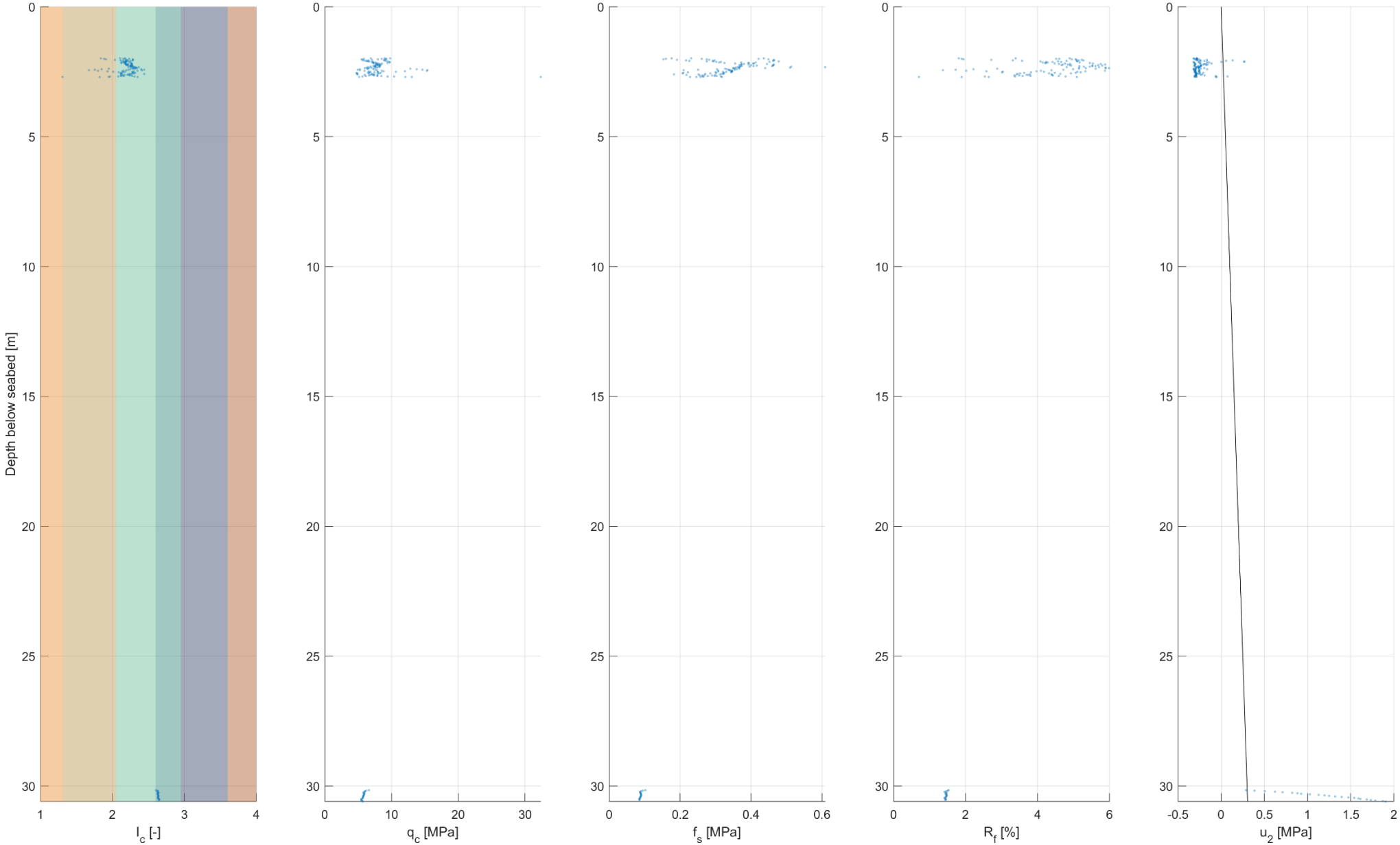

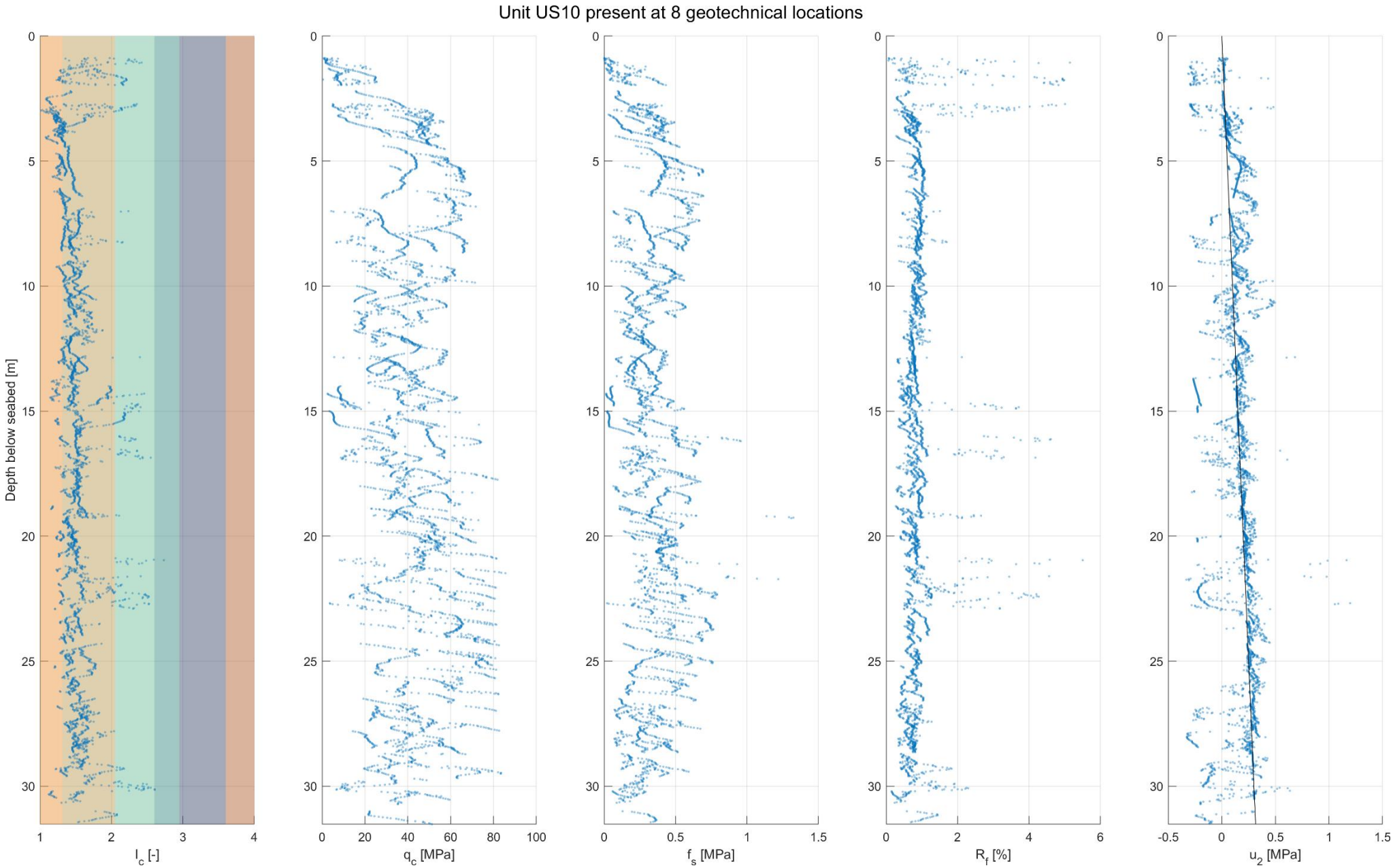
Unit US10 present at 8 geotechnical locations
Depth below seabed [m]
0
5
10
15
20
25
30
1
2
3
4
I_c [-]
0
20
40
60
80
100
q_c [MPa]
0
0.5
1
1.5
f_s [MPa]
0
2
4
6
R_f [%]
-0.5
0
0.5
1
1.5
u_2 [MPa]

Unit UC11 present at 9 geotechnical locations

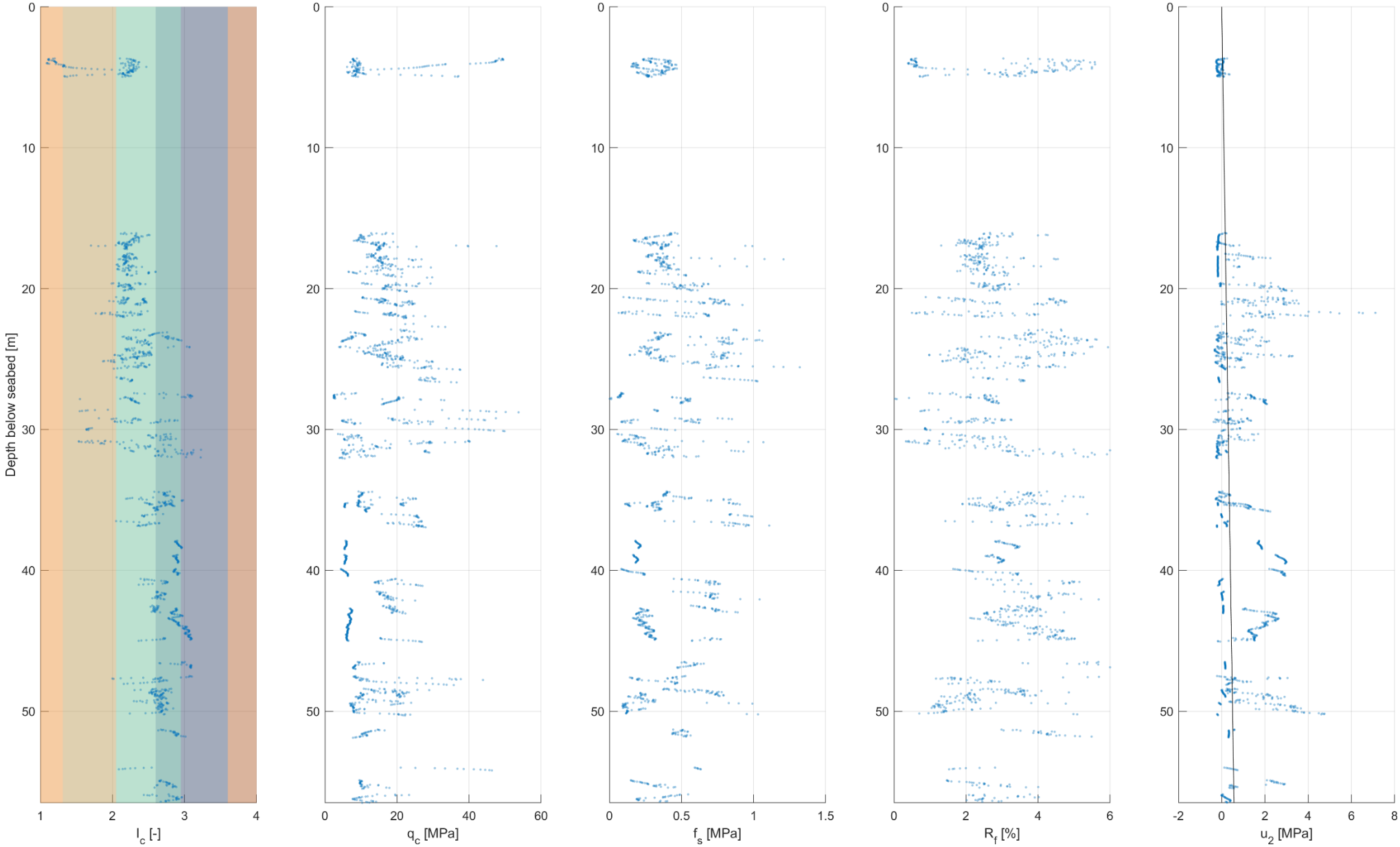

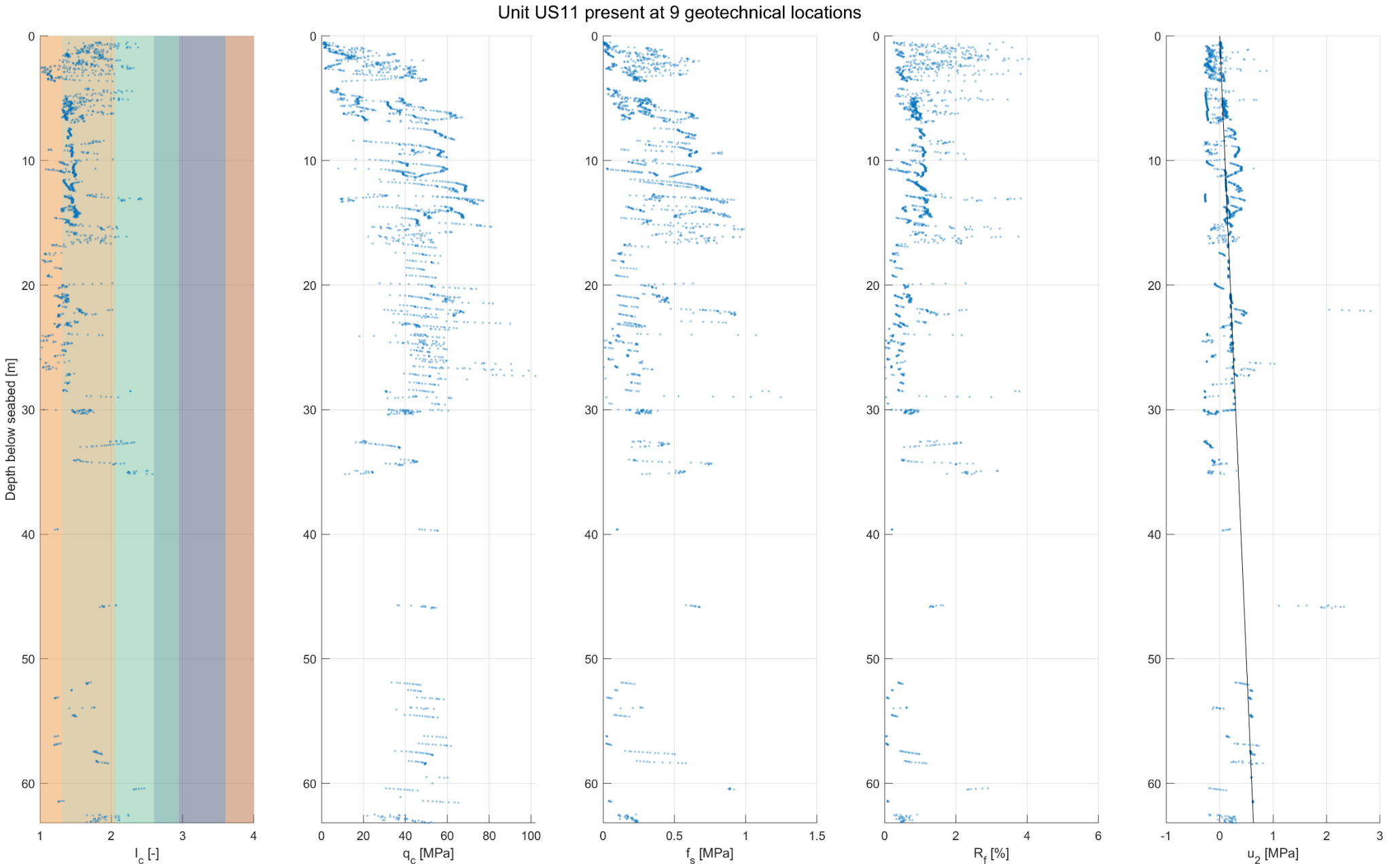
Unit US11 present at 9 geotechnical locations
Depth below seabed [m]
0
10
20
30
40
50
60
1
2
3
4
I_c [-]
0
20
40
60
80
100
q_c [MPa]
0
0.5
1
1.5
f_s [MPa]
0
2
4
6
R_f [%]
-1
0
1
2
3
u_2 [MPa]

Unit UC12 present at 3 geotechnical locations

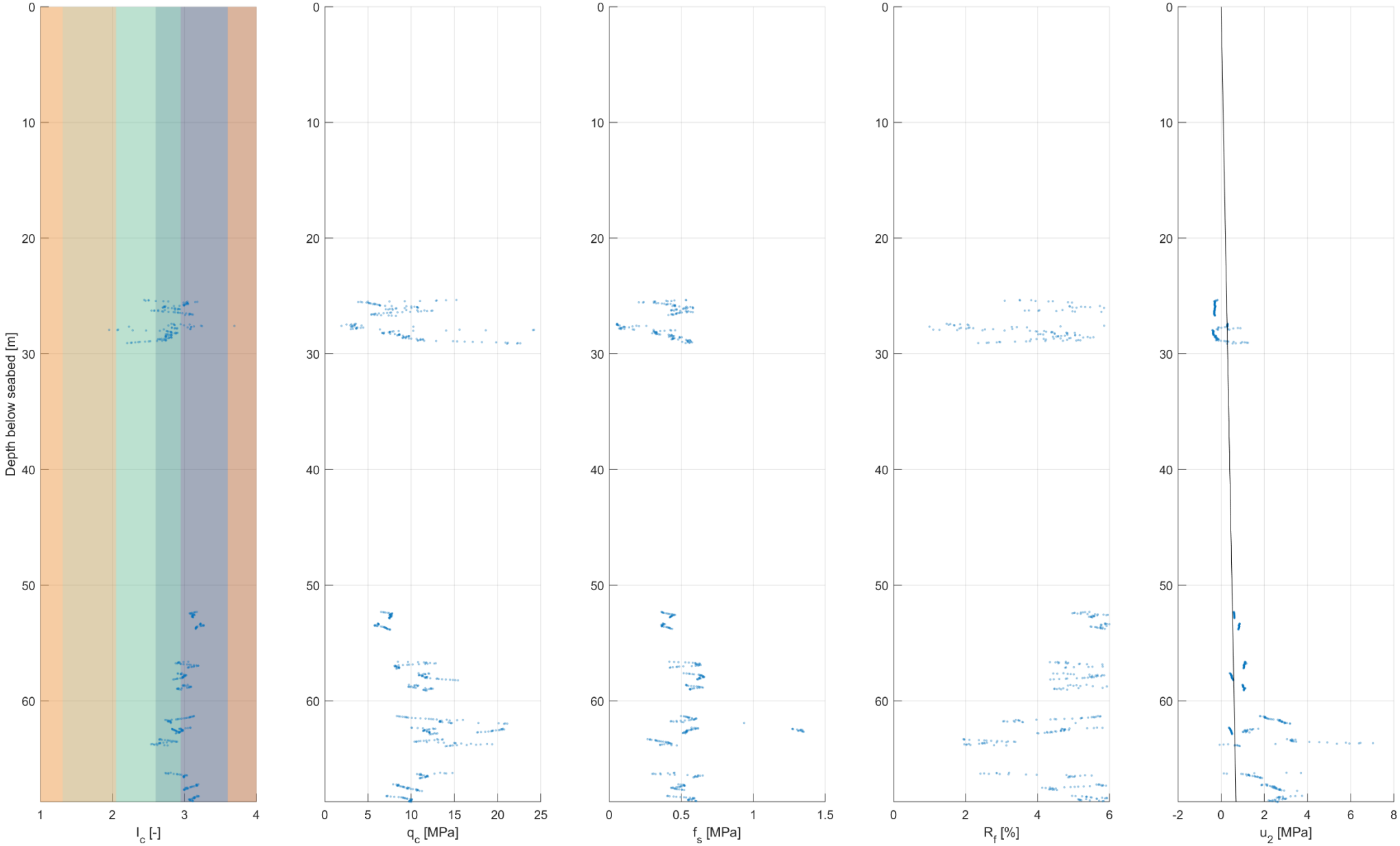

B.2 Presentation of geotechnical unit groupings by Robertson charts

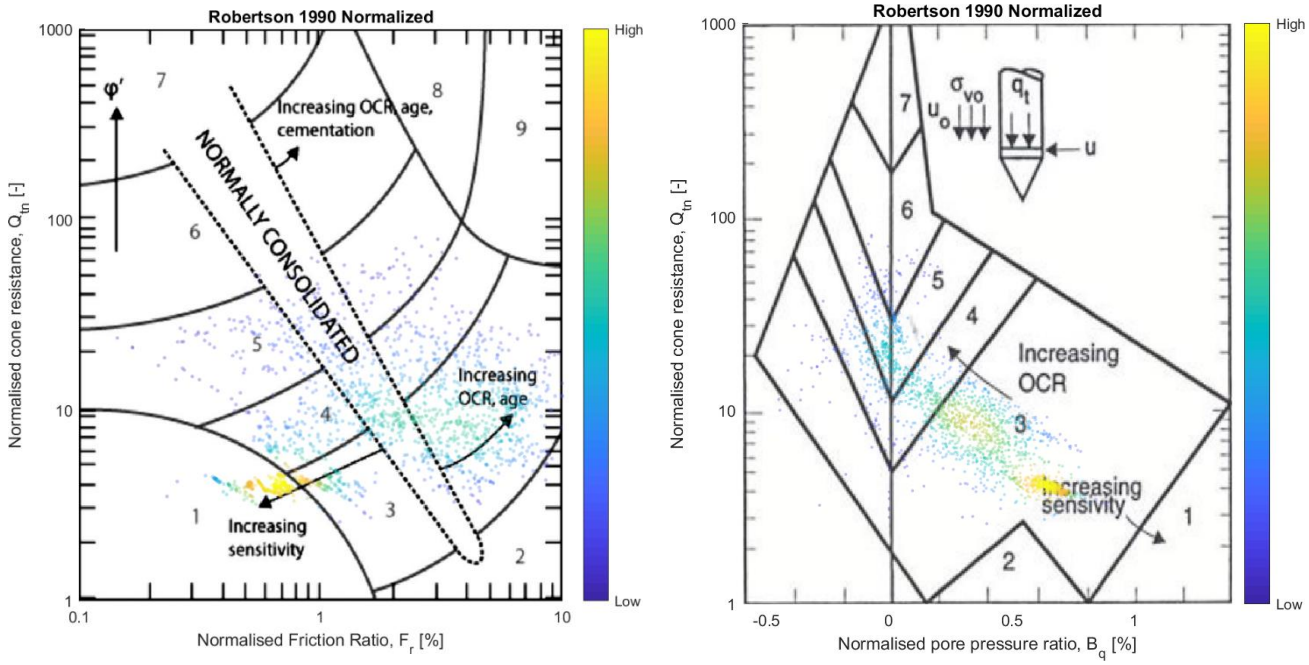

Figure B - 1 CPT data plotted in Robertson SBT chart for UC01.

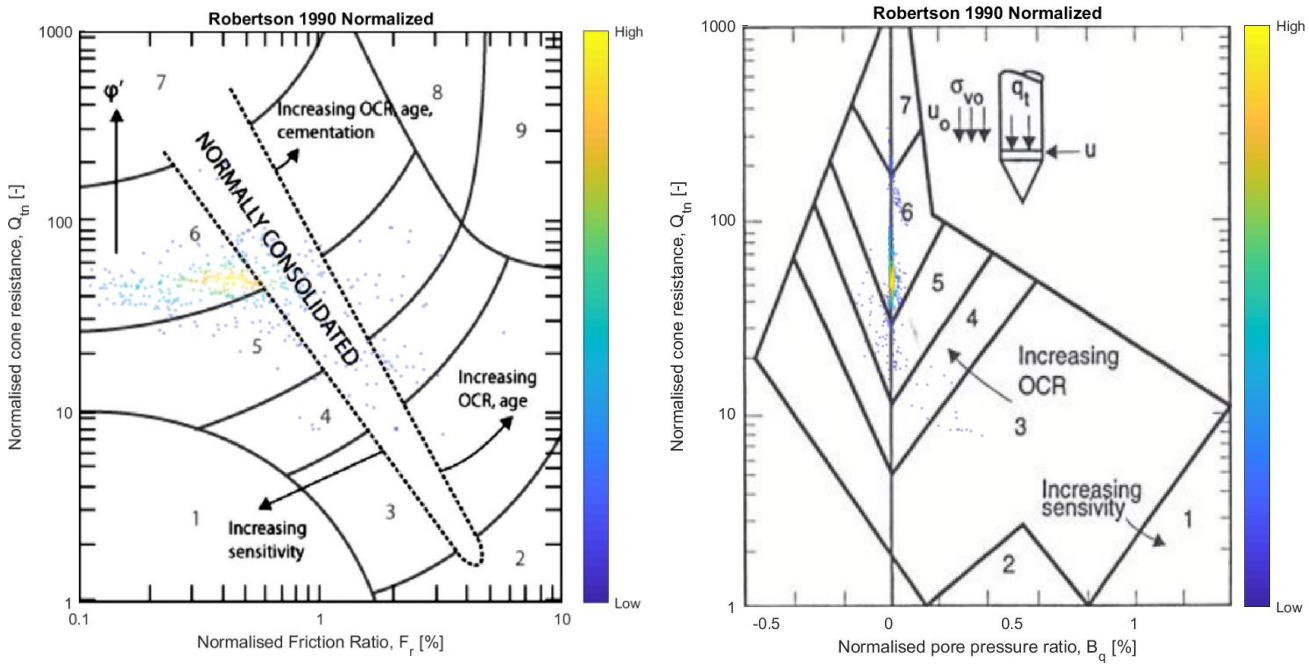

Figure B - 2 CPT data plotted in Robertson SBT chart for US01.

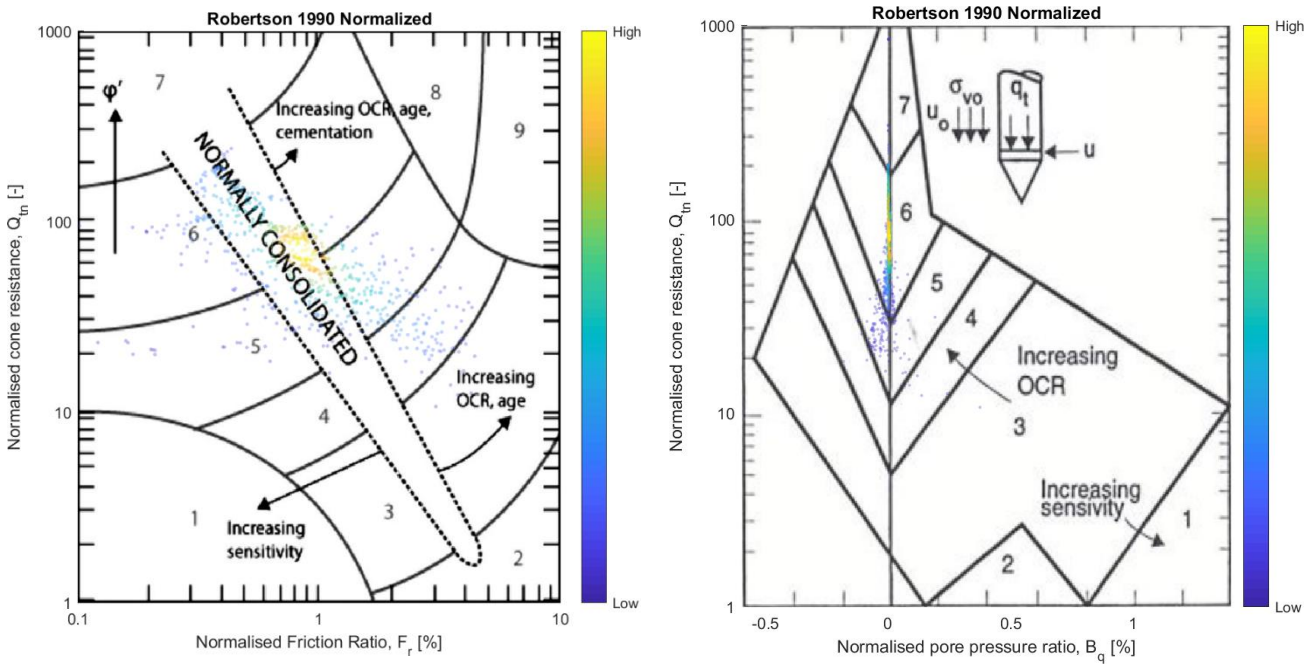

Figure B - 3 CPT data plotted in Robertson SBT chart for US02.

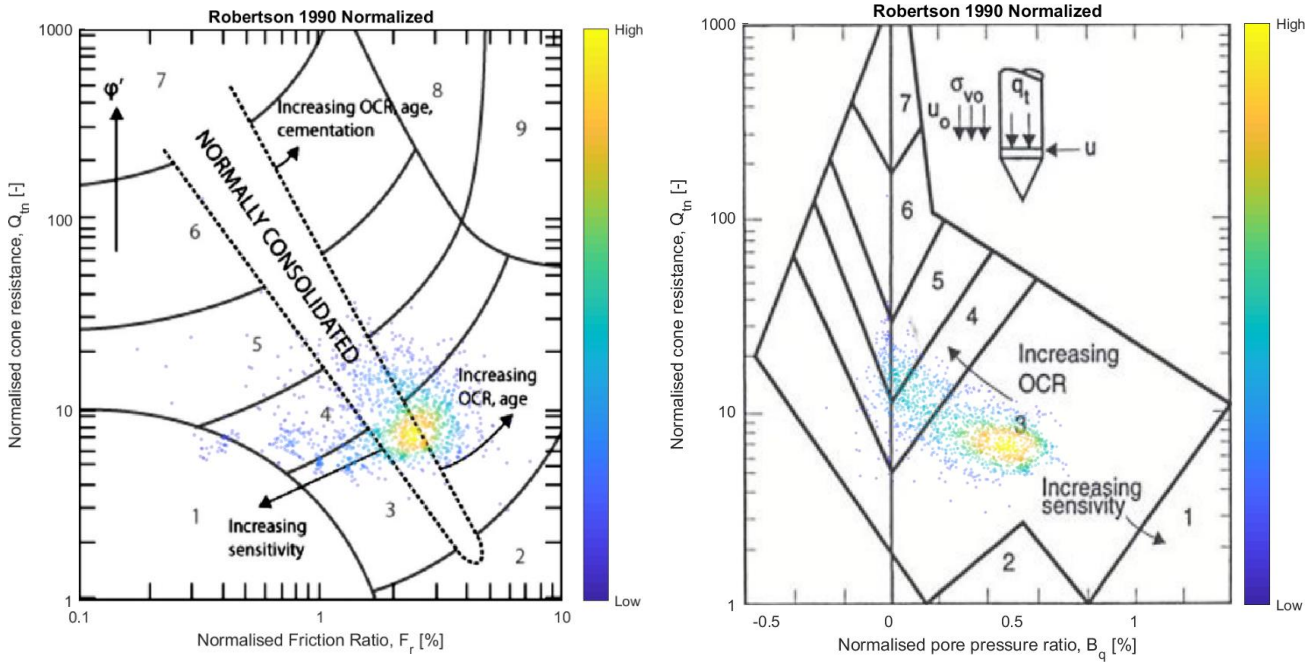

Figure B - 4 CPT data plotted in Robertson SBT chart for UC03.

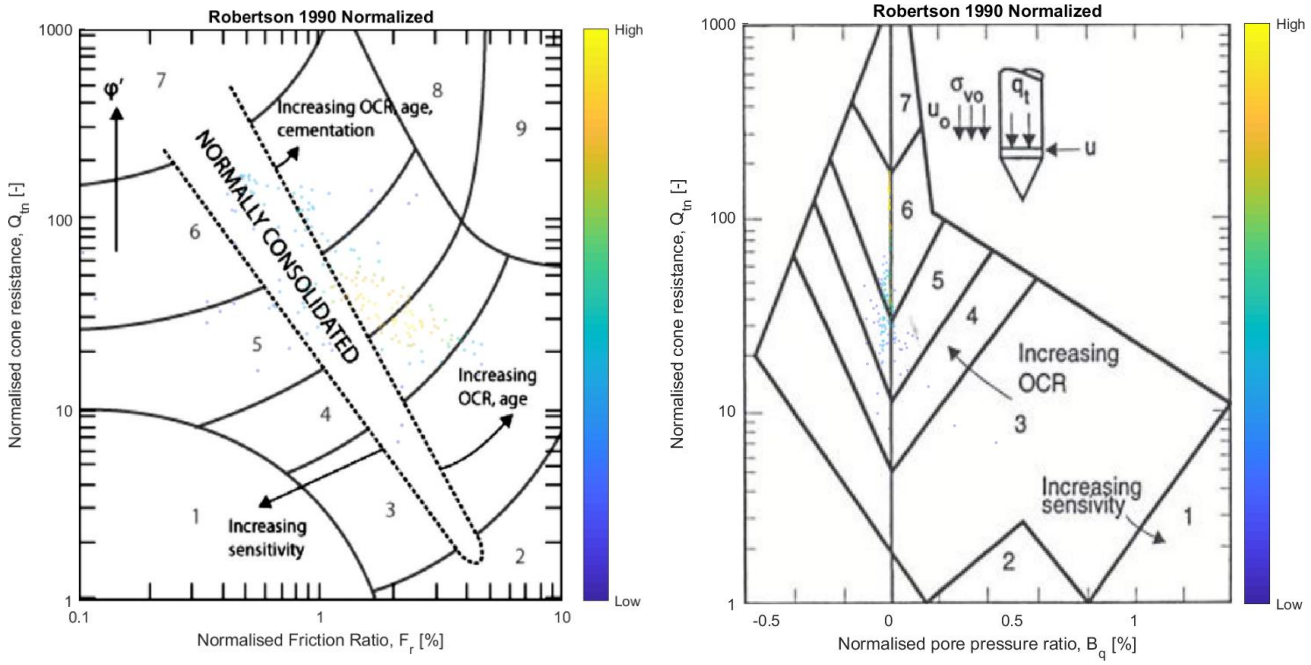

Figure B -

5 CPT data plotted in Robertson SBT chart for US03.

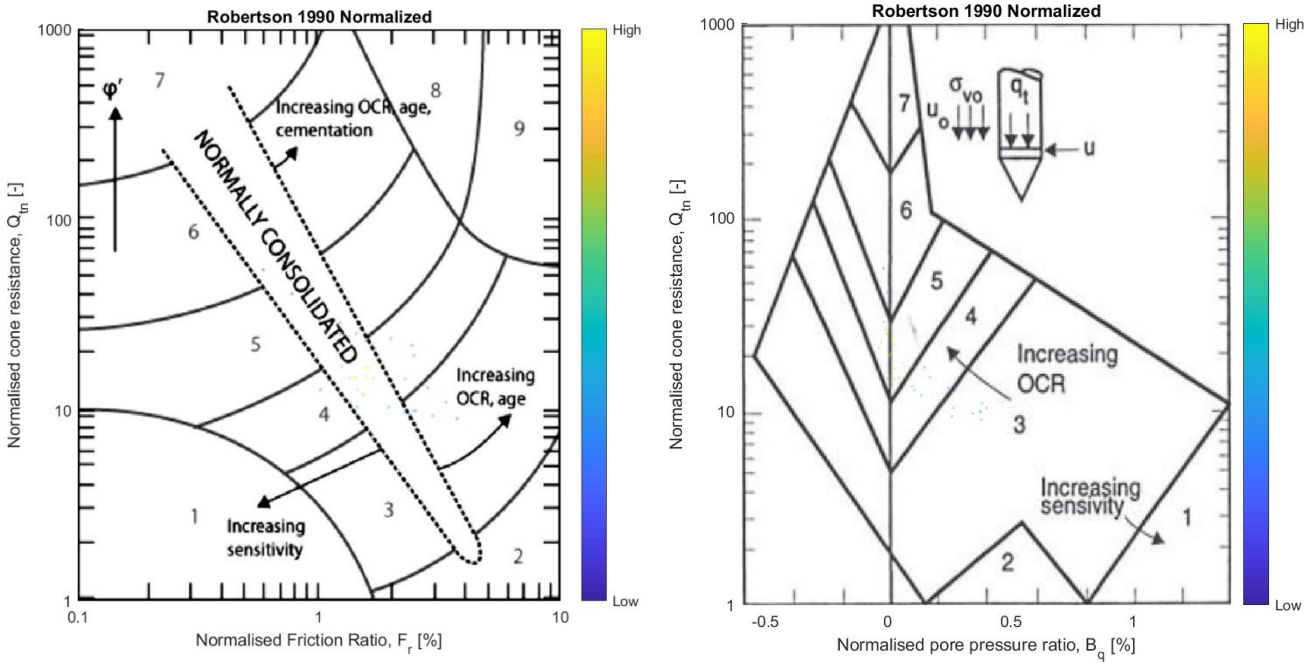

Figure B - 6 CPT data plotted in Robertson SBT chart for UC04.

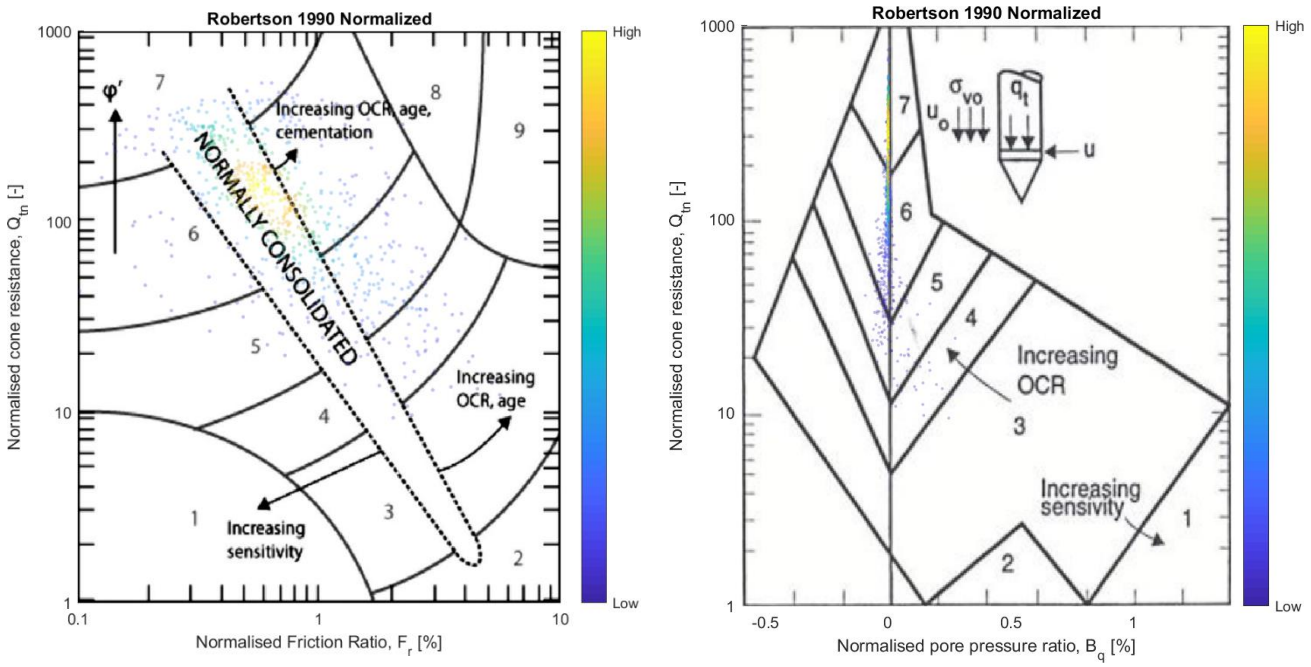

Figure B - 7 CPT data plotted in Robertson SBT chart for US04.

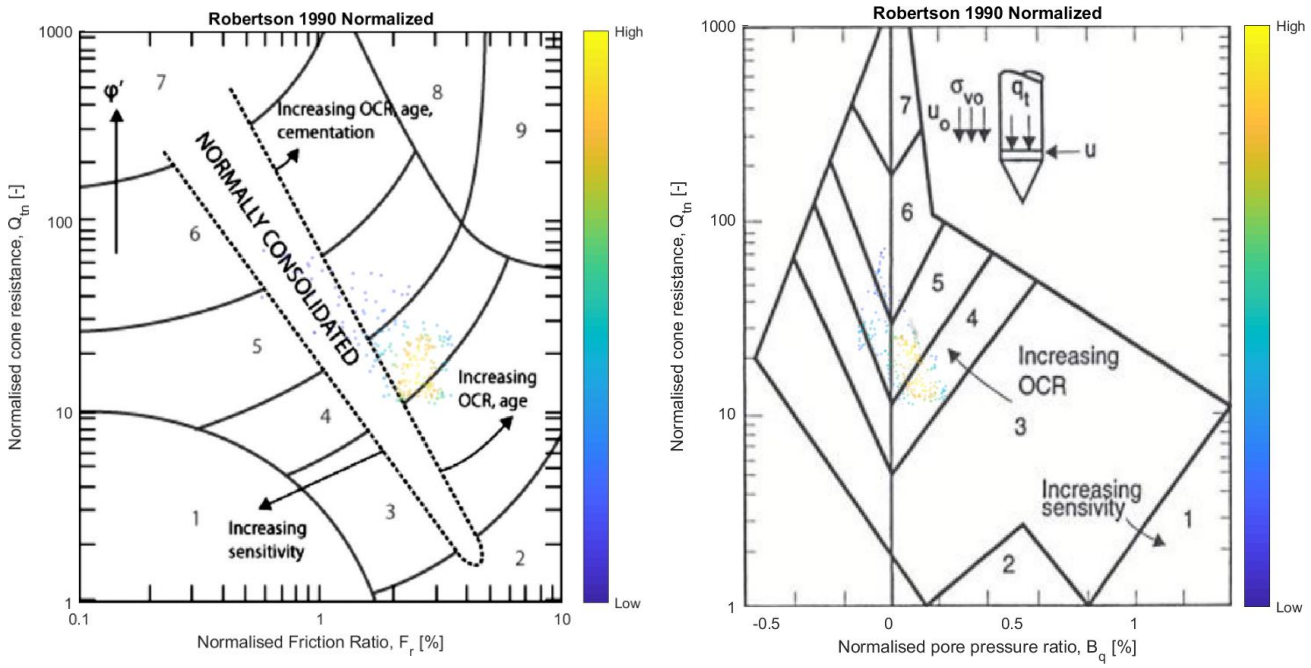

Figure B - 8 CPT data plotted in Robertson SBT chart for UC05.

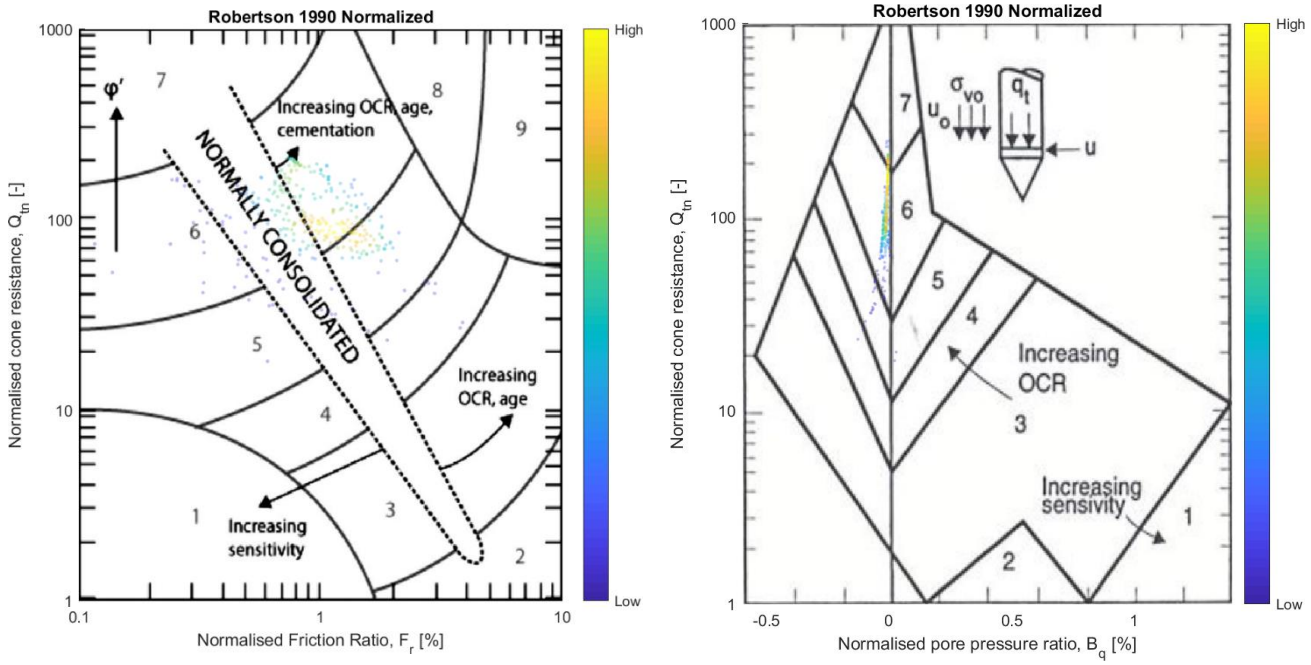

Figure B -

9 CPT data plotted in Robertson SBT chart for US05.

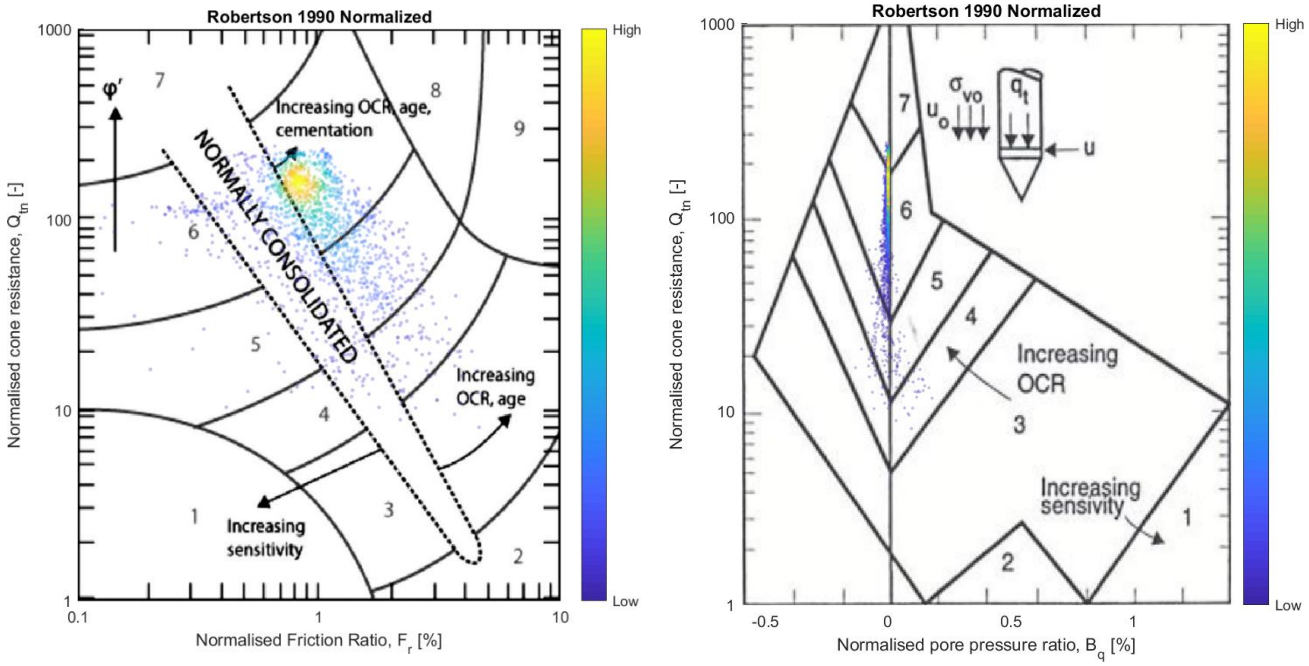

Figure B - 10 CPT data plotted in Robertson SBT chart for US06.

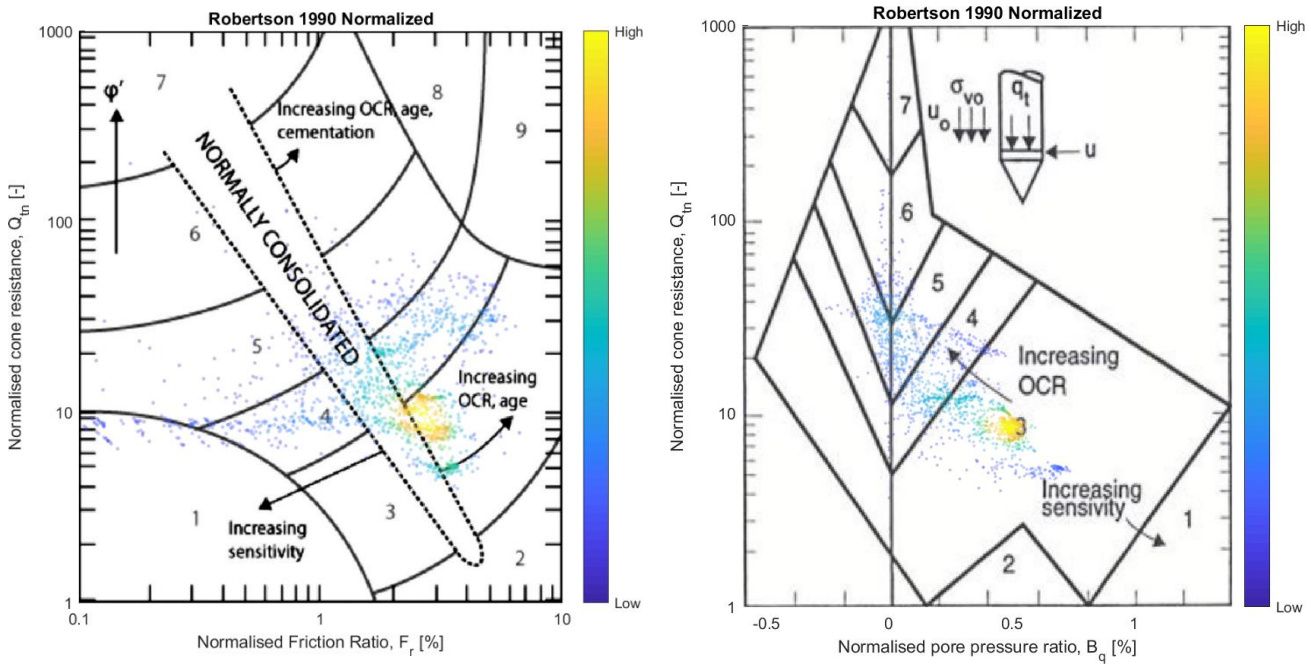

Figure B - 11 CPT data plotted in Robertson SBT chart for UC07.

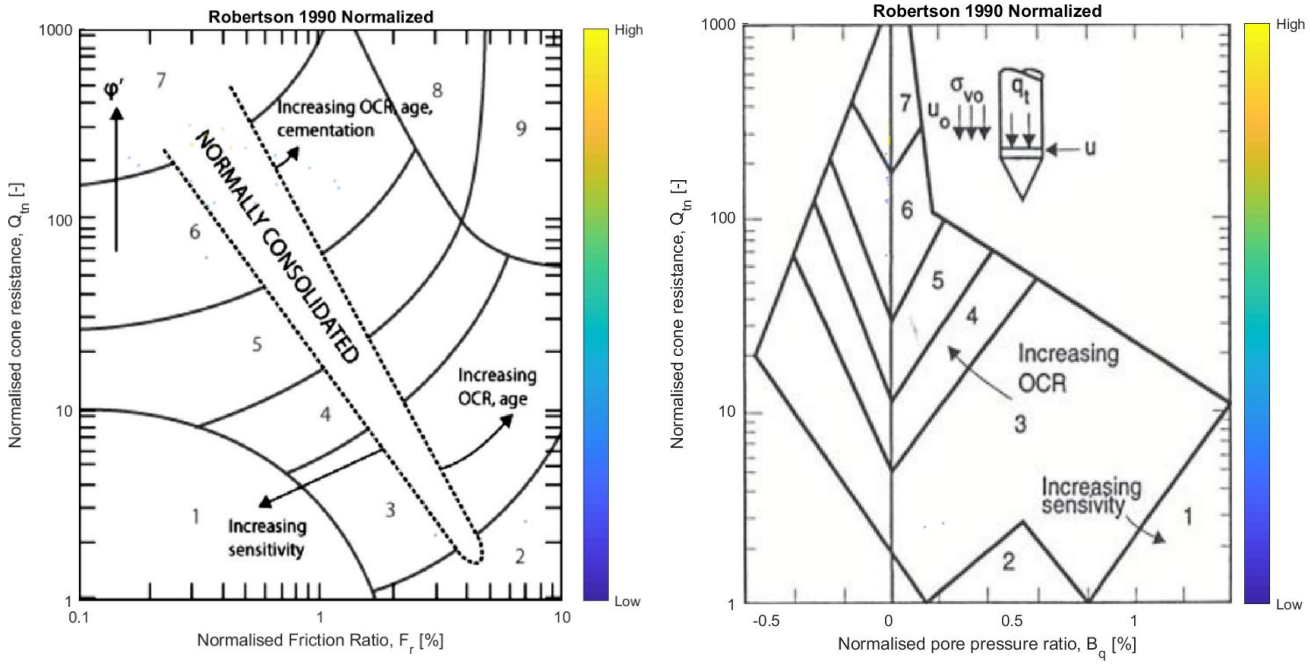

Figure B - 12 CPT data plotted in Robertson SBT chart for US07.

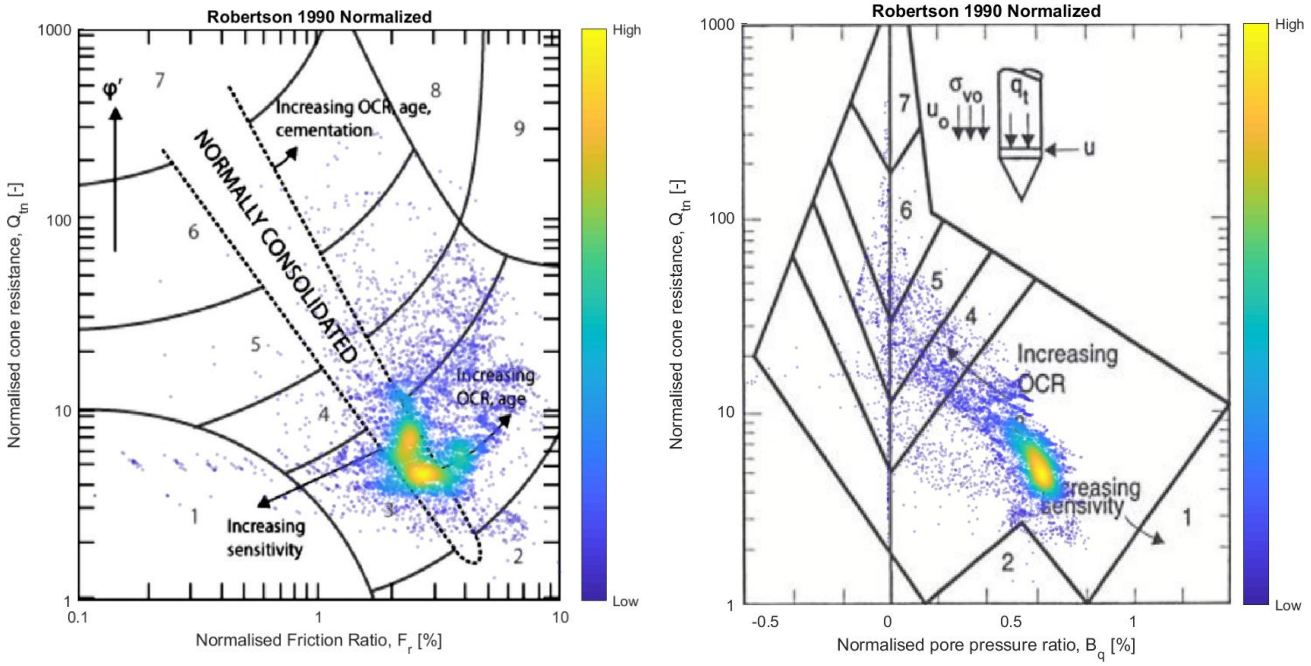

Figure B - 13 CPT data plotted in Robertson SBT chart for UC08.

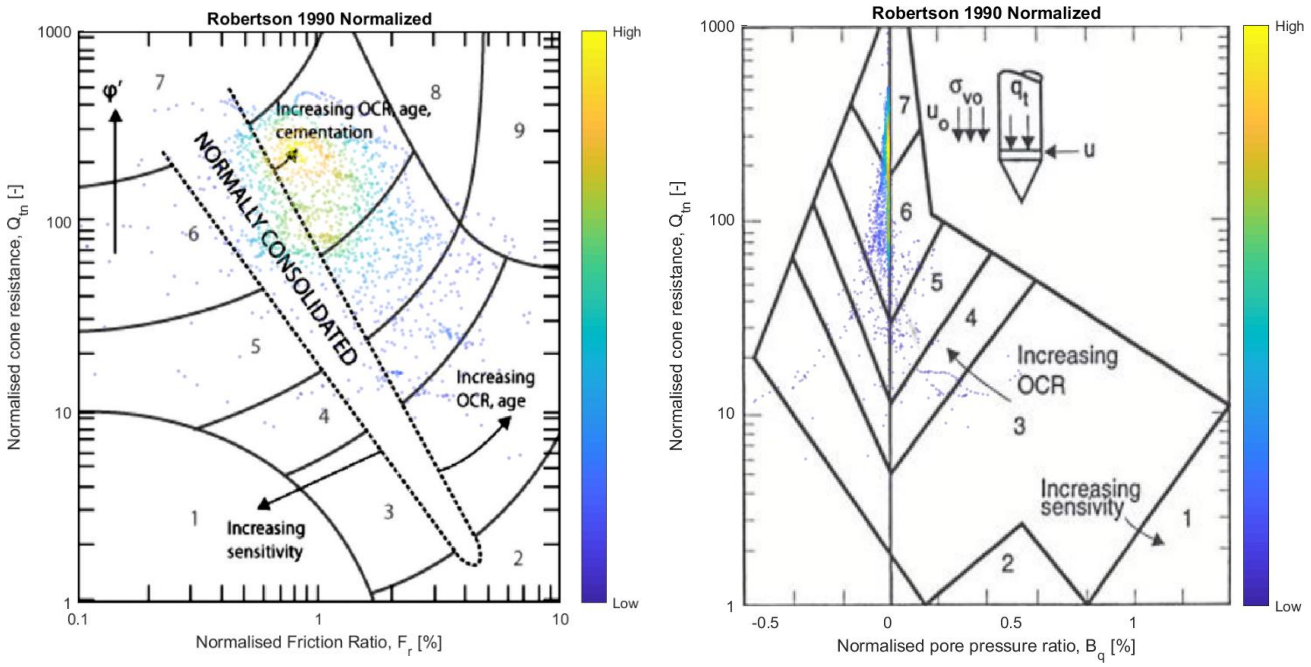

Figure B - 14 CPT data plotted in Robertson SBT chart for US08.

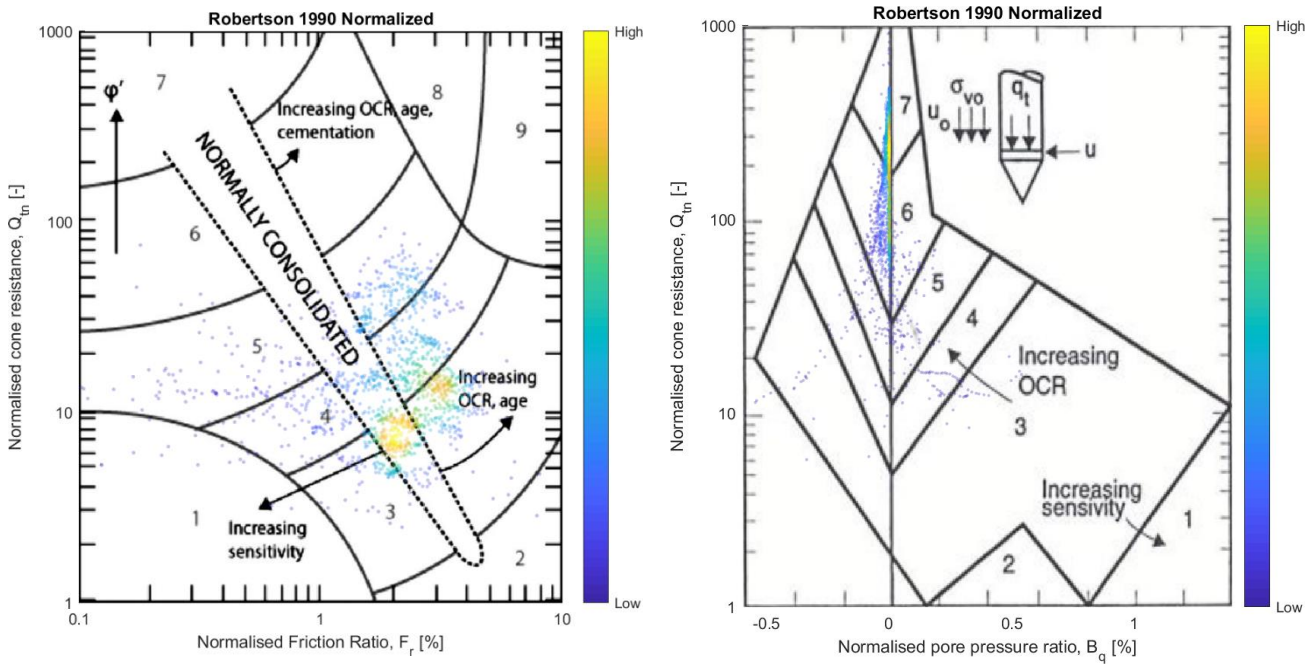

Figure B - 15 CPT data plotted in Robertson SBT chart for UC09.

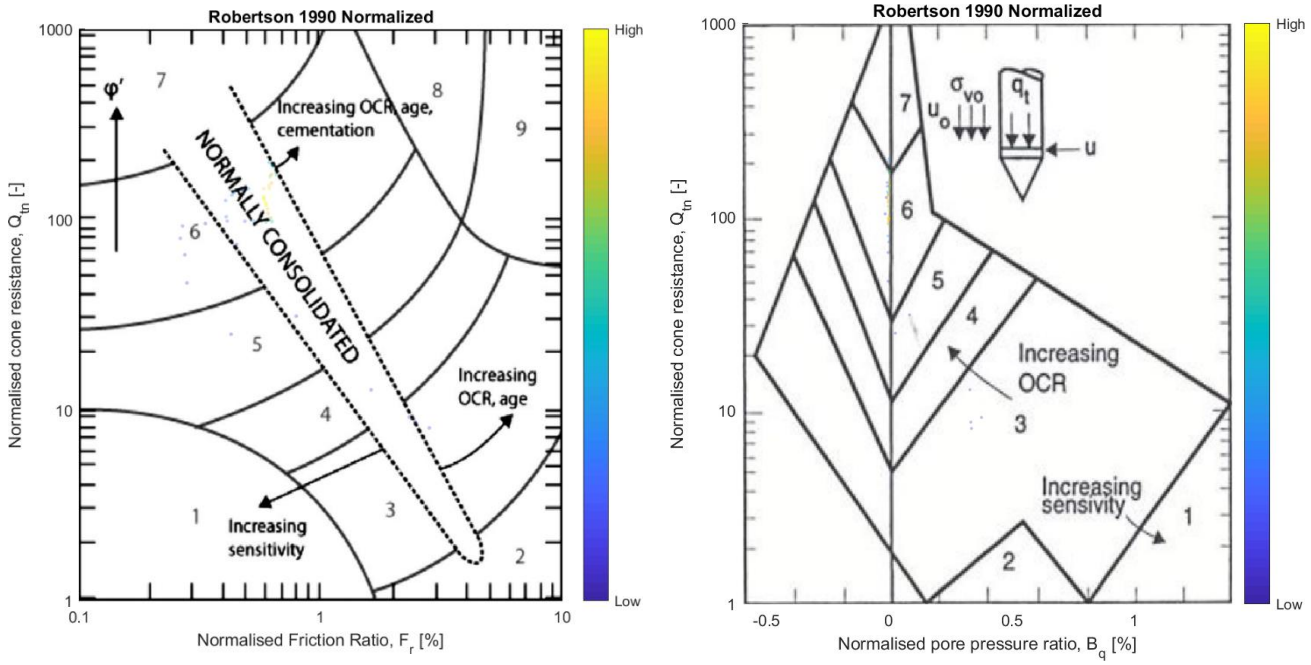

Figure B - 16 CPT data plotted in Robertson SBT chart for US09.

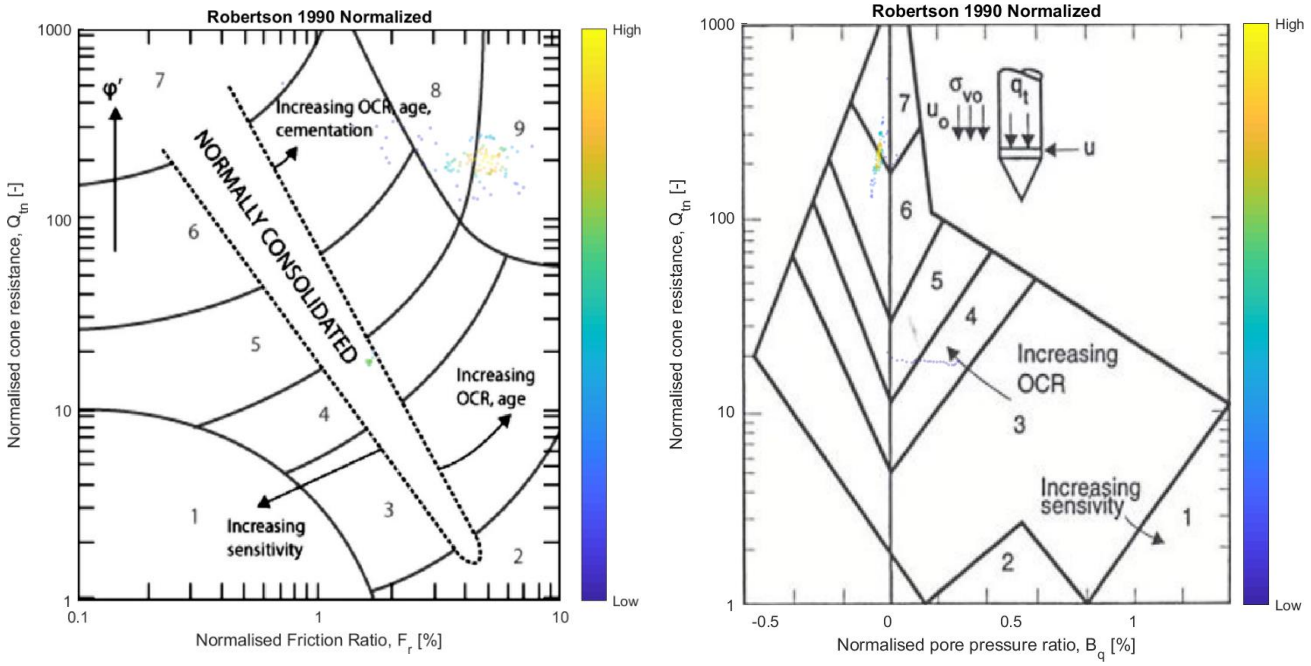

Figure B - 17 CPT data plotted in Robertson SBT chart for UC10.

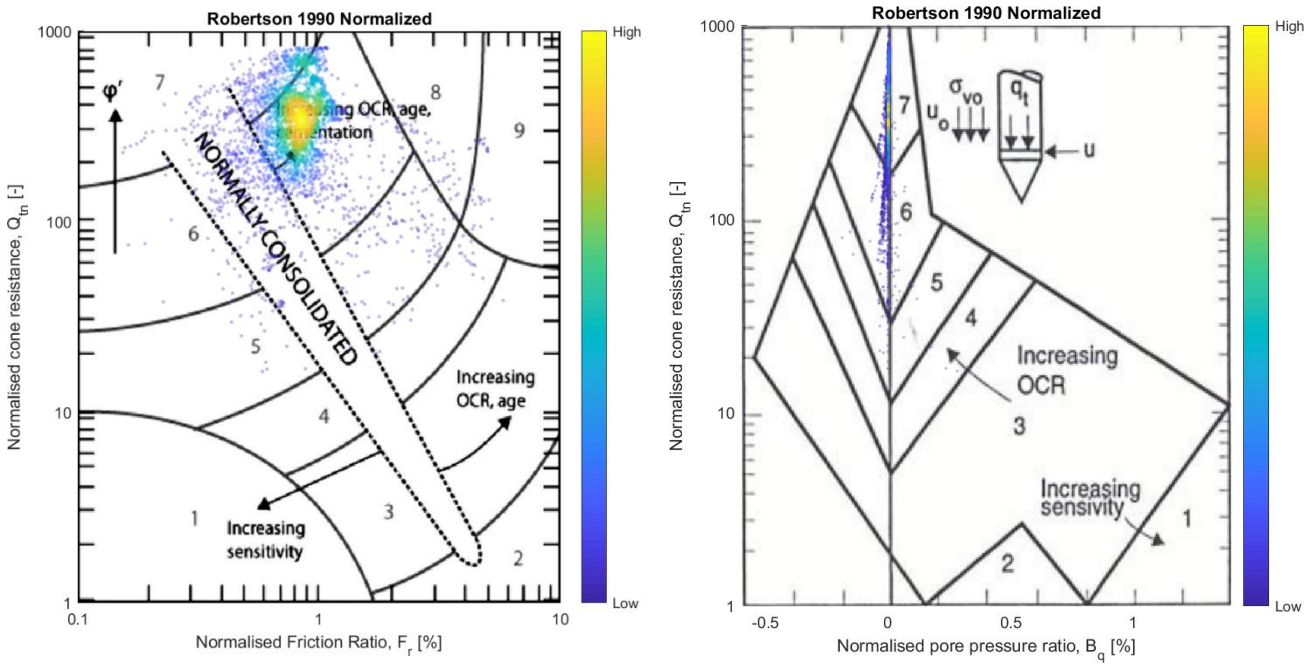

Figure B - 18 CPT data plotted in Robertson SBT chart for US10.

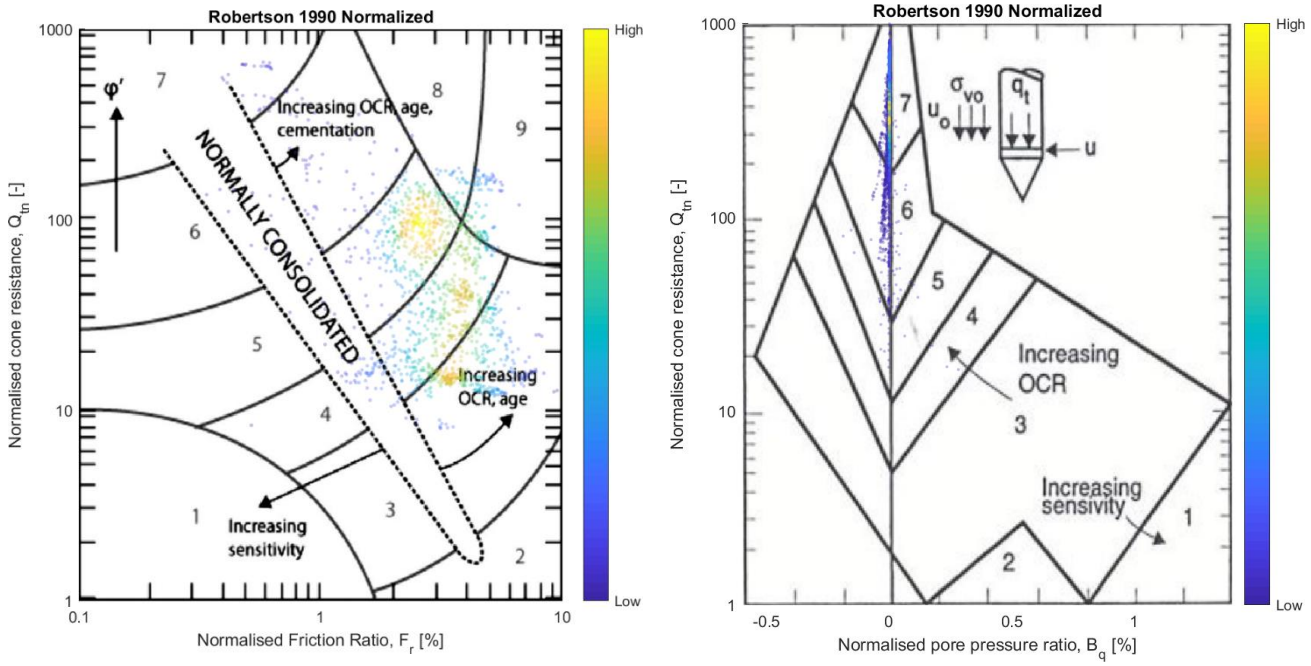

Figure B - 19 CPT data plotted in Robertson SBT chart for UC11.

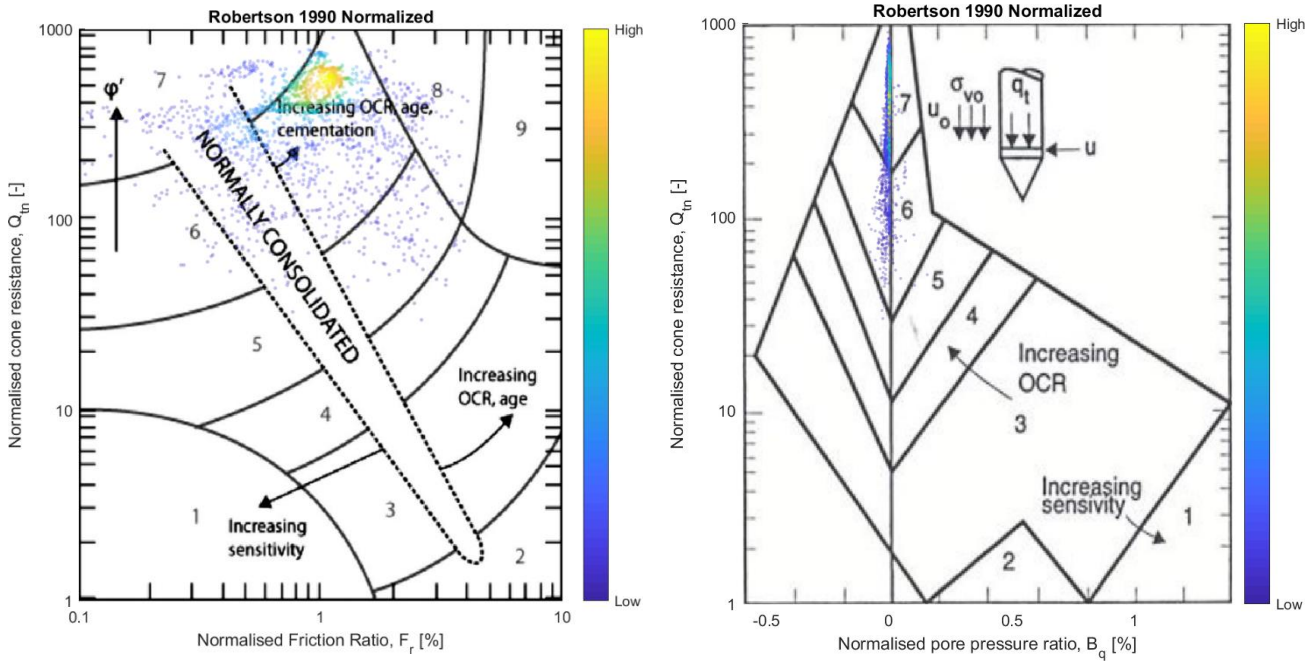

Figure B - 20 CPT data plotted in Robertson SBT chart for US11.

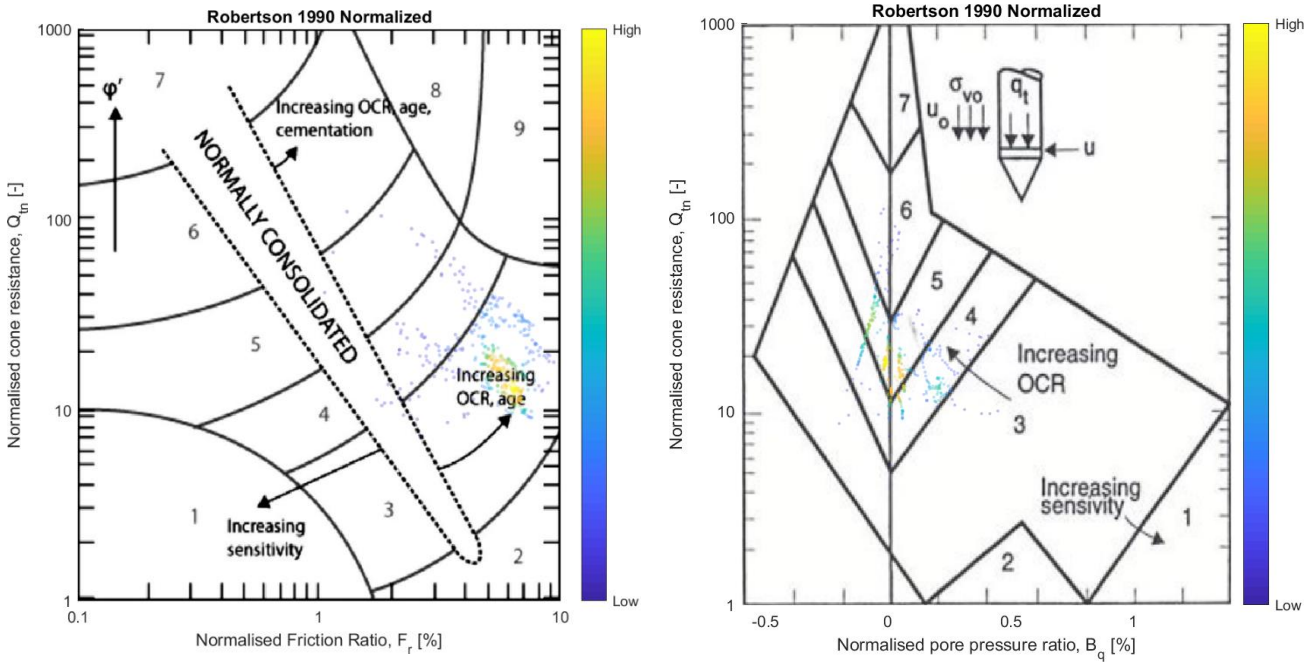

Figure B - 21 CPT data plotted in Robertson SBT chart for UC12.

Appendix C Calculated soil properties per CPT location

This appendix presents the state-, stiffness- and strength properties with depth per geotechnical test location. An example for one location can be seen in Figure C-1. The parameters presented in the figures are derived from the methodology presented in section 8. The red horizontal lines represent the interpreted stratigraphy at the location. It is noticeable that the undrained shear strength, c_u, is only interpreted for clay units, whereas the friction angle, φ', is interpreted for sand units.

The friction angle subplots show a vertical line "I_D limit". This line indicates a maximum value of φ' provided that the relative density used to interpret the friction angle has been limited to I_D = 100%. Nevertheless, CPT-interpretation of the relative density may estimate values above 100%, hence in this case, φ' exceeds the limit line. This description also applies for the figures presented in D.3.

All figures per geotechnical test location are presented in the following pages.

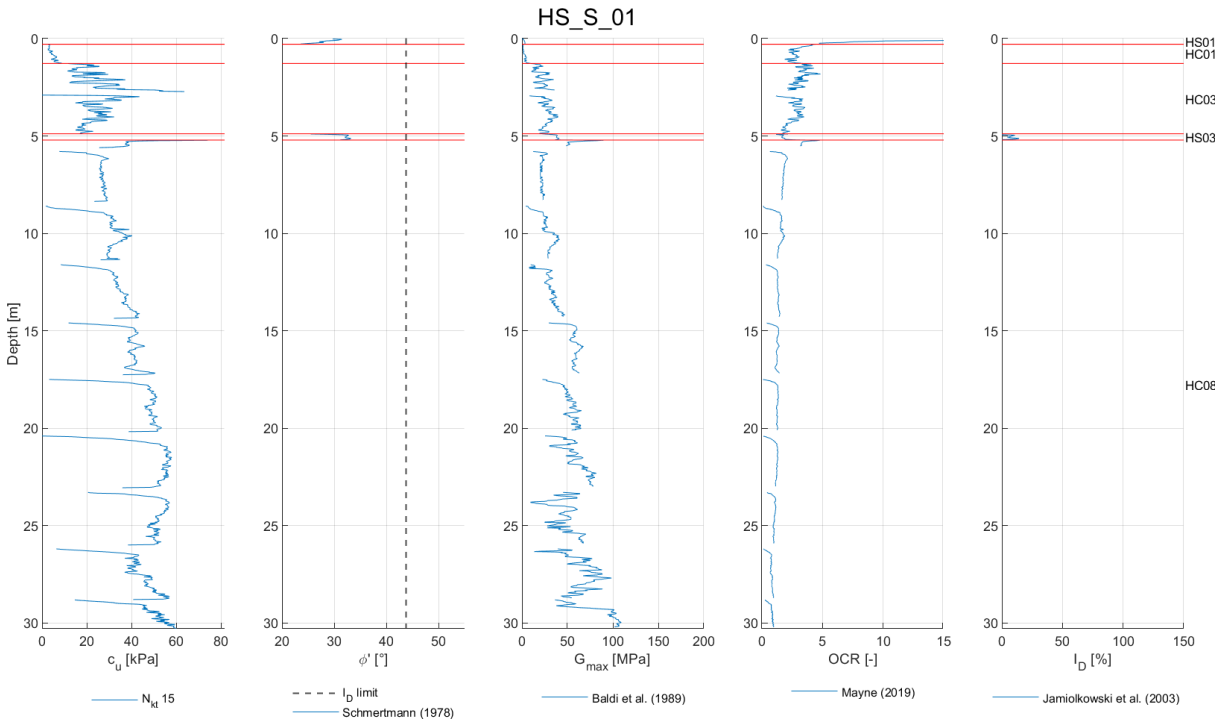

Figure C-1 Example of interpreted properties for HS_S_01

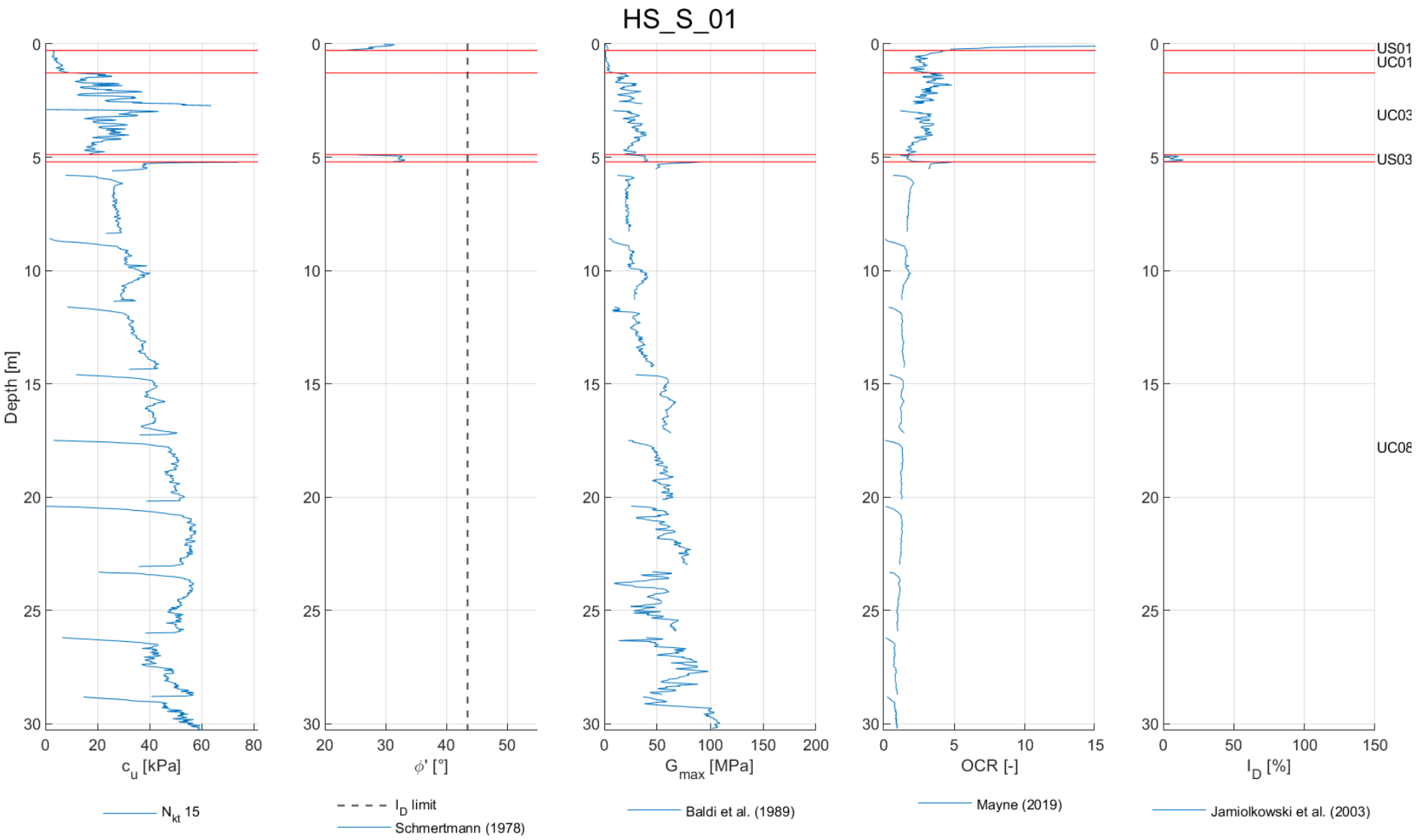
HS_S_01
Depth [m]
c_u [kPa]
N_{kt} 15
ϕ' [°]
I_D limit
Schmertmann (1978)
G_{max} [MPa]
Baldi et al. (1989)
OCR [-]
Mayne (2019)
I_D [%]
Jamiolkowski et al. (2003)
US01
UC01
UC03
US03
UC08

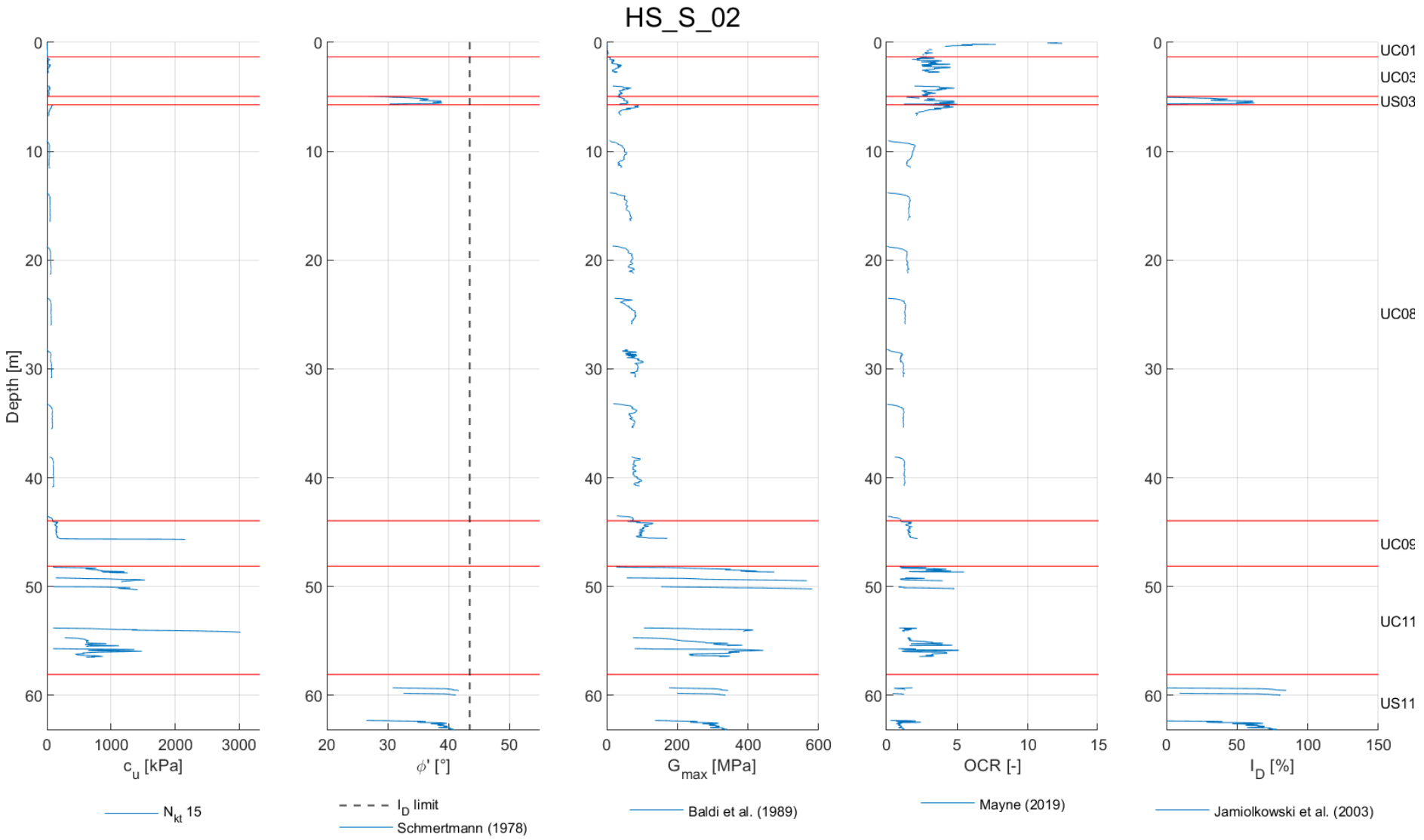
HS_S_02
Depth [m]
c_u [kPa]
ϕ' [°]
G_{max} [MPa]
OCR [-]
I_D [%]
UC01
UC03
US03
UC08
UC09
UC11
US11
N_{kt} 15
I_D limit
Schmertmann (1978)
Baldi et al. (1989)
Mayne (2019)
Jamiolkowski et al. (2003)

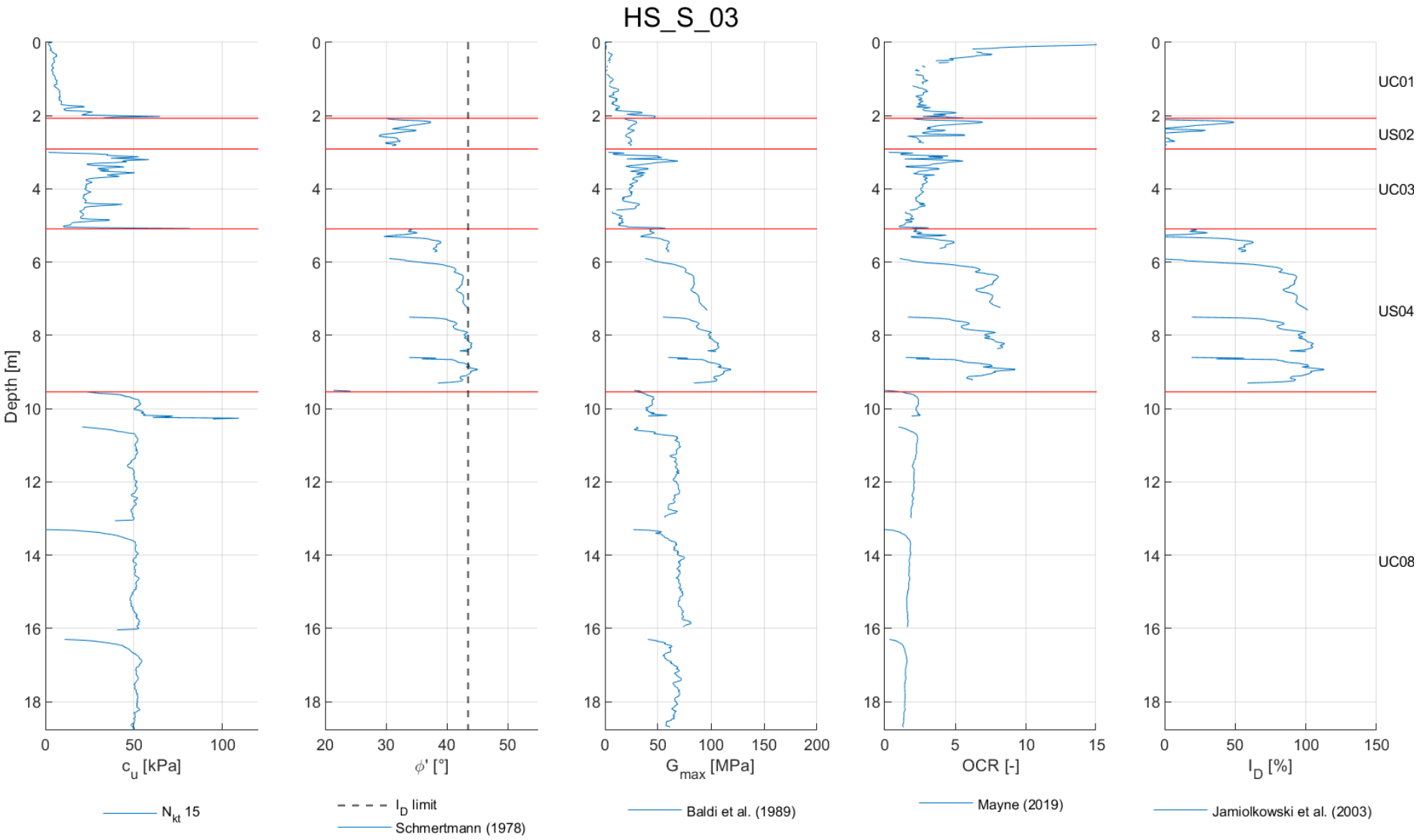
HS_S_03
Depth [m]
c_u [kPa]
N_{kt} 15
ϕ' [°]
I_D limit
Schmertmann (1978)
G_{max} [MPa]
Baldi et al. (1989)
OCR [-]
Mayne (2019)
I_D [%]
Jamiolkowski et al. (2003)
UC01
US02
UC03
US04
UC08

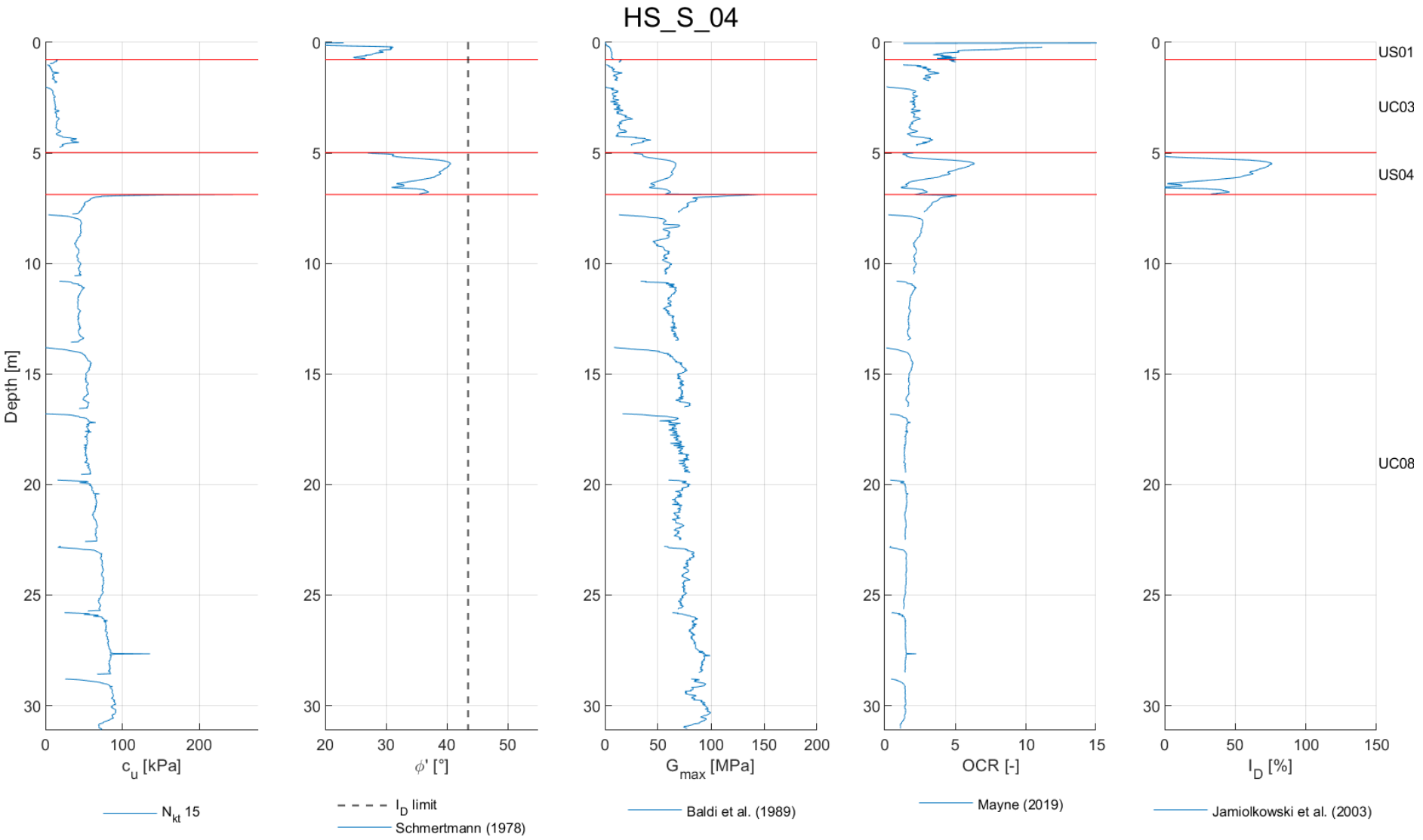
HS_S_04
Depth [m]
0
5
10
15
20
25
30
US01
UC03
US04
UC08
0
100
200
c_u [kPa]
N_{kt} 15
20
30
40
50
ϕ' [°]
I_D limit
Schmertmann (1978)
0
50
100
150
200
G_{max} [MPa]
Baldi et al. (1989)
0
5
10
15
OCR [-]
Mayne (2019)
0
50
100
150
I_D [%]
Jamiolkowski et al. (2003)

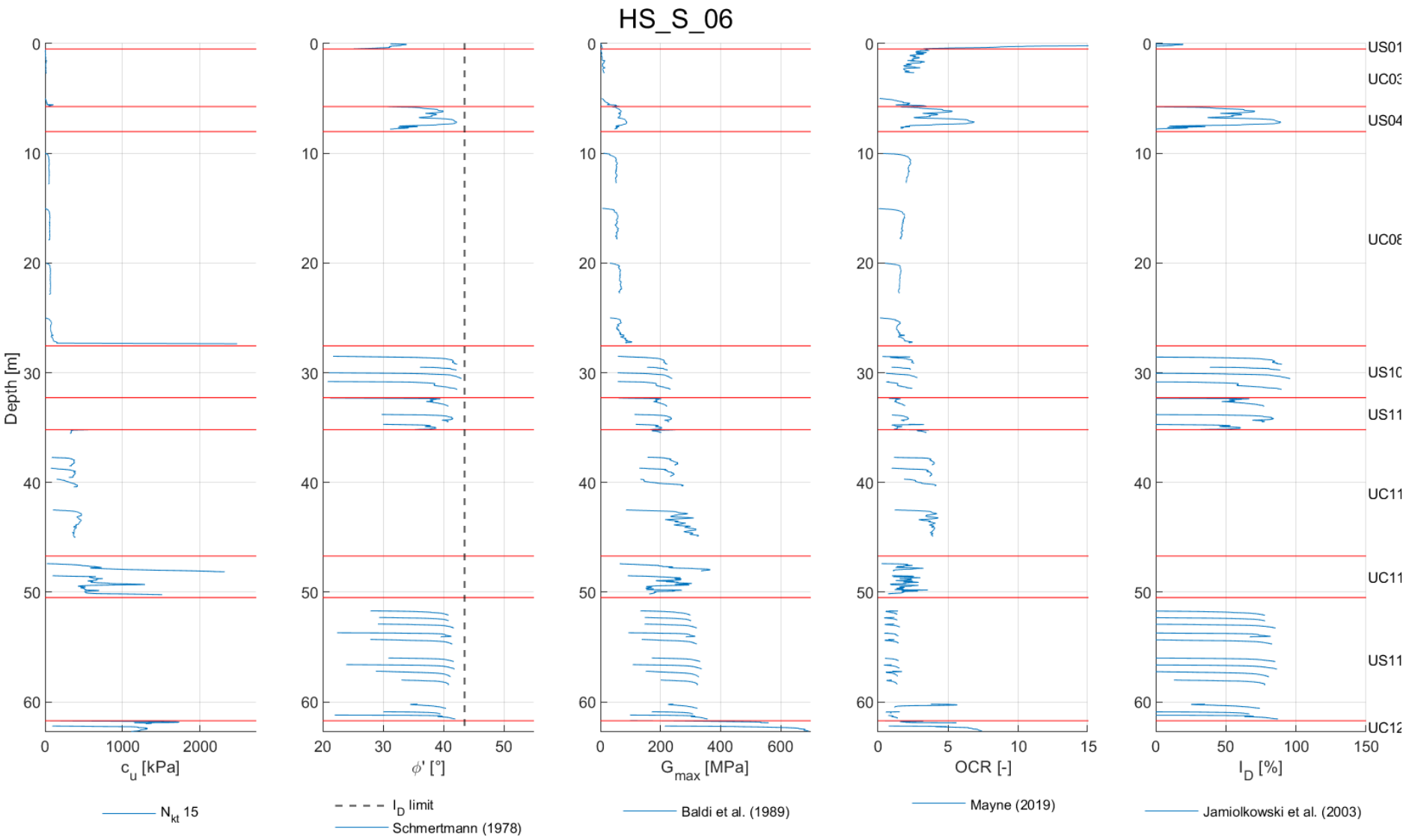
HS_S_06
Depth [m]
c_u [kPa]
ϕ' [°]
G_{max} [MPa]
OCR [-]
I_D [%]
US01
UC03
US04
UC08
US10
US11
UC11
UC11
US11
UC12
N_{kt} 15
I_D limit
Schmertmann (1978)
Baldi et al. (1989)
Mayne (2019)
Jamiolkowski et al. (2003)

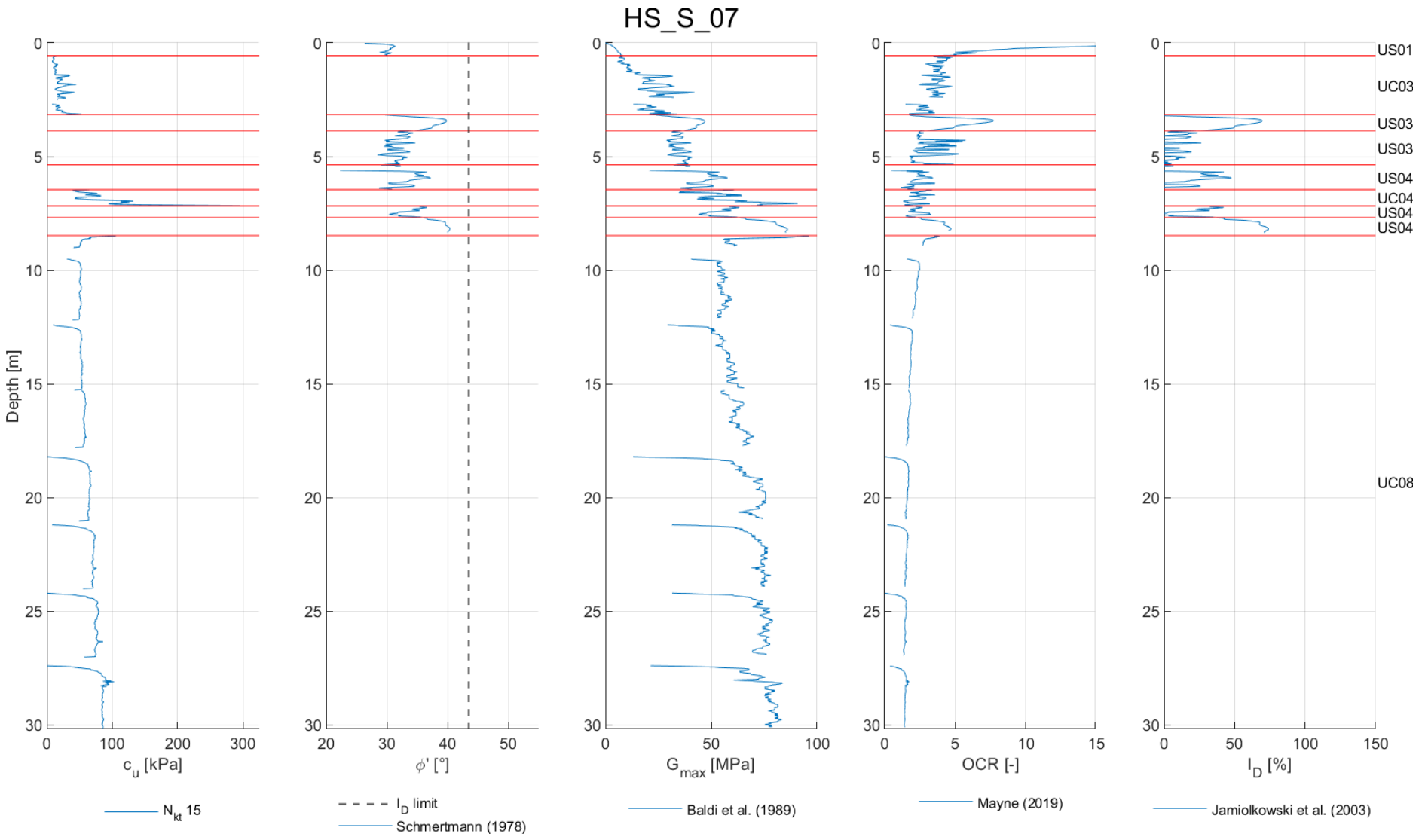
HS_S_07
Depth [m]
c_u [kPa]
ϕ' [°]
G_{max} [MPa]
OCR [-]
I_D [%]
US01
UC03
US03
US03
US04
UC04
US04
US04
UC08
N_{kt} 15
I_D limit
Schmertmann (1978)
Baldi et al. (1989)
Mayne (2019)
Jamiolkowski et al. (2003)

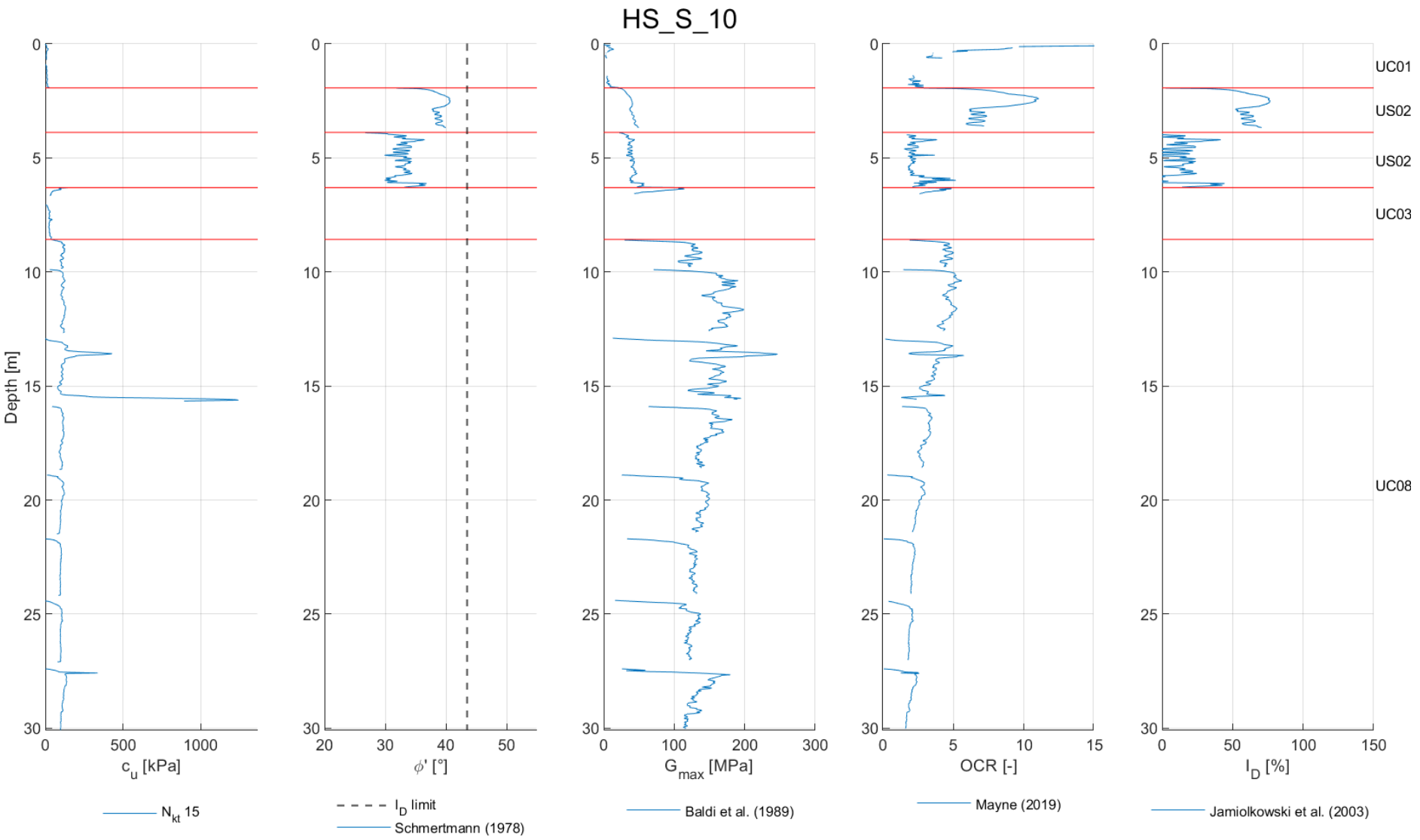
HS_S_10
Depth [m]
c_u [kPa]
N_{kt} 15
ϕ' [°]
I_D limit
Schmertmann (1978)
G_{max} [MPa]
Baldi et al. (1989)
OCR [-]
Mayne (2019)
I_D [%]
Jamiolkowski et al. (2003)
UC01
US02
US02
UC03
UC08

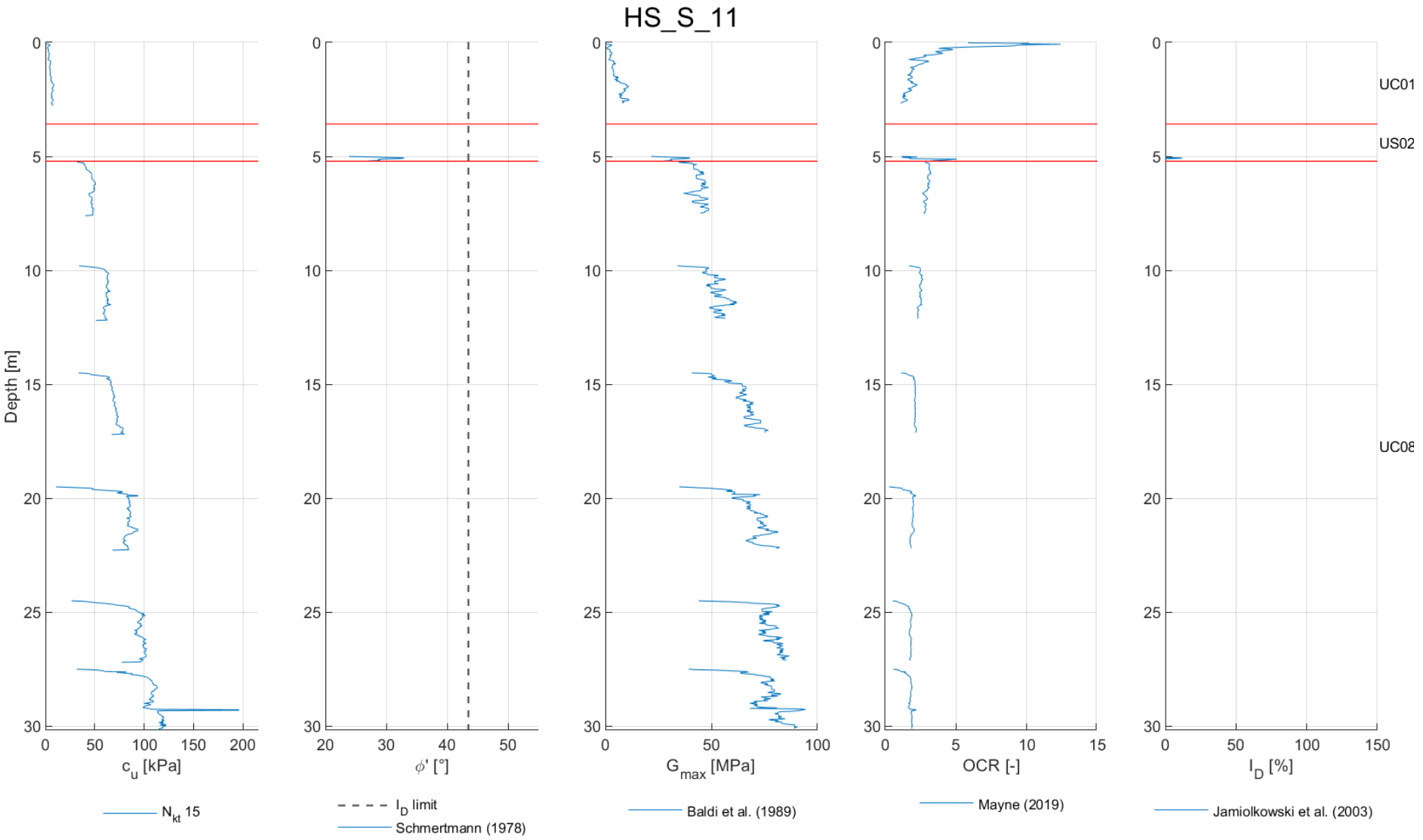
HS_S_11
Depth [m]
c_u [kPa]
ϕ' [°]
G_{max} [MPa]
OCR [-]
I_D [%]
UC01
US02
UC08
N_{kt} 15
I_D limit
Schmertmann (1978)
Baldi et al. (1989)
Mayne (2019)
Jamiolkowski et al. (2003)

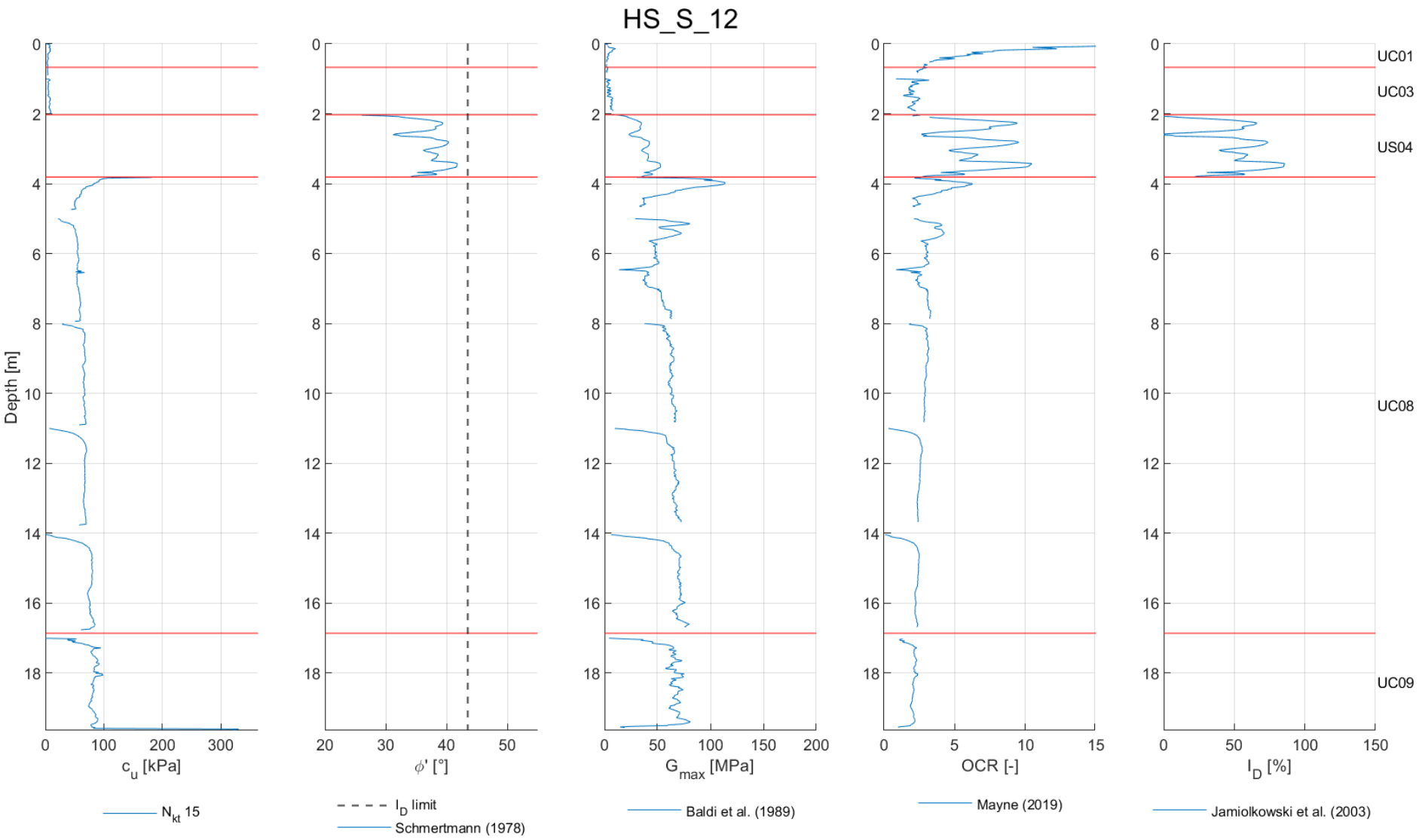
HS_S_12
Depth [m]
c_u [kPa]
ϕ' [°]
G_{max} [MPa]
OCR [-]
I_D [%]
UC01
UC03
US04
UC08
UC09
N_{kt} 15
I_D limit
Schmertmann (1978)
Baldi et al. (1989)
Mayne (2019)
Jamiolkowski et al. (2003)

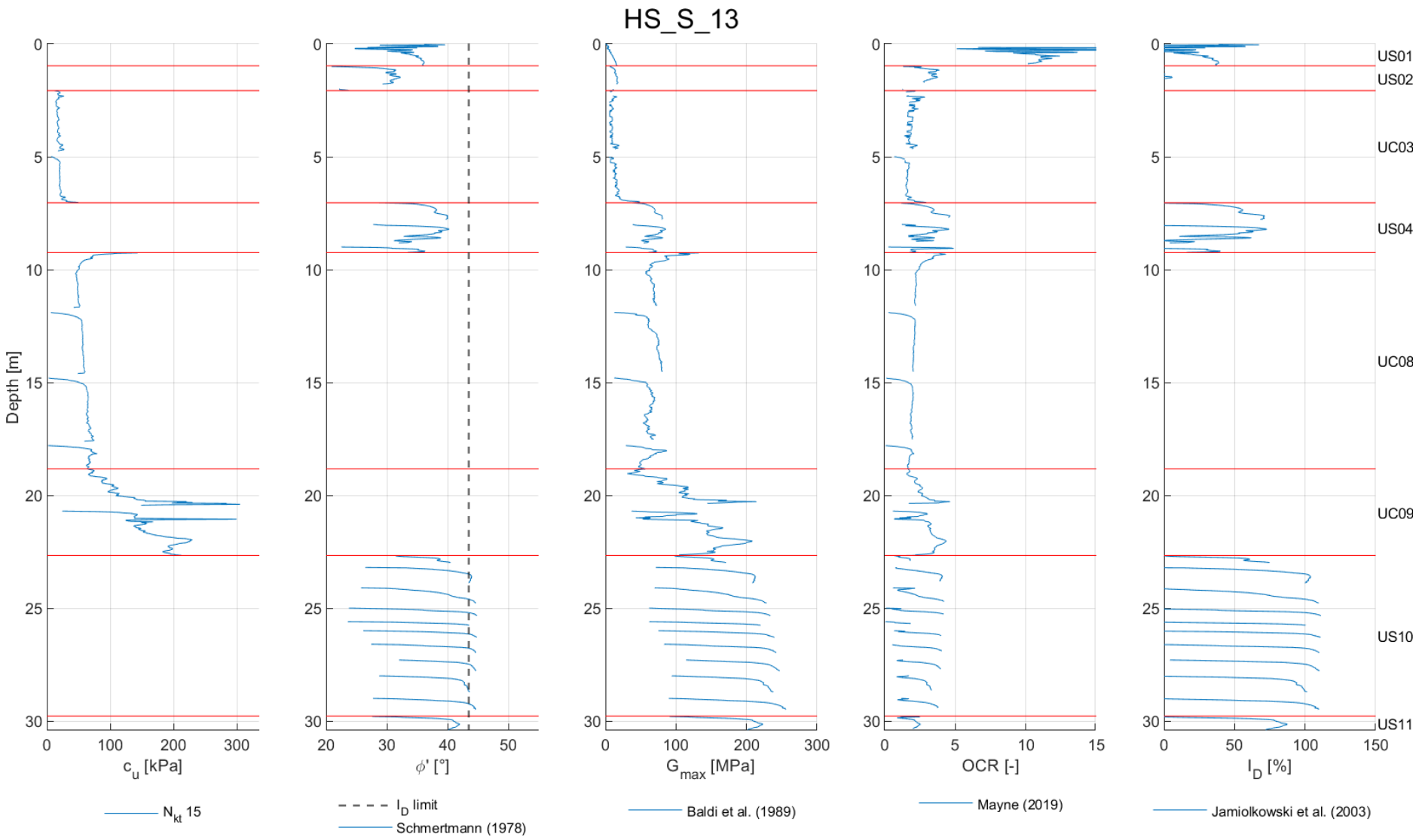
HS_S_13
Depth [m]
c_u [kPa]
ϕ' [°]
G_{max} [MPa]
OCR [-]
I_D [%]
US01
US02
UC03
US04
UC08
UC09
US10
US11
N_{kt} 15
I_D limit
Schmertmann (1978)
Baldi et al. (1989)
Mayne (2019)
Jamiolkowski et al. (2003)

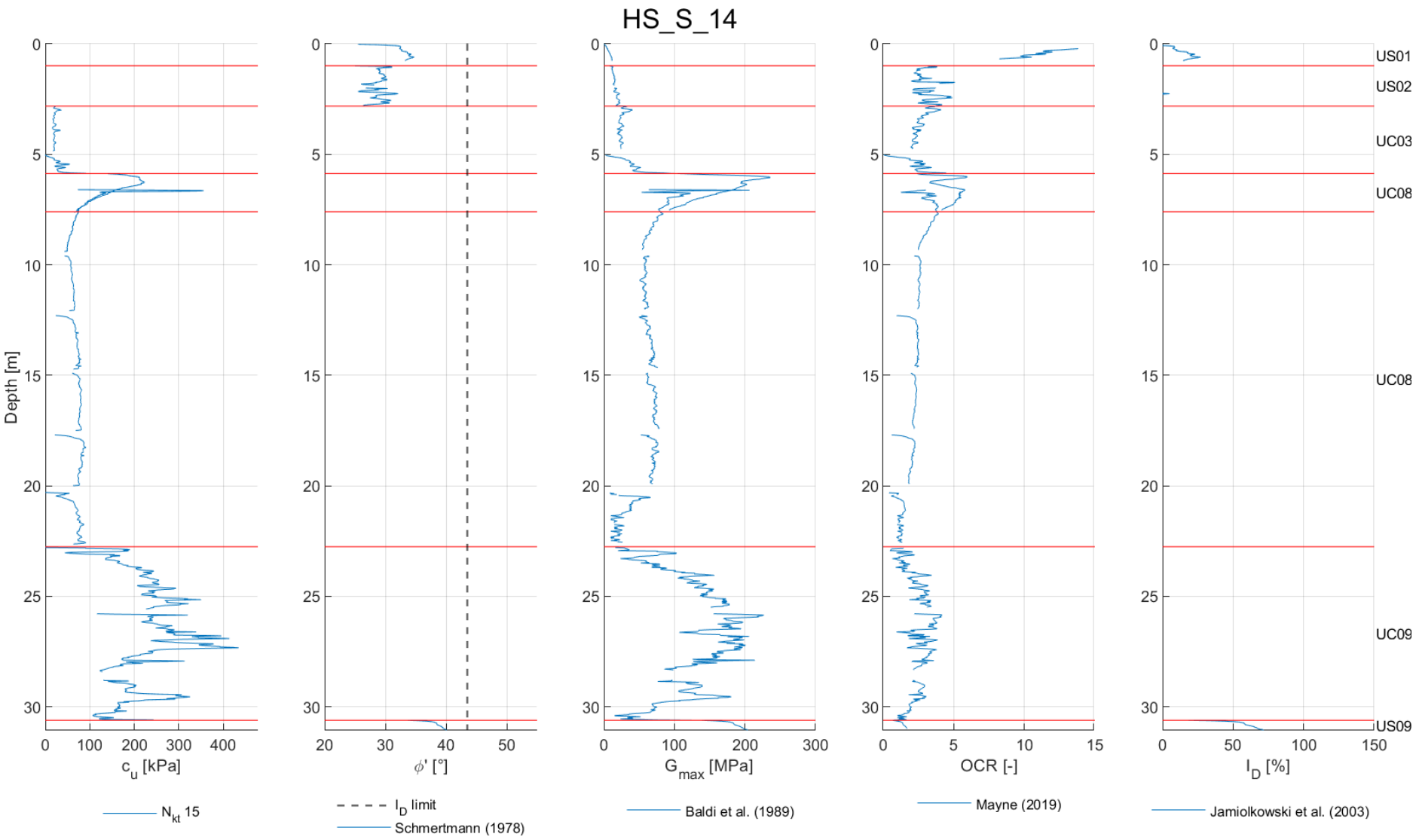
HS_S_14
Depth [m]
c_u [kPa]
ϕ' [°]
G_{max} [MPa]
OCR [-]
I_D [%]
US01
US02
UC03
UC08
UC08
UC09
US09
N_{kt} 15
I_D limit
Schmertmann (1978)
Baldi et al. (1989)
Mayne (2019)
Jamiolkowski et al. (2003)

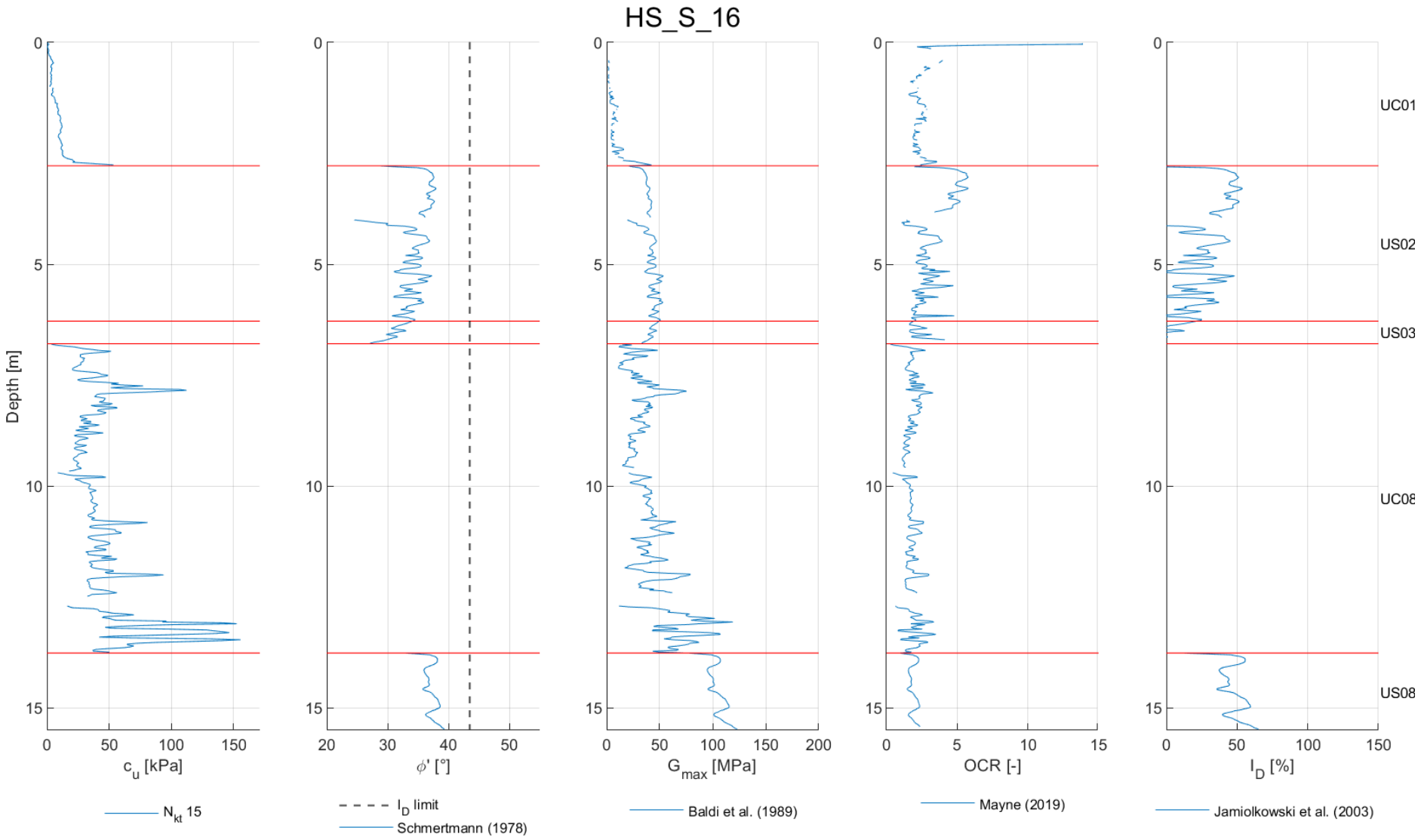
HS_S_16
Depth [m]
0
5
10
15
0
50
100
150
c_u [kPa]
N_{kt} 15
20
30
40
50
ϕ' [°]
I_D limit
Schmertmann (1978)
0
50
100
150
200
G_{max} [MPa]
Baldi et al. (1989)
0
5
10
15
OCR [-]
Mayne (2019)
0
50
100
150
I_D [%]
Jamiolkowski et al. (2003)
UC01
US02
US03
UC08
US08

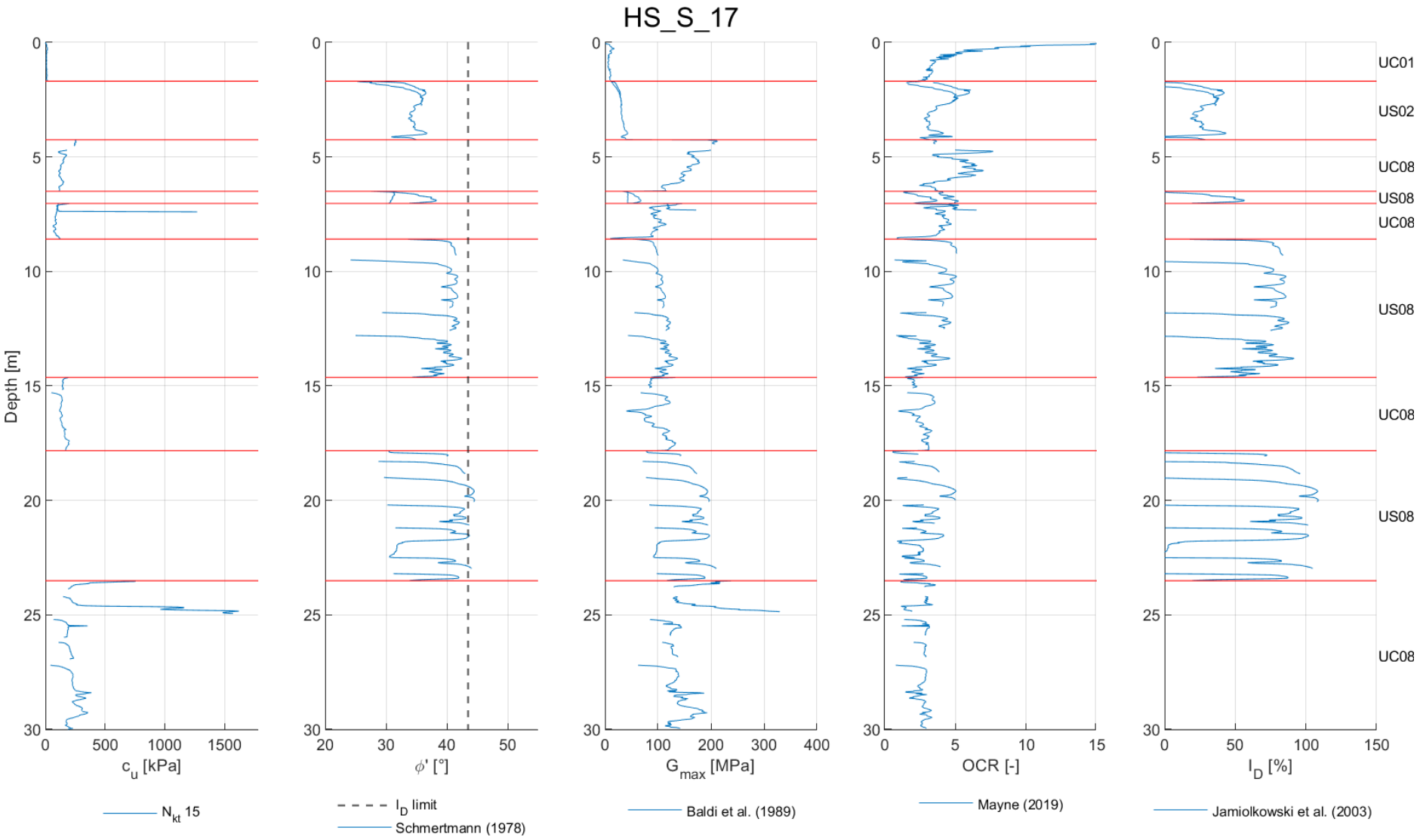
HS_S_17
Depth [m]
c_u [kPa]
N_{kt} 15
ϕ' [°]
I_D limit
Schmertmann (1978)
G_{max} [MPa]
Baldi et al. (1989)
OCR [-]
Mayne (2019)
I_D [%]
Jamiolkowski et al. (2003)
UC01
US02
UC08
US08
UC08
US08
UC08
US08
UC08

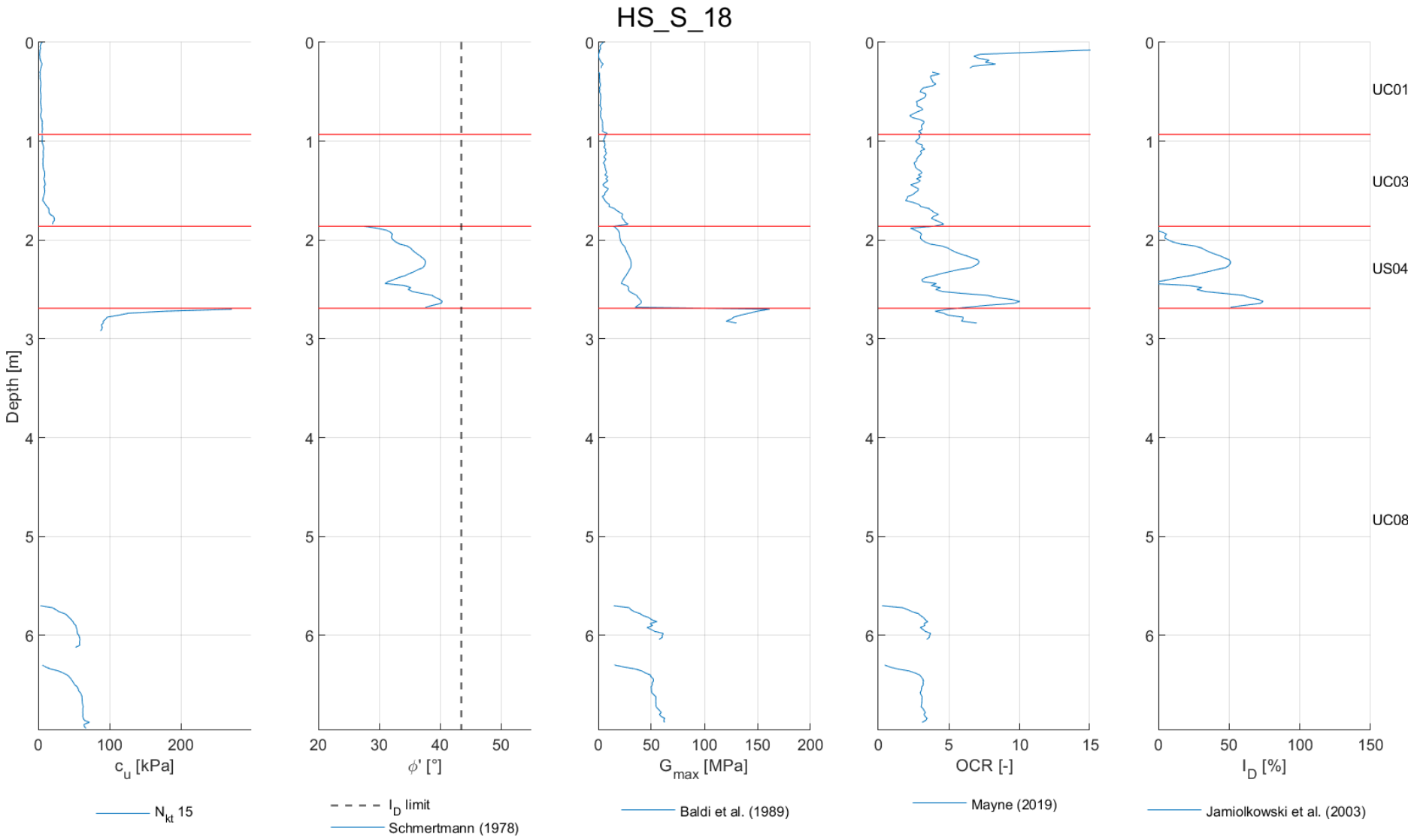
HS_S_18
Depth [m]
c_u [kPa]
ϕ' [°]
G_{max} [MPa]
OCR [-]
I_D [%]
UC01
UC03
US04
UC08
N_{kt} 15
I_D limit
Schmertmann (1978)
Baldi et al. (1989)
Mayne (2019)
Jamiolkowski et al. (2003)

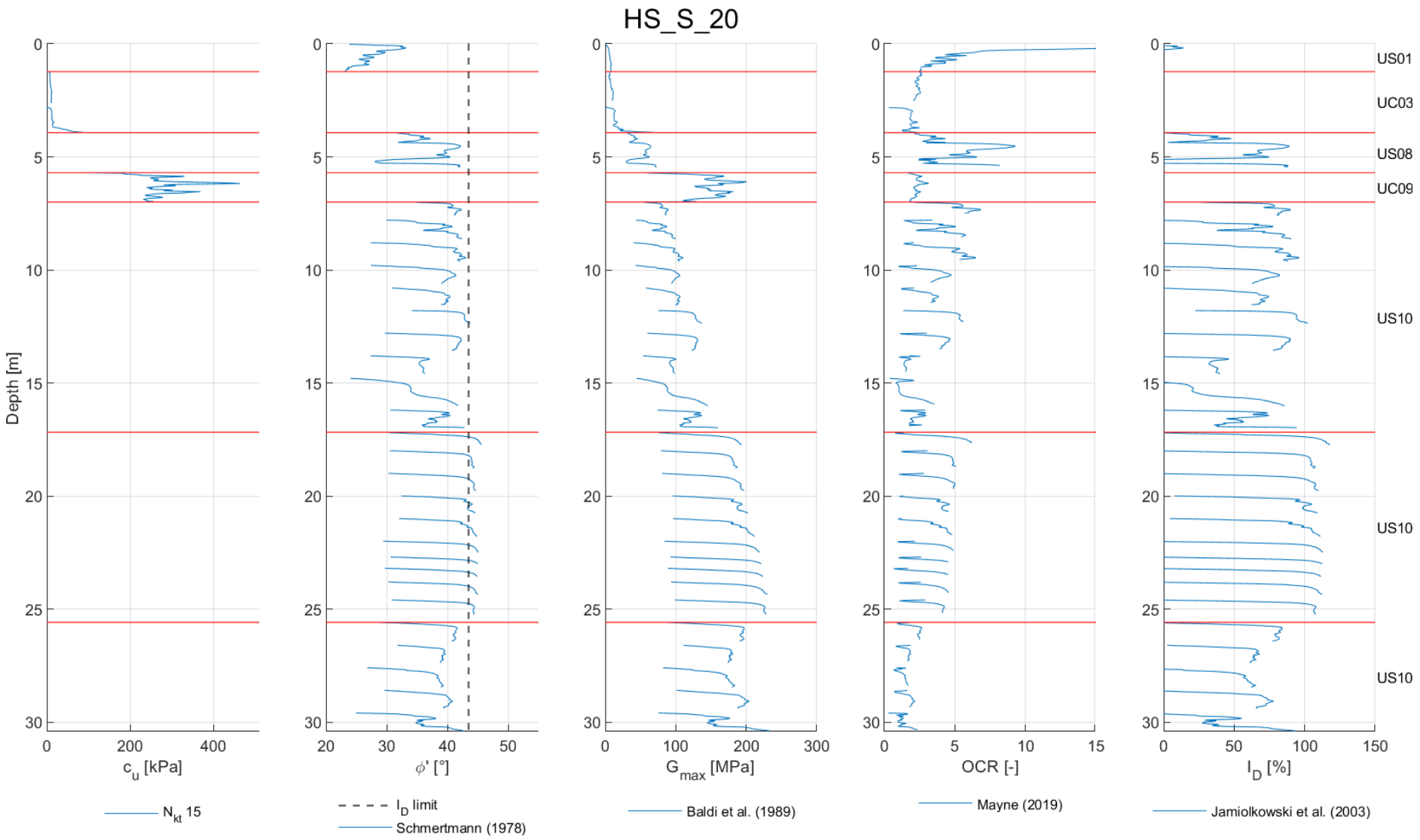
HS_S_20
Depth [m]
c_u [kPa]
ϕ' [°]
G_{max} [MPa]
OCR [-]
I_D [%]
US01
UC03
US08
UC09
US10
US10
US10
N_{kt} 15
I_D limit
Schmertmann (1978)
Baldi et al. (1989)
Mayne (2019)
Jamiolkowski et al. (2003)

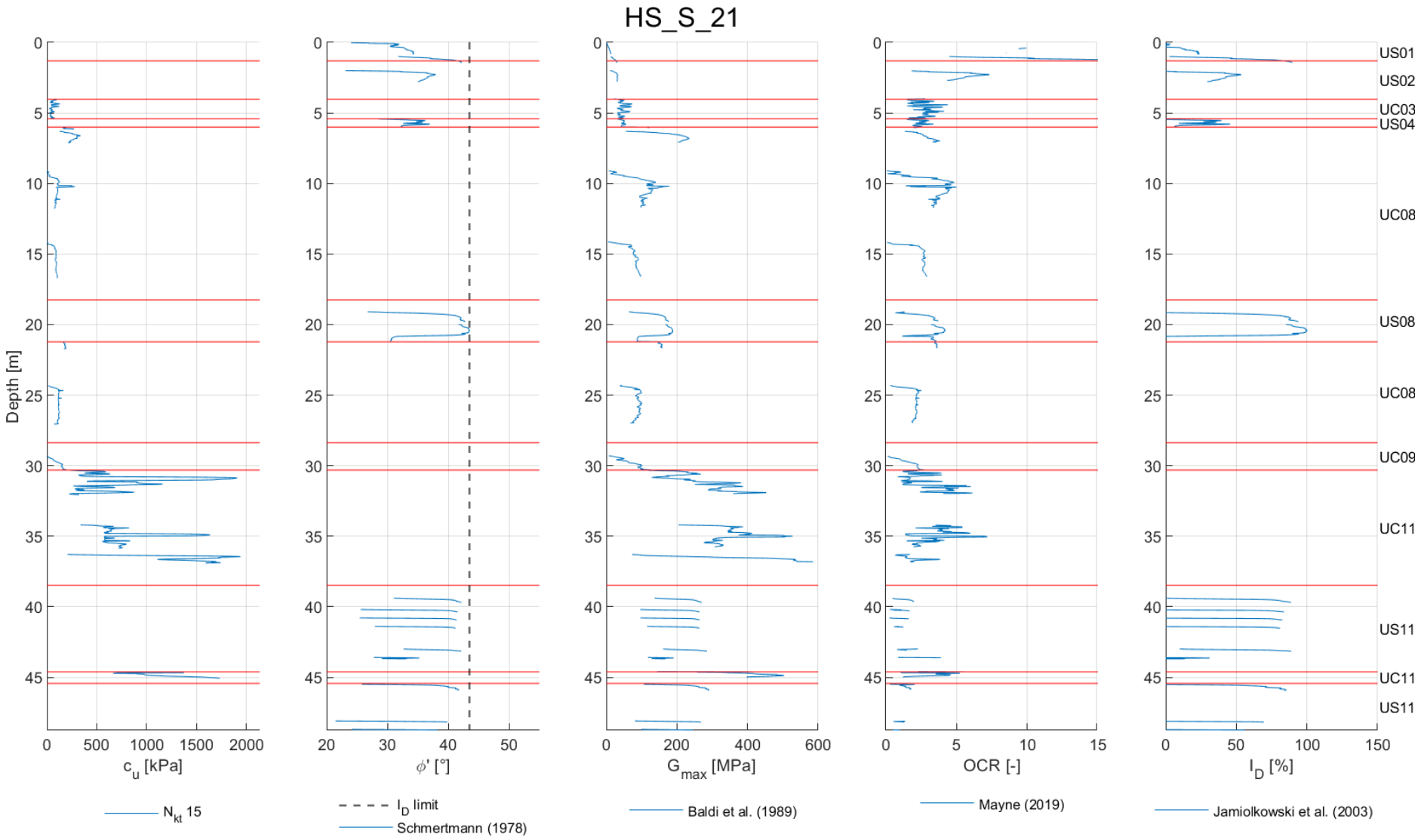
HS_S_21
Depth [m]
c_u [kPa]
ϕ' [°]
G_{max} [MPa]
OCR [-]
I_D [%]
US01
US02
UC03
US04
UC08
US08
UC08
UC09
UC11
US11
UC11
US11
N_{kt} 15
I_D limit
Schmertmann (1978)
Baldi et al. (1989)
Mayne (2019)
Jamiolkowski et al. (2003)

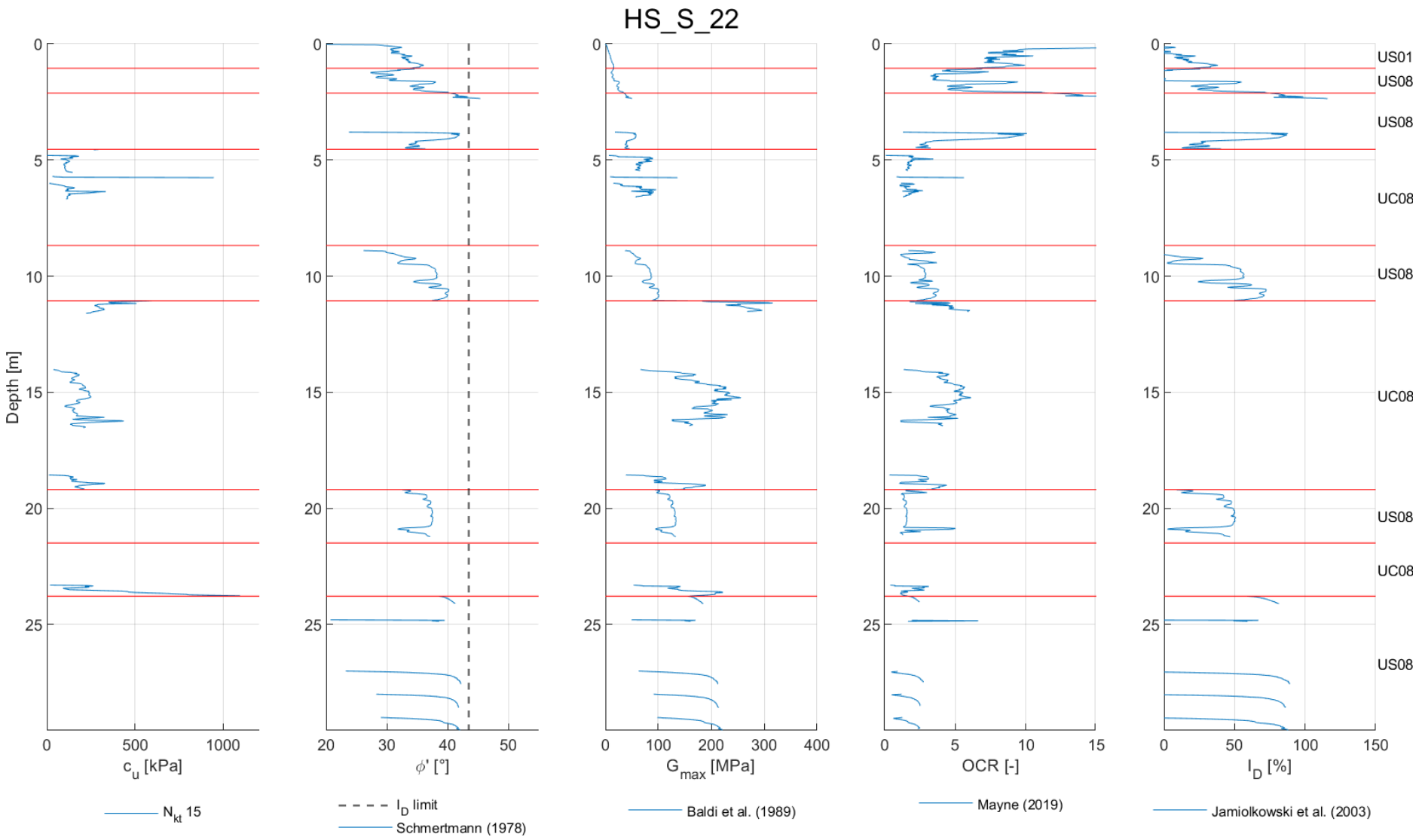
HS_S_22
Depth [m]
c_u [kPa]
ϕ' [°]
G_{max} [MPa]
OCR [-]
I_D [%]
US01
US08
US08
UC08
US08
UC08
US08
UC08
US08
N_{kt} 15
I_D limit
Schmertmann (1978)
Baldi et al. (1989)
Mayne (2019)
Jamiolkowski et al. (2003)

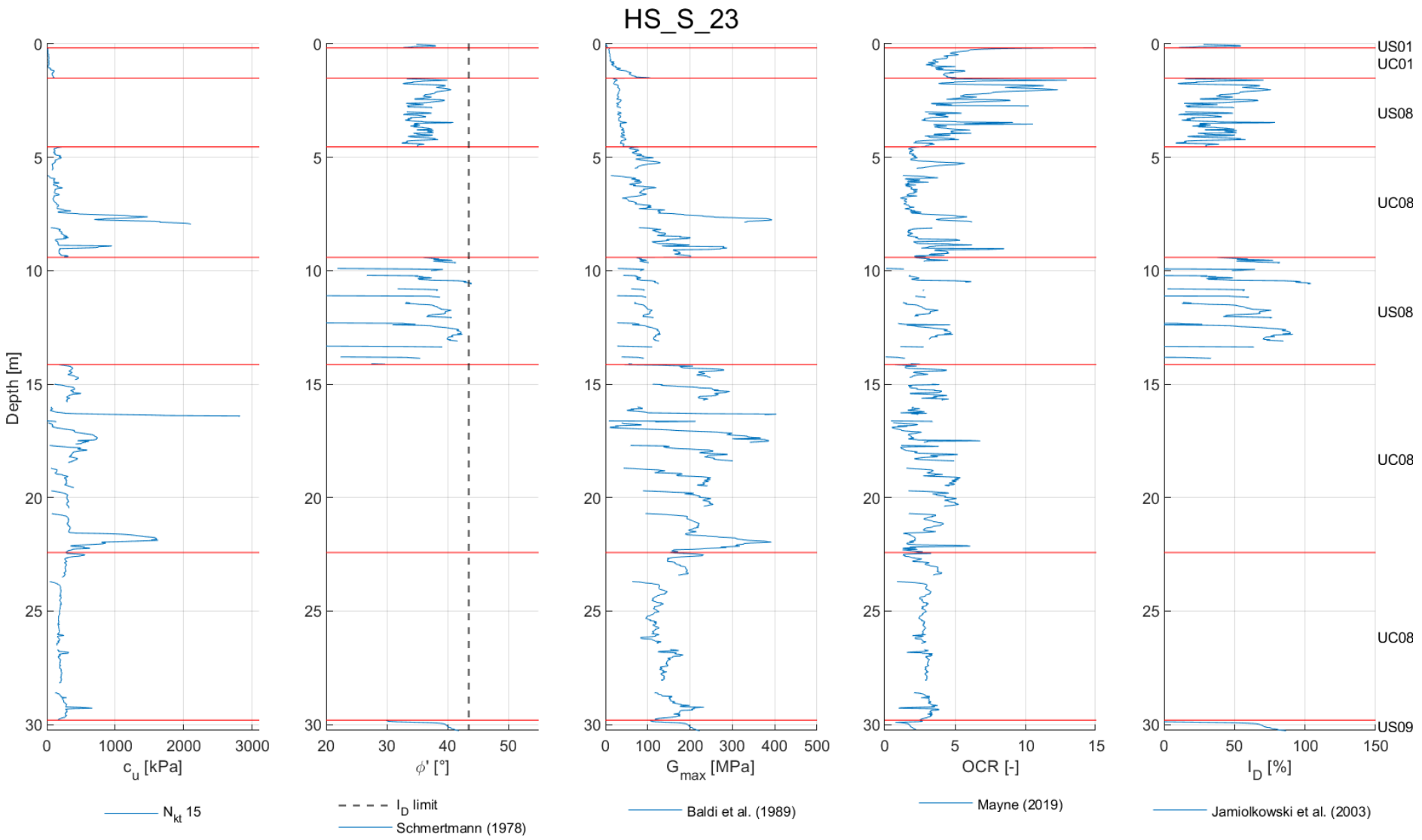
HS_S_23
Depth [m]
0
5
10
15
20
25
30
0
1000
2000
3000
c_u [kPa]
N_{kt} 15
20
30
40
50
ϕ' [°]
I_D limit
Schmertmann (1978)
0
100
200
300
400
500
G_{max} [MPa]
Baldi et al. (1989)
0
5
10
15
OCR [-]
Mayne (2019)
0
50
100
150
I_D [%]
Jamiolkowski et al. (2003)
US01
UC01
US08
UC08
US08
UC08
UC08
US09

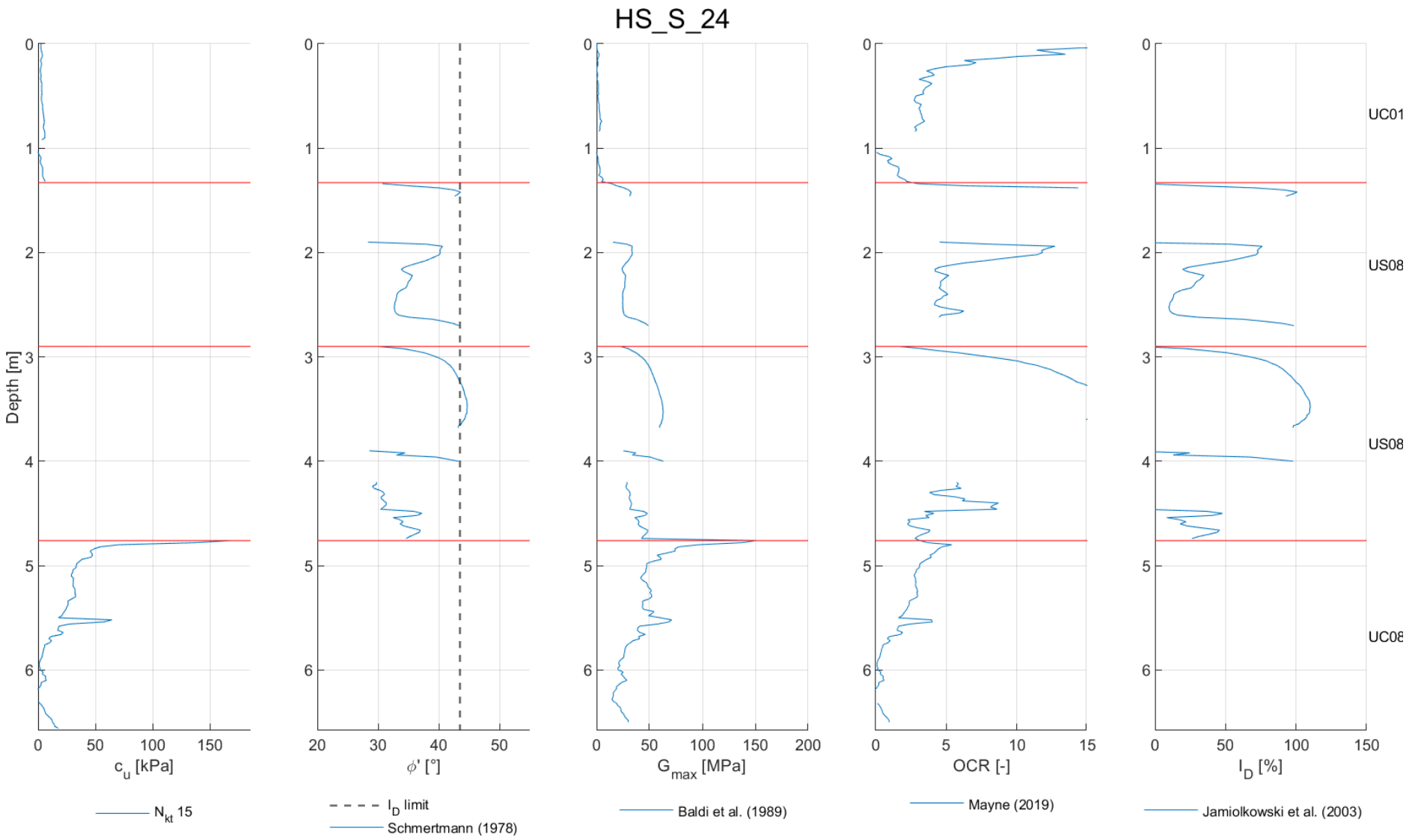
HS_S_24
Depth [m]
c_u [kPa]
ϕ' [°]
G_{max} [MPa]
OCR [-]
I_D [%]
UC01
US08
US08
UC08
N_{kt} 15
I_D limit
Schmertmann (1978)
Baldi et al. (1989)
Mayne (2019)
Jamiolkowski et al. (2003)

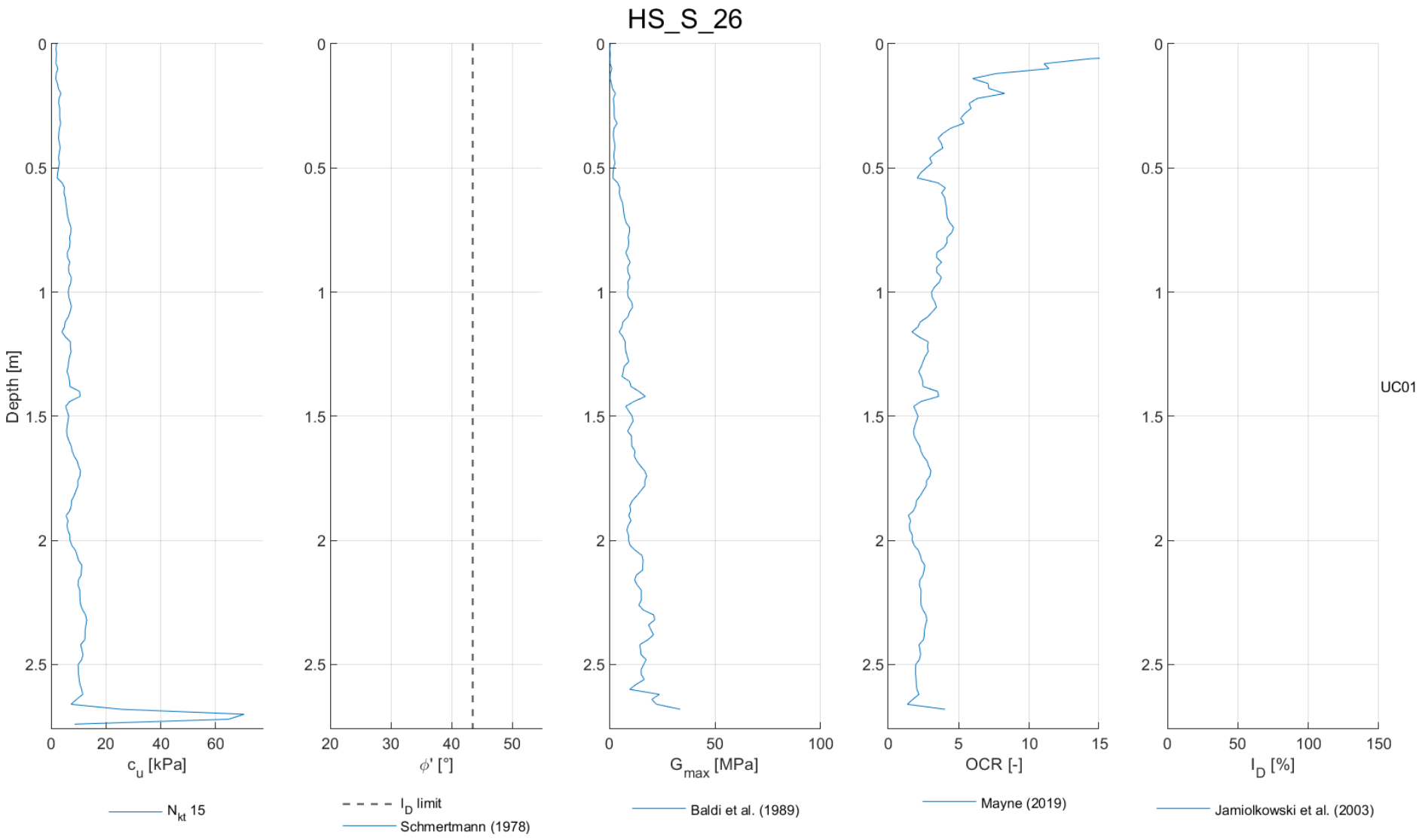
HS_S_26
Depth [m]
0
0.5
1
1.5
2
2.5
0
20
40
60
c_u [kPa]
N_{kt} 15
20
30
40
50
ϕ' [°]
I_D limit
Schmertmann (1978)
0
50
100
G_{max} [MPa]
Baldi et al. (1989)
0
5
10
15
OCR [-]
Mayne (2019)
0
50
100
150
I_D [%]
Jamiolkowski et al. (2003)
UC01

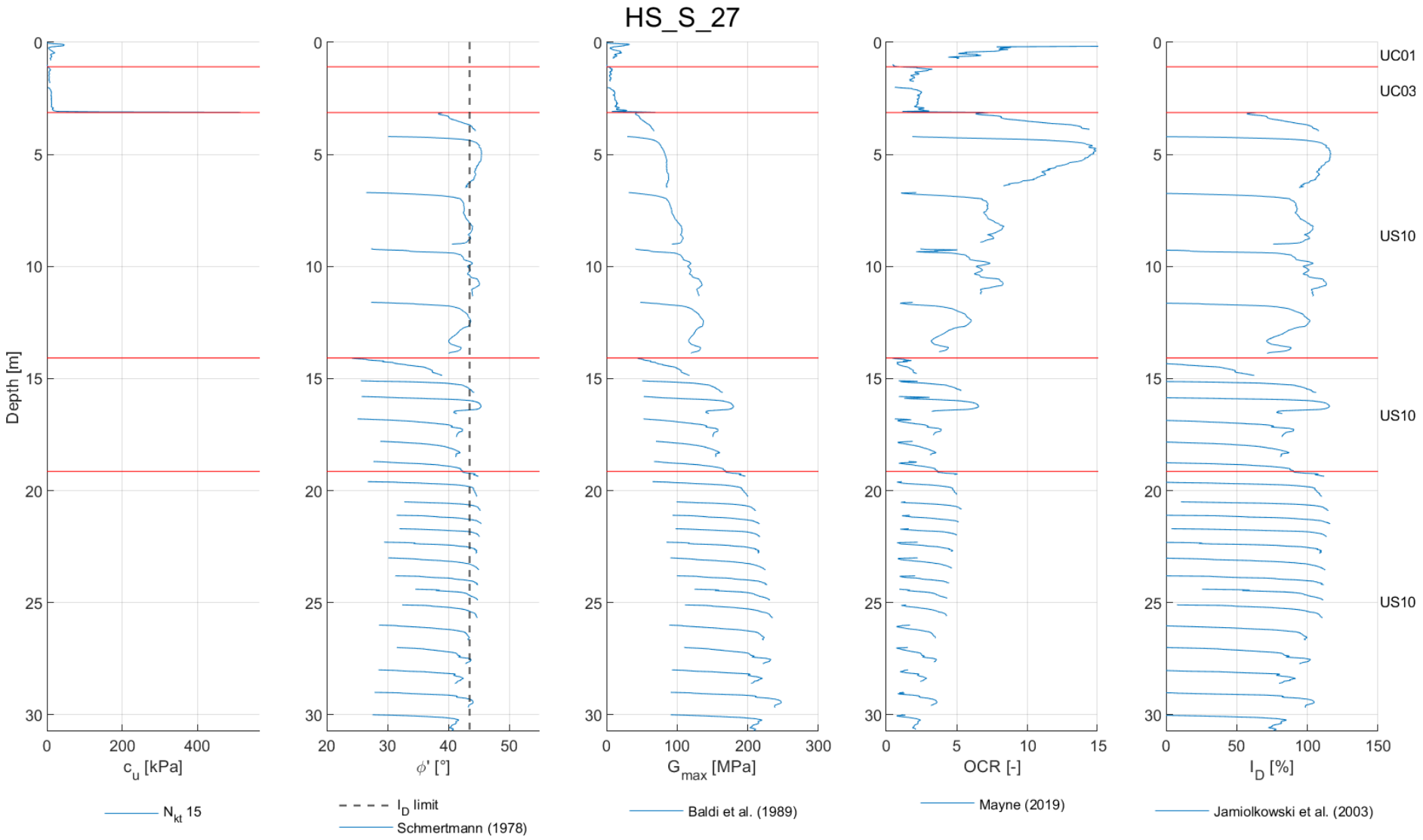
HS_S_27
Depth [m]
c_u [kPa]
ϕ' [°]
G_{max} [MPa]
OCR [-]
I_D [%]
UC01
UC03
US10
US10
US10
N_{kt} 15
I_D limit
Schmertmann (1978)
Baldi et al. (1989)
Mayne (2019)
Jamiolkowski et al. (2003)

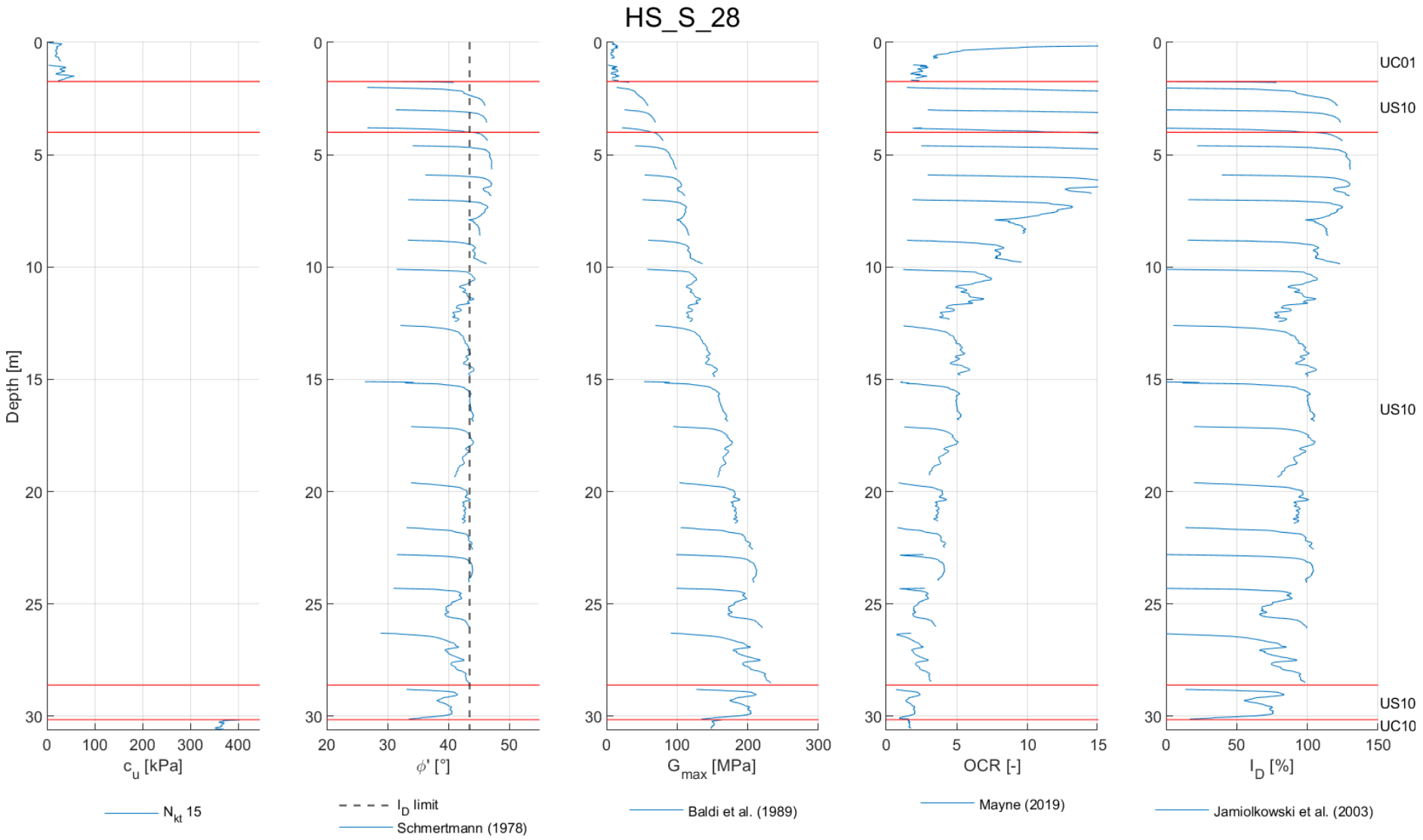
HS_S_28
Depth [m]
c_u [kPa]
ϕ' [°]
G_{max} [MPa]
OCR [-]
I_D [%]
UC01
US10
US10
US10
UC10
N_{kt} 15
I_D limit
Schmertmann (1978)
Baldi et al. (1989)
Mayne (2019)
Jamiolkowski et al. (2003)

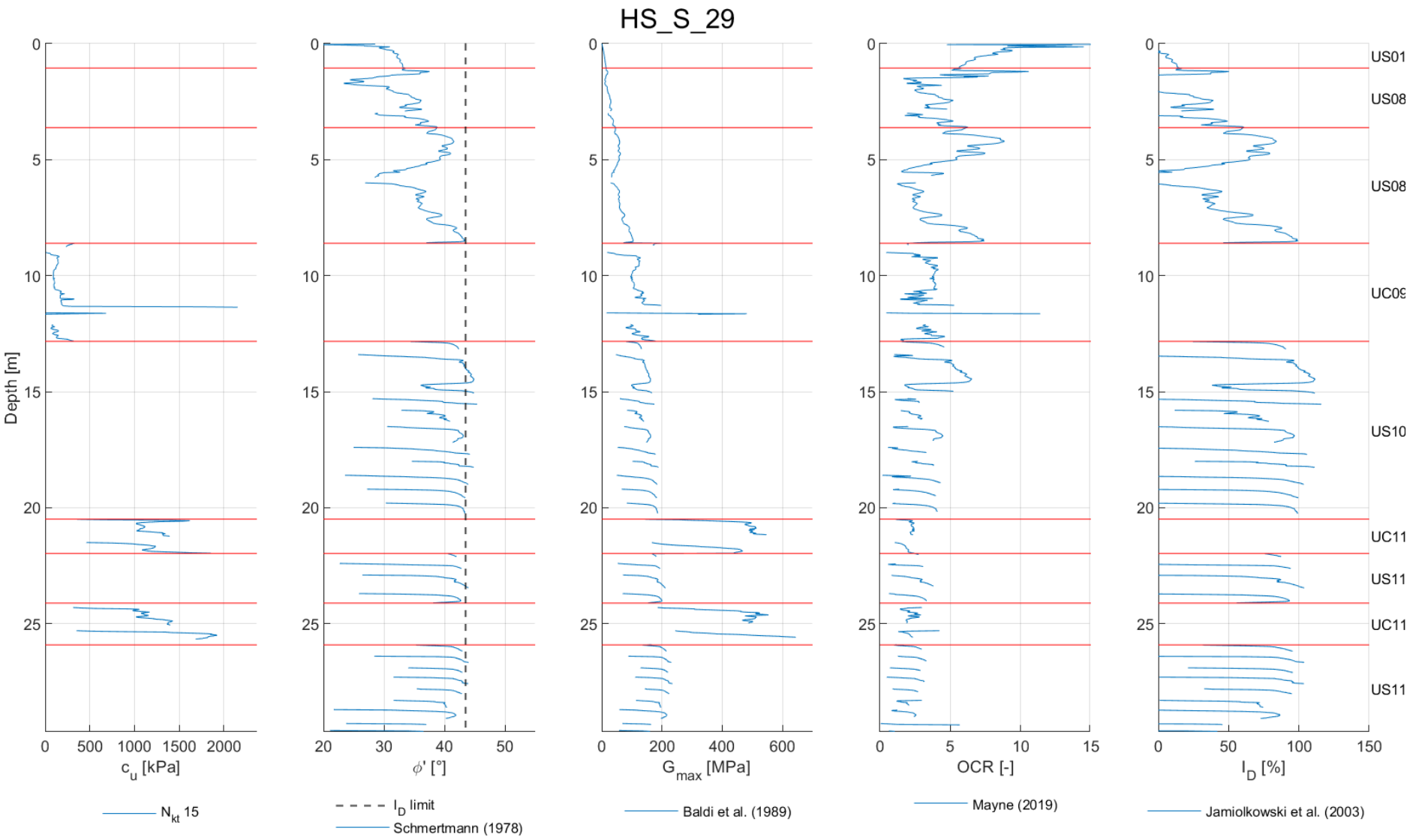
HS_S_29
Depth [m]
0
5
10
15
20
25
0 500 1000 1500 2000
c_u [kPa]
N_{kt} 15
20 30 40 50
ϕ' [°]
I_D limit
Schmertmann (1978)
0 200 400 600
G_{max} [MPa]
Baldi et al. (1989)
0 5 10 15
OCR [-]
Mayne (2019)
0 50 100 150
I_D [%]
Jamiolkowski et al. (2003)
US01
US08
US08
UC09
US10
UC11
US11
UC11
US11

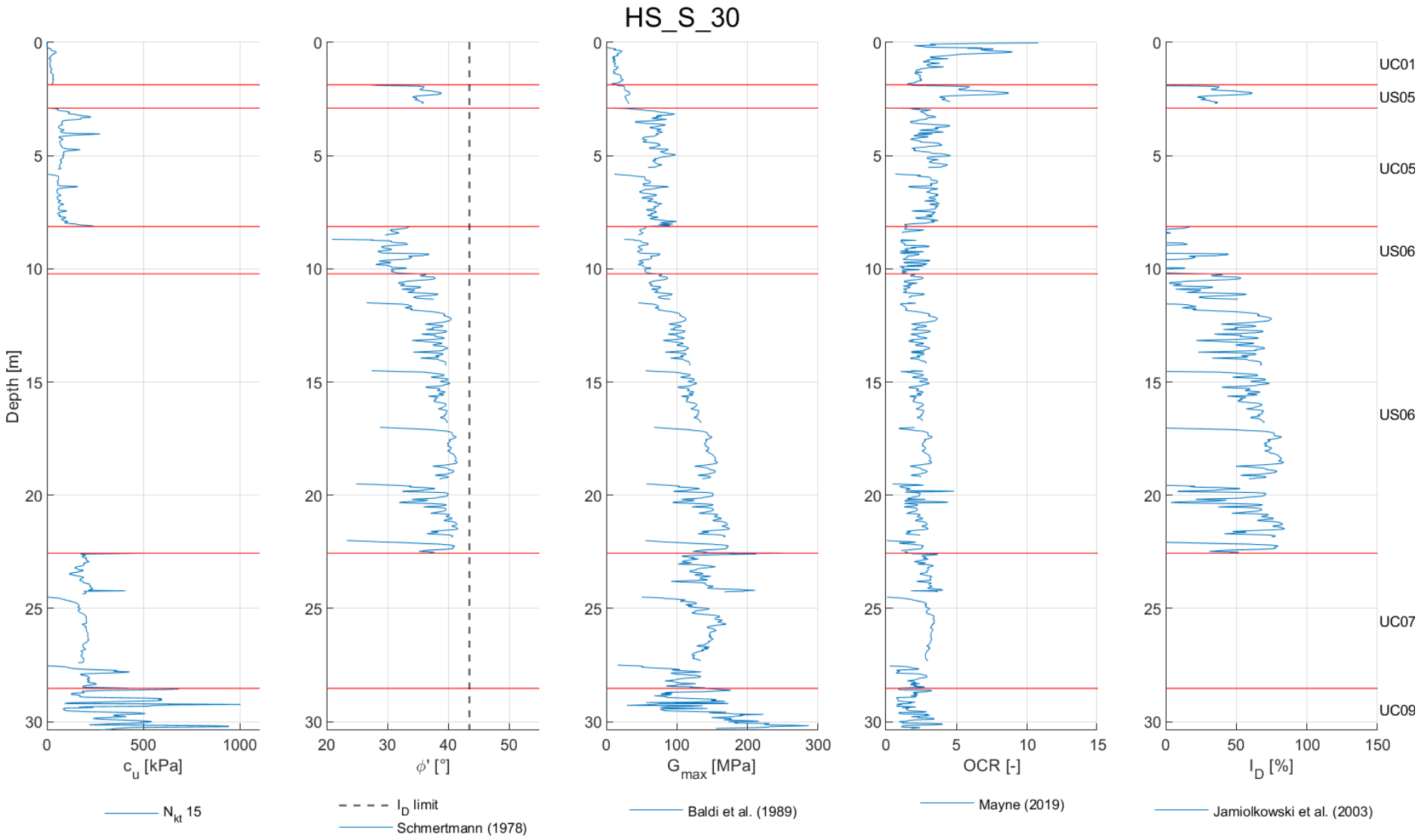
HS_S_30
Depth [m]
c_u [kPa]
ϕ' [°]
G_{max} [MPa]
OCR [-]
I_D [%]
UC01
US05
UC05
US06
US06
UC07
UC09
N_{kt} 15
I_D limit
Schmertmann (1978)
Baldi et al. (1989)
Mayne (2019)
Jamiolkowski et al. (2003)

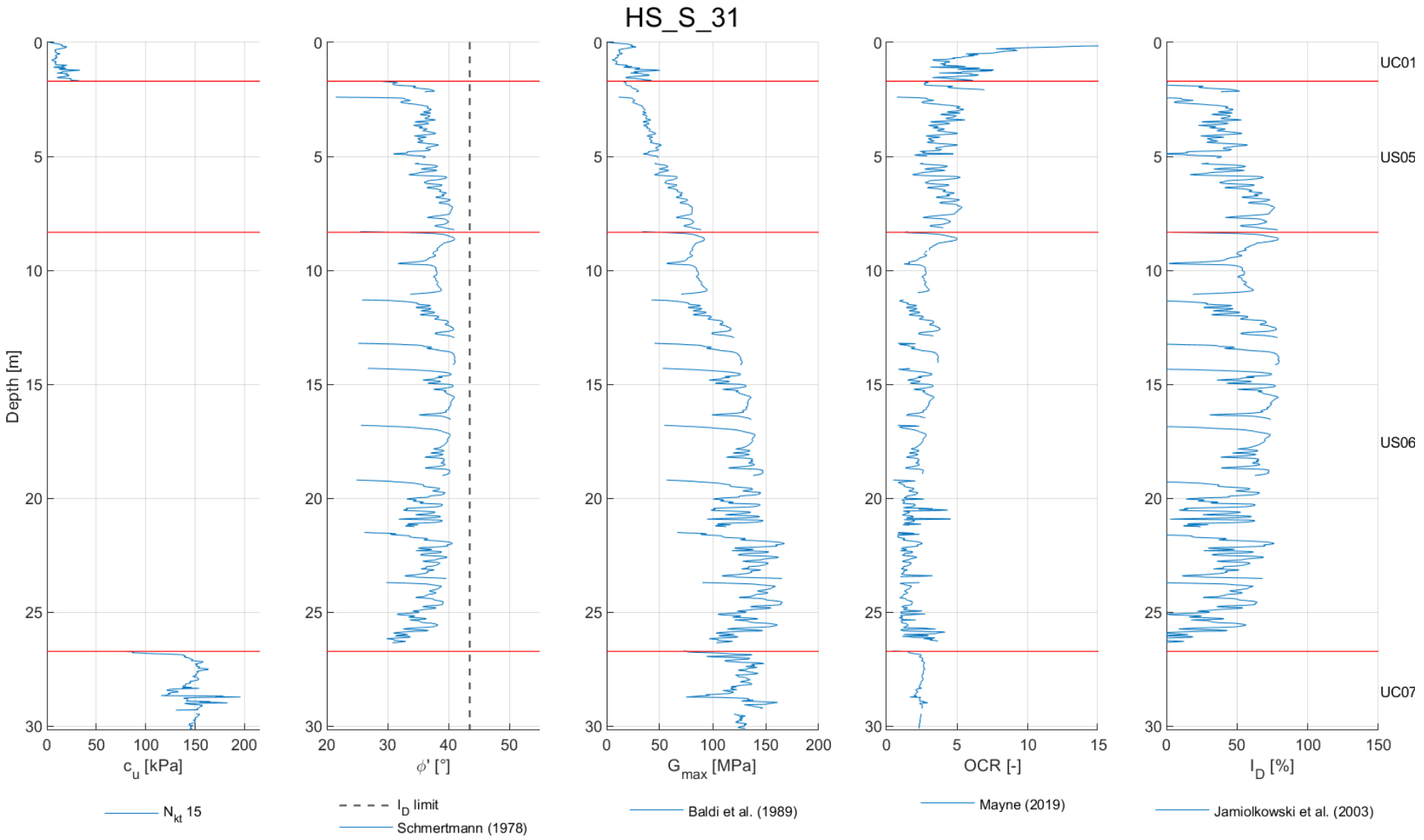
HS_S_31
Depth [m]
c_u [kPa]
ϕ' [°]
G_{max} [MPa]
OCR [-]
I_D [%]
UC01
US05
US06
UC07
N_{kt} 15
I_D limit
Schmertmann (1978)
Baldi et al. (1989)
Mayne (2019)
Jamiolkowski et al. (2003)

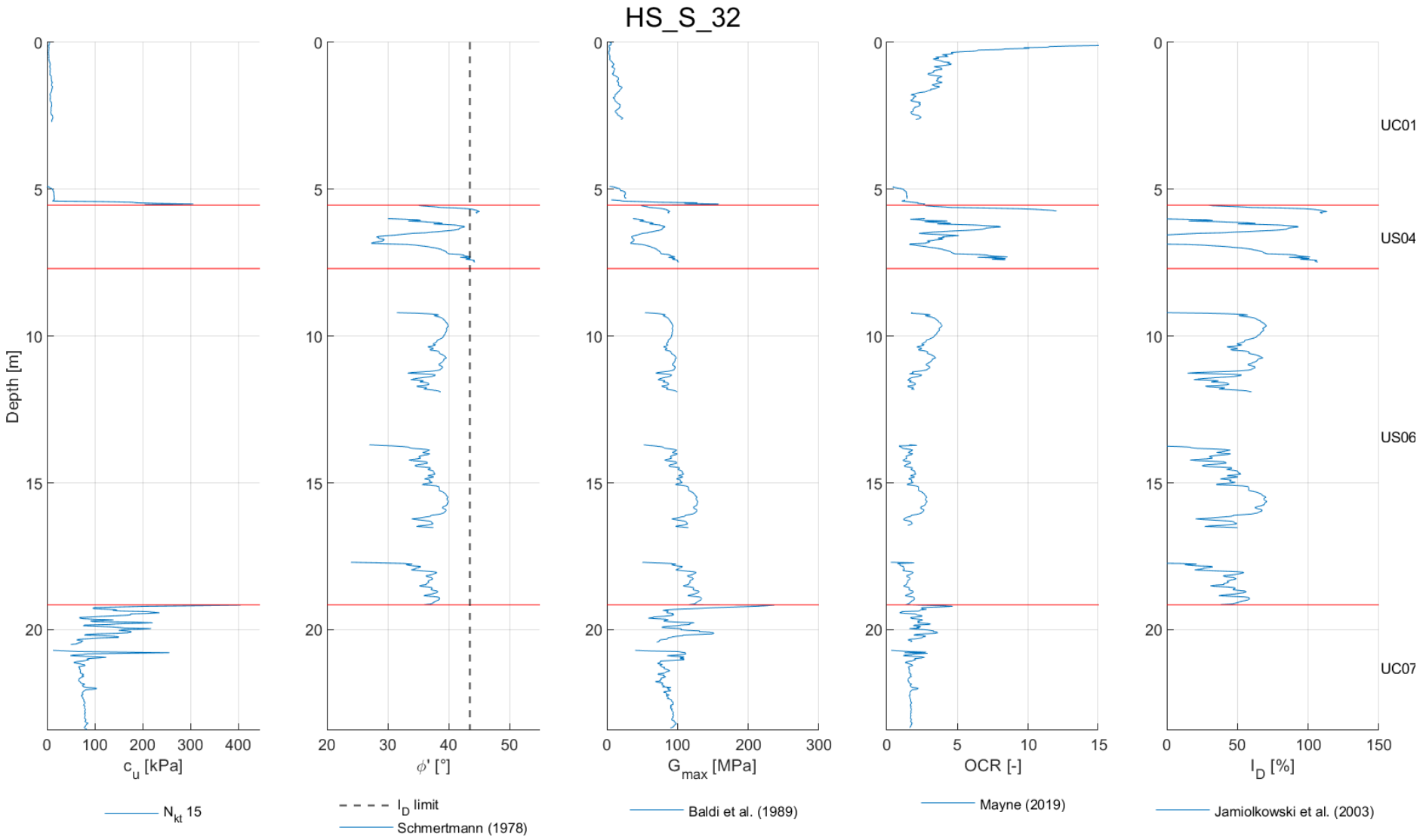
HS_S_32
Depth [m]
0
5
10
15
20
0
100
200
300
400
c_u [kPa]
N_{kt} 15
20
30
40
50
ϕ' [°]
I_D limit
Schmertmann (1978)
0
100
200
300
G_{max} [MPa]
Baldi et al. (1989)
0
5
10
15
OCR [-]
Mayne (2019)
0
50
100
150
I_D [%]
Jamiolkowski et al. (2003)
UC01
US04
US06
UC07

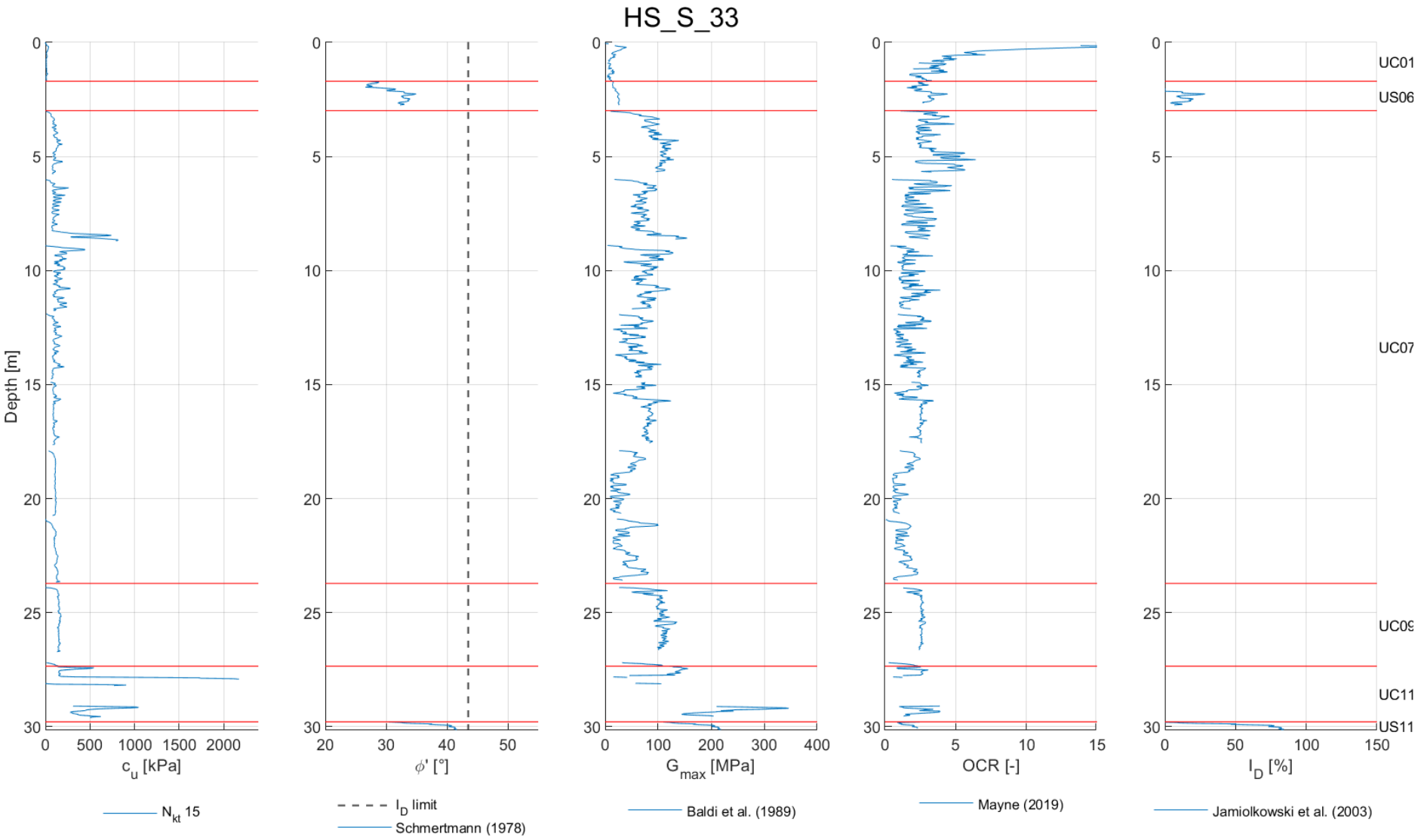
HS_S_33
Depth [m]
0
5
10
15
20
25
30
0
500
1000
1500
2000
c_u [kPa]
N_{kt} 15
20
30
40
50
ϕ' [°]
I_D limit
Schmertmann (1978)
0
100
200
300
400
G_{max} [MPa]
Baldi et al. (1989)
0
5
10
15
OCR [-]
Mayne (2019)
0
50
100
150
I_D [%]
Jamiolkowski et al. (2003)
UC01
US06
UC07
UC09
UC11
US11

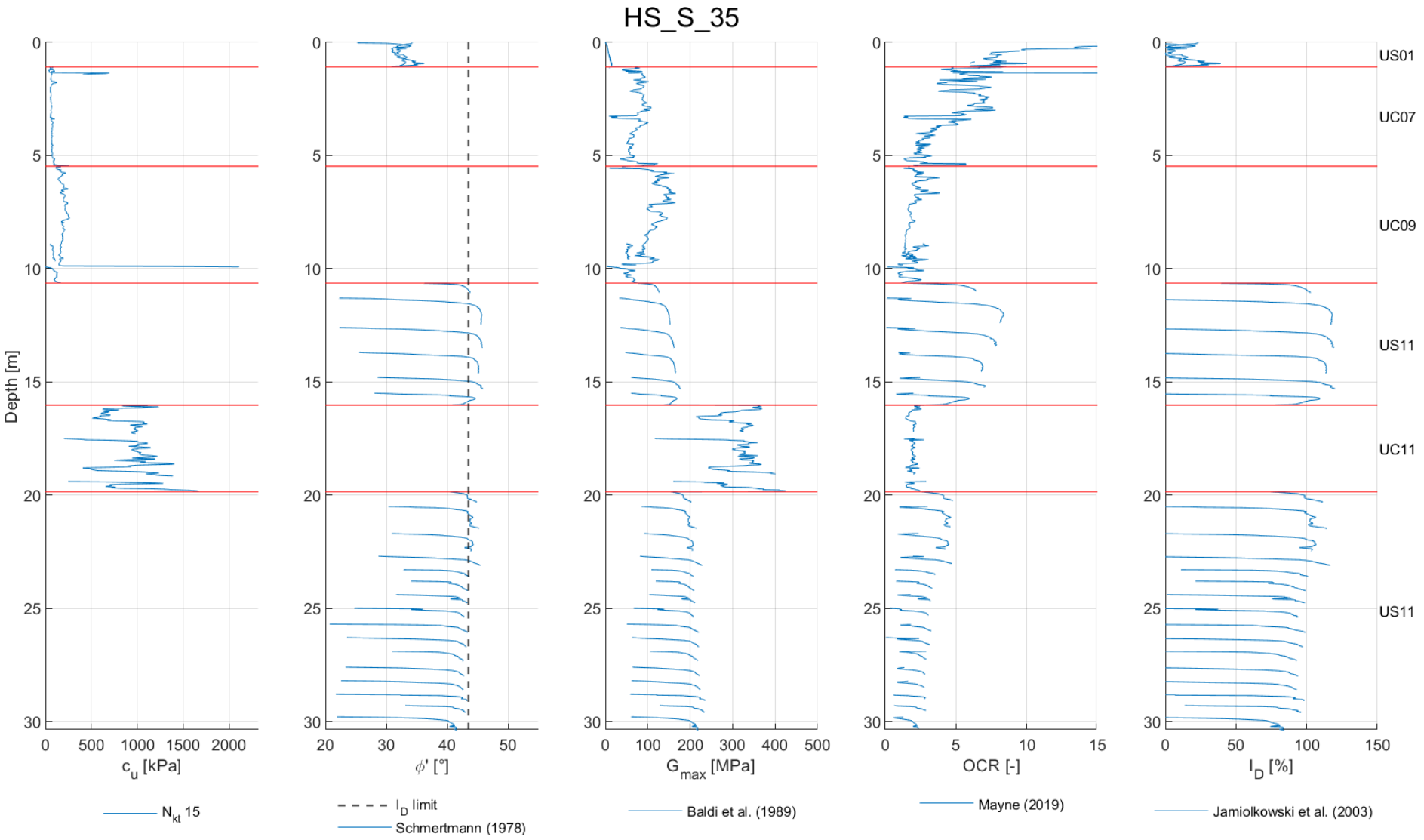
HS_S_35
Depth [m]
c_u [kPa]
N_{kt} 15
ϕ' [°]
I_D limit
Schmertmann (1978)
G_{max} [MPa]
Baldi et al. (1989)
OCR [-]
Mayne (2019)
I_D [%]
Jamiolkowski et al. (2003)
US01
UC07
UC09
US11
UC11
US11

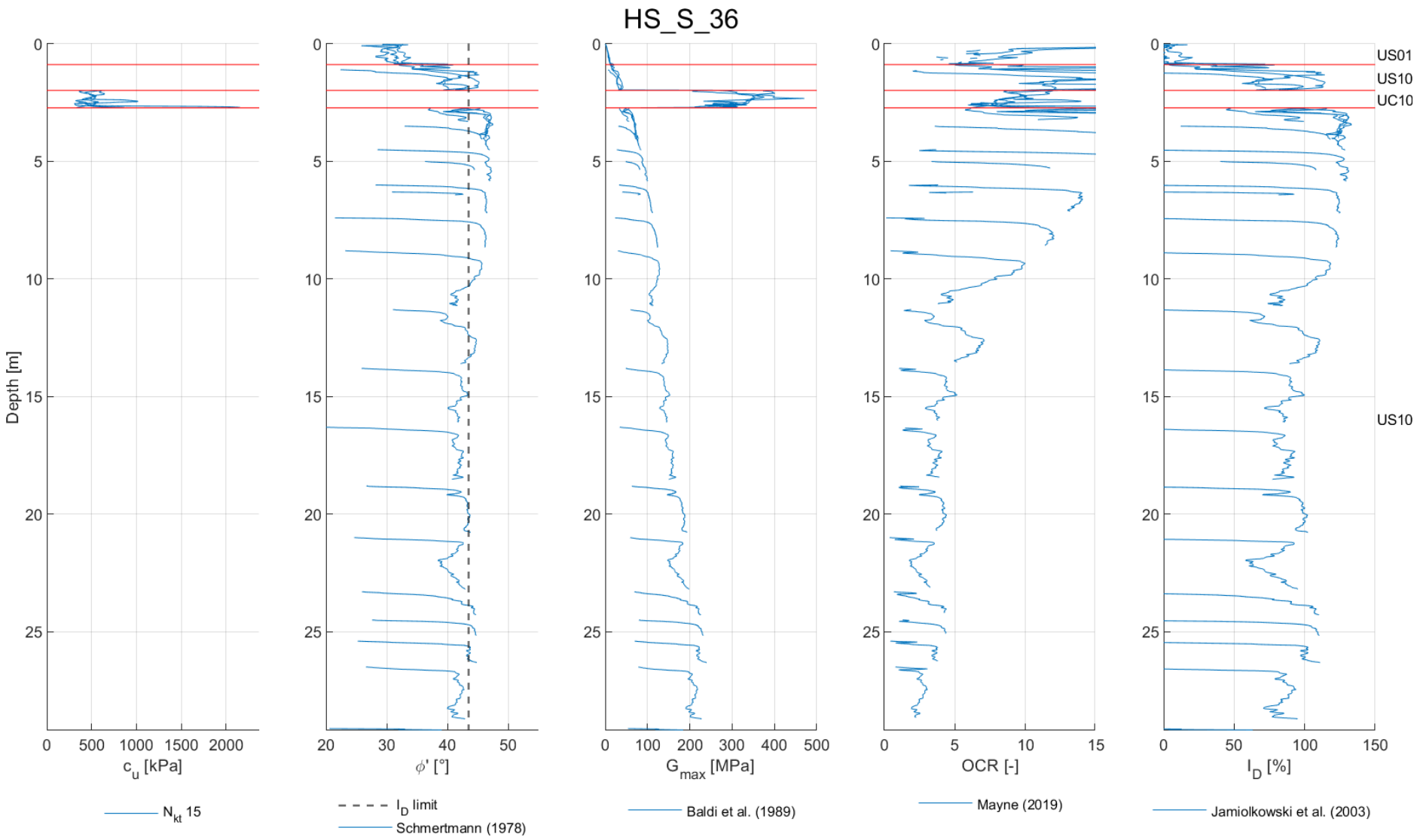
HS_S_36
Depth [m]
0
5
10
15
20
25
0 500 1000 1500 2000
c_u [kPa]
N_{kt} 15
20 30 40 50
ϕ' [°]
I_D limit
Schmertmann (1978)
0 100 200 300 400 500
G_{max} [MPa]
Baldi et al. (1989)
0 5 10 15
OCR [-]
Mayne (2019)
0 50 100 150
I_D [%]
Jamiolkowski et al. (2003)
US01
US10
UC10
US10

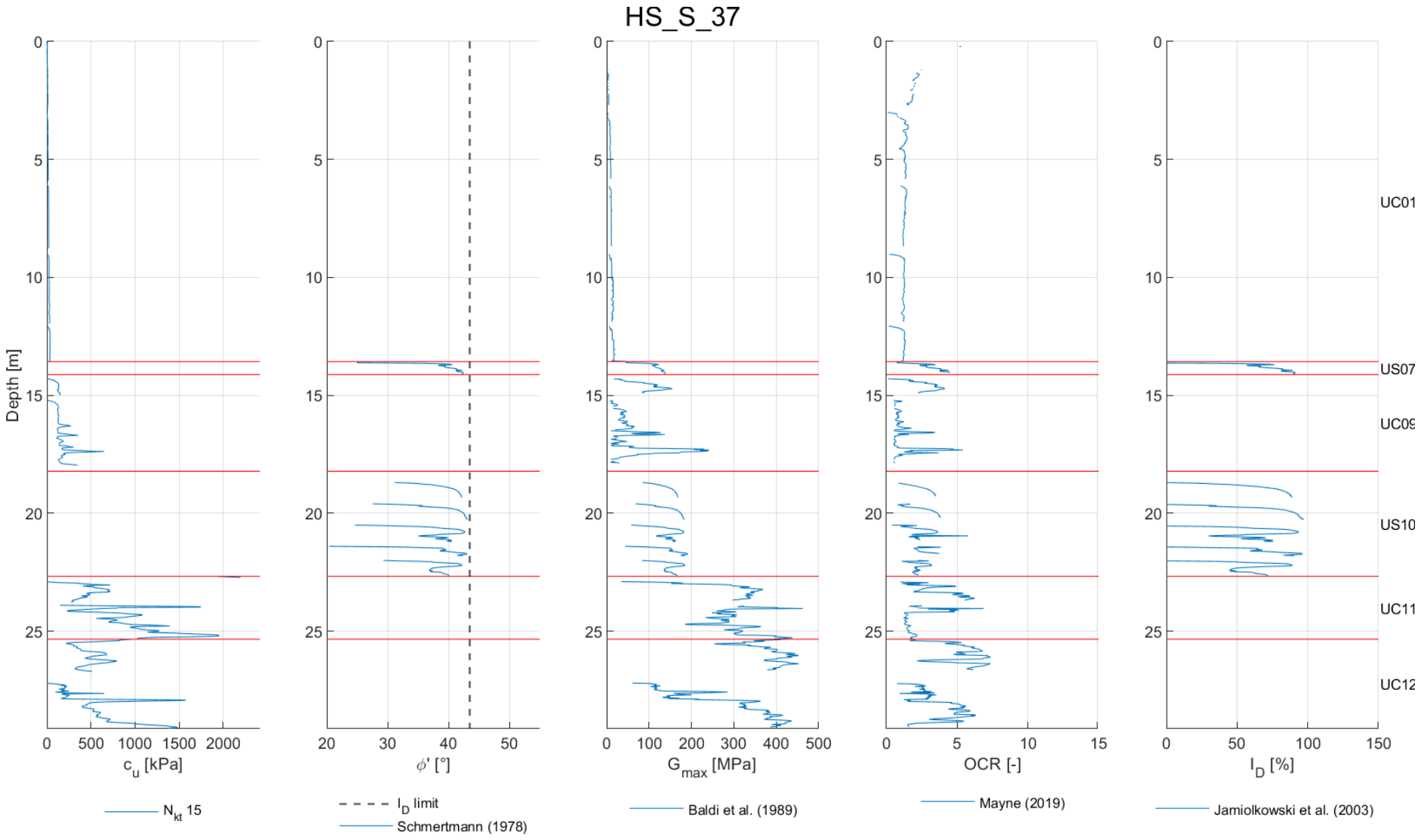
HS_S_37
Depth [m]
0
5
10
15
20
25
0 500 1000 1500 2000
c_u [kPa]
N_{kt} 15
20 30 40 50
ϕ' [°]
I_D limit
Schmertmann (1978)
0 100 200 300 400 500
G_{max} [MPa]
Baldi et al. (1989)
0 5 10 15
OCR [-]
Mayne (2019)
0 50 100 150
I_D [%]
Jamiolkowski et al. (2003)
UC01
US07
UC09
US10
UC11
UC12

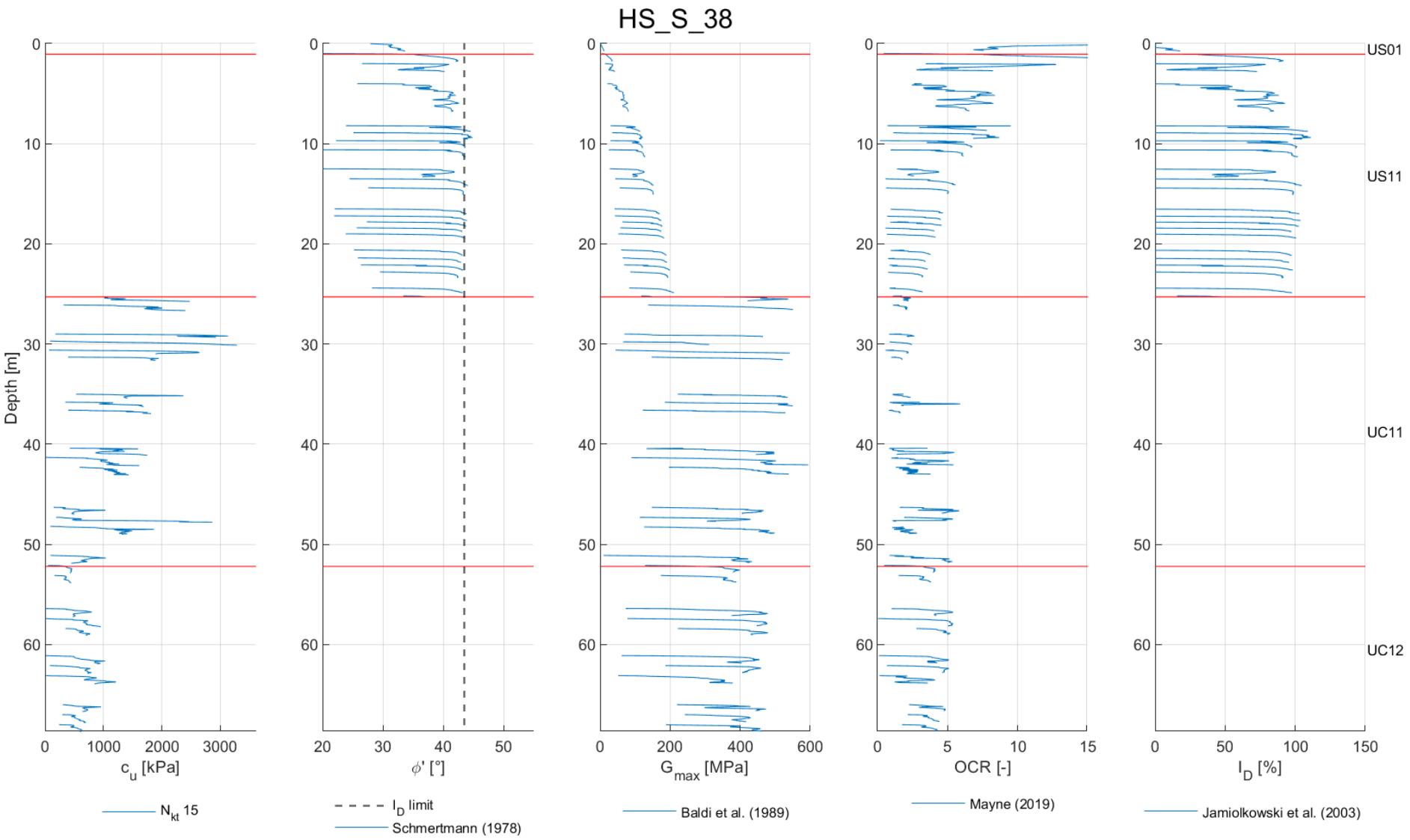
HS_S_38
Depth [m]
0
10
20
30
40
50
60
0
1000
2000
3000
c_u [kPa]
N_{kt} 15
20
30
40
50
ϕ' [°]
I_D limit
Schmertmann (1978)
0
200
400
600
G_{max} [MPa]
Baldi et al. (1989)
0
5
10
15
OCR [-]
Mayne (2019)
0
50
100
150
I_D [%]
Jamiolkowski et al. (2003)
US01
US11
UC11
UC12

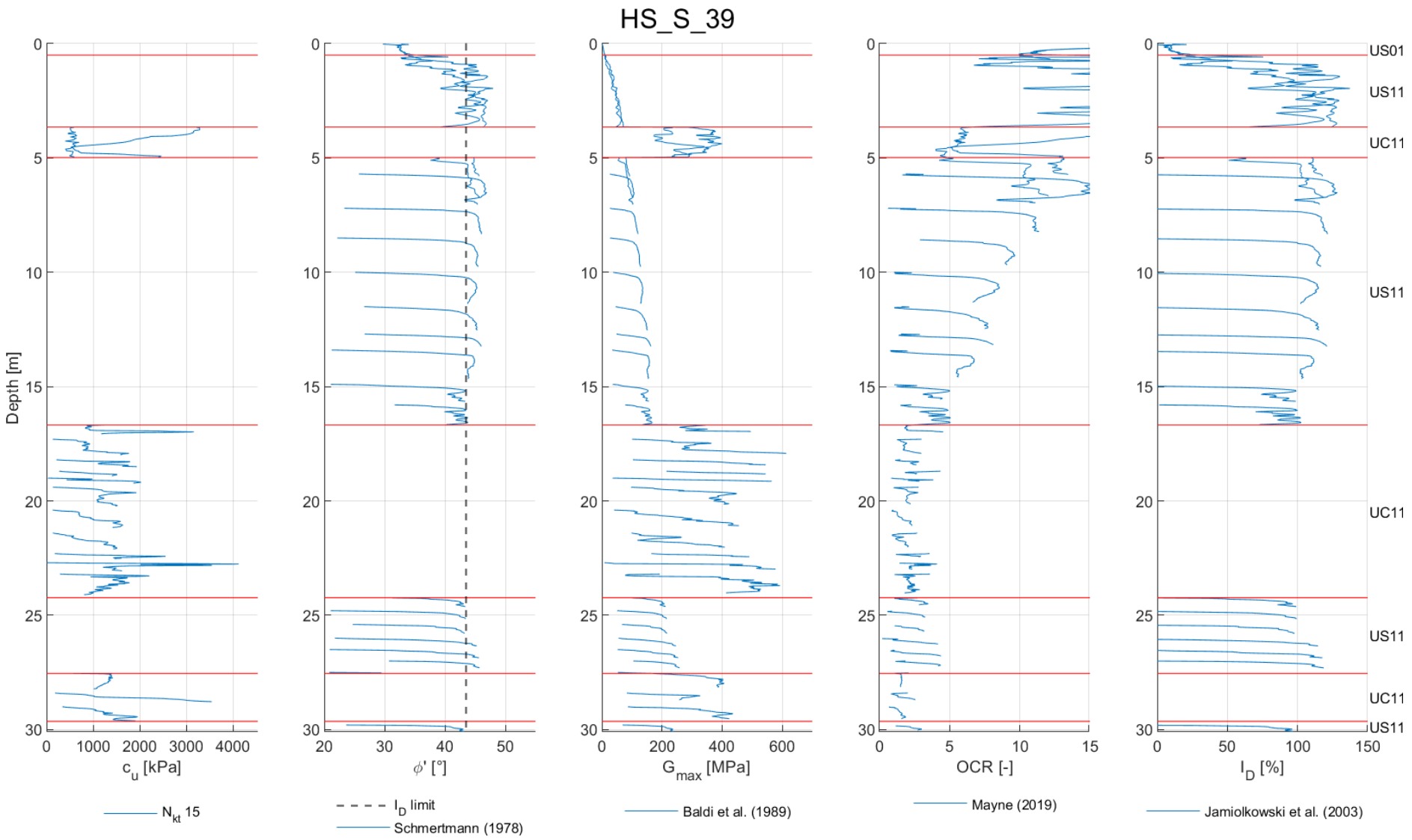
HS_S_39
Depth [m]
0
5
10
15
20
25
30
0 1000 2000 3000 4000
c_u [kPa]
N_{kt} 15
20 30 40 50
ϕ' [°]
I_D limit
Schmertmann (1978)
0 200 400 600
G_{max} [MPa]
Baldi et al. (1989)
0 5 10 15
OCR [-]
Mayne (2019)
0 50 100 150
I_D [%]
Jamiolkowski et al. (2003)
US01
US11
UC11
US11
UC11
US11
UC11
US11

Appendix D CPT plots per geotechnical unit including properties from laboratory testing

This appendix presents the derived soil properties per unit. For presenting the data per unit, the first 20 cm of each CPT push has been removed from the data sample as these are not found representative for the actual unit properties.

D.1 Over-consolidation ratio

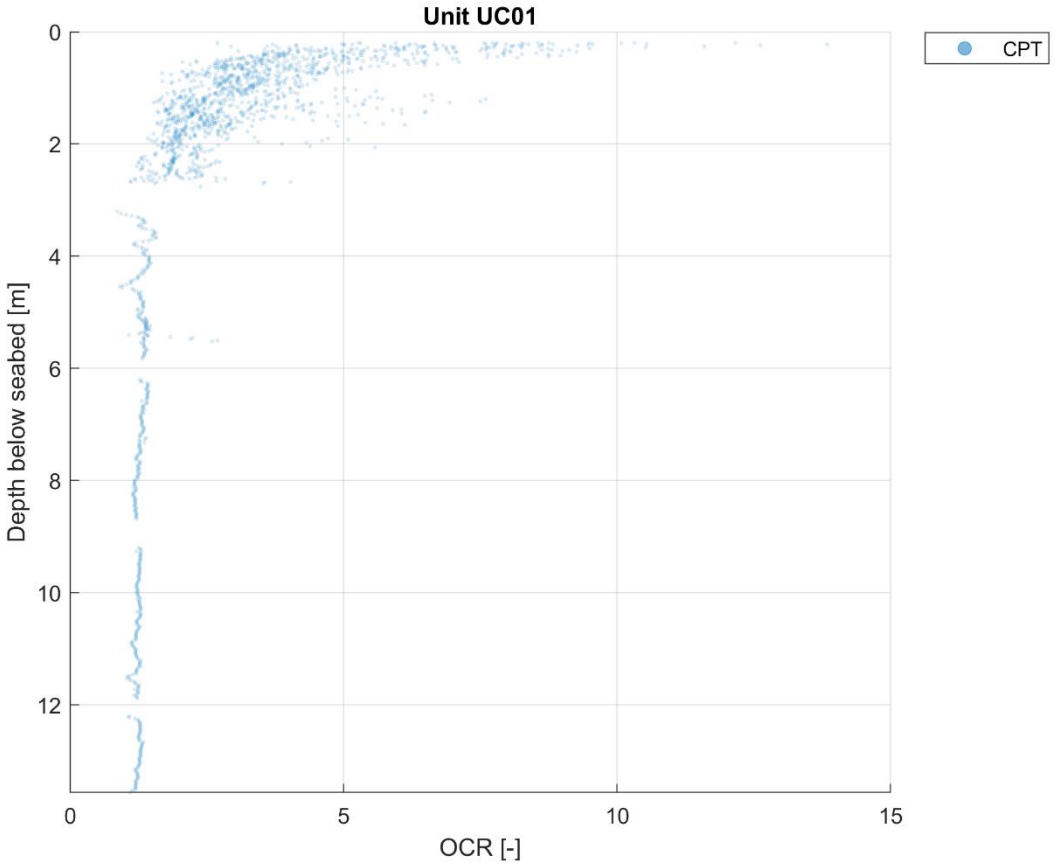

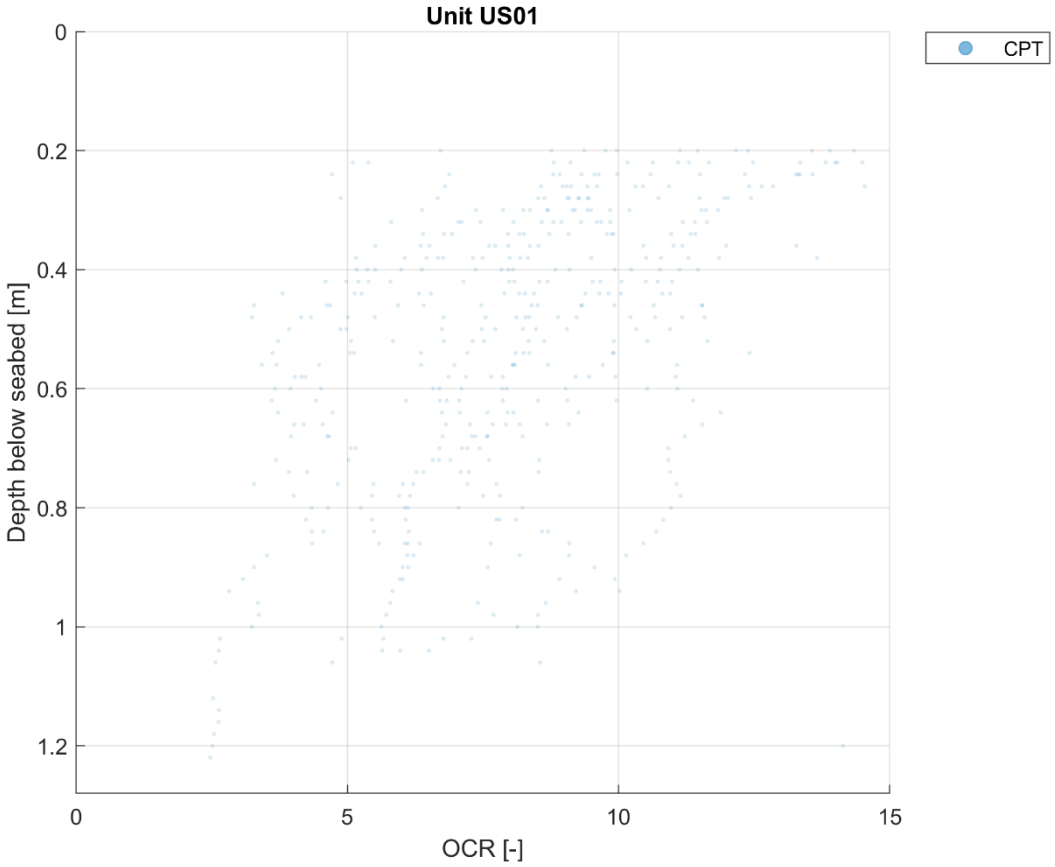

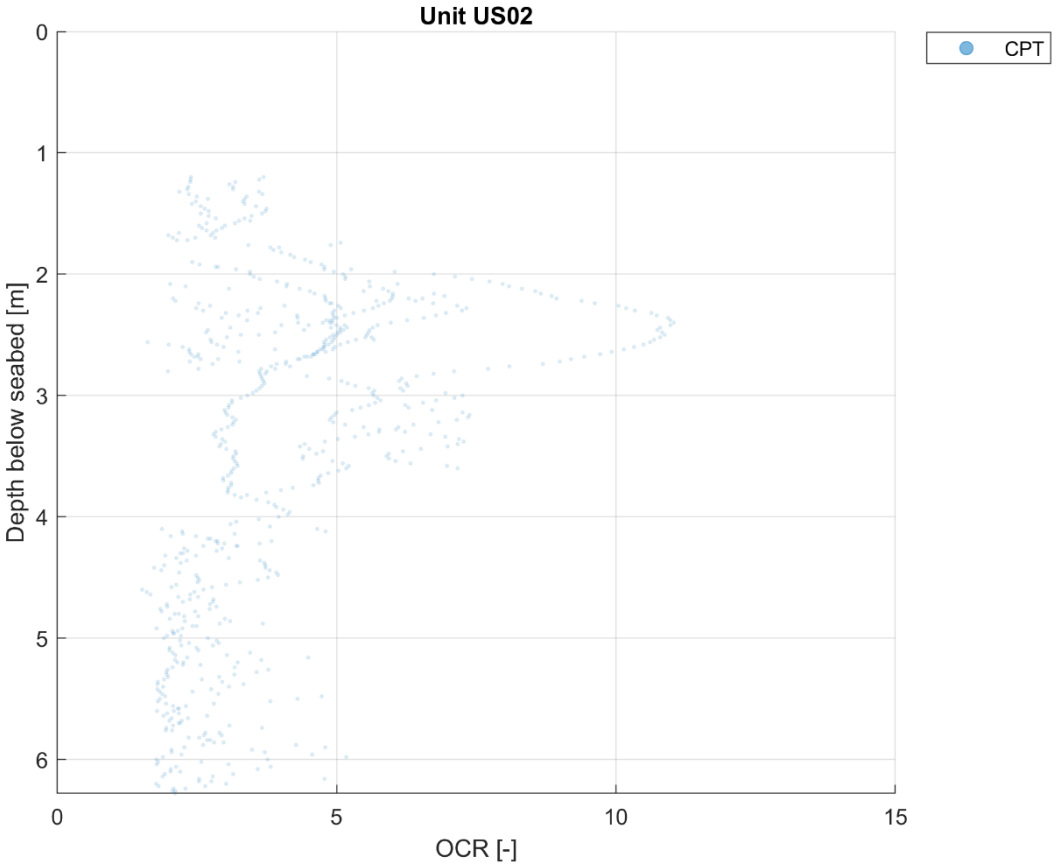
Unit US02
CPT
Depth below seabed [m]
OCR [-]
0
1
2
3
4
5
6
0
5
10
15

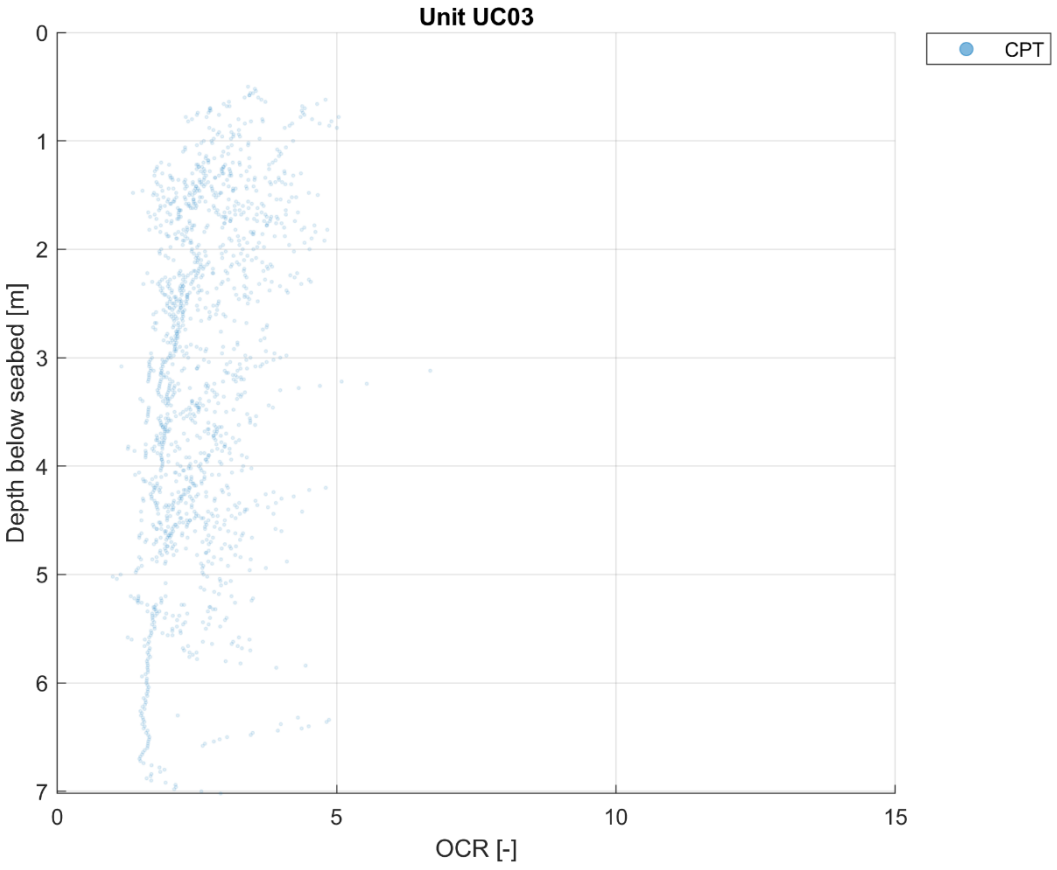
Unit UC03
CPT
Depth below seabed [m]
OCR [-]
0
1
2
3
4
5
6
7
0
5
10
15

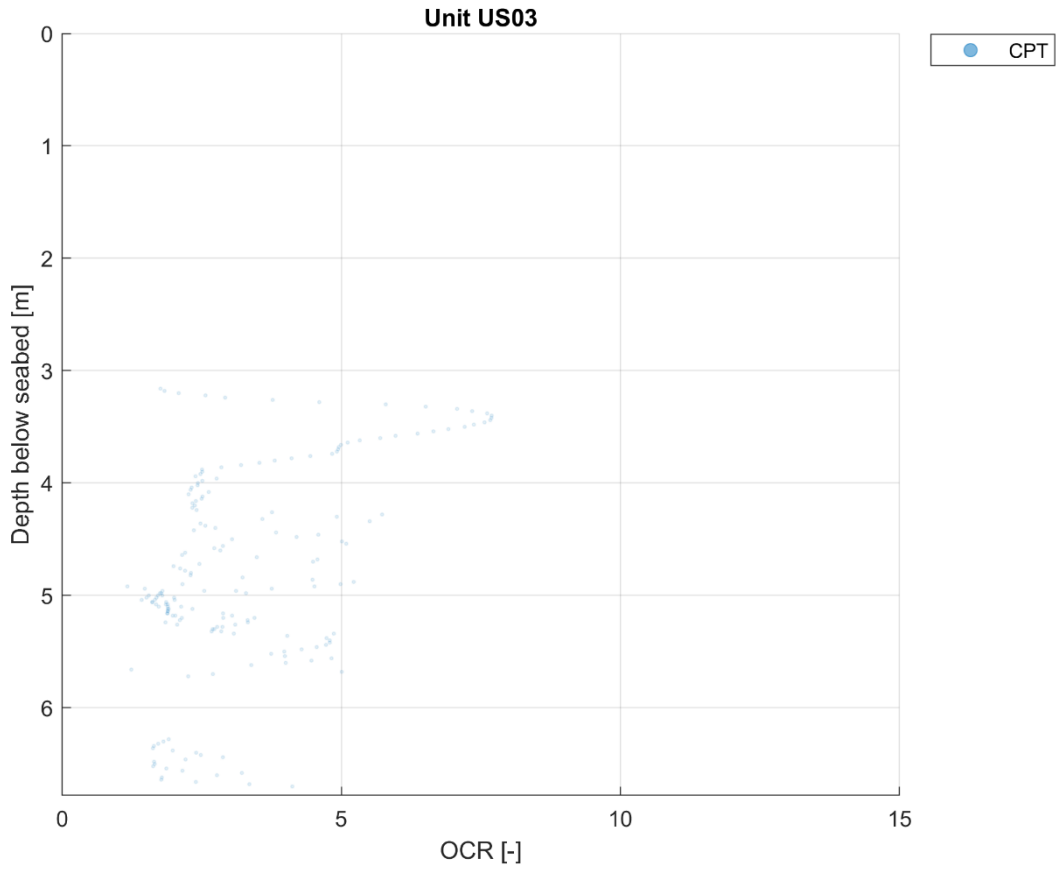
Unit US03
CPT
Depth below seabed [m]
OCR [-]
0
1
2
3
4
5
6
0
5
10
15

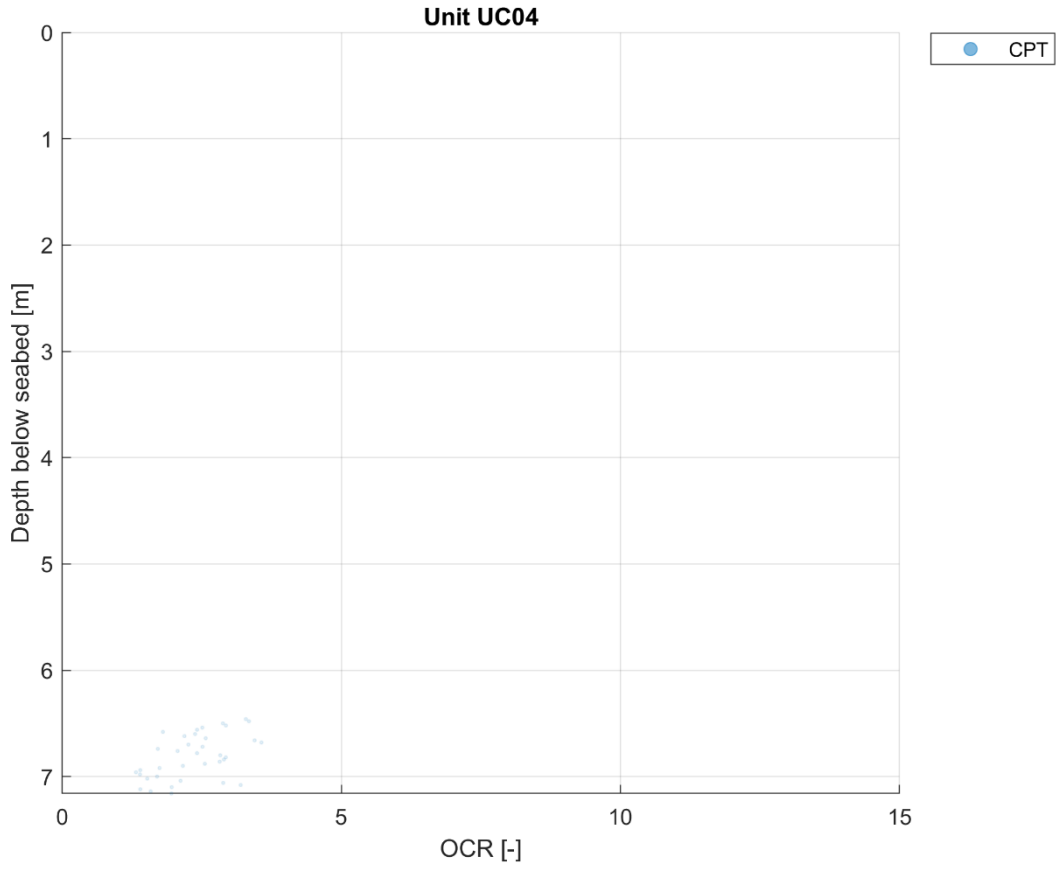
Unit UC04
CPT
Depth below seabed [m]
OCR [-]
0
1
2
3
4
5
6
7
0
5
10
15

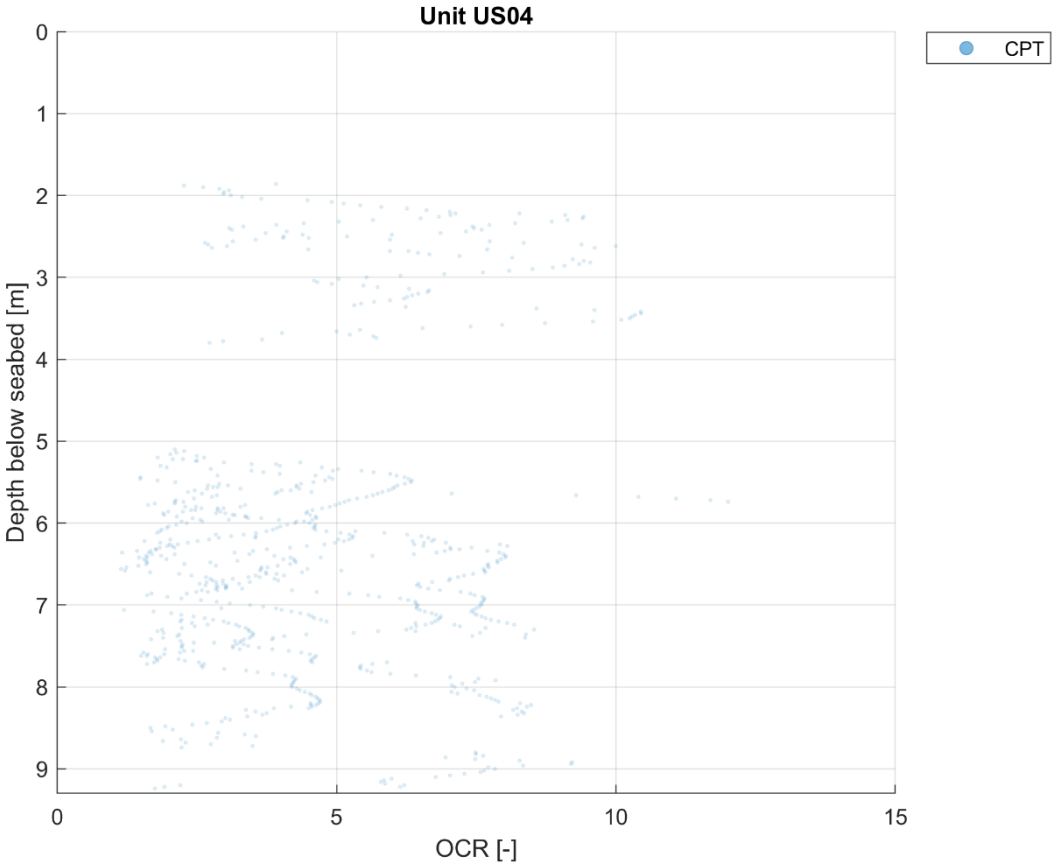
Unit US04
CPT
Depth below seabed [m]
OCR [-]
0
1
2
3
4
5
6
7
8
9
0
5
10
15

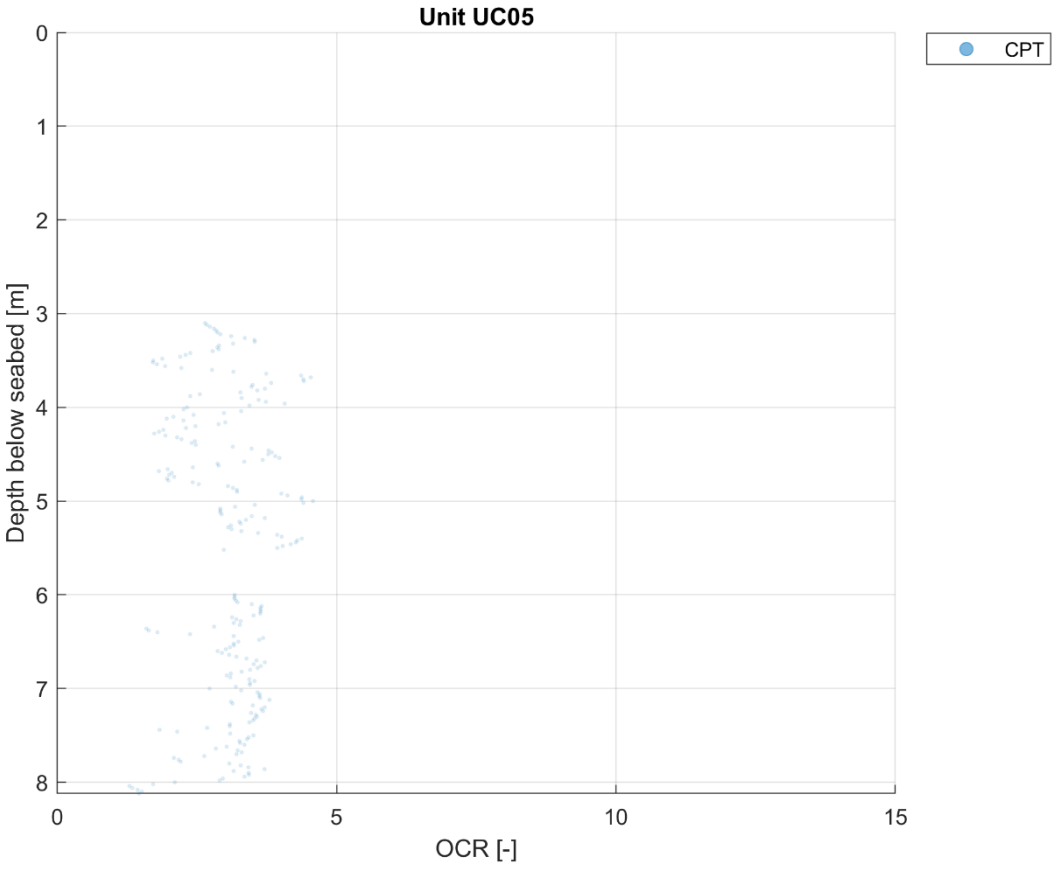
Unit UC05
CPT
Depth below seabed [m]
OCR [-]
0
1
2
3
4
5
6
7
8
0
5
10
15

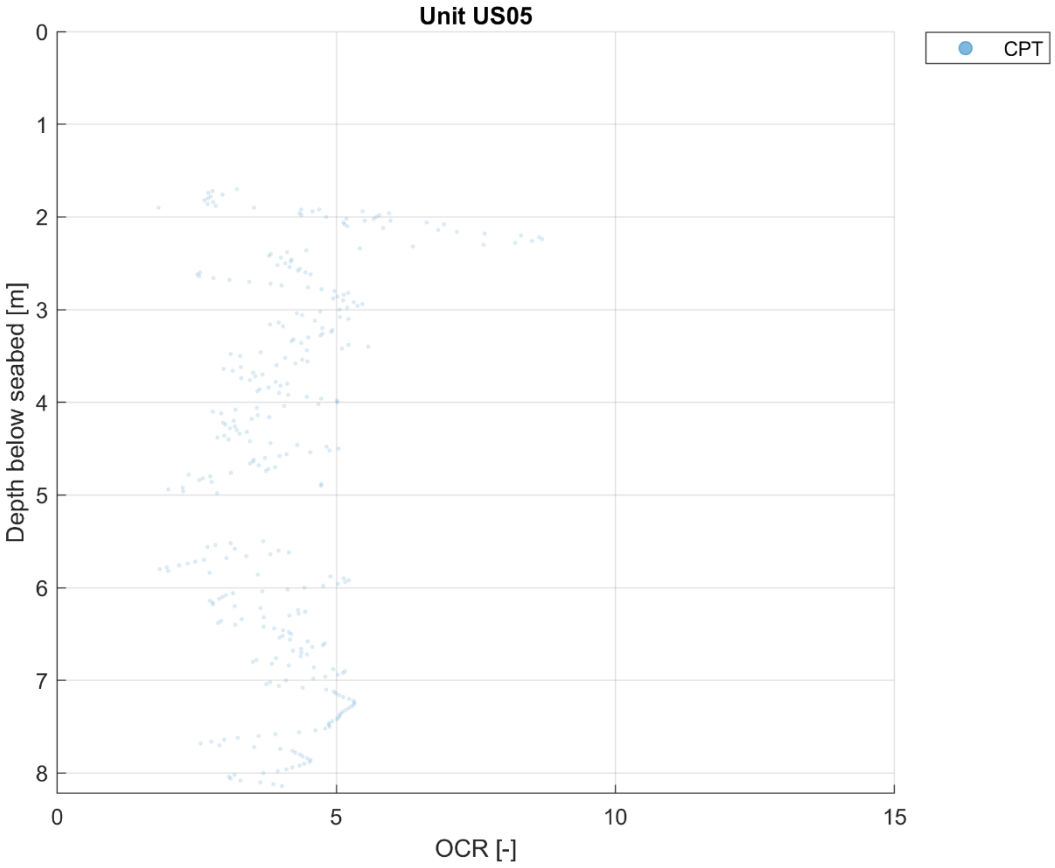
Unit US05
CPT
Depth below seabed [m]
OCR [-]
0
1
2
3
4
5
6
7
8
0
5
10
15

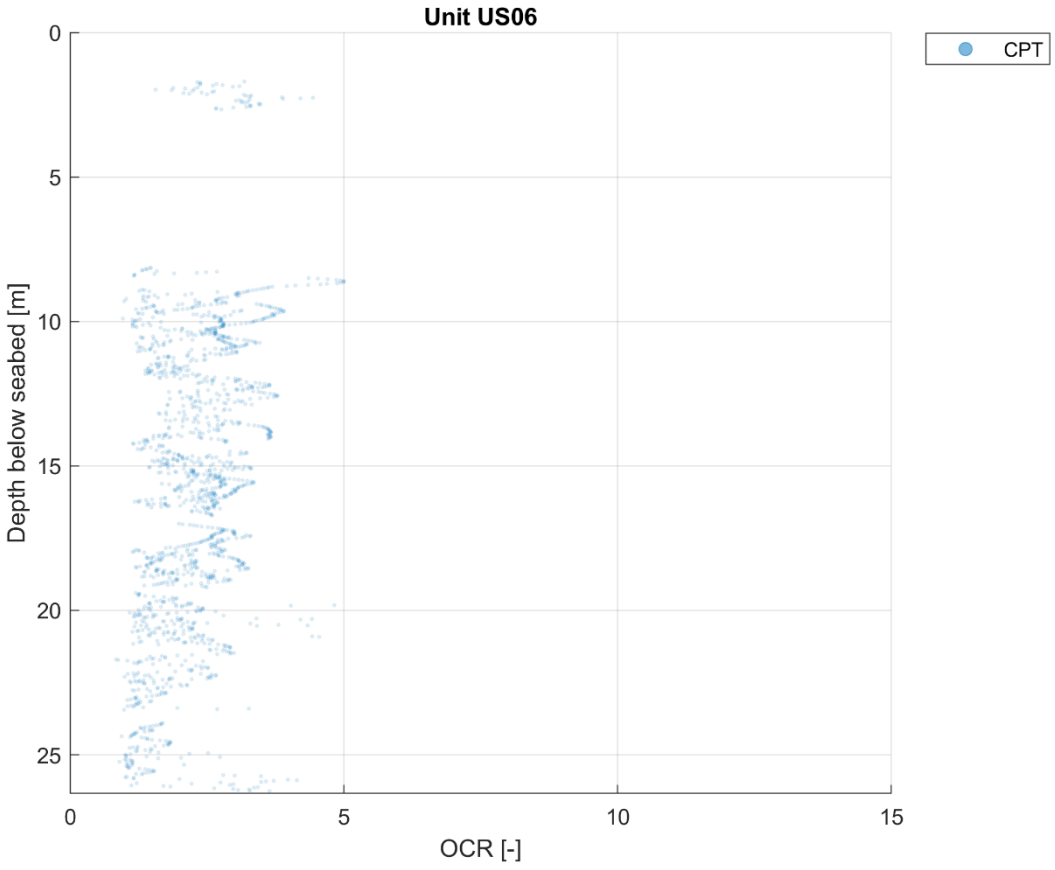
Unit US06
CPT
Depth below seabed [m]
OCR [-]
0
5
10
15
20
25
0
5
10
15

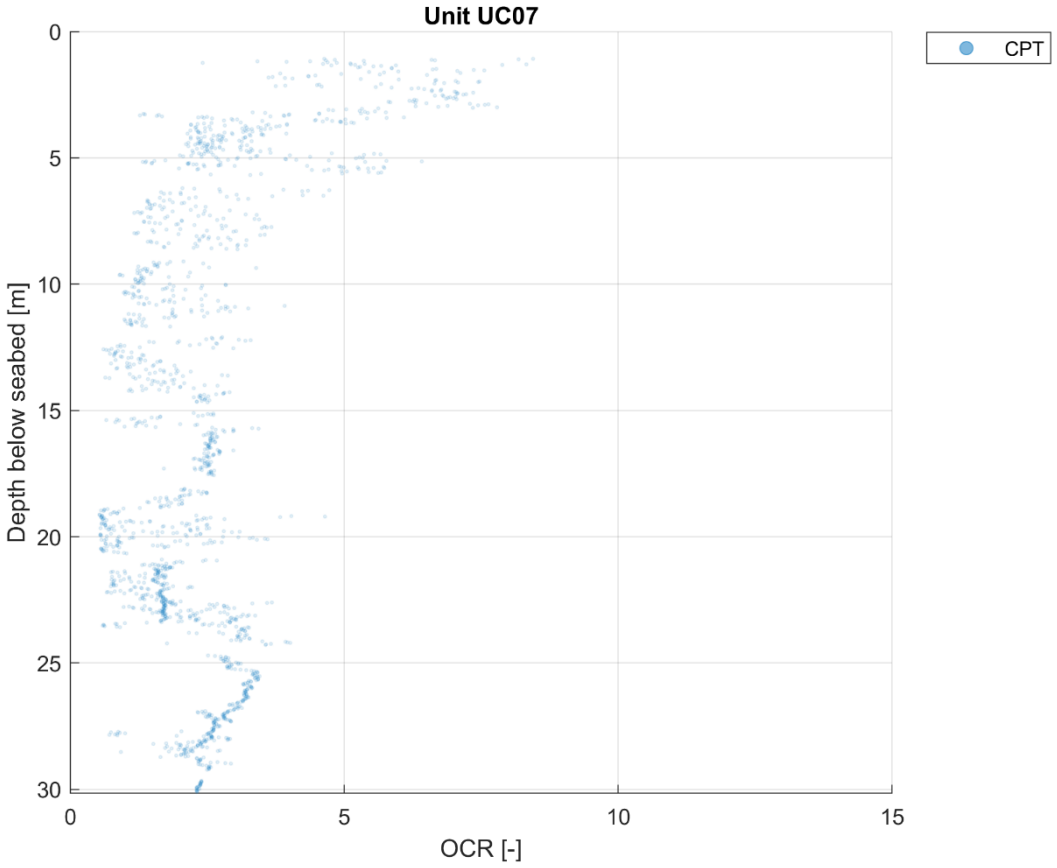
Unit UC07
CPT
Depth below seabed [m]
0
5
10
15
20
25
30
OCR [-]
0
5
10
15

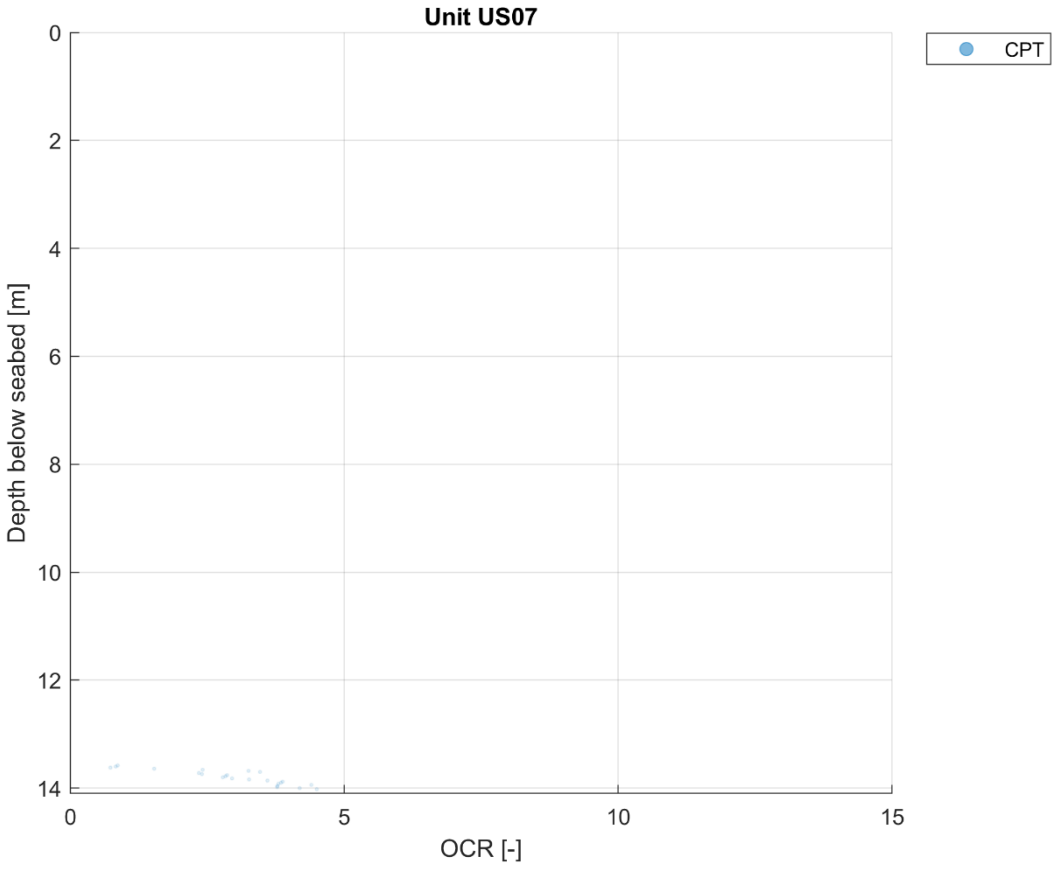
Unit US07
CPT
Depth below seabed [m]
0
2
4
6
8
10
12
14
OCR [-]
0
5
10
15

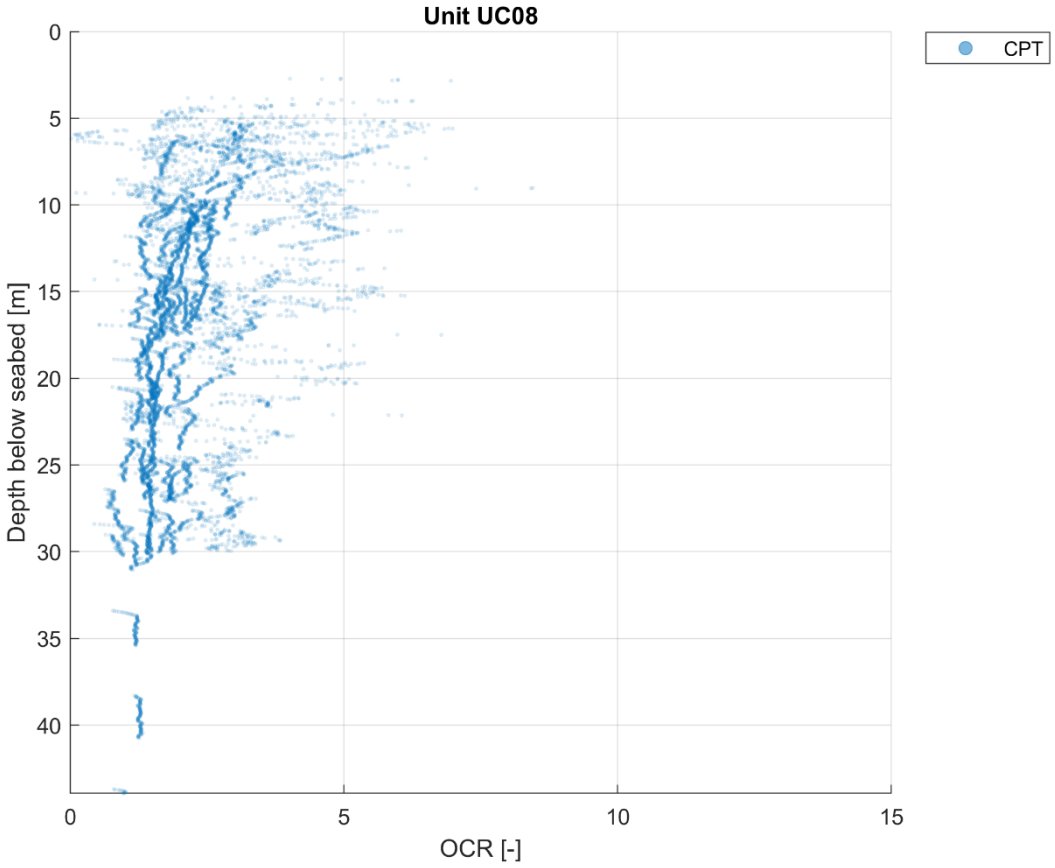
Unit UC08
CPT
Depth below seabed [m]
OCR [-]
0
5
10
15
20
25
30
35
40

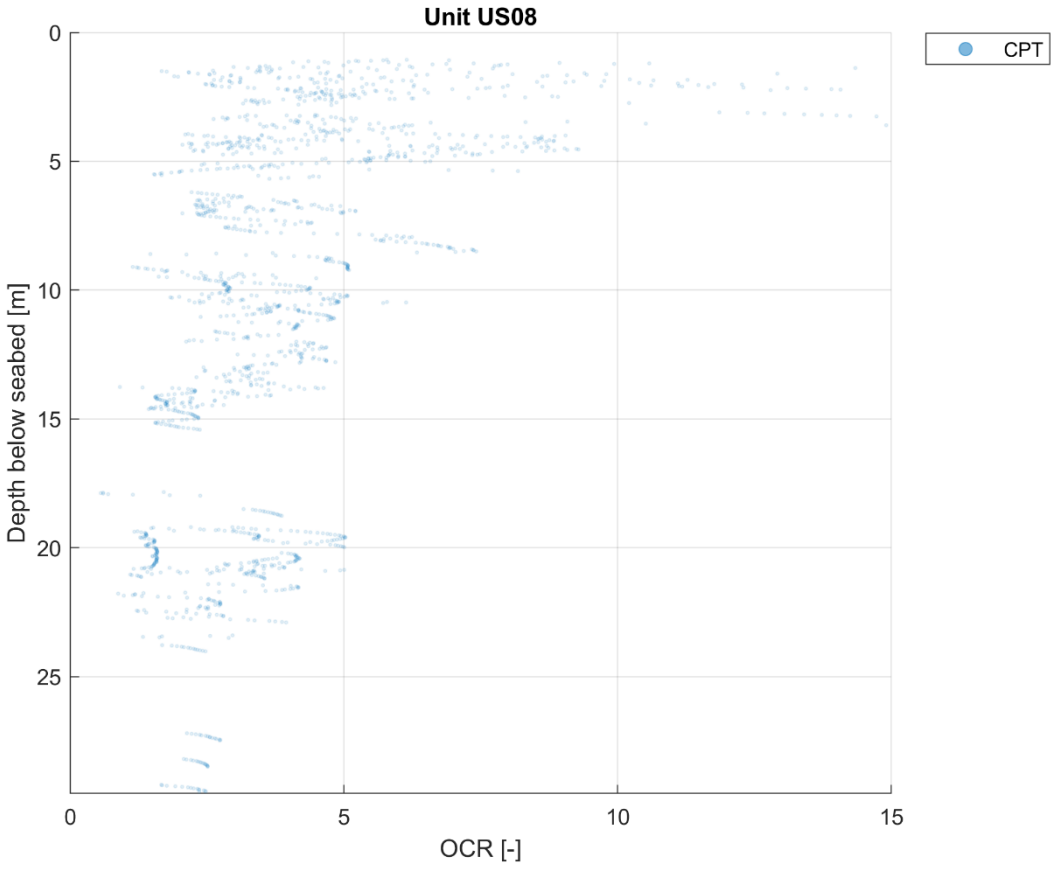
Unit US08
CPT
Depth below seabed [m]
OCR [-]
0
5
10
15
20
25

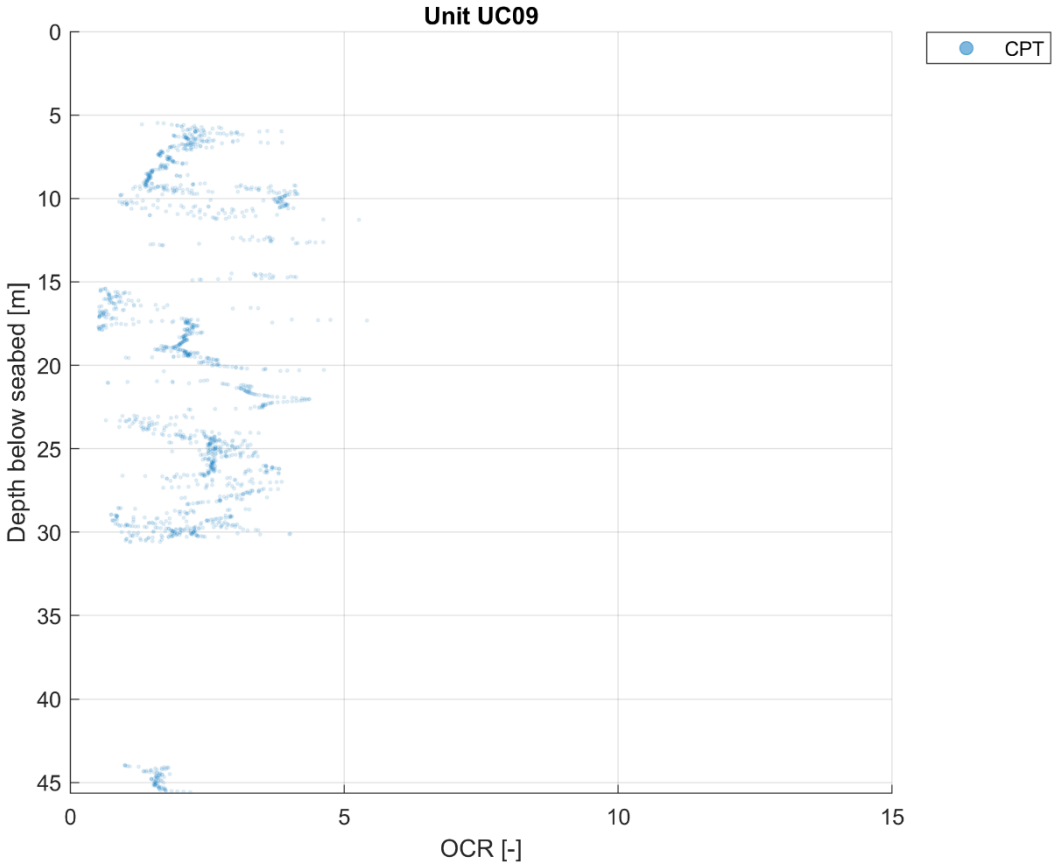
Unit UC09
CPT
Depth below seabed [m]
0
5
10
15
20
25
30
35
40
45
0
5
10
15
OCR [-]

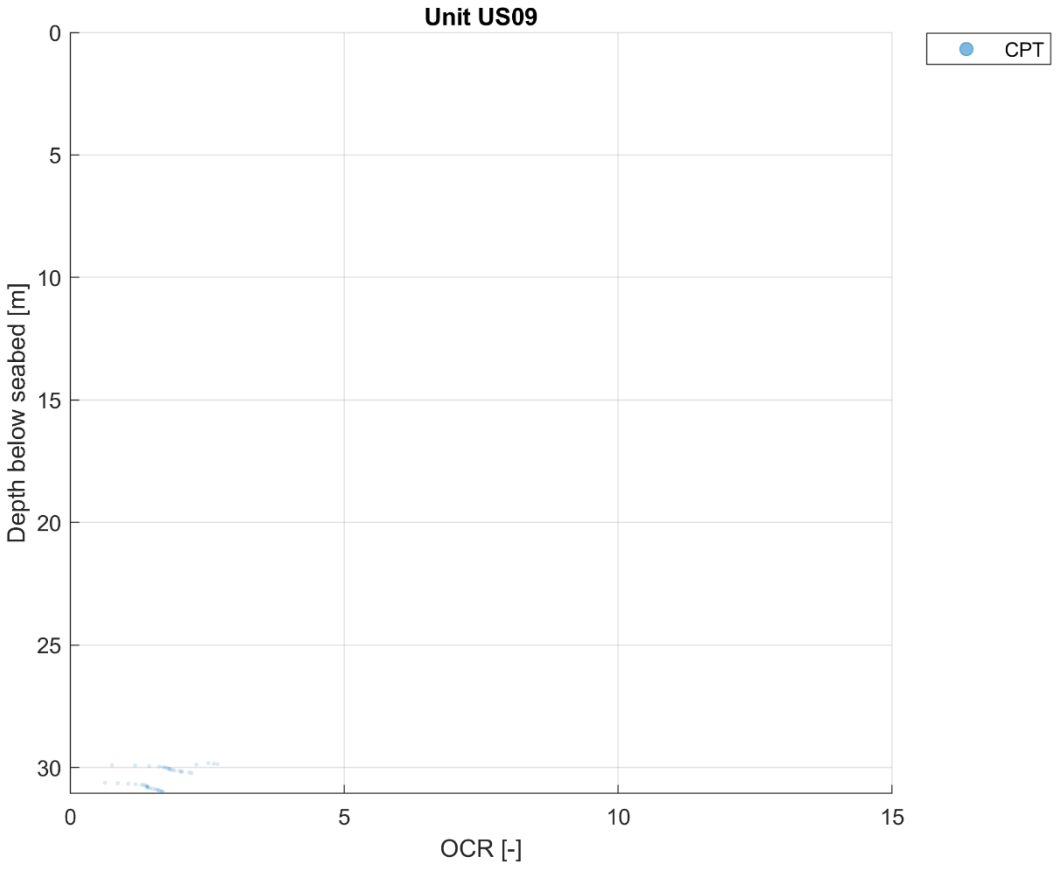
Unit US09
CPT
Depth below seabed [m]
0
5
10
15
20
25
30
0
5
10
15
OCR [-]

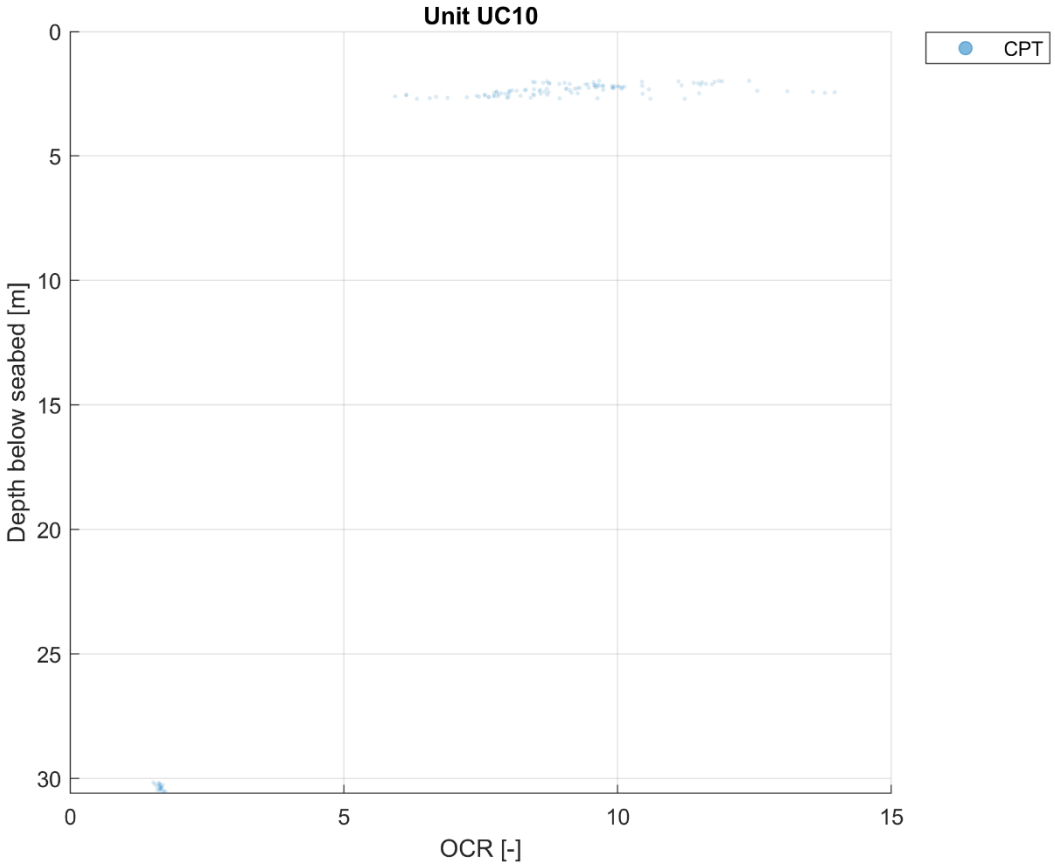
Unit UC10
CPT
Depth below seabed [m]
OCR [-]
0
5
10
15
20
25
30

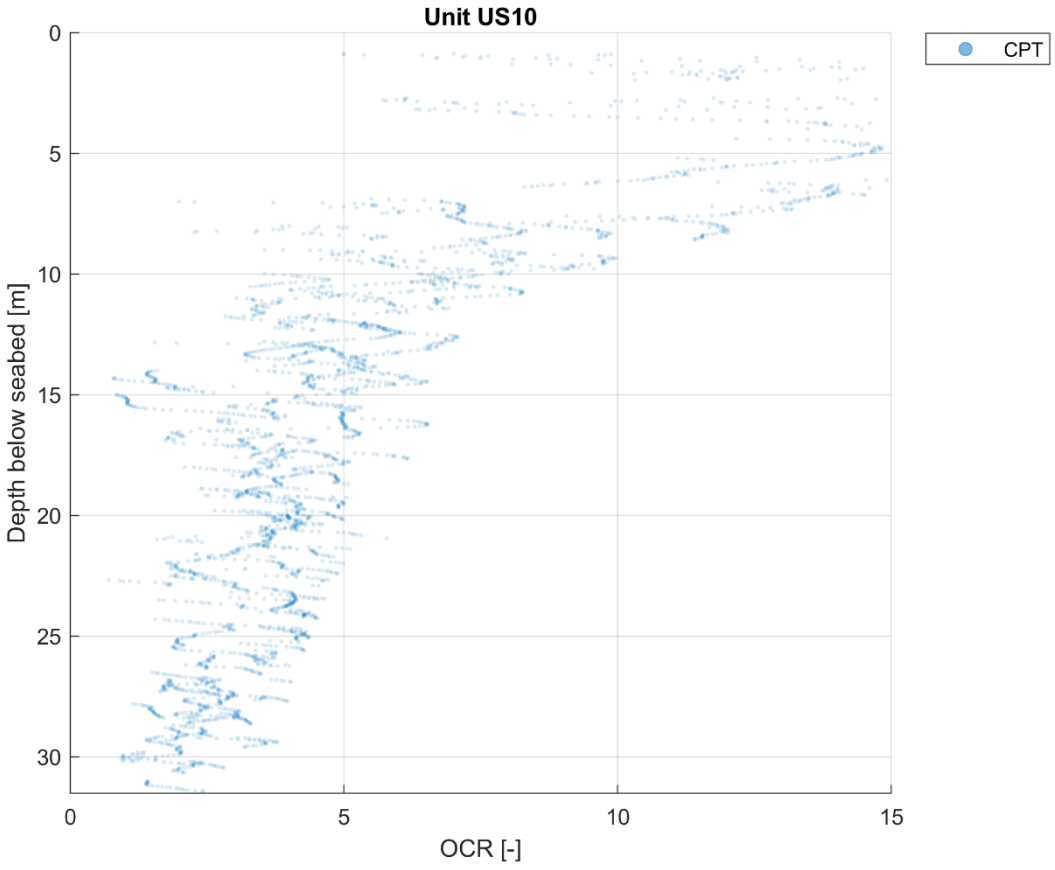
Unit US10
CPT
Depth below seabed [m]
OCR [-]
0
5
10
15
20
25
30

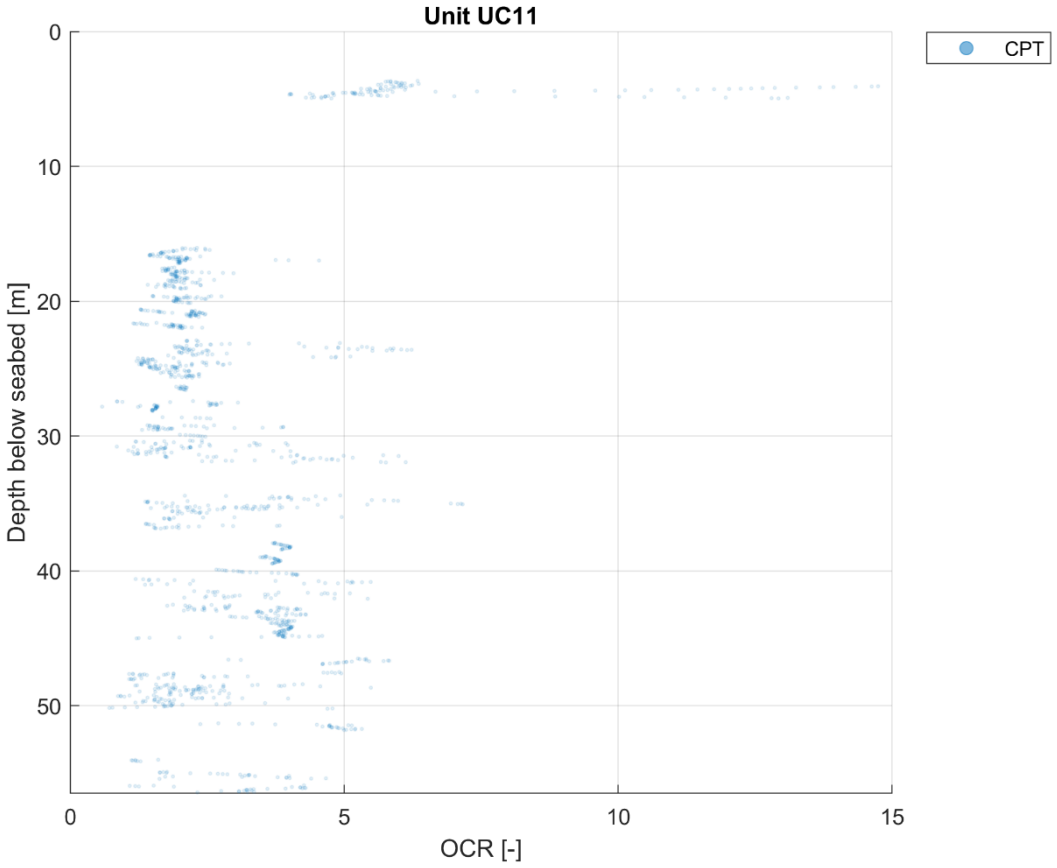
Unit UC11
CPT
Depth below seabed [m]
0
10
20
30
40
50
0
5
10
15
OCR [-]

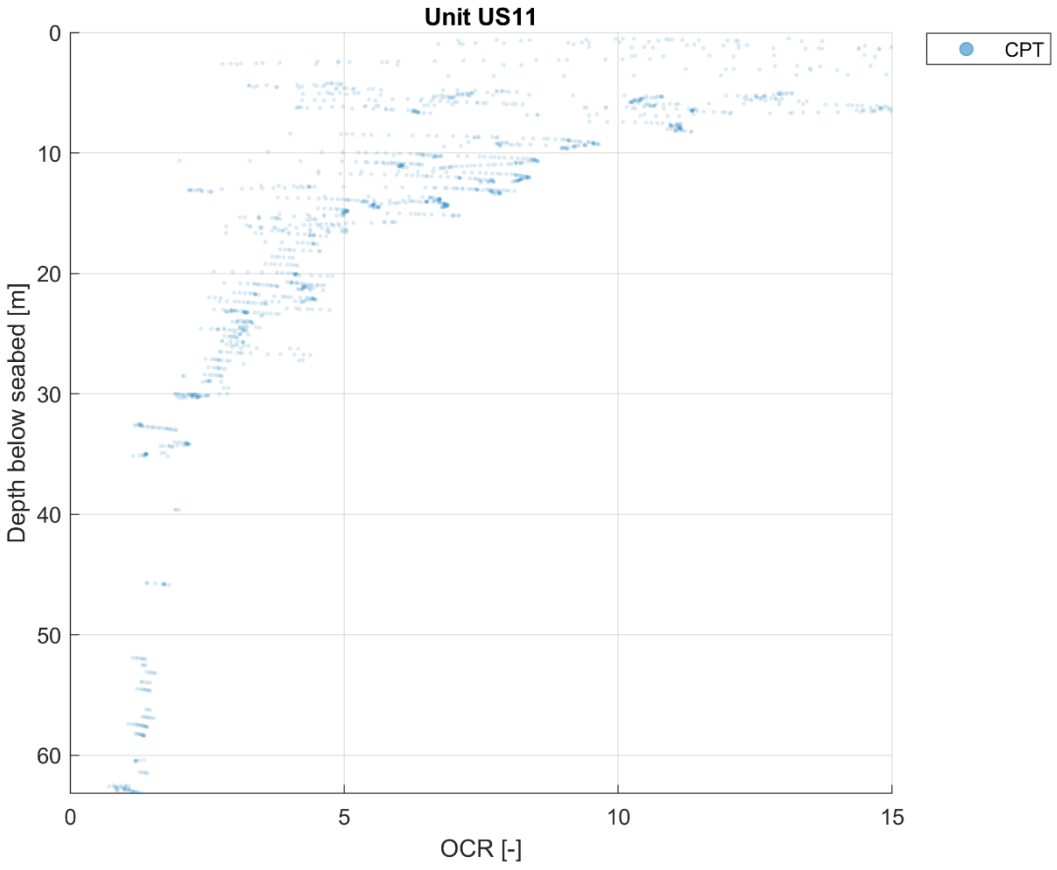
Unit US11
CPT
Depth below seabed [m]
0
10
20
30
40
50
60
0
5
10
15
OCR [-]

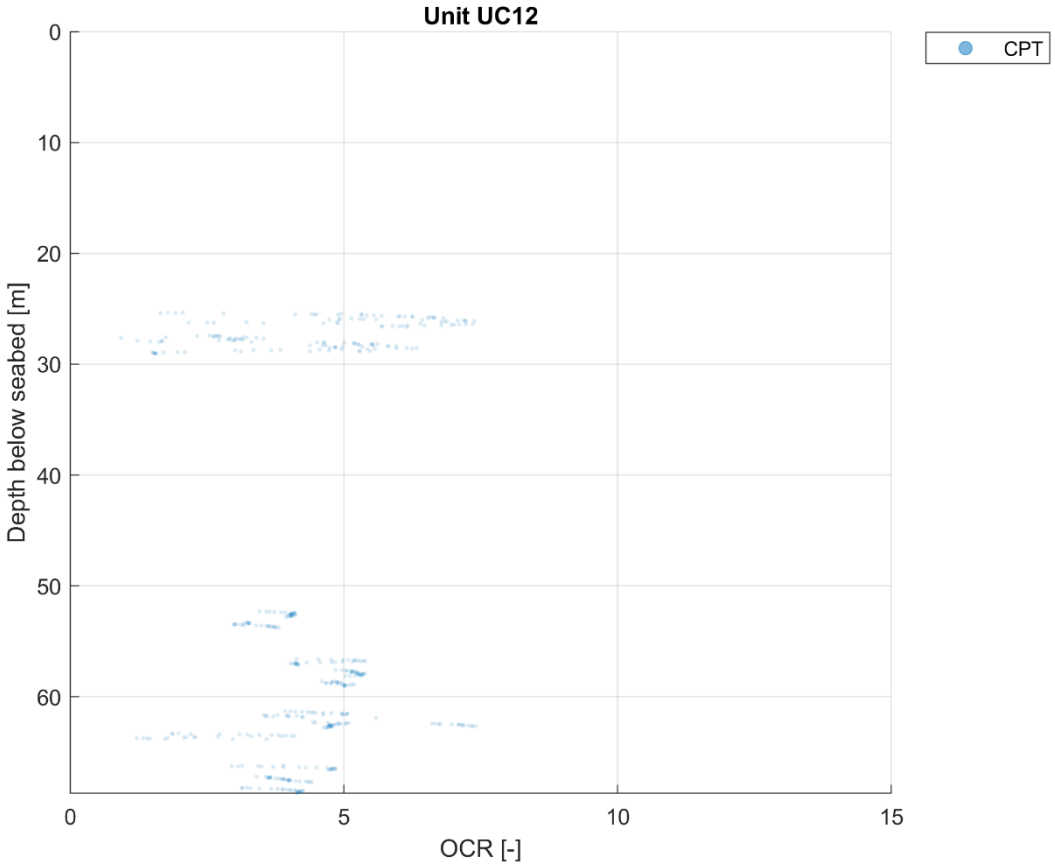
Unit UC12
CPT
Depth below seabed [m]
0
10
20
30
40
50
60
0
5
10
15
OCR [-]

D.2 Relative density

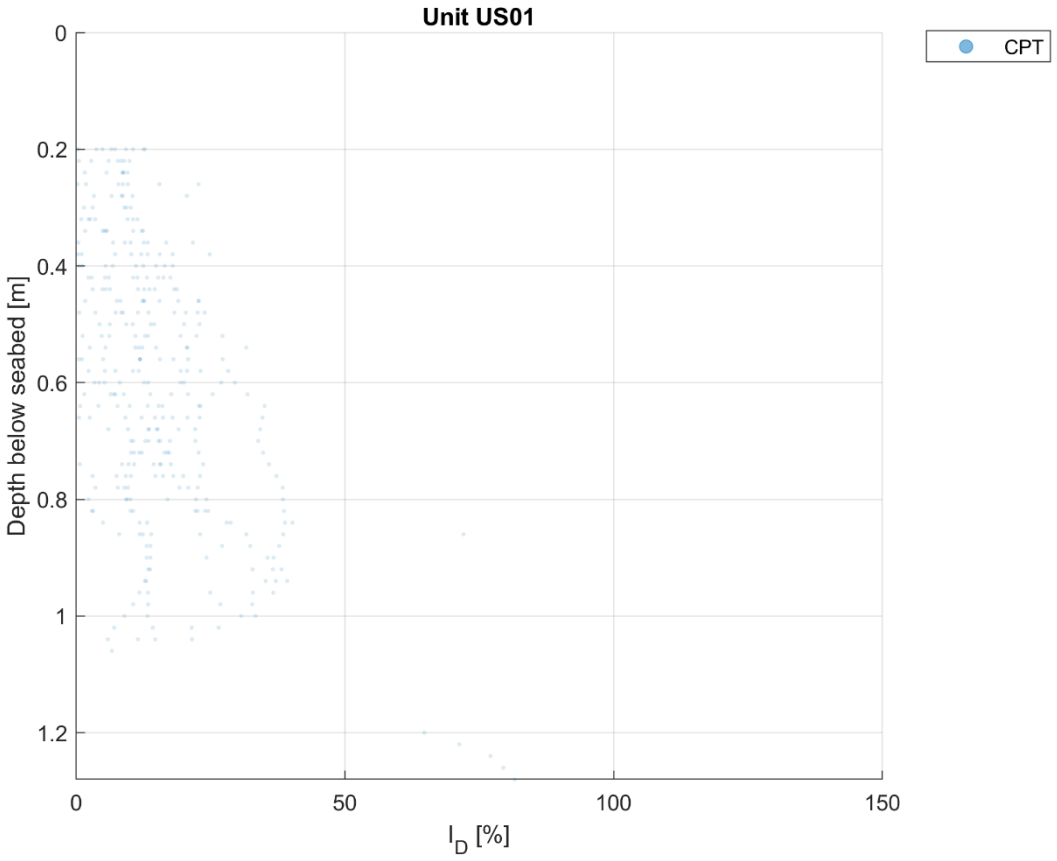

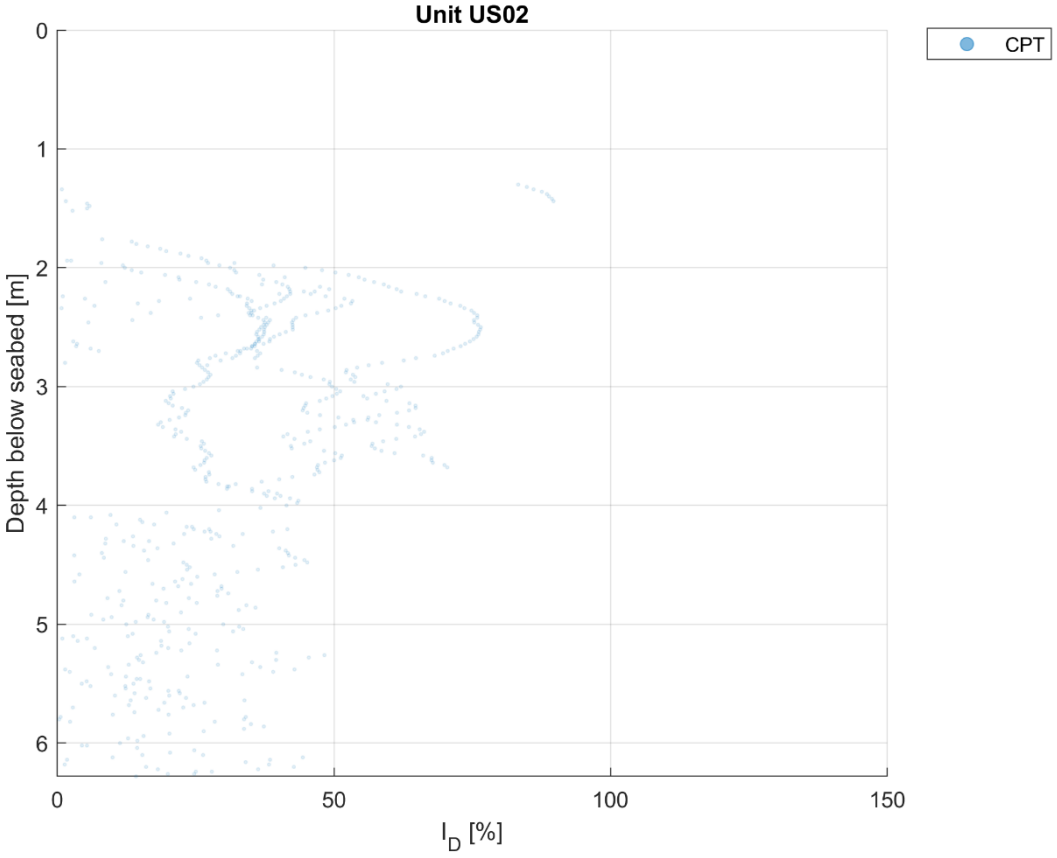

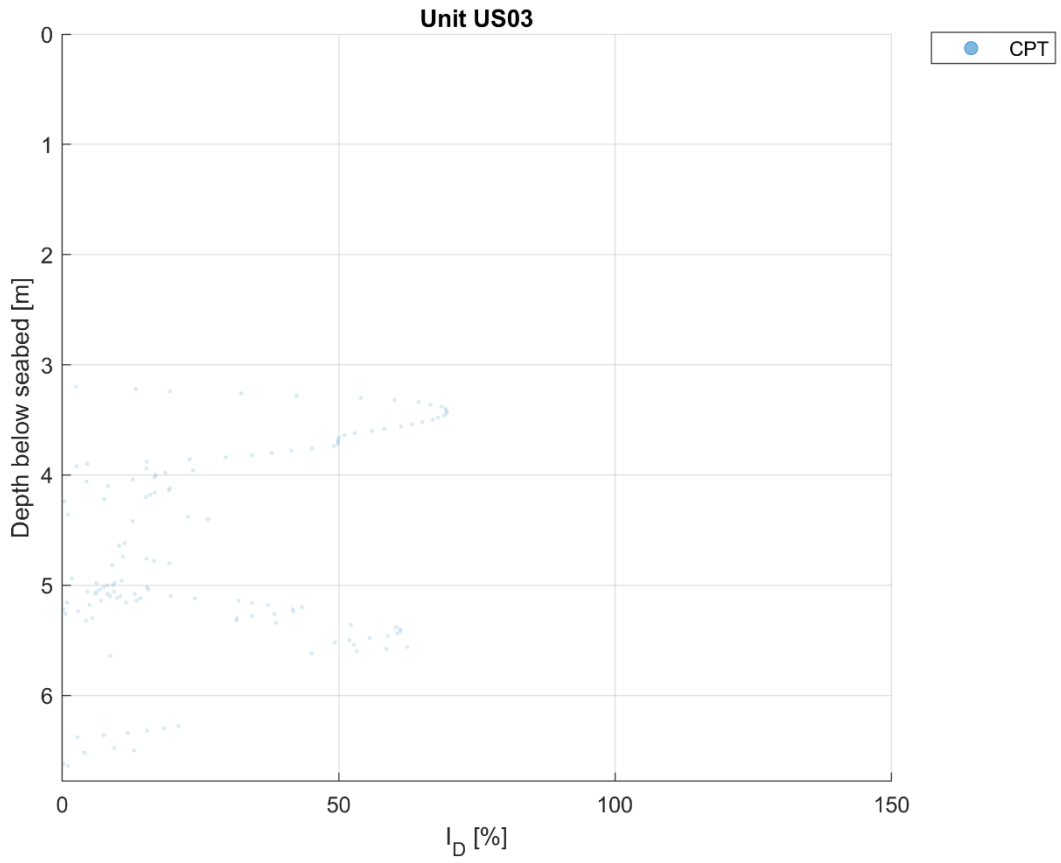
Unit US03
CPT
Depth below seabed [m]
0
1
2
3
4
5
6
0
50
100
150
I_D [%]

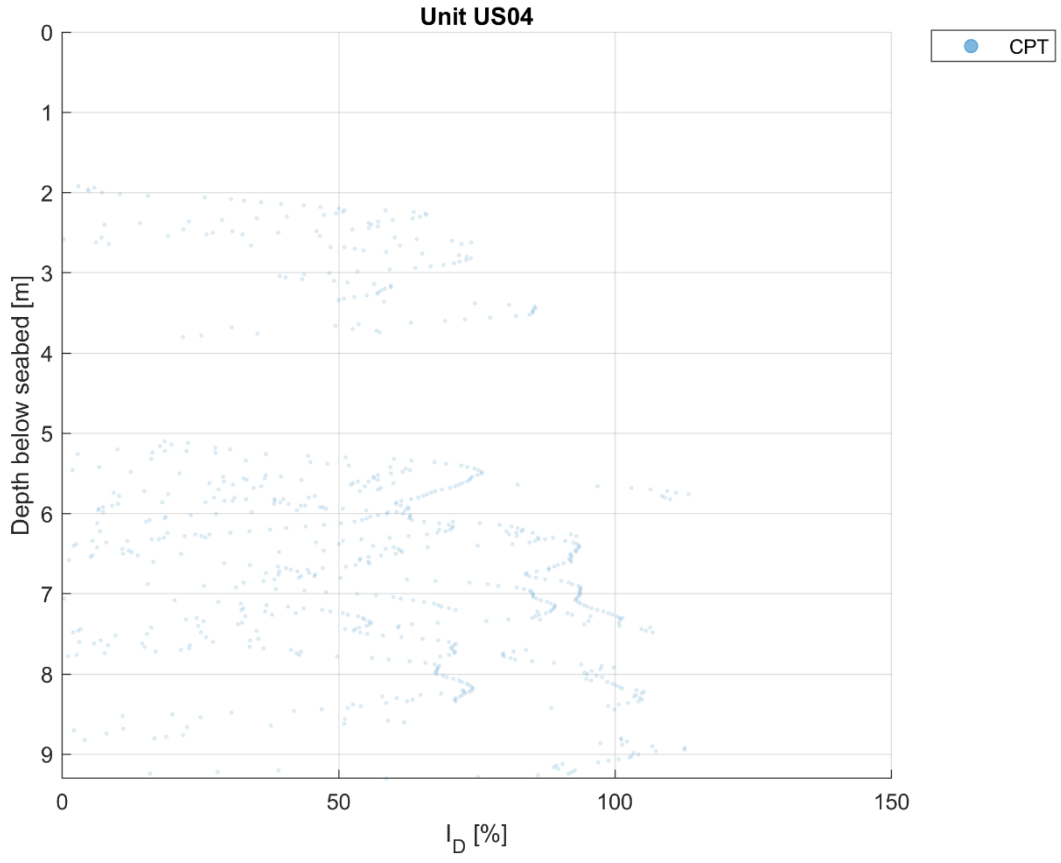
Unit US04
CPT
Depth below seabed [m]
0
1
2
3
4
5
6
7
8
9
0
50
100
150
I_D [%]

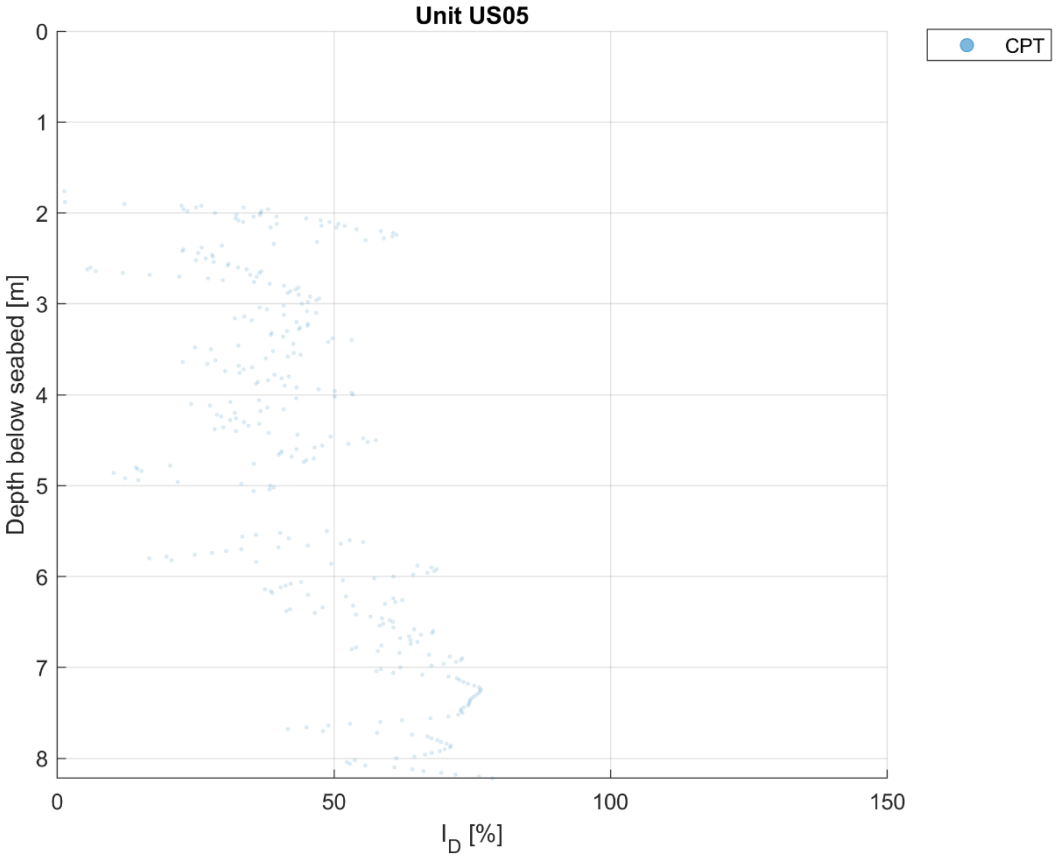
Unit US05
CPT
Depth below seabed [m]
0
1
2
3
4
5
6
7
8
0
50
100
150
I_D [%]

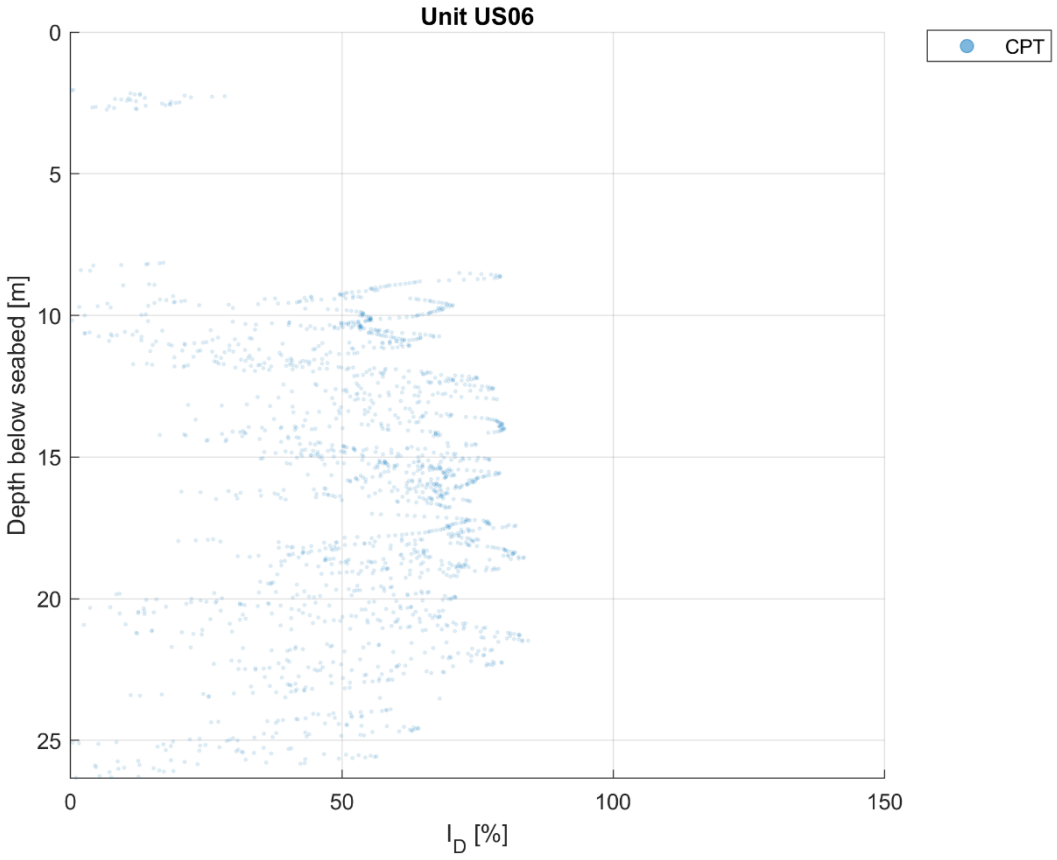
Unit US06
CPT
Depth below seabed [m]
0
5
10
15
20
25
0
50
100
150
I_D [%]

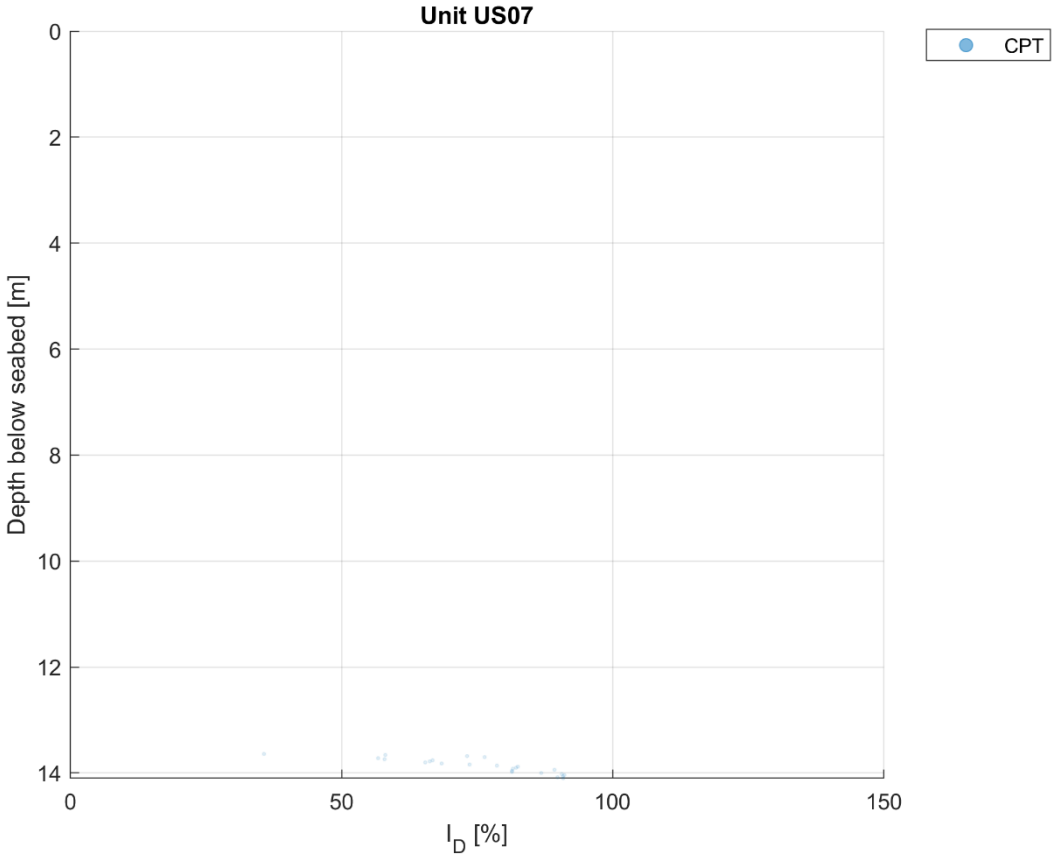
Unit US07
CPT
Depth below seabed [m]
0
2
4
6
8
10
12
14
0
50
100
150
I_D [%]

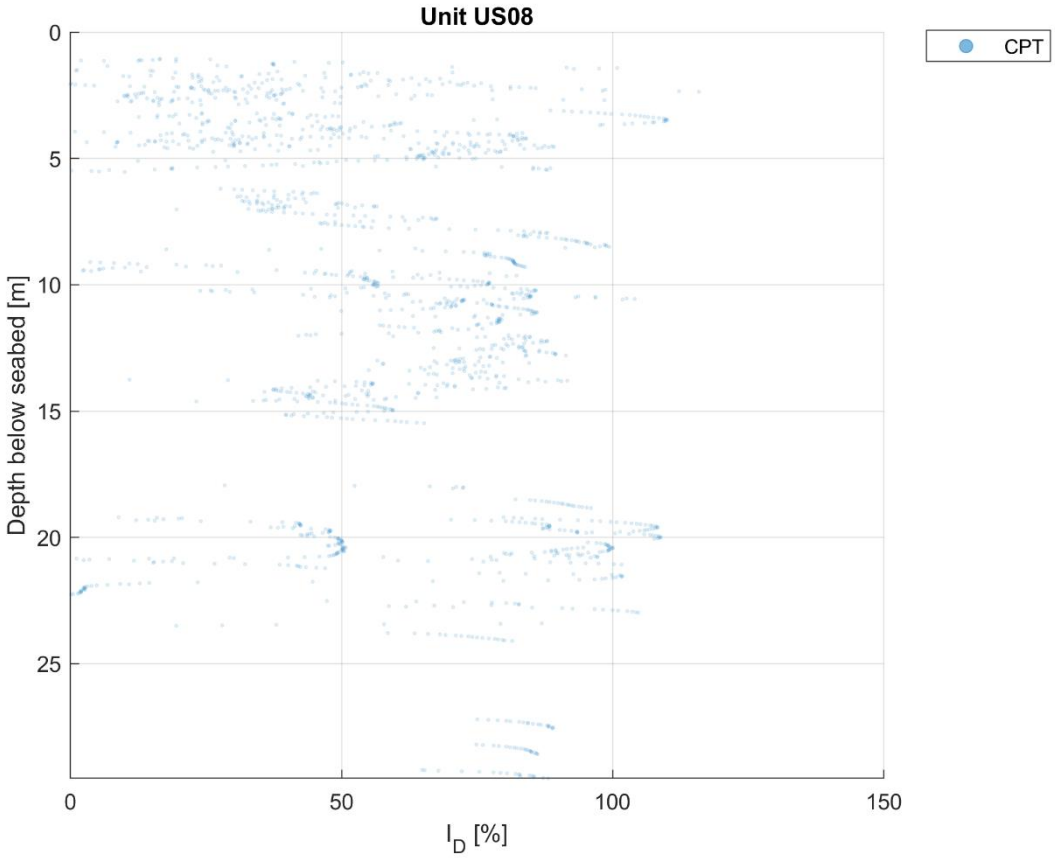
Unit US08
CPT
Depth below seabed [m]
0
5
10
15
20
25
0
50
100
150
I_D [%]

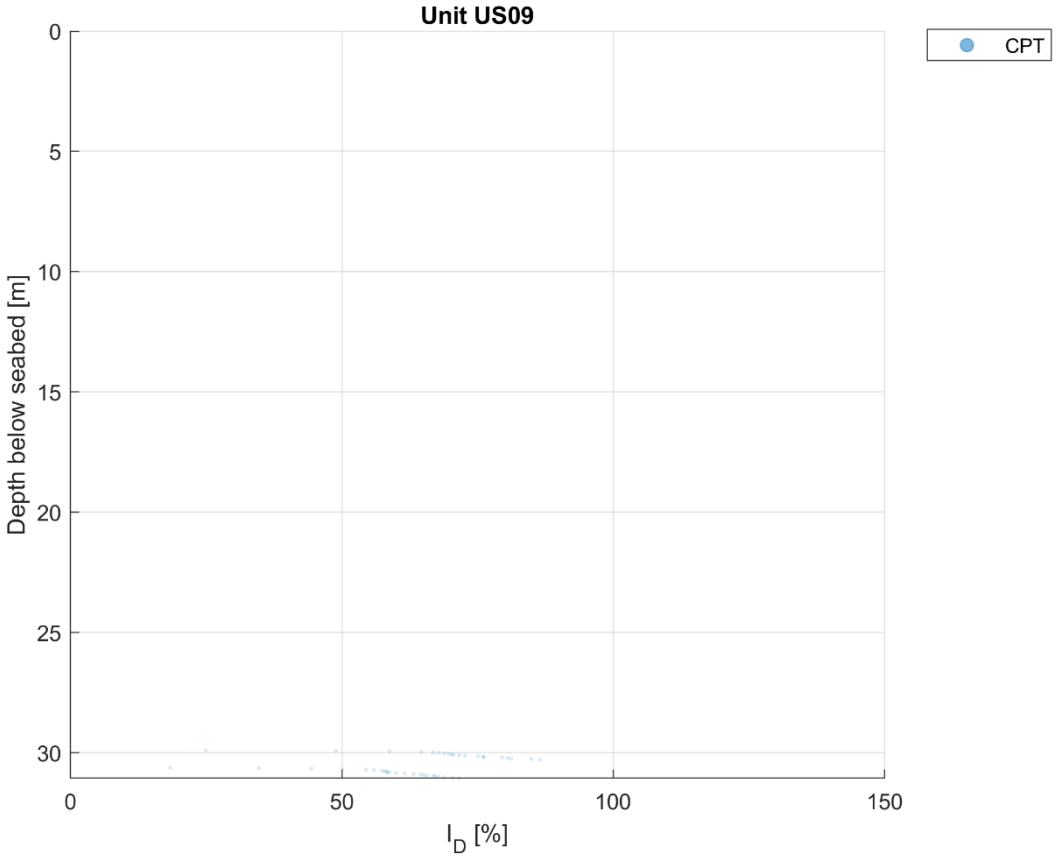
Unit US09
CPT
Depth below seabed [m]
0
5
10
15
20
25
30
0
50
100
150
I_D [%]

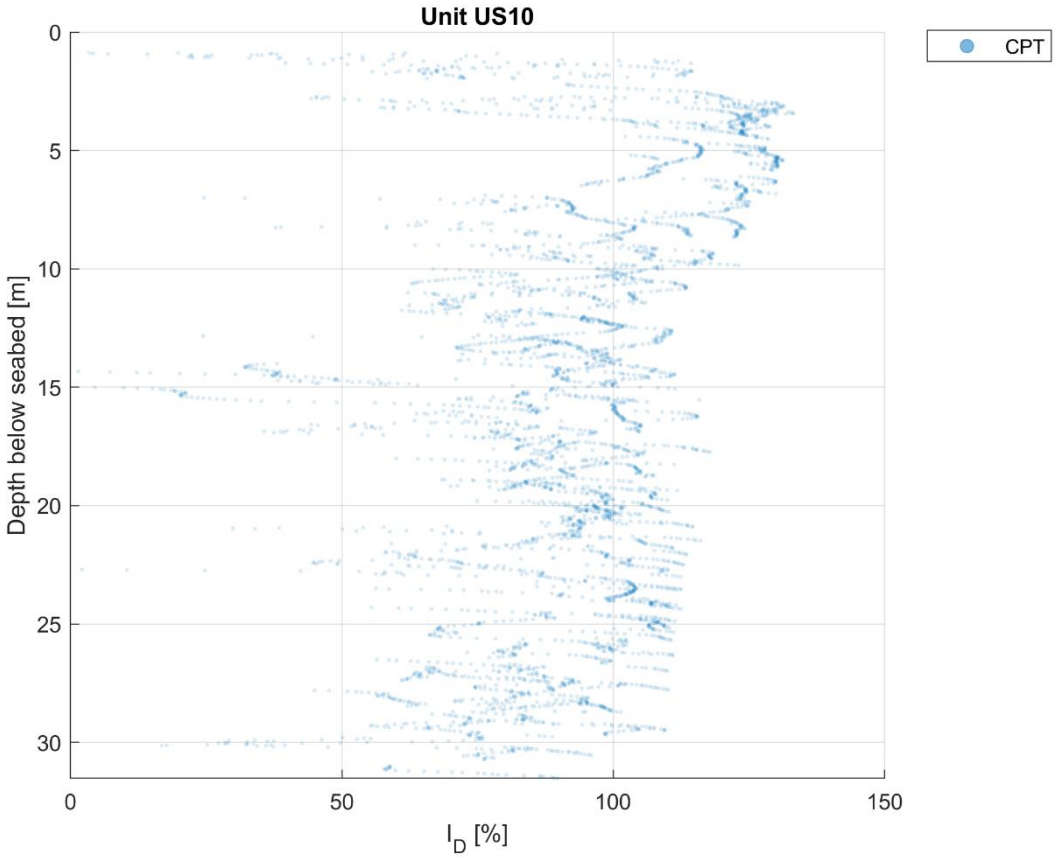
Unit US10
CPT
Depth below seabed [m]
0
5
10
15
20
25
30
0
50
100
150
I_D [%]

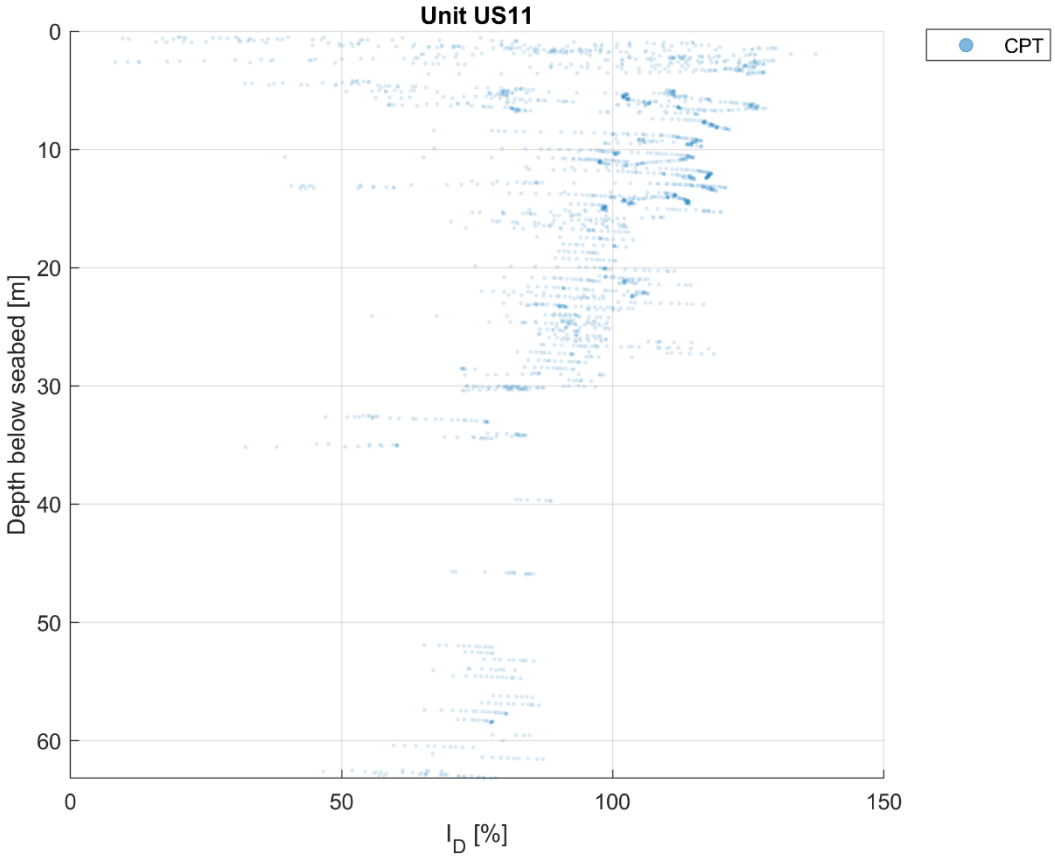
Unit US11
CPT
Depth below seabed [m]
0
10
20
30
40
50
60
0
50
100
150
I_D [%]

D.3 Friction angle

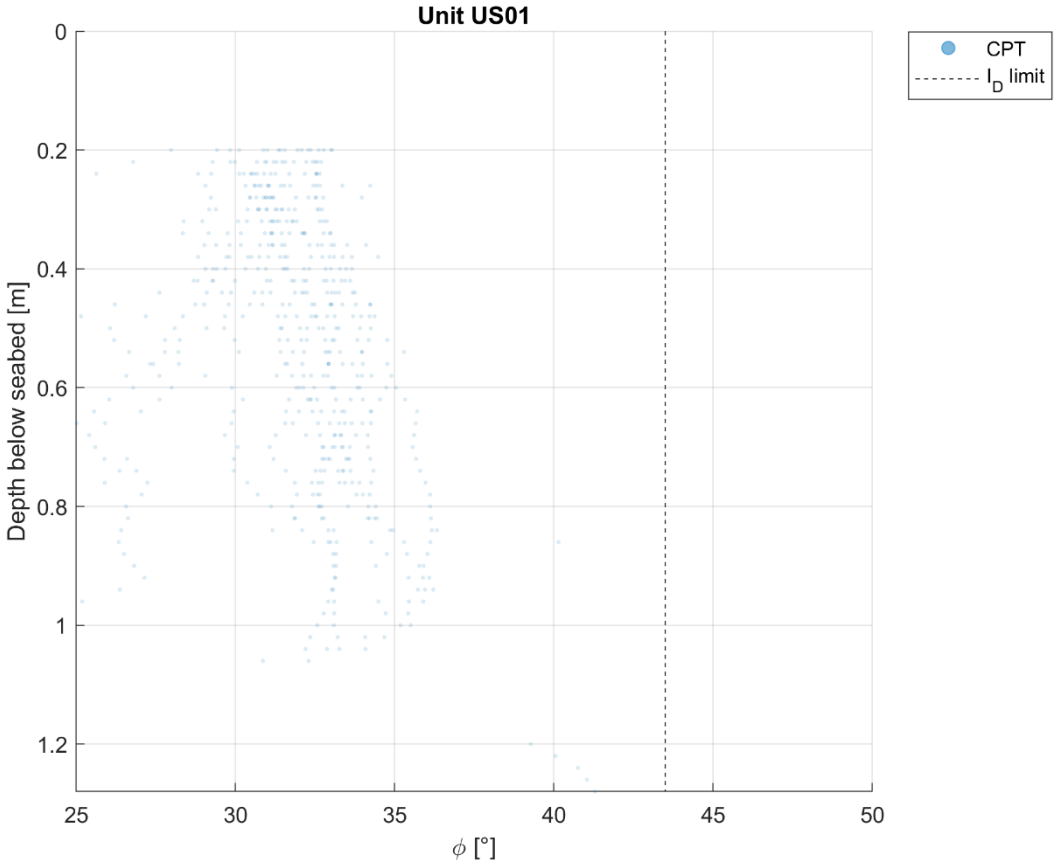

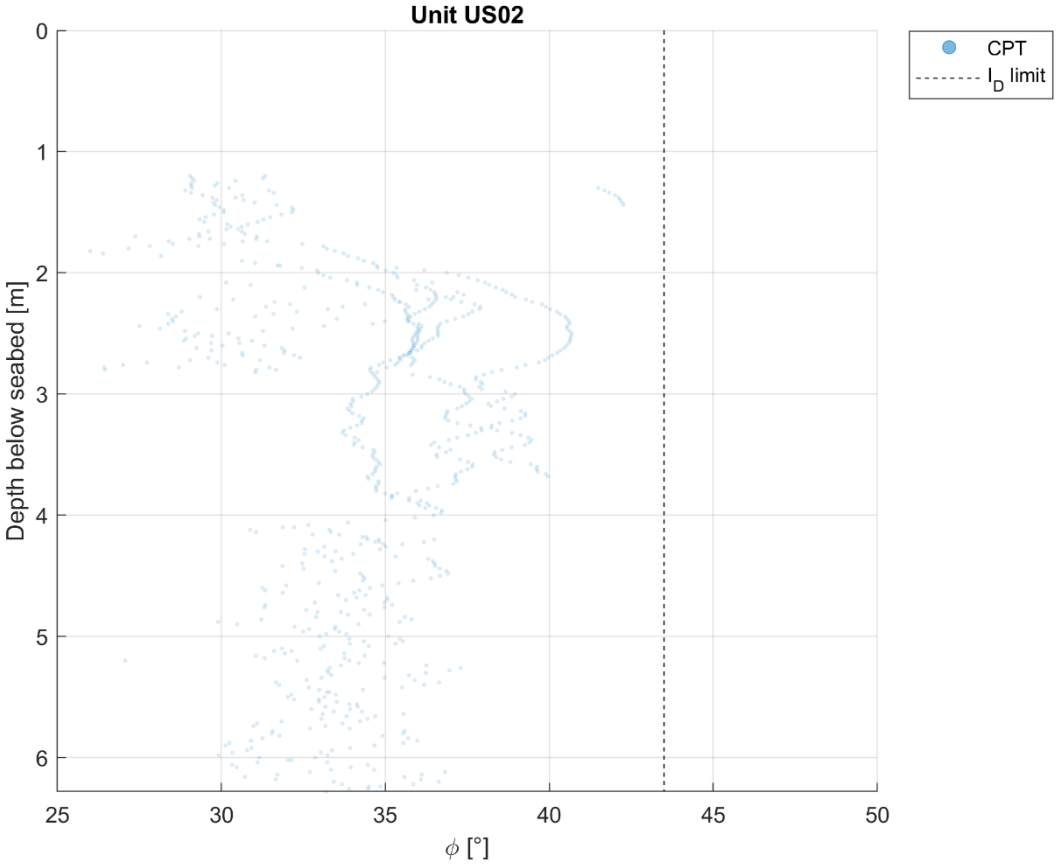

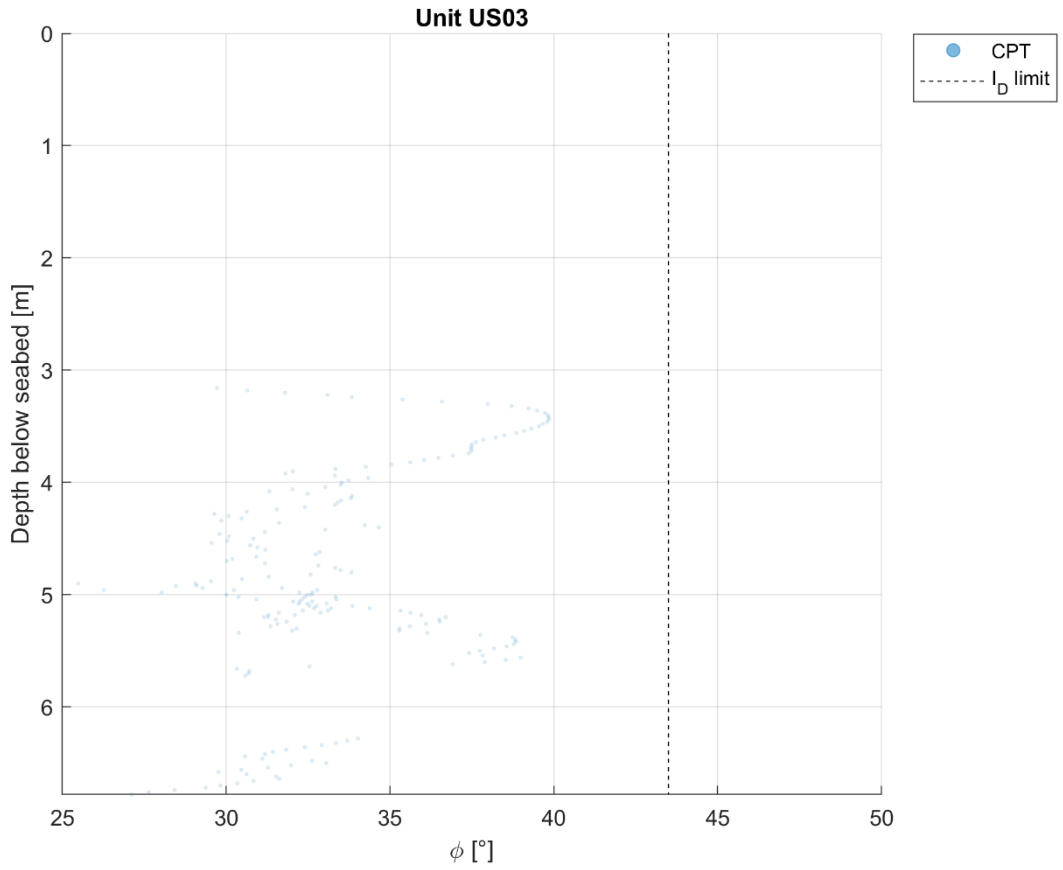
Unit US03
CPT
I_D limit
Depth below seabed [m]
ϕ [°]
0
1
2
3
4
5
6
25
30
35
40
45
50

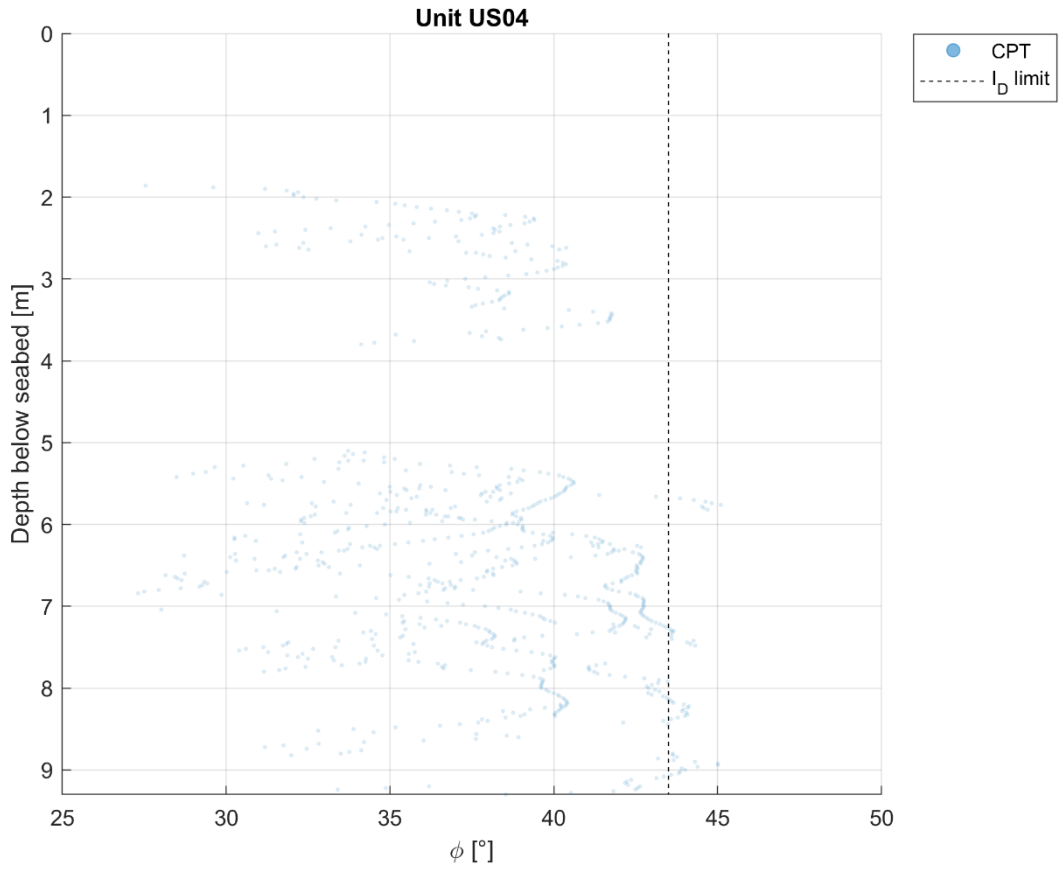
Unit US04
CPT
I_D limit
Depth below seabed [m]
ϕ [°]
0
1
2
3
4
5
6
7
8
9
25
30
35
40
45
50

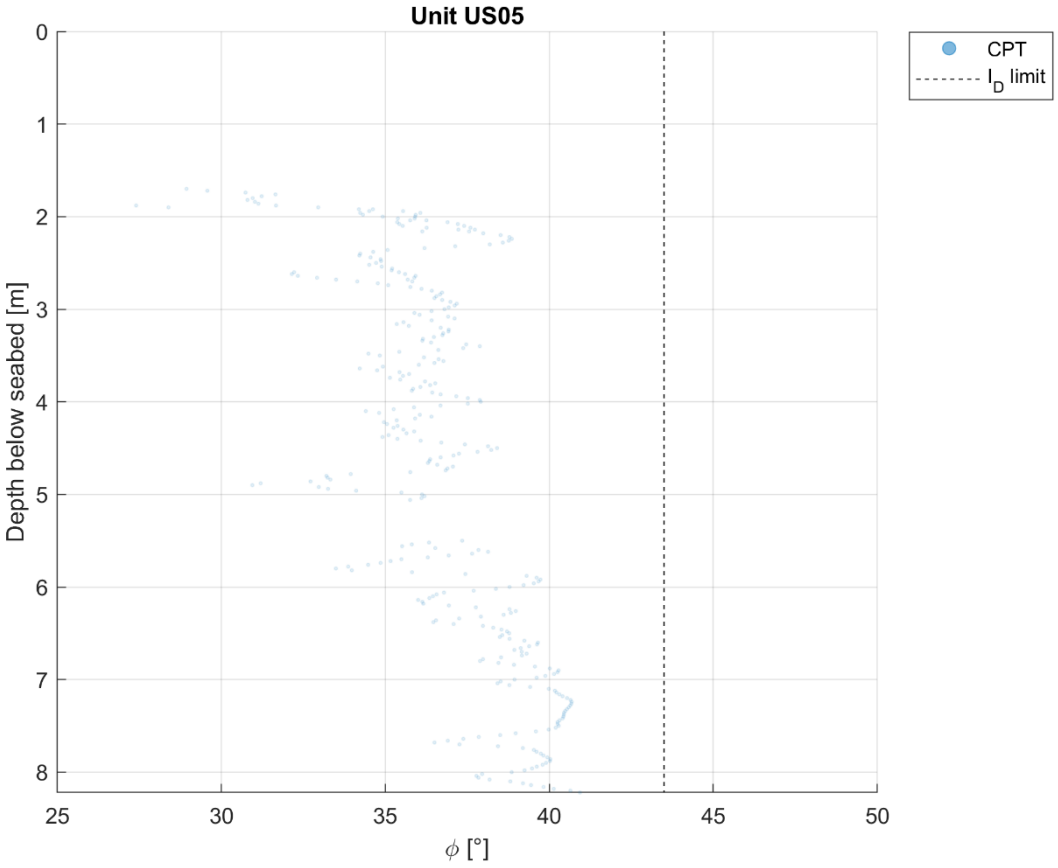
Unit US05
CPT
I_D limit
Depth below seabed [m]
0
1
2
3
4
5
6
7
8
25
30
35
40
45
50
ϕ [°]

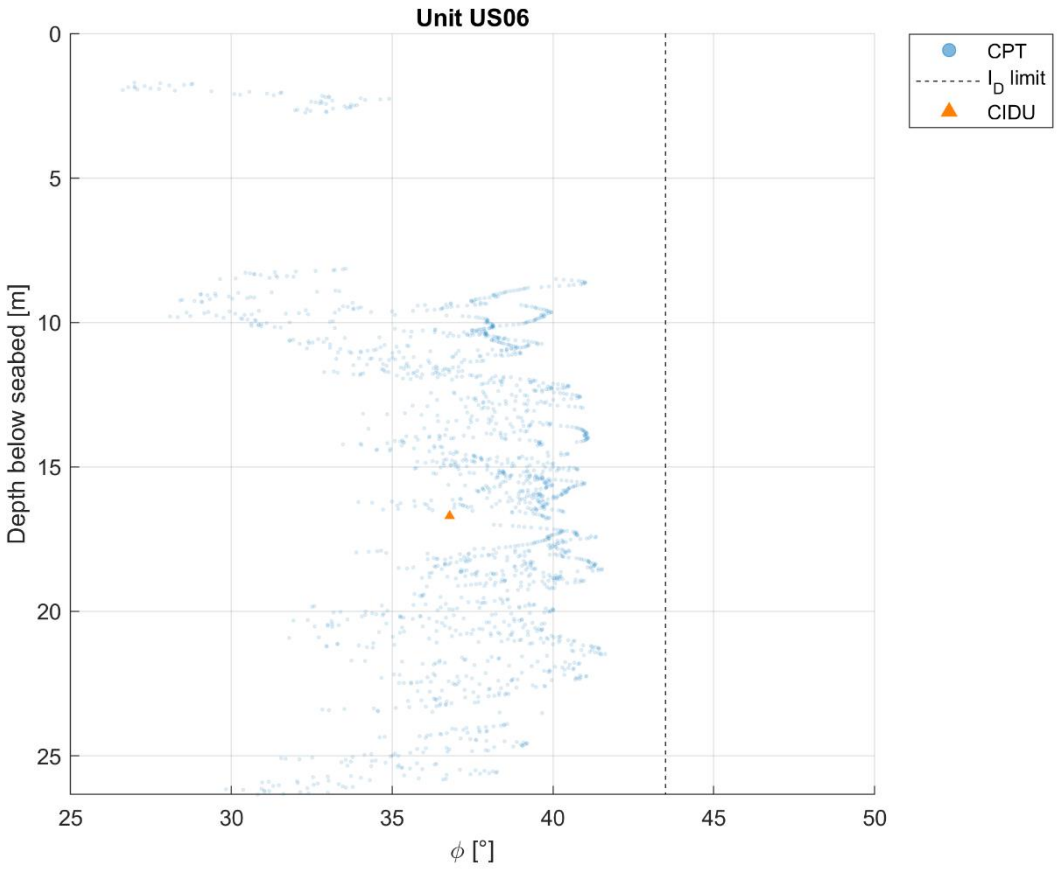
Unit US06
CPT
I_D limit
CIDU
Depth below seabed [m]
0
5
10
15
20
25
25
30
35
40
45
50
ϕ [°]

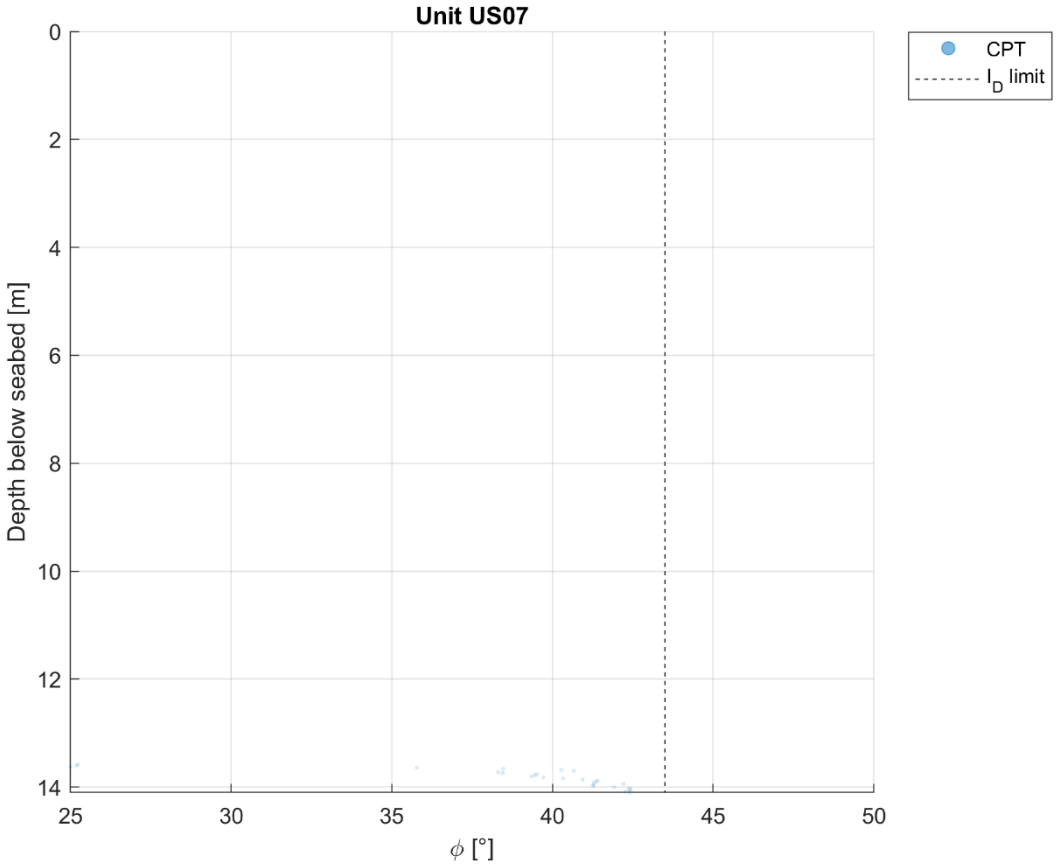
Unit US07
CPT
I_D limit
Depth below seabed [m]
0
2
4
6
8
10
12
14
25
30
35
40
45
50
ϕ [°]

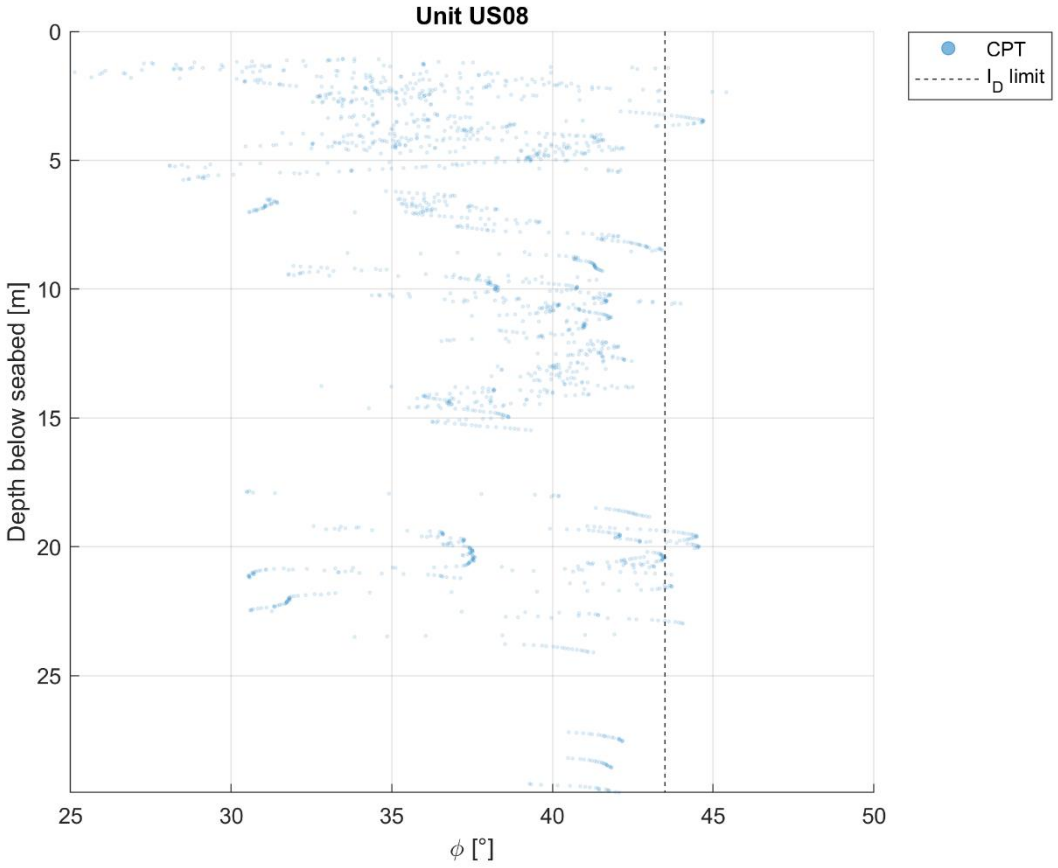
Unit US08
CPT
I_D limit
Depth below seabed [m]
0
5
10
15
20
25
25
30
35
40
45
50
ϕ [°]

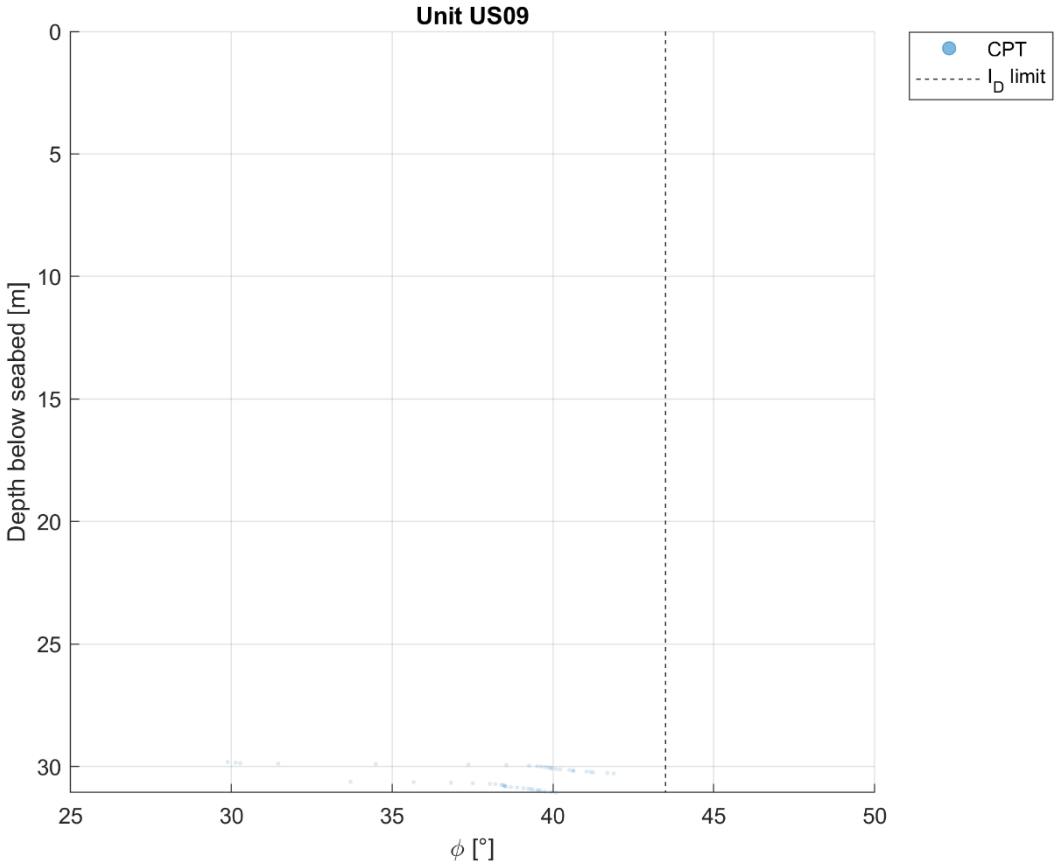
Unit US09
CPT
I_D limit
Depth below seabed [m]
0
5
10
15
20
25
30
25
30
35
40
45
50
ϕ [°]

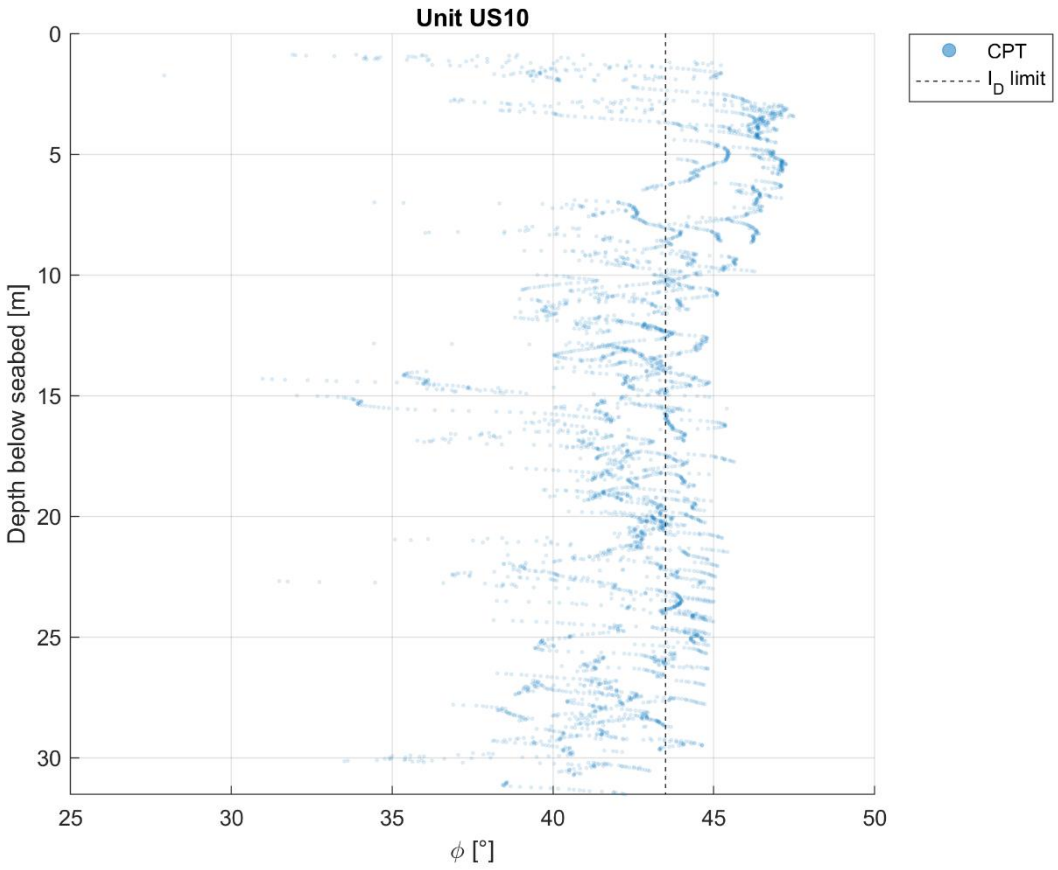
Unit US10
CPT
I_D limit
Depth below seabed [m]
0
5
10
15
20
25
30
25
30
35
40
45
50
ϕ [°]

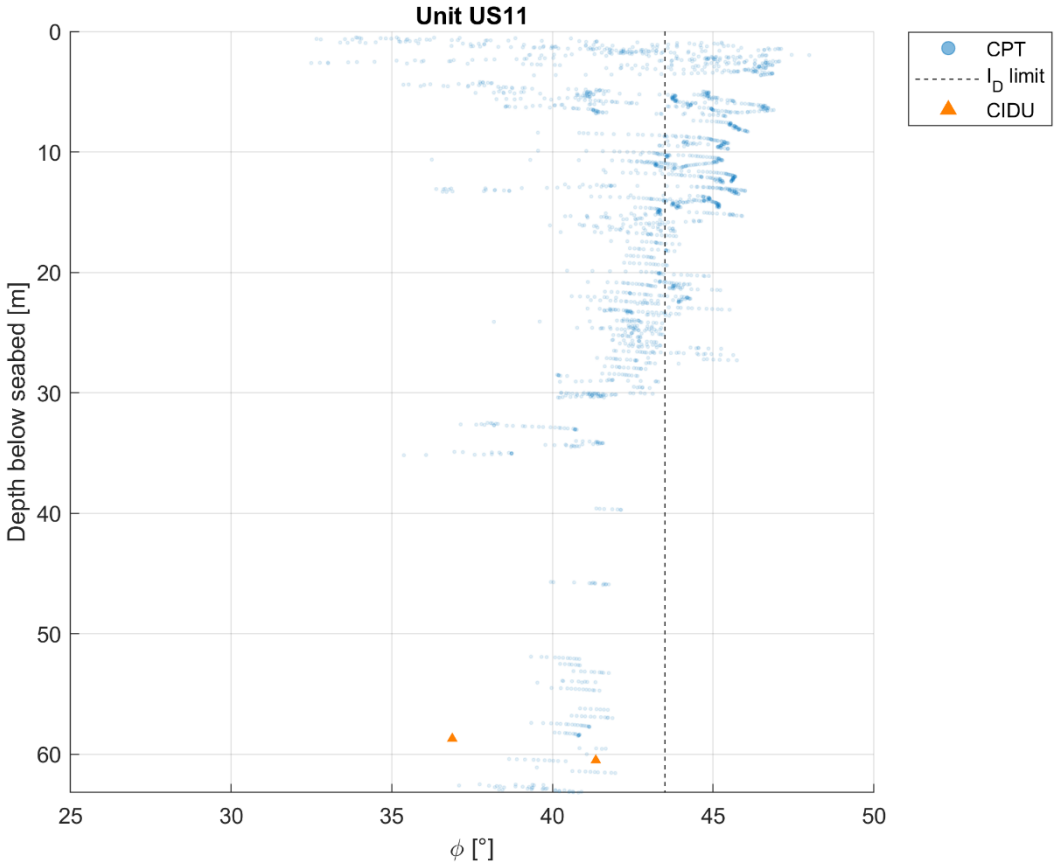
Unit US11
Depth below seabed [m]
0
10
20
30
40
50
60
25
30
35
40
45
50
ϕ [°]
CPT
I_D limit
CIDU

D.4 Undrained shear strength

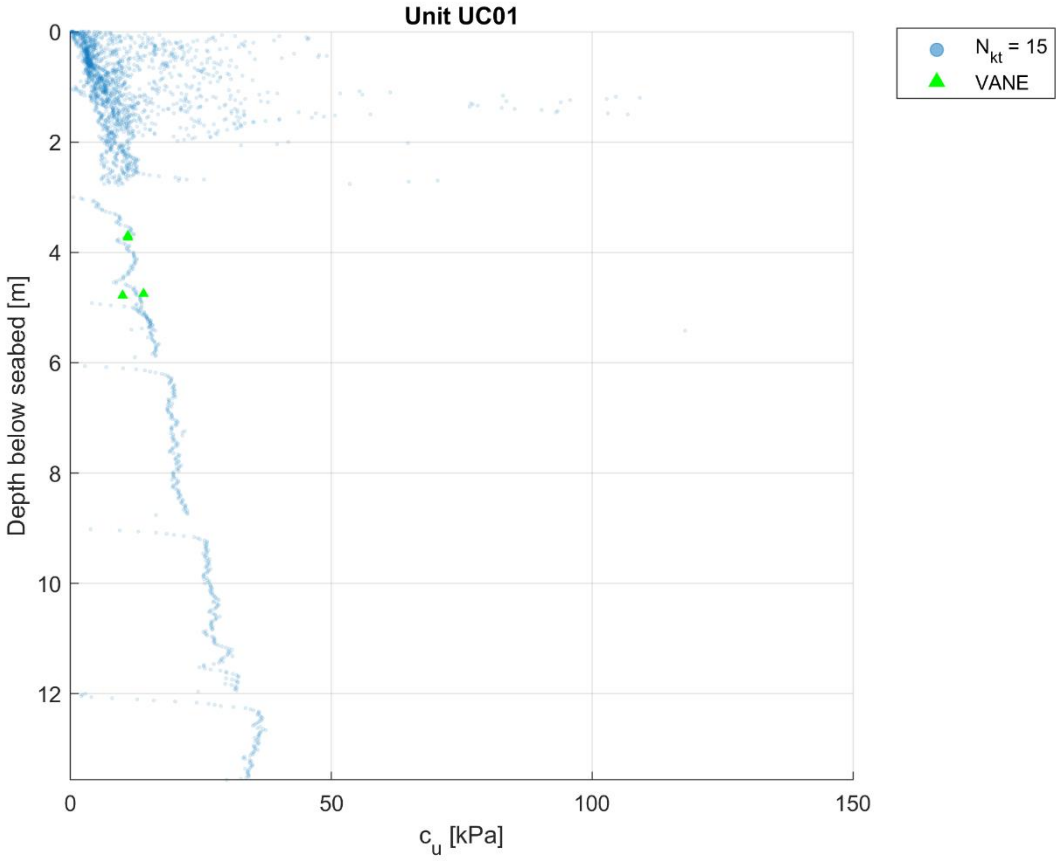

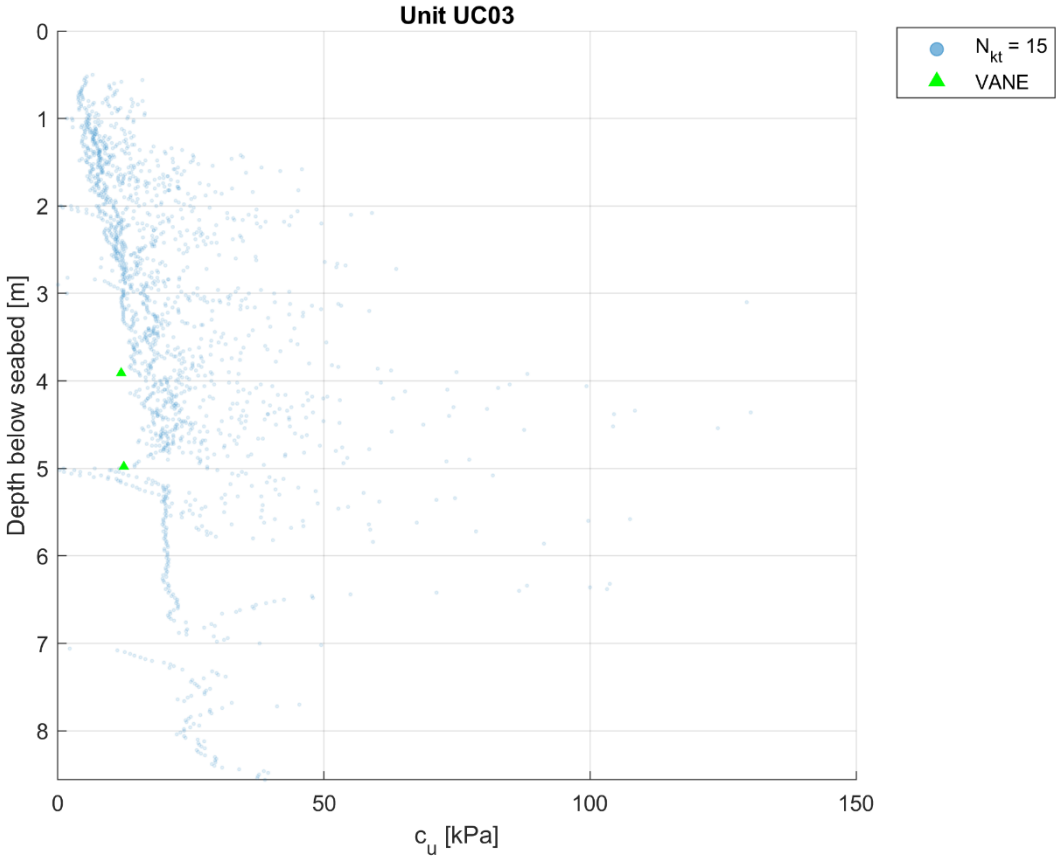

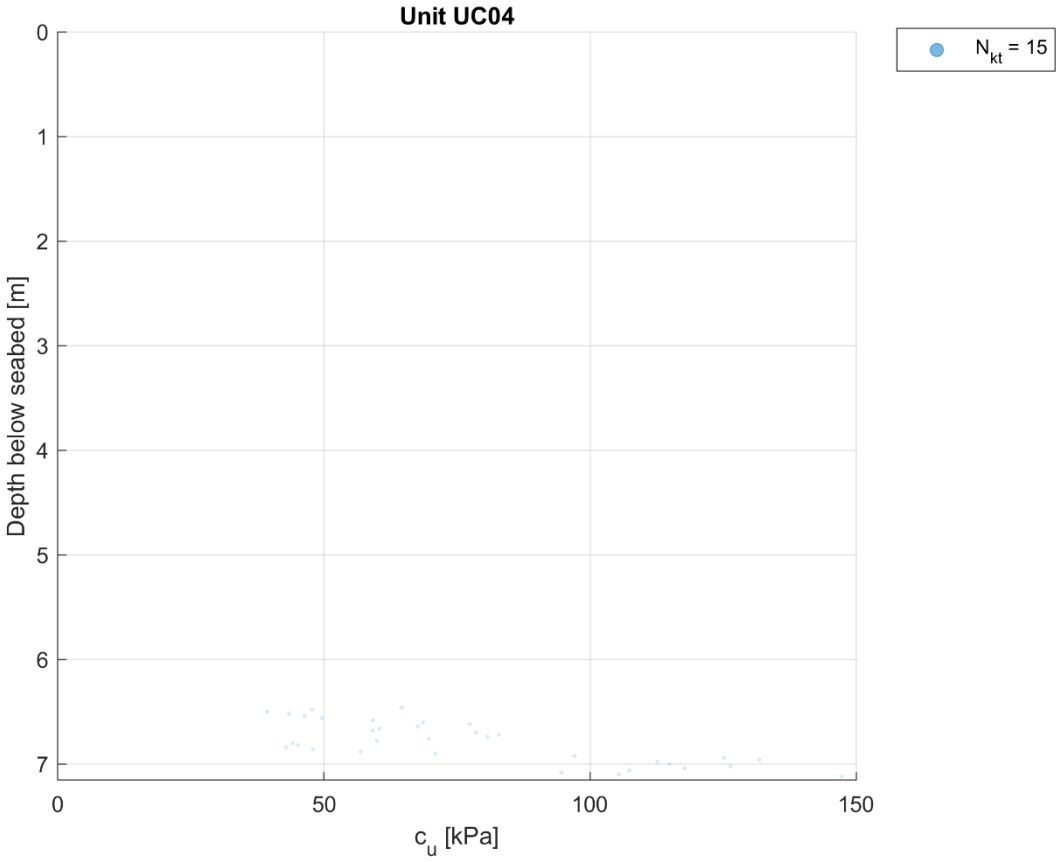
Unit UC04
N_kt = 15
Depth below seabed [m]
0
1
2
3
4
5
6
7
0
50
100
150
c_u [kPa]

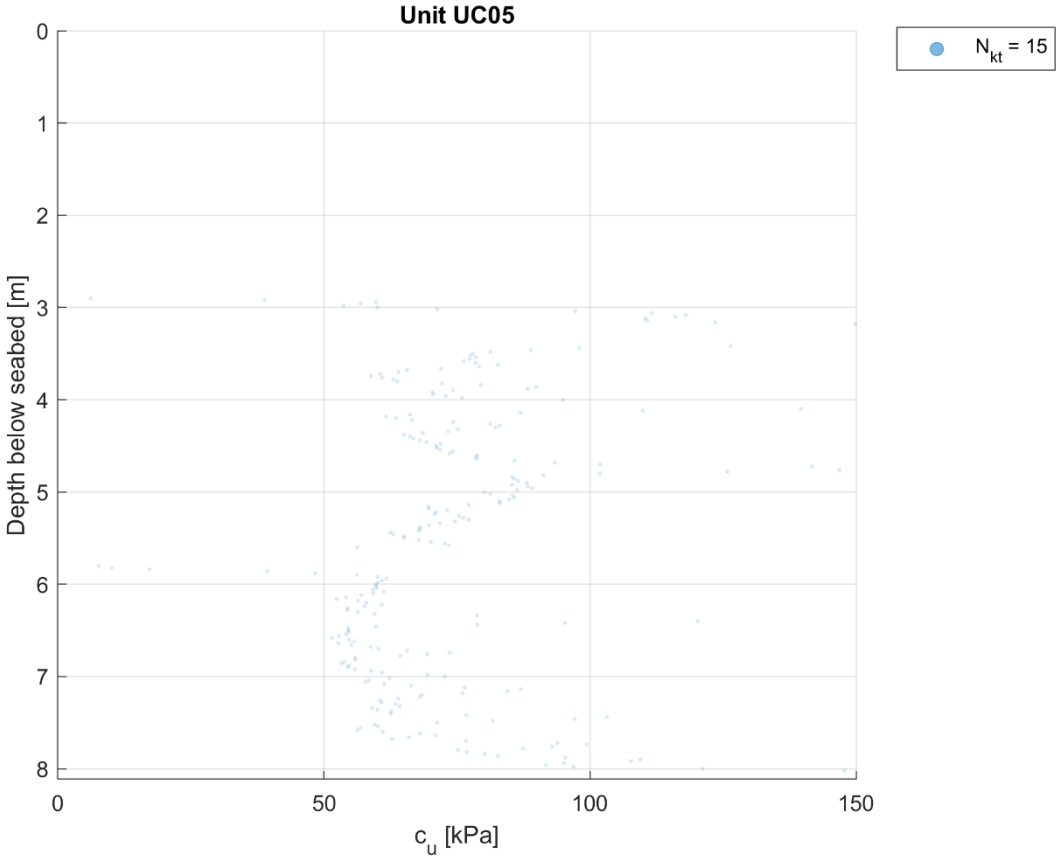
Unit UC05
N_kt = 15
Depth below seabed [m]
0
1
2
3
4
5
6
7
8
0
50
100
150
c_u [kPa]

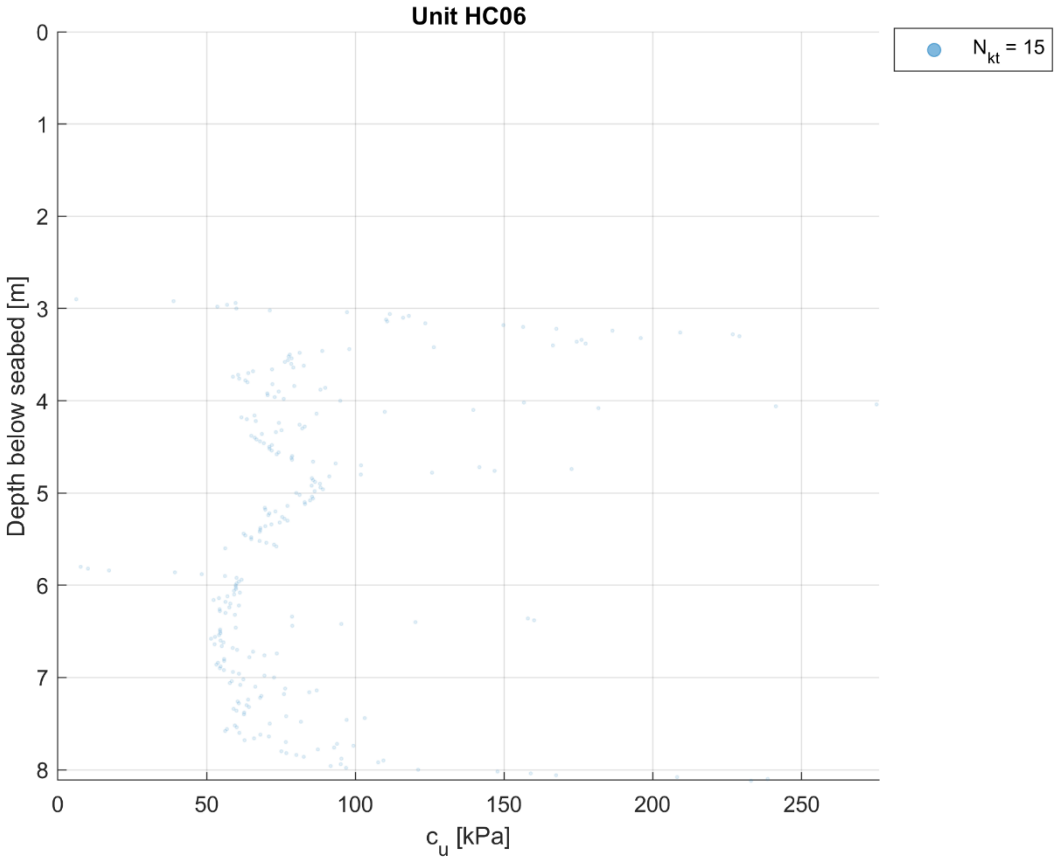
Unit HC06
N_kt = 15
Depth below seabed [m]
c_u [kPa]
0
1
2
3
4
5
6
7
8
0
50
100
150
200
250

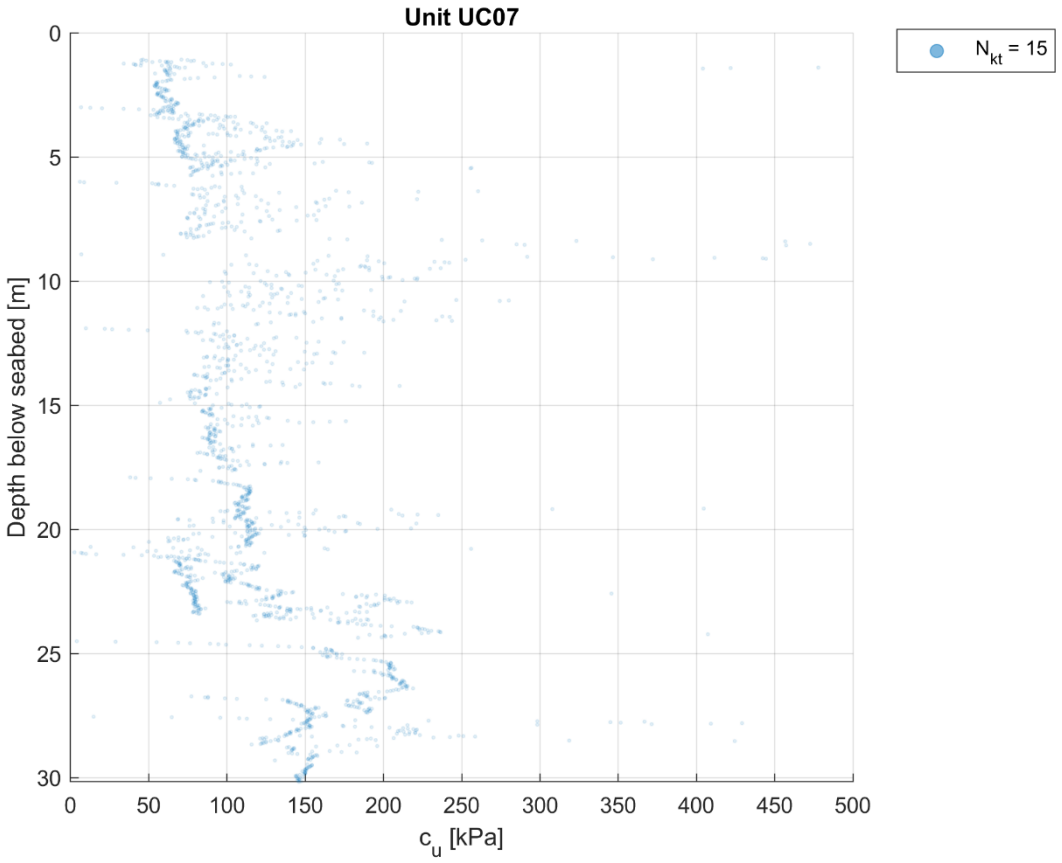
Unit UC07
N_kt = 15
Depth below seabed [m]
c_u [kPa]
0
5
10
15
20
25
30
0
50
100
150
200
250
300
350
400
450
500

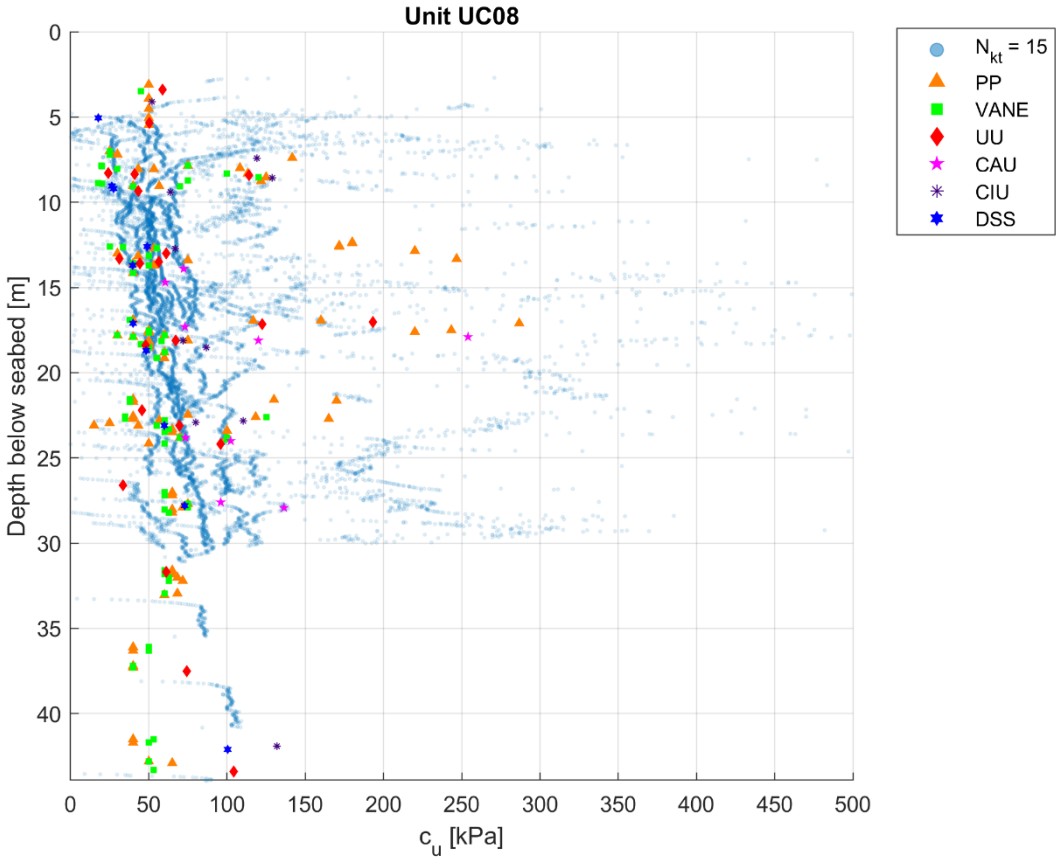
Unit UC08
Depth below seabed [m]
c_u [kPa]
N_{kt} = 15
PP
VANE
UU
CAU
CIU
DSS

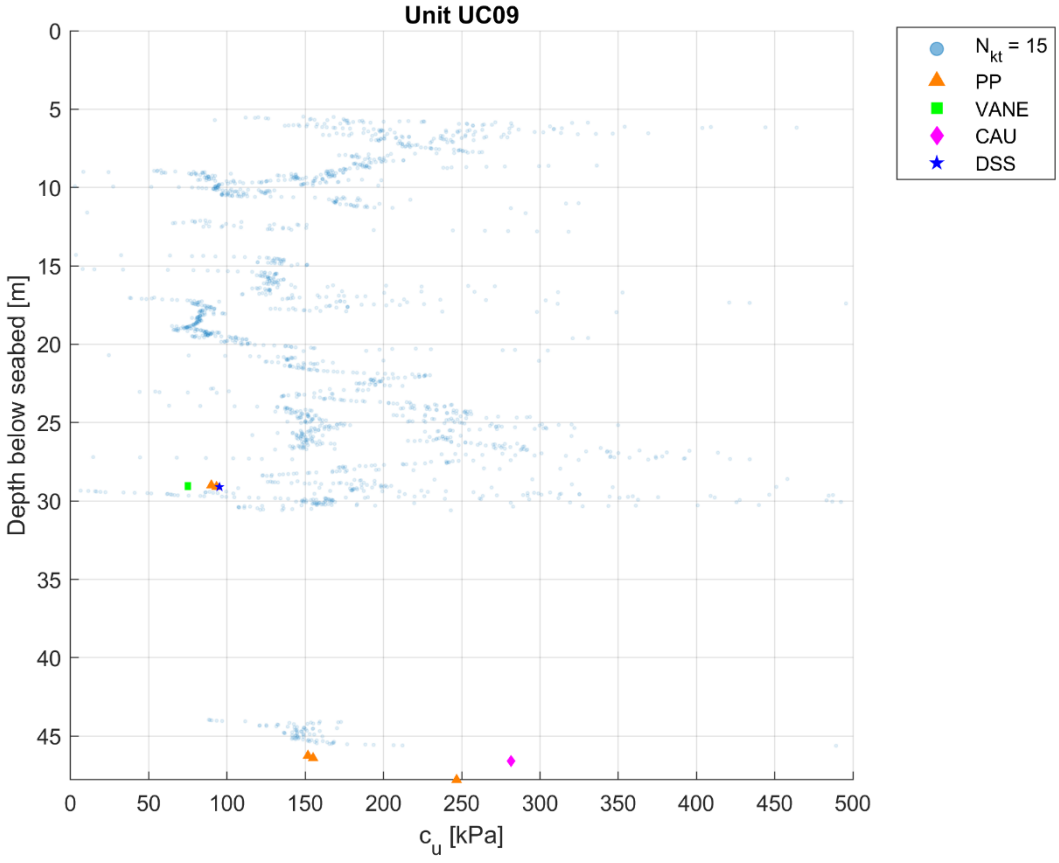
Unit UC09
Depth below seabed [m]
c_u [kPa]
N_{kt} = 15
PP
VANE
CAU
DSS

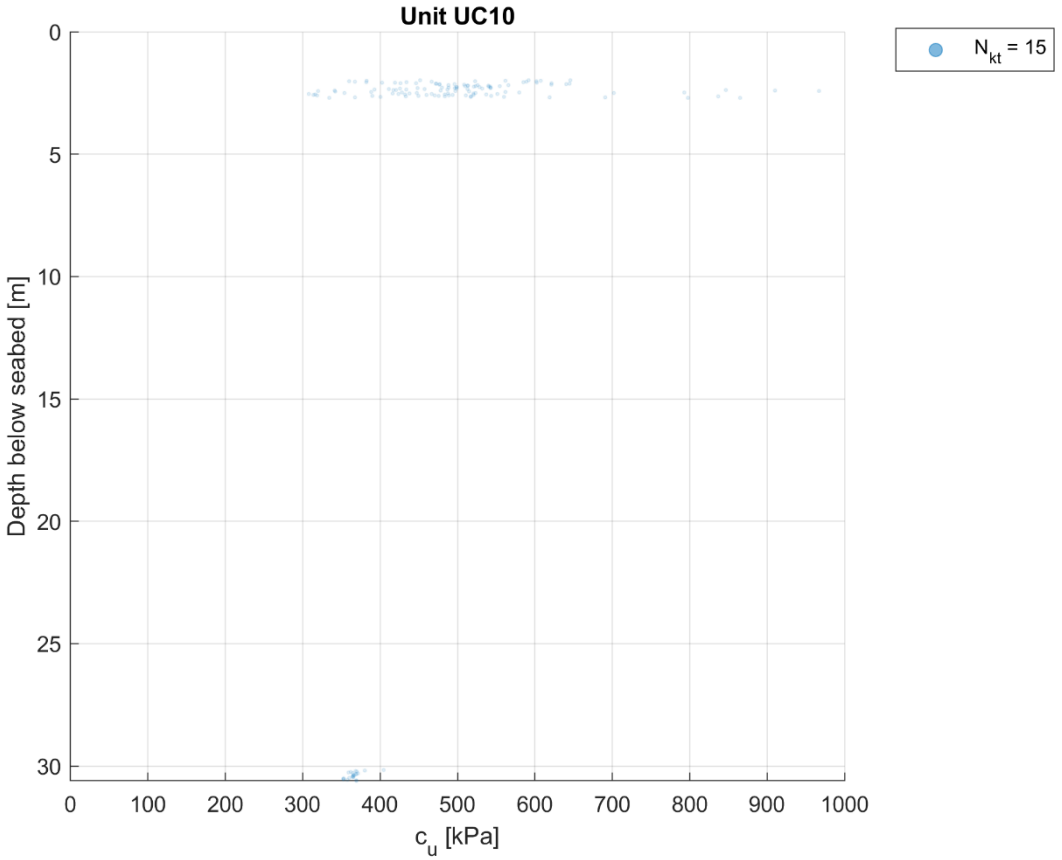
Unit UC10
Depth below seabed [m]
0
5
10
15
20
25
30
0
100
200
300
400
500
600
700
800
900
1000
c_u [kPa]
N_kt = 15

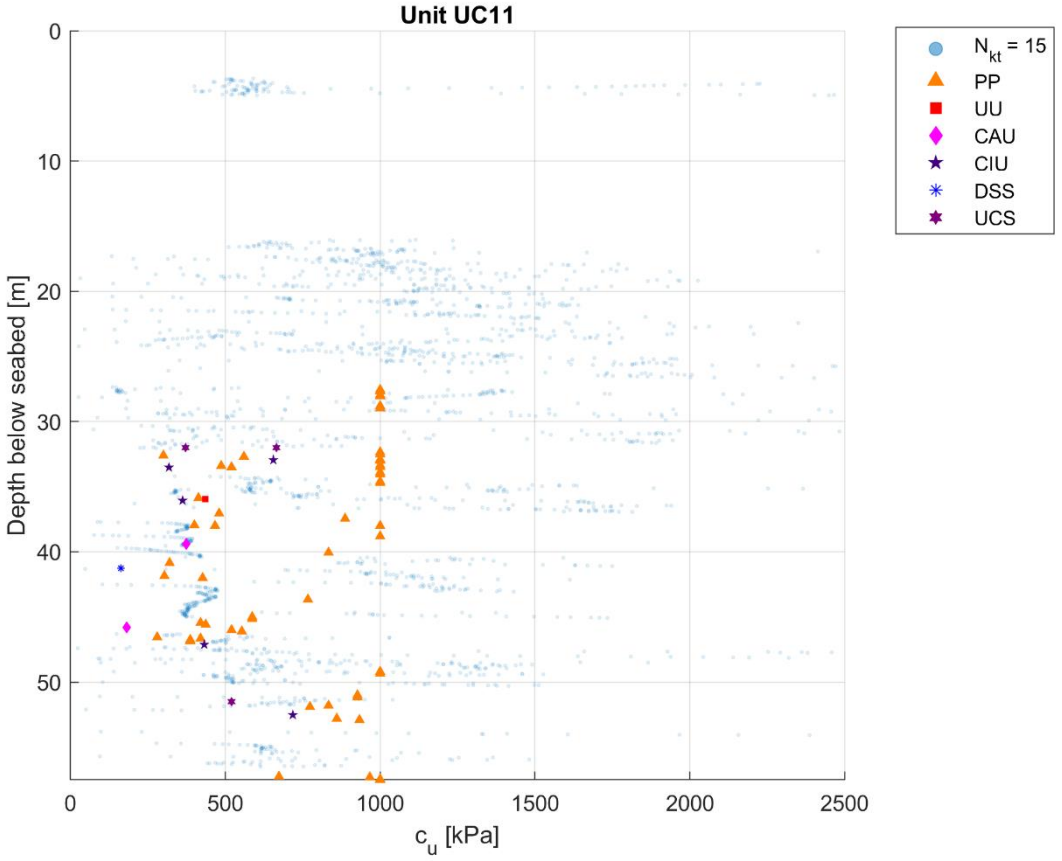
Unit UC11
Depth below seabed [m]
0
10
20
30
40
50
0
500
1000
1500
2000
2500
c_u [kPa]
N_kt = 15
PP
UU
CAU
CIU
DSS
UCS

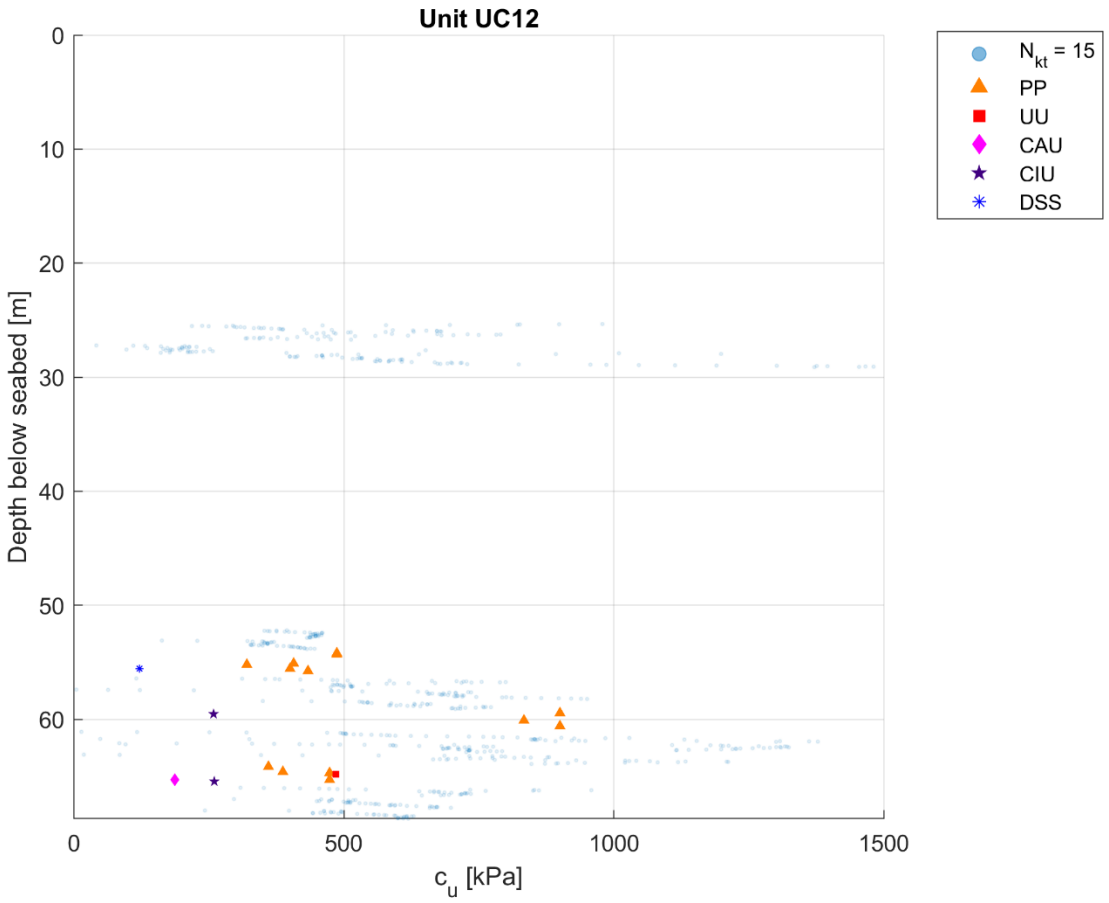
Unit UC12
Depth below seabed [m]
0
10
20
30
40
50
60
0
500
1000
1500
c_u [kPa]
N_kt = 15
PP
UU
CAU
CIU
DSS

D.5 Small-strain shear modulus

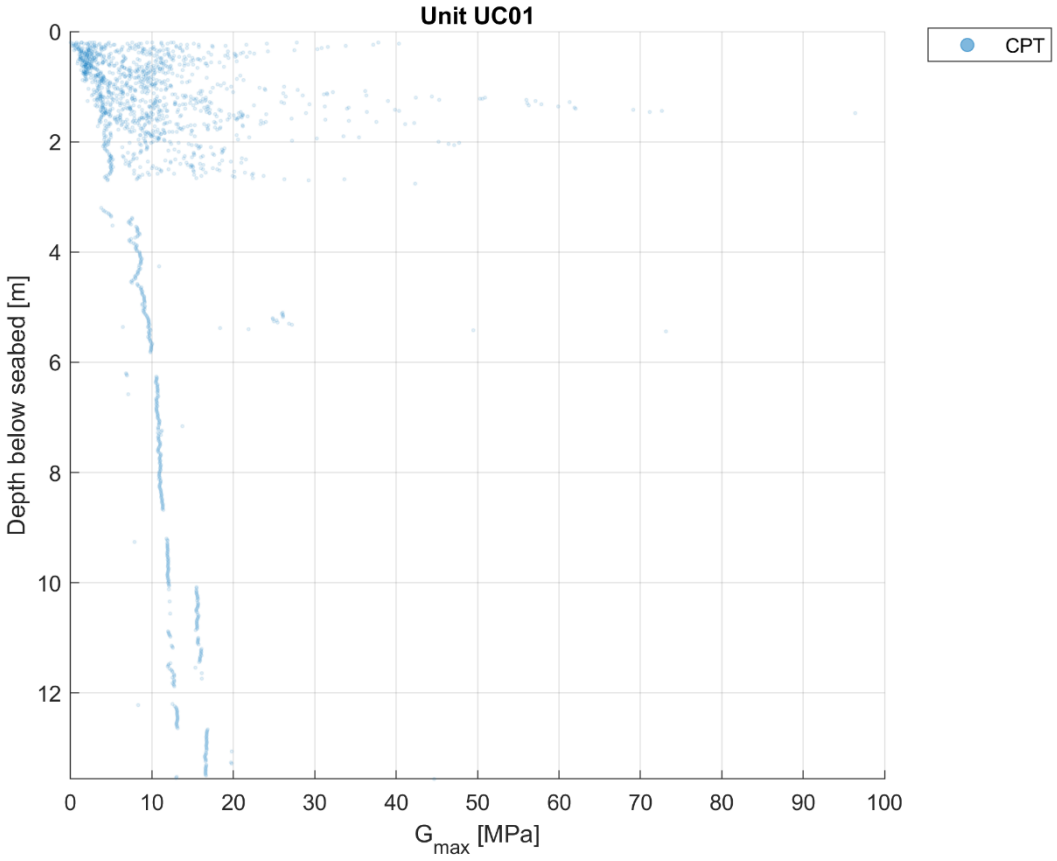

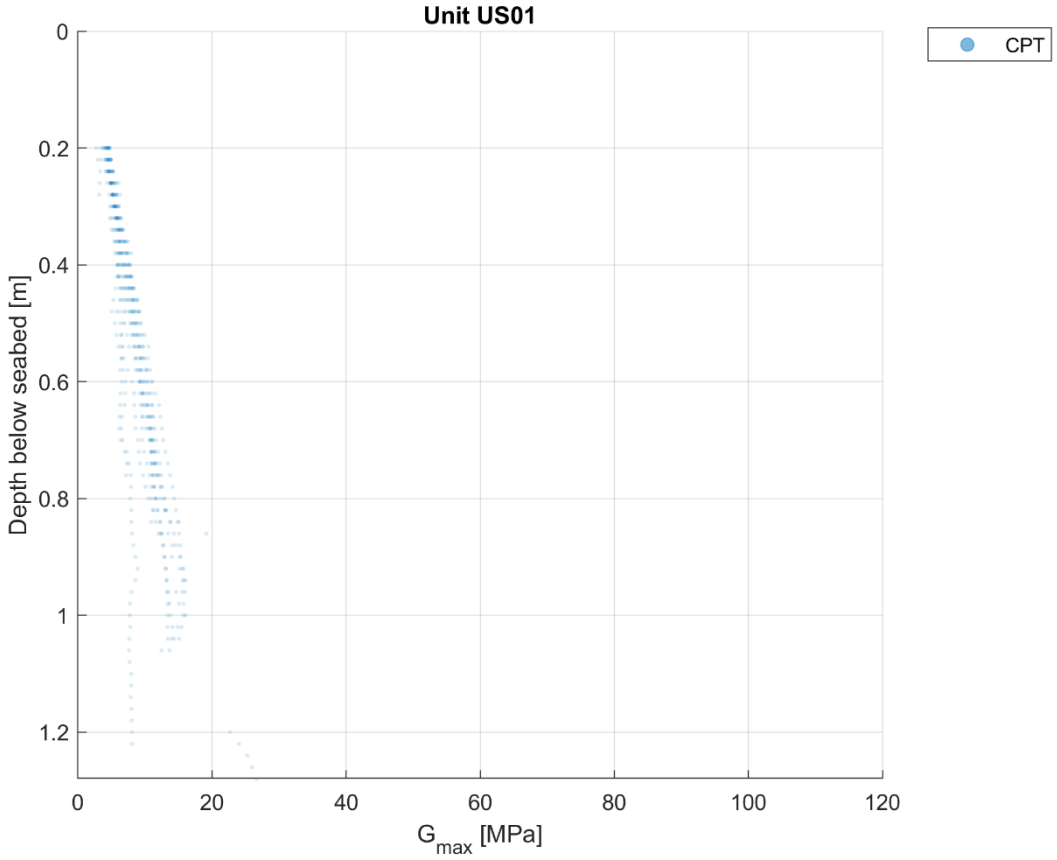

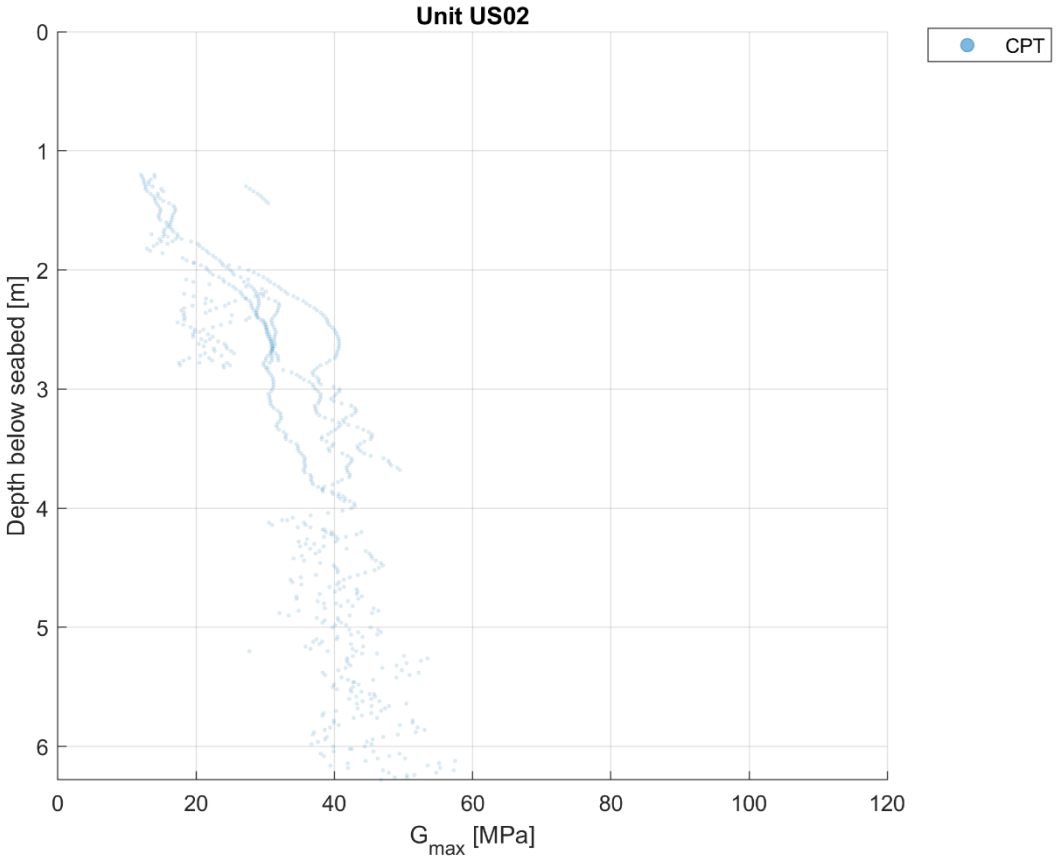
Unit US02
CPT
Depth below seabed [m]
0
1
2
3
4
5
6
0
20
40
60
80
100
120
G max [MPa]

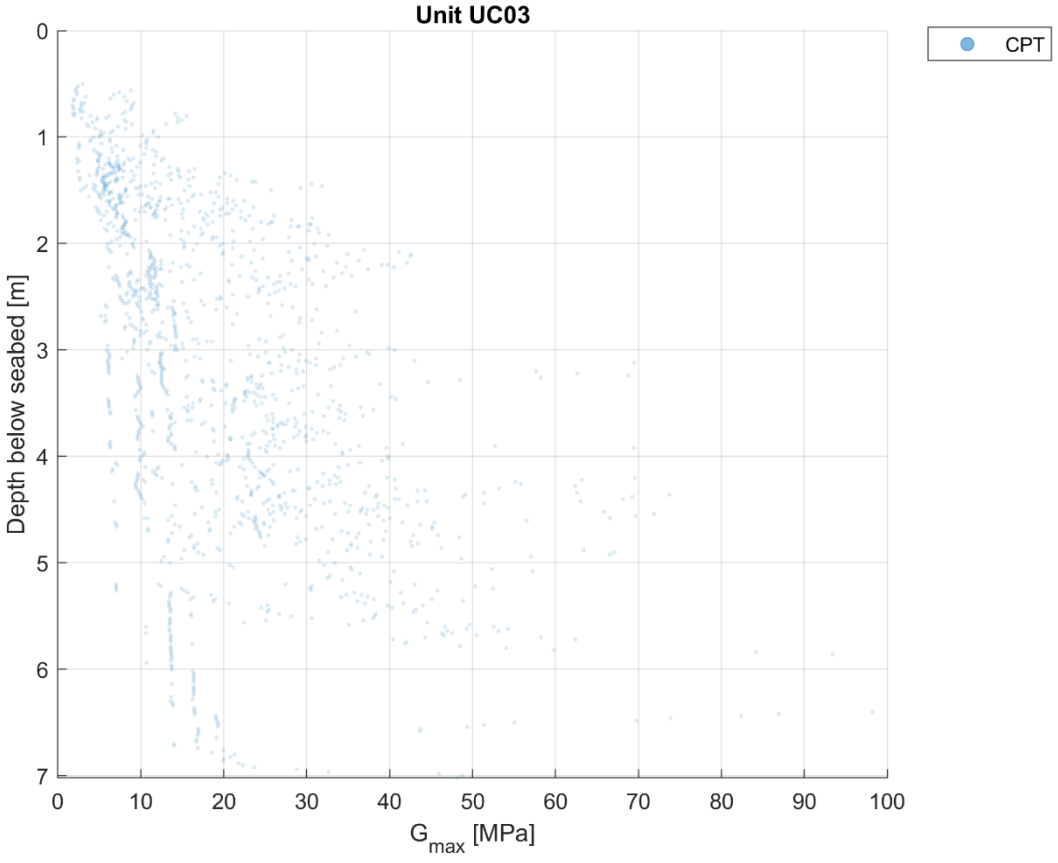
Unit UC03
CPT
Depth below seabed [m]
0
1
2
3
4
5
6
7
0
10
20
30
40
50
60
70
80
90
100
G max [MPa]

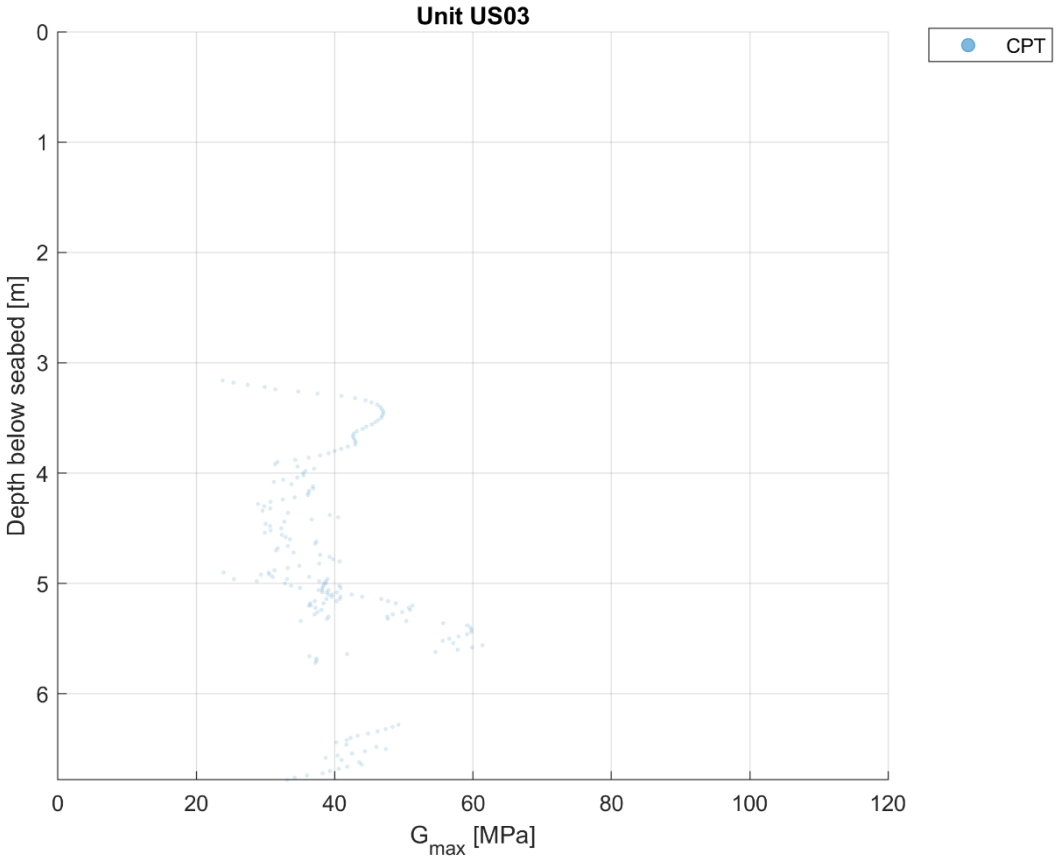
Unit US03
CPT
Depth below seabed [m]
0
1
2
3
4
5
6
0
20
40
60
80
100
120
G_{max} [MPa]

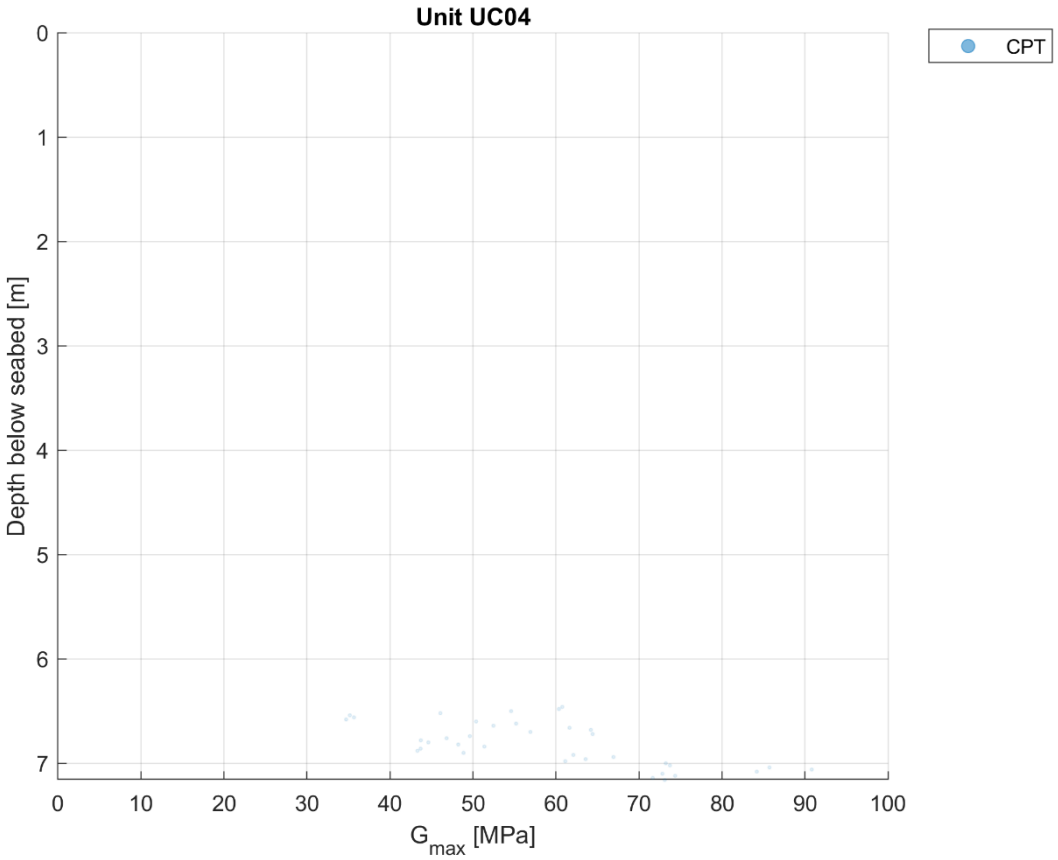
Unit UC04
CPT
Depth below seabed [m]
0
1
2
3
4
5
6
7
0
10
20
30
40
50
60
70
80
90
100
G_{max} [MPa]

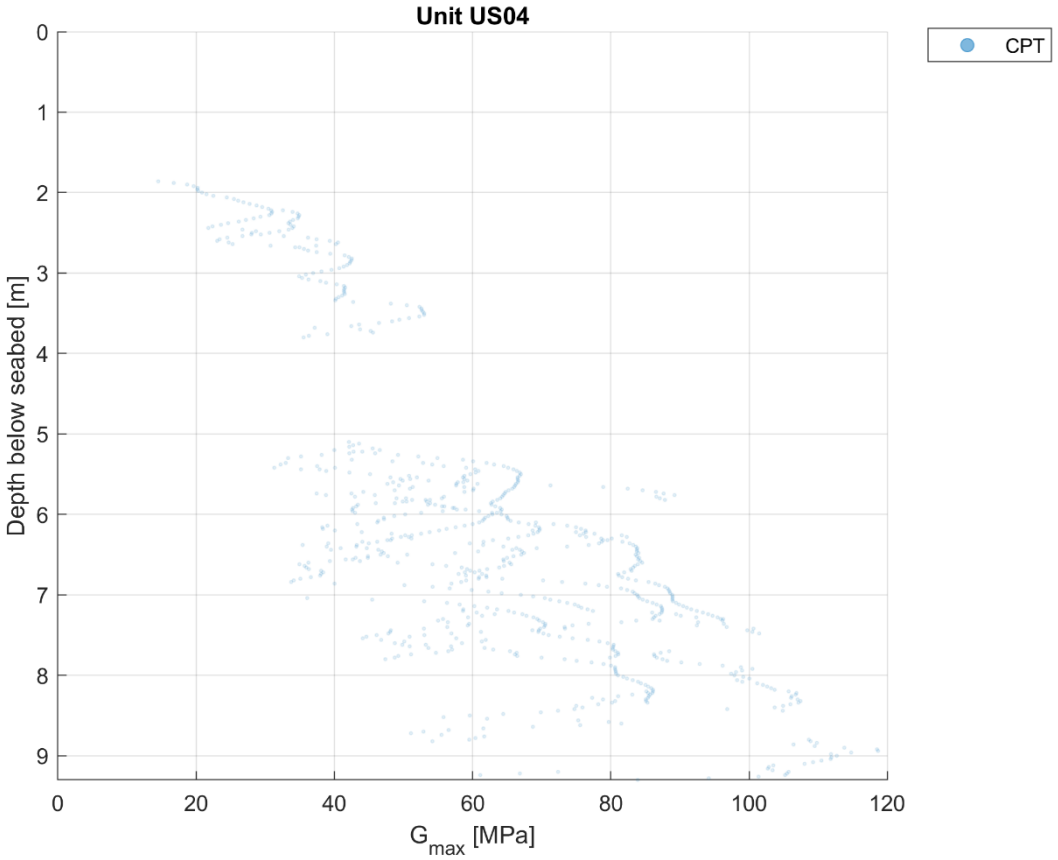
Unit US04
CPT
Depth below seabed [m]
0
1
2
3
4
5
6
7
8
9
0
20
40
60
80
100
120
G max [MPa]

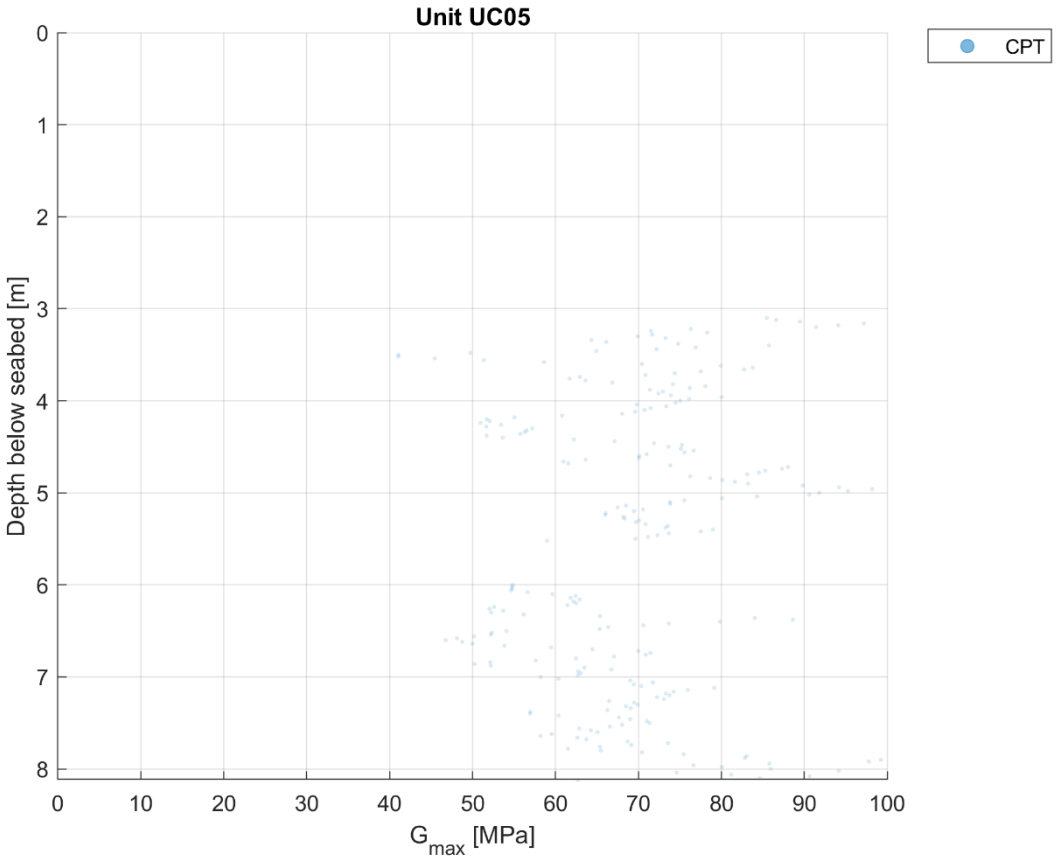
Unit UC05
CPT
Depth below seabed [m]
0
1
2
3
4
5
6
7
8
0
10
20
30
40
50
60
70
80
90
100
G max [MPa]

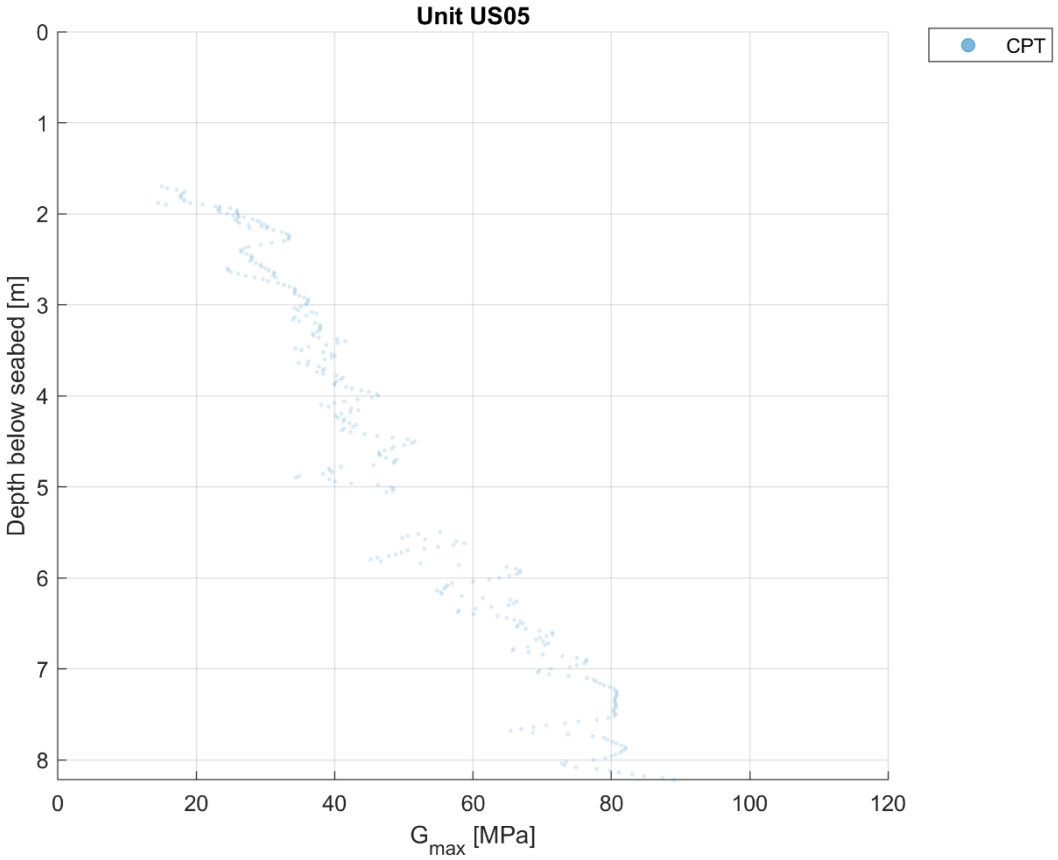
Unit US05
CPT
Depth below seabed [m]
0
1
2
3
4
5
6
7
8
0
20
40
60
80
100
120
G max [MPa]

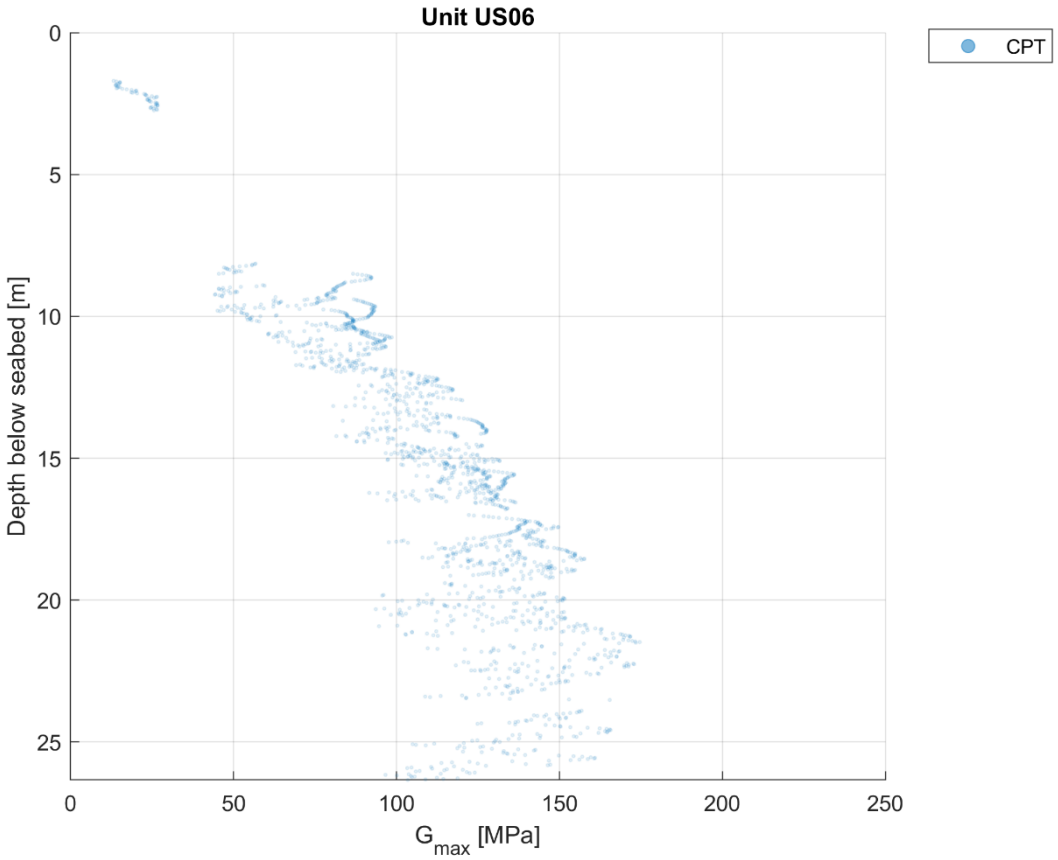
Unit US06
CPT
Depth below seabed [m]
0
5
10
15
20
25
0
50
100
150
200
250
G max [MPa]

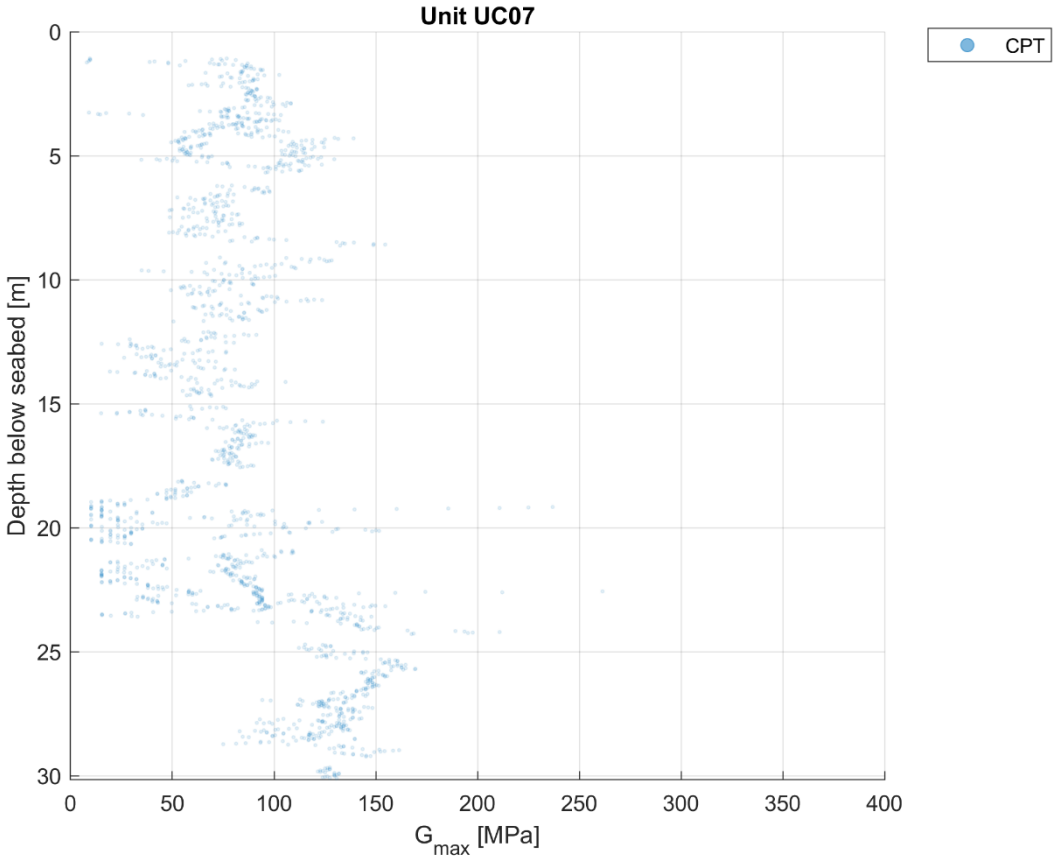
Unit UC07
CPT
Depth below seabed [m]
0
5
10
15
20
25
30
0
50
100
150
200
250
300
350
400
G_{max} [MPa]

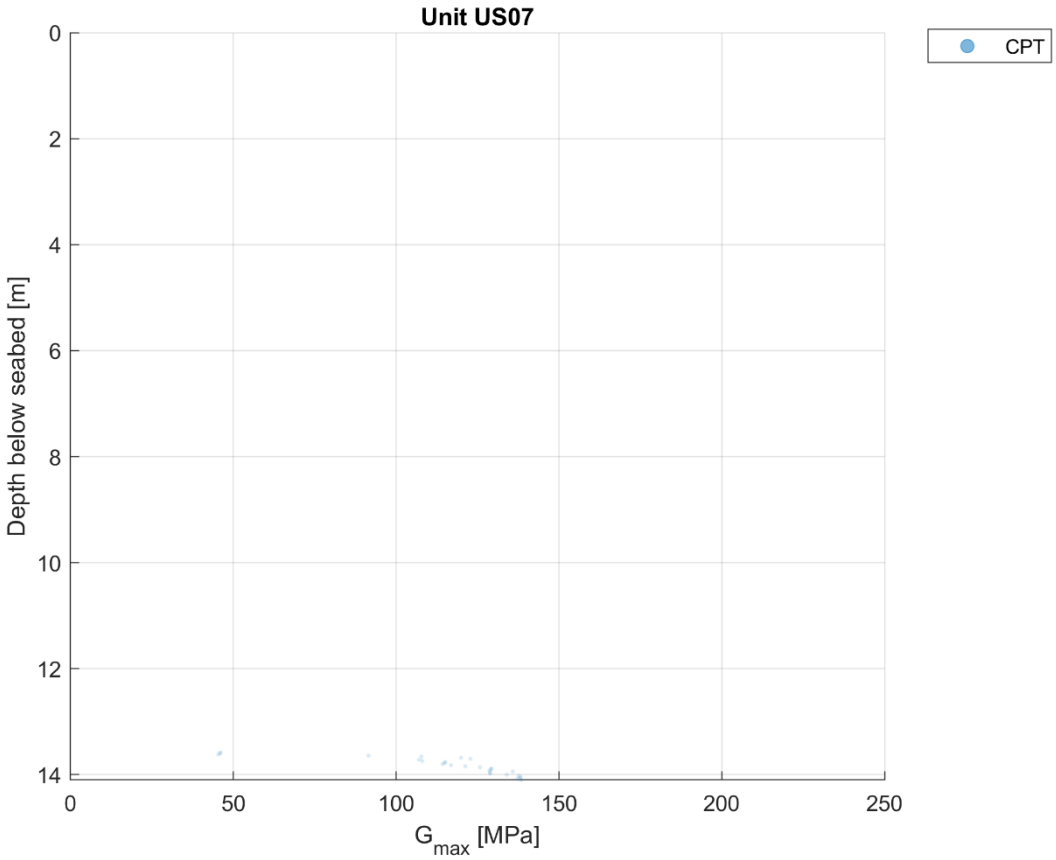
Unit US07
CPT
Depth below seabed [m]
0
2
4
6
8
10
12
14
0
50
100
150
200
250
G_{max} [MPa]

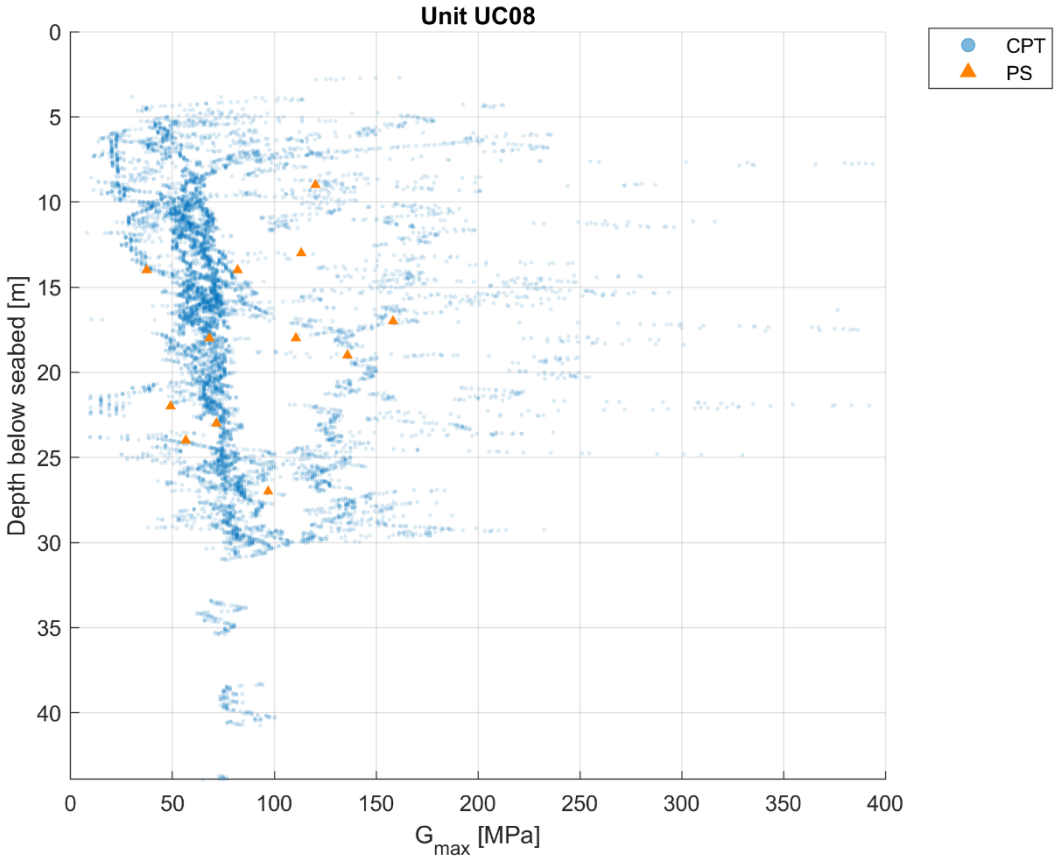
Unit UC08
CPT
PS
Depth below seabed [m]
0
5
10
15
20
25
30
35
40
0
50
100
150
200
250
300
350
400
G max [MPa]

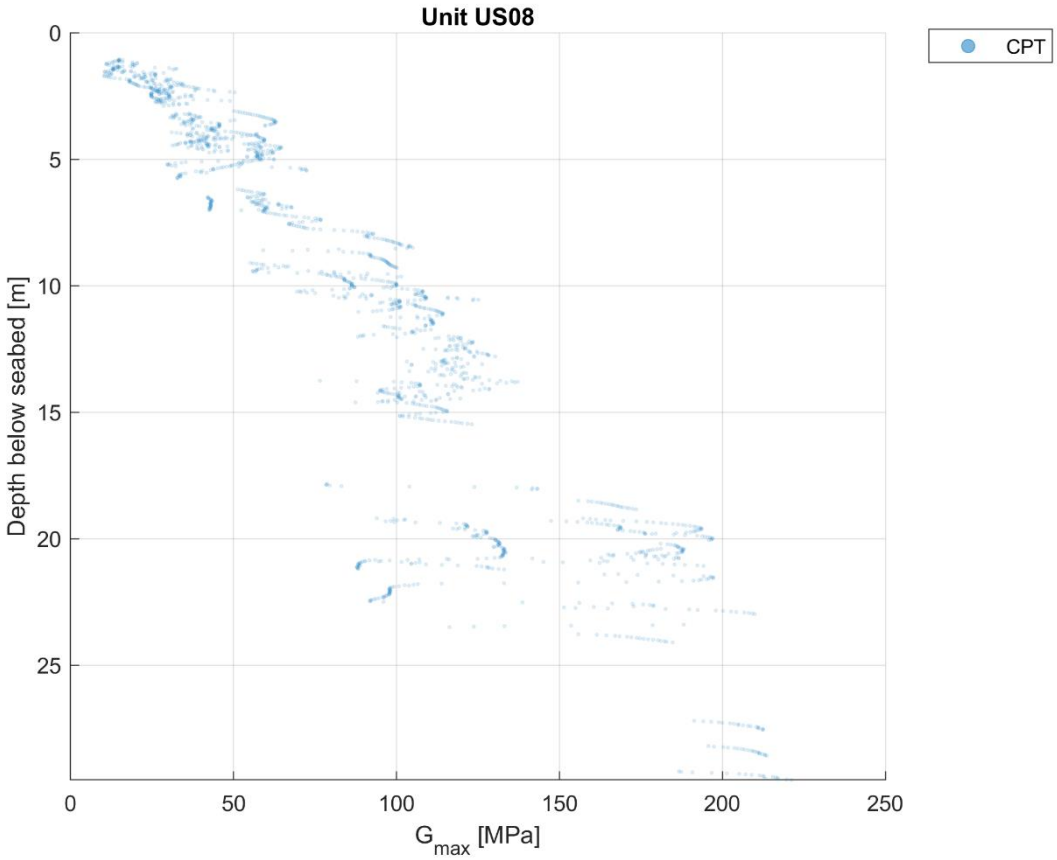
Unit US08
CPT
Depth below seabed [m]
0
5
10
15
20
25
0
50
100
150
200
250
G max [MPa]

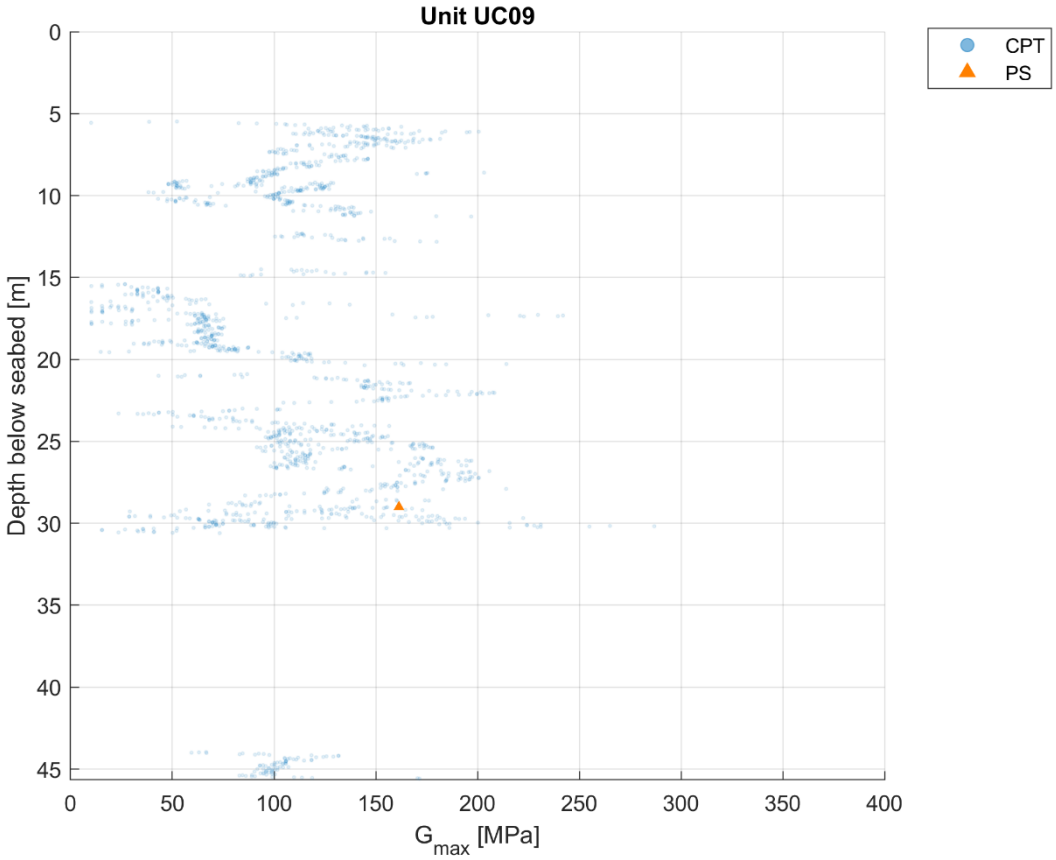
Unit UC09
CPT
PS
Depth below seabed [m]
0
5
10
15
20
25
30
35
40
45
0
50
100
150
200
250
300
350
400
G_{max} [MPa]

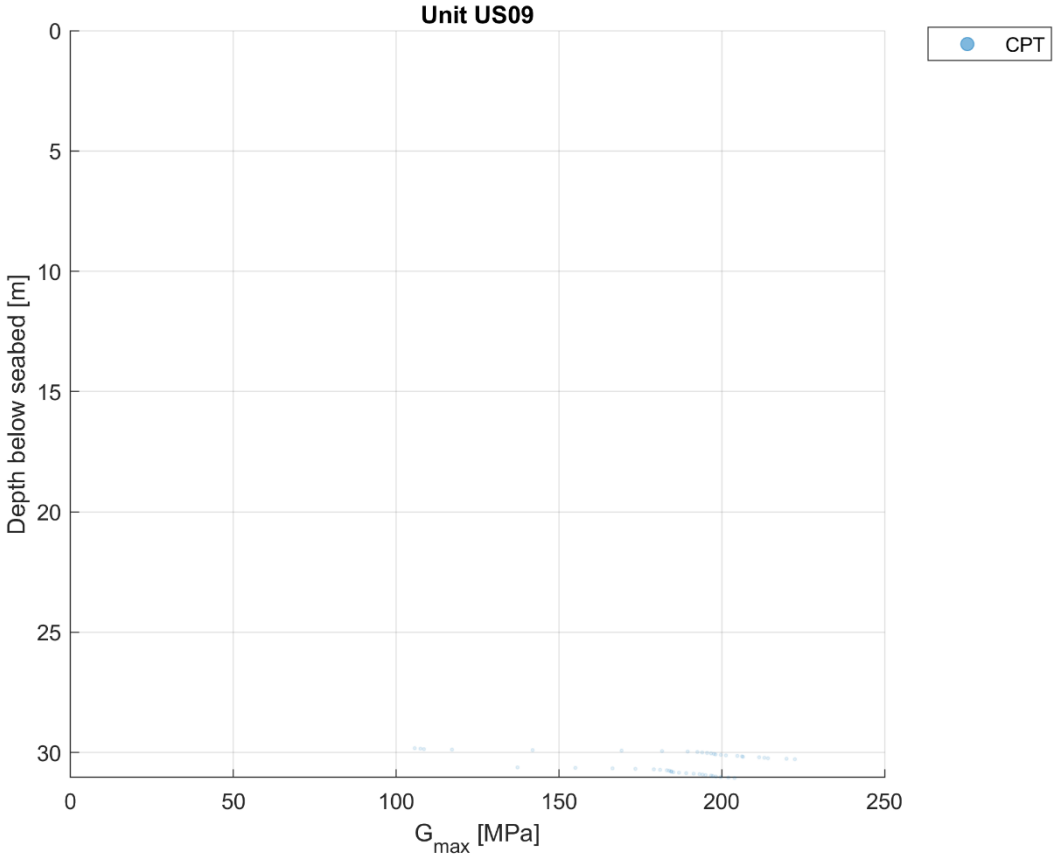
Unit US09
CPT
Depth below seabed [m]
0
5
10
15
20
25
30
0
50
100
150
200
250
G_{max} [MPa]

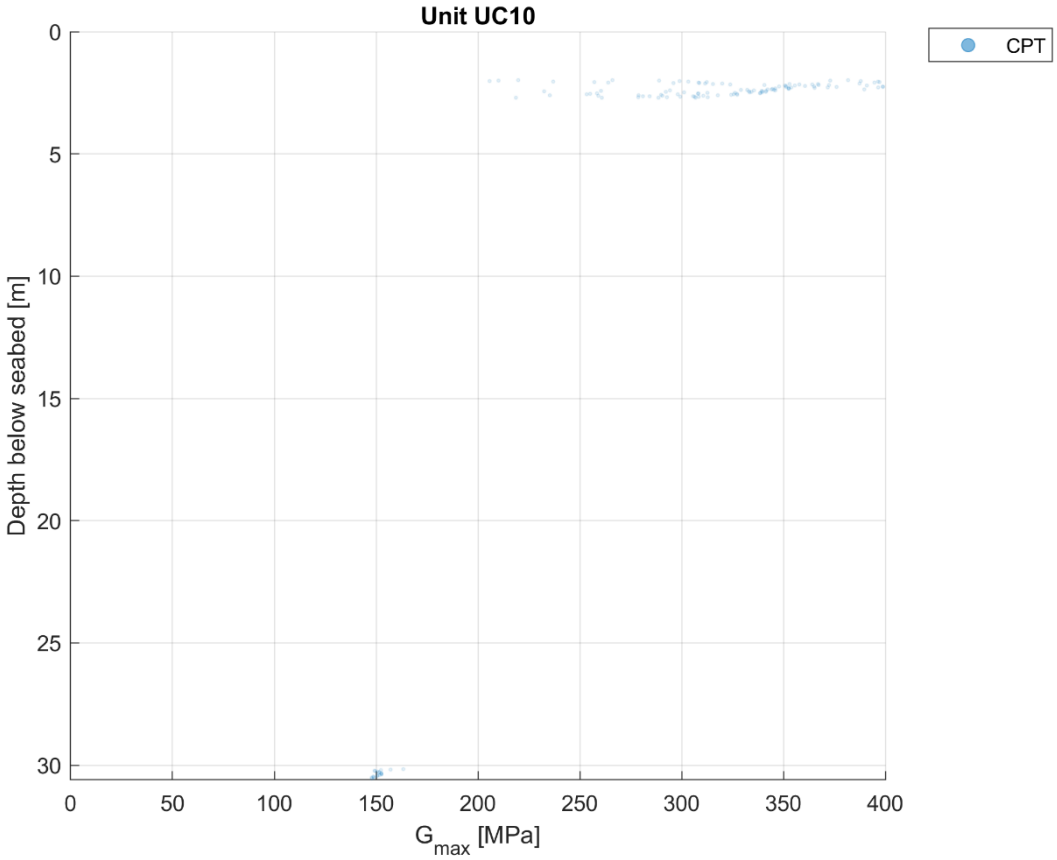
Unit UC10
CPT
Depth below seabed [m]
0
5
10
15
20
25
30
0
50
100
150
200
250
300
350
400
G_{max} [MPa]

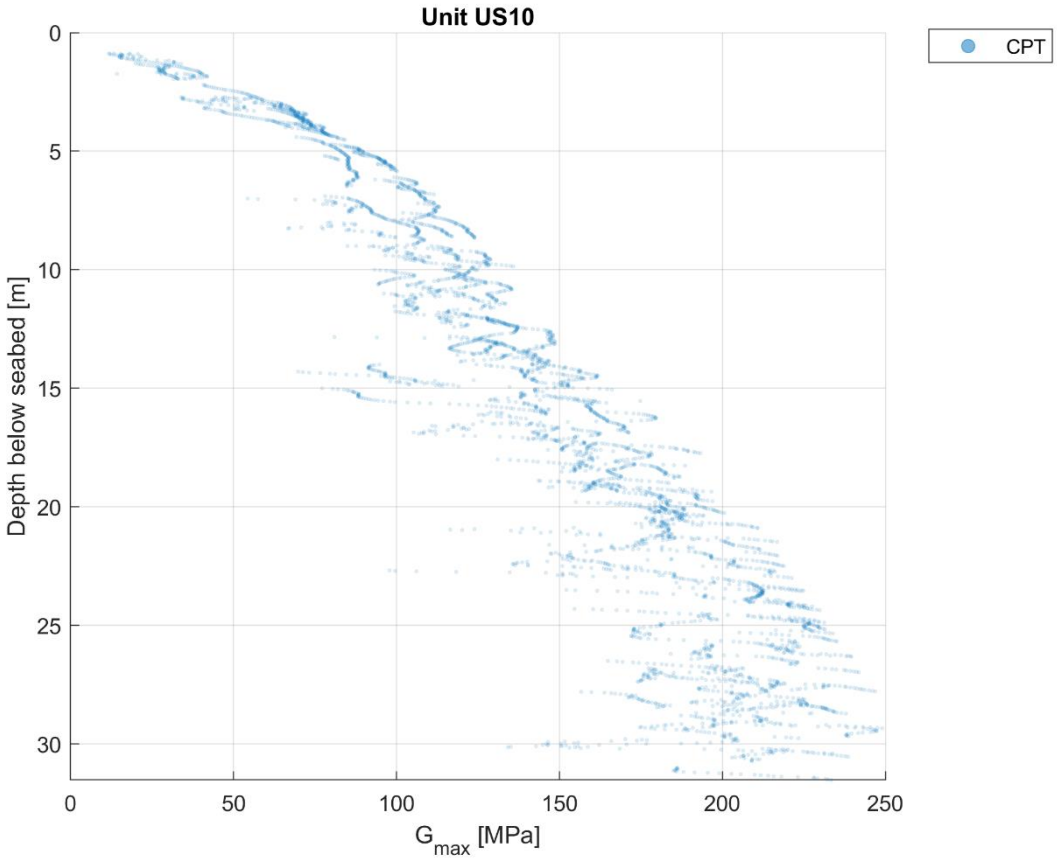
Unit US10
CPT
Depth below seabed [m]
0
5
10
15
20
25
30
0
50
100
150
200
250
G_{max} [MPa]

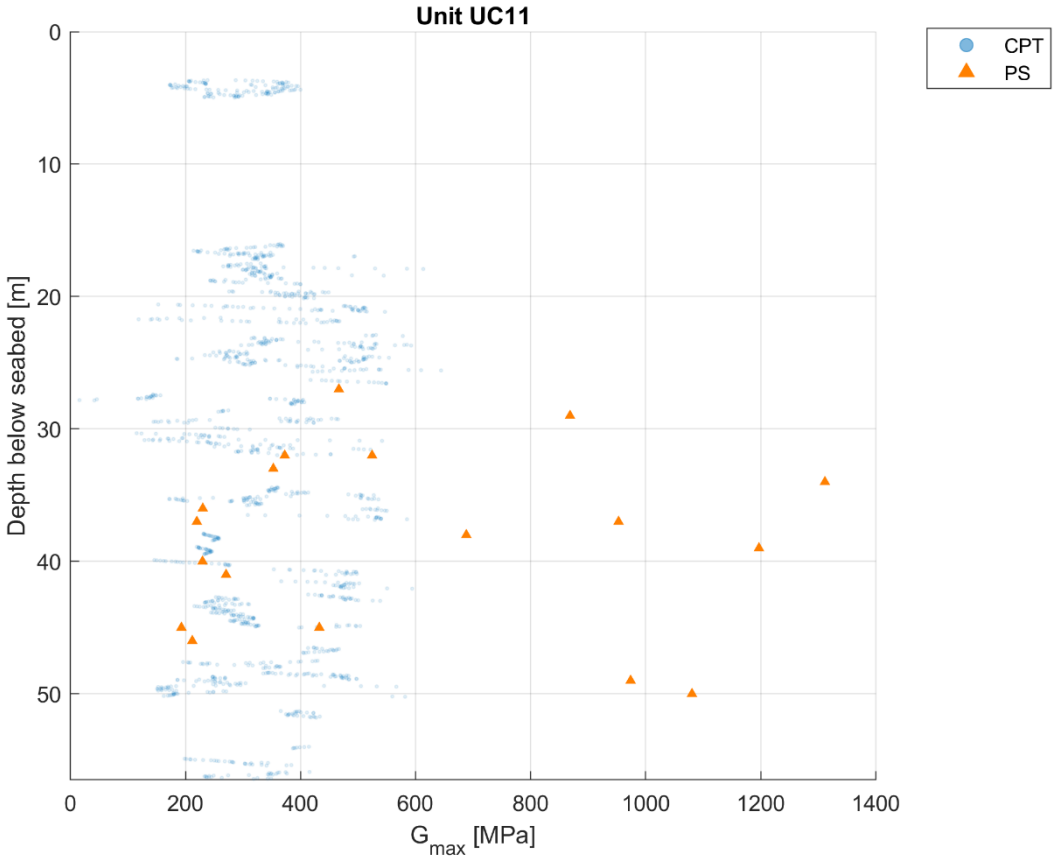
Unit UC11
CPT
PS
Depth below seabed [m]
0
10
20
30
40
50
0
200
400
600
800
1000
1200
1400
G max [MPa]

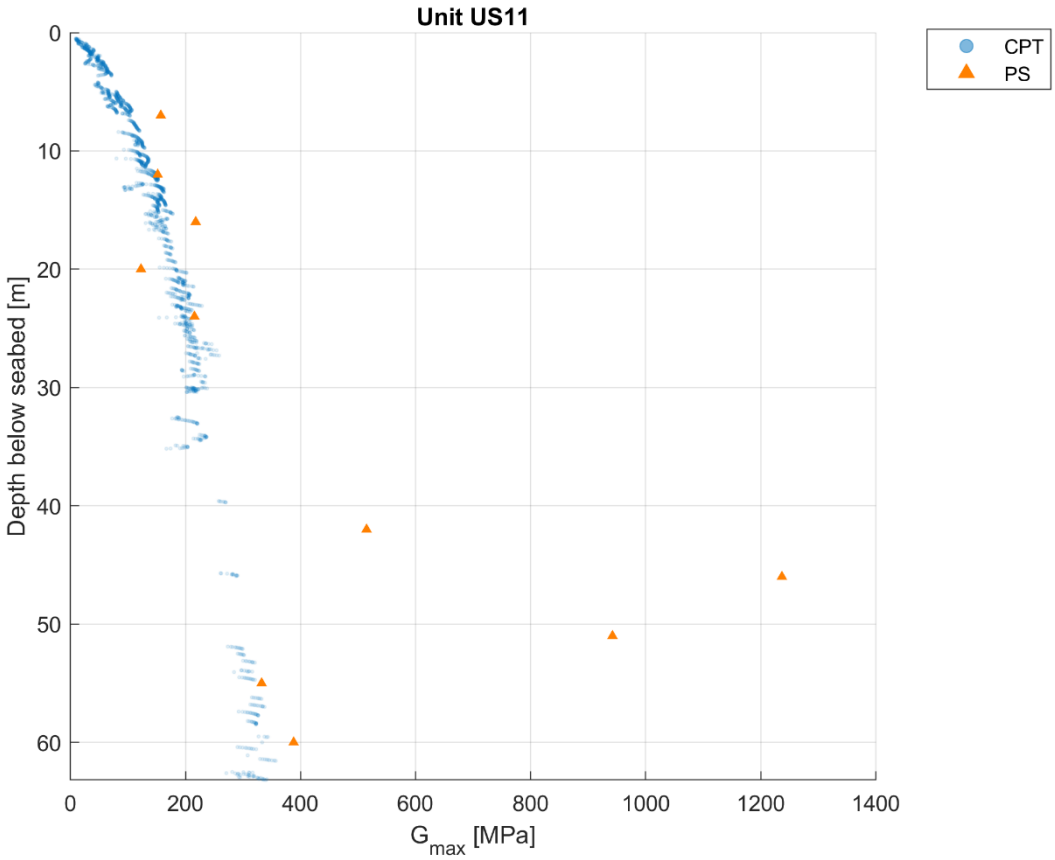
Unit US11
CPT
PS
Depth below seabed [m]
0
10
20
30
40
50
60
0
200
400
600
800
1000
1200
1400
G max [MPa]

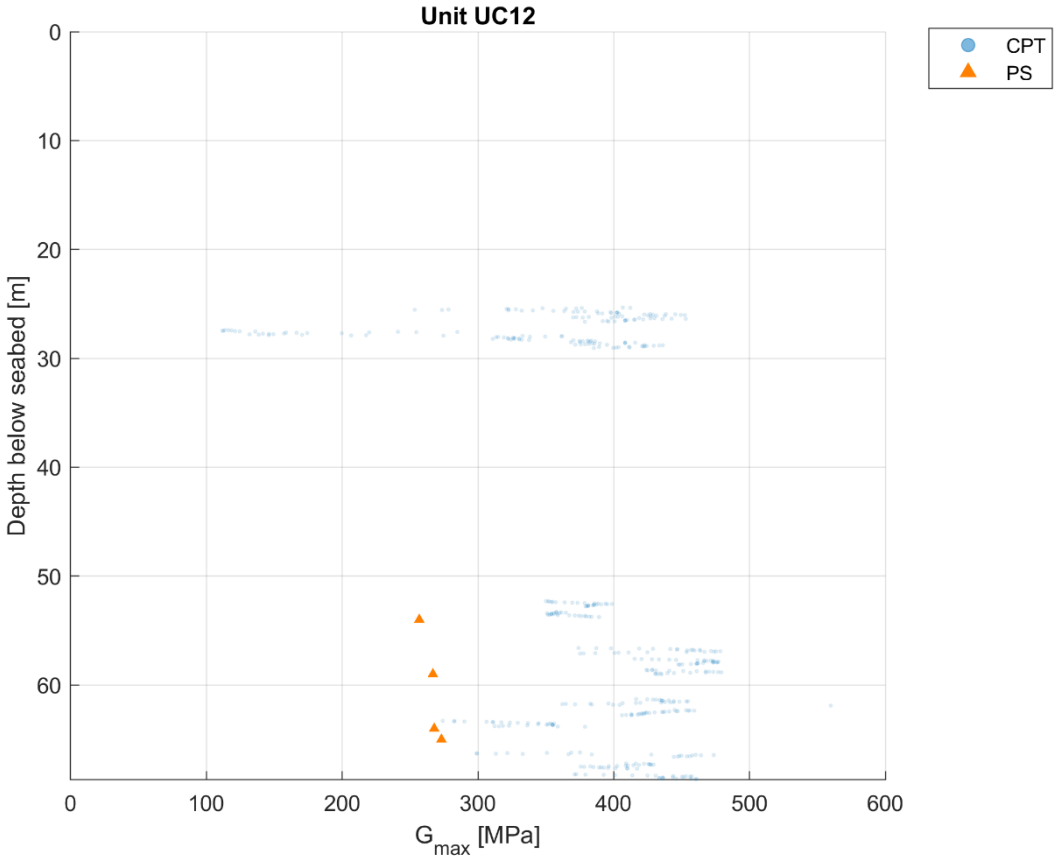
Unit UC12
CPT
PS
Depth below seabed [m]
0
10
20
30
40
50
60
0
100
200
300
400
500
600
G max [MPa]

Appendix E Cone factor assessment

To derive undrained shear strength properties from the CPT measurements, a high-level assessment is performed to determine a cone factor, N_{kt}, to be used for correlating the CPT to undrained shear strength, where a factor of 15 is found representative.

The N_{kt} factor is selected from visual inspections and engineering judgement on which value suits best for fitting the data. Below figures present the assessment for N_{kt} values of 10, 15, 20 and 25 for units where laboratory tests being of the considered types used for calibration is available.

Below figures contain of two subplots. The left subplot shows the correlation between CPT derived values and laboratory values. The CPT values are determined with specified N_{kt} value and considering measurements within ±25 cm of the test sample depth. The blue line presents the best linear fit to the measurements, while the black line presents one-to-one values between laboratory values and CPT correlated values, hence scatter located above the line represent values determined from CPT correlation is higher than comparable test value from laboratory test, and values below the line represent values from laboratory testing results are higher than comparable values from CPT correlation. The right subplot presents the difference between laboratory tests and derived parameter from CPT correlation with respect to depth.

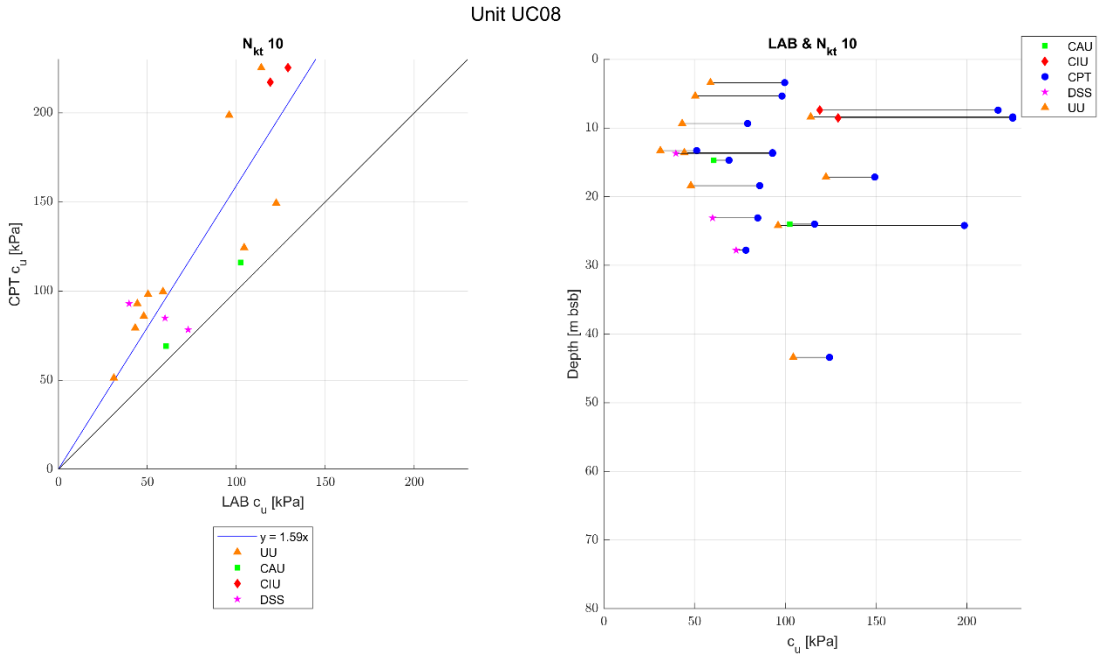

Unit UC08

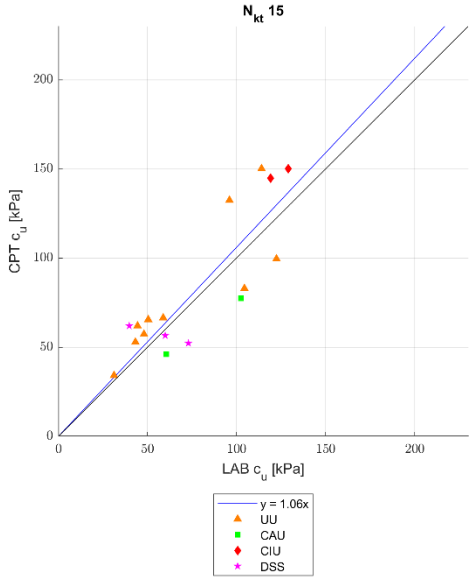

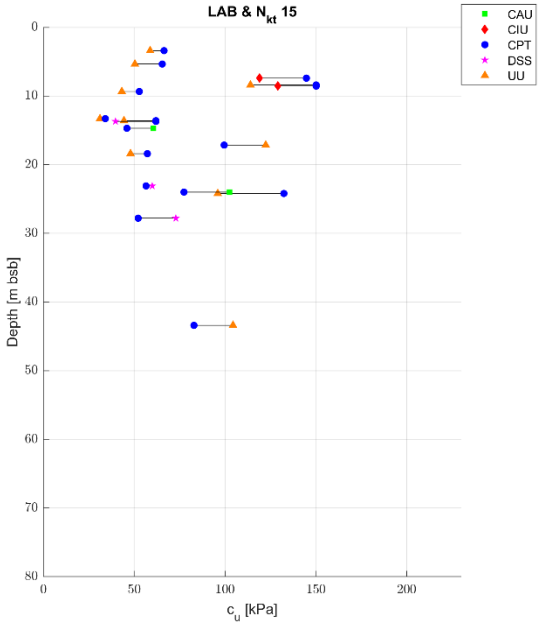

Unit UC08

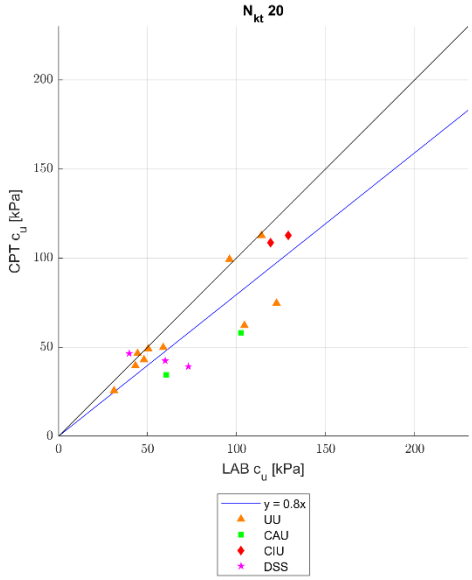

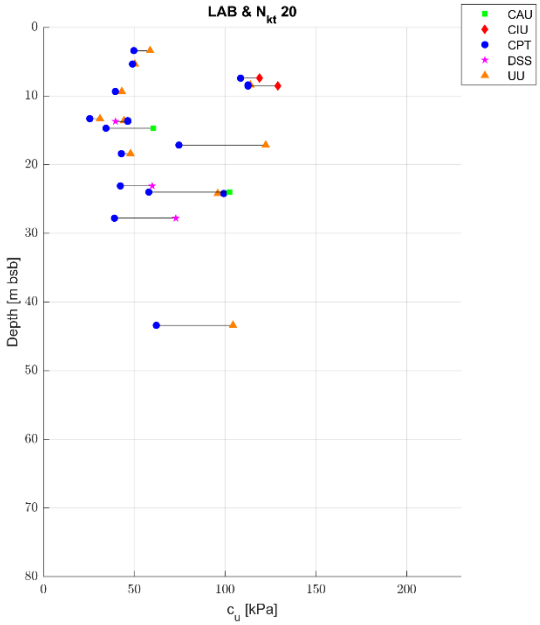

Unit UC08

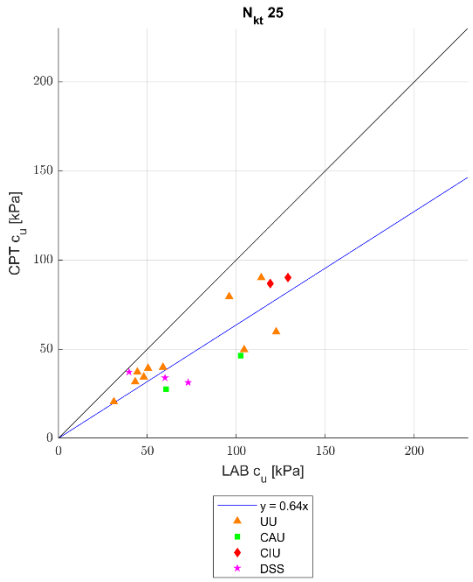

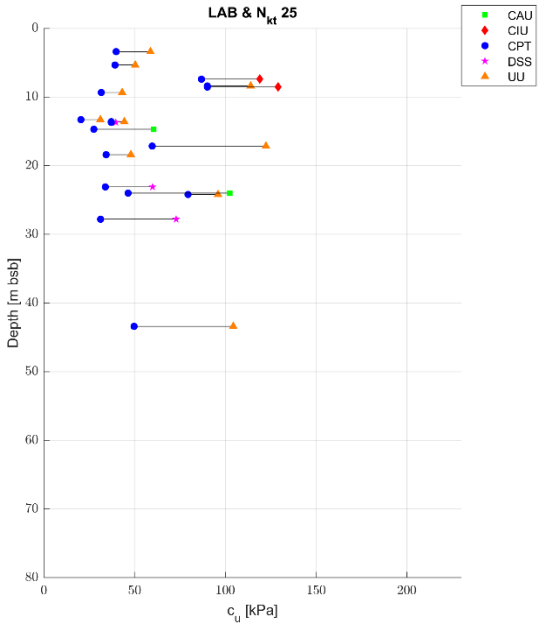

Unit UC09

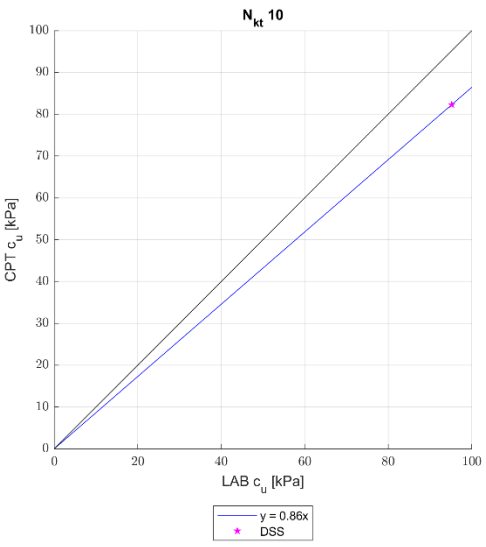

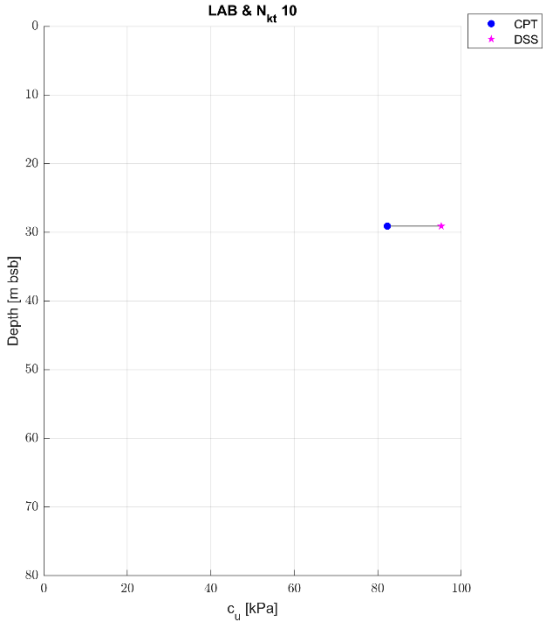

Unit UC09

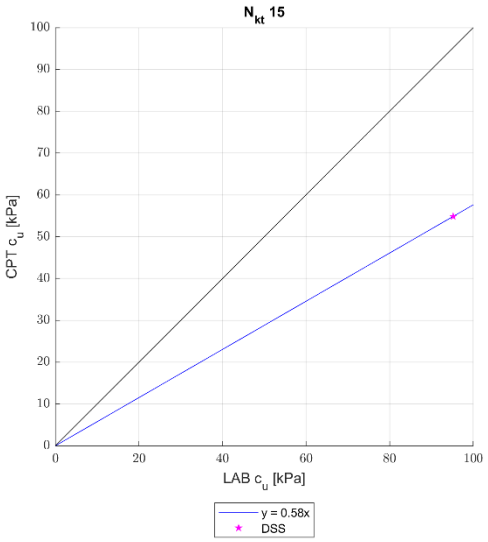

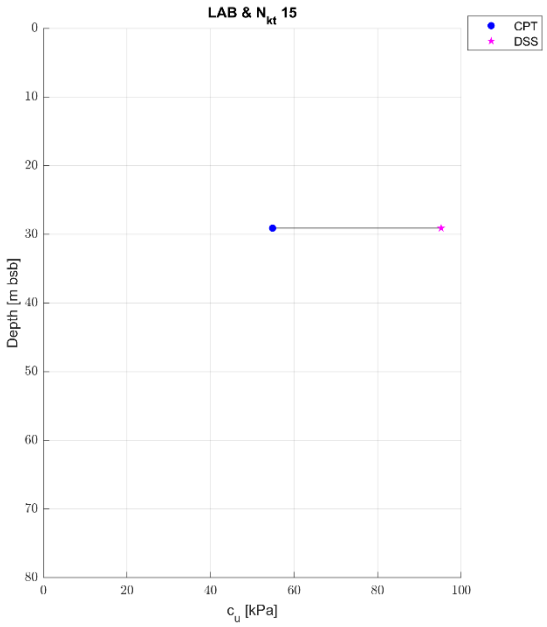

Unit UC09

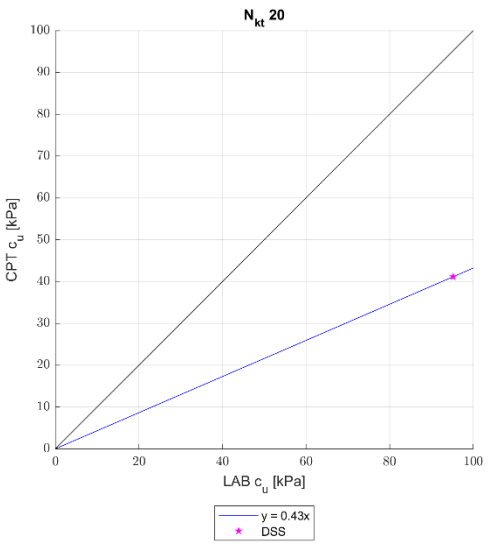

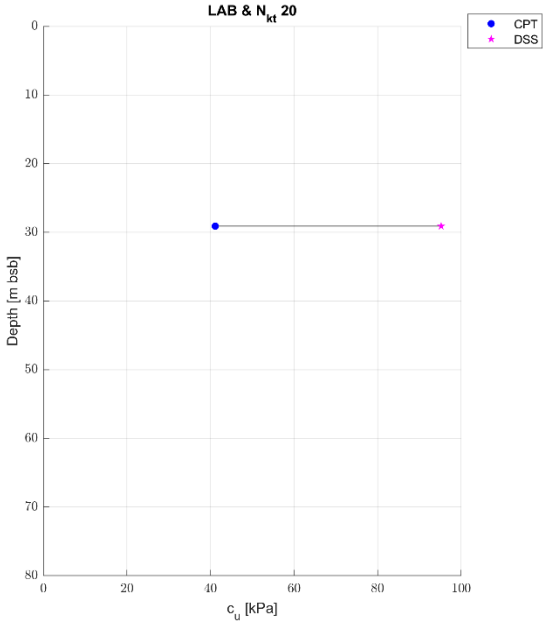

Unit UC09

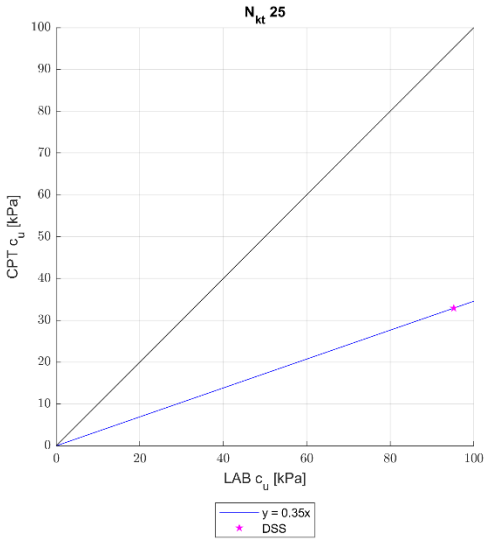

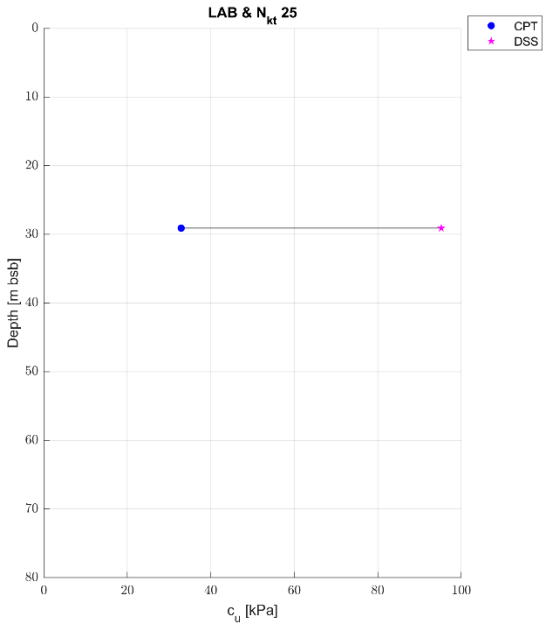

Unit UC11

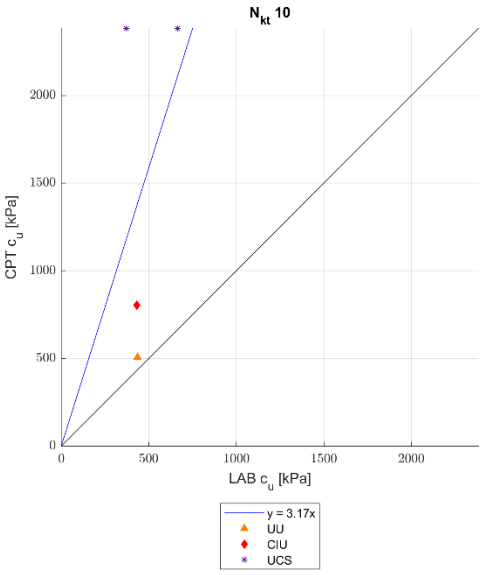

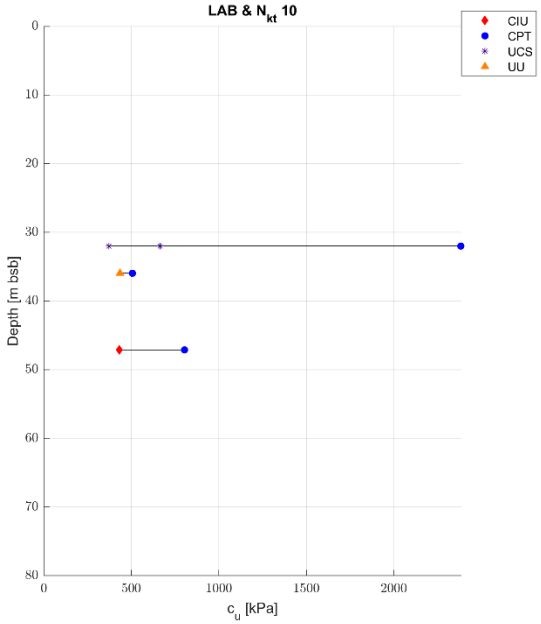

Unit UC11

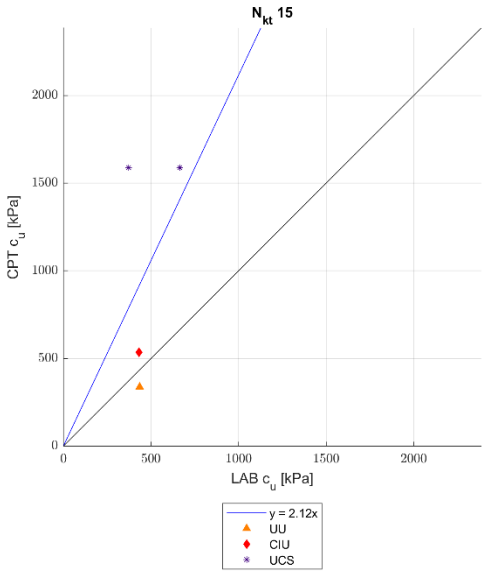

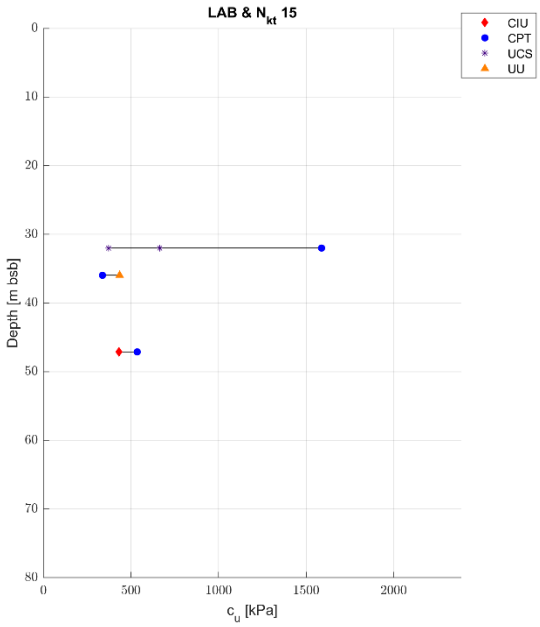

Unit UC11

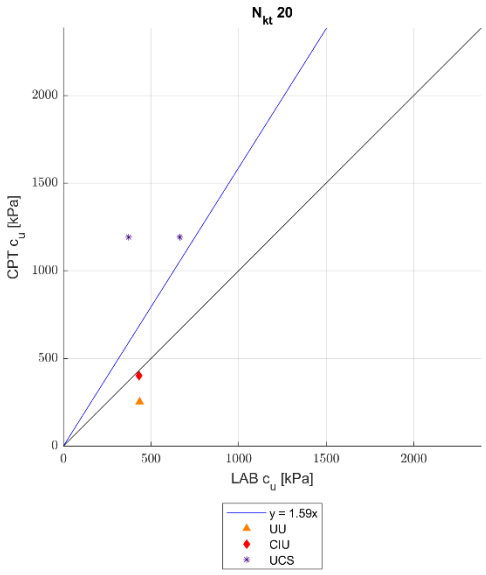

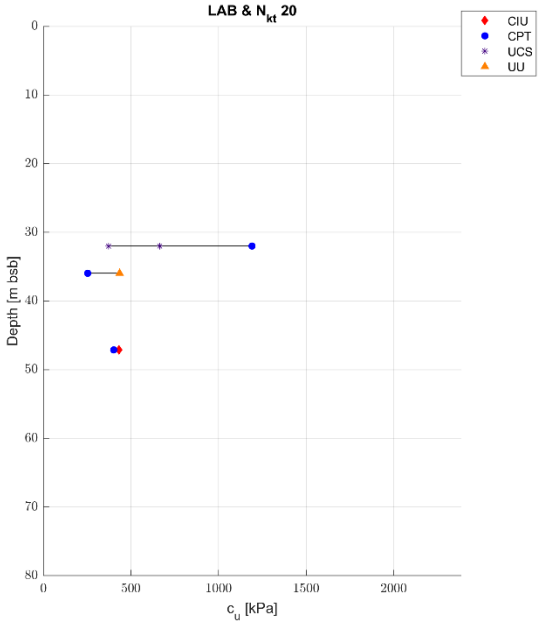

Unit UC11

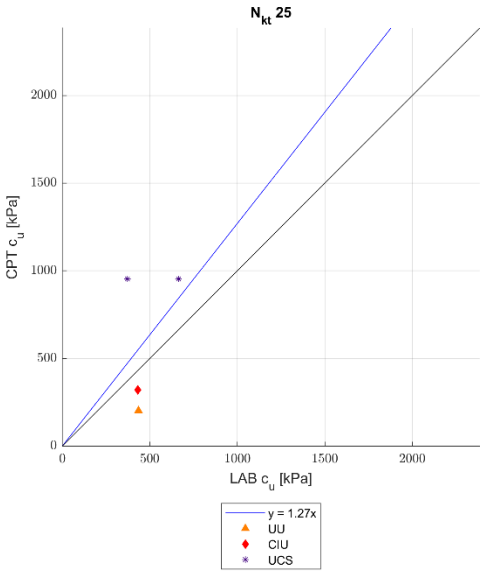
N_kt 25
CPT c_u [kPa]
LAB c_u [kPa]
y = 1.27x
UU
CIU
UCS

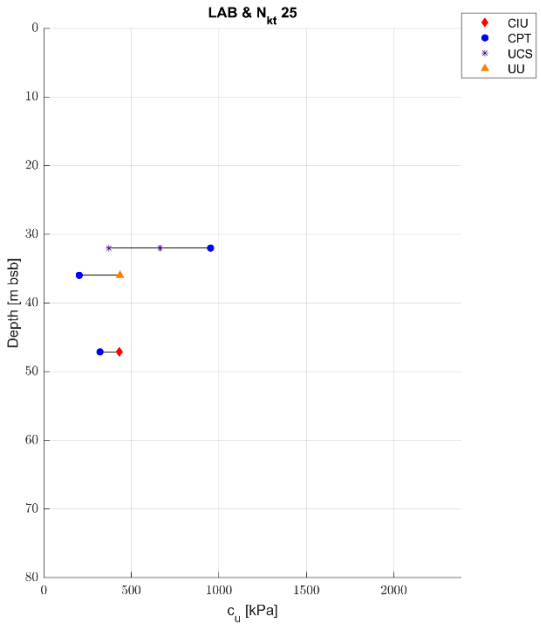
LAB & N_kt 25
Depth [m bsb]
c_u [kPa]
CIU
CPT
UCS
UU

Appendix F Range of soil properties per soil unit

This appendix presents the range of soil properties per geotechnical unit. The values presented are in the format:

min / max / average / standard deviation (number of tests)

Standard deviation is calculated based on sample size formulation and is not determined when only one (1) test is available.

Table F-1 Statistical overview of the strength parameter undrained shear strength per geotechnical unit based on available laboratory tests. Note, that the geotechnical units are based on CPT measurements and geophysical data. Hence, some test results are also given for sand units (i.e., tests performed on clayey/silty specimens present within a sand unit).

Geotechnical unit	Undrained shear strength [kPa]						
	DSS	CAU	CIU	UU	UCS	PP	Vane
UC01	-/-/-/- (0)	-/-/-/- (0)	-/-/-/- (0)	-/-/-/- (0)	-/-/-/- (0)	-/-/-/- (0)	10/14/11.5/1.7 (4)
UC03	-/-/-/- (0)	-/-/-/- (0)	-/-/-/- (0)	-/-/-/- (0)	-/-/-/- (0)	-/-/-/- (0)	11.9/12.4/12.2/0.4 (2)
UC04	-/-/-/- (0)	-/-/-/- (0)	-/-/-/- (0)	-/-/-/- (0)	-/-/-/- (0)	-/-/-/- (0)	-/-/-/- (0)
UC05	-/-/-/- (0)	-/-/-/- (0)	-/-/-/- (0)	-/-/-/- (0)	-/-/-/- (0)	-/-/-/- (0)	-/-/-/- (0)
UC07	-/-/-/- (0)	-/-/-/- (0)	-/-/-/- (0)	-/-/-/- (0)	-/-/-/- (0)	-/-/-/- (0)	-/-/-/- (0)
UC08	17.8/100.4/48.2/24.6 (10)	60.5/254/109.8/59.5 (9)	52/131.9/91.1/29.1 (10)	24/193.2/68.6/39.2 (21)	-/-/-/- (0)	15/286.7/80.4/56.5 (87)	17.7/125/53.7/22.0 (64)
UC09	95.2/95.2/95.2/- (1)	281.6/281.6/281.6/- (1)	-/-/-/- (0)	-/-/-/- (0)	-/-/-/- (0)	90/246.7/147.3/63.6 (5)	75/75/75/0 (2)
UC10	-/-/-/- (0)	-/-/-/- (0)	-/-/-/- (0)	-/-/-/- (0)	-/-/-/- (0)	-/-/-/- (0)	-/-/-/- (0)
UC11	162.5/162.5/162.5/- (1)	181.3/373/277.1/135.6 (2)	318/718/497/179.1 (5)	435.6/435.6/435.6/- (1)	371.5/665/518.8/146.8 (3)	280/1000/752.5/266.1 (54)	-/-/-/- (0)
UC12	121.0/121.0/121.0/- (1)	187/187/187/- (1)	258.3/259.7/259/1.0 (2)	484.8/484.8/484.8/- (1)	-/-/-/- (0)	320/900/527.7/206.3 (13)	-/-/-/- (0)
US01	-/-/-/- (0)	-/-/-/- (0)	-/-/-/- (0)	-/-/-/- (0)	-/-/-/- (0)	-/-/-/- (0)	-/-/-/- (0)
US02	-/-/-/- (0)	-/-/-/- (0)	-/-/-/- (0)	-/-/-/- (0)	-/-/-/- (0)	-/-/-/- (0)	-/-/-/- (0)
US03	-/-/-/- (0)	-/-/-/- (0)	-/-/-/- (0)	-/-/-/- (0)	-/-/-/- (0)	-/-/-/- (0)	-/-/-/- (0)
US04	-/-/-/- (0)	-/-/-/- (0)	-/-/-/- (0)	-/-/-/- (0)	-/-/-/- (0)	-/-/-/- (0)	-/-/-/- (0)
US05	-/-/-/- (0)	-/-/-/- (0)	-/-/-/- (0)	-/-/-/- (0)	-/-/-/- (0)	-/-/-/- (0)	-/-/-/- (0)
US06	-/-/-/- (0)	-/-/-/- (0)	-/-/-/- (0)	-/-/-/- (0)	-/-/-/- (0)	-/-/-/- (0)	-/-/-/- (0)
US07	-/-/-/- (0)	-/-/-/- (0)	-/-/-/- (0)	-/-/-/- (0)	-/-/-/- (0)	-/-/-/- (0)	-/-/-/- (0)
US08	-/-/-/- (0)	-/-/-/- (0)	-/-/-/- (0)	-/-/-/- (0)	-/-/-/- (0)	-/-/-/- (0)	-/-/-/- (0)
US09	-/-/-/- (0)	-/-/-/- (0)	-/-/-/- (0)	-/-/-/- (0)	-/-/-/- (0)	-/-/-/- (0)	-/-/-/- (0)
US10	-/-/-/- (0)	-/-/-/- (0)	-/-/-/- (0)	-/-/-/- (0)	-/-/-/- (0)	-/-/-/- (0)	-/-/-/- (0)
US11	415.2/415.2/415.2/- (1)	-/-/-/- (0)	2554.2/2554.2/2554.2/- (1)	-/-/-/- (0)	-/-/-/- (0)	141.7/141.7/141.7/- (1)	-/-/-/- (0)

Table F-2 Statistical overview of the friction angle and small-strain shear modulus per geotechnical unit. Note, that the geotechnical units are based on CPT measurements and geophysical data. Hence, some CID tests are also performed for clay units.

Geotechnical unit	Friction angle [°]	Small-strain shear modulus [MPa]
	CIDU	P-S logging
UC01	-/-/-/- (0)	-/-/-/- (0)
UC03	-/-/-/- (0)	-/-/-/- (0)
UC04	-/-/-/- (0)	-/-/-/- (0)
UC05	-/-/-/- (0)	-/-/-/- (0)
UC07	-/-/-/- (0)	-/-/-/- (0)
UC08	27.2/39.5/33.1/2.9 (19)	37.4/158.3/91.7/37.1 (12)
UC09	36.7/36.7/36.7/- (1)	161.4/161.4/161.4/- (1)
UC10	-/-/-/- (0)	-/-/-/- (0)
UC11	22.5/37.3/32.4/4.8 (7)	192.8/1311.7/587.5/379.1 (18)
UC12	20.9/24.8/22.3/2.1 (3)	256.8/273.1/266.1/6.8 (4)
US01	-/-/-/- (0)	-/-/-/- (0)
US02	-/-/-/- (0)	-/-/-/- (0)
US03	-/-/-/- (0)	-/-/-/- (0)
US04	-/-/-/- (0)	-/-/-/- (0)
US05	-/-/-/- (0)	-/-/-/- (0)
US06	36.8/36.8/36.8/- (1)	-/-/-/- (0)
US07	-/-/-/- (0)	-/-/-/- (0)
US08	-/-/-/- (0)	-/-/-/- (0)
US09	-/-/-/- (0)	-/-/-/- (0)
US10	-/-/-/- (0)	-/-/-/- (0)
US11	36.9/41.3/39.1/3.2 (2)	122.5/1236.9/427.9/375.6 (10)

Table F-3 Statistical overview of particle size distribution per geotechnical unit based on available laboratory tests.

Geotechnical unit	Gravel content [%]	Sand content [%]	Silt content [%]	Clay content [%]	Fines content [%]
UC01	0/0/0/- (1)	4/4/4/- (1)	60/60/60/- (1)	36/36/36/- (1)	96/96/96/- (1)
UC03	-/-/-/- (0)	-/-/-/- (0)	-/-/-/- (0)	-/-/-/- (0)	-/-/-/- (0)
UC04	-/-/-/- (0)	-/-/-/- (0)	-/-/-/- (0)	-/-/-/- (0)	-/-/-/- (0)
UC05	-/-/-/- (0)	-/-/-/- (0)	-/-/-/- (0)	-/-/-/- (0)	-/-/-/- (0)
UC07	-/-/-/- (0)	-/-/-/- (0)	-/-/-/- (0)	-/-/-/- (0)	-/-/-/- (0)
UC08	0/10/1.5/2.6 (20)	1/46/15.2/13.4 (20)	30/53/43.3/5.4 (20)	14/56/40.1/12 (20)	44/99/83.4/15.5 (20)
UC09	4/4/4/- (1)	41/41/41/- (1)	30/30/30/- (1)	25/25/25/- (1)	55/55/55/- (1)
UC10	-/-/-/- (0)	-/-/-/- (0)	-/-/-/- (0)	-/-/-/- (0)	-/-/-/- (0)
UC11	1/8/4.2/2.1 (9)	5/53/37.8/16.4 (9)	28/46/33.4/5.3 (9)	14/48/24.6/12.8 (9)	42/94/58/17.6 (9)
UC12	0/2/1/1.4 (2)	0/1/0.5/0.7 (2)	28/33/30.5/3.5 (2)	67/69/68/1.4 (2)	97/100/98.5/2.1 (2)
US01	-/-/-/- (0)	-/-/-/- (0)	-/-/-/- (0)	-/-/-/- (0)	-/-/-/- (0)
US02	1/14/7.5/9.2 (2)	77/79/78/1.4 (2)	9/13/11/2.8 (2)	0/7/3.5/4.9 (2)	9/20/14.5/7.8 (2)
US03	-/-/-/- (0)	-/-/-/- (0)	-/-/-/- (0)	-/-/-/- (0)	-/-/-/- (0)
US04	-/-/-/- (0)	-/-/-/- (0)	-/-/-/- (0)	-/-/-/- (0)	-/-/-/- (0)
US05	-/-/-/- (0)	-/-/-/- (0)	-/-/-/- (0)	-/-/-/- (0)	-/-/-/- (0)
US06	1/1/1/0 (2)	67/83/75/11.3 (2)	14/18/16/2.8 (2)	2/14/8/8.5 (2)	16/32/24/11.3 (2)
US07	-/-/-/- (0)	-/-/-/- (0)	-/-/-/- (0)	-/-/-/- (0)	-/-/-/- (0)
US08	0/0/0/0 (2)	81/97/89/11.3 (2)	3/15/9/8.5 (2)	0/4/2/2.8 (2)	3/19/11/11.3 (2)
US09	-/-/-/- (0)	-/-/-/- (0)	-/-/-/- (0)	-/-/-/- (0)	-/-/-/- (0)
US10	0/0/0/- (1)	92/92/92/- (1)	8/8/8/- (1)	0/0/0/- (1)	8/8/8/- (1)
US11	0/5/1.6/2.2 (11)	7/94/40.5/26.2 (11)	1/82/49.2/23.6 (11)	0/20/8.6/6.5 (11)	1/93/57.8/27.7 (11)

Table F-4 Statistical overview of densities from classification tests per geotechnical unit based on available laboratory tests.

Geotechnical unit	Bulk density [Mg/m^3]	Dry density [Mg/m^3]	Particle density [Mg/m^3]	Maximum dry density [Mg/m^3]	Minimum dry density [Mg/m^3]
UC01	1.69/1.8/1.74/0.06 (3)	1.1/1.34/1.18/0.14 (3)	2.65/2.65/2.65/- (1)	-/-/-/- (0)	-/-/-/- (0)
UC03	1.58/1.85/1.71/0.12 (4)	1/1.41/1.15/0.18 (4)	-/-/-/- (0)	-/-/-/- (0)	-/-/-/- (0)
UC04	-/-/-/- (0)	-/-/-/- (0)	-/-/-/- (0)	-/-/-/- (0)	-/-/-/- (0)
UC05	-/-/-/- (0)	-/-/-/- (0)	-/-/-/- (0)	-/-/-/- (0)	-/-/-/- (0)
UC07	-/-/-/- (0)	-/-/-/- (0)	-/-/-/- (0)	-/-/-/- (0)	-/-/-/- (0)
UC08	1.38/2.37/2.01/0.17 (55)	1.39/2.03/1.69/0.23 (8)	2.69/2.71/2.7/0.01 (7)	-/-/-/- (0)	-/-/-/- (0)
UC09	2.1/2.12/2.11/0.01 (2)	-/-/-/- (0)	2.57/2.57/2.57/- (1)	-/-/-/- (0)	-/-/-/- (0)
UC10	-/-/-/- (0)	-/-/-/- (0)	-/-/-/- (0)	-/-/-/- (0)	-/-/-/- (0)
UC11	1.93/2.49/2.24/0.13 (35)	1.85/1.85/1.85/- (1)	2.51/2.72/2.64/0.07 (6)	-/-/-/- (0)	-/-/-/- (0)
UC12	1.78/2.15/2.04/0.09 (14)	-/-/-/- (0)	-/-/-/- (0)	-/-/-/- (0)	-/-/-/- (0)
US01	-/-/-/- (0)	-/-/-/- (0)	-/-/-/- (0)	-/-/-/- (0)	-/-/-/- (0)
US02	1.78/1.93/1.87/0.08 (3)	1.24/1.6/1.41/0.18 (3)	2.62/2.62/2.62/- (1)	-/-/-/- (0)	-/-/-/- (0)
US03	-/-/-/- (0)	-/-/-/- (0)	-/-/-/- (0)	-/-/-/- (0)	-/-/-/- (0)
US04	1.86/1.86/1.86/- (1)	1.31/1.31/1.31/- (1)	-/-/-/- (0)	-/-/-/- (0)	-/-/-/- (0)
US05	-/-/-/- (0)	-/-/-/- (0)	-/-/-/- (0)	-/-/-/- (0)	-/-/-/- (0)
US06	1.99/2.04/2.02/0.02 (6)	1.6/1.68/1.64/0.03 (6)	2.65/2.65/2.65/- (1)	1.73/1.73/1.73/1.73 (1)	1.31/1.31/1.31/- (1)
US07	-/-/-/- (0)	-/-/-/- (0)	-/-/-/- (0)	-/-/-/- (0)	-/-/-/- (0)
US08	1.91/2.13/2.01/0.08 (8)	1.57/1.81/1.65/0.09 (8)	2.63/2.65/2.64/0.01 (3)	1.78/1.78/1.78/- (1)	1.3/1.3/1.3/- (1)
US09	-/-/-/- (0)	-/-/-/- (0)	-/-/-/- (0)	-/-/-/- (0)	-/-/-/- (0)
US10	-/-/-/- (0)	-/-/-/- (0)	2.62/2.62/2.62/- (1)	-/-/-/- (0)	-/-/-/- (0)
US11	1.76/2.34/2.09/0.13 (39)	1.61/2.08/1.77/0.15 (19)	2.6/2.68/2.64/0.02 (12)	-/-/-/- (0)	-/-/-/- (0)

Table F-5 Statistical overview of classification properties per geotechnical unit based on available laboratory tests. Note, that the geotechnical units are based on CPT measurements and geophysical data. Hence, some test results are also given for sand units (i.e., tests performed on clayey/silty specimens present within a sand unit) even though Atterberg limits are generally only performed on silty/clayey soils.

Geotechnical unit	Liquid limit [%]	Plastic limit [%]	Plasticity index [%]
UC01	53/53/53/- (1)	21/21/21/- (1)	32/32/32/- (1)
UC03	-/-/-/- (0)	-/-/-/- (0)	-/-/-/- (0)
UC04	-/-/-/- (0)	-/-/-/- (0)	-/-/-/- (0)
UC05	-/-/-/- (0)	-/-/-/- (0)	-/-/-/- (0)
UC07	-/-/-/- (0)	-/-/-/- (0)	-/-/-/- (0)
UC08	20/62/44.6/11.3 (19)	11/23/18.7/3.5 (19)	9/39/25.9/7.9 (19)
UC09	39/39/39/- (1)	18/18/18/- (1)	21/21/21/- (1)
UC10	-/-/-/- (0)	-/-/-/- (0)	-/-/-/- (0)
UC11	20/49/31.9/11.3 (11)	11/23/15.5/4.6 (11)	7/28/16.5/7.1 (11)
UC12	57/71/65.4/5.5 (5)	23/28/24.8/2 (5)	34/45/40.6/4.5 (5)
US01	-/-/-/- (0)	-/-/-/- (0)	-/-/-/- (0)
US02	-/-/-/- (0)	-/-/-/- (0)	-/-/-/- (0)
US03	-/-/-/- (0)	-/-/-/- (0)	-/-/-/- (0)
US04	-/-/-/- (0)	-/-/-/- (0)	-/-/-/- (0)
US05	-/-/-/- (0)	-/-/-/- (0)	-/-/-/- (0)
US06	-/-/-/- (0)	-/-/-/- (0)	-/-/-/- (0)
US07	-/-/-/- (0)	-/-/-/- (0)	-/-/-/- (0)
US08	-/-/-/- (0)	-/-/-/- (0)	-/-/-/- (0)
US09	-/-/-/- (0)	-/-/-/- (0)	-/-/-/- (0)
US10	-/-/-/- (0)	-/-/-/- (0)	-/-/-/- (0)
US11	27/27/27/- (1)	19/19/19/- (1)	8/8/8/- (1)

Table F-6 Statistical overview of classification properties per geotechnical unit based on available laboratory tests.

Geotechnical unit	Carbonate content [%]	Organic matter content [%]	Water soluble chloride [g/l]	Total acid sulphate [%]	Thermal conductivity [W/(mK)]
UC01	2.9/2.9/2.9/- (1)	-/-/-/- (0)	3.7/3.7/3.7/- (1)	0.09/0.09/0.09/- (1)	-/-/-/- (0)
UC03	3.5/3.5/3.5/- (1)	2.5/2.5/2.5/- (1)	2.5/2.5/2.5/- (1)	0.08/0.08/0.08/- (1)	-/-/-/- (0)
UC04	-/-/-/- (0)	-/-/-/- (0)	-/-/-/- (0)	-/-/-/- (0)	-/-/-/- (0)
UC05	-/-/-/- (0)	-/-/-/- (0)	-/-/-/- (0)	-/-/-/- (0)	-/-/-/- (0)
UC07	-/-/-/- (0)	-/-/-/- (0)	-/-/-/- (0)	-/-/-/- (0)	-/-/-/- (0)
UC08	1.9/32/14.4/13.7 (6)	3.1/4.5/3.8/1 (2)	1.6/2.4/1.8/0.3 (6)	0.08/0.59/0.24/0.19 (6)	1.27/2.64/1.63/0.57 (5)
UC09	-/-/-/- (0)	-/-/-/- (0)	-/-/-/- (0)	-/-/-/- (0)	-/-/-/- (0)
UC10	-/-/-/- (0)	-/-/-/- (0)	-/-/-/- (0)	-/-/-/- (0)	-/-/-/- (0)
UC11	3.5/19/9/8.6 (3)	-/-/-/- (0)	0.5/0.6/0.5/0.1 (3)	0.09/0.2/0.14/0.06 (3)	-/-/-/- (0)
UC12	0/0/0/- (1)	-/-/-/- (0)	2.6/2.6/2.6/- (1)	0.07/0.07/0.07/- (1)	-/-/-/- (0)
US01	-/-/-/- (0)	-/-/-/- (0)	-/-/-/- (0)	-/-/-/- (0)	-/-/-/- (0)
US02	1.4/1.4/1.4/- (1)	3.5/3.5/3.5/- (1)	2.3/2.3/2.3/- (1)	0.14/0.14/0.14/- (1)	-/-/-/- (0)
US03	-/-/-/- (0)	-/-/-/- (0)	-/-/-/- (0)	-/-/-/- (0)	-/-/-/- (0)
US04	29/29/29/- (1)	-/-/-/- (0)	1.6/1.6/1.6/- (1)	0.1/0.1/0.1/- (1)	-/-/-/- (0)
US05	-/-/-/- (0)	-/-/-/- (0)	-/-/-/- (0)	-/-/-/- (0)	-/-/-/- (0)
US06	16/16/16/- (1)	0.7/0.7/0.7/- (1)	2.4/2.4/2.4/- (1)	0.14/0.14/0.14/- (1)	-/-/-/- (0)
US07	-/-/-/- (0)	-/-/-/- (0)	-/-/-/- (0)	-/-/-/- (0)	-/-/-/- (0)
US08	2.6/12/7.3/6.6 (2)	0.9/0.9/0.9/- (1)	1.8/2/1.9/0.1 (2)	0.11/0.14/0.13/0.02 (2)	-/-/-/- (0)
US09	-/-/-/- (0)	-/-/-/- (0)	-/-/-/- (0)	-/-/-/- (0)	-/-/-/- (0)
US10	-/-/-/- (0)	-/-/-/- (0)	-/-/-/- (0)	-/-/-/- (0)	-/-/-/- (0)
US11	5.6/5.6/5.6/- (1)	1.9/3.4/2.7/1.1 (2)	1.5/1.5/1.5/- (1)	0.24/0.24/0.24/- (1)	2.05/2.05/2.05/- (1)

Appendix G Conceptual Geological Model

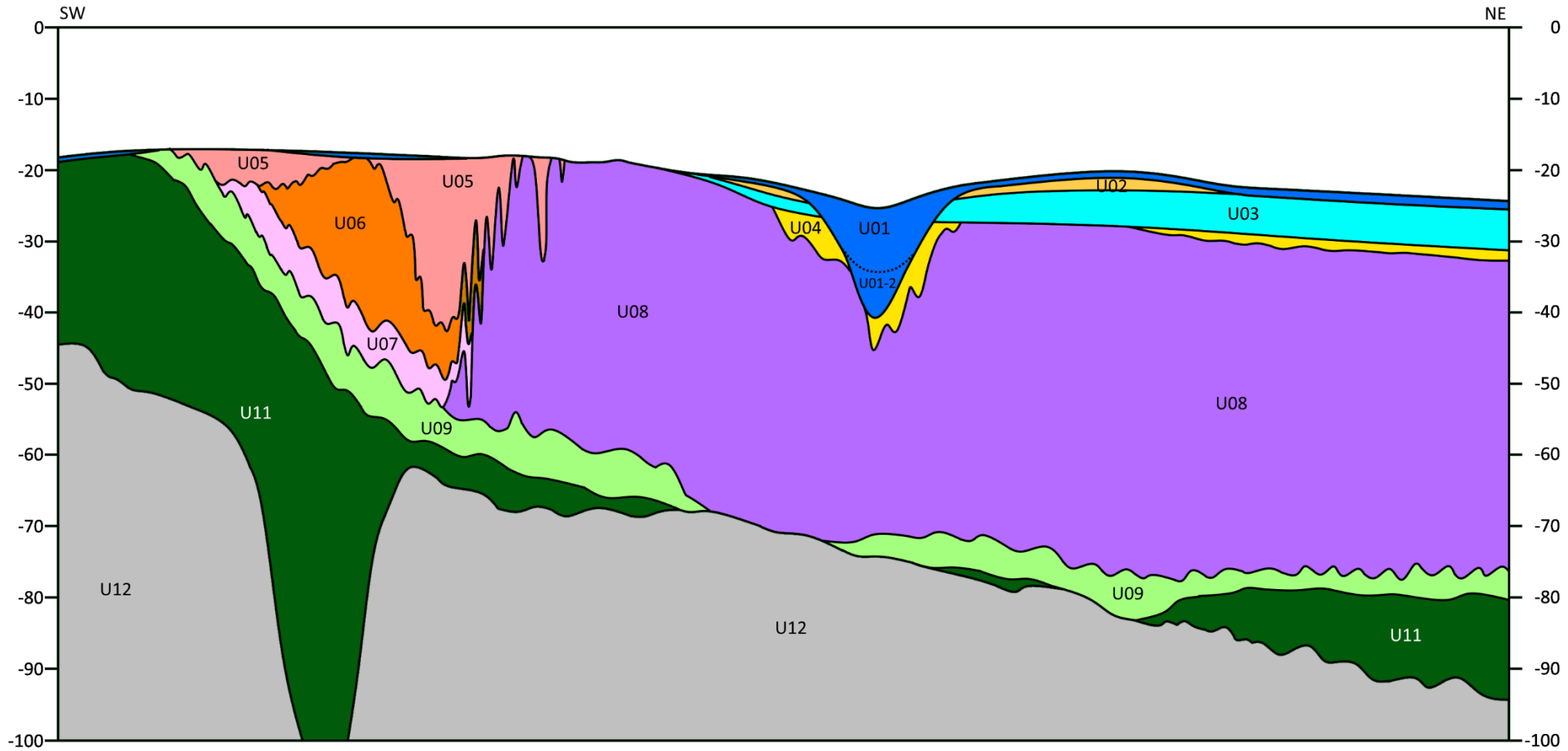

Figure G-1 Conceptual model cross section oriented from southwest to northeast through the central part of the site.

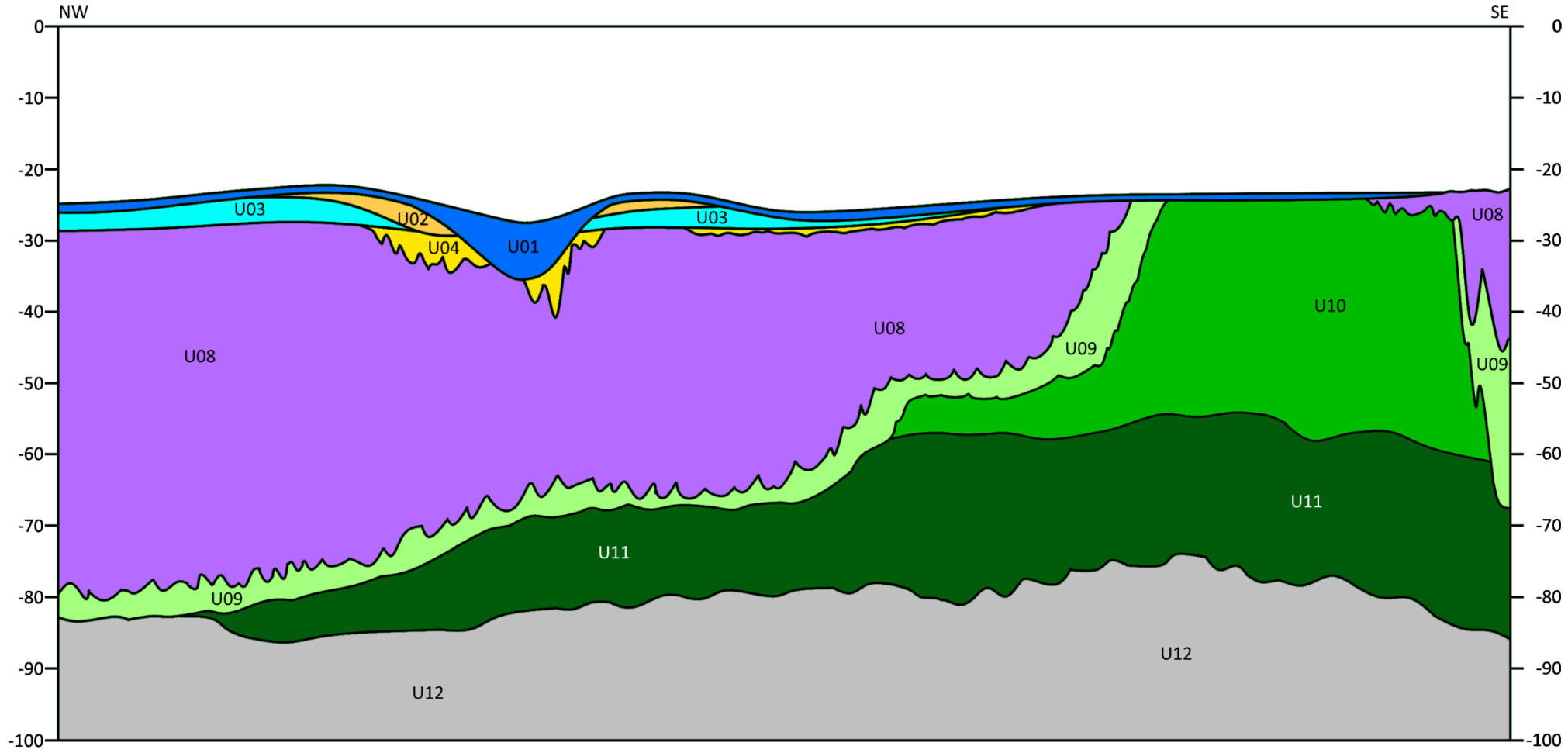

Figure G-2 Conceptual model cross section oriented from northwest to southeast through the central to northern part of the site.

Appendix H Soil profiles for LPA assessment

As stated in section 11.3, constant strength parameters are required as input for the high-level LPA assessment per geotechnical location. For estimating the required strength parameters for the different layers, the following procedure is used:

- For clay layers, the undrained shear strength is estimated for each individual layer by disregarding the highest and lowest 10% of the data. This is done to remove potential smaller outliers from the considered data sample from the layer. After, the average value from the remaining 80% of the measurements are determined and used as representative value for the layer.

- For sand layers, the undrained friction angle is estimated for each individual layer by disregarding the highest and lowest 10% of the data. This is done to remove potential smaller outliers from the considered data sample from the layer. After, the average value from the remaining 80% of the measurements are determined and used as representative value for the layer.

- For all type of layers, in case a startup of new CPT push is present in the layer, the first 20 cm (10 measurements) from the CPT push are removed for the strength value to not be wrongfully lowered due to the effect from this.

Table H-1 Soil stratigraphy per geotechnical location considered for e analyses.

Location	Unit	Top [m]	Bottom [m]	Material	Undrained shear strength [kPa]	Friction angle [°]
HS_S_01	US01	0.0	0.3	SAND	-	25.7
HS_S_01	UC01	0.3	1.3	CLAY	4.5	-
HS_S_01	UC03	1.3	4.9	CLAY	22.5	-
HS_S_01	US03	4.9	5.2	SAND	-	32.3
HS_S_01	UC08	5.2	30.3	CLAY	42.8	-
HS_S_02	UC01	0.0	1.3	CLAY	6.0	-
HS_S_02	UC03	1.3	5.0	CLAY	25.6	-
HS_S_02	US03	5.0	5.7	SAND	-	35.3
HS_S_02	UC08	5.7	44.0	CLAY	64.2	-
HS_S_02	UC09	44.0	48.1	CLAY	149.5	-
HS_S_02	UC11	48.1	58.1	CLAY	890.1	-
HS_S_02	US11	58.1	63.2	SAND	-	39.6
HS_S_03	UC01	0.0	2.1	CLAY	7.3	-
HS_S_03	US02	2.1	2.9	SAND	-	32.3
HS_S_03	UC03	2.9	5.1	CLAY	26.3	-
HS_S_03	US04	5.1	9.5	SAND	-	41.9
HS_S_03	UC08	9.5	18.8	CLAY	50.8	-
HS_S_04	US01	0.0	0.8	SAND	-	28.3

Location	Unit	Top [m]	Bottom [m]	Material	Undrained shear strength [kPa]	Friction angle [°]
HS_S_04	UC03	0.8	5.0	CLAY	14.1	-
HS_S_04	US04	5.0	6.9	SAND	-	37.1
HS_S_04	UC08	6.9	31.1	CLAY	60.9	-
HS_S_06	US01	0.0	0.5	SAND	-	30.2
HS_S_06	UC03	0.5	5.7	CLAY	10.8	-
HS_S_06	US04	5.7	8.0	SAND	-	38.3
HS_S_06	UC08	8.0	27.6	CLAY	63.4	-
HS_S_06	US10	27.6	32.3	SAND	-	41.3
HS_S_06	US11	32.3	35.2	SAND	-	39.7
HS_S_06	UC11	35.2	46.7	CLAY	388.9	-
HS_S_06	UC11	46.7	50.5	CLAY	699.4	-
HS_S_06	US11	50.5	61.7	SAND	-	40.8
HS_S_06	UC12	61.7	62.7	CLAY	1253.4	-
HS_S_07	US01	0.0	0.6	SAND	-	30.2
HS_S_07	UC03	0.6	3.2	CLAY	17.7	-
HS_S_07	US03	3.2	3.9	SAND	-	37.6
HS_S_07	US03	3.9	5.4	SAND	-	31.9
HS_S_07	US04	5.4	6.5	SAND	-	33.1
HS_S_07	UC04	6.5	7.2	CLAY	78.4	-
HS_S_07	US04	7.2	7.7	SAND	-	33.7
HS_S_07	US04	7.7	8.5	SAND	-	39.5
HS_S_07	UC08	8.5	30.2	CLAY	64.5	-
HS_S_10	UC01	0.0	1.9	CLAY	10.5	-
HS_S_10	US02	1.9	3.9	SAND	-	39.1
HS_S_10	US02	3.9	6.3	SAND	-	33.1
HS_S_10	UC03	6.3	8.6	CLAY	30.6	-
HS_S_10	UC08	8.6	30.1	CLAY	107.5	-
HS_S_11	UC01	0.0	3.6	CLAY	5.5	-
HS_S_11	US02	3.6	5.2	SAND	-	27.1
HS_S_11	UC08	5.2	30.2	CLAY	78.5	-
HS_S_12	UC01	0.0	0.7	CLAY	4.5	-
HS_S_12	UC03	0.7	2.0	CLAY	6.0	-
HS_S_12	US04	2.0	3.8	SAND	-	38.3
HS_S_12	UC08	3.8	16.9	CLAY	66.2	-
HS_S_12	UC09	16.9	19.6	CLAY	83.0	-
HS_S_13	US01	0.0	1.0	SAND	-	34.7
HS_S_13	US02	1.0	2.1	SAND	-	30.9
HS_S_13	UC03	2.1	7.0	CLAY	19.3	-
HS_S_13	US04	7.0	9.3	SAND	-	37.3
HS_S_13	UC08	9.3	18.8	CLAY	59.1	-
HS_S_13	UC09	18.8	22.7	CLAY	144.9	-
HS_S_13	US10	22.7	29.8	SAND	-	43.3
HS_S_13	US11	29.8	30.4	SAND	-	41.2
HS_S_14	US01	0.0	1.0	SAND	-	33.6
HS_S_14	US02	1.0	2.8	SAND	-	29.3
HS_S_14	UC03	2.8	5.9	CLAY	22.2	-
HS_S_14	UC08	5.9	7.6	CLAY	126.2	-

Location	Unit	Top [m]	Bottom [m]	Material	Undrained shear strength [kPa]	Friction angle [°]
HS_S_14	UC08	7.6	22.8	CLAY	71.3	-
HS_S_14	UC09	22.8	30.6	CLAY	221.9	-
HS_S_14	US09	30.6	31.1	SAND	-	38.7
HS_S_16	UC01	0.0	2.8	CLAY	8.1	-
HS_S_16	US02	2.8	6.3	SAND	-	35.3
HS_S_16	US03	6.3	6.8	SAND	-	31.2
HS_S_16	UC08	6.8	13.8	CLAY	40.0	-
HS_S_16	US08	13.8	15.5	SAND	-	37.3
HS_S_17	UC01	0.0	1.7	CLAY	11.2	-
HS_S_17	US02	1.7	4.3	SAND	-	35.0
HS_S_17	UC08	4.3	6.5	CLAY	144.9	-
HS_S_17	US08	6.5	7.0	SAND	-	33.1
HS_S_17	UC08	7.0	8.6	CLAY	93.8	-
HS_S_17	US08	8.6	14.6	SAND	-	40.7
HS_S_17	UC08	14.6	17.8	CLAY	148.7	-
HS_S_17	US08	17.8	23.5	SAND	-	40.4
HS_S_17	UC08	23.5	30.0	CLAY	242.5	-
HS_S_18	UC01	0.0	0.9	CLAY	4.0	-
HS_S_18	UC03	0.9	1.9	CLAY	8.9	-
HS_S_18	US04	1.9	2.7	SAND	-	35.2
HS_S_18	UC08	2.7	7.0	CLAY	66.2	-
HS_S_20	US01	0.0	1.2	SAND	-	26.6
HS_S_20	UC03	1.2	3.9	CLAY	11.2	-
HS_S_20	US08	3.9	5.7	SAND	-	37.6
HS_S_20	UC09	5.7	7.0	CLAY	274.4	-
HS_S_20	US10	7.0	17.2	SAND	-	39.7
HS_S_20	US10	17.2	25.6	SAND	-	44.2
HS_S_20	US10	25.6	30.4	SAND	-	39.6
HS_S_21	US01	0.0	1.3	SAND	-	33.5
HS_S_21	US02	1.3	4.0	SAND	-	37.4
HS_S_21	UC03	4.0	5.4	CLAY	50.3	-
HS_S_21	US04	5.4	6.0	SAND	-	34.1
HS_S_21	UC08	6.0	18.3	CLAY	105.2	-
HS_S_21	US08	18.3	21.2	SAND	-	40.0
HS_S_21	UC08	21.2	28.4	CLAY	123.5	-
HS_S_21	UC09	28.4	30.3	CLAY	127.6	-
HS_S_21	UC11	30.3	38.5	CLAY	776.0	-
HS_S_21	US11	38.5	44.6	SAND	-	41.8
HS_S_21	UC11	44.6	45.4	CLAY	1318.2	-
HS_S_21	US11	45.4	48.8	SAND	-	41.2
HS_S_22	US01	0.0	1.1	SAND	-	33.2
HS_S_22	US08	1.1	2.1	SAND	-	33.1
HS_S_22	US08	2.1	4.5	SAND	-	38.1
HS_S_22	UC08	4.5	8.7	CLAY	121.5	-
HS_S_22	US08	8.7	11.1	SAND	-	37.4
HS_S_22	UC08	11.1	19.2	CLAY	204.9	-
HS_S_22	US08	19.2	21.5	SAND	-	36.5

Location	Unit	Top [m]	Bottom [m]	Material	Undrained shear strength [kPa]	Friction angle [°]
HS_S_22	UC08	21.5	23.8	CLAY	576.3	-
HS_S_22	US08	23.8	29.6	SAND	-	41.2
HS_S_23	US01	0.0	0.2	SAND	-	41.0
HS_S_23	UC01	0.2	1.5	CLAY	40.0	-
HS_S_23	US08	1.5	4.5	SAND	-	36.1
HS_S_23	UC08	4.5	9.4	CLAY	192.2	-
HS_S_23	US08	9.4	14.1	SAND	-	40.2
HS_S_23	UC08	14.1	22.4	CLAY	392.0	-
HS_S_23	UC08	22.4	29.8	CLAY	215.0	-
HS_S_23	US09	29.8	30.3	SAND	-	38.8
HS_S_24	UC01	0.0	1.3	CLAY	3.9	-
HS_S_24	US08	1.3	2.9	SAND	-	35.4
HS_S_24	US08	2.9	4.8	SAND	-	40.9
HS_S_24	UC08	4.8	6.6	CLAY	17.8	-
HS_S_26	UC01	0.0	2.8	CLAY	7.4	-
HS_S_27	UC01	0.0	1.1	CLAY	11.0	-
HS_S_27	UC03	1.1	3.1	CLAY	10.3	-
HS_S_27	US10	3.1	14.1	SAND	-	43.3
HS_S_27	US10	14.1	19.1	SAND	-	41.2
HS_S_27	US10	19.1	30.7	SAND	-	43.4
HS_S_28	UC01	0.0	1.7	CLAY	25.9	-
HS_S_28	US10	1.7	4.0	SAND	-	45.1
HS_S_28	US10	4.0	28.6	SAND	-	43.3
HS_S_28	US10	28.6	30.2	SAND	-	39.6
HS_S_28	UC10	30.2	30.6	CLAY	364.9	-
HS_S_29	US01	0.0	1.1	SAND	-	32.4
HS_S_29	US08	1.1	3.6	SAND	-	33.3
HS_S_29	US08	3.6	8.6	SAND	-	38.4
HS_S_29	UC09	8.6	12.8	CLAY	141.5	-
HS_S_29	US10	12.8	20.5	SAND	-	42.6
HS_S_29	UC11	20.5	22.0	CLAY	1181.6	-
HS_S_29	US11	22.0	24.1	SAND	-	42.3
HS_S_29	UC11	24.1	25.9	CLAY	1350.1	-
HS_S_29	US11	25.9	29.7	SAND	-	42.1
HS_S_30	UC01	0.0	1.9	CLAY	24.4	-
HS_S_30	US05	1.9	2.9	SAND	-	35.8
HS_S_30	UC05	2.9	8.1	CLAY	78.0	-
HS_S_30	US06	8.1	10.2	SAND	-	31.2
HS_S_30	US06	10.2	22.6	SAND	-	38.8
HS_S_30	UC07	22.6	28.5	CLAY	195.4	-
HS_S_30	UC09	28.5	30.4	CLAY	353.8	-
HS_S_31	UC01	0.0	1.7	CLAY	13.4	-
HS_S_31	US05	1.7	8.3	SAND	-	37.1
HS_S_31	US06	8.3	26.7	SAND	-	38.0
HS_S_31	UC07	26.7	30.2	CLAY	147.6	-
HS_S_32	UC01	0.0	5.5	CLAY	8.8	-
HS_S_32	US04	5.5	7.7	SAND	-	38.5

Location	Unit	Top [m]	Bottom [m]	Material	Undrained shear strength [kPa]	Friction angle [°]
HS_S_32	US06	7.7	19.2	SAND	-	37.7
HS_S_32	UC07	19.2	23.4	CLAY	88.3	-
HS_S_33	UC01	0.0	1.7	CLAY	13.8	-
HS_S_33	US06	1.7	3.0	SAND	-	31.4
HS_S_33	UC07	3.0	23.7	CLAY	112.7	-
HS_S_33	UC09	23.7	27.4	CLAY	151.5	-
HS_S_33	UC11	27.4	29.8	CLAY	348.6	-
HS_S_33	US11	29.8	30.2	SAND	-	41.3
HS_S_35	US01	0.0	1.1	SAND	-	32.5
HS_S_35	UC07	1.1	5.5	CLAY	68.3	-
HS_S_35	UC09	5.5	10.6	CLAY	172.6	-
HS_S_35	US11	10.6	16.0	SAND	-	44.9
HS_S_35	UC11	16.0	19.9	CLAY	944.2	-
HS_S_35	US11	19.9	30.4	SAND	-	43
HS_S_36	US01	0.0	0.9	SAND	-	31.4
HS_S_36	US10	0.9	2.0	SAND	-	40.6
HS_S_36	UC10	2.0	2.7	CLAY	499.9	-
HS_S_36	US10	2.7	29.2	SAND	-	43.6
HS_S_37	UC01	0.0	13.6	CLAY	18.7	-
HS_S_37	US07	13.6	14.1	SAND	-	40.3
HS_S_37	UC09	14.1	18.2	CLAY	148.2	-
HS_S_37	US10	18.2	22.7	SAND	-	40.9
HS_S_37	UC11	22.7	25.3	CLAY	818.6	-
HS_S_37	UC12	25.3	29.1	CLAY	510.1	-
HS_S_38	US01	0.0	1.1	SAND	-	32.2
HS_S_38	US11	1.1	25.3	SAND	-	41.9
HS_S_38	UC11	25.3	52.2	CLAY	1321.7	-
HS_S_38	UC12	52.2	68.7	CLAY	641.3	-
HS_S_39	US01	0.0	0.5	SAND	-	33.0
HS_S_39	US11	0.5	3.7	SAND	-	43.8
HS_S_39	UC11	3.7	5.0	CLAY	1083.9	-
HS_S_39	US11	5.0	16.7	SAND	-	44.6
HS_S_39	UC11	16.7	24.2	CLAY	1254.4	-
HS_S_39	US11	24.2	27.5	SAND	-	43.5
HS_S_39	UC11	27.5	29.6	CLAY	1473.7	-
HS_S_39	US11	29.6	30.1	SAND	-	42.7